

Rivet user manual

version 2.1.2

Andy Buckley

PPE Group, School of Physics, University of Edinburgh, UK.
E-mail: andy.buckley@ed.ac.uk

Jonathan Butterworth

HEP Group, Dept. of Physics and Astronomy, UCL, London, UK.
E-mail: J.Butterworth@ucl.ac.uk

David Grellscheid

IPPP, Durham University, UK.
E-mail: david.grellscheid@durham.ac.uk

Hendrik Hoeth

IPPP, Durham University, UK.
E-mail: hendrik.hoeth@cern.ch

Leif Lönnblad

Theoretical Physics, Lund University, Sweden.
E-mail: lonnblad@thep.lu.se

James Monk

Experimental Particle Physics, Niels Bohr Institute, Copenhagen, Denmark.
E-mail: jmonk@cern.ch

Holger Schulz

Institut für Physik, Berlin Humboldt University, Germany.
E-mail: holger.schulz@physik.hu-berlin.de

Jan Eike von Seggern

Institut für Physik, Berlin Humboldt University, Germany.
E-mail: vsegger@physik.hu-berlin.de

Frank Siegert

Physikalisches Institut, Freiburg University, Germany.
E-mail: frank.siegert@cern.ch

ABSTRACT: This is the manual and user guide for the Rivet system for the validation and tuning of Monte Carlo event generators. As well as the core Rivet library, this manual describes the usage of the `rivet` program and the AGILE generator interface library. The depth and level of description is chosen for users of the system, starting with the basics of using validation code written by others, and then covering sufficient details to write new Rivet analyses and calculational components.

KEYWORDS: Event generator, simulation, validation, tuning, QCD.

Contents

1. Introduction	9
1.1 Typographic conventions	10
I Getting started with Rivet	11
2. Quickstart	11
2.1 Getting generators for AGILE	12
2.2 Command completion	13
3. Running Rivet analyses	13
3.1 The FIFO idiom	13
3.2 Analysis status	14
3.3 Example <code>rivet</code> commands	15
4. Using analysis data	16
4.1 Histogram formats	16
4.2 Plotting and comparing data	17
4.3 Merging histograms from different Rivet runs	17
5. Outdated information for AIDA in Rivet 1.x	18
5.1 Chopping histograms	18
5.2 Normalising histograms	18
II Standard Rivet analyses	20
6. LEP and SLC analyses	20
6.1 ALEPH_1991_S2435284	20
6.2 ALEPH_1996_S3196992	21
6.3 ALEPH_1996_S3486095	22
6.4 ALEPH_1999_S4193598	25
6.5 ALEPH_2001_S4656318	26
6.6 ALEPH_2002_S4823664	27
6.7 ALEPH_2004_S5765862	28
6.8 DELPHI_1995_S3137023	38
6.9 DELPHI_1996_S3430090	39
6.10 DELPHI_1999_S3960137	42
6.11 DELPHI_2000_S4328825	43
6.12 DELPHI_2002_069_CONF_603	44
6.13 DELPHI_2003_WUD_03_11	45

6.14	JADE_OPAL_2000_S4300807	46
6.15	OPAL_1993_S2692198	51
6.16	OPAL_1994_S2927284	52
6.17	OPAL_1995_S3198391	53
6.18	OPAL_1996_S3257789	54
6.19	OPAL_1997_S3396100	55
6.20	OPAL_1997_S3608263	56
6.21	OPAL_1998_S3702294	57
6.22	OPAL_1998_S3749908	58
6.23	OPAL_1998_S3780481	59
6.24	OPAL_2000_S4418603	60
6.25	OPAL_2001_S4553896	61
6.26	OPAL_2002_S5361494	62
6.27	OPAL_2004_S6132243	63
6.28	SLD_1996_S3398250	68
6.29	SLD_1999_S3743934	69
6.30	SLD_2002_S4869273	74
6.31	SLD_2004_S5693039	75
7.	Tevatron analyses	78
7.1	CDF_1988_S1865951	78
7.2	CDF_1990_S2089246	79
7.3	CDF_1993_S2742446	80
7.4	CDF_1994_S2952106	81
7.5	CDF_1996_S3108457	82
7.6	CDF_1996_S3349578	83
7.7	CDF_1996_S3418421	85
7.8	CDF_1997_S3541940	86
7.9	CDF_1998_S3618439	88
7.10	CDF_2000_S4155203	89
7.11	CDF_2000_S4266730	90
7.12	CDF_2001_S4517016	91
7.13	CDF_2001_S4563131	92
7.14	CDF_2001_S4751469	93
7.15	CDF_2002_S4796047	95
7.16	CDF_2004_S5839831	96
7.17	CDF_2005_S6080774	98
7.18	CDF_2005_S6217184	100
7.19	CDF_2006_S6450792	102
7.20	CDF_2006_S6653332	103
7.21	CDF_2007_S7057202	104
7.22	CDF_2008_S7540469	105
7.23	CDF_2008_S7541902	106

7.24	CDF_2008_S7782535	108
7.25	CDF_2008_S7828950	109
7.26	CDF_2008_S8093652	110
7.27	CDF_2008_S8095620	111
7.28	CDF_2009_NOTE_9936	112
7.29	CDF_2009_S8233977	113
7.30	CDF_2009_S8383952	114
7.31	CDF_2009_S8436959	115
7.32	CDF_2010_S8591881_DY	116
7.33	CDF_2010_S8591881_QCD	118
7.34	CDF_2012_NOTE10874	120
7.35	D0_1996_S3214044	122
7.36	D0_1996_S3324664	124
7.37	D0_2000_I499943	125
7.38	D0_2000_S4480767	126
7.39	D0_2001_S4674421	127
7.40	D0_2004_S5992206	128
7.41	D0_2006_S6438750	129
7.42	D0_2007_S7075677	130
7.43	D0_2008_S6879055	131
7.44	D0_2008_S7554427	132
7.45	D0_2008_S7662670	133
7.46	D0_2008_S7719523	134
7.47	D0_2008_S7837160	136
7.48	D0_2008_S7863608	137
7.49	D0_2009_S8202443	138
7.50	D0_2009_S8320160	139
7.51	D0_2009_S8349509	140
7.52	D0_2010_S8566488	141
7.53	D0_2010_S8570965	142
7.54	D0_2010_S8671338	144
7.55	D0_2010_S8821313	145
7.56	D0_2011_I895662	146
7.57	E735_1998_S3905616	147
8.	LHC analyses	148
8.1	ALICE_2010_S8624100	148
8.2	ALICE_2010_S8625980	149
8.3	ALICE_2010_S8706239	150
8.4	ALICE_2011_S8909580	151
8.5	ALICE_2011_S8945144	152
8.6	ALICE_2012_I1181770	153
8.7	ATLAS_2010_CONF_2010_049	155

8.8	ATLAS_2010_S8591806	157
8.9	ATLAS_2010_S8817804	158
8.10	ATLAS_2010_S8894728	161
8.11	ATLAS_2010_S8914702	165
8.12	ATLAS_2010_S8918562	166
8.13	ATLAS_2010_S8919674	169
8.14	ATLAS_2011_CONF_2011_090	170
8.15	ATLAS_2011_CONF_2011_098	171
8.16	ATLAS_2011_I894867	172
8.17	ATLAS_2011_I919017	173
8.18	ATLAS_2011_I925932	184
8.19	ATLAS_2011_I926145	185
8.20	ATLAS_2011_I930220	186
8.21	ATLAS_2011_I944826	188
8.22	ATLAS_2011_I945498	190
8.23	ATLAS_2011_I954993	193
8.24	ATLAS_2011_S8924791	194
8.25	ATLAS_2011_S8971293	199
8.26	ATLAS_2011_S8983313	200
8.27	ATLAS_2011_S8994773	201
8.28	ATLAS_2011_S9002537	202
8.29	ATLAS_2011_S9019561	203
8.30	ATLAS_2011_S9035664	204
8.31	ATLAS_2011_S9041966	205
8.32	ATLAS_2011_S9108483	206
8.33	ATLAS_2011_S9120807	207
8.34	ATLAS_2011_S9126244	208
8.35	ATLAS_2011_S9128077	212
8.36	ATLAS_2011_S9131140	214
8.37	ATLAS_2011_S9212183	215
8.38	ATLAS_2011_S9212353	216
8.39	ATLAS_2011_S9225137	217
8.40	ATLAS_2012_CONF_2012_001	220
8.41	ATLAS_2012_CONF_2012_103	221
8.42	ATLAS_2012_CONF_2012_104	222
8.43	ATLAS_2012_CONF_2012_105	223
8.44	ATLAS_2012_CONF_2012_109	224
8.45	ATLAS_2012_CONF_2012_153	225
8.46	ATLAS_2012_I1082009	226
8.47	ATLAS_2012_I1082936	227
8.48	ATLAS_2012_I1083318	230
8.49	ATLAS_2012_I1084540	233
8.50	ATLAS_2012_I1091481	243

8.51	ATLAS_2012_I1093734	245
8.52	ATLAS_2012_I1093738	247
8.53	ATLAS_2012_I1094564	248
8.54	ATLAS_2012_I1094568	251
8.55	ATLAS_2012_I1095236	252
8.56	ATLAS_2012_I1112263	253
8.57	ATLAS_2012_I1117704	254
8.58	ATLAS_2012_I1118269	255
8.59	ATLAS_2012_I1119557	256
8.60	ATLAS_2012_I1124167	257
8.61	ATLAS_2012_I1125575	259
8.62	ATLAS_2012_I1125961	272
8.63	ATLAS_2012_I1126136	273
8.64	ATLAS_2012_I1180197	274
8.65	ATLAS_2012_I1183818	275
8.66	ATLAS_2012_I1186556	277
8.67	ATLAS_2012_I1188891	278
8.68	ATLAS_2012_I1190891	279
8.69	ATLAS_2012_I1203852	280
8.70	ATLAS_2012_I1204447	281
8.71	ATLAS_2012_I1204784	282
8.72	ATLAS_2012_I943401	284
8.73	ATLAS_2012_I946427	286
8.74	ATLAS_2013_I1190187	287
8.75	ATLAS_2013_I1217867	288
8.76	ATLAS_2013_I1230812	289
8.77	ATLAS_2013_I1230812_EL	291
8.78	ATLAS_2013_I1230812_MU	293
8.79	ATLAS_2013_I1243871	295
8.80	CMS_2010_S8547297	296
8.81	CMS_2010_S8656010	298
8.82	CMS_2011_I954992	300
8.83	CMS_2011_S8884919	301
8.84	CMS_2011_S8941262	303
8.85	CMS_2011_S8950903	304
8.86	CMS_2011_S8957746	305
8.87	CMS_2011_S8968497	306
8.88	CMS_2011_S8973270	308
8.89	CMS_2011_S8978280	309
8.90	CMS_2011_S9086218	311
8.91	CMS_2011_S9088458	312
8.92	CMS_2011_S9120041	313
8.93	CMS_2011_S9215166	315

8.94 CMS_2012_I1087342	316
8.95 CMS_2012_I1090423	317
8.96 CMS_2012_I1102908	319
8.97 CMS_2012_I1107658	321
8.98 CMS_2012_I1184941	323
8.99 CMS_2012_I1193338	324
8.100CMS_2012_I941555	325
8.101CMS_2012_PAS_QCD_11_010	326
8.102CMS_2013_I1209721	327
8.103CMS_2013_I1218372	329
8.104CMS_2013_I1224539_DIJET	330
8.105CMS_2013_I1224539_WJET	332
8.106CMS_2013_I1224539_ZJET	334
8.107CMS_2013_I1256943	336
8.108CMS_2013_I1258128	338
8.109CMS_2013_I1261026	340
8.110CMS_2013_I1265659	342
8.111CMS_2013_I1272853	343
8.112CMS_2013_I1273574	344
8.113CMS_QCD_10_024	346
8.114LHCb_2010_I867355	347
8.115LHCb_2010_S8758301	348
8.116LHCb_2011_I917009	349
8.117LHCb_2011_I919315	351
8.118LHCb_2012_I1119400	352
8.119LHCb_2013_I1208105	355
8.120LHCb_2013_I1218996	357
8.121LHCF_2012_I1115479	360
8.122TOTEM_2012_002	361
8.123TOTEM_2012_I1115294	362
9. SPS analyses	363
9.1 UA1_1990_S2044935	363
9.2 UA5_1982_S875503	365
9.3 UA5_1986_S1583476	366
9.4 UA5_1987_S1640666	368
9.5 UA5_1988_S1867512	369
9.6 UA5_1989_S1926373	370
10. HERA analyses	372
10.1 H1_1994_S2919893	372
10.2 H1_1995_S3167097	373
10.3 H1_2000_S4129130	374

10.4 ZEUS_2001_S4815815	376
11. RHIC analyses	377
11.1 STAR_2006_S6500200	377
11.2 STAR_2006_S6860818	378
11.3 STAR_2006_S6870392	379
11.4 STAR_2008_S7869363	380
11.5 STAR_2008_S7993412	381
11.6 STAR_2009_UE_HELEN	382
12. Monte Carlo analyses	383
12.1 MC_DIJET	383
12.2 MC_DIPHOTON	384
12.3 MC_GENERIC	385
12.4 MC_HINC	386
12.5 MC_HJETS	387
12.6 MC_HKTSPATTERINGS	388
12.7 MC_IDENTIFIED	389
12.8 MC_JETS	390
12.9 MC_LEADJETUE	391
12.10MC_PDFs	392
12.11MC_PHOTONINC	393
12.12MC_PHOTONJETS	394
12.13MC_PHOTONJETUE	395
12.14MC_PHOTONKTSPATTERINGS	396
12.15MC_PHOTONS	397
12.16MC_PRINTEVENT	398
12.17MC_QCD_PARTONS	399
12.18MC_SUSY	400
12.19MC_TTBAR	401
12.20MC_VH2BB	402
12.21MC_WINC	403
12.22MC_WJETS	404
12.23MC_WKTSPATTERINGS	405
12.24MC_WPOL	406
12.25MC_WWINC	407
12.26MC_WWJETS	408
12.27MC_WWKTSPATTERINGS	409
12.28MC_XS	410
12.29MC_ZINC	411
12.30MC_ZJETS	412
12.31MC_ZKTSPATTERINGS	413
12.32MC_ZZINC	414

12.33	MC_ZZJETS	415
12.34	MC_ZZKTSPLITTINGS	416
13.	Example analyses	417
13.1	EXAMPLE	417
14.	Misc. analyses	418
14.1	ARGUS_1993_S2653028	418
14.2	ARGUS_1993_S2669951	419
14.3	ARGUS_1993_S2789213	420
14.4	ATLAS_2012_I1199269	422
14.5	BABAR_2003_I593379	423
14.6	BABAR_2005_S6181155	424
14.7	BABAR_2007_S6895344	425
14.8	BABAR_2007_S7266081	426
14.9	BELLE_2001_S4598261	428
14.10	BELLE_2006_S6265367	429
14.11	CLEO_2004_S5809304	431
14.12	JADE_1998_S3612880	433
14.13	PDG_HADRON_MULTIPLICITIES	434
14.14	PDG_HADRON_MULTIPLICITIES RATIOS	439
14.15	SFM_1984_S1178091	445
14.16	TASSO_1990_S2148048	446
III	How Rivet works	448
15.	The science and art of physically valid MC analysis	448
16.	Projections	450
16.1	Projection caching	450
16.2	Using projection caching	451
17.	Analyses	452
17.1	Writing a new analysis	452
17.2	Utility classes	454
17.2.1	FourMomentum	454
17.2.2	Particle	454
17.2.3	Jet	455
17.2.4	Mathematical utilities	455
17.3	Histogramming	455
17.4	Analysis metadata	456
17.4.1	Analysis info files	456
17.4.2	Plot styling files	456

17.5	Pluggable analyses	457
17.5.1	Plugin paths	457
18.	Using Rivet as a library	458
IV	Appendices	463
A.	Typical <code>agile-runmc</code> commands	463
B.	Acknowledgements	463
V	Bibliography	465

1. Introduction

This manual is a users’ guide to using the Rivet generator validation system. Rivet is a C++ class library, which provides the infrastructure and calculational tools for particle-level analyses for high energy collider experiments, enabling physicists to validate event generator models and tunings with minimal effort and maximum portability. Rivet is designed to scale effectively to large numbers of analyses for truly global validation, by transparent use of an automated result caching system.

The Rivet ethos, if it may be expressed succinctly, is that user analysis code should be extremely clean and easy to write — ideally it should be sufficiently self-explanatory to in itself be a reference to the experimental analysis algorithm — without sacrificing power or extensibility. The machinery to make this possible is intentionally hidden from the view of all but the most prying users. Generator independence is explicitly required by virtue of all analyses operating on the generic “HepMC” event record.

The simplest way to use Rivet is via the `rivet` command line tool, which analyses textual HepMC event records as they are generated and produces output distributions in a structured textual format. The input events are generated using the generator’s own steering program, if one is provided; for generators which provide no default way to produce HepMC output, the AGILE generator interface library, and in particular the `agile-runmc` command which it provides, may be useful. For those who wish to embed their analyses in some larger framework, Rivet can also be used as a library to run programmatically on HepMC event objects with no special executable being required.

Before we get started, a declaration of intent: this manual is intended to be a guide to using Rivet, rather than a comprehensive and painstakingly maintained reference to the application programming interface (API) of the Rivet library. For that purpose the online documentation at <http://rivet.hepforge.org> should be sufficient – in case of confusion

please contact the authors at `rivet@projects.hepforge.org`. Similar API documentation is maintained for AGILE at <http://agile.hepforge.org>.

1.1 Typographic conventions

As is normal in computer user manuals, the typography in this manual is used to indicate whether we are describing source code elements, commands to be run in a terminal, the output of a command etc.

The main such clue will be the use of **typewriter-style** text: this indicates the name of a command or code element — class names, function names etc. Typewriter font is also used for commands to be run in a terminal, but in this case it will be prefixed by a dollar sign, as in `$ echo "Hello" | cat`. The output of such a command on the terminal will be typeset in **sans-serif** font. When we are documenting a code feature in detail (which is not the main point of this manual), we will use square brackets to indicate optional arguments, and italic font between angle brackets to represent an argument name which should be replaced by a value, e.g. `Event::applyProjection(<proj>)`.

Part I

Getting started with Rivet

As with many things, Rivet may be meaningfully approached at several distinct levels of detail:

- The simplest, and we hope the most common, is to use the analyses which are already in the library to study events from a variety of generators and tunes: this is enormously valuable in itself and we encourage all manner of experimentalists and phenomenologists alike to use Rivet in this mode.
- A more involved level of usage is to write your own Rivet analyses — this may be done without affecting the installed standard analyses by use of a “plugin” system (although we encourage users who develop analyses to submit them to the Rivet developers for inclusion into a future release of the main package). This approach requires some understanding of programming within Rivet but you don’t *need* to know about exactly what the system is doing with the objects that you have defined.
- Finally, Rivet developers and people who want to do non-standard things with their analyses will need to know something about the messy details of what Rivet’s infrastructure is doing behind the scenes. But you’d probably rather be doing some physics!

The current part of this manual is for the first sort of user, who wants to get on with studying some observables with a generator or tune, or comparing several such models. Since everyone will fall into this category at some point, our present interest is to get you to that all-important “physics plots” stage as quickly as possible. Analysis authors and Rivet service-mechanics will find the more detailed information that they crave in Part III.

2. Quickstart

The point of this section is to get you up and running with Rivet as soon as possible. Doing this by hand may be rather frustrating, as Rivet depends on several external libraries — you’ll get bored downloading and building them by hand in the right order. Here we recommend a much simpler way — for the full details of how to build Rivet by hand, please consult the Rivet Web page.

Bootstrap script We have written a bootstrapping script which will download tarballs of Rivet, AGILE and the other required libraries, expand them and build them in the right order with the correct build flags. This is generally nicer than doing it all by hand, and virtually essential if you want to use the existing versions of FastJet, HepMC, generator libraries, and so on from CERN AFS: there are issues with these versions which the script works around, which you won’t find easy to do yourself.

To run the script, we recommend that you choose a personal installation directory, i.e. make a `~/local` directory for this purpose, to avoid polluting your home directory with a lot of files. If you already use a directory of the same name, you might want to use a separate one, say `~/rivetlocal`, such that if you need to delete everything in the installation area you can do so without difficulties.

Now, change directory to your build area (you may also want to make this, e.g. `~/build`), and download the script:

```
$ wget http://rivet.hepforge.org/svn/bootstrap/rivet-bootstrap  
$ chmod +x rivet-bootstrap
```

Now run it to get some help: `$./rivet-bootstrap --help`

Now to actually do the install: for example, to bootstrap Rivet and AGILE to the install area specified as the prefix argument, run this:

```
$ ./rivet-bootstrap --install-agile --prefix=<localdir>
```

If you are running on a system where the CERN AFS area is mounted as `/afs/cern.ch`, then the bootstrap script will attempt to use the pre-built HepMC[1], LHAPDF[2], FastJet[3, 4] and GSL libraries from the LCG software area. Either way, finally the bootstrap script will write out a file containing the environment settings which will make the system useable. You can source this file, e.g. `source rivetenv.sh` to make your current shell ready-to-go for a Rivet run (use `rivetenv.csh` if you are a C shell user).

You now have a working, installed copy of the Rivet and AGILE libraries, and the `rivet` and `agile-runmc` executables: respectively these are the command-line frontend to the Rivet analysis library, and a convenient steering command for generators which do not provide their own main program with HepMC output. To test that they work as expected, source the setup scripts as above, if you've not already done so, and run this:

```
$ rivet --help
```

This should print a quick-reference user guide for the `rivet` command to the terminal. Similarly, for `agile-runmc`,

```
$ agile-runmc --help  
$ agile-runmc --list-gens  
$ agile-runmc --beams=pp:14000 Pythia6:425
```

which should respectively print the help, list the available generators and make 10 LHC-type events using the Fortran Pythia[5] 6.423 generator. You're on your way! If no generators are listed, you probably need to install a local Genser-type generator repository: see section 2.1.

In this manual, because of its convenience, we will use `agile-runmc` as our canonical way of producing a stream of HepMC event data; if your interest is in running a generator like Sherpa[6], Pythia 8[7, 8], or Herwig++[9] which provides their own native way to make HepMC output, or a generator like PHOJET which is not currently supported by AGILE, then substitute the appropriate command in what follows. We'll discuss using these commands in detail in section 3.

2.1 Getting generators for AGILE

One last thing before continuing, though: the generators themselves. Again, if you're running on a system with the CERN LCG AFS area mounted, then `agile-runmc` will

attempt to automatically use the generators packaged by the LCG Genser team.

Otherwise, you’ll have to build your own mirror of the LCG generators. This process is evolving with time, and so, rather than provide information in this manual which will be outdated by the time you read it, we simply refer you to the relevant page on the Rivet wiki: <http://rivet.hepforge.org/trac/wiki/GenserMirror>.

If you are interested in using a generator not currently supported by AGILE, which does not output HepMC events in its native state, then please contact the authors (via the Rivet developer contact email address) and hopefully we can help.

2.2 Command completion

A final installation point worth considering is using the supplied bash-shell programmable completion setup for the `rivet` and `agile-runmc` commands. Despite being cosmetic and semi-trivial, programmable completion makes using `rivet` positively pleasant, especially since you no longer need to remember the somewhat cryptic analysis names¹!

To use programmable completion, source the appropriate files from the install location:

```
$ . <localdir>/share/Rivet/rivet-completion
$ . <localdir>/share/AGILE/agile-completion
```

(if you are using the setup script `rivetenv.sh` this is automatically done for you). If there is already a `<localdir>/etc/bash_completion.d` directory in your install path, Rivet and AGILE’s installation scripts will install extra copies into that location, since automatically sourcing all completion files in such a path is quite standard.

3. Running Rivet analyses

The `rivet` executable is the easiest way to use Rivet, and will be our example throughout this manual. This command reads HepMC events in the standard ASCII format, either from file or from a text stream.

3.1 The FIFO idiom

Since you rarely want to store simulated HepMC events and they are computationally cheap to produce (at least when compared to the remainder of experiment simulation chains), we recommend using a Unix *named pipe* (or “FIFO” — first-in, first-out) to stream the events. While this may seem unusual at first, it is just a nice way of “pretending” that we are writing to and reading from a file, without actually involving any slow disk access or building of huge files: a 1M event LHC run would occupy $\sim 60GB$ on disk, and typically it takes twice as long to make and analyse the events when the filesystem is involved! Here is an example:

```
$ mkfifo fifo.hepmc
$ agile-runmc Pythia6:425 -o fifo.hepmc &
$ rivet -a EXAMPLE fifo.hepmc
```

¹Standard Rivet analyses have names which, as well as the publication date and experiment name, incorporate the 8-digit Spires/Inspire ID code.

Note that the generator process (`agile-runmc` in this case) is *backgrounded* before `rivet` is run.

Notably, `mkfifo` will not work if applied to a directory mounted via the AFS distributed filesystem, as widely used in HEP. This is not a big problem: just make your FIFO object somewhere not mounted via AFS, e.g. `/tmp`. There is no performance penalty, as the filesystem object is not written to during the streaming process.

In the following command examples, we will assume that a generator has been set up to write to the `fifo.hepmc` FIFO, and just list the `rivet` command that reads from that location. Some typical `agile-runmc` commands are listed in [A](#).

3.2 Analysis status

The standard Rivet analyses are divided into four status classes: validated, preliminary, obsolete, and unvalidated (in roughly decreasing order of academic acceptability).

The Rivet “validation procedure” is not formally defined, but generally implies that an analysis has been checked to ensure reproduction of MC points shown in the paper where possible, and is believed to have no outstanding issues with analysis procedure or cuts. Additionally, analyses marked as “validated” and distributed with Rivet should normally have been code-checked by an experienced developer to ensure that the code is a good example of Rivet usage and is not more complex than required or otherwise difficult to read or maintain. Such analyses are regarded as fully ready for use in any MC validation or tuning studies.

Validated analyses which implement an unfinished piece of experimental work are considered to be trustworthy in their implementation of a conference note or similar “informal” publication, but do not have the magic stamp of approval that comes from a journal publication. This remains the standard mark of experimental respectability and accordingly we do not include such analyses in the Rivet standard analysis libraries, but in a special “preliminary” library. While preliminary analyses may be used for physics studies, please be aware of the incomplete status of the corresponding experimental study, and also be aware that the histograms in such analyses may be renamed or removed entirely, as may the analysis itself.

Preliminary analyses will not have a Spires/Inspire ID, and hence on their move into the standard Rivet analysis library they will normally undergo a name change: please ensure when you upgrade between Rivet versions that any scripts or programs which were using preliminary analyses are not broken by the disappearance or change of that analysis in the newer version. The minor perils of using preliminary analyses can be avoided by the cautious by building Rivet with the `--disable-preliminary` configuration flag, in which case their temptation will not even be offered.

To make transitions between Rivet versions more smooth and predictable for users of preliminary analyses, preliminary analyses which are superseded by a validated version will be reclassified as obsolete and will be retained for one major version of Rivet with a status of ”obsolete” before being removed, to give users time to migrate their run scripts, i.e. if an analysis is marked as obsolete in version 1.4.2, it will remain in Rivet’s distribution until version 1.5.0. Obsolete analyses may have different reference histograms from the

final version and will not be maintained. Obsolete analyses will not be built if either the `--disable-obsolete` configuration flag is specified at build time: for convenience, the default value of this flag is the value of the `--disable-preliminary` flag.

Finally, unvalidated analyses are those whose implementation is incomplete, flawed or just troubled by doubts. Running such analyses is not a good idea if you aren’t trying to fix them, and Rivet’s command line tools will print copious warning messages if you do. Unvalidated analyses in the Rivet distribution are not built by default, as they are only of interest to developers and would be distracting clutter for the majority of users: if you *really* need them, building Rivet with the `--enable-unvalidated` configuration flag will slake your thirst for danger.

3.3 Example `rivet` commands

- **Getting help:** `rivet --help` will print a (hopefully) helpful list of options which may be used with the `rivet` command, as well as other information such as environment variables which may affect the run.
- **Choosing analyses:** `rivet --list-analyses` will list the available analyses, including both those in the Rivet distribution and any plugins which are found at runtime. `rivet --show-analysis <patt>` will show a lot of details about any analyses whose name match the `<patt>` regular expression pattern — simple bits of analysis name are a perfectly valid subset of this. For example, `rivet --show-analysis CDF_200` exploits the standard Rivet analysis naming scheme to show details of all available CDF experiment analyses published in the “noughties.”
- **Running analyses:** `rivet -a DELPHI_1996_S3430090 fifo.hepmc` will run the Rivet `DELPHI_1996_S3430090` [10] analysis on the events in the `fifo.hepmc` file (which, from the name, is probably a filesystem named pipe rather than a normal *file*). This analysis is the one originally used for the DELPHI “PROFESSOR” generator tuning. If the first event in the data file does not have appropriate beam particles, the analysis will be disabled; since there is only one analysis in this case, the command will exit immediately with a warning if the first event is not an e^+e^- event.
- **Histogramming:** `rivet fifo.hepmc -H foo.yoda` will read all the events in the `fifo.hepmc` file. The `-H` switch is used to specify that the output histogram file will be named `foo.yoda`. By default the output file is called `Rivet.yoda`.
- **Fine-grained logging:**

```
rivet fifo.hepmc -A -l Rivet.Analysis=DEBUG \
-l Rivet.Projection=DEBUG -l Rivet.Projection.FinalState=TRACE \
-l NEvt=WARN will analyse events as before, but will print different status information
as the run progresses. Hierarchical logging control is possible down to the level of
individual analyses and projections as shown above; this is useful for debugging
without getting overloaded with debug information from all the components at once.
```

The default level is “INFO”, which lies between “DEBUG” and “WARNING”; the “TRACE” level is for very low level information, and probably isn’t needed by normal users.

4. Using analysis data

In this section, we summarise how to use the data files which Rivet produces for plotting, validation and tuning.

4.1 Histogram formats

Rivet produces output data in the YODA text-based format. This is a significant change from versions of Rivet before 2.0.0, which used the AIDA programming interface and XML format. If you do not want to use the plotting tools that come with Rivet (cf. Sec. 4.2), you might wish to convert the YODA files to a different format for plotting: the YODA package itself provides several scripts for this purpose.

Conversion to ROOT For many people, the first question will be “how do I plot my Rivet histograms using ROOT?” [11]. Setting aside the suggestion of masochism that this raises, be assured that the `yoda2root` script (installed by YODA if built with ROOT support enabled) will do a direct conversion of a `.yoda` file into an equivalent `.root` file. Equivalent, that is, as far as ROOT can represent the information in a YODA histogram: YODA stores far more information about weights and distribution moments within bins than ROOT can handle. For programmatic conversion, both the C++ and Python interfaces to YODA can convert YODA objects into their ROOT equivalents (and vice versa).

Conversion to “flat format” Most of our histogramming is based around a “flat” plain text format, which can easily be read (and written) by hand. YODA provides a script called `yoda2flat` to do this conversion. Run `yoda2flat -h` to get usage instructions. Aside from anything else, this is useful for simply checking the contents of an YODA file, with `yoda2flat Rivet.yoda - | less`.



We’re often asked why we don’t use ROOT internally. It’s a natural question, given how dominant ROOT is in (experimental) particle physics data analysis and plotting. Rivet’s not using ROOT was originally historical, but is now a matter of our requirements. ROOT is a very monolithic system, and when we started writing Rivet, many theorists (who we needed to be on-side) were unhappy about introducing such a large dependency – so we settled on using the AIDA/LWH system, which could be fully embedded in the Rivet code.

Eventually we decided that AIDA had run its course, due to such things as the awkwardness of histogram addition and division, confusion between bin heights and areas, and lack of support for gaps in binning (needed by several analyses). ROOT was the obvious replacement, but after detailed consideration we decided that it wouldn’t solve the problems: we would re-encounter many of the same weighted statistics issues we had already dealt with in AIDA (as well as weight-handling not being enabled by default), binning gaps

still wouldn't be supported, and we would block future development thanks to ROOT's notorious thread-unsafe and object ownership issues. Plus, how hard can histogramming be? Having thought a lot about histogramming over the years, we decided to write YODA. It's taken several years (admittedly with very low manpower fractions on that task!) to iterate to a design that we're really happy with, but we think YODA is a *really* pleasant way to do histogramming. It's object oriented but without the global state issues of ROOT, or the factory-based weirdnesses of AIDA. Weights are handled naturally, bins store enough distribution moments to do some pretty advanced stuff, overflows are handled by default, scalings (of weights or axes) and histogram arithmetic are easy and natural, and it's computationally efficient. It's also not finished – completed 2D histogramming and abstract binning ideas are still to be implemented – but that means that your desired enhancements stand a chance of getting implemented. So let us know your thoughts!

4.2 Plotting and comparing data

Rivet comes with three commands — `rivet-mkhtml`, `rivet-cmphistos` and `make-plots` — for comparing and plotting data files. These commands produce nice comparison plots of publication quality from the YODA format text files.

The high level program `rivet-mkhtml` will automatically create a plot webpage from the given YODA files. It searches for reference data automatically and uses the other two commands internally. Example:

```
$ rivet-mkhtml withUE.yoda:'Title=With UE' withoutUE.yoda:'LineColor=blue'  
Run rivet-mkhtml --help to find out about all features and options.
```

You can also run the other two commands separately:

- `rivet-cmphistos` will accept a number of YODA files as input (ending in `.yoda`), identify which plots are available in them, and combine the MC and reference plots appropriately into a set of plot data files ending with `.dat`. More options are described by running `rivet-cmphistos --help`.

Incidentally, the reference files for each Rivet analysis are to be found in the installed Rivet shared data directory, `<installdir>/share/Rivet`. You can find the location of this by using the `rivet-config` command:

```
$ rivet-config --datadir
```

- You can plot the created data files using the `make-plots` command:

```
$ make-plots --pdf *.dat
```

The `--pdf` flag makes the output plots in PDF format: by default the output is in PostScript (`.ps`), and flags for conversion to EPS and PNG are also available.

4.3 Merging histograms from different Rivet runs

The `yodamerge` script will take several YODA files and merge them together into a single one. If a histogram path only occurs in one of the input files, it is copied directly to the output. If it occurs more than once, the statistics of those histograms will be merged with full accuracy, producing the same output as would have been obtained from a single long

run containing all the same events. Run `yodamerge -h` to get instructions on using the script.



This exact merging only applies for *histograms*, of either normal or profile type. There are heuristics in the merging script to detect whether or not there should be a common normalization, but as with all heuristics they are not 100% guaranteed. Also, more complex objects such as histogrammed asymmetries, of the form $H_1 - H_2 / H_1 + H_2$, are not really histograms: in YODA the division operation will automatically convert them to the `Scatter2D` type, for which no moments are stored. It's not possible to combine the statistics of such objects in a straightforward way – so for now only one of the input copies will be output. Watch Rivet 2.x for developments which will finally *properly* solve the run combination problem, by allowing the `finalize()` step to be re-run on combined Rivet run outputs!

5. Outdated information for AIDA in Rivet 1.x



The following information applies to the Rivet 1.x series and the tools provided for AIDA histogramming. YODA should make many of these features unnecessary, since its Python interface is far more powerful and precise... but this is subject to evolution.

5.1 Chopping histograms

In some cases you don't want to keep the complete histograms produced by Rivet. For generator tuning purposes, for example, you want to get rid of the bins you already know your generator is incapable of describing. You can use the script `rivet-chopbins` to specify those bin-ranges you want to keep individually for each histogram in a Rivet output-file. The bin-ranges have to be specified using the corresponding x-values of that histogram. The usage is very simple. You can specify bin ranges of histograms to keep on the command-line via the `-b` switch, which can be given multiple times, e.g.

```
rivet-chopbins -b /CDF_2001_S4751469/d03-x01-y01:5:13 Rivet.aida
```

will chop all bins with $x < 5$ and $x > 13$ from the histogram `/CDF_2001_S4751469/d03-x01y01` in the file `Rivet.aida`. (In this particular case, x would be a leading jet p_\perp .)

5.2 Normalising histograms

Sometimes you want to use histograms normalised to, e.g., the generator cross-section or the area of a reference-data histogram. The script `rivet-rescale` was designed for these purposes. The usage is the following:

```
rivet-rescale -O observables -r RIVETDATA -o normalised Rivet.aida
```

By default, the normalised histograms are written to file in the AIDA-XML format. You can also give the `-f` switch on the command line to produce flat histograms.

Normalising to reference data You will need an output-file of Rivet, `Rivet.aida`, a folder that contains the reference-data histograms (e.g. `rivet-config --datadir`) and optionally, a text-file, `observables` that contains the names of the histograms you would like to normalise - those not given in the file will remain un-normalised. These are examples of how your `observables` file might look like:

```
/CDF_2000_S4155203/d01-x01-y01
```

If a histogram `/CDF_2000_S4155203/d01-x01-y01` is found in one of the reference-data files in the folder specified via the `-r` switch, then this will result in a histogram `/CDF_2000_S4155203/d01-x01-y01` being normalised to the area of the corresponding reference-data histogram. You can further specify a certain range of bins to normalise:

```
/CDF_2000_S4155203/d01-x01-y01:2:35
```

will chop off the bins with $x < 2$ and $x > 35$ of both, the histogram in your `Rivet.aida` and the reference-data histogram. The remaining MC histogram is then normalised to the remaining area of the reference-data histogram.

Normalising to arbitrary areas In the file `observables` you can further specify an arbitrary number, e.g. a generator cross-section, as follows:

```
/CDF_2000_S4155203/d01-x01-y01 1.0
```

will result in the histogram `/CDF_2000_S4155203/d01-x01-y01` being normalised to 1.0, and

```
/CDF_2000_S4155203/d01-x01-y01:2:35 1.0
```

will chop off the bins with $x < 2$ and $x > 35$ of the histogram

`/CDF_2000_S4155203/d01-x01-y01` first and normalise the remaining histogram to one.

Part II

Standard Rivet analyses

In this section we describe the standard experimental analyses included with the Rivet library. To maintain synchronisation with the code, these descriptions are generated automatically from the metadata in the analysis objects themselves.

6. LEP and SLC analyses

6.1 ALEPH_1991_S2435284 [12]

Hadronic Z decay charged multiplicity measurement

Beams: $e^+ e^-$

Energies: (45.6, 45.6) GeV

Experiment: ALEPH (LEP 1)

Spires ID: [2435284](#)

Status: VALIDATED

Authors:

- Andy Buckley (andy.buckley@cern.ch)

References:

- Phys. Lett. B, 273, 181 (1991)

Run details:

- Hadronic Z decay events generated on the Z pole ($\sqrt{s} = 91.2$ GeV)

The charged particle multiplicity distribution of hadronic Z decays, as measured on the peak of the Z resonance using the ALEPH detector at LEP. The unfolding procedure was model independent, and the distribution was found to have a mean of 20.85 ± 0.24 , Comparison with lower energy data supports the KNO scaling hypothesis. The shape of the multiplicity distribution is well described by a log-normal distribution, as predicted from a cascading model for multi-particle production.

Histograms (1):

- Total charged multiplicity (/REF/ALEPH_1991_S2435284/d01-x01-y01)

6.2 ALEPH_1996_S3196992 [13]

Measurement of the quark to photon fragmentation function

Beams: $e^+ e^-$

Energies: (45.6, 45.6) GeV

Experiment: ALEPH (LEP Run 1)

Spires ID: 3196992

Status: VALIDATED

Authors:

- Frank Siegert <frank.siegert@cern.ch>

References:

- Z.Phys.C69:365-378,1996
- DOI: [10.1007/s002880050037](https://doi.org/10.1007/s002880050037)

Run details:

- $e^+ e^- \rightarrow$ jets with π and η decays turned off.

Earlier measurements at LEP of isolated hard photons in hadronic Z decays, attributed to radiation from primary quark pairs, have been extended in the ALEPH experiment to include hard photon production inside hadron jets. Events are selected where all particles combine democratically to form hadron jets, one of which contains a photon with a fractional energy $z > 0.7$. After statistical subtraction of non-prompt photons, the quark-to-photon fragmentation function, $D(z)$, is extracted directly from the measured 2-jet rate.

Histograms (8):

- Photon Fragmentation in 2-jet events with $y_{\text{cut}} = 0.01$ ([/REF/ALEPH_1996_S3196992/d01-x01-y01](#))
- Photon Fragmentation in 2-jet events with $y_{\text{cut}} = 0.06$ ([/REF/ALEPH_1996_S3196992/d02-x01-y01](#))
- Photon Fragmentation in 2-jet events with $y_{\text{cut}} = 0.1$ ([/REF/ALEPH_1996_S3196992/d03-x01-y01](#))
- Photon Fragmentation in 2-jet events with $y_{\text{cut}} = 0.33$ ([/REF/ALEPH_1996_S3196992/d04-x01-y01](#))
- Photon Fragmentation in 3-jet events with $y_{\text{cut}} = 0.01$ ([/REF/ALEPH_1996_S3196992/d05-x01-y01](#))
- Photon Fragmentation in 3-jet events with $y_{\text{cut}} = 0.06$ ([/REF/ALEPH_1996_S3196992/d06-x01-y01](#))
- Photon Fragmentation in 3-jet events with $y_{\text{cut}} = 0.1$ ([/REF/ALEPH_1996_S3196992/d07-x01-y01](#))
- Photon Fragmentation in 4-jet events with $y_{\text{cut}} = 0.01$ ([/REF/ALEPH_1996_S3196992/d08-x01-y01](#))

6.3 ALEPH_1996_S3486095 [14]

Studies of QCD with the ALEPH detector.

Beams: $e^+ e^-$

Energies: (45.6, 45.6) GeV

Experiment: ALEPH (LEP 1)

Spires ID: 3486095

Status: VALIDATED

Authors:

- Holger Schulz [⟨ holger.schulz@physik.hu-berlin.de ⟩](mailto:holger.schulz@physik.hu-berlin.de)

References:

- Phys. Rept., 294, 1–165 (1998)

Run details:

- Hadronic Z decay events generated on the Z pole ($\sqrt{s} = 91.2$ GeV)

Summary paper of QCD results as measured by ALEPH at LEP 1. The publication includes various event shape variables, multiplicities (identified particles and inclusive), and particle spectra.

Histograms (51):

- Sphericity, S (charged) (/REF/ALEPH_1996_S3486095/d01-x01-y01)
- Aplanarity, A (charged) (/REF/ALEPH_1996_S3486095/d02-x01-y01)
- 1-Thrust, $1 - T$ (charged) (/REF/ALEPH_1996_S3486095/d03-x01-y01)
- Thrust minor, m (charged) (/REF/ALEPH_1996_S3486095/d04-x01-y01)
- Two-jet resolution variable, Y_3 (charged) (/REF/ALEPH_1996_S3486095/d05-x01-y01)
- Heavy jet mass (charged) (/REF/ALEPH_1996_S3486095/d06-x01-y01)
- C parameter (charged) (/REF/ALEPH_1996_S3486095/d07-x01-y01)
- Oblateness, $M - m$ (charged) (/REF/ALEPH_1996_S3486095/d08-x01-y01)
- Scaled momentum, $x_p = |p|/|p_{\text{beam}}|$ (charged) (/REF/ALEPH_1996_S3486095/d09-x01-y01)
- Rapidity w.r.t. thrust axes, y_T (charged) (/REF/ALEPH_1996_S3486095/d10-x01-y01)
- In-plane p_T in GeV w.r.t. sphericity axes (charged) (/REF/ALEPH_1996_S3486095/d11-x01-y01)
- Out-of-plane p_T in GeV w.r.t. sphericity axes (charged) (/REF/ALEPH_1996_S3486095/d12-x01-y01)
- Log of scaled momentum, $\log(1/x_p)$ (charged) (/REF/ALEPH_1996_S3486095/d17-x01-y01)

- Charged multiplicity distribution (/REF/ALEPH_1996_S3486095/d18-x01-y01)
- Mean charged multiplicity (/REF/ALEPH_1996_S3486095/d19-x01-y01)
- Mean charged multiplicity for rapidity $|Y| < 0.5$ (/REF/ALEPH_1996_S3486095/d20-x01-y01)
- Mean charged multiplicity for rapidity $|Y| < 1.0$ (/REF/ALEPH_1996_S3486095/d21-x01-y01)
- Mean charged multiplicity for rapidity $|Y| < 1.5$ (/REF/ALEPH_1996_S3486095/d22-x01-y01)
- Mean charged multiplicity for rapidity $|Y| < 2.0$ (/REF/ALEPH_1996_S3486095/d23-x01-y01)
- π^\pm spectrum (/REF/ALEPH_1996_S3486095/d25-x01-y01)
- K^\pm spectrum (/REF/ALEPH_1996_S3486095/d26-x01-y01)
- p spectrum (/REF/ALEPH_1996_S3486095/d27-x01-y01)
- γ spectrum (/REF/ALEPH_1996_S3486095/d28-x01-y01)
- π^0 spectrum (/REF/ALEPH_1996_S3486095/d29-x01-y01)
- η spectrum (/REF/ALEPH_1996_S3486095/d30-x01-y01)
- η' spectrum (/REF/ALEPH_1996_S3486095/d31-x01-y01)
- K^0 spectrum (/REF/ALEPH_1996_S3486095/d32-x01-y01)
- Λ^0 spectrum (/REF/ALEPH_1996_S3486095/d33-x01-y01)
- Ξ^- spectrum (/REF/ALEPH_1996_S3486095/d34-x01-y01)
- $\Sigma^\pm(1385)$ spectrum (/REF/ALEPH_1996_S3486095/d35-x01-y01)
- $\Xi^0(1530)$ spectrum (/REF/ALEPH_1996_S3486095/d36-x01-y01)
- ρ spectrum (/REF/ALEPH_1996_S3486095/d37-x01-y01)
- $\omega(782)$ spectrum (/REF/ALEPH_1996_S3486095/d38-x01-y01)
- $K^{*0}(892)$ spectrum (/REF/ALEPH_1996_S3486095/d39-x01-y01)
- ϕ spectrum (/REF/ALEPH_1996_S3486095/d40-x01-y01)
- $K^{*\pm}(892)$ spectrum (/REF/ALEPH_1996_S3486095/d43-x01-y01)
- Mean π^0 multiplicity (/REF/ALEPH_1996_S3486095/d44-x01-y02)
- Mean η multiplicity (/REF/ALEPH_1996_S3486095/d44-x01-y03)
- Mean η' multiplicity (/REF/ALEPH_1996_S3486095/d44-x01-y04)
- Mean $K_S + K_L$ multiplicity (/REF/ALEPH_1996_S3486095/d44-x01-y05)

- Mean ρ^0 multiplicity (/REF/ALEPH_1996_S3486095/d44-x01-y06)
- Mean $\omega(782)$ multiplicity (/REF/ALEPH_1996_S3486095/d44-x01-y07)
- Mean ϕ multiplicity (/REF/ALEPH_1996_S3486095/d44-x01-y08)
- Mean $K^{*\pm}$ multiplicity (/REF/ALEPH_1996_S3486095/d44-x01-y09)
- Mean K^{*0} multiplicity (/REF/ALEPH_1996_S3486095/d44-x01-y10)
- Mean Λ multiplicity (/REF/ALEPH_1996_S3486095/d44-x01-y11)
- Mean Σ multiplicity (/REF/ALEPH_1996_S3486095/d44-x01-y12)
- Mean Ξ multiplicity (/REF/ALEPH_1996_S3486095/d44-x01-y13)
- Mean $\Sigma(1385)$ multiplicity (/REF/ALEPH_1996_S3486095/d44-x01-y14)
- Mean $\Xi(1530)$ multiplicity (/REF/ALEPH_1996_S3486095/d44-x01-y15)
- Mean Ω^\mp multiplicity (/REF/ALEPH_1996_S3486095/d44-x01-y16)

6.4 ALEPH_1999_S4193598 [15]

Scaled energy distribution of D^* at LEP

Beams: $e^+ e^-$

Energies: (45.6, 45.6) GeV

Experiment: ALEPH (LEP)

Spires ID: 4193598

Status: VALIDATED

Authors:

- Holger Schulz [⟨ hschulz@physik.hu-berlin.de ⟩](mailto:hschulz@physik.hu-berlin.de)

References:

- Eur.Phys.J.C16:597-611,2000
- hep-ex/9909032
- CERN-EP-99-094

Run details:

- Hadronic Z decays at 91.2 GeV.

Study of charm production in Z decays. Here, only the scaled energy distribution of $D^{*\pm}$ is implemented. Should be very important for fragmentation tuning.

Histograms (1):

- Scaled energy of $D^{*\pm}$ in $e^+e^- \rightarrow Z \rightarrow$ hadronic at $\sqrt{s} = 91.2$ GeV ([/REF/ALEPH_1999_-S4193598/d01-x01-y01](#))

6.5 ALEPH_2001_S4656318 [16]

Study of the fragmentation of b quarks into B mesons at the Z peak

Beams: $e^+ e^-$

Energies: (45.6, 45.6) GeV

Experiment: ALEPH (LEP 1)

Spires ID: [4656318](#)

Status: VALIDATED

Authors:

- Peter Richardson (Peter.Richardson@durham.ac.uk)

References:

- Phys.Lett.B512:30-48,2001.
- hep-ex/0106051

Run details:

- Hadronic Z decay events generated on the Z pole ($\sqrt{s} = 91.2$ GeV)

Measurement of the b -quark fragmentation function by ALEPH using LEP 1 data. The fragmentation function for both weakly decaying and leading b -quarks has been determined. The data used for the plots has been renormalised to give a differential distribution rather than the bin-by-bin average in HEPDATA.

Histograms (1):

- Mean of b quark fragmentation function $f(x_B^{\text{weak}})$ ([/REF/ALEPH_2001_S4656318/d06-x01-y01](#))

6.6 ALEPH_2002_S4823664 [17]

η and ω Production in Hadronic Z^0 Decays

Beams: $e^+ e^-$

Energies: (45.6, 45.6) GeV

Experiment: OPAL (LEP 1)

Spires ID: [4823664](#)

Status: VALIDATED

Authors:

- Peter Richardson (Peter.Richardson@durham.ac.uk)

References:

- Phys.Lett. B528 (2002) 19-33
- hep-ex/0201012

Run details:

- Hadronic Z decay events generated on the Z pole ($\sqrt{s} = 91.2$ GeV)

The production of η and ω mesons measured using 4 million Z^0 events by the ALEPH experiment at LEP. Only the fragmentation functions are implemented.

Histograms (2):

- η scaled momentum ([/REF/ALEPH_2002_S4823664/d02-x01-y02](#))
- ω scaled momentum ([/REF/ALEPH_2002_S4823664/d03-x01-y02](#))

6.7 ALEPH_2004_S5765862 [18]

Jet rates and event shapes at LEP I and II

Beams: $e^+ e^-$

Energies: (45.6, 45.6), (66.5, 66.5), (80.5, 80.5), (86.0, 86.0), (91.5, 91.5), (94.5, 94.5), (98.5, 98.5), (100.0, 100.0), (103.0, 103.0) GeV

Experiment: ALEPH (LEP Run 1 and 2)

Spires ID: [5765862](#)

Status: VALIDATED

Authors:

- Frank Siegert <frank.siegert@cern.ch>

References:

- Eur.Phys.J.C35:457-486,2004
- DOI: [10.1140/epjc/s2004-01891-4](https://doi.org/10.1140/epjc/s2004-01891-4)
- <http://cdsweb.cern.ch/record/690637/files/ep-2003-084.pdf>

Run details:

- $e^+ e^- \rightarrow \text{jet jet (+ jets)}$

Jet rates, event-shape variables and inclusive charged particle spectra are measured in $e^+ e^-$ collisions at CMS energies between 91 and 209 GeV. The previously published data at 91.2 GeV and 133 GeV have been re-processed and the higher energy data are presented here for the first time. Note that the data have been corrected to include neutrinos.

Histograms (231):

- Charged multiplicity at a function of energy ([/REF/ALEPH_2004_S5765862/d01-x01-y01](#))
- Charged particle spectrum ($E_{\text{CMS}} = 133$ GeV) ([/REF/ALEPH_2004_S5765862/d02-x01-y01](#))
- Charged particle spectrum ($E_{\text{CMS}} = 161$ GeV) ([/REF/ALEPH_2004_S5765862/d03-x01-y01](#))
- Charged particle spectrum ($E_{\text{CMS}} = 172$ GeV) ([/REF/ALEPH_2004_S5765862/d04-x01-y01](#))
- Charged particle spectrum ($E_{\text{CMS}} = 183$ GeV) ([/REF/ALEPH_2004_S5765862/d05-x01-y01](#))
- Charged particle spectrum ($E_{\text{CMS}} = 189$ GeV) ([/REF/ALEPH_2004_S5765862/d06-x01-y01](#))
- Charged particle spectrum ($E_{\text{CMS}} = 196$ GeV) ([/REF/ALEPH_2004_S5765862/d07-x01-y01](#))
- Charged particle spectrum ($E_{\text{CMS}} = 200$ GeV) ([/REF/ALEPH_2004_S5765862/d08-x01-y01](#))
- Charged particle spectrum ($E_{\text{CMS}} = 206$ GeV) ([/REF/ALEPH_2004_S5765862/d09-x01-y01](#))
- Thrust major ($E_{\text{CMS}} = 200$ GeV) ([/REF/ALEPH_2004_S5765862/d100-x01-y01](#))

- Thrust major ($E_{\text{CMS}} = 206$ GeV) (/REF/ALEPH_2004_S5765862/d101-x01-y01)
- Thrust minor ($E_{\text{CMS}} = 91.2$ GeV) (/REF/ALEPH_2004_S5765862/d102-x01-y01)
- Thrust minor ($E_{\text{CMS}} = 133$ GeV) (/REF/ALEPH_2004_S5765862/d103-x01-y01)
- Thrust minor ($E_{\text{CMS}} = 161$ GeV) (/REF/ALEPH_2004_S5765862/d104-x01-y01)
- Thrust minor ($E_{\text{CMS}} = 172$ GeV) (/REF/ALEPH_2004_S5765862/d105-x01-y01)
- Thrust minor ($E_{\text{CMS}} = 183$ GeV) (/REF/ALEPH_2004_S5765862/d106-x01-y01)
- Thrust minor ($E_{\text{CMS}} = 189$ GeV) (/REF/ALEPH_2004_S5765862/d107-x01-y01)
- Thrust minor ($E_{\text{CMS}} = 200$ GeV) (/REF/ALEPH_2004_S5765862/d108-x01-y01)
- Thrust minor ($E_{\text{CMS}} = 206$ GeV) (/REF/ALEPH_2004_S5765862/d109-x01-y01)
- Charged particle spectrum ($E_{\text{CMS}} = 133$ GeV) (/REF/ALEPH_2004_S5765862/d11-x01-y01)
- Jet mass difference ($E_{\text{CMS}} = 91.2$ GeV) (/REF/ALEPH_2004_S5765862/d110-x01-y01)
- Jet mass difference ($E_{\text{CMS}} = 133$ GeV) (/REF/ALEPH_2004_S5765862/d111-x01-y01)
- Jet mass difference ($E_{\text{CMS}} = 161$ GeV) (/REF/ALEPH_2004_S5765862/d112-x01-y01)
- Jet mass difference ($E_{\text{CMS}} = 1722$ GeV) (/REF/ALEPH_2004_S5765862/d113-x01-y01)
- Jet mass difference ($E_{\text{CMS}} = 183$ GeV) (/REF/ALEPH_2004_S5765862/d114-x01-y01)
- Jet mass difference ($E_{\text{CMS}} = 189$ GeV) (/REF/ALEPH_2004_S5765862/d115-x01-y01)
- Jet mass difference ($E_{\text{CMS}} = 200$ GeV) (/REF/ALEPH_2004_S5765862/d116-x01-y01)
- Jet mass difference ($E_{\text{CMS}} = 206$ GeV) (/REF/ALEPH_2004_S5765862/d117-x01-y01)
- Aplanarity ($E_{\text{CMS}} = 91.2$ GeV) (/REF/ALEPH_2004_S5765862/d118-x01-y01)
- Aplanarity ($E_{\text{CMS}} = 133$ GeV) (/REF/ALEPH_2004_S5765862/d119-x01-y01)
- Charged particle spectrum ($E_{\text{CMS}} = 161$ GeV) (/REF/ALEPH_2004_S5765862/d12-x01-y01)
- Aplanarity ($E_{\text{CMS}} = 161$ GeV) (/REF/ALEPH_2004_S5765862/d120-x01-y01)
- Aplanarity ($E_{\text{CMS}} = 172$ GeV) (/REF/ALEPH_2004_S5765862/d121-x01-y01)
- Aplanarity ($E_{\text{CMS}} = 183$ GeV) (/REF/ALEPH_2004_S5765862/d122-x01-y01)
- Aplanarity ($E_{\text{CMS}} = 189$ GeV) (/REF/ALEPH_2004_S5765862/d123-x01-y01)
- Aplanarity ($E_{\text{CMS}} = 200$ GeV) (/REF/ALEPH_2004_S5765862/d124-x01-y01)
- Aplanarity ($E_{\text{CMS}} = 206$ GeV) (/REF/ALEPH_2004_S5765862/d125-x01-y01)

- Planarity ($E_{\text{CMS}} = 133$ GeV) (/REF/ALEPH_2004_S5765862/d126-x01-y01)
- Planarity ($E_{\text{CMS}} = 161$ GeV) (/REF/ALEPH_2004_S5765862/d127-x01-y01)
- Planarity ($E_{\text{CMS}} = 172$ GeV) (/REF/ALEPH_2004_S5765862/d128-x01-y01)
- Planarity ($E_{\text{CMS}} = 183$ GeV) (/REF/ALEPH_2004_S5765862/d129-x01-y01)
- Charged particle spectrum ($E_{\text{CMS}} = 172$ GeV) (/REF/ALEPH_2004_S5765862/d13-x01-y01)
- Planarity ($E_{\text{CMS}} = 189$ GeV) (/REF/ALEPH_2004_S5765862/d130-x01-y01)
- Planarity ($E_{\text{CMS}} = 200$ GeV) (/REF/ALEPH_2004_S5765862/d131-x01-y01)
- Planarity ($E_{\text{CMS}} = 206$ GeV) (/REF/ALEPH_2004_S5765862/d132-x01-y01)
- Oblateness ($E_{\text{CMS}} = 91.2$ GeV) (/REF/ALEPH_2004_S5765862/d133-x01-y01)
- Oblateness ($E_{\text{CMS}} = 133$ GeV) (/REF/ALEPH_2004_S5765862/d134-x01-y01)
- Oblateness ($E_{\text{CMS}} = 161$ GeV) (/REF/ALEPH_2004_S5765862/d135-x01-y01)
- Oblateness ($E_{\text{CMS}} = 172$ GeV) (/REF/ALEPH_2004_S5765862/d136-x01-y01)
- Oblateness ($E_{\text{CMS}} = 183$ GeV) (/REF/ALEPH_2004_S5765862/d137-x01-y01)
- Oblateness ($E_{\text{CMS}} = 189$ GeV) (/REF/ALEPH_2004_S5765862/d138-x01-y01)
- Oblateness ($E_{\text{CMS}} = 200$ GeV) (/REF/ALEPH_2004_S5765862/d139-x01-y01)
- Charged particle spectrum ($E_{\text{CMS}} = 183$ GeV) (/REF/ALEPH_2004_S5765862/d14-x01-y01)
- Oblateness ($E_{\text{CMS}} = 206$ GeV) (/REF/ALEPH_2004_S5765862/d140-x01-y01)
- Sphericity ($E_{\text{CMS}} = 91.2$ GeV) (/REF/ALEPH_2004_S5765862/d141-x01-y01)
- Sphericity ($E_{\text{CMS}} = 133$ GeV) (/REF/ALEPH_2004_S5765862/d142-x01-y01)
- Sphericity ($E_{\text{CMS}} = 161$ GeV) (/REF/ALEPH_2004_S5765862/d143-x01-y01)
- Sphericity ($E_{\text{CMS}} = 172$ GeV) (/REF/ALEPH_2004_S5765862/d144-x01-y01)
- Sphericity ($E_{\text{CMS}} = 183$ GeV) (/REF/ALEPH_2004_S5765862/d145-x01-y01)
- Sphericity ($E_{\text{CMS}} = 189$ GeV) (/REF/ALEPH_2004_S5765862/d146-x01-y01)
- Sphericity ($E_{\text{CMS}} = 200$ GeV) (/REF/ALEPH_2004_S5765862/d147-x01-y01)
- Sphericity ($E_{\text{CMS}} = 206$ GeV) (/REF/ALEPH_2004_S5765862/d148-x01-y01)
- Durham jet resolution $2 \rightarrow 1$ ($E_{\text{CMS}} = 91.2$ GeV) (/REF/ALEPH_2004_S5765862/d149-x01-y01)
- Charged particle spectrum ($E_{\text{CMS}} = 189$ GeV) (/REF/ALEPH_2004_S5765862/d15-x01-y01)

- Durham jet resolution $2 \rightarrow 1$ ($E_{\text{CMS}} = 133$ GeV) (/REF/ALEPH_2004_S5765862/d150-x01-y01)
- Durham jet resolution $2 \rightarrow 1$ ($E_{\text{CMS}} = 161$ GeV) (/REF/ALEPH_2004_S5765862/d151-x01-y01)
- Durham jet resolution $2 \rightarrow 1$ ($E_{\text{CMS}} = 173$ GeV) (/REF/ALEPH_2004_S5765862/d152-x01-y01)
- Durham jet resolution $2 \rightarrow 1$ ($E_{\text{CMS}} = 183$ GeV) (/REF/ALEPH_2004_S5765862/d153-x01-y01)
- Durham jet resolution $2 \rightarrow 1$ ($E_{\text{CMS}} = 189$ GeV) (/REF/ALEPH_2004_S5765862/d154-x01-y01)
- Durham jet resolution $2 \rightarrow 1$ ($E_{\text{CMS}} = 200$ GeV) (/REF/ALEPH_2004_S5765862/d155-x01-y01)
- Durham jet resolution $2 \rightarrow 1$ ($E_{\text{CMS}} = 206$ GeV) (/REF/ALEPH_2004_S5765862/d156-x01-y01)
- Durham jet resolution $3 \rightarrow 2$ ($E_{\text{CMS}} = 91.2$ GeV) (/REF/ALEPH_2004_S5765862/d157-x01-y01)
- Durham jet resolution $3 \rightarrow 2$ ($E_{\text{CMS}} = 133$ GeV) (/REF/ALEPH_2004_S5765862/d158-x01-y01)
- Durham jet resolution $3 \rightarrow 2$ ($E_{\text{CMS}} = 161$ GeV) (/REF/ALEPH_2004_S5765862/d159-x01-y01)
- Charged particle spectrum ($E_{\text{CMS}} = 196$ GeV) (/REF/ALEPH_2004_S5765862/d16-x01-y01)
- Durham jet resolution $3 \rightarrow 2$ ($E_{\text{CMS}} = 172$ GeV) (/REF/ALEPH_2004_S5765862/d160-x01-y01)
- Durham jet resolution $3 \rightarrow 2$ ($E_{\text{CMS}} = 183$ GeV) (/REF/ALEPH_2004_S5765862/d161-x01-y01)
- Durham jet resolution $3 \rightarrow 2$ ($E_{\text{CMS}} = 189$ GeV) (/REF/ALEPH_2004_S5765862/d162-x01-y01)
- Durham jet resolution $3 \rightarrow 2$ ($E_{\text{CMS}} = 200$ GeV) (/REF/ALEPH_2004_S5765862/d163-x01-y01)
- Durham jet resolution $3 \rightarrow 2$ ($E_{\text{CMS}} = 206$ GeV) (/REF/ALEPH_2004_S5765862/d164-x01-y01)
- Durham jet resolution $4 \rightarrow 3$ ($E_{\text{CMS}} = 91.2$ GeV) (/REF/ALEPH_2004_S5765862/d165-x01-y01)
- Durham jet resolution $4 \rightarrow 3$ ($E_{\text{CMS}} = 133$ GeV) (/REF/ALEPH_2004_S5765862/d166-x01-y01)
- Durham jet resolution $4 \rightarrow 3$ ($E_{\text{CMS}} = 161$ GeV) (/REF/ALEPH_2004_S5765862/d167-x01-y01)
- Durham jet resolution $4 \rightarrow 3$ ($E_{\text{CMS}} = 172$ GeV) (/REF/ALEPH_2004_S5765862/d168-x01-y01)
- Durham jet resolution $4 \rightarrow 3$ ($E_{\text{CMS}} = 183$ GeV) (/REF/ALEPH_2004_S5765862/d169-x01-y01)
- Charged particle spectrum ($E_{\text{CMS}} = 200$ GeV) (/REF/ALEPH_2004_S5765862/d17-x01-y01)
- Durham jet resolution $4 \rightarrow 3$ ($E_{\text{CMS}} = 189$ GeV) (/REF/ALEPH_2004_S5765862/d170-x01-y01)
- Durham jet resolution $4 \rightarrow 3$ ($E_{\text{CMS}} = 200$ GeV) (/REF/ALEPH_2004_S5765862/d171-x01-y01)
- Durham jet resolution $4 \rightarrow 3$ ($E_{\text{CMS}} = 206$ GeV) (/REF/ALEPH_2004_S5765862/d172-x01-y01)
- Durham jet resolution $5 \rightarrow 4$ ($E_{\text{CMS}} = 91.2$ GeV) (/REF/ALEPH_2004_S5765862/d173-x01-y01)
- Durham jet resolution $5 \rightarrow 4$ ($E_{\text{CMS}} = 133$ GeV) (/REF/ALEPH_2004_S5765862/d174-x01-y01)

- Durham jet resolution $5 \rightarrow 4$ ($E_{\text{CMS}} = 161$ GeV) (/REF/ALEPH_2004_S5765862/d175-x01-y01)
- Durham jet resolution $5 \rightarrow 4$ ($E_{\text{CMS}} = 172$ GeV) (/REF/ALEPH_2004_S5765862/d176-x01-y01)
- Durham jet resolution $5 \rightarrow 4$ ($E_{\text{CMS}} = 183$ GeV) (/REF/ALEPH_2004_S5765862/d177-x01-y01)
- Durham jet resolution $5 \rightarrow 4$ ($E_{\text{CMS}} = 189$ GeV) (/REF/ALEPH_2004_S5765862/d178-x01-y01)
- Durham jet resolution $5 \rightarrow 4$ ($E_{\text{CMS}} = 200$ GeV) (/REF/ALEPH_2004_S5765862/d179-x01-y01)
- Charged particle spectrum ($E_{\text{CMS}} = 206$ GeV) (/REF/ALEPH_2004_S5765862/d18-x01-y01)
- Durham jet resolution $6 \rightarrow 5$ ($E_{\text{CMS}} = 91.2$ GeV) (/REF/ALEPH_2004_S5765862/d180-x01-y01)
- Durham jet resolution $6 \rightarrow 5$ ($E_{\text{CMS}} = 133$ GeV) (/REF/ALEPH_2004_S5765862/d181-x01-y01)
- Durham jet resolution $6 \rightarrow 5$ ($E_{\text{CMS}} = 161$ GeV) (/REF/ALEPH_2004_S5765862/d182-x01-y01)
- Durham jet resolution $6 \rightarrow 5$ ($E_{\text{CMS}} = 172$ GeV) (/REF/ALEPH_2004_S5765862/d183-x01-y01)
- Durham jet resolution $6 \rightarrow 5$ ($E_{\text{CMS}} = 183$ GeV) (/REF/ALEPH_2004_S5765862/d184-x01-y01)
- Durham jet resolution $6 \rightarrow 5$ ($E_{\text{CMS}} = 189$ GeV) (/REF/ALEPH_2004_S5765862/d185-x01-y01)
- Durham jet resolution $6 \rightarrow 5$ ($E_{\text{CMS}} = 200$ GeV) (/REF/ALEPH_2004_S5765862/d186-x01-y01)
- 1-jet fraction ($E_{\text{CMS}} = 91.2$ GeV) (/REF/ALEPH_2004_S5765862/d187-x01-y01)
- 1-jet fraction ($E_{\text{CMS}} = 133$ GeV) (/REF/ALEPH_2004_S5765862/d188-x01-y01)
- 1-jet fraction ($E_{\text{CMS}} = 161$ GeV) (/REF/ALEPH_2004_S5765862/d189-x01-y01)
- Charged particle spectrum ($E_{\text{CMS}} = 133$ GeV) (/REF/ALEPH_2004_S5765862/d19-x01-y01)
- 1-jet fraction ($E_{\text{CMS}} = 172$ GeV) (/REF/ALEPH_2004_S5765862/d190-x01-y01)
- 1-jet fraction ($E_{\text{CMS}} = 183$ GeV) (/REF/ALEPH_2004_S5765862/d191-x01-y01)
- 1-jet fraction ($E_{\text{CMS}} = 189$ GeV) (/REF/ALEPH_2004_S5765862/d192-x01-y01)
- 1-jet fraction ($E_{\text{CMS}} = 200$ GeV) (/REF/ALEPH_2004_S5765862/d193-x01-y01)
- 1-jet fraction ($E_{\text{CMS}} = 206$ GeV) (/REF/ALEPH_2004_S5765862/d194-x01-y01)
- 2-jet fraction ($E_{\text{CMS}} = 91.2$ GeV) (/REF/ALEPH_2004_S5765862/d195-x01-y01)
- 2-jet fraction ($E_{\text{CMS}} = 133$ GeV) (/REF/ALEPH_2004_S5765862/d196-x01-y01)
- 2-jet fraction ($E_{\text{CMS}} = 161$ GeV) (/REF/ALEPH_2004_S5765862/d197-x01-y01)
- 2-jet fraction ($E_{\text{CMS}} = 172$ GeV) (/REF/ALEPH_2004_S5765862/d198-x01-y01)
- 2-jet fraction ($E_{\text{CMS}} = 183$ GeV) (/REF/ALEPH_2004_S5765862/d199-x01-y01)

- Charged particle spectrum ($E_{\text{CMS}} = 161$ GeV) (/REF/ALEPH_2004_S5765862/d20-x01-y01)
- 2-jet fraction ($E_{\text{CMS}} = 189$ GeV) (/REF/ALEPH_2004_S5765862/d200-x01-y01)
- 2-jet fraction ($E_{\text{CMS}} = 200$ GeV) (/REF/ALEPH_2004_S5765862/d201-x01-y01)
- 2-jet fraction ($E_{\text{CMS}} = 206$ GeV) (/REF/ALEPH_2004_S5765862/d202-x01-y01)
- 3-jet fraction ($E_{\text{CMS}} = 91.2$ GeV) (/REF/ALEPH_2004_S5765862/d203-x01-y01)
- 3-jet fraction ($E_{\text{CMS}} = 133$ GeV) (/REF/ALEPH_2004_S5765862/d204-x01-y01)
- 3-jet fraction ($E_{\text{CMS}} = 161$ GeV) (/REF/ALEPH_2004_S5765862/d205-x01-y01)
- 3-jet fraction ($E_{\text{CMS}} = 172$ GeV) (/REF/ALEPH_2004_S5765862/d206-x01-y01)
- 3-jet fraction ($E_{\text{CMS}} = 183$ GeV) (/REF/ALEPH_2004_S5765862/d207-x01-y01)
- 3-jet fraction ($E_{\text{CMS}} = 189$ GeV) (/REF/ALEPH_2004_S5765862/d208-x01-y01)
- 3-jet fraction ($E_{\text{CMS}} = 200$ GeV) (/REF/ALEPH_2004_S5765862/d209-x01-y01)
- Charged particle spectrum ($E_{\text{CMS}} = 172$ GeV) (/REF/ALEPH_2004_S5765862/d21-x01-y01)
- 3-jet fraction ($E_{\text{CMS}} = 206$ GeV) (/REF/ALEPH_2004_S5765862/d210-x01-y01)
- 4-jet fraction ($E_{\text{CMS}} = 91.2$ GeV) (/REF/ALEPH_2004_S5765862/d211-x01-y01)
- 4-jet fraction ($E_{\text{CMS}} = 133$ GeV) (/REF/ALEPH_2004_S5765862/d212-x01-y01)
- 4-jet fraction ($E_{\text{CMS}} = 161$ GeV) (/REF/ALEPH_2004_S5765862/d213-x01-y01)
- 4-jet fraction ($E_{\text{CMS}} = 172$ GeV) (/REF/ALEPH_2004_S5765862/d214-x01-y01)
- 4-jet fraction ($E_{\text{CMS}} = 183$ GeV) (/REF/ALEPH_2004_S5765862/d215-x01-y01)
- 4-jet fraction ($E_{\text{CMS}} = 189$ GeV) (/REF/ALEPH_2004_S5765862/d216-x01-y01)
- 4-jet fraction ($E_{\text{CMS}} = 200$ GeV) (/REF/ALEPH_2004_S5765862/d217-x01-y01)
- 4-jet fraction ($E_{\text{CMS}} = 206$ GeV) (/REF/ALEPH_2004_S5765862/d218-x01-y01)
- 5-jet fraction ($E_{\text{CMS}} = 91.2$ GeV) (/REF/ALEPH_2004_S5765862/d219-x01-y01)
- Charged particle spectrum ($E_{\text{CMS}} = 183$ GeV) (/REF/ALEPH_2004_S5765862/d22-x01-y01)
- 5-jet fraction ($E_{\text{CMS}} = 133$ GeV) (/REF/ALEPH_2004_S5765862/d220-x01-y01)
- 5-jet fraction ($E_{\text{CMS}} = 161$ GeV) (/REF/ALEPH_2004_S5765862/d221-x01-y01)
- 5-jet fraction ($E_{\text{CMS}} = 172$ GeV) (/REF/ALEPH_2004_S5765862/d222-x01-y01)
- 5-jet fraction ($E_{\text{CMS}} = 183$ GeV) (/REF/ALEPH_2004_S5765862/d223-x01-y01)

- 5-jet fraction ($E_{\text{CMS}} = 189$ GeV) (/REF/ALEPH_2004_S5765862/d224-x01-y01)
- 5-jet fraction ($E_{\text{CMS}} = 200$ GeV) (/REF/ALEPH_2004_S5765862/d225-x01-y01)
- 5-jet fraction ($E_{\text{CMS}} = 206$ GeV) (/REF/ALEPH_2004_S5765862/d226-x01-y01)
- ≥ 6 -jet fraction ($E_{\text{CMS}} = 91.2$ GeV) (/REF/ALEPH_2004_S5765862/d227-x01-y01)
- ≥ 6 -jet fraction ($E_{\text{CMS}} = 133$ GeV) (/REF/ALEPH_2004_S5765862/d228-x01-y01)
- ≥ 6 -jet fraction ($E_{\text{CMS}} = 161$ GeV) (/REF/ALEPH_2004_S5765862/d229-x01-y01)
- Charged particle spectrum ($E_{\text{CMS}} = 189$ GeV) (/REF/ALEPH_2004_S5765862/d23-x01-y01)
- ≥ 6 -jet fraction ($E_{\text{CMS}} = 172$ GeV) (/REF/ALEPH_2004_S5765862/d230-x01-y01)
- ≥ 6 -jet fraction ($E_{\text{CMS}} = 183$ GeV) (/REF/ALEPH_2004_S5765862/d231-x01-y01)
- ≥ 6 -jet fraction ($E_{\text{CMS}} = 189$ GeV) (/REF/ALEPH_2004_S5765862/d232-x01-y01)
- ≥ 6 -jet fraction ($E_{\text{CMS}} = 200$ GeV) (/REF/ALEPH_2004_S5765862/d233-x01-y01)
- ≥ 6 -jet fraction ($E_{\text{CMS}} = 206$ GeV) (/REF/ALEPH_2004_S5765862/d234-x01-y01)
- Charged particle spectrum ($E_{\text{CMS}} = 196$ GeV) (/REF/ALEPH_2004_S5765862/d24-x01-y01)
- Charged particle spectrum ($E_{\text{CMS}} = 200$ GeV) (/REF/ALEPH_2004_S5765862/d25-x01-y01)
- Charged particle spectrum ($E_{\text{CMS}} = 206$ GeV) (/REF/ALEPH_2004_S5765862/d26-x01-y01)
- In-plane p_{\perp} in GeV w.r.t. thrust axes ($E_{\text{CMS}} = 133$ GeV) (/REF/ALEPH_2004_S5765862/d27-x01-y01)
- In-plane p_{\perp} in GeV w.r.t. thrust axes ($E_{\text{CMS}} = 161$ GeV) (/REF/ALEPH_2004_S5765862/d28-x01-y01)
- In-plane p_{\perp} in GeV w.r.t. thrust axes ($E_{\text{CMS}} = 172$ GeV) (/REF/ALEPH_2004_S5765862/d29-x01-y01)
- In-plane p_{\perp} in GeV w.r.t. thrust axes ($E_{\text{CMS}} = 183$ GeV) (/REF/ALEPH_2004_S5765862/d30-x01-y01)
- In-plane p_{\perp} in GeV w.r.t. thrust axes ($E_{\text{CMS}} = 189$ GeV) (/REF/ALEPH_2004_S5765862/d31-x01-y01)
- In-plane p_{\perp} in GeV w.r.t. thrust axes ($E_{\text{CMS}} = 196$ GeV) (/REF/ALEPH_2004_S5765862/d32-x01-y01)
- In-plane p_{\perp} in GeV w.r.t. thrust axes ($E_{\text{CMS}} = 200$ GeV) (/REF/ALEPH_2004_S5765862/d33-x01-y01)
- In-plane p_{\perp} in GeV w.r.t. thrust axes ($E_{\text{CMS}} = 206$ GeV) (/REF/ALEPH_2004_S5765862/d34-x01-y01)
- Out-of-plane p_{\perp} in GeV w.r.t. thrust axes ($E_{\text{CMS}} = 206$ GeV) (/REF/ALEPH_2004_S5765862/d35-x01-y01)
- Rapidity w.r.t. thrust axes, y_T ($E_{\text{CMS}} = 133$ GeV) (/REF/ALEPH_2004_S5765862/d36-x01-y01)
- Rapidity w.r.t. thrust axes, y_T ($E_{\text{CMS}} = 161$ GeV) (/REF/ALEPH_2004_S5765862/d37-x01-y01)

- Rapidity w.r.t. thrust axes, y_T ($E_{\text{CMS}} = 172 \text{ GeV}$) (/REF/ALEPH_2004_S5765862/d38-x01-y01)
- Rapidity w.r.t. thrust axes, y_T ($E_{\text{CMS}} = 183 \text{ GeV}$) (/REF/ALEPH_2004_S5765862/d39-x01-y01)
- Rapidity w.r.t. thrust axes, y_T ($E_{\text{CMS}} = 189 \text{ GeV}$) (/REF/ALEPH_2004_S5765862/d40-x01-y01)
- Rapidity w.r.t. thrust axes, y_T ($E_{\text{CMS}} = 196 \text{ GeV}$) (/REF/ALEPH_2004_S5765862/d41-x01-y01)
- Rapidity w.r.t. thrust axes, y_T ($E_{\text{CMS}} = 200 \text{ GeV}$) (/REF/ALEPH_2004_S5765862/d42-x01-y01)
- Rapidity w.r.t. thrust axes, y_T ($E_{\text{CMS}} = 206 \text{ GeV}$) (/REF/ALEPH_2004_S5765862/d43-x01-y01)
- Rapidity w.r.t. sphericity axes, y_S ($E_{\text{CMS}} = 133 \text{ GeV}$) (/REF/ALEPH_2004_S5765862/d44-x01-y01)
- Rapidity w.r.t. sphericity axes, y_S ($E_{\text{CMS}} = 161 \text{ GeV}$) (/REF/ALEPH_2004_S5765862/d45-x01-y01)
- Rapidity w.r.t. sphericity axes, y_S ($E_{\text{CMS}} = 172 \text{ GeV}$) (/REF/ALEPH_2004_S5765862/d46-x01-y01)
- Rapidity w.r.t. sphericity axes, y_S ($E_{\text{CMS}} = 183 \text{ GeV}$) (/REF/ALEPH_2004_S5765862/d47-x01-y01)
- Rapidity w.r.t. sphericity axes, y_S ($E_{\text{CMS}} = 189 \text{ GeV}$) (/REF/ALEPH_2004_S5765862/d48-x01-y01)
- Rapidity w.r.t. sphericity axes, y_S ($E_{\text{CMS}} = 196 \text{ GeV}$) (/REF/ALEPH_2004_S5765862/d49-x01-y01)
- Rapidity w.r.t. sphericity axes, y_S ($E_{\text{CMS}} = 200 \text{ GeV}$) (/REF/ALEPH_2004_S5765862/d50-x01-y01)
- Rapidity w.r.t. sphericity axes, y_S ($E_{\text{CMS}} = 206 \text{ GeV}$) (/REF/ALEPH_2004_S5765862/d51-x01-y01)
- Thrust ($E_{\text{CMS}} = 91.2 \text{ GeV}$) (/REF/ALEPH_2004_S5765862/d54-x01-y01)
- Thrust ($E_{\text{CMS}} = 133 \text{ GeV}$) (/REF/ALEPH_2004_S5765862/d55-x01-y01)
- Thrust ($E_{\text{CMS}} = 161 \text{ GeV}$) (/REF/ALEPH_2004_S5765862/d56-x01-y01)
- Thrust ($E_{\text{CMS}} = 172 \text{ GeV}$) (/REF/ALEPH_2004_S5765862/d57-x01-y01)
- Thrust ($E_{\text{CMS}} = 183 \text{ GeV}$) (/REF/ALEPH_2004_S5765862/d58-x01-y01)
- Thrust ($E_{\text{CMS}} = 189 \text{ GeV}$) (/REF/ALEPH_2004_S5765862/d59-x01-y01)
- Thrust ($E_{\text{CMS}} = 200 \text{ GeV}$) (/REF/ALEPH_2004_S5765862/d60-x01-y01)
- Thrust ($E_{\text{CMS}} = 206 \text{ GeV}$) (/REF/ALEPH_2004_S5765862/d61-x01-y01)
- Heavy jet mass ($E_{\text{CMS}} = 91.2 \text{ GeV}$) (/REF/ALEPH_2004_S5765862/d62-x01-y01)
- Heavy jet mass ($E_{\text{CMS}} = 133 \text{ GeV}$) (/REF/ALEPH_2004_S5765862/d63-x01-y01)
- Heavy jet mass ($E_{\text{CMS}} = 161 \text{ GeV}$) (/REF/ALEPH_2004_S5765862/d64-x01-y01)
- Heavy jet mass ($E_{\text{CMS}} = 172 \text{ GeV}$) (/REF/ALEPH_2004_S5765862/d65-x01-y01)
- Heavy jet mass ($E_{\text{CMS}} = 183 \text{ GeV}$) (/REF/ALEPH_2004_S5765862/d66-x01-y01)

- Heavy jet mass ($E_{\text{CMS}} = 189$ GeV) (/REF/ALEPH_2004_S5765862/d67-x01-y01)
- Heavy jet mass ($E_{\text{CMS}} = 200$ GeV) (/REF/ALEPH_2004_S5765862/d68-x01-y01)
- Heavy jet mass ($E_{\text{CMS}} = 206$ GeV) (/REF/ALEPH_2004_S5765862/d69-x01-y01)
- Total jet broadening ($E_{\text{CMS}} = 91.2$ GeV) (/REF/ALEPH_2004_S5765862/d70-x01-y01)
- Total jet broadening ($E_{\text{CMS}} = 133$ GeV) (/REF/ALEPH_2004_S5765862/d71-x01-y01)
- Total jet broadening ($E_{\text{CMS}} = 161$ GeV) (/REF/ALEPH_2004_S5765862/d72-x01-y01)
- Total jet broadening ($E_{\text{CMS}} = 172$ GeV) (/REF/ALEPH_2004_S5765862/d73-x01-y01)
- Total jet broadening ($E_{\text{CMS}} = 183$ GeV) (/REF/ALEPH_2004_S5765862/d74-x01-y01)
- Total jet broadening ($E_{\text{CMS}} = 189$ GeV) (/REF/ALEPH_2004_S5765862/d75-x01-y01)
- Total jet broadening ($E_{\text{CMS}} = 200$ GeV) (/REF/ALEPH_2004_S5765862/d76-x01-y01)
- Total jet broadening ($E_{\text{CMS}} = 206$ GeV) (/REF/ALEPH_2004_S5765862/d77-x01-y01)
- Wide jet broadening ($E_{\text{CMS}} = 91.2$ GeV) (/REF/ALEPH_2004_S5765862/d78-x01-y01)
- Wide jet broadening ($E_{\text{CMS}} = 133$ GeV) (/REF/ALEPH_2004_S5765862/d79-x01-y01)
- Wide jet broadening ($E_{\text{CMS}} = 161$ GeV) (/REF/ALEPH_2004_S5765862/d80-x01-y01)
- Wide jet broadening ($E_{\text{CMS}} = 172$ GeV) (/REF/ALEPH_2004_S5765862/d81-x01-y01)
- Wide jet broadening ($E_{\text{CMS}} = 183$ GeV) (/REF/ALEPH_2004_S5765862/d82-x01-y01)
- Wide jet broadening ($E_{\text{CMS}} = 189$ GeV) (/REF/ALEPH_2004_S5765862/d83-x01-y01)
- Wide jet broadening ($E_{\text{CMS}} = 200$ GeV) (/REF/ALEPH_2004_S5765862/d84-x01-y01)
- Wide jet broadening ($E_{\text{CMS}} = 206$ GeV) (/REF/ALEPH_2004_S5765862/d85-x01-y01)
- C-Parameter ($E_{\text{CMS}} = 91.2$ GeV) (/REF/ALEPH_2004_S5765862/d86-x01-y01)
- C-Parameter ($E_{\text{CMS}} = 133$ GeV) (/REF/ALEPH_2004_S5765862/d87-x01-y01)
- C-Parameter ($E_{\text{CMS}} = 161$ GeV) (/REF/ALEPH_2004_S5765862/d88-x01-y01)
- C-Parameter ($E_{\text{CMS}} = 172$ GeV) (/REF/ALEPH_2004_S5765862/d89-x01-y01)
- C-Parameter ($E_{\text{CMS}} = 183$ GeV) (/REF/ALEPH_2004_S5765862/d90-x01-y01)
- C-Parameter ($E_{\text{CMS}} = 189$ GeV) (/REF/ALEPH_2004_S5765862/d91-x01-y01)
- C-Parameter ($E_{\text{CMS}} = 200$ GeV) (/REF/ALEPH_2004_S5765862/d92-x01-y01)
- C-Parameter ($E_{\text{CMS}} = 206$ GeV) (/REF/ALEPH_2004_S5765862/d93-x01-y01)

- Thrust major ($E_{\text{CMS}} = 91.2 \text{ GeV}$) ([/REF/ALEPH_2004_S5765862/d94-x01-y01](#))
- Thrust major ($E_{\text{CMS}} = 133 \text{ GeV}$) ([/REF/ALEPH_2004_S5765862/d95-x01-y01](#))
- Thrust major ($E_{\text{CMS}} = 161 \text{ GeV}$) ([/REF/ALEPH_2004_S5765862/d96-x01-y01](#))
- Thrust major ($E_{\text{CMS}} = 172 \text{ GeV}$) ([/REF/ALEPH_2004_S5765862/d97-x01-y01](#))
- Thrust major ($E_{\text{CMS}} = 183 \text{ GeV}$) ([/REF/ALEPH_2004_S5765862/d98-x01-y01](#))
- Thrust major ($E_{\text{CMS}} = 189 \text{ GeV}$) ([/REF/ALEPH_2004_S5765862/d99-x01-y01](#))

6.8 DELPHI_1995_S3137023 [19]

Strange baryon production in Z hadronic decays at Delphi

Beams: $e^+ e^-$

Energies: (45.6, 45.6) GeV

Experiment: DELPHI (LEP 1)

Spires ID: [3137023](#)

Status: VALIDATED

Authors:

- Hendrik Hoeth (hendrik.hoeth@cern.ch)

References:

- Z. Phys. C, 67, 543–554 (1995)

Run details:

- Hadronic Z decay events generated on the Z pole ($\sqrt{s} = 91.2$ GeV)

Measurement of the Ξ^- and $\Sigma^+(1385)/\Sigma^-(1385)$ scaled momentum distributions by DELPHI at LEP 1. The paper also has the production cross-sections of these particles, but that's not implemented in Rivet.

Histograms (2):

- Ξ^- scaled momentum ([/REF/DELPHI_1995_S3137023/d02-x01-y01](#))
- $\Sigma^\pm(1385)$ scaled momentum ([/REF/DELPHI_1995_S3137023/d03-x01-y01](#))

6.9 DELPHI_1996_S3430090 [10]

Delphi MC tuning on event shapes and identified particles.

Beams: $e^+ e^-$

Energies: (45.6, 45.6) GeV

Experiment: DELPHI (LEP 1)

Spires ID: [3430090](#)

Status: VALIDATED

Authors:

- Andy Buckley <andy.buckley@cern.ch>
- Hendrik Hoeth <hendrik.hoeth@cern.ch>

References:

- Z.Phys.C73:11-60,1996
- DOI: [10.1007/s002880050295](https://doi.org/10.1007/s002880050295)

Run details:

- $\sqrt{s} = 91.2$ GeV, $e^+e^- \rightarrow Z^0$ production with hadronic decays only

Event shape and charged particle inclusive distributions measured using 750000 decays of Z bosons to hadrons from the DELPHI detector at LEP. This data, combined with identified particle distributions from all LEP experiments, was used for tuning of shower-hadronisation event generators by the original PROFESSOR method. This is a critical analysis for MC event generator tuning of final state radiation and both flavour and kinematic aspects of hadronisation models.

Histograms (60):

- In-plane p_\perp in GeV w.r.t. thrust axes ([/REF/DELPHI_1996_S3430090/d01-x01-y01](#))
- Out-of-plane p_\perp in GeV w.r.t. thrust axes ([/REF/DELPHI_1996_S3430090/d02-x01-y01](#))
- In-plane p_\perp in GeV w.r.t. sphericity axes ([/REF/DELPHI_1996_S3430090/d03-x01-y01](#))
- Out-of-plane p_\perp in GeV w.r.t. sphericity axes ([/REF/DELPHI_1996_S3430090/d04-x01-y01](#))
- Rapidity w.r.t. thrust axes, y_T ([/REF/DELPHI_1996_S3430090/d05-x01-y01](#))
- Rapidity w.r.t. sphericity axes, y_S ([/REF/DELPHI_1996_S3430090/d06-x01-y01](#))
- Scaled momentum, $x_p = |p|/|p_{\text{beam}}|$ ([/REF/DELPHI_1996_S3430090/d07-x01-y01](#))
- Log of scaled momentum, $\log(1/x_p)$ ([/REF/DELPHI_1996_S3430090/d08-x01-y01](#))
- Mean out-of-plane p_\perp in GeV w.r.t. thrust axes vs. x_p ([/REF/DELPHI_1996_S3430090/d09-x01-y01](#))

- Mean p_\perp in GeV vs. x_p (/REF/DELPHI_1996_S3430090/d10-x01-y01)
- 1 – Thrust (/REF/DELPHI_1996_S3430090/d11-x01-y01)
- Thrust major, M (/REF/DELPHI_1996_S3430090/d12-x01-y01)
- Thrust minor, m (/REF/DELPHI_1996_S3430090/d13-x01-y01)
- Oblateness = $M - m$ (/REF/DELPHI_1996_S3430090/d14-x01-y01)
- Sphericity, S (/REF/DELPHI_1996_S3430090/d15-x01-y01)
- Aplanarity, A (/REF/DELPHI_1996_S3430090/d16-x01-y01)
- Planarity, P (/REF/DELPHI_1996_S3430090/d17-x01-y01)
- C parameter (/REF/DELPHI_1996_S3430090/d18-x01-y01)
- D parameter (/REF/DELPHI_1996_S3430090/d19-x01-y01)
- Heavy hemisphere masses, M_h^2/E_{vis}^2 (/REF/DELPHI_1996_S3430090/d20-x01-y01)
- Light hemisphere masses, M_l^2/E_{vis}^2 (/REF/DELPHI_1996_S3430090/d21-x01-y01)
- Difference in hemisphere masses, M_d^2/E_{vis}^2 (/REF/DELPHI_1996_S3430090/d22-x01-y01)
- Wide hemisphere broadening, B_{\max} (/REF/DELPHI_1996_S3430090/d23-x01-y01)
- Narrow hemisphere broadening, B_{\min} (/REF/DELPHI_1996_S3430090/d24-x01-y01)
- Total hemisphere broadening, B_{\sum} (/REF/DELPHI_1996_S3430090/d25-x01-y01)
- Difference in hemisphere broadening, B_{diff} (/REF/DELPHI_1996_S3430090/d26-x01-y01)
- Differential 3-jet rate with Durham algorithm, D_2^{Durham} (/REF/DELPHI_1996_S3430090/d27-x01-y01)
- Differential 3-jet rate with Jade algorithm, D_2^{Jade} (/REF/DELPHI_1996_S3430090/d28-x01-y01)
- Differential 4-jet rate with Durham algorithm, D_3^{Durham} (/REF/DELPHI_1996_S3430090/d29-x01-y01)
- Differential 4-jet rate with Jade algorithm, D_3^{Jade} (/REF/DELPHI_1996_S3430090/d30-x01-y01)
- Differential 5-jet rate with Durham algorithm, D_4^{Durham} (/REF/DELPHI_1996_S3430090/d31-x01-y01)
- Differential 5-jet rate with Jade algorithm, D_4^{Jade} (/REF/DELPHI_1996_S3430090/d32-x01-y01)
- Energy-energy correlation, EEC (/REF/DELPHI_1996_S3430090/d33-x01-y01)
- Asymmetry of the energy-energy correlation, AEEC (/REF/DELPHI_1996_S3430090/d34-x01-y01)
- Mean charged multiplicity (/REF/DELPHI_1996_S3430090/d35-x01-y01)
- Mean π^+/π^- multiplicity (/REF/DELPHI_1996_S3430090/d36-x01-y01)

- Mean π^0 multiplicity (/REF/DELPHI_1996_S3430090/d36-x01-y02)
- Mean K^+/K^- multiplicity (/REF/DELPHI_1996_S3430090/d36-x01-y03)
- Mean K^0 multiplicity (/REF/DELPHI_1996_S3430090/d36-x01-y04)
- Mean η multiplicity (/REF/DELPHI_1996_S3430090/d36-x01-y05)
- Mean η' multiplicity (/REF/DELPHI_1996_S3430090/d36-x01-y06)
- Mean D^+ multiplicity (/REF/DELPHI_1996_S3430090/d36-x01-y07)
- Mean D^0 multiplicity (/REF/DELPHI_1996_S3430090/d36-x01-y08)
- Mean $B^+/B^-/B^0$ multiplicity (/REF/DELPHI_1996_S3430090/d36-x01-y09)
- Mean $f_0(980)$ multiplicity (/REF/DELPHI_1996_S3430090/d37-x01-y01)
- Mean ρ multiplicity (/REF/DELPHI_1996_S3430090/d38-x01-y01)
- Mean $K^*(892)^+/K^*(892)^-$ multiplicity (/REF/DELPHI_1996_S3430090/d38-x01-y02)
- Mean $K^*(892)^0$ multiplicity (/REF/DELPHI_1996_S3430090/d38-x01-y03)
- Mean ϕ multiplicity (/REF/DELPHI_1996_S3430090/d38-x01-y04)
- Mean $D^*(2010)^+/D^*(2010)^-$ multiplicity (/REF/DELPHI_1996_S3430090/d38-x01-y05)
- Mean $f_2(1270)$ multiplicity (/REF/DELPHI_1996_S3430090/d39-x01-y01)
- Mean $K_2^*(1430)^0$ multiplicity (/REF/DELPHI_1996_S3430090/d39-x01-y02)
- Mean p multiplicity (/REF/DELPHI_1996_S3430090/d40-x01-y01)
- Mean Λ^0 multiplicity (/REF/DELPHI_1996_S3430090/d40-x01-y02)
- Mean Ξ^- multiplicity (/REF/DELPHI_1996_S3430090/d40-x01-y03)
- Mean Ω^- multiplicity (/REF/DELPHI_1996_S3430090/d40-x01-y04)
- Mean $\Delta(1232)^{++}$ multiplicity (/REF/DELPHI_1996_S3430090/d40-x01-y05)
- Mean $\Sigma(1385)^+/\Sigma(1385)^-$ multiplicity (/REF/DELPHI_1996_S3430090/d40-x01-y06)
- Mean $\Xi(1530)^0$ multiplicity (/REF/DELPHI_1996_S3430090/d40-x01-y07)
- Mean Λ_b^0 multiplicity (/REF/DELPHI_1996_S3430090/d40-x01-y08)

6.10 DELPHI_1999_S3960137 [20]

Measurement of inclusive ρ^0 , $f_0(980)$, $f_2(1270)$, $K_2^{*0}(1430)$ and $f'_2(1525)$ production in Z^0 decays

Beams: $e^+ e^-$

Energies: (45.6, 45.6) GeV

Experiment: DELPHI (LEP 1)

Spires ID: [3960137](#)

Status: VALIDATED

Authors:

- Peter Richardson (Peter.Richardson@durham.ac.uk)

References:

- Phys.Lett.B449:364-382,1999

Run details:

- Hadronic Z decay events generated on the Z pole ($\sqrt{s} = 91.2$ GeV)

DELPHI results for the production of ρ^0 , $f_0(980)$, $f_2(1270)$, $K_2^{*0}(1430)$ and $f'_2(1525)$ in Z^0 decays. Only the identified particle spectra for ρ^0 , $f_0(980)$ and $f_2(1270)$ are implemented.

Histograms (3):

- ρ^0 scaled momentum ([/REF/DELPHI_1999_S3960137/d01-x01-y01](#))
- $f^0(980)$ scaled momentum ([/REF/DELPHI_1999_S3960137/d01-x01-y02](#))
- $f_2(1270)$ scaled momentum ([/REF/DELPHI_1999_S3960137/d01-x01-y03](#))

6.11 DELPHI_2000_S4328825 [21]

Hadronization properties of b quarks compared to light quarks in $e^+e^- \rightarrow q\bar{q}$ from 183 GeV to 200 GeV

Beams: e^+e^-

Energies: (91.5, 91.5), (94.5, 94.5), (96.0, 96.0), (98.0, 98.0), (100.0, 100.0), (103.0, 103.0) GeV

Experiment: OPAL (LEP 2)

Spires ID: [4328825](#)

Status: VALIDATED

Authors:

- Peter Richardson (Peter.Richardson@durham.ac.uk)

References:

- Phys.Lett.B479:118-128,2000
- hep-ex/0103022
- DELPHI 2002-052 CONF 586

Run details:

- Hadronic Z decay events generated on the Z pole ($\sqrt{s} = 91.2$ GeV)

Measurements of the mean charged multiplicities separately for $b\bar{b}$, $c\bar{c}$ and light quark (uds) initiated events in e^+e^- interactions at energies above the Z^0 mass. In addition to the energy points in the original paper one additional point at 206;GeV is included from a later preliminary result.

Histograms (4):

- Charged multiplicity as a function of energy in b events (/REF/DELPHI_2000_S4328825/d01-x01-y01)
- Charged multiplicity as a function of energy in c events (/REF/DELPHI_2000_S4328825/d01-x01-y02)
- Charged multiplicity as a function of energy in uds events (/REF/DELPHI_2000_S4328825/d01-x01-y03)
- Difference in Charged multiplicity as a function of energy between b and uds events (/REF/DELPHI_2000_S4328825/d01-x01-y04)

6.12 DELPHI_2002_069_CONF_603

Study of the b-quark fragmentation function at LEP 1

Beams: $e^+ e^-$

Energies: (45.6, 45.6) GeV

Experiment: DELPHI (LEP 1)

Status: PRELIMINARY

Authors:

- Hendrik Hoeth hendrik.hoeth@cern.ch

References:

- DELPHI note 2002-069-CONF-603 (ICHEP 2002)

Run details:

- Hadronic Z decay events generated on the Z pole ($\sqrt{s} = 91.2$ GeV)

Measurement of the b -quark fragmentation function by DELPHI using 1994 LEP 1 data. The fragmentation function for both weakly decaying and primary b -quarks has been determined in a model independent way. Nevertheless the authors trust $f(x_B^{\text{weak}})$ more than $f(x_B^{\text{prim}})$.

Histograms (4):

- b quark fragmentation function $f(x_B^{\text{prim}})$ (/REF/DELPHI_2002_069_CONF_603/d01-x01-y01)
- b quark fragmentation function $f(x_B^{\text{weak}})$ (/REF/DELPHI_2002_069_CONF_603/d02-x01-y01)
- Mean of b quark fragmentation function $f(x_B^{\text{prim}})$ (/REF/DELPHI_2002_069_CONF_603/d04-x01-y01)
- Mean of b quark fragmentation function $f(x_B^{\text{weak}})$ (/REF/DELPHI_2002_069_CONF_603/d05-x01-y01)

6.13 DELPHI_2003_WUD_03_11

4-jet angular distributions at LEP (note)

Beams: $e^+ e^-$

Energies: (45.6, 45.6) GeV

Experiment: DELPHI (LEP 1)

Status: UNVALIDATED

Authors:

- Hendrik Hoeth hendrik.hoeth@cern.ch

References:

- Diploma thesis WUD-03-11, University of Wuppertal

Run details:

- Hadronic Z decay events generated on the Z pole ($\sqrt{s} = 91.2$ GeV)

The 4-jet angular distributions (Bengtsson-Zerwas, Körner-Schierholz- Willrodt, Nachtmann-Reiter, and α_{34}) have been measured with DELPHI at LEP 1 using Jade and Durham cluster algorithms.

Histograms (8):

- Bengtsson-Zerwas $|\cos(\chi_{BZ})|$, Durham $y_{\text{cut}} = 0.008$ ([/REF/DELPHI_2003_WUD_03_11/d01-x01-y01](#))
- Bengtsson-Zerwas $|\cos(\chi_{BZ})|$, Jade $y_{\text{cut}} = 0.015$ ([/REF/DELPHI_2003_WUD_03_11/d01-x02-y01](#))
- Körner-Schierholz-Willrodt $\cos(\phi_{KSW})$, Durham $y_{\text{cut}} = 0.008$ ([/REF/DELPHI_2003_WUD_03_11/d02-x01-y01](#))
- Körner-Schierholz-Willrodt $\cos(\phi_{KSW})$, Jade $y_{\text{cut}} = 0.015$ ([/REF/DELPHI_2003_WUD_03_11/d02-x02-y01](#))
- Nachtmann-Reiter (mod.) $|\cos(\theta_{\text{NR}}^*)|$, Durham $y_{\text{cut}} = 0.008$ ([/REF/DELPHI_2003_WUD_03_11/d03-x01-y01](#))
- Nachtmann-Reiter (mod.) $|\cos(\theta_{\text{NR}}^*)|$, Jade $y_{\text{cut}} = 0.015$ ([/REF/DELPHI_2003_WUD_03_11/d03-x02-y01](#))
- $\cos(\alpha_{34})$, Durham $y_{\text{cut}} = 0.008$ ([/REF/DELPHI_2003_WUD_03_11/d04-x01-y01](#))
- $\cos(\alpha_{34})$, Jade $y_{\text{cut}} = 0.015$ ([/REF/DELPHI_2003_WUD_03_11/d04-x02-y01](#))

6.14 JADE_OPAL_2000_S4300807 [22]

Jet rates in e^+e^- at JADE [35–44 GeV] and OPAL [91–189 GeV].

Beams: e^+e^-

Energies: (17.5, 17.5), (22.0, 22.0), (45.6, 45.6), (66.5, 66.5), (80.5, 80.5), (86.0, 86.0), (91.5, 91.5), (94.5, 94.5) GeV

Experiment: JADE_OPAL (PETRA and LEP)

Spires ID: [4300807](#)

Status: VALIDATED

Authors:

- Frank Siegert [⟨frank.siegert@cern.ch⟩](mailto:frank.siegert@cern.ch)
- Andy Buckley [⟨andy.buckley@cern.ch⟩](mailto:andy.buckley@cern.ch)

References:

- Eur.Phys.J.C17:19-51,2000
- arXiv: [hep-ex/0001055](#)

Run details:

- $e^+e^- \rightarrow \text{jet jet (+ jets)}$

Differential and integrated jet rates for Durham and JADE jet algorithms. The integration cut value used for the integrated rate observables is not well-defined in the paper: the midpoint of the differential bin has been used thanks to information from Stefan Kluth and Christoph Pahl. We anyway recommend that the differential plots be preferred over the integrated ones for MC generator validation and tuning, to minimise correlations.

Histograms (112):

- Integrated 2-jet rate with Jade algorithm (35 GeV) ([/REF/JADE_OPAL_2000_S4300807/d07-x01-y01](#))
- Integrated 3-jet rate with Jade algorithm (35 GeV) ([/REF/JADE_OPAL_2000_S4300807/d07-x01-y02](#))
- Integrated 4-jet rate with Jade algorithm (35 GeV) ([/REF/JADE_OPAL_2000_S4300807/d07-x01-y03](#))
- Integrated 5-jet rate with Jade algorithm (35 GeV) ([/REF/JADE_OPAL_2000_S4300807/d07-x01-y04](#))
- Integrated ≥ 6 -jet rate with Jade algorithm (35 GeV) ([/REF/JADE_OPAL_2000_S4300807/d07-x01-y05](#))
- Integrated 2-jet rate with Jade algorithm (44 GeV) ([/REF/JADE_OPAL_2000_S4300807/d08-x01-y01](#))
- Integrated 3-jet rate with Jade algorithm (44 GeV) ([/REF/JADE_OPAL_2000_S4300807/d08-x01-y02](#))
- Integrated 4-jet rate with Jade algorithm (44 GeV) ([/REF/JADE_OPAL_2000_S4300807/d08-x01-y03](#))
- Integrated 5-jet rate with Jade algorithm (44 GeV) ([/REF/JADE_OPAL_2000_S4300807/d08-x01-y04](#))

- Integrated ≥ 6 -jet rate with Jade algorithm (44 GeV) (/REF/JADE_OPAL_2000_S4300807/d08-x01-y05)
- Integrated 2-jet rate with Jade algorithm (91.2 GeV) (/REF/JADE_OPAL_2000_S4300807/d09-x01-y01)
- Integrated 3-jet rate with Jade algorithm (91.2 GeV) (/REF/JADE_OPAL_2000_S4300807/d09-x01-y02)
- Integrated 4-jet rate with Jade algorithm (91.2 GeV) (/REF/JADE_OPAL_2000_S4300807/d09-x01-y03)
- Integrated 5-jet rate with Jade algorithm (91.2 GeV) (/REF/JADE_OPAL_2000_S4300807/d09-x01-y04)
- Integrated ≥ 6 -jet rate with Jade algorithm (91.2 GeV) (/REF/JADE_OPAL_2000_S4300807/d09-x01-y05)
- Integrated 2-jet rate with Jade algorithm (133 GeV) (/REF/JADE_OPAL_2000_S4300807/d10-x01-y01)
- Integrated 3-jet rate with Jade algorithm (133 GeV) (/REF/JADE_OPAL_2000_S4300807/d10-x01-y02)
- Integrated 4-jet rate with Jade algorithm (133 GeV) (/REF/JADE_OPAL_2000_S4300807/d10-x01-y03)
- Integrated 5-jet rate with Jade algorithm (133 GeV) (/REF/JADE_OPAL_2000_S4300807/d10-x01-y04)
- Integrated ≥ 6 -jet rate with Jade algorithm (133 GeV) (/REF/JADE_OPAL_2000_S4300807/d10-x01-y05)
- Integrated 2-jet rate with Jade algorithm (161 GeV) (/REF/JADE_OPAL_2000_S4300807/d11-x01-y01)
- Integrated 3-jet rate with Jade algorithm (161 GeV) (/REF/JADE_OPAL_2000_S4300807/d11-x01-y02)
- Integrated 4-jet rate with Jade algorithm (161 GeV) (/REF/JADE_OPAL_2000_S4300807/d11-x01-y03)
- Integrated 5-jet rate with Jade algorithm (161 GeV) (/REF/JADE_OPAL_2000_S4300807/d11-x01-y04)
- Integrated ≥ 6 -jet rate with Jade algorithm (161 GeV) (/REF/JADE_OPAL_2000_S4300807/d11-x01-y05)
- Integrated 2-jet rate with Jade algorithm (172 GeV) (/REF/JADE_OPAL_2000_S4300807/d12-x01-y01)
- Integrated 3-jet rate with Jade algorithm (172 GeV) (/REF/JADE_OPAL_2000_S4300807/d12-x01-y02)
- Integrated 4-jet rate with Jade algorithm (172 GeV) (/REF/JADE_OPAL_2000_S4300807/d12-x01-y03)
- Integrated 5-jet rate with Jade algorithm (172 GeV) (/REF/JADE_OPAL_2000_S4300807/d12-x01-y04)
- Integrated ≥ 6 -jet rate with Jade algorithm (172 GeV) (/REF/JADE_OPAL_2000_S4300807/d12-x01-y05)
- Integrated 2-jet rate with Jade algorithm (183 GeV) (/REF/JADE_OPAL_2000_S4300807/d13-x01-y01)
- Integrated 3-jet rate with Jade algorithm (183 GeV) (/REF/JADE_OPAL_2000_S4300807/d13-x01-y02)
- Integrated 4-jet rate with Jade algorithm (183 GeV) (/REF/JADE_OPAL_2000_S4300807/d13-x01-y03)
- Integrated 5-jet rate with Jade algorithm (183 GeV) (/REF/JADE_OPAL_2000_S4300807/d13-x01-y04)
- Integrated ≥ 6 -jet rate with Jade algorithm (183 GeV) (/REF/JADE_OPAL_2000_S4300807/d13-x01-y05)
- Integrated 2-jet rate with Jade algorithm (189 GeV) (/REF/JADE_OPAL_2000_S4300807/d14-x01-y01)

- Integrated 3-jet rate with Jade algorithm (189 GeV) (/REF/JADE_OPAL_2000_S4300807/d14-x01-y02)
- Integrated 4-jet rate with Jade algorithm (189 GeV) (/REF/JADE_OPAL_2000_S4300807/d14-x01-y03)
- Integrated 5-jet rate with Jade algorithm (189 GeV) (/REF/JADE_OPAL_2000_S4300807/d14-x01-y04)
- Integrated ≥ 6 -jet rate with Jade algorithm (189 GeV) (/REF/JADE_OPAL_2000_S4300807/d14-x01-y05)
- Integrated 2-jet rate with Durham algorithm (35 GeV) (/REF/JADE_OPAL_2000_S4300807/d16-x01-y01)
- Integrated 3-jet rate with Durham algorithm (35 GeV) (/REF/JADE_OPAL_2000_S4300807/d16-x01-y02)
- Integrated 4-jet rate with Durham algorithm (35 GeV) (/REF/JADE_OPAL_2000_S4300807/d16-x01-y03)
- Integrated 5-jet rate with Durham algorithm (35 GeV) (/REF/JADE_OPAL_2000_S4300807/d16-x01-y04)
- Integrated ≥ 6 -jet rate with Durham algorithm (35 GeV) (/REF/JADE_OPAL_2000_S4300807/d16-x01-y05)
- Integrated 2-jet rate with Durham algorithm (44 GeV) (/REF/JADE_OPAL_2000_S4300807/d17-x01-y01)
- Integrated 3-jet rate with Durham algorithm (44 GeV) (/REF/JADE_OPAL_2000_S4300807/d17-x01-y02)
- Integrated 4-jet rate with Durham algorithm (44 GeV) (/REF/JADE_OPAL_2000_S4300807/d17-x01-y03)
- Integrated 5-jet rate with Durham algorithm (44 GeV) (/REF/JADE_OPAL_2000_S4300807/d17-x01-y04)
- Integrated ≥ 6 -jet rate with Durham algorithm (44 GeV) (/REF/JADE_OPAL_2000_S4300807/d17-x01-y05)
- Integrated 2-jet rate with Durham algorithm (91.2 GeV) (/REF/JADE_OPAL_2000_S4300807/d18-x01-y01)
- Integrated 3-jet rate with Durham algorithm (91.2 GeV) (/REF/JADE_OPAL_2000_S4300807/d18-x01-y02)
- Integrated 4-jet rate with Durham algorithm (91.2 GeV) (/REF/JADE_OPAL_2000_S4300807/d18-x01-y03)
- Integrated 5-jet rate with Durham algorithm (91.2 GeV) (/REF/JADE_OPAL_2000_S4300807/d18-x01-y04)
- Integrated ≥ 6 -jet rate with Durham algorithm (91.2 GeV) (/REF/JADE_OPAL_2000_-S4300807/d18-x01-y05)
- Integrated 2-jet rate with Durham algorithm (133 GeV) (/REF/JADE_OPAL_2000_S4300807/d19-x01-y01)
- Integrated 3-jet rate with Durham algorithm (133 GeV) (/REF/JADE_OPAL_2000_S4300807/d19-x01-y02)
- Integrated 4-jet rate with Durham algorithm (133 GeV) (/REF/JADE_OPAL_2000_S4300807/d19-x01-y03)
- Integrated 5-jet rate with Durham algorithm (133 GeV) (/REF/JADE_OPAL_2000_S4300807/d19-x01-y04)
- Integrated ≥ 6 -jet rate with Durham algorithm (133 GeV) (/REF/JADE_OPAL_2000_-S4300807/d19-x01-y05)
- Integrated 2-jet rate with Durham algorithm (161 GeV) (/REF/JADE_OPAL_2000_S4300807/d20-x01-y01)
- Integrated 3-jet rate with Durham algorithm (161 GeV) (/REF/JADE_OPAL_2000_S4300807/d20-x01-y02)

- Integrated 4-jet rate with Durham algorithm (161 GeV) (/REF/JADE_OPAL_2000_S4300807/d20-x01-y03)
- Integrated 5-jet rate with Durham algorithm (161 GeV) (/REF/JADE_OPAL_2000_S4300807/d20-x01-y04)
- Integrated ≥ 6 -jet rate with Durham algorithm (161 GeV) (/REF/JADE_OPAL_2000_S4300807/d20-x01-y05)
- Integrated 2-jet rate with Durham algorithm (172 GeV) (/REF/JADE_OPAL_2000_S4300807/d21-x01-y01)
- Integrated 3-jet rate with Durham algorithm (172 GeV) (/REF/JADE_OPAL_2000_S4300807/d21-x01-y02)
- Integrated 4-jet rate with Durham algorithm (172 GeV) (/REF/JADE_OPAL_2000_S4300807/d21-x01-y03)
- Integrated 5-jet rate with Durham algorithm (172 GeV) (/REF/JADE_OPAL_2000_S4300807/d21-x01-y04)
- Integrated ≥ 6 -jet rate with Durham algorithm (172 GeV) (/REF/JADE_OPAL_2000_S4300807/d21-x01-y05)
- Integrated 2-jet rate with Durham algorithm (183 GeV) (/REF/JADE_OPAL_2000_S4300807/d22-x01-y01)
- Integrated 3-jet rate with Durham algorithm (183 GeV) (/REF/JADE_OPAL_2000_S4300807/d22-x01-y02)
- Integrated 4-jet rate with Durham algorithm (183 GeV) (/REF/JADE_OPAL_2000_S4300807/d22-x01-y03)
- Integrated 5-jet rate with Durham algorithm (183 GeV) (/REF/JADE_OPAL_2000_S4300807/d22-x01-y04)
- Integrated ≥ 6 -jet rate with Durham algorithm (183 GeV) (/REF/JADE_OPAL_2000_S4300807/d22-x01-y05)
- Integrated 2-jet rate with Durham algorithm (189 GeV) (/REF/JADE_OPAL_2000_S4300807/d23-x01-y01)
- Integrated 3-jet rate with Durham algorithm (189 GeV) (/REF/JADE_OPAL_2000_S4300807/d23-x01-y02)
- Integrated 4-jet rate with Durham algorithm (189 GeV) (/REF/JADE_OPAL_2000_S4300807/d23-x01-y03)
- Integrated 5-jet rate with Durham algorithm (189 GeV) (/REF/JADE_OPAL_2000_S4300807/d23-x01-y04)
- Integrated ≥ 6 -jet rate with Durham algorithm (189 GeV) (/REF/JADE_OPAL_2000_S4300807/d23-x01-y05)
- Differential 2-jet rate with Durham algorithm (35 GeV) (/REF/JADE_OPAL_2000_S4300807/d24-x01-y01)
- Differential 3-jet rate with Durham algorithm (35 GeV) (/REF/JADE_OPAL_2000_S4300807/d24-x01-y02)
- Differential 4-jet rate with Durham algorithm (35 GeV) (/REF/JADE_OPAL_2000_S4300807/d24-x01-y03)
- Differential 5-jet rate with Durham algorithm (35 GeV) (/REF/JADE_OPAL_2000_S4300807/d24-x01-y04)
- Differential 2-jet rate with Durham algorithm (44 GeV) (/REF/JADE_OPAL_2000_S4300807/d25-x01-y01)
- Differential 3-jet rate with Durham algorithm (44 GeV) (/REF/JADE_OPAL_2000_S4300807/d25-x01-y02)
- Differential 4-jet rate with Durham algorithm (44 GeV) (/REF/JADE_OPAL_2000_S4300807/d25-x01-y03)

- Differential 5-jet rate with Durham algorithm (44 GeV) (/REF/JADE_OPAL_2000_S4300807/d25-x01-y04)
- Differential 2-jet rate with Durham algorithm (91.2 GeV) (/REF/JADE_OPAL_2000_-S4300807/d26-x01-y01)
- Differential 3-jet rate with Durham algorithm (91.2 GeV) (/REF/JADE_OPAL_2000_-S4300807/d26-x01-y02)
- Differential 4-jet rate with Durham algorithm (91.2 GeV) (/REF/JADE_OPAL_2000_-S4300807/d26-x01-y03)
- Differential 5-jet rate with Durham algorithm (91.2 GeV) (/REF/JADE_OPAL_2000_-S4300807/d26-x01-y04)
- Differential 2-jet rate with Durham algorithm (133 GeV) (/REF/JADE_OPAL_2000_S4300807/d27-x01-y01)
- Differential 3-jet rate with Durham algorithm (133 GeV) (/REF/JADE_OPAL_2000_S4300807/d27-x01-y02)
- Differential 4-jet rate with Durham algorithm (133 GeV) (/REF/JADE_OPAL_2000_S4300807/d27-x01-y03)
- Differential 5-jet rate with Durham algorithm (133 GeV) (/REF/JADE_OPAL_2000_S4300807/d27-x01-y04)
- Differential 2-jet rate with Durham algorithm (161 GeV) (/REF/JADE_OPAL_2000_S4300807/d28-x01-y01)
- Differential 3-jet rate with Durham algorithm (161 GeV) (/REF/JADE_OPAL_2000_S4300807/d28-x01-y02)
- Differential 4-jet rate with Durham algorithm (161 GeV) (/REF/JADE_OPAL_2000_S4300807/d28-x01-y03)
- Differential 5-jet rate with Durham algorithm (161 GeV) (/REF/JADE_OPAL_2000_S4300807/d28-x01-y04)
- Differential 2-jet rate with Durham algorithm (172 GeV) (/REF/JADE_OPAL_2000_S4300807/d29-x01-y01)
- Differential 3-jet rate with Durham algorithm (172 GeV) (/REF/JADE_OPAL_2000_S4300807/d29-x01-y02)
- Differential 4-jet rate with Durham algorithm (172 GeV) (/REF/JADE_OPAL_2000_S4300807/d29-x01-y03)
- Differential 5-jet rate with Durham algorithm (172 GeV) (/REF/JADE_OPAL_2000_S4300807/d29-x01-y04)
- Differential 2-jet rate with Durham algorithm (183 GeV) (/REF/JADE_OPAL_2000_S4300807/d30-x01-y01)
- Differential 3-jet rate with Durham algorithm (183 GeV) (/REF/JADE_OPAL_2000_S4300807/d30-x01-y02)
- Differential 4-jet rate with Durham algorithm (183 GeV) (/REF/JADE_OPAL_2000_S4300807/d30-x01-y03)
- Differential 5-jet rate with Durham algorithm (183 GeV) (/REF/JADE_OPAL_2000_S4300807/d30-x01-y04)
- Differential 2-jet rate with Durham algorithm (189 GeV) (/REF/JADE_OPAL_2000_S4300807/d31-x01-y01)
- Differential 3-jet rate with Durham algorithm (189 GeV) (/REF/JADE_OPAL_2000_S4300807/d31-x01-y02)
- Differential 4-jet rate with Durham algorithm (189 GeV) (/REF/JADE_OPAL_2000_S4300807/d31-x01-y03)
- Differential 5-jet rate with Durham algorithm (189 GeV) (/REF/JADE_OPAL_2000_S4300807/d31-x01-y04)

6.15 OPAL_1993_S2692198 [23]

Measurement of photon production at LEP 1

Beams: $e^+ e^-$

Energies: (45.6, 45.6) GeV

Experiment: OPAL (LEP Run 1)

Spires ID: [2692198](#)

Status: UNVALIDATED

Authors:

- Peter Richardson (Peter.Richardson@durham.ac.uk)

References:

- Z.Phys.C58:405-418,1993
- DOI: [10.1007/BF01557697](https://doi.org/10.1007/BF01557697)

Run details:

- $e^+ e^- \rightarrow \text{jet jet} (+ \text{ photons})$

Measurement of the production of photons in $e^+ e^- \rightarrow q\bar{q}$ events at LEP 1.

Histograms (10):

- Number of photon vs y_{cut} , Jade ([/REF/OPAL_1993_S2692198/d01-x01-y01](#))
- Number of photon vs y_{cut} , Durham ([/REF/OPAL_1993_S2692198/d02-x01-y01](#))
- Number of 1 jet events vs y_{cut} , Jade ([/REF/OPAL_1993_S2692198/d03-x01-y01](#))
- Number of 2 jet events vs y_{cut} , Jade ([/REF/OPAL_1993_S2692198/d03-x01-y02](#))
- Number of 3 jet events vs y_{cut} , Jade ([/REF/OPAL_1993_S2692198/d03-x01-y03](#))
- Number of > 3 jet events vs y_{cut} , Jade ([/REF/OPAL_1993_S2692198/d03-x01-y04](#))
- Number of 1 jet events vs y_{cut} , Durham ([/REF/OPAL_1993_S2692198/d04-x01-y01](#))
- Number of 2 jet events vs y_{cut} , Durham ([/REF/OPAL_1993_S2692198/d04-x01-y02](#))
- Number of 3 jet events vs y_{cut} , Durham ([/REF/OPAL_1993_S2692198/d04-x01-y03](#))
- Number of > 3 jet events vs y_{cut} , Durham ([/REF/OPAL_1993_S2692198/d04-x01-y04](#))

6.16 OPAL_1994_S2927284 [24]

Measurement of the production rates of charged hadrons in e^+e^- annihilation at the Z^0

Beams: e^+e^-

Energies: (45.6, 45.6) GeV

Experiment: OPAL (LEP 1)

Spires ID: [2927284](#)

Status: VALIDATED

Authors:

- Peter Richardson (Peter.Richardson@durham.ac.uk)

References:

- Z.Phys.C63:181-196,1994

Run details:

- Hadronic Z decay events generated on the Z pole ($\sqrt{s} = 91.2$ GeV)

The inclusive production rates of π^\pm , K^\pm and $p\bar{p}$ in Z^0 decays measured using the OPAL detector at LEP. Only the differential cross sections are currently implemented.

Histograms (3):

- π^\pm momentum ([/REF/OPAL_1994_S2927284/d01-x01-y01](#))
- K^\pm momentum ([/REF/OPAL_1994_S2927284/d02-x01-y01](#))
- p, \bar{p} momentum ([/REF/OPAL_1994_S2927284/d03-x01-y01](#))

6.17 OPAL_1995_S3198391 [25]

Δ^{++} Production in Hadronic Z^0 Decays

Beams: $e^+ e^-$

Energies: (45.6, 45.6) GeV

Experiment: OPAL (LEP 1)

Spires ID: 3198391

Status: VALIDATED

Authors:

- Peter Richardson (Peter.Richardson@durham.ac.uk)

References:

- Phys.Lett.B358:162-172,1995

Run details:

- Hadronic Z decay events generated on the Z pole ($\sqrt{s} = 91.2$ GeV)

The production of Δ^{++} baryons measured using 3.5 million Z^0 events by the OPAL experiment at LEP. Only the fragmentation function is implemented.

Histograms (1):

- Δ^{++} scaled momentum ([/REF/OPAL_1995_S3198391/d01-x01-y01](#))

6.18 OPAL_1996_S3257789 [26]

J/ψ and ψ' Production in Hadronic Z^0 Decays

Beams: $e^+ e^-$

Energies: (45.6, 45.6) GeV

Experiment: OPAL (LEP 1)

Spires ID: [3257789](#)

Status: VALIDATED

Authors:

- Peter Richardson (Peter.Richardson@durham.ac.uk)

References:

- Z.Phys. C70 (1996) 197-210

Run details:

- Hadronic Z decay events generated on the Z pole ($\sqrt{s} = 91.2$ GeV)

The production of J/ψ and ψ' mesons measured by the OPAL experiment at LEP. The fragmentation function for J/ψ and the multiplicities of J/ψ and ψ' are included.

Histograms (3):

- J/ψ scaled momentum ([/REF/OPAL_1996_S3257789/d01-x01-y01](#))
- J/ψ Multiplicity ([/REF/OPAL_1996_S3257789/d02-x01-y01](#))
- ψ' Multiplicity ([/REF/OPAL_1996_S3257789/d02-x01-y02](#))

6.19 OPAL_1997_S3396100 [27]

Strange baryon production in Z hadronic decays at OPAL

Beams: $e^+ e^-$

Energies: (45.6, 45.6) GeV

Experiment: OPAL (LEP 1)

Spires ID: 3396100

Status: VALIDATED

Authors:

- Peter Richardson (Peter.Richardson@durham.ac.uk)

References:

- Z. Phys. C, 73, 569–586 (1997)

Run details:

- Hadronic Z decay events generated on the Z pole ($\sqrt{s} = 91.2$ GeV)

Measurement of the Ξ^- , Λ^0 , $\Sigma^+(1385)$, $\Sigma^-(1385)$, $\Xi^0(1530)$ and $\Lambda^0(1520)$ scaled momentum distributions by OPAL at LEP 1. The paper also has the production cross-sections of these particles, but that is not implemented in Rivet.

Histograms (12):

- Λ^0 scaled momentum (/REF/OPAL_1997_S3396100/d01-x01-y01)
- Λ^0 scaled momentum (/REF/OPAL_1997_S3396100/d02-x01-y01)
- Ξ^- scaled momentum (/REF/OPAL_1997_S3396100/d03-x01-y01)
- Ξ^- scaled momentum (/REF/OPAL_1997_S3396100/d04-x01-y01)
- $\Sigma^+(1385)$ scaled momentum (/REF/OPAL_1997_S3396100/d05-x01-y01)
- $\Sigma^+(1385)$ scaled momentum (/REF/OPAL_1997_S3396100/d06-x01-y01)
- $\Sigma^-(1385)$ scaled momentum (/REF/OPAL_1997_S3396100/d07-x01-y01)
- $\Sigma^-(1385)$ scaled momentum (/REF/OPAL_1997_S3396100/d08-x01-y01)
- $\Xi^0(1530)$ scaled momentum (/REF/OPAL_1997_S3396100/d09-x01-y01)
- $\Xi^0(1530)$ scaled momentum (/REF/OPAL_1997_S3396100/d10-x01-y01)
- $\Lambda^0(1520)$ scaled momentum (/REF/OPAL_1997_S3396100/d11-x01-y01)
- $\Lambda^0(1520)$ scaled momentum (/REF/OPAL_1997_S3396100/d12-x01-y01)

6.20 OPAL_1997_S3608263 [28]

K^{*0} meson production measured by OPAL at LEP 1.

Beams: $e^+ e^-$

Energies: (45.6, 45.6) GeV

Experiment: OPAL (LEP 1)

Spires ID: 3608263

Status: VALIDATED

Authors:

- Peter Richardson (Peter.Richardson@durham.ac.uk)

References:

- Phys.Lett.B412:210-224,1997
- hep-ex/9708022

Run details:

- Hadronic Z decay events generated on the Z pole ($\sqrt{s} = 91.2$ GeV)

The K^{*0} fragmentation function has been measured in hadronic Z^0 decays. In addition the helicity density matrix elements for inclusive $K^*(892)^0$ mesons from hadronic Z^0 decays have been measured over the full range of K^{*0} momentum using data taken with the OPAL experiment at LEP. Only the fragmentation function measurement is currently implemented.

Histograms (1):

- K^{*0} scaled momentum (/REF/OPAL_1997_S3608263/d01-x01-y01)

6.21 OPAL_1998_S3702294 [29]

Production of $f_0(980)$, $f_2(1270)$ and $\phi(1020)$ in hadronic Z^0 decay

Beams: $e^+ e^-$

Energies: (45.6, 45.6) GeV

Experiment: OPAL (LEP 1)

Spires ID: [3702294](#)

Status: VALIDATED

Authors:

- Peter Richardson (Peter.Richardson@durham.ac.uk)

References:

- Eur.Phys.J.C4:19-28,1998
- hep-ex/9802013

Run details:

- Hadronic Z decay events generated on the Z pole ($\sqrt{s} = 91.2$ GeV)

Inclusive production of the $f_0(980)$, $f_2(1270)$ and $\phi(1020)$ resonances studied in a sample of 4.3 million hadronic Z^0 decays from the OPAL experiment at LEP. Fragmentation functions are reported for the three states.

Histograms (3):

- $f_0(980)$ scaled momentum ([/REF/OPAL_1998_S3702294/d02-x01-y01](#))
- $f_2(1270)$ scaled momentum ([/REF/OPAL_1998_S3702294/d02-x01-y02](#))
- $\phi(1020)$ scaled momentum ([/REF/OPAL_1998_S3702294/d02-x01-y03](#))

6.22 OPAL_1998_S3749908 [30]

Photon and Light Meson Production in Hadronic Z^0 Decays

Beams: $e^+ e^-$

Energies: (45.6, 45.6) GeV

Experiment: OPAL (LEP 1)

Spires ID: [3749908](#)

Status: VALIDATED

Authors:

- Peter Richardson (Peter.Richardson@durham.ac.uk)

References:

- Eur.Phys.J.C5:411-437,1998
- hep-ex/9805011

Run details:

- Hadronic Z decay events generated on the Z pole ($\sqrt{s} = 91.2$ GeV)

The inclusive production rates and differential cross sections of photons and mesons with a final state containing photons have been measured with the OPAL detector at LEP. The light mesons covered by the measurements are the π^0 , η , $\rho(770)^{\pm}$, $\omega(782)$, $\eta'(958)$ and $a_0(980)^{\pm}$.

Histograms (14):

- Photon scaled momentum ([/REF/OPAL_1998_S3749908/d02-x01-y01](#))
- Photon scaled momentum ([/REF/OPAL_1998_S3749908/d03-x01-y01](#))
- π^0 scaled momentum ([/REF/OPAL_1998_S3749908/d04-x01-y01](#))
- π^0 scaled momentum ([/REF/OPAL_1998_S3749908/d05-x01-y01](#))
- η scaled momentum ([/REF/OPAL_1998_S3749908/d06-x01-y01](#))
- η scaled momentum ([/REF/OPAL_1998_S3749908/d07-x01-y01](#))
- ρ^{\pm} scaled momentum ([/REF/OPAL_1998_S3749908/d08-x01-y01](#))
- ρ^{\pm} scaled momentum ([/REF/OPAL_1998_S3749908/d09-x01-y01](#))
- ω scaled momentum ([/REF/OPAL_1998_S3749908/d10-x01-y01](#))
- ω scaled momentum ([/REF/OPAL_1998_S3749908/d11-x01-y01](#))
- η' scaled momentum ([/REF/OPAL_1998_S3749908/d12-x01-y01](#))
- η' scaled momentum ([/REF/OPAL_1998_S3749908/d13-x01-y01](#))
- a_0^{\pm} scaled momentum ([/REF/OPAL_1998_S3749908/d14-x01-y01](#))
- a_0^{\pm} scaled momentum ([/REF/OPAL_1998_S3749908/d15-x01-y01](#))

6.23 OPAL_1998_S3780481 [31]

Measurements of flavor dependent fragmentation functions in $Z^0 \rightarrow q\bar{q}$ events

Beams: $e^+ e^-$

Energies: (45.6, 45.6) GeV

Experiment: OPAL (LEP 1)

Spires ID: [3780481](#)

Status: VALIDATED

Authors:

- Hendrik Hoeth (hendrik.hoeth@cern.ch)

References:

- Eur. Phys. J, C7, 369–381 (1999)
- hep-ex/9807004

Run details:

- Hadronic Z decay events generated on the Z pole ($\sqrt{s} = 91.2$ GeV)

Measurement of scaled momentum distributions and total charged multiplicities in flavour tagged events at LEP 1. OPAL measured these observables in uds-, c-, and b-events separately. An inclusive measurement is also included.

Histograms (12):

- *uds* events scaled momentum ([/REF/OPAL_1998_S3780481/d01-x01-y01](#))
- *c* events scaled momentum ([/REF/OPAL_1998_S3780481/d02-x01-y01](#))
- *b* events scaled momentum ([/REF/OPAL_1998_S3780481/d03-x01-y01](#))
- All events scaled momentum ([/REF/OPAL_1998_S3780481/d04-x01-y01](#))
- *uds* events $\ln(1/x_p)$ ([/REF/OPAL_1998_S3780481/d05-x01-y01](#))
- *c* events $\ln(1/x_p)$ ([/REF/OPAL_1998_S3780481/d06-x01-y01](#))
- *b* events $\ln(1/x_p)$ ([/REF/OPAL_1998_S3780481/d07-x01-y01](#))
- All events $\ln(1/x_p)$ ([/REF/OPAL_1998_S3780481/d08-x01-y01](#))
- *uds* events mean charged multiplicity ([/REF/OPAL_1998_S3780481/d09-x01-y01](#))
- *c* events mean charged multiplicity ([/REF/OPAL_1998_S3780481/d09-x01-y02](#))
- *b* events mean charged multiplicity ([/REF/OPAL_1998_S3780481/d09-x01-y03](#))
- All events mean charged multiplicity ([/REF/OPAL_1998_S3780481/d09-x01-y04](#))

6.24 OPAL_2000_S4418603 [32]

Multiplicities of π^0 , η , K^0 and of charged particles in quark and gluon jets

Beams: $e^+ e^-$

Energies: (45.6, 45.6) GeV

Experiment: OPAL (LEP 1)

Spires ID: [4418603](#)

Status: VALIDATED

Authors:

- Peter Richardson (Peter.Richardson@durham.ac.uk)

References:

- Eur.Phys.J.C17:373-387,2000
- hep-ex/0007017

Run details:

- Hadronic Z decay events generated on the Z pole ($\sqrt{s} = 91.2$ GeV)

Multiplicities of π^0 , η , K^0 and of charged particles in quark and gluon jets in 3-jet events, as measured by the OPAL experiment at LEP. The main implemented measurement is the K^0 fragmentation function.

Histograms (1):

- K^0 scaled momentum ([/REF/OPAL_2000_S4418603/d03-x01-y01](#))

6.25 OPAL_2001_S4553896 [33]

Four-jet angles using Durham algorithm

Beams: $e^+ e^-$

Energies: (45.6, 45.6) GeV

Experiment: OPAL (LEP Run 1)

Spires ID: [4553896](#)

Status: VALIDATED

Authors:

- Frank Siegert <frank.siegert@cern.ch>

References:

- Eur.Phys.J.C20:601-615,2001
- DOI: [10.1007/s100520100699](https://doi.org/10.1007/s100520100699)
- arXiv: [hep-ex/0101044](https://arxiv.org/abs/hep-ex/0101044)

Run details:

- Hadronic Z decay events generated on the Z pole ($\sqrt{s} = 91.2$ GeV) Hadronisation should be turned off because the data is corrected back to the parton level.

Angles between the leading (in energy) four jets defined using the Durham algorithm with $y_{\text{cut}} = 0.008$. The data is presented at the parton level and includes the Bengtsson-Zerwas, Körner-Schierholz-Willrodt and Nachtmann-Reiter angles as well as the angle between the two softest jets.

Histograms (4):

- Bengtsson-Zerwas angle (parton level) ([/REF/OPAL_2001_S4553896/d03-x01-y01](#))
- Körner-Schierholz-Willrodt angle (parton level) ([/REF/OPAL_2001_S4553896/d04-x01-y01](#))
- Modified Nachtmann-Reiter angle (parton level) ([/REF/OPAL_2001_S4553896/d05-x01-y01](#))
- Angle between the two softest jets (parton level) ([/REF/OPAL_2001_S4553896/d06-x01-y01](#))

6.26 OPAL_2002_S5361494 [34]

Charged particle multiplicities in heavy and light quark initiated events above the Z^0 peak

Beams: $e^+ e^-$

Energies: (65.0, 65.0), (68.0, 68.0), (80.5, 80.5), (86.0, 86.0), (91.5, 91.5), (94.5, 94.5), (96.0, 96.0), (98.0, 98.0), (100.0, 100.0), (101.0, 101.0), (103.0, 103.0) GeV

Experiment: OPAL (LEP 2)

Spires ID: [5361494](#)

Status: VALIDATED

Authors:

- Peter Richardson (Peter.Richardson@durham.ac.uk)

References:

- Phys.Lett. B550 (2002) 33-46
- hep-ex/0211007

Run details:

- Hadronic Z decay events generated on the Z pole ($\sqrt{s} = 91.2$ GeV)

Measurements of the mean charged multiplicities separately for $b\bar{b}$, $c\bar{c}$ and light quark (uds) initiated events in e^+e^- interactions at energies above the Z^0 mass. The data is from the LEP running periods between 1995 and 2000.

Histograms (4):

- Charged multiplicity as a function of energy in b events (/REF/OPAL_2002_S5361494/d01-x01-y01)
- Charged multiplicity as a function of energy in c events (/REF/OPAL_2002_S5361494/d01-x01-y02)
- Charged multiplicity as a function of energy in uds events (/REF/OPAL_2002_S5361494/d01-x01-y03)
- Difference in Charged multiplicity as a function of energy between b and uds events (/REF/OPAL_2002_S5361494/d01-x01-y04)

6.27 OPAL_2004_S6132243 [35]

Event shape distributions and moments in $e^+e^- \rightarrow$ hadrons at 91–209 GeV

Beams: e^+e^-

Energies: (45.6, 45.6), (66.5, 66.5), (88.5, 88.5), (98.5, 98.5) GeV

Experiment: OPAL (LEP 1 & 2)

Spires ID: [6132243](#)

Status: VALIDATED

Authors:

- Andy Buckley (andy.buckley@cern.ch)

References:

- Eur.Phys.J.C40:287-316,2005
- arXiv: [hep-ex/0503051](#)

Run details:

- Hadronic e^+e^- events at 4 representative energies (91, 133, 177, 197). Runs need to have ISR suppressed, since the analysis was done using a cut of $\sqrt{s} - \sqrt{s_{\text{reco}}} < 1$ GeV. Particles with a livetime $> 3 \cdot 10^{-10}$ s are considered to be stable.

Measurement of e^+e^- event shape variable distributions and their 1st to 5th moments in LEP running from the Z pole to the highest LEP 2 energy of 209 GeV.

Histograms (104):

- Thrust, $1 - T$, at 91 GeV ([/REF/OPAL_2004_S6132243/d01-x01-y01](#))
- Thrust, $1 - T$, at 133 GeV ([/REF/OPAL_2004_S6132243/d01-x01-y02](#))
- Thrust, $1 - T$, at 177 (161–183) GeV ([/REF/OPAL_2004_S6132243/d01-x01-y03](#))
- Thrust, $1 - T$, at 197 (189–209) GeV ([/REF/OPAL_2004_S6132243/d01-x01-y04](#))
- Heavy hemisphere mass, M_H , at 91 GeV ([/REF/OPAL_2004_S6132243/d02-x01-y01](#))
- Heavy hemisphere mass, M_H , at 133 GeV ([/REF/OPAL_2004_S6132243/d02-x01-y02](#))
- Heavy hemisphere mass, M_H , at 177 (161–183) GeV ([/REF/OPAL_2004_S6132243/d02-x01-y03](#))
- Heavy hemisphere mass, M_H , at 197 (189–209) GeV ([/REF/OPAL_2004_S6132243/d02-x01-y04](#))
- C parameter at 91 GeV ([/REF/OPAL_2004_S6132243/d03-x01-y01](#))
- C parameter at 133 GeV ([/REF/OPAL_2004_S6132243/d03-x01-y02](#))
- C parameter at 177 (161–183) GeV ([/REF/OPAL_2004_S6132243/d03-x01-y03](#))
- C parameter at 197 (189–209) GeV ([/REF/OPAL_2004_S6132243/d03-x01-y04](#))

- Total hemisphere broadening, B_{sum} , at 91 GeV (/REF/OPAL_2004_S6132243/d04-x01-y01)
- Total hemisphere broadening, B_{sum} , at 133 GeV (/REF/OPAL_2004_S6132243/d04-x01-y02)
- Total hemisphere broadening, B_{sum} , at 177 (161–183) GeV (/REF/OPAL_2004_S6132243/d04-x01-y03)
- Total hemisphere broadening, B_{sum} , at 197 (189–209) GeV (/REF/OPAL_2004_S6132243/d04-x01-y04)
- Wide hemisphere broadening, B_{max} , at 91 GeV (/REF/OPAL_2004_S6132243/d05-x01-y01)
- Wide hemisphere broadening, B_{max} , at 133 GeV (/REF/OPAL_2004_S6132243/d05-x01-y02)
- Wide hemisphere broadening, B_{max} , at 177 (161–183) GeV (/REF/OPAL_2004_S6132243/d05-x01-y03)
- Wide hemisphere broadening, B_{max} , at 197 (189–209) GeV (/REF/OPAL_2004_S6132243/d05-x01-y04)
- Durham jet 2 → 3 transition parameter, y_{23} , at 91 GeV (/REF/OPAL_2004_S6132243/d06-x01-y01)
- Durham jet 2 → 3 transition parameter, y_{23} , at 133 GeV (/REF/OPAL_2004_S6132243/d06-x01-y02)
- Durham jet 2 → 3 transition parameter, y_{23} , at 177 (161–183) GeV (/REF/OPAL_2004_-
S6132243/d06-x01-y03)
- Durham jet 2 → 3 transition parameter, y_{23} , at 197 (189–209) GeV (/REF/OPAL_2004_-
S6132243/d06-x01-y04)
- Thrust major, T_{maj} , at 91 GeV (/REF/OPAL_2004_S6132243/d07-x01-y01)
- Thrust major, T_{maj} , at 133 GeV (/REF/OPAL_2004_S6132243/d07-x01-y02)
- Thrust major, T_{maj} , at 177 (161–183) GeV (/REF/OPAL_2004_S6132243/d07-x01-y03)
- Thrust major, T_{maj} , at 197 (189–209) GeV (/REF/OPAL_2004_S6132243/d07-x01-y04)
- Thrust minor, T_{min} , at 91 GeV (/REF/OPAL_2004_S6132243/d08-x01-y01)
- Thrust minor, T_{min} , at 133 GeV (/REF/OPAL_2004_S6132243/d08-x01-y02)
- Thrust minor, T_{min} , at 177 (161–183) GeV (/REF/OPAL_2004_S6132243/d08-x01-y03)
- Thrust minor, T_{min} , at 197 (189–209) GeV (/REF/OPAL_2004_S6132243/d08-x01-y04)
- Aplanarity, A , at 91 GeV (/REF/OPAL_2004_S6132243/d09-x01-y01)
- Aplanarity, A , at 133 GeV (/REF/OPAL_2004_S6132243/d09-x01-y02)
- Aplanarity, A , at 177 (161–183) GeV (/REF/OPAL_2004_S6132243/d09-x01-y03)
- Aplanarity, A , at 197 (189–209) GeV (/REF/OPAL_2004_S6132243/d09-x01-y04)
- Sphericity, S , at 91 GeV (/REF/OPAL_2004_S6132243/d10-x01-y01)
- Sphericity, S , at 133 GeV (/REF/OPAL_2004_S6132243/d10-x01-y02)

- Sphericity, S , at 177 (161–183) GeV (/REF/OPAL_2004_S6132243/d10-x01-y03)
- Sphericity, S , at 197 (189–209) GeV (/REF/OPAL_2004_S6132243/d10-x01-y04)
- Oblateness, O , at 91 GeV (/REF/OPAL_2004_S6132243/d11-x01-y01)
- Oblateness, O , at 133 GeV (/REF/OPAL_2004_S6132243/d11-x01-y02)
- Oblateness, O , at 177 (161–183) GeV (/REF/OPAL_2004_S6132243/d11-x01-y03)
- Oblateness, O , at 197 (189–209) GeV (/REF/OPAL_2004_S6132243/d11-x01-y04)
- Light hemisphere mass, M_L , at 91 GeV (/REF/OPAL_2004_S6132243/d12-x01-y01)
- Light hemisphere mass, M_L , at 133 GeV (/REF/OPAL_2004_S6132243/d12-x01-y02)
- Light hemisphere mass, M_L , at 177 (161–183) GeV (/REF/OPAL_2004_S6132243/d12-x01-y03)
- Light hemisphere mass, M_L , at 197 (189–209) GeV (/REF/OPAL_2004_S6132243/d12-x01-y04)
- Narrow hemisphere broadening, B_{\min} , at 91 GeV (/REF/OPAL_2004_S6132243/d13-x01-y01)
- Narrow hemisphere broadening, B_{\min} , at 133 GeV (/REF/OPAL_2004_S6132243/d13-x01-y02)
- Narrow hemisphere broadening, B_{\min} , at 177 (161–183) GeV (/REF/OPAL_2004_S6132243/d13-x01-y03)
- Narrow hemisphere broadening, B_{\min} , at 197 (189–209) GeV (/REF/OPAL_2004_S6132243/d13-x01-y04)
- D parameter at 91 GeV (/REF/OPAL_2004_S6132243/d14-x01-y01)
- D parameter at 133 GeV (/REF/OPAL_2004_S6132243/d14-x01-y02)
- D parameter at 177 (161–183) GeV (/REF/OPAL_2004_S6132243/d14-x01-y03)
- D parameter at 197 (189–209) GeV (/REF/OPAL_2004_S6132243/d14-x01-y04)
- Moments of $1 - T$ at 91 GeV (/REF/OPAL_2004_S6132243/d15-x01-y01)
- Moments of $1 - T$ at 133 GeV (/REF/OPAL_2004_S6132243/d15-x01-y02)
- Moments of $1 - T$ at 177 (161–183) GeV (/REF/OPAL_2004_S6132243/d15-x01-y03)
- Moments of $1 - T$ at 197 (189–209) GeV (/REF/OPAL_2004_S6132243/d15-x01-y04)
- Moments of M_H at 91 GeV (/REF/OPAL_2004_S6132243/d16-x01-y01)
- Moments of M_H at 133 GeV (/REF/OPAL_2004_S6132243/d16-x01-y02)
- Moments of M_H at 177 (161–183) GeV (/REF/OPAL_2004_S6132243/d16-x01-y03)
- Moments of M_H at 197 (189–209) GeV (/REF/OPAL_2004_S6132243/d16-x01-y04)
- Moments of C at 91 GeV (/REF/OPAL_2004_S6132243/d17-x01-y01)

- Moments of C at 133 GeV (/REF/OPAL_2004_S6132243/d17-x01-y02)
- Moments of C at 177 (161–183) GeV (/REF/OPAL_2004_S6132243/d17-x01-y03)
- Moments of C at 197 (189–209) GeV (/REF/OPAL_2004_S6132243/d17-x01-y04)
- Moments of B_{sum} at 91 GeV (/REF/OPAL_2004_S6132243/d18-x01-y01)
- Moments of B_{sum} at 133 GeV (/REF/OPAL_2004_S6132243/d18-x01-y02)
- Moments of B_{sum} at 177 (161–183) GeV (/REF/OPAL_2004_S6132243/d18-x01-y03)
- Moments of B_{sum} at 197 (189–209) GeV (/REF/OPAL_2004_S6132243/d18-x01-y04)
- Moments of B_{max} at 91 GeV (/REF/OPAL_2004_S6132243/d19-x01-y01)
- Moments of B_{max} at 133 GeV (/REF/OPAL_2004_S6132243/d19-x01-y02)
- Moments of B_{max} at 177 (161–183) GeV (/REF/OPAL_2004_S6132243/d19-x01-y03)
- Moments of B_{max} at 197 (189–209) GeV (/REF/OPAL_2004_S6132243/d19-x01-y04)
- Moments of y_{23} at 91 GeV (/REF/OPAL_2004_S6132243/d20-x01-y01)
- Moments of y_{23} at 133 GeV (/REF/OPAL_2004_S6132243/d20-x01-y02)
- Moments of y_{23} at 177 (161–183) GeV (/REF/OPAL_2004_S6132243/d20-x01-y03)
- Moments of y_{23} at 197 (189–209) GeV (/REF/OPAL_2004_S6132243/d20-x01-y04)
- Moments of T_{maj} at 91 GeV (/REF/OPAL_2004_S6132243/d21-x01-y01)
- Moments of T_{maj} at 133 GeV (/REF/OPAL_2004_S6132243/d21-x01-y02)
- Moments of T_{maj} at 177 (161–183) GeV (/REF/OPAL_2004_S6132243/d21-x01-y03)
- Moments of T_{maj} at 197 (189–209) GeV (/REF/OPAL_2004_S6132243/d21-x01-y04)
- Moments of T_{min} at 91 GeV (/REF/OPAL_2004_S6132243/d22-x01-y01)
- Moments of T_{min} at 133 GeV (/REF/OPAL_2004_S6132243/d22-x01-y02)
- Moments of T_{min} at 177 (161–183) GeV (/REF/OPAL_2004_S6132243/d22-x01-y03)
- Moments of T_{min} at 197 (189–209) GeV (/REF/OPAL_2004_S6132243/d22-x01-y04)
- Moments of S at 91 GeV (/REF/OPAL_2004_S6132243/d23-x01-y01)
- Moments of S at 133 GeV (/REF/OPAL_2004_S6132243/d23-x01-y02)
- Moments of S at 177 (161–183) GeV (/REF/OPAL_2004_S6132243/d23-x01-y03)
- Moments of S at 197 (189–209) GeV (/REF/OPAL_2004_S6132243/d23-x01-y04)

- Moments of O at 91 GeV (/REF/OPAL_2004_S6132243/d24-x01-y01)
- Moments of O at 133 GeV (/REF/OPAL_2004_S6132243/d24-x01-y02)
- Moments of O at 177 (161–183) GeV (/REF/OPAL_2004_S6132243/d24-x01-y03)
- Moments of O at 197 (189–209) GeV (/REF/OPAL_2004_S6132243/d24-x01-y04)
- Moments of M_L at 91 GeV (/REF/OPAL_2004_S6132243/d25-x01-y01)
- Moments of M_L at 133 GeV (/REF/OPAL_2004_S6132243/d25-x01-y02)
- Moments of M_L at 177 (161–183) GeV (/REF/OPAL_2004_S6132243/d25-x01-y03)
- Moments of M_L at 197 (189–209) GeV (/REF/OPAL_2004_S6132243/d25-x01-y04)
- Moments of B_{\min} at 91 GeV (/REF/OPAL_2004_S6132243/d26-x01-y01)
- Moments of B_{\min} at 133 GeV (/REF/OPAL_2004_S6132243/d26-x01-y02)
- Moments of B_{\min} at 177 (161–183) GeV (/REF/OPAL_2004_S6132243/d26-x01-y03)
- Moments of B_{\min} at 197 (189–209) GeV (/REF/OPAL_2004_S6132243/d26-x01-y04)

6.28 SLD_1996_S3398250 [36]

Charged particle multiplicities in heavy and light quark initiated events on the Z^0 peak

Beams: $e^+ e^-$

Energies: (45.6, 45.6) GeV

Experiment: SLD (SLC)

Spires ID: [3398250](#)

Status: VALIDATED

Authors:

- Peter Richardson (Peter.Richardson@durham.ac.uk)

References:

- Phys.Lett.B386:475-485,1996
- hep-ex/9608008

Run details:

- Hadronic Z decay events generated on the Z pole ($\sqrt{s} = 91.2$ GeV)

Measurements of the mean charged multiplicities separately for $b\bar{b}$, $c\bar{c}$ and light quark (uds) initiated events in e^+e^- interactions at the Z^0 mass.

Histograms (5):

- Charged multiplicity in b events (/REF/SLD_1996_S3398250/d01-x01-y01)
- Charged multiplicity in c events (/REF/SLD_1996_S3398250/d02-x01-y01)
- Charged multiplicity in uds events (/REF/SLD_1996_S3398250/d03-x01-y01)
- Difference in Charged multiplicity between c and uds events (/REF/SLD_1996_S3398250/d04-x01-y01)
- Difference in Charged multiplicity between b and uds events (/REF/SLD_1996_S3398250/d05-x01-y01)

6.29 SLD_1999_S3743934 [37]

Production of π^+ , K^+ , K^0 , K^{*0} , Φ , p and Λ^0 in hadronic Z^0 decay

Beams: $e^+ e^-$

Energies: (45.6, 45.6) GeV

Experiment: SLD (SLC)

Spires ID: 3743934

Status: VALIDATED

Authors:

- Peter Richardson (Peter.Richardson@durham.ac.uk)

References:

- Phys.Rev.D59:052001,1999
- hep-ex/9805029

Run details:

- Hadronic Z decay events generated on the Z pole ($\sqrt{s} = 91.2$ GeV)

Measurement of scaled momentum distributions and fragmentation functions in flavour tagged events at SLC. SLD measured these observables in uds-, c-, and b-events separately. An inclusive measurement is also included.

Histograms (103):

- Ratio $N_{\pi^+}/N_{\text{charged}}$ (/REF/SLD_1999_S3743934/d01-x01-y01)
- π^+ scaled momentum (/REF/SLD_1999_S3743934/d01-x01-y02)
- Ratio $N_{K^+}/N_{\text{charged}}$ (/REF/SLD_1999_S3743934/d02-x01-y01)
- K^+ scaled momentum (/REF/SLD_1999_S3743934/d02-x01-y02)
- Ratio $N_{p^+}/N_{\text{charged}}$ (/REF/SLD_1999_S3743934/d03-x01-y01)
- p^+ scaled momentum (/REF/SLD_1999_S3743934/d03-x01-y02)
- Charged Particle scaled momentum (/REF/SLD_1999_S3743934/d04-x01-y01)
- K^0 scaled momentum (/REF/SLD_1999_S3743934/d05-x01-y01)
- Λ^0 scaled momentum (/REF/SLD_1999_S3743934/d07-x01-y01)
- K^{*0} scaled momentum (/REF/SLD_1999_S3743934/d08-x01-y01)
- ϕ^0 scaled momentum (/REF/SLD_1999_S3743934/d09-x01-y01)
- π^+ scaled momentum, (uds) events (/REF/SLD_1999_S3743934/d10-x01-y01)

- π^+ scaled momentum, c events ([/REF/SLD_1999_S3743934/d10-x01-y02](#))
- π^+ scaled momentum, b events ([/REF/SLD_1999_S3743934/d10-x01-y03](#))
- π^+ scaled momentum, ratio c to uds events ([/REF/SLD_1999_S3743934/d11-x01-y01](#))
- π^+ scaled momentum, ratio b to uds events ([/REF/SLD_1999_S3743934/d11-x01-y02](#))
- K^+ scaled momentum, (uds) events ([/REF/SLD_1999_S3743934/d12-x01-y01](#))
- K^+ scaled momentum, c events ([/REF/SLD_1999_S3743934/d12-x01-y02](#))
- K^+ scaled momentum, b events ([/REF/SLD_1999_S3743934/d12-x01-y03](#))
- K^+ scaled momentum, ratio c to uds events ([/REF/SLD_1999_S3743934/d13-x01-y01](#))
- K^+ scaled momentum, ratio b to uds events ([/REF/SLD_1999_S3743934/d13-x01-y02](#))
- K^{*0} scaled momentum, (uds) events ([/REF/SLD_1999_S3743934/d14-x01-y01](#))
- K^{*0} scaled momentum, c events ([/REF/SLD_1999_S3743934/d14-x01-y02](#))
- K^{*0} scaled momentum, b events ([/REF/SLD_1999_S3743934/d14-x01-y03](#))
- K^{*0} scaled momentum, ratio c to uds events ([/REF/SLD_1999_S3743934/d15-x01-y01](#))
- K^{*0} scaled momentum, ratio b to uds events ([/REF/SLD_1999_S3743934/d15-x01-y02](#))
- p^+ scaled momentum, (uds) events ([/REF/SLD_1999_S3743934/d16-x01-y01](#))
- p^+ scaled momentum, c events ([/REF/SLD_1999_S3743934/d16-x01-y02](#))
- p^+ scaled momentum, b events ([/REF/SLD_1999_S3743934/d16-x01-y03](#))
- p^+ scaled momentum, ratio c to uds events ([/REF/SLD_1999_S3743934/d17-x01-y01](#))
- p^+ scaled momentum, ratio b to uds events ([/REF/SLD_1999_S3743934/d17-x01-y02](#))
- Λ^0 scaled momentum, (uds) events ([/REF/SLD_1999_S3743934/d18-x01-y01](#))
- Λ^0 scaled momentum, c events ([/REF/SLD_1999_S3743934/d18-x01-y02](#))
- Λ^0 scaled momentum, b events ([/REF/SLD_1999_S3743934/d18-x01-y03](#))
- Λ^0 scaled momentum, ratio c to uds events ([/REF/SLD_1999_S3743934/d19-x01-y01](#))
- Λ^0 scaled momentum, ratio b to uds events ([/REF/SLD_1999_S3743934/d19-x01-y02](#))
- K^0 scaled momentum, (uds) events ([/REF/SLD_1999_S3743934/d20-x01-y01](#))
- K^0 scaled momentum, c events ([/REF/SLD_1999_S3743934/d20-x01-y02](#))
- K^0 scaled momentum, b events ([/REF/SLD_1999_S3743934/d20-x01-y03](#))

- K^0 scaled momentum, ratio c to uds events (/REF/SLD_1999_S3743934/d21-x01-y01)
- K^0 scaled momentum, ratio b to uds events (/REF/SLD_1999_S3743934/d21-x01-y02)
- ϕ^0 scaled momentum, (uds) events (/REF/SLD_1999_S3743934/d22-x01-y01)
- ϕ^0 scaled momentum, c events (/REF/SLD_1999_S3743934/d22-x01-y02)
- ϕ^0 scaled momentum, b events (/REF/SLD_1999_S3743934/d22-x01-y03)
- ϕ^0 scaled momentum, ratio c to uds events (/REF/SLD_1999_S3743934/d23-x01-y01)
- ϕ^0 scaled momentum, ratio b to uds events (/REF/SLD_1999_S3743934/d23-x01-y02)
- Multiplicity of π^\pm (/REF/SLD_1999_S3743934/d24-x01-y01)
- Multiplicity of π^\pm in (uds) events (/REF/SLD_1999_S3743934/d24-x01-y02)
- Multiplicity of π^\pm in c events (/REF/SLD_1999_S3743934/d24-x01-y03)
- Multiplicity of π^\pm in b events (/REF/SLD_1999_S3743934/d24-x01-y04)
- Multiplicity of K^\pm (/REF/SLD_1999_S3743934/d24-x02-y01)
- Multiplicity of K^\pm in (uds) events (/REF/SLD_1999_S3743934/d24-x02-y02)
- Multiplicity of K^\pm in c events (/REF/SLD_1999_S3743934/d24-x02-y03)
- Multiplicity of K^\pm in b events (/REF/SLD_1999_S3743934/d24-x02-y04)
- Multiplicity of K^0, \bar{K}^0 (/REF/SLD_1999_S3743934/d24-x03-y01)
- Multiplicity of K^0, \bar{K}^0 in (uds) events (/REF/SLD_1999_S3743934/d24-x03-y02)
- Multiplicity of K^0, \bar{K}^0 in c events (/REF/SLD_1999_S3743934/d24-x03-y03)
- Multiplicity of K^0, \bar{K}^0 in b events (/REF/SLD_1999_S3743934/d24-x03-y04)
- Multiplicity of K^{*0}, \bar{K}^{*0} (/REF/SLD_1999_S3743934/d24-x04-y01)
- Multiplicity of K^{*0}, \bar{K}^{*0} in (uds) events (/REF/SLD_1999_S3743934/d24-x04-y02)
- Multiplicity of K^{*0}, \bar{K}^{*0} in c events (/REF/SLD_1999_S3743934/d24-x04-y03)
- Multiplicity of K^{*0}, \bar{K}^{*0} in b events (/REF/SLD_1999_S3743934/d24-x04-y04)
- Multiplicity of ϕ (/REF/SLD_1999_S3743934/d24-x05-y01)
- Multiplicity of ϕ in (uds) events (/REF/SLD_1999_S3743934/d24-x05-y02)
- Multiplicity of ϕ in c events (/REF/SLD_1999_S3743934/d24-x05-y03)
- Multiplicity of ϕ in b events (/REF/SLD_1999_S3743934/d24-x05-y04)

- Multiplicity of p, \bar{p} (/REF/SLD_1999_S3743934/d24-x06-y01)
- Multiplicity of p, \bar{p} in (*uds*) events (/REF/SLD_1999_S3743934/d24-x06-y02)
- Multiplicity of p, \bar{p} in *c* events (/REF/SLD_1999_S3743934/d24-x06-y03)
- Multiplicity of p, \bar{p} in *b* events (/REF/SLD_1999_S3743934/d24-x06-y04)
- Multiplicity of $\Lambda^0, \bar{\Lambda}^0$ (/REF/SLD_1999_S3743934/d24-x07-y01)
- Multiplicity of $\Lambda^0, \bar{\Lambda}^0$ in (*uds*) events (/REF/SLD_1999_S3743934/d24-x07-y02)
- Multiplicity of $\Lambda^0, \bar{\Lambda}^0$ in *c* events (/REF/SLD_1999_S3743934/d24-x07-y03)
- Multiplicity of $\Lambda^0, \bar{\Lambda}^0$ in *b* events (/REF/SLD_1999_S3743934/d24-x07-y04)
- Multiplicity difference *c-uds* for π^\pm (/REF/SLD_1999_S3743934/d25-x01-y01)
- Multiplicity difference *b-uds* for π^\pm (/REF/SLD_1999_S3743934/d25-x01-y02)
- Multiplicity difference *c-uds* for K^\pm (/REF/SLD_1999_S3743934/d25-x02-y01)
- Multiplicity difference *b-uds* for K^\pm (/REF/SLD_1999_S3743934/d25-x02-y02)
- Multiplicity difference *c-uds* for K^0, \bar{K}^0 (/REF/SLD_1999_S3743934/d25-x03-y01)
- Multiplicity difference *b-uds* for K^0, \bar{K}^0 (/REF/SLD_1999_S3743934/d25-x03-y02)
- Multiplicity difference *c-uds* for K^{*0}, \bar{K}^{*0} (/REF/SLD_1999_S3743934/d25-x04-y01)
- Multiplicity difference *b-uds* for K^{*0}, \bar{K}^{*0} (/REF/SLD_1999_S3743934/d25-x04-y02)
- Multiplicity difference *c-uds* for ϕ (/REF/SLD_1999_S3743934/d25-x05-y01)
- Multiplicity difference *b-uds* for ϕ (/REF/SLD_1999_S3743934/d25-x05-y02)
- Multiplicity difference *c-uds* for p, \bar{p} (/REF/SLD_1999_S3743934/d25-x06-y01)
- Multiplicity difference *b-uds* for p, \bar{p} (/REF/SLD_1999_S3743934/d25-x06-y02)
- Multiplicity difference *c-uds* for $\Lambda^0, \bar{\Lambda}^0$ (/REF/SLD_1999_S3743934/d25-x07-y01)
- Multiplicity difference *b-uds* for $\Lambda^0, \bar{\Lambda}^0$ (/REF/SLD_1999_S3743934/d25-x07-y02)
- $R_{\pi^+}^q = \frac{1}{2N_{\text{events}}} \frac{d}{dx_p} [N(q \rightarrow \pi^+) + N(\bar{q} \rightarrow \pi^-)]$ (/REF/SLD_1999_S3743934/d26-x01-y01)
- $R_{\pi^-}^q = \frac{1}{2N_{\text{events}}} \frac{d}{dx_p} [N(q \rightarrow \pi^-) + N(\bar{q} \rightarrow \pi^+)]$ (/REF/SLD_1999_S3743934/d26-x01-y02)
- $D_{\pi^-}^q = (R_{\pi^-}^q - R_{\pi^+}^q) / (R_{\pi^-}^q + R_{\pi^+}^q)$ (/REF/SLD_1999_S3743934/d27-x01-y01)
- $R_{K^{*0}}^q = \frac{1}{2N_{\text{events}}} \frac{d}{dx_p} [N(q \rightarrow K^{*0}) + N(\bar{q} \rightarrow \bar{K}^{*0})]$ (/REF/SLD_1999_S3743934/d28-x01-y01)
- $R_{\bar{K}^{*0}}^q = \frac{1}{2N_{\text{events}}} \frac{d}{dx_p} [N(q \rightarrow \bar{K}^{*0}) + N(\bar{q} \rightarrow K^{*0})]$ (/REF/SLD_1999_S3743934/d28-x01-y02)

- $D_{\bar{K}^{*0}}^q = (R_{\bar{K}^{*0}}^q - R_{K^{*0}}^q) / (R_{\bar{K}^{*0}}^q + R_{K^{*0}}^q)$ (/REF/SLD_1999_S3743934/d29-x01-y01)
- $R_{K^+}^q = \frac{1}{2N_{\text{events}}} \frac{d}{dx_p} [N(q \rightarrow K^+) + N(\bar{q} \rightarrow K^-)]$ (/REF/SLD_1999_S3743934/d30-x01-y01)
- $R_{K^-}^q = \frac{1}{2N_{\text{events}}} \frac{d}{dx_p} [N(q \rightarrow K^-) + N(\bar{q} \rightarrow K^+)]$ (/REF/SLD_1999_S3743934/d30-x01-y02)
- $D_{K^-}^q = (R_{K^-}^q - R_{K^+}^q) / (R_{K^-}^q + R_{K^+}^q)$ (/REF/SLD_1999_S3743934/d31-x01-y01)
- $R_p^q = \frac{1}{2N_{\text{events}}} \frac{d}{dx_p} [N(q \rightarrow p) + N(\bar{q} \rightarrow \bar{p})]$ (/REF/SLD_1999_S3743934/d32-x01-y01)
- $R_{\bar{p}}^q = \frac{1}{2N_{\text{events}}} \frac{d}{dx_p} [N(q \rightarrow \bar{p}) + N(\bar{q} \rightarrow p)]$ (/REF/SLD_1999_S3743934/d32-x01-y02)
- $D_p^q = (R_p^q - R_{\bar{p}}^q) / (R_p^q + R_{\bar{p}}^q)$ (/REF/SLD_1999_S3743934/d33-x01-y01)
- $R_{\Lambda^0}^q = \frac{1}{2N_{\text{events}}} \frac{d}{dx_p} [N(q \rightarrow \Lambda^0) + N(\bar{q} \rightarrow \bar{\Lambda}^0)]$ (/REF/SLD_1999_S3743934/d34-x01-y01)
- $R_{\bar{\Lambda}^0}^q = \frac{1}{2N_{\text{events}}} \frac{d}{dx_p} [N(q \rightarrow \bar{\Lambda}^0) + N(\bar{q} \rightarrow \Lambda^0)]$ (/REF/SLD_1999_S3743934/d34-x01-y02)
- $D_{\Lambda^0}^q = (R_{\Lambda^0}^q - R_{\bar{\Lambda}^0}^q) / (R_{\Lambda^0}^q + R_{\bar{\Lambda}^0}^q)$ (/REF/SLD_1999_S3743934/d35-x01-y01)

6.30 SLD_2002_S4869273 [38]

Measurement of the b-quark fragmentation function in Z^0 decays

Beams: $e^+ e^-$

Energies: (45.6, 45.6) GeV

Experiment: SLD (SLC)

Spires ID: [4869273](#)

Status: VALIDATED

Authors:

- Peter Richardson (Peter.Richardson@durham.ac.uk)

References:

- Phys. Rev.D65:092006,2002
- hep-ex/0202031

Run details:

- Hadronic Z decay events generated on the Z pole ($\sqrt{s} = 91.2$ GeV)

Measurement of the b -quark fragmentation function by SLC. The fragmentation function for weakly decaying b -quarks has been measured.

Histograms (1):

- b quark fragmentation function $f(x_B^{\text{weak}})$ ([/REF/SLD_2002_S4869273/d01-x01-y01](#))

6.31 SLD_2004_S5693039 [39]

Production of π^+ , π^- , K^+ , K^- , p and \bar{p} in Light (uds), c and b Jets from Z Decays

Beams: $e^+ e^-$

Energies: (45.6, 45.6) GeV

Experiment: SLD (SLC)

Spires ID: [5693039](#)

Status: VALIDATED

Authors:

- Peter Richardson (Peter.Richardson@durham.ac.uk)

References:

- Phys.Rev.D69:072003,2004
- arXiv: [hep-ex/0310017](#)

Run details:

- Hadronic Z decay events generated on the Z pole ($\sqrt{s} = 91.2$ GeV)

Measurements of the differential production rates of stable charged particles in hadronic Z^0 decays, and of charged pions, kaons and protons identified over a wide momentum range. In addition to flavour-inclusive Z^0 decays, measurements are made for Z^0 decays into light (u, d, s), c and b primary flavors.

Histograms (42):

- Charged Particle Momentum ([/REF/SLD_2004_S5693039/d01-x01-y01](#))
- π^\pm scaled Momentum ([/REF/SLD_2004_S5693039/d02-x01-y02](#))
- π^\pm multiplicity ([/REF/SLD_2004_S5693039/d02-x02-y02](#))
- K^\pm scaled Momentum ([/REF/SLD_2004_S5693039/d03-x01-y02](#))
- K^\pm multiplicity ([/REF/SLD_2004_S5693039/d03-x02-y02](#))
- p, \bar{p} scaled Momentum ([/REF/SLD_2004_S5693039/d04-x01-y02](#))
- p, \bar{p} multiplicity ([/REF/SLD_2004_S5693039/d04-x02-y02](#))
- π^\pm scaled Momentum, (uds) events ([/REF/SLD_2004_S5693039/d05-x01-y01](#))
- π^\pm scaled Momentum, c events ([/REF/SLD_2004_S5693039/d05-x01-y02](#))
- π^\pm scaled Momentum, b events ([/REF/SLD_2004_S5693039/d05-x01-y03](#))
- π^\pm multiplicity, (uds) events ([/REF/SLD_2004_S5693039/d05-x02-y01](#))

- π^\pm multiplicity, c events ([/REF/SLD_2004_S5693039/d05-x02-y02](#))
- π^\pm multiplicity, b events ([/REF/SLD_2004_S5693039/d05-x02-y03](#))
- K^\pm scaled Momentum, (uds) events ([/REF/SLD_2004_S5693039/d06-x01-y01](#))
- K^\pm scaled Momentum, c events ([/REF/SLD_2004_S5693039/d06-x01-y02](#))
- K^\pm scaled Momentum, b events ([/REF/SLD_2004_S5693039/d06-x01-y03](#))
- K^\pm multiplicity, (uds) events ([/REF/SLD_2004_S5693039/d06-x02-y01](#))
- K^\pm multiplicity, c events ([/REF/SLD_2004_S5693039/d06-x02-y02](#))
- K^\pm multiplicity, b events ([/REF/SLD_2004_S5693039/d06-x02-y03](#))
- p, \bar{p} scaled Momentum, (uds) events ([/REF/SLD_2004_S5693039/d07-x01-y01](#))
- p, \bar{p} scaled Momentum, c events ([/REF/SLD_2004_S5693039/d07-x01-y02](#))
- p, \bar{p} scaled Momentum, b events ([/REF/SLD_2004_S5693039/d07-x01-y03](#))
- p, \bar{p} multiplicity, (uds) events ([/REF/SLD_2004_S5693039/d07-x02-y01](#))
- p, \bar{p} multiplicity, c events ([/REF/SLD_2004_S5693039/d07-x02-y02](#))
- p, \bar{p} multiplicity, b events ([/REF/SLD_2004_S5693039/d07-x02-y03](#))
- Charged particle scaled Momentum, (uds) events ([/REF/SLD_2004_S5693039/d08-x01-y01](#))
- Charged particle scaled Momentum, c events ([/REF/SLD_2004_S5693039/d08-x01-y02](#))
- Charged particle scaled Momentum, b events ([/REF/SLD_2004_S5693039/d08-x01-y03](#))
- Charged particle multiplicity, (uds) events ([/REF/SLD_2004_S5693039/d08-x02-y01](#))
- Charged particle multiplicity, c events ([/REF/SLD_2004_S5693039/d08-x02-y02](#))
- Charged particle multiplicity, b events ([/REF/SLD_2004_S5693039/d08-x02-y03](#))
- Difference in Charged multiplicity between c and uds events ([/REF/SLD_2004_S5693039/d08-x03-y02](#))
- Difference in Charged multiplicity between b and uds events ([/REF/SLD_2004_S5693039/d08-x03-y03](#))
- $R_{\pi^+}^q = \frac{1}{2N_{\text{events}}} \frac{d}{dx_p} [N(q \rightarrow \pi^+) + N(\bar{q} \rightarrow \pi^-)]$ ([/REF/SLD_2004_S5693039/d09-x01-y01](#))
- $R_{\pi^-}^q = \frac{1}{2N_{\text{events}}} \frac{d}{dx_p} [N(q \rightarrow \pi^-) + N(\bar{q} \rightarrow \pi^+)]$ ([/REF/SLD_2004_S5693039/d09-x01-y02](#))
- $D_{\pi^-}^q = (R_{\pi^-}^q - R_{\pi^+}^q) / (R_{\pi^-}^q + R_{\pi^+}^q)$ ([/REF/SLD_2004_S5693039/d09-x01-y03](#))
- $R_{K^+}^q = \frac{1}{2N_{\text{events}}} \frac{d}{dx_p} [N(q \rightarrow K^+) + N(\bar{q} \rightarrow K^-)]$ ([/REF/SLD_2004_S5693039/d10-x01-y01](#))
- $R_{K^-}^q = \frac{1}{2N_{\text{events}}} \frac{d}{dx_p} [N(q \rightarrow K^-) + N(\bar{q} \rightarrow K^+)]$ ([/REF/SLD_2004_S5693039/d10-x01-y02](#))

- $D_{K^-}^q = (R_{K^-}^q - R_{K^+}^q)/(R_{K^-}^q + R_{K^+}^q)$ (/REF/SLD_2004_S5693039/d10-x01-y03)
- $R_p^q = \frac{1}{2N_{\text{events}}} \frac{d}{dx_p} [N(q \rightarrow p) + N(\bar{q} \rightarrow \bar{p})]$ (/REF/SLD_2004_S5693039/d11-x01-y01)
- $R_{\bar{p}}^q = \frac{1}{2N_{\text{events}}} \frac{d}{dx_{\bar{p}}} [N(q \rightarrow \bar{p}) + N(\bar{q} \rightarrow p)]$ (/REF/SLD_2004_S5693039/d11-x01-y02)
- $D_{\bar{p}}^q = (R_p^q - R_{\bar{p}}^q)/(R_p^q + R_{\bar{p}}^q)$ (/REF/SLD_2004_S5693039/d11-x01-y03)

7. Tevatron analyses

7.1 CDF_1988_S1865951 [40]

CDF transverse momentum distributions at 630 GeV and 1800 GeV.

Beams: $\bar{p}p$

Energies: (315.0, 315.0), (900.0, 900.0) GeV

Experiment: CDF (Tevatron Run I)

Spires ID: [1865951](#)

Status: VALIDATED

Authors:

- Christophe Vaillant (c.l.j.j.vaillant@durham.ac.uk)
- Andy Buckley (andy.buckley@cern.ch)

References:

- Phys.Rev.Lett.61:1819,1988
- DOI: [10.1103/PhysRevLett.61.1819](https://doi.org/10.1103/PhysRevLett.61.1819)

Run details:

- QCD min bias events at $\sqrt{s} = 630$ GeV and 1800 GeV, $|\eta| < 1.0$.

Transverse momentum distributions at 630 GeV and 1800 GeV based on data from the CDF experiment at the Tevatron collider.

Histograms (2):

- p_{\perp} distribution at $\sqrt{s} = 1800$ GeV ([/REF/CDF_1988_S1865951/d01-x01-y01](#))
- p_{\perp} distribution at $\sqrt{s} = 630$ GeV ([/REF/CDF_1988_S1865951/d02-x01-y01](#))

7.2 CDF_1990_S2089246 [41]

CDF pseudorapidity distributions at 630 and 1800 GeV

Beams: $\bar{p}p$

Energies: (315.0, 315.0), (900.0, 900.0) GeV

Experiment: CDF (Tevatron Run 0)

Spires ID: [2089246](#)

Status: VALIDATED

Authors:

- Andy Buckley <andy.buckley@cern.ch>

References:

- Phys.Rev.D41:2330,1990
- DOI: [10.1103/PhysRevD.41.2330](https://doi.org/10.1103/PhysRevD.41.2330)

Run details:

- QCD min bias events at $\sqrt{s} = 630$ and 1800 GeV. Particles with $c\tau > 10$ mm should be set stable.

Pseudorapidity distributions based on the CDF 630 and 1800 GeV runs from 1987. All data is detector corrected. The data confirms the UA5 measurement of a $dN/d\eta$ rise with energy faster than $\ln \sqrt{s}$, and as such this analysis is important for constraining the energy evolution of minimum bias and underlying event characteristics in MC simulations.

Histograms (2):

- Pseudorapidity distribution at $\sqrt{s} = 1800$ GeV ([/REF/CDF_1990_S2089246/d03-x01-y01](#))
- Pseudorapidity distribution at $\sqrt{s} = 630$ GeV ([/REF/CDF_1990_S2089246/d04-x01-y01](#))

7.3 CDF_1993_S2742446 [42]

Angular distribution of prompt photon

Beams: $\bar{p}p$

Energies: (900.0, 900.0) GeV

Experiment: CDF (Tevatron Run 1)

Spires ID: [2742446](#)

Status: UNVALIDATED

Authors:

- Frank Siegert <frank.siegert@cern.ch>

References:

- Phys.Rev.Lett.71:679-683,1993
- DOI: [10.1103/PhysRevLett.71.679](https://doi.org/10.1103/PhysRevLett.71.679)

Run details:

- All prompt photon production processes in $p\bar{p}$ at 1800 GeV. Hadronisation should be switched off, because non-prompt photon production has been corrected for.

Data taken with the Collider Detector at Fermilab (CDF) during the 1988-1989 run of the Tevatron are used to measure the distribution of the center-of-mass (rest frame of the initial state partons) angle between isolated prompt photons and the beam direction.

Histograms (1):

- Angular distribution of prompt photons ([/REF/CDF_1993_S2742446/d01-x01-y01](#))

7.4 CDF_1994_S2952106 [43]

CDF Run I color coherence analysis.

Beams: $\bar{p}p$

Energies: (900.0, 900.0) GeV

Experiment: CDF (Tevatron Run 1)

Spires ID: [2952106](#)

Status: VALIDATED

Authors:

- Lars Sonnenschein (Lars.Sonnenschein@cern.ch)
- Andy Buckley (andy.buckley@cern.ch)

References:

- Phys.Rev.D50,5562,1994
- DOI: [10.1103/PhysRevD.50.5562](https://doi.org/10.1103/PhysRevD.50.5562)

Run details:

- QCD events at $\sqrt{s} = 1800$ GeV. Leading jet $p_{\perp \min} = 100$ GeV.

CDF Run I color coherence analysis. Events with ≥ 3 jets are selected and Et distributions of the three highest- p_{\perp} jets are obtained. The plotted quantities are the ΔR between the 2nd and 3rd leading jets in the p_{\perp} and pseudorapidity of the 3rd jet, and $\alpha = d\eta/d\phi$, where $d\eta$ is the pseudorapidity difference between the 2nd and 3rd jets and $d\phi$ is their azimuthal angle difference. Since the data has not been detector-corrected, a bin by bin correction is applied, based on the distributions with ideal and CDF simulation as given in the publication.

Histograms (5):

- E_{\perp} of leading jet ([/REF/CDF_1994_S2952106/d01-x01-y01](#))
- E_{\perp} of 2nd leading jet ([/REF/CDF_1994_S2952106/d02-x01-y01](#))
- Pseudorapidity, η , of 3rd jet ([/REF/CDF_1994_S2952106/d03-x01-y01](#))
- R distance between 2nd and 3rd jet ([/REF/CDF_1994_S2952106/d04-x01-y01](#))
- α ([/REF/CDF_1994_S2952106/d05-x01-y01](#))

7.5 CDF_1996_S3108457 [44]

Properties of High-Mass Multijet Events

Beams: $\bar{p}p$

Energies: (900.0, 900.0) GeV

Experiment: CDF (Tevatron Run 1)

Spires ID: [3108457](#)

Status: UNVALIDATED

Authors:

- Frank Siegert <frank.siegert@cern.ch>

References:

- Phys.Rev.Lett.75:608-612,1995
- DOI: [10.1103/PhysRevLett.75.608](https://doi.org/10.1103/PhysRevLett.75.608)

Run details:

- Pure QCD events without underlying event.

Properties of two-, three-, four-, five-, and six-jet events... Multijet-mass, leading jet angle, jet p_\perp .

Histograms (15):

- Multijet mass in 2-jet events ([/REF/CDF_1996_S3108457/d01-x01-y01](#))
- Multijet mass in 3-jet events ([/REF/CDF_1996_S3108457/d02-x01-y01](#))
- Multijet mass in 4-jet events ([/REF/CDF_1996_S3108457/d03-x01-y01](#))
- Multijet mass in 5-jet events ([/REF/CDF_1996_S3108457/d04-x01-y01](#))
- Multijet mass in 6-jet events ([/REF/CDF_1996_S3108457/d05-x01-y01](#))
- Leading jet angle in 2-jet events ([/REF/CDF_1996_S3108457/d10-x01-y01](#))
- Leading jet angle in 3-jet events ([/REF/CDF_1996_S3108457/d11-x01-y01](#))
- Leading jet angle in 4-jet events ([/REF/CDF_1996_S3108457/d12-x01-y01](#))
- Leading jet angle in 5-jet events ([/REF/CDF_1996_S3108457/d13-x01-y01](#))
- Leading jet angle in 6-jet events ([/REF/CDF_1996_S3108457/d14-x01-y01](#))
- Inclusive jet p_\perp in 2-jet events ([/REF/CDF_1996_S3108457/d15-x01-y01](#))
- Inclusive jet p_\perp in 3-jet events ([/REF/CDF_1996_S3108457/d16-x01-y01](#))
- Inclusive jet p_\perp in 4-jet events ([/REF/CDF_1996_S3108457/d17-x01-y01](#))
- Inclusive jet p_\perp in 5-jet events ([/REF/CDF_1996_S3108457/d18-x01-y01](#))
- Inclusive jet p_\perp in 6-jet events ([/REF/CDF_1996_S3108457/d19-x01-y01](#))

7.6 CDF_1996_S3349578 [45]

Further properties of high-mass multijet events

Beams: $\bar{p}p$

Energies: (900.0, 900.0) GeV

Experiment: CDF (Tevatron Run 1)

Spires ID: [3349578](#)

Status: UNVALIDATED

Authors:

- Frank Siegert (frank.siegert@cern.ch)

References:

- Phys.Rev.D54:4221-4233,1996
- DOI: [10.1103/PhysRevD.54.4221](https://doi.org/10.1103/PhysRevD.54.4221)
- arXiv: [hep-ex/9605004](https://arxiv.org/abs/hep-ex/9605004)

Run details:

- Pure QCD events without underlying event.

Multijet distributions corresponding to $(4N - 4)$ variables that span the N -body parameter space in inclusive $N = 3$ -, 4-, and 5-jet events.

Histograms (36):

- Multijet mass in inclusive 3-jet events ([/REF/CDF_1996_S3349578/d01-x01-y01](#))
- Multijet mass in inclusive 4-jet events ([/REF/CDF_1996_S3349578/d01-x01-y02](#))
- Multijet mass in inclusive 5-jet events ([/REF/CDF_1996_S3349578/d01-x01-y03](#))
- Dalitz distribution in inclusive 3-jet events ([/REF/CDF_1996_S3349578/d02-x01-y01](#))
- Dalitz distribution in inclusive 3-jet events ([/REF/CDF_1996_S3349578/d03-x01-y01](#))
- Dalitz distribution in inclusive 4-jet events ([/REF/CDF_1996_S3349578/d04-x01-y01](#))
- Dalitz distribution in inclusive 4-jet events ([/REF/CDF_1996_S3349578/d05-x01-y01](#))
- Dalitz distribution in inclusive 5-jet events ([/REF/CDF_1996_S3349578/d06-x01-y01](#))
- Dalitz distribution in inclusive 5-jet events ([/REF/CDF_1996_S3349578/d07-x01-y01](#))
- Leading jet angle in inclusive 3-jet events ([/REF/CDF_1996_S3349578/d08-x01-y01](#))
- Angular distribution in inclusive 3-jet events ([/REF/CDF_1996_S3349578/d09-x01-y01](#))
- Leading jet angle in inclusive 4-jet events ([/REF/CDF_1996_S3349578/d10-x01-y01](#))

- Angular distribution in inclusive 4-jet events ([/REF/CDF_1996_S3349578/d11-x01-y01](#))
- Leading jet angle in inclusive 5-jet events ([/REF/CDF_1996_S3349578/d12-x01-y01](#))
- Angular distribution in inclusive 5-jet events ([/REF/CDF_1996_S3349578/d13-x01-y01](#))
- Single-jet mass fraction in inclusive 3-jet events ([/REF/CDF_1996_S3349578/d14-x01-y01](#))
- Single-jet mass fraction in inclusive 3-jet events ([/REF/CDF_1996_S3349578/d14-x01-y02](#))
- Single-jet mass fraction in inclusive 3-jet events ([/REF/CDF_1996_S3349578/d14-x01-y03](#))
- Single-jet mass fraction in inclusive 4-jet events ([/REF/CDF_1996_S3349578/d15-x01-y01](#))
- Single-jet mass fraction in inclusive 4-jet events ([/REF/CDF_1996_S3349578/d15-x01-y02](#))
- Single-jet mass fraction in inclusive 4-jet events ([/REF/CDF_1996_S3349578/d15-x01-y03](#))
- Single-jet mass fraction in inclusive 5-jet events ([/REF/CDF_1996_S3349578/d16-x01-y01](#))
- Single-jet mass fraction in inclusive 5-jet events ([/REF/CDF_1996_S3349578/d16-x01-y02](#))
- Single-jet mass fraction in inclusive 5-jet events ([/REF/CDF_1996_S3349578/d16-x01-y03](#))
- Two-body energy sharing in inclusive 4-jet events ([/REF/CDF_1996_S3349578/d17-x01-y01](#))
- Two-body energy sharing in inclusive 5-jet events ([/REF/CDF_1996_S3349578/d18-x01-y01](#))
- Two-body energy sharing in inclusive 5-jet events ([/REF/CDF_1996_S3349578/d18-x01-y02](#))
- Two-body angular distribution in inclusive 4-jet events ([/REF/CDF_1996_S3349578/d19-x01-y01](#))
- Two-body angular distribution in inclusive 5-jet events ([/REF/CDF_1996_S3349578/d20-x01-y01](#))
- Two-body angular distribution in inclusive 5-jet events ([/REF/CDF_1996_S3349578/d20-x01-y02](#))
- Single-body mass fraction in inclusive 4-jet events ([/REF/CDF_1996_S3349578/d21-x01-y01](#))
- Single-body mass fraction in inclusive 4-jet events ([/REF/CDF_1996_S3349578/d21-x01-y02](#))
- Single-body mass fraction in inclusive 5-jet events ([/REF/CDF_1996_S3349578/d22-x01-y01](#))
- Single-body mass fraction in inclusive 5-jet events ([/REF/CDF_1996_S3349578/d23-x01-y01](#))
- Single-body mass fraction in inclusive 5-jet events ([/REF/CDF_1996_S3349578/d24-x01-y01](#))
- Single-body mass fraction in inclusive 5-jet events ([/REF/CDF_1996_S3349578/d25-x01-y01](#))

7.7 CDF_1996_S3418421 [46]

Dijet angular distributions

Beams: $\bar{p}p$

Energies: (900.0, 900.0) GeV

Experiment: CDF (Tevatron Run 1)

Spires ID: 3418421

Status: VALIDATED

Authors:

- Frank Siegert <frank.siegert@cern.ch>

References:

- Phys.Rev.Lett.77:5336-5341,1996
- DOI: [10.1103/PhysRevLett.77.5336](https://doi.org/10.1103/PhysRevLett.77.5336)
- arXiv: [hep-ex/9609011](https://arxiv.org/abs/hep-ex/9609011)

Run details:

- QCD dijet events at Tevatron $\sqrt{s} = 1.8$ TeV without MPI.

Measurement of jet angular distributions in events with two jets in the final state in 5 bins of dijet invariant mass. Based on 106pb^{-1}

Histograms (6):

- Dijet events with $241 < m_{\text{dijet}}/\text{GeV} < 300$ ([/REF/CDF_1996_S3418421/d01-x01-y01](#))
- Dijet events with $300 < m_{\text{dijet}}/\text{GeV} < 400$ ([/REF/CDF_1996_S3418421/d01-x01-y02](#))
- Dijet events with $400 < m_{\text{dijet}}/\text{GeV} < 517$ ([/REF/CDF_1996_S3418421/d01-x01-y03](#))
- Dijet events with $517 < m_{\text{dijet}}/\text{GeV} < 625$ ([/REF/CDF_1996_S3418421/d01-x01-y04](#))
- Dijet events with $625 < m_{\text{dijet}}/\text{GeV} < 1000$ ([/REF/CDF_1996_S3418421/d01-x01-y05](#))
- Dijet angular ratio as function of dijet mass ([/REF/CDF_1996_S3418421/d02-x01-y01](#))

7.8 CDF_1997_S3541940 [47]

Properties of six jet events with large six jet mass

Beams: $\bar{p}p$

Energies: (900.0, 900.0) GeV

Experiment: CDF (Tevatron Run 1)

Spires ID: [3541940](#)

Status: UNVALIDATED

Authors:

- Frank Siegert <frank.siegert@cern.ch>

References:

- Phys.Rev.D56:2532-2543,1997
- DOI: [10.1103/PhysRevD.56.2532](https://doi.org/10.1103/PhysRevD.56.2532)
- <http://lss.fnal.gov/archive/1997/pub/Pub-97-093-E.pdf>

Run details:

- Pure QCD events without underlying event.

Multijet distributions corresponding to 20 variables that span the 6-body parameter space in inclusive 6-jet events.

Histograms (20):

- Multijet mass (/REF/CDF_1997_S3541940/d01-x01-y01)
- Dalitz distribution (/REF/CDF_1997_S3541940/d02-x01-y01)
- Dalitz distribution (/REF/CDF_1997_S3541940/d03-x01-y01)
- Leading jet angle (/REF/CDF_1997_S3541940/d04-x01-y01)
- Angular distribution (/REF/CDF_1997_S3541940/d05-x01-y01)
- Single-jet mass fraction (/REF/CDF_1997_S3541940/d06-x01-y01)
- Single-jet mass fraction (/REF/CDF_1997_S3541940/d06-x01-y02)
- Single-jet mass fraction (/REF/CDF_1997_S3541940/d06-x01-y03)
- Two-body energy sharing (/REF/CDF_1997_S3541940/d07-x01-y01)
- Two-body energy sharing (/REF/CDF_1997_S3541940/d08-x01-y01)
- Two-body energy sharing (/REF/CDF_1997_S3541940/d09-x01-y01)
- Two-body angular distribution (/REF/CDF_1997_S3541940/d10-x01-y01)

- Two-body angular distribution (/REF/CDF_1997_S3541940/d11-x01-y01)
- Two-body angular distribution (/REF/CDF_1997_S3541940/d12-x01-y01)
- Single-body mass fraction (/REF/CDF_1997_S3541940/d13-x01-y01)
- Single-body mass fraction (/REF/CDF_1997_S3541940/d14-x01-y01)
- Single-body mass fraction (/REF/CDF_1997_S3541940/d15-x01-y01)
- Single-body mass fraction (/REF/CDF_1997_S3541940/d16-x01-y01)
- Single-body mass fraction (/REF/CDF_1997_S3541940/d17-x01-y01)
- Single-body mass fraction (/REF/CDF_1997_S3541940/d18-x01-y01)

7.9 CDF_1998_S3618439 [48]

Differential cross-section for events with large total transverse energy

Beams: $\bar{p}p$

Energies: (900.0, 900.0) GeV

Experiment: CDF (Tevatron Run 1)

Spires ID: [3618439](#)

Status: UNVALIDATED

Authors:

- Frank Siegert <frank.siegert@cern.ch>

References:

- Phys.Rev.Lett.80:3461-3466,1998
- [10.1103/PhysRevLett.80.3461](https://doi.org/10.1103/PhysRevLett.80.3461)

Run details:

- QCD events at Tevatron with $\sqrt{s} = 1.8$ TeV without MPI.

Measurement of the differential cross section $d\sigma/dE_{\perp}^j$ for the production of multijet events in $p\bar{p}$ collisions where the sum is over all jets with transverse energy $E_{\perp}^j > E_{\perp}^{\min}$.

Histograms (2):

- E_{\perp} sum for jets with $E_{\perp} > 20$ GeV ([/REF/CDF_1998_S3618439/d01-x01-y01](#))
- E_{\perp} sum for jets with $E_{\perp} > 100$ GeV ([/REF/CDF_1998_S3618439/d01-x01-y02](#))

7.10 CDF_2000_S4155203 [49]

Z p_\perp measurement in CDF Z $\rightarrow e^+e^-$ events

Beams: $\bar{p}p$

Energies: (900.0, 900.0) GeV

Experiment: CDF (Tevatron Run 1)

Spires ID: 4155203

Status: VALIDATED

Authors:

- Hendrik Hoeth (hendrik.hoeth@cern.ch)

References:

- Phys.Rev.Lett.84:845-850,2000
- arXiv: [hep-ex/0001021](#)
- DOI: [10.1103/PhysRevLett.84.845](https://doi.org/10.1103/PhysRevLett.84.845)

Run details:

- $p\bar{p}$ collisions at 1800 GeV. Z/ γ^* Drell-Yan events with e^+e^- decay mode only. Restrict Z/ γ^* mass range to roughly $50 \text{ GeV}/c^2 < m_{ee} < 120 \text{ GeV}/c^2$ for efficiency.

Measurement of transverse momentum and total cross section of e^+e^- pairs in the Z-boson region of $66 \text{ GeV}/c^2 < m_{ee} < 116 \text{ GeV}/c^2$ from pbar-p collisions at $\sqrt{s} = 1.8 \text{ TeV}$, with the Tevatron CDF detector. The Z p_\perp , in a fully-factorised picture, is generated by the momentum balance against initial state radiation (ISR) and the primordial/intrinsic p_\perp of the Z's parent partons in the incoming hadrons. The Z p_\perp is important in generator tuning to fix the interplay of ISR and multi-parton interactions (MPI) in generating ‘underlying event’ activity. This analysis is subject to ambiguities in the experimental Z p_\perp definition, since the Rivet implementation reconstructs the Z momentum from the dilepton pair with finite cones for QED bremsstrahlung summation, rather than non-portable direct use of the (sometimes absent) Z in the event record.

Histograms (1):

- $p_\perp(Z)$ in Z $\rightarrow e^+e^-$ events ([/REF/CDF_2000_S4155203/d01-x01-y01](#))

7.11 CDF_2000_S4266730 [50]

Inclusive jet cross section differential in dijet mass

Beams: $\bar{p}p$

Energies: (900.0, 900.0) GeV

Experiment: CDF (Tevatron Run 1)

Spires ID: [4266730](#)

Status: VALIDATED

Authors:

- Frank Siegert <frank.siegert@cern.ch>

References:

- Phys.Rev.D61:091101,2000
- DOI: [10.1103/PhysRevD.61.091101](https://doi.org/10.1103/PhysRevD.61.091101)
- arXiv: [hep-ex/9912022](https://arxiv.org/abs/hep-ex/9912022)

Run details:

- Dijet events at Tevatron with $\sqrt{s} = 1.8$ TeV

Measurement of the cross section for production of two or more jets as a function of dijet mass in the range 180 to 1000 GeV. It is based on an integrated luminosity of 86pb^{-1} .

Histograms (1):

- Dijet mass ([/REF/CDF_2000_S4266730/d01-x01-y01](#))

7.12 CDF_2001_S4517016 [51]

Two jet triply-differential cross-section

Beams: $\bar{p}p$

Energies: (900.0, 900.0) GeV

Experiment: CDF (Tevatron Run 1)

Spires ID: 4517016

Status: UNVALIDATED

Authors:

- Frank Siegert <frank.siegert@cern.ch>

References:

- Phys.Rev.D64:012001,2001
- DOI: [10.1103/PhysRevD.64.012001](https://doi.org/10.1103/PhysRevD.64.012001)
- arXiv: [hep-ex/0012013](https://arxiv.org/abs/hep-ex/0012013)

Run details:

- Dijet events at Tevatron with $\sqrt{s} = 1.8$ TeV

A measurement of the two-jet differential cross section, $d^3\sigma/dE_T d\eta_1 d\eta_2$, based on an integrated luminosity of 86pb^{-1} . The differential cross section is measured as a function of the transverse energy, E_\perp , of a jet in the pseudorapidity region $0.1 < |\eta_1| < 0.7$ for four different pseudorapidity bins of a second jet restricted to $0.1 < |\eta_2| < 3.0$.

Histograms (4):

- E_\perp of leading jet for events with $0.1 < |\eta_2| < 0.7$ ([/REF/CDF_2001_S4517016/d01-x01-y01](#))
- E_\perp of leading jet for events with $0.7 < |\eta_2| < 1.4$ ([/REF/CDF_2001_S4517016/d02-x01-y01](#))
- E_\perp of leading jet for events with $1.4 < |\eta_2| < 2.1$ ([/REF/CDF_2001_S4517016/d03-x01-y01](#))
- E_\perp of leading jet for events with $2.1 < |\eta_2| < 3.0$ ([/REF/CDF_2001_S4517016/d04-x01-y01](#))

7.13 CDF_2001_S4563131 [52]

Inclusive jet cross section

Beams: $\bar{p}p$

Energies: (900.0, 900.0) GeV

Experiment: CDF (Tevatron Run 1)

Spires ID: 4563131

Status: UNVALIDATED

Authors:

- Frank Siegert <frank.siegert@cern.ch>

References:

- Phys.Rev.D64:032001,2001
- DOI: [10.1103/PhysRevD.64.032001](https://doi.org/10.1103/PhysRevD.64.032001)
- arXiv: [hep-ph/0102074](https://arxiv.org/abs/hep-ph/0102074)

Run details:

- Dijet events at Tevatron with $\sqrt{s} = 1.8$ TeV

Measurement of the inclusive jet cross section for jet transverse energies from 40 to 465 GeV in the pseudo-rapidity range $0.1 < |\eta| < 0.7$. The results are based on 87 pb^{-1} of data.

Histograms (1):

- Inclusive jet cross section ([/REF/CDF_2001_S4563131/d01-x01-y01](#))

7.14 CDF_2001_S4751469 [53]

Field & Stuart Run I underlying event analysis.

Beams: $\bar{p}p$

Energies: (900.0, 900.0) GeV

Experiment: CDF (Tevatron Run 1)

Spires ID: [4751469](#)

Status: VALIDATED

Authors:

- Andy Buckley ⟨andy.buckley@cern.ch⟩

References:

- Phys.Rev.D65:092002,2002
- FNAL-PUB 01/211-E

Run details:

- $p\bar{p}$ QCD interactions at 1800 GeV. The leading jet is binned from 0–49 GeV, and histos can usually be filled with a single generator run without kinematic sub-samples.

The original CDF underlying event analysis, based on decomposing each event into a transverse structure with “toward”, “away” and “transverse” regions defined relative to the azimuthal direction of the leading jet in the event. Since the toward region is by definition dominated by the hard process, as is the away region by momentum balance in the matrix element, the transverse region is most sensitive to multi-parton interactions. The transverse regions occupy $|\phi| \in [60^\circ, 120^\circ]$ for $|\eta| < 1$. The p_\perp ranges for the leading jet are divided experimentally into the ‘min-bias’ sample from 0–20 GeV, and the ‘JET20’ sample from 18–49 GeV.

Histograms (21):

- $\langle N_{\text{ch}} \rangle$ vs. $\Delta\phi$ from leading jet ($p_\perp^{\text{lead}} > 2$ GeV) ([/REF/CDF_2001_S4751469/d01-x01-y01](#))
- $\langle N_{\text{ch}} \rangle$ vs. $\Delta\phi$ from leading jet ($p_\perp^{\text{lead}} > 5$ GeV) ([/REF/CDF_2001_S4751469/d01-x01-y02](#))
- $\langle N_{\text{ch}} \rangle$ vs. $\Delta\phi$ from leading jet ($p_\perp^{\text{lead}} > 30$ GeV) ([/REF/CDF_2001_S4751469/d01-x01-y03](#))
- $\langle p_\perp^{\text{sum}} \rangle$ vs. $\Delta\phi$ from leading jet ($p_\perp^{\text{lead}} > 2$ GeV) ([/REF/CDF_2001_S4751469/d02-x01-y01](#))
- $\langle p_\perp^{\text{sum}} \rangle$ vs. $\Delta\phi$ from leading jet ($p_\perp^{\text{lead}} > 5$ GeV) ([/REF/CDF_2001_S4751469/d02-x01-y02](#))
- $\langle p_\perp^{\text{sum}} \rangle$ vs. $\Delta\phi$ from leading jet ($p_\perp^{\text{lead}} > 30$ GeV) ([/REF/CDF_2001_S4751469/d02-x01-y03](#))
- N_{ch} (toward) for min-bias ([/REF/CDF_2001_S4751469/d03-x01-y01](#))
- N_{ch} (transverse) for min-bias ([/REF/CDF_2001_S4751469/d03-x01-y02](#))
- N_{ch} (away) for min-bias ([/REF/CDF_2001_S4751469/d03-x01-y03](#))

- N_{ch} (toward) for JET20 (/REF/CDF_2001_S4751469/d04-x01-y01)
- N_{ch} (transverse) for JET20 (/REF/CDF_2001_S4751469/d04-x01-y02)
- N_{ch} (away) for JET20 (/REF/CDF_2001_S4751469/d04-x01-y03)
- p_{\perp}^{sum} (toward) for min-bias (/REF/CDF_2001_S4751469/d05-x01-y01)
- p_{\perp}^{sum} (transverse) for min-bias (/REF/CDF_2001_S4751469/d05-x01-y02)
- p_{\perp}^{sum} (away) for min-bias (/REF/CDF_2001_S4751469/d05-x01-y03)
- p_{\perp}^{sum} (toward) for JET20 (/REF/CDF_2001_S4751469/d06-x01-y01)
- p_{\perp}^{sum} (transverse) for JET20 (/REF/CDF_2001_S4751469/d06-x01-y02)
- p_{\perp}^{sum} (away) for JET20 (/REF/CDF_2001_S4751469/d06-x01-y03)
- p_{\perp} distribution (transverse, $p_{\perp}^{\text{lead}} > 2$ GeV) (/REF/CDF_2001_S4751469/d07-x01-y01)
- p_{\perp} distribution (transverse, $p_{\perp}^{\text{lead}} > 5$ GeV) (/REF/CDF_2001_S4751469/d07-x01-y02)
- p_{\perp} distribution (transverse, $p_{\perp}^{\text{lead}} > 30$ GeV) (/REF/CDF_2001_S4751469/d07-x01-y03)

7.15 CDF_2002_S4796047 [54]

CDF Run 1 charged multiplicity measurement

Beams: $\bar{p}p$

Energies: (315.0, 315.0), (900.0, 900.0) GeV

Experiment: CDF (Tevatron Run 1)

Spires ID: [4796047](#)

Status: VALIDATED

Authors:

- Hendrik Hoeth (hendrik.hoeth@cern.ch)

References:

- Phys.Rev.D65:072005,2002
- DOI: [10.1103/PhysRevD.65.072005](https://doi.org/10.1103/PhysRevD.65.072005)

Run details:

- QCD events at $\sqrt{s} = 630$ and 1800 GeV.

A study of $p\bar{p}$ collisions at $\sqrt{s} = 1800$ and 630 GeV collected using a minimum bias trigger in which the data set is divided into two classes corresponding to ‘soft’ and ‘hard’ interactions. For each subsample, the analysis includes measurements of the multiplicity, transverse momentum (p_{\perp}) spectra, and the average p_{\perp} and event-by-event p_{\perp} dispersion as a function of multiplicity. A comparison of results shows distinct differences in the behavior of the two samples as a function of the center of mass energy. The properties of the soft sample are invariant as a function of c.m. energy. It should be noticed that minimum bias tunings of PYTHIA made by ATLAS in early 2010, which used this among all other available data from CDF and from ATLAS at 900 GeV and 7 TeV, found an unavoidable tension between this data and the rest. Accordingly, this data was excluded from the fits. Whether this reflects a problem with this dataset or with the PYTHIA MPI model is a judgement for users to make!

Histograms (4):

- Charged multiplicity at $\sqrt{s} = 630$ GeV, $|\eta| < 1$, $p_T > 0.4$ GeV ([/REF/CDF_2002_-S4796047/d01-x01-y01](#))
- Charged multiplicity at $\sqrt{s} = 1800$ GeV, $|\eta| < 1$, $p_T > 0.4$ GeV ([/REF/CDF_2002_-S4796047/d02-x01-y01](#))
- $\langle p_{\perp} \rangle$ vs. multiplicity at $\sqrt{s} = 630$ GeV, $|\eta| < 1$, $p_T > 0.4$ GeV ([/REF/CDF_2002_-S4796047/d03-x01-y01](#))
- $\langle p_{\perp} \rangle$ vs. multiplicity at $\sqrt{s} = 1800$ GeV, $|\eta| < 1$, $p_T > 0.4$ GeV ([/REF/CDF_2002_-S4796047/d04-x01-y01](#))

7.16 CDF_2004_S5839831 [55]

Transverse cone and ‘Swiss cheese’ underlying event studies

Beams: $\bar{p}p$

Energies: (315.0, 315.0), (900.0, 900.0) GeV

Experiment: CDF (Tevatron Run 1)

Spires ID: [5839831](#)

Status: VALIDATED

Authors:

- Andy Buckley <andy.buckley@cern.ch>

References:

- Phys. Rev. D70, 072002 (2004)
- arXiv: [hep-ex/0404004](#)

Run details:

- QCD events at $\sqrt{s} = 630$ & 1800 GeV. Several p_{\perp}^{\min} cutoffs are probably required to fill the profile histograms, e.g. 0 (min bias), 30, 90, 150 GeV at 1800 GeV, and 0 (min bias), 20, 90, 150 GeV at 630 GeV.

This analysis studies the underlying event via transverse cones of $R = 0.7$ at 90 degrees in ϕ relative to the leading (highest E) jet, at $\sqrt{s} = 630$ and 1800 GeV. This is similar to the 2001 CDF UE analysis, except that cones, rather than the whole central η range are used. The transverse cones are categorised as ‘TransMIN’ and ‘TransMAX’ on an event-by-event basis, to give greater sensitivity to the UE component. ‘Swiss Cheese’ distributions, where cones around the leading n jets are excluded from the distributions, are also included for $n = 2, 3$. This analysis is useful for constraining the energy evolution of the underlying event, since it performs the same analyses at two distinct CoM energies. WARNING! The p_{\perp} plots are normalised to raw number of events. The min bias data have not been reproduced by MC, and are not recommended for tuning.

Histograms (23):

- Transverse cone $\langle\langle p_{\perp}^{\max}\rangle\rangle$ vs. E_{\perp}^{lead} at $\sqrt{s} = 1800$ GeV ([/REF/CDF_2004_S5839831/d01-x01-y01](#))
- Transverse cone $\langle\langle p_{\perp}^{\min}\rangle\rangle$ vs. E_{\perp}^{lead} at $\sqrt{s} = 1800$ GeV ([/REF/CDF_2004_S5839831/d01-x01-y02](#))
- Transverse cone $\langle p_{\perp}^{\max}\rangle$ vs. E_{\perp}^{lead} at $\sqrt{s} = 1800$ GeV ([/REF/CDF_2004_S5839831/d02-x01-y01](#))
- Transverse cone $\langle p_{\perp}^{\min}\rangle$ vs. E_{\perp}^{lead} at $\sqrt{s} = 1800$ GeV ([/REF/CDF_2004_S5839831/d02-x01-y02](#))
- Transverse cone $\langle p_{\perp}^{\text{diff}}\rangle$ vs. E_{\perp}^{lead} at $\sqrt{s} = 1800$ GeV ([/REF/CDF_2004_S5839831/d02-x01-y03](#))
- Transverse cone p_{\perp} ($40 < E_{\perp}^{\text{lead}} < 80$ GeV, $\sqrt{s}=1.8$ TeV) ([/REF/CDF_2004_S5839831/d03-x01-y01](#))
- Transverse cone p_{\perp} ($80 < E_{\perp}^{\text{lead}} < 120$ GeV, $\sqrt{s}=1.8$ TeV) ([/REF/CDF_2004_S5839831/d03-x01-y02](#))

- Transverse cone p_{\perp} ($120 < E_{\perp}^{\text{lead}} < 160$ GeV, $\sqrt{s}=1.8$ TeV) (/REF/CDF_2004_S5839831/d03-x01-y03)
- Transverse cone p_{\perp} ($160 < E_{\perp}^{\text{lead}} < 200$ GeV, $\sqrt{s}=1.8$ TeV) (/REF/CDF_2004_S5839831/d03-x01-y04)
- Transverse cone p_{\perp} ($200 < E_{\perp}^{\text{lead}} < 270$ GeV, $\sqrt{s}=1.8$ TeV) (/REF/CDF_2004_S5839831/d03-x01-y05)
- Transverse cone N_{\max} vs. E_{\perp}^{lead} at $\sqrt{s} = 1800$ GeV (/REF/CDF_2004_S5839831/d04-x01-y01)
- Transverse cone N_{\min} vs. E_{\perp}^{lead} at $\sqrt{s} = 1800$ GeV (/REF/CDF_2004_S5839831/d04-x01-y02)
- Min bias track multiplicity distribution at $\sqrt{s} = 1800$ GeV (/REF/CDF_2004_S5839831/d05-x01-y01)
- Min bias p_{\perp} distribution at $\sqrt{s} = 1800$ GeV (/REF/CDF_2004_S5839831/d06-x01-y01)
- Swiss Cheese p_{\perp}^{sum} vs. E_{\perp}^{lead} (2 jets removed) at $\sqrt{s} = 1800$ GeV (/REF/CDF_2004_S5839831/d07-x01-y01)
- Swiss Cheese p_{\perp}^{sum} vs. E_{\perp}^{lead} (3 jets removed) at $\sqrt{s} = 1800$ GeV (/REF/CDF_2004_S5839831/d07-x01-y02)
- Transverse cone $\langle p_{\perp}^{\max} \rangle$ vs. E_{\perp}^{lead} at $\sqrt{s} = 630$ GeV (/REF/CDF_2004_S5839831/d08-x01-y01)
- Transverse cone $\langle p_{\perp}^{\min} \rangle$ vs. E_{\perp}^{lead} at $\sqrt{s} = 630$ GeV (/REF/CDF_2004_S5839831/d08-x01-y02)
- Transverse cone $\langle p_{\perp}^{\text{diff}} \rangle$ vs. E_{\perp}^{lead} at $\sqrt{s} = 630$ GeV (/REF/CDF_2004_S5839831/d08-x01-y03)
- Swiss Cheese p_{\perp}^{sum} vs. E_{\perp}^{lead} (2 jets removed) at $\sqrt{s} = 630$ GeV (/REF/CDF_2004_S5839831/d09-x01-y01)
- Swiss Cheese p_{\perp}^{sum} vs. E_{\perp}^{lead} (3 jets removed) at $\sqrt{s} = 630$ GeV (/REF/CDF_2004_S5839831/d09-x01-y02)
- Min bias track multiplicity distribution at $\sqrt{s} = 630$ GeV (/REF/CDF_2004_S5839831/d10-x01-y01)
- Min bias p_{\perp} distribution at $\sqrt{s} = 630$ GeV (/REF/CDF_2004_S5839831/d11-x01-y01)

7.17 CDF_2005_S6080774 [56]

Differential cross sections for prompt diphoton production

Beams: $p\bar{p}$

Energies: (980.0, 980.0) GeV

Experiment: CDF (Tevatron Run 2)

Spires ID: [6080774](#)

Status: VALIDATED

Authors:

- Frank Siegert (frank.siegert@cern.ch)

References:

- Phys. Rev. Lett. 95, 022003
- DOI: [10.1103/PhysRevLett.95.022003](https://doi.org/10.1103/PhysRevLett.95.022003)
- arXiv: [hep-ex/0412050](https://arxiv.org/abs/hep-ex/0412050)

Run details:

- $p\bar{p} \rightarrow \gamma\gamma$ [+ jets] at 1960 GeV. The analysis uses photons with p_{\perp} larger than 13 GeV. To allow for shifts in the shower, the ME cut on the transverse photon momentum shouldn't be too hard, e.g. 5 GeV.

Measurement of the cross section of prompt diphoton production in $p\bar{p}$ collisions at $\sqrt{s} = 1.96$ TeV using a data sample of 207 pb^{-1} as a function of the diphoton mass, the transverse momentum of the diphoton system, and the azimuthal angle between the two photons.

Histograms (12):

- Invariant mass of diphoton pair ([/REF/CDF_2005_S6080774/d01-x01-y01](#))
- Invariant mass of diphoton pair (compared to DIPHOX) ([/REF/CDF_2005_S6080774/d01-x01-y02](#))
- Invariant mass of diphoton pair (compared to RESBOS) ([/REF/CDF_2005_S6080774/d01-x01-y03](#))
- Invariant mass of diphoton pair (compared to PYTHIA) ([/REF/CDF_2005_S6080774/d01-x01-y04](#))
- Transverse momentum of diphoton pair ([/REF/CDF_2005_S6080774/d02-x01-y01](#))
- Transverse momentum of diphoton pair (compared to DIPHOX) ([/REF/CDF_2005_S6080774/d02-x01-y02](#))
- Transverse momentum of diphoton pair (compared to RESBOS) ([/REF/CDF_2005_S6080774/d02-x01-y03](#))
- Transverse momentum of diphoton pair (compared to PYTHIA) ([/REF/CDF_2005_S6080774/d02-x01-y04](#))

- Azimuthal angle between photons ([/REF/CDF_2005_S6080774/d03-x01-y01](#))
- Azimuthal angle between photons (compared to DIPHOX) ([/REF/CDF_2005_S6080774/d03-x01-y02](#))
- Azimuthal angle between photons (compared to RESBOS) ([/REF/CDF_2005_S6080774/d03-x01-y03](#))
- Azimuthal angle between photons (compared to PYTHIA) ([/REF/CDF_2005_S6080774/d03-x01-y04](#))

7.18 CDF_2005_S6217184 [57]

CDF Run II jet shape analysis

Beams: $p\bar{p}$

Energies: (980.0, 980.0) GeV

Experiment: CDF (Tevatron Run 2)

Spires ID: 6217184

Status: VALIDATED

Authors:

- Lars Sonnenschein (Lars.Sonnenschein@cern.ch)
- Andy Buckley (andy.buckley@cern.ch)

References:

- Phys.Rev.D71:112002,2005
- DOI: [10.1103/PhysRevD.71.112002](https://doi.org/10.1103/PhysRevD.71.112002)
- arXiv: [hep-ex/0505013](https://arxiv.org/abs/hep-ex/0505013)

Run details:

- QCD events at $\sqrt{s} = 1960$ GeV. Jet p_{\perp}^{\min} in plots is 37 GeV/ c – choose a generator min p_{\perp} well below this.

Measurement of jet shapes in inclusive jet production in $p\bar{p}$ collisions at center-of-mass energy $\sqrt{s} = 1.96$ TeV. The data cover jet transverse momenta from 37–380 GeV and absolute jet rapidities in the range 0.1–0.7.

Histograms (37):

- Differential jet shape ρ , $37 \text{ GeV}/c < p_{\perp}^{\text{jet}} < 45 \text{ GeV}/c$ ([/REF/CDF_2005_S6217184/d01-x01-y01](#))
- Differential jet shape ρ , $45 \text{ GeV}/c < p_{\perp}^{\text{jet}} < 55 \text{ GeV}/c$ ([/REF/CDF_2005_S6217184/d01-x01-y02](#))
- Differential jet shape ρ , $55 \text{ GeV}/c < p_{\perp}^{\text{jet}} < 63 \text{ GeV}/c$ ([/REF/CDF_2005_S6217184/d01-x01-y03](#))
- Differential jet shape ρ , $63 \text{ GeV}/c < p_{\perp}^{\text{jet}} < 73 \text{ GeV}/c$ ([/REF/CDF_2005_S6217184/d02-x01-y01](#))
- Differential jet shape ρ , $73 \text{ GeV}/c < p_{\perp}^{\text{jet}} < 84 \text{ GeV}/c$ ([/REF/CDF_2005_S6217184/d02-x01-y02](#))
- Differential jet shape ρ , $84 \text{ GeV}/c < p_{\perp}^{\text{jet}} < 97 \text{ GeV}/c$ ([/REF/CDF_2005_S6217184/d02-x01-y03](#))
- Differential jet shape ρ , $97 \text{ GeV}/c < p_{\perp}^{\text{jet}} < 112 \text{ GeV}/c$ ([/REF/CDF_2005_S6217184/d03-x01-y01](#))
- Differential jet shape ρ , $112 \text{ GeV}/c < p_{\perp}^{\text{jet}} < 128 \text{ GeV}/c$ ([/REF/CDF_2005_S6217184/d03-x01-y02](#))
- Differential jet shape ρ , $128 \text{ GeV}/c < p_{\perp}^{\text{jet}} < 148 \text{ GeV}/c$ ([/REF/CDF_2005_S6217184/d03-x01-y03](#))
- Differential jet shape ρ , $148 \text{ GeV}/c < p_{\perp}^{\text{jet}} < 166 \text{ GeV}/c$ ([/REF/CDF_2005_S6217184/d04-x01-y01](#))

- Differential jet shape ρ , $166 \text{ GeV}/c < p_{\perp}^{\text{jet}} < 186 \text{ GeV}/c$ (/REF/CDF_2005_S6217184/d04-x01-y02)
- Differential jet shape ρ , $186 \text{ GeV}/c < p_{\perp}^{\text{jet}} < 208 \text{ GeV}/c$ (/REF/CDF_2005_S6217184/d04-x01-y03)
- Differential jet shape ρ , $208 \text{ GeV}/c < p_{\perp}^{\text{jet}} < 229 \text{ GeV}/c$ (/REF/CDF_2005_S6217184/d05-x01-y01)
- Differential jet shape ρ , $229 \text{ GeV}/c < p_{\perp}^{\text{jet}} < 250 \text{ GeV}/c$ (/REF/CDF_2005_S6217184/d05-x01-y02)
- Differential jet shape ρ , $250 \text{ GeV}/c < p_{\perp}^{\text{jet}} < 277 \text{ GeV}/c$ (/REF/CDF_2005_S6217184/d05-x01-y03)
- Differential jet shape ρ , $277 \text{ GeV}/c < p_{\perp}^{\text{jet}} < 304 \text{ GeV}/c$ (/REF/CDF_2005_S6217184/d06-x01-y01)
- Differential jet shape ρ , $304 \text{ GeV}/c < p_{\perp}^{\text{jet}} < 340 \text{ GeV}/c$ (/REF/CDF_2005_S6217184/d06-x01-y02)
- Differential jet shape ρ , $340 \text{ GeV}/c < p_{\perp}^{\text{jet}} < 380 \text{ GeV}/c$ (/REF/CDF_2005_S6217184/d06-x01-y03)
- Integral jet shape Ψ , $37 \text{ GeV}/c < p_{\perp}^{\text{jet}} < 45 \text{ GeV}/c$ (/REF/CDF_2005_S6217184/d07-x01-y01)
- Integral jet shape Ψ , $45 \text{ GeV}/c < p_{\perp}^{\text{jet}} < 55 \text{ GeV}/c$ (/REF/CDF_2005_S6217184/d07-x01-y02)
- Integral jet shape Ψ , $55 \text{ GeV}/c < p_{\perp}^{\text{jet}} < 63 \text{ GeV}/c$ (/REF/CDF_2005_S6217184/d07-x01-y03)
- Integral jet shape Ψ , $63 \text{ GeV}/c < p_{\perp}^{\text{jet}} < 73 \text{ GeV}/c$ (/REF/CDF_2005_S6217184/d08-x01-y01)
- Integral jet shape Ψ , $73 \text{ GeV}/c < p_{\perp}^{\text{jet}} < 84 \text{ GeV}/c$ (/REF/CDF_2005_S6217184/d08-x01-y02)
- Integral jet shape Ψ , $84 \text{ GeV}/c < p_{\perp}^{\text{jet}} < 97 \text{ GeV}/c$ (/REF/CDF_2005_S6217184/d08-x01-y03)
- Integral jet shape Ψ , $97 \text{ GeV}/c < p_{\perp}^{\text{jet}} < 112 \text{ GeV}/c$ (/REF/CDF_2005_S6217184/d09-x01-y01)
- Integral jet shape Ψ , $112 \text{ GeV}/c < p_{\perp}^{\text{jet}} < 128 \text{ GeV}/c$ (/REF/CDF_2005_S6217184/d09-x01-y02)
- Integral jet shape Ψ , $128 \text{ GeV}/c < p_{\perp}^{\text{jet}} < 148 \text{ GeV}/c$ (/REF/CDF_2005_S6217184/d09-x01-y03)
- Integral jet shape Ψ , $148 \text{ GeV}/c < p_{\perp}^{\text{jet}} < 166 \text{ GeV}/c$ (/REF/CDF_2005_S6217184/d10-x01-y01)
- Integral jet shape Ψ , $166 \text{ GeV}/c < p_{\perp}^{\text{jet}} < 186 \text{ GeV}/c$ (/REF/CDF_2005_S6217184/d10-x01-y02)
- Integral jet shape Ψ , $186 \text{ GeV}/c < p_{\perp}^{\text{jet}} < 208 \text{ GeV}/c$ (/REF/CDF_2005_S6217184/d10-x01-y03)
- Integral jet shape Ψ , $208 \text{ GeV}/c < p_{\perp}^{\text{jet}} < 229 \text{ GeV}/c$ (/REF/CDF_2005_S6217184/d11-x01-y01)
- Integral jet shape Ψ , $229 \text{ GeV}/c < p_{\perp}^{\text{jet}} < 250 \text{ GeV}/c$ (/REF/CDF_2005_S6217184/d11-x01-y02)
- Integral jet shape Ψ , $250 \text{ GeV}/c < p_{\perp}^{\text{jet}} < 277 \text{ GeV}/c$ (/REF/CDF_2005_S6217184/d11-x01-y03)
- Integral jet shape Ψ , $277 \text{ GeV}/c < p_{\perp}^{\text{jet}} < 304 \text{ GeV}/c$ (/REF/CDF_2005_S6217184/d12-x01-y01)
- Integral jet shape Ψ , $304 \text{ GeV}/c < p_{\perp}^{\text{jet}} < 340 \text{ GeV}/c$ (/REF/CDF_2005_S6217184/d12-x01-y02)
- Integral jet shape Ψ , $340 \text{ GeV}/c < p_{\perp}^{\text{jet}} < 380 \text{ GeV}/c$ (/REF/CDF_2005_S6217184/d12-x01-y03)
- Integral jet shape, $\Psi(0.3/R)$, vs. p_{\perp}^{jet} (/REF/CDF_2005_S6217184/d13-x01-y01)

7.19 CDF_2006_S6450792 [58]

Inclusive jet cross section differential in p_{\perp}

Beams: $p\bar{p}$

Energies: (980.0, 980.0) GeV

Experiment: CDF (Tevatron Run 2)

Spires ID: [6450792](#)

Status: VALIDATED

Authors:

- Frank Siegert (frank.siegert@cern.ch)

References:

- Phys.Rev.D74:071103,2006
- DOI: [10.1103/PhysRevD.74.071103](https://doi.org/10.1103/PhysRevD.74.071103)
- arXiv: [hep-ex/0512020](https://arxiv.org/abs/hep-ex/0512020)

Run details:

- $p\bar{p} \rightarrow$ jets at 1960 GeV

Measurement of the inclusive jet cross section in ppbar interactions at $\sqrt{s} = 1.96$ TeV using 385 pb $^{-1}$ of data. The data cover the jet transverse momentum range from 61 to 620 GeV/c in $0.1 < |y| < 0.7$. This analysis has been updated with more data in more rapidity bins in CDF_2008_S7828950.

Histograms (1):

- Inclusive jet differential cross section (hadron level) ([/REF/CDF_2006_S6450792/d01-x01-y01](#))

7.20 CDF_2006_S6653332 [59]

b-jet cross section in $Z + \text{jets}$ events

Beams: $p\bar{p}$

Energies: (980.0, 980.0) GeV

Experiment: CDF (Tevatron Run 2)

Spires ID: [6653332](#)

Status: VALIDATED

Authors:

- Lars Sonnenschein (Lars.Sonnenschein@cern.ch)
- Steffen Schumann [js.schumann\(at\)thphys.uni-heidelberg.de](mailto:js.schumann(at)thphys.uni-heidelberg.de)

References:

- Phys.Rev.D.74:032008,2006
- DOI: [10.1103/PhysRevD.74.032008](https://doi.org/10.1103/PhysRevD.74.032008)
- arXiv: [hep-ex/0605099v2](https://arxiv.org/abs/hep-ex/0605099v2)

Run details:

- $Z + \text{jets}$ events at $\sqrt{s} = 1960$ GeV. Jets min p_{\perp} cut = 20 GeV, leptons min p_{\perp} cut = 10 GeV

Measurement of the b -jet cross section in events with Z boson in $p\bar{p}$ collisions at center-of-mass energy $\sqrt{s} = 1.96$ TeV. The data cover jet transverse momenta above 20 GeV and jet pseudorapidities in the range -1.5 to 1.5. Z bosons are identified in their electron and muon decay modes in an invariant dilepton mass range between 66 and 116 GeV.

Histograms (3):

- $\sigma(Z + b \text{ jet})$ ([/REF/CDF_2006_S6653332/d01-x01-y01](#))
- $\sigma(Z + b \text{ jet})/\sigma(Z)$ ([/REF/CDF_2006_S6653332/d02-x01-y01](#))
- $\sigma(Z + b \text{ jet})/\sigma(Z + \text{jet})$ ([/REF/CDF_2006_S6653332/d03-x01-y01](#))

7.21 CDF_2007_S7057202 [60]

CDF Run II inclusive jet cross-section using the kT algorithm

Beams: $\bar{p}p$

Energies: (980.0, 980.0) GeV

Experiment: CDF (Tevatron Run 2)

Spires ID: [7057202](#)

Status: VALIDATED

Authors:

- David Voong
- Frank Siegert (frank.siegert@cern.ch)

References:

- Phys.Rev.D75:092006,2007
- Erratum-ibid.D75:119901,2007
- FNAL-PUB 07/026-E
- hep-ex/0701051

Run details:

- p-pbar collisions at 1960 GeV. Jet p_{\perp} bins from 54 GeV to 700 GeV. Jet rapidity $< |2.1|$.

CDF Run II measurement of inclusive jet cross sections at a p-pbar collision energy of 1.96 TeV. Jets are reconstructed in the central part of the detector ($|y| < 2.1$) using the kT algorithm with an R parameter of 0.7. The minimum jet p_{\perp} considered is 54 GeV, with a maximum around 700 GeV. The inclusive jet p_{\perp} is plotted in bins of rapidity $|y| < 0.1$, $0.1 < |y| < 0.7$, $0.7 < |y| < 1.1$, $1.1 < |y| < 1.6$ and $1.6 < |y| < 2.1$.

Histograms (7):

- Inclusive jet cross-section vs p_T for $|\eta| < 0.1$, $D = 0.7$ ([/REF/CDF_2007_S7057202/d01-x01-y01](#))
- Inclusive jet cross-section vs p_T for $0.1 < |\eta| < 0.7$, $D = 0.7$ ([/REF/CDF_2007_S7057202/d02-x01-y01](#))
- Inclusive jet cross-section vs p_T for $0.7 < |\eta| < 1.1$, $D = 0.7$ ([/REF/CDF_2007_S7057202/d03-x01-y01](#))
- Inclusive jet cross-section vs p_T for $1.1 < |\eta| < 1.6$, $D = 0.7$ ([/REF/CDF_2007_S7057202/d04-x01-y01](#))
- Inclusive jet cross-section vs p_T for $1.6 < |\eta| < 2.1$, $D = 0.7$ ([/REF/CDF_2007_S7057202/d05-x01-y01](#))
- Inclusive jet cross-section vs p_T for $0.1 < |\eta| < 0.7$, $D = 0.5$ ([/REF/CDF_2007_S7057202/d06-x01-y01](#))
- Inclusive jet cross-section vs p_T for $0.1 < |\eta| < 0.7$, $D = 1.0$ ([/REF/CDF_2007_S7057202/d07-x01-y01](#))

7.22 CDF_2008_S7540469 [61]

Measurement of differential $Z/\gamma^* + \text{jet} + X$ cross sections

Beams: $p\bar{p}$

Energies: (980.0, 980.0) GeV

Experiment: CDF (Tevatron Run 2)

Spires ID: [7540469](#)

Status: VALIDATED

Authors:

- Frank Siegert (frank.siegert@cern.ch)

References:

- Phys.Rev.Lett.100:102001,2008
- arXiv: [0711.3717](#)

Run details:

- $p\bar{p} \rightarrow e^+e^- + \text{jets}$ at 1960 GeV. Needs mass cut on lepton pair to avoid photon singularity, looser than $66 < m_{ee} < 116$

Cross sections as a function of jet transverse momentum in 1 and 2 jet events, and jet multiplicity in $p\bar{p}$ collisions at $\sqrt{s} = 1.96$ TeV, based on an integrated luminosity of 1.7 fb^{-1} . The measurements cover the rapidity region $|y_{\text{jet}}| < 2.1$ and the transverse momentum range $p_{\perp}^{\text{jet}} > 30 \text{ GeV}/c$.

Histograms (3):

- Jet multiplicity ([/REF/CDF_2008_S7540469/d01-x01-y01](#))
- Jet p_{\perp} for inclusive $N_{\text{jet}} \geq 1$ ([/REF/CDF_2008_S7540469/d02-x01-y01](#))
- Jet p_{\perp} for inclusive $N_{\text{jet}} \geq 2$ ([/REF/CDF_2008_S7540469/d03-x01-y01](#))

7.23 CDF_2008_S7541902 [62]

Jet p_{\perp} and multiplicity distributions in $W + \text{jets}$ events

Beams: $p\bar{p}$

Energies: (980.0, 980.0) GeV

Experiment: CDF (Tevatron Run 2)

Spires ID: [7541902](#)

Status: UNVALIDATED

Authors:

- Ben Cooper (b.d.cooper@qmul.ac.uk)
- Emily Nurse (nurse@hep.ucl.ac.uk)

References:

- arXiv: [0711.4044](#)
- Phys.Rev.D77:011108,2008

Run details:

- Requires the process $p\bar{p} \rightarrow W \rightarrow e\nu$. Additional hard jets will also have to be included to get a good description. The LO process in Herwig is set with IPROC=1451.

Measurement of the cross section for W boson production in association with jets in $p\bar{p}$ collisions at $\sqrt{s} = 1.96$ TeV. The analysis uses 320 pb^{-1} of data collected with the CDF II detector. W bosons are identified in their $e\nu$ decay channel and jets are reconstructed using an $R < 0.4$ cone algorithm. For each $W + \geq n$ -jet sample (where $n = 1-4$) a measurement of $d\sigma(p\bar{p} \rightarrow W + \geq n \text{ jet})/dE_T(n^{\text{th}}\text{-jet}) \times \text{BR}(W \rightarrow e\nu)$ is made, where $dE_T(n^{\text{th}}\text{-jet})$ is the Et of the n^{th} -highest Et jet above 20 GeV. A measurement of the total cross section, $\sigma(p\bar{p} \rightarrow W + \geq n\text{-jet}) \times \text{BR}(W \rightarrow e\nu)$ with $E_T(n^{\text{th}} - \text{jet}) > 25$ GeV is also made. Both measurements are made for jets with $|\eta| < 2$ and for a limited region of the $W \rightarrow e\nu$ decay phase space; $|\eta^e| < 1.1$, $p_T^e > 20$ GeV, $p_T^\nu > 30$ GeV and $M_T > 20$ GeV. The cross sections are corrected for all detector effects and can be directly compared to particle level $W + \text{jet(s)}$ predictions. These measurements can be used to test and tune QCD predictions for the number of jets in and kinematics of $W + \text{jets}$ events.

Histograms (12):

- E_{\perp} of jet #1 ([/REF/CDF_2008_S7541902/d01-x01-y01](#))
- E_{\perp} of jet #2 ([/REF/CDF_2008_S7541902/d02-x01-y01](#))
- E_{\perp} of jet #3 ([/REF/CDF_2008_S7541902/d03-x01-y01](#))
- E_{\perp} of jet #4 ([/REF/CDF_2008_S7541902/d04-x01-y01](#))
- $\sigma(1 \text{ jets})/\sigma(0 \text{ jets})$ ([/REF/CDF_2008_S7541902/d05-x01-y01](#))

- $\sigma(2 \text{ jets})/\sigma(1 \text{ jets})$ ([/REF/CDF_2008_S7541902/d05-x01-y02](#))
- $\sigma(3 \text{ jets})/\sigma(2 \text{ jets})$ ([/REF/CDF_2008_S7541902/d05-x01-y03](#))
- $\sigma(4 \text{ jets})/\sigma(3 \text{ jets})$ ([/REF/CDF_2008_S7541902/d05-x01-y04](#))
- $\sigma(1 \text{ jets})$ ([/REF/CDF_2008_S7541902/d06-x01-y01](#))
- $\sigma(2 \text{ jets})$ ([/REF/CDF_2008_S7541902/d07-x01-y01](#))
- $\sigma(3 \text{ jets})$ ([/REF/CDF_2008_S7541902/d08-x01-y01](#))
- $\sigma(4 \text{ jets})$ ([/REF/CDF_2008_S7541902/d09-x01-y01](#))

7.24 CDF_2008_S7782535 [63]

CDF Run II b -jet shape paper

Beams: $\bar{p}p$

Energies: (980.0, 980.0) GeV

Experiment: CDF (Tevatron Run 2)

Spires ID: 7782535

Status: UNVALIDATED

Authors:

- Alison Lister ⟨ alister@fnal.gov ⟩
- Emily Nurse ⟨ nurse@hep.ucl.ac.uk ⟩
- Andy Buckley ⟨ andy.buckley@cern.ch ⟩

References:

- arXiv: [0806.1699](#)
- Phys.Rev.D78:072005,2008

Run details:

- Requires $2 \rightarrow 2$ QCD scattering processes. The minimum jet E_\perp is 52 GeV, so kinematic cuts on p_\perp may be required for statistical validity.

A measurement of the shapes of b -jets using 300 pb^{-1} of data obtained with CDF II in $p\bar{p}$ collisions at $\sqrt{s} = 1.96 \text{ TeV}$. The measured quantity is the average integrated jet shape, which is computed over an ensemble of jets. This quantity is expressed as $\Psi(r/R) = \langle \frac{p_\perp(0 \rightarrow r)}{p_\perp(0 \rightarrow R)} \rangle$, where $p_\perp(0 \rightarrow r)$ is the scalar sum of the transverse momenta of all objects inside a sub-cone of radius r around the jet axis. The integrated shapes are by definition normalized such that $\Psi(r/R = 1) = 1$. The measurement is done in bins of jet p_\perp in the range 52 to 300 GeV/c . The jets have $|\eta| < 0.7$. The b -jets are expected to be broader than inclusive jets. Moreover, b -jets containing a single b -quark are expected to be narrower than those containing a $b\bar{b}$ pair from gluon splitting.

Histograms (5):

- Integral jet shape Ψ for $52 < p_\perp < 80$ ([/REF/CDF_2008_S7782535/d01-x02-y01](#))
- Integral jet shape Ψ for $80 < p_\perp < 104$ ([/REF/CDF_2008_S7782535/d02-x02-y01](#))
- Integral jet shape Ψ for $104 < p_\perp < 142$ ([/REF/CDF_2008_S7782535/d03-x02-y01](#))
- Integral jet shape Ψ for $142 < p_\perp < 300$ ([/REF/CDF_2008_S7782535/d04-x02-y01](#))
- $1 - \Psi$ vs jet p_\perp ([/REF/CDF_2008_S7782535/d05-x01-y01](#))

7.25 CDF_2008_S7828950 [64]

CDF Run II inclusive jet cross-section using the Midpoint algorithm

Beams: $\bar{p}p$

Energies: (980.0, 980.0) GeV

Experiment: CDF (Tevatron Run 2)

Spires ID: 7828950

Status: VALIDATED

Authors:

- Craig Group ⟨group@fnal.gov⟩
- Frank Siegert ⟨frank.siegert@cern.ch⟩

References:

- arXiv: 0807.2204
- Phys.Rev.D78:052006,2008

Run details:

- Requires $2 \rightarrow 2$ QCD scattering processes. The minimum jet E_{\perp} is 62 GeV, so a cut on kinematic p_{\perp} may be required for good statistics.

Measurement of the inclusive jet cross section in $p\bar{p}$ collisions at $\sqrt{s} = 1.96$ TeV as a function of jet E_{\perp} , for $E_{\perp} > 62$ GeV. The data is collected by the CDF II detector and has an integrated luminosity of 1.13 fb^{-1} . The measurement was made using the cone-based Midpoint jet clustering algorithm in rapidity bins within $|y| < 2.1$. This measurement can be used to provide increased precision in PDFs at high parton momentum fraction x .

Histograms (5):

- $\eta < 0.1, R = 0.7$ (/REF/CDF_2008_S7828950/d01-x01-y01)
- $0.1 < \eta < 0.7, R = 0.7$ (/REF/CDF_2008_S7828950/d02-x01-y01)
- $0.7 < \eta < 1.1, R = 0.7$ (/REF/CDF_2008_S7828950/d03-x01-y01)
- $1.1 < \eta < 1.6, R = 0.7$ (/REF/CDF_2008_S7828950/d04-x01-y01)
- $1.6 < \eta < 2.1, R = 0.7$ (/REF/CDF_2008_S7828950/d05-x01-y01)

7.26 CDF_2008_S8093652 [65]

Dijet mass spectrum

Beams: $p\bar{p}$

Energies: (980.0, 980.0) GeV

Experiment: CDF (Tevatron Run 2)

Spires ID: [8093652](#)

Status: VALIDATED

Authors:

- Frank Siegert <frank.siegert@cern.ch>

References:

- arXiv: [0812.4036](#)

Run details:

- $p\bar{p} \rightarrow$ jets at 1960 GeV

Dijet mass spectrum from 0.2 TeV to 1.4 TeV in $p\bar{p}$ collisions at $\sqrt{s} = 1.96$ TeV, based on an integrated luminosity of 1.13 fb^{-1} .

Histograms (1):

- Dijet mass spectrum ([/REF/CDF_2008_S8093652/d01-x01-y01](#))

7.27 CDF_2008_S8095620 [66]

CDF Run II Z+b-jet cross section paper, 2 fb⁻¹

Beams: $p\bar{p}$

Energies: (980.0, 980.0) GeV

Experiment: CDF (Tevatron Run 2)

Spires ID: 8095620

Status: VALIDATED

Authors:

- Emily Nurse <nurse@hep.ucl.ac.uk>
- Steffen Schumann [js.schumann\(at\)thphys.uni-heidelberg.de](mailto:js.schumann(at)thphys.uni-heidelberg.de)

References:

- arXiv: [0812.4458](#)

Run details:

- Requires the process $p\bar{p} \rightarrow Z \rightarrow \ell\ell$, where ℓ is e or μ . Additional hard jets will also have to be included to get a good description.

Measurement of the b-jet production cross section for events containing a Z boson produced in $p\bar{p}$ collisions at $\sqrt{s} = 1.96$ TeV, using data corresponding to an integrated luminosity of 2 fb^{-1} collected by the CDF II detector at the Tevatron. Z bosons are selected in the electron and muon decay modes. Jets are considered with transverse energy $E_T > 20$ GeV and pseudorapidity $|\eta| < 1.5$. The ratio of the integrated $Z + \text{b-jet}$ cross section to the inclusive Z production cross section is measured differentially in jet E_T , jet η , Z -boson transverse momentum, number of jets, and number of b-jets. The first two measurements have an entry for each b-jet in the event, the last three measurements have one entry per event.

Histograms (6):

- ([/REF/CDF_2008_S8095620/d01-x01-y01](#))
- ([/REF/CDF_2008_S8095620/d02-x01-y01](#))
- ([/REF/CDF_2008_S8095620/d03-x01-y01](#))
- ([/REF/CDF_2008_S8095620/d04-x01-y01](#))
- ([/REF/CDF_2008_S8095620/d05-x01-y01](#))
- ([/REF/CDF_2008_S8095620/d06-x01-y01](#))

7.28 CDF_2009_NOTE_9936

CDF Run 2 min bias charged multiplicity analysis

Beams: $p\bar{p}$

Energies: (980.0, 980.0) GeV

Experiment: CDF (Tevatron Run 2)

Spires ID: None

Status: OBSOLETE

Authors:

- Holger Schulz (holger.schulz@physik.hu-berlin.de)

References:

- CDF public note 9936
- http://www-cdf.fnal.gov/physics/new/qcd/minbias_mult09/multpage.html

Run details:

- $p\bar{p}$ QCD interactions at 1960 GeV. Particles with $c\tau > 10$ mm should be set stable.

Niccolo Moggi's min bias analysis. Minimum bias events are used to measure the charged multiplicity distribution. The multiplicity distribution was not published in S8233977 but the numbers and a public note are available from the CDF website given above. Note: the systematic and statistical errors in Rivet were added in quadrature.

Histograms (1):

- MinBias Charged multiplicity in $p\bar{p}$ events at $\sqrt{s} = 1.96$ TeV ([/REF/CDF_2009_NOTE_9936/d01-x01-y01](#))

7.29 CDF_2009_S8233977 [67]

CDF Run 2 min bias cross-section analysis

Beams: $p\bar{p}$

Energies: (980.0, 980.0) GeV

Experiment: CDF (Tevatron Run 2)

Spires ID: [8233977](#)

Status: VALIDATED

Authors:

- Hendrik Hoeth (hendrik.hoeth@cern.ch)
- Niccolo' Moggi (niccolo.moggi@bo.infn.it)

References:

- Phys.Rev.D79:112005,2009
- DOI: [10.1103/PhysRevD.79.112005](https://doi.org/10.1103/PhysRevD.79.112005)
- arXiv: [0904.1098](https://arxiv.org/abs/0904.1098)

Run details:

- $p\bar{p}$ QCD interactions at 1960 GeV. Particles with $c\tau > 10$ mm should be set stable.

Niccolo Moggi's min bias analysis. Minimum bias events are used to measure the average track p_\perp vs. charged multiplicity, a track p_\perp distribution and an inclusive $\sum E_T$ distribution.

Histograms (3):

- track p_T , $|\eta| < 1$, $p_\perp > 0.4$ GeV ([/REF/CDF_2009_S8233977/d01-x01-y01](#))
- Mean track p_T vs multiplicity, $|\eta| < 1$, $p_\perp > 0.4$ GeV ([/REF/CDF_2009_S8233977/d02-x01-y01](#))
- $\sum E_T$, $|\eta| < 1$ ([/REF/CDF_2009_S8233977/d03-x01-y01](#))

7.30 CDF_2009_S8383952 [68]

Z rapidity measurement

Beams: $\bar{p}p$

Energies: (980.0, 980.0) GeV

Experiment: CDF (Tevatron Run 2)

Spires ID: 8383952

Status: VALIDATED

Authors:

- Frank Siegert <frank.siegert@cern.ch>

References:

- arXiv: [0908.3914](#)

Run details:

- $p\bar{p} \rightarrow e^+e^- + \text{jets}$ at 1960 GeV. Needs mass cut on lepton pair to avoid photon singularity, looser than $66 < m_{ee} < 116$ GeV

CDF measurement of the total cross section and rapidity distribution, $d\sigma/dy$, for $q\bar{q} \rightarrow \gamma^*/Z \rightarrow e^+e^-$ events in the Z boson mass region ($66 < M_{ee} < 116$ GeV/c 2) produced in $p\bar{p}$ collisions at $\sqrt{s} = 1.96$ TeV with 2.1 fb^{-1} of integrated luminosity.

Histograms (2):

- Total XS for $66 < M_{ee}/\text{GeV} < 116$ ([/REF/CDF_2009_S8383952/d01-x01-y01](#))
- e^+e^- pair rapidity ([/REF/CDF_2009_S8383952/d02-x01-y01](#))

7.31 CDF_2009_S8436959 [69]

Measurement of the inclusive isolated prompt photon cross-section

Beams: $\bar{p}p$

Energies: (980.0, 980.0) GeV

Experiment: CDF (Tevatron Run 2)

Spires ID: [8436959](#)

Status: VALIDATED

Authors:

- Frank Siegert [⟨frank.siegert@cern.ch⟩](mailto:frank.siegert@cern.ch)

References:

- arXiv: [0910.3623](#)

Run details:

- $\gamma + \text{jet}$ processes in ppbar collisions at $\sqrt{s} = 1960$ GeV. Minimum p_{\perp} cut on the photon in the analysis is 30 GeV.

A measurement of the cross section for the inclusive production of isolated photons. The measurement covers the pseudorapidity region $|\eta^{\gamma}| < 1.0$ and the transverse energy range $E_T^{\gamma} > 30$ GeV and is based on 2.5 fb^{-1} of integrated luminosity. The cross section is measured differential in $E_{\perp}(\gamma)$.

Histograms (1):

- Transverse energy of isolated prompt photon ([/REF/CDF_2009_S8436959/d01-x01-y01](#))

7.32 CDF_2010_S8591881_DY

CDF Run 2 underlying event in Drell-Yan

Beams: $\bar{p}p$

Energies: (980.0, 980.0) GeV

Experiment: CDF (Tevatron Run 2)

Spires ID: [8591881](#)

Status: VALIDATED

Authors:

- Hendrik Hoeth (hendrik.hoeth@cern.ch)

References:

- Phys.Rev.D82:034001,2010

Run details:

- ppbar collisions at 1960 GeV.
- Drell-Yan events with $Z/\gamma^* \rightarrow ee$ and $Z/\gamma^* \rightarrow \mu\mu$.
- A mass cut $m_{ll} > 70$ GeV can be applied on generator level.
- Particles with $c\tau > 10$ mm should be set stable.

Deepak Kar and Rick Field's measurement of the underlying event in Drell-Yan events. $Z \rightarrow ee$ and $Z \rightarrow \mu\mu$ events are selected using a Z mass window cut between 70 and 110 GeV. "Toward", "away" and "transverse" regions are defined in the same way as in the original (2001) CDF underlying event analysis. The reconstructed Z defines the ϕ direction of the toward region. The leptons are ignored after the Z has been reconstructed. Thus the region most sensitive to the underlying event is the toward region (the recoil jet is boosted into the away region).

Histograms (19):

- Toward region charged particle density ([/REF/CDF_2010_S8591881_DY/d01-x01-y01](#))
- Transverse region charged particle density ([/REF/CDF_2010_S8591881_DY/d01-x01-y02](#))
- Away region charged particle density ([/REF/CDF_2010_S8591881_DY/d01-x01-y03](#))
- TransMAX region charged particle density ([/REF/CDF_2010_S8591881_DY/d02-x01-y01](#))
- TransMIN region charged particle density ([/REF/CDF_2010_S8591881_DY/d02-x01-y02](#))
- TransDIF region charged particle density ([/REF/CDF_2010_S8591881_DY/d02-x01-y03](#))
- Toward region charged p_{\perp}^{sum} density ([/REF/CDF_2010_S8591881_DY/d03-x01-y01](#))
- Transverse region charged p_{\perp}^{sum} density ([/REF/CDF_2010_S8591881_DY/d03-x01-y02](#))

- Away region charged p_{\perp}^{sum} density ([/REF/CDF_2010_S8591881_DY/d03-x01-y03](#))
- TransMAX region charged p_{\perp}^{sum} density ([/REF/CDF_2010_S8591881_DY/d04-x01-y01](#))
- TransMIN region charged p_{\perp}^{sum} density ([/REF/CDF_2010_S8591881_DY/d04-x01-y02](#))
- TransDIF region charged p_{\perp}^{sum} density ([/REF/CDF_2010_S8591881_DY/d04-x01-y03](#))
- Toward region charged p_{\perp} average ([/REF/CDF_2010_S8591881_DY/d05-x01-y01](#))
- Transverse region charged p_{\perp} average ([/REF/CDF_2010_S8591881_DY/d05-x01-y02](#))
- Toward region charged p_{\perp} maximum ([/REF/CDF_2010_S8591881_DY/d06-x01-y01](#))
- Transverse region charged p_{\perp} maximum ([/REF/CDF_2010_S8591881_DY/d06-x01-y02](#))
- Average lepton-pair p_{\perp} versus charged multiplicity ([/REF/CDF_2010_S8591881_DY/d07-x01-y01](#))
- Average charged p_{\perp} vs charged multiplicity ([/REF/CDF_2010_S8591881_DY/d08-x01-y01](#))
- Average charged p_{\perp} vs charged multiplicity, $p_{\perp}(Z) < 10 \text{ GeV}$ ([/REF/CDF_2010_S8591881_DY/d09-x01-y01](#))

7.33 CDF_2010_S8591881_QCD

CDF Run 2 underlying event in leading jet events

Beams: $\bar{p}p$

Energies: (980.0, 980.0) GeV

Experiment: CDF (Tevatron Run 2)

Spires ID: 8591881

Status: VALIDATED

Authors:

- Hendrik Hoeth (hendrik.hoeth@cern.ch)

References:

- Phys.Rev.D82:034001,2010

Run details:

- $p\bar{p}$ QCD interactions at 1960 GeV. Particles with $c\tau > 10$ mm should be set stable. Several p_{\perp}^{\min} cutoffs are probably required to fill the profile histograms. $p_{\perp}^{\min} = 0$ (min bias), 10, 20, 50, 100, 150 GeV. The corresponding merging points are at $p_T = 0, 30, 50, 80, 130, 180$ GeV

Rick Field's measurement of the underlying event in leading jet events. If the leading jet of the event is within $|\eta| < 2$, the event is accepted and "toward", "away" and "transverse" regions are defined in the same way as in the original (2001) CDF underlying event analysis. The leading jet defines the ϕ direction of the toward region. The transverse regions are most sensitive to the underlying event.

Histograms (14):

- Toward region charged particle density ([/REF/CDF_2010_S8591881_QCD/d10-x01-y01](#))
- Transverse region charged particle density ([/REF/CDF_2010_S8591881_QCD/d10-x01-y02](#))
- Away region charged particle density ([/REF/CDF_2010_S8591881_QCD/d10-x01-y03](#))
- TransMAX region charged particle density ([/REF/CDF_2010_S8591881_QCD/d11-x01-y01](#))
- TransMIN region charged particle density ([/REF/CDF_2010_S8591881_QCD/d11-x01-y02](#))
- TransDIF region charged particle density ([/REF/CDF_2010_S8591881_QCD/d11-x01-y03](#))
- Toward region charged $\sum p_{\perp}$ density ([/REF/CDF_2010_S8591881_QCD/d12-x01-y01](#))
- Transverse region charged $\sum p_{\perp}$ density ([/REF/CDF_2010_S8591881_QCD/d12-x01-y02](#))
- Away region charged $\sum p_{\perp}$ density ([/REF/CDF_2010_S8591881_QCD/d12-x01-y03](#))
- TransMAX region charged $\sum p_{\perp}$ density ([/REF/CDF_2010_S8591881_QCD/d13-x01-y01](#))

- TransMIN region charged $\sum p_\perp$ density (`/REF/CDF_2010_S8591881_QCD/d13-x01-y02`)
- TransDIF region charged $\sum p_\perp$ density (`/REF/CDF_2010_S8591881_QCD/d13-x01-y03`)
- Transverse region charged p_\perp average (`/REF/CDF_2010_S8591881_QCD/d14-x01-y01`)
- Transverse region charged p_\perp max (`/REF/CDF_2010_S8591881_QCD/d15-x01-y01`)

7.34 CDF_2012_NOTE10874

CDF energy scan underlying event analysis

Beams: $p\bar{p}$

Energies: (150.0, 150.0), (450.0, 450.0), (980.0, 980.0) GeV

Experiment: CDF (Tevatron energy scan)

Status: VALIDATED

Authors:

- Rick Field rfield@phys.ufl.edu

References:

- CDF Note 10874

Run details:

- $p\bar{p}$ QCD interactions at 300, 900, and 1960 GeV. Particles with $c\tau > 10$ mm should be set stable.

In this analysis the behavior of the underlying event in hard scattering proton-antiproton collisions at 300 GeV, 900 GeV, and 1.96 TeV is studied. The 300 GeV and 900 GeV data are a result of the Tevatron Energy Scan which was performed just before the Tevatron was shut down. The energy ratio histograms can be created from different runs with a merging script available in the Rivet bin directory.

Histograms (18):

- Transverse Charged Particle Density (/REF/CDF_2012_NOTE10874/d01-x01-y01)
- Transverse Charged Particle Density (/REF/CDF_2012_NOTE10874/d01-x01-y02)
- Transverse Charged Particle Density (/REF/CDF_2012_NOTE10874/d01-x01-y03)
- Transverse Charged Particle Density (/REF/CDF_2012_NOTE10874/d01-x01-y04)
- Transverse Charged Particle Density (/REF/CDF_2012_NOTE10874/d01-x01-y05)
- Transverse Charged Particle Density (/REF/CDF_2012_NOTE10874/d01-x01-y06)
- Transverse Charged $\sum p_\perp$ density (/REF/CDF_2012_NOTE10874/d02-x01-y01)
- Transverse Charged $\sum p_\perp$ density (/REF/CDF_2012_NOTE10874/d02-x01-y02)
- Transverse Charged $\sum p_\perp$ density (/REF/CDF_2012_NOTE10874/d02-x01-y03)
- Transverse Charged $\sum p_\perp$ density (/REF/CDF_2012_NOTE10874/d02-x01-y04)
- Transverse Charged $\sum p_\perp$ density (/REF/CDF_2012_NOTE10874/d02-x01-y05)
- Transverse Charged $\sum p_\perp$ density (/REF/CDF_2012_NOTE10874/d02-x01-y06)

- Transverse Charged Particle Average p_{\perp} (/REF/CDF_2012_NOTE10874/d03-x01-y01)
- Transverse Charged Particle Average p_{\perp} (/REF/CDF_2012_NOTE10874/d03-x01-y02)
- Transverse Charged Particle Average p_{\perp} (/REF/CDF_2012_NOTE10874/d03-x01-y03)
- Transverse Charged Particle Average p_{\perp} (/REF/CDF_2012_NOTE10874/d03-x01-y04)
- Transverse Charged Particle Average p_{\perp} (/REF/CDF_2012_NOTE10874/d03-x01-y05)
- Transverse Charged Particle Average p_{\perp} (/REF/CDF_2012_NOTE10874/d03-x01-y06)

7.35 D0_1996_S3214044 [70]

Topological distributions of inclusive three- and four-jet events

Beams: $p\bar{p}$

Energies: (900.0, 900.0) GeV

Experiment: D0 (Tevatron Run 1)

Spires ID: 3214044

Status: UNVALIDATED - currently wrong jet algorithm!

Authors:

- Frank Siegert ⟨ frank.siegert@cern.ch ⟩

References:

- Phys.Rev.D53:6000-6016,1996
- DOI: [10.1103/PhysRevD.53.6000](https://doi.org/10.1103/PhysRevD.53.6000)
- arXiv: [hep-ex/9509005](https://arxiv.org/abs/hep-ex/9509005)

Run details:

- $p\bar{p} \rightarrow$ jets at 1800 GeV with minimum jet p_\perp in analysis = 20 GeV

The global topologies of inclusive three- and four-jet events produced in pbar p interactions are described. The three- and four-jet events are selected from data recorded by the D0 detector at the Fermilab Tevatron Collider operating at a center-of-mass energy of $\sqrt{s}=1800$ GeV. The studies also show that the topological distributions of the different subprocesses involving different numbers of quarks are very similar and reproduce the measured distributions well. The parton-shower Monte Carlo generators provide a less satisfactory description of the topologies of the three- and four-jet events.

Histograms (29):

- Energy fraction of hardest jet in 3-jet events ([/REF/D0_1996_S3214044/d01-x01-y01](#))
- Energy fraction of 3rd jet in 3-jet events ([/REF/D0_1996_S3214044/d02-x01-y01](#))
- Leading jet polar angle ([/REF/D0_1996_S3214044/d03-x01-y01](#))
- ψ^* angle ([/REF/D0_1996_S3214044/d04-x01-y01](#))
- Scaled invariant mass of jet pair ([/REF/D0_1996_S3214044/d05-x01-y01](#))
- Scaled invariant mass of jet pair ([/REF/D0_1996_S3214044/d06-x01-y01](#))
- Scaled invariant mass of jet pair ([/REF/D0_1996_S3214044/d07-x01-y01](#))
- Energy fraction of hardest jet in 4-jet events ([/REF/D0_1996_S3214044/d08-x01-y01](#))
- Energy fraction of 2nd jet in 4-jet events ([/REF/D0_1996_S3214044/d09-x01-y01](#))

- Energy fraction of 3rd jet in 4-jet events (/REF/D0_1996_S3214044/d10-x01-y01)
- Energy fraction of 4th jet in 4-jet events (/REF/D0_1996_S3214044/d11-x01-y01)
- Polar angle of leading jet (/REF/D0_1996_S3214044/d12-x01-y01)
- Polar angle of 2nd jet (/REF/D0_1996_S3214044/d13-x01-y01)
- Polar angle of 3rd jet (/REF/D0_1996_S3214044/d14-x01-y01)
- Polar angle of 4th jet (/REF/D0_1996_S3214044/d15-x01-y01)
- Space angle between jet pair (/REF/D0_1996_S3214044/d16-x01-y01)
- Space angle between jet pair (/REF/D0_1996_S3214044/d17-x01-y01)
- Space angle between jet pair (/REF/D0_1996_S3214044/d18-x01-y01)
- Space angle between jet pair (/REF/D0_1996_S3214044/d19-x01-y01)
- Space angle between jet pair (/REF/D0_1996_S3214044/d20-x01-y01)
- Space angle between jet pair (/REF/D0_1996_S3214044/d21-x01-y01)
- Scaled invariant mass of jet pair (/REF/D0_1996_S3214044/d22-x01-y01)
- Scaled invariant mass of jet pair (/REF/D0_1996_S3214044/d23-x01-y01)
- Scaled invariant mass of jet pair (/REF/D0_1996_S3214044/d24-x01-y01)
- Scaled invariant mass of jet pair (/REF/D0_1996_S3214044/d25-x01-y01)
- Scaled invariant mass of jet pair (/REF/D0_1996_S3214044/d26-x01-y01)
- Scaled invariant mass of jet pair (/REF/D0_1996_S3214044/d27-x01-y01)
- Angle between jet planes (/REF/D0_1996_S3214044/d28-x01-y01)
- Angle between jet planes (/REF/D0_1996_S3214044/d29-x01-y01)

7.36 D0_1996_S3324664 [71]

Azimuthal decorrelation of jets widely separated in rapidity

Beams: $p\bar{p}$

Energies: (900.0, 900.0) GeV

Experiment: D0 (Tevatron Run 1)

Spires ID: 3324664

Status: UNVALIDATED - currently uses wrong jet algorithm!

Authors:

- Frank Siegert <frank.siegert@cern.ch>

References:

- Phys.Rev.Lett.77:595-600,1996
- DOI: [10.1103/PhysRevLett.77.595](https://doi.org/10.1103/PhysRevLett.77.595)
- arXiv: [hep-ex/9603010](https://arxiv.org/abs/hep-ex/9603010)

Run details:

- $p\bar{p} \rightarrow$ jets at 1800 GeV

First measurement of the azimuthal decorrelation between jets with pseudorapidity separation up to five units. The data were accumulated using the D0 detector during Tevatron Run 1 at $\sqrt{s} = 1.8$ TeV.

Histograms (5):

- Pseudorapidity difference of the two opposite jets ([/REF/D0_1996_S3324664/d01-x01-y01](#))
- Azimuthal angle difference for $0 < \Delta\eta < 2$ ([/REF/D0_1996_S3324664/d02-x01-y01](#))
- Azimuthal angle difference for $2 < \Delta\eta < 4$ ([/REF/D0_1996_S3324664/d02-x01-y02](#))
- Azimuthal angle difference for $4 < \Delta\eta < 6$ ([/REF/D0_1996_S3324664/d02-x01-y03](#))
- Correlation of the jets ([/REF/D0_1996_S3324664/d03-x01-y01](#))

7.37 D0_2000_I499943 [72]

The $b\bar{b}$ production cross-section and angular correlations

Beams: $p\bar{p}$

Energies: (900.0, 900.0) GeV

Experiment: D0 (Tevatron Run 1)

Inspire ID: 499943

Status: UNVALIDATED

Authors:

- Simone Amoroso (amoroso@cern.ch)

References:

- Phys.Lett.B487:264-272,2000
- DOI: [10.1016/PhysLettB.487.264](https://doi.org/10.1016/PhysLettB.487.264)
- arXiv: [hep-ex/9905024v2](https://arxiv.org/abs/hep-ex/9905024v2)

Run details:

- $p\bar{p}$ dijet events at 1.8 TeV, with a minimum p_T of 12 GeV.

Measurements of the $b\bar{b}$ production cross-section and angular correlations using the D0 detector at the Fermilab Tevatron $p\bar{p}$ collider operating at $\sqrt{s} = 1.8$ TeV. The b quark production cross-section and the angular correlations between b -quark pairs, for $|y(b)| < 1.0$ and $p_T(b) > 6$ GeV/ c , are extracted from single muon and dimuon data samples.

Histograms (2):

- Leading muon p_T spectrum for $b\bar{b}$ production ([/REF/D0_2000_I499943/d01-x01-y01](#))
- $\Delta\phi_{\mu\mu}$ spectrum for $b\bar{b}$ production ([/REF/D0_2000_I499943/d03-x01-y01](#))

7.38 D0_2000_S4480767 [73]

Transverse momentum of the W boson

Beams: $\bar{p}p$

Energies: (900.0, 900.0) GeV

Experiment: D0 (Tevatron Run 1)

Spires ID: 4480767

Status: VALIDATED

Authors:

- Frank Siegert <frank.siegert@cern.ch>

References:

- Phys.Lett. B513 (2001) 292-300
- DOI: [10.1016/S0370-2693\(01\)00628-1](https://doi.org/10.1016/S0370-2693(01)00628-1)
- arXiv: [hep-ex/0010026](https://arxiv.org/abs/hep-ex/0010026)

Run details:

- Production of W+ and W- decaying into the electron channel.

Measurement of the differential cross section for W boson production as a function of its transverse momentum. The data were collected by the D0 experiment at the Fermilab Tevatron Collider during 1994-1995 and correspond to an integrated luminosity of 85 pb^{-1} .

Histograms (1):

- W boson pT ([/REF/D0_2000_S4480767/d01-x01-y01](#))

7.39 D0_2001_S4674421 [74]

Tevatron Run I differential W/Z boson cross-section analysis

Beams: $p\bar{p}$

Energies: (900.0, 900.0) GeV

Experiment: D0 (Tevatron Run 1)

Spires ID: 4674421

Status: VALIDATED

Authors:

- Lars Sonnenschein (Lars.Sonnenschein@cern.ch)

References:

- Phys.Lett.B517:299-308,2001
- DOI: [10.1016/S0370-2693\(01\)01020-6](https://doi.org/10.1016/S0370-2693(01)01020-6)
- arXiv: [hep-ex/0107012v2](https://arxiv.org/abs/hep-ex/0107012v2)

Run details:

- W/Z events with decays to first generation leptons, in $p\bar{p}$ collisions at $\sqrt{s} = 1800$ GeV

Measurement of differential W/Z boson cross section and ratio in $p\bar{p}$ collisions at center-of-mass energy $\sqrt{s} = 1.8$ TeV. The data cover electrons and neutrinos in a pseudorapidity range of -2.5 to 2.5.

Histograms (3):

- $d\sigma/dp_{\perp}(W)$ (/REF/D0_2001_S4674421/d01-x01-y01)
- $d\sigma/dp_{\perp}(Z)$ (/REF/D0_2001_S4674421/d01-x01-y02)
- W/Z differential cross section ratio (/REF/D0_2001_S4674421/d02-x01-y01)

7.40 D0_2004_S5992206 [75]

Run II jet azimuthal decorrelation analysis

Beams: $\bar{p}p$

Energies: (980.0, 980.0) GeV

Experiment: D0 (Tevatron Run 2)

Spires ID: 5992206

Status: VALIDATED

Authors:

- Lars Sonnenschein ⟨ lars.sonnenschein@cern.ch ⟩

References:

- Phys. Rev. Lett., 94, 221801 (2005)
- arXiv: [hep-ex/0409040](#)

Run details:

- QCD events in ppbar interactions at $\sqrt{s} = 1960$ GeV.

Correlations in the azimuthal angle between the two largest p_{\perp} jets have been measured using the D0 detector in ppbar collisions at 1960 GeV. The analysis is based on an inclusive dijet event sample in the central rapidity region. The correlations are determined for four different p_{\perp} intervals.

Histograms (4):

- Jet–jet azimuthal angle, $p_{\perp}^{\max} \in [75, 100]$ GeV ([/REF/D0_2004_S5992206/d01-x02-y01](#))
- Jet–jet azimuthal angle, $p_{\perp}^{\max} \in [100..130]$ GeV ([/REF/D0_2004_S5992206/d02-x02-y01](#))
- Jet–jet azimuthal angle, $p_{\perp}^{\max} \in [130..180]$ GeV ([/REF/D0_2004_S5992206/d03-x02-y01](#))
- Jet–jet azimuthal angle, $p_{\perp}^{\max} > 180$ GeV ([/REF/D0_2004_S5992206/d04-x02-y01](#))

7.41 D0_2006_S6438750 [76]

Inclusive isolated photon cross-section, differential in p_{\perp} (gamma)

Beams: $\bar{p}p$

Energies: (980.0, 980.0) GeV

Experiment: D0 (Tevatron Run 2)

Spires ID: 6438750

Status: VALIDATED

Authors:

- Andy Buckley <andy.buckley@cern.ch>
- Gavin Hesketh <gavin.hesketh@cern.ch>
- Frank Siegert <frank.siegert@cern.ch>

References:

- Phys.Lett.B639:151-158,2006, Erratum-ibid.B658:285-289,2008
- DOI: [10.1016/j.physletb.2006.04.048](https://doi.org/10.1016/j.physletb.2006.04.048)
- arXiv: [hep-ex/0511054](https://arxiv.org/abs/hep-ex/0511054)

Run details:

- ppbar collisions at $\sqrt{s} = 1960$ GeV. Requires gamma + jet (q,qbar,g) hard processes, which for Pythia 6 means MSEL=10 for with MSUB indices 14, 18, 29, 114, 115 enabled.

Measurement of differential cross section for inclusive production of isolated photons in p pbar collisions at $\sqrt{s} = 1.96$ TeV with the DØdetector at the Fermilab Tevatron collider. The photons span transverse momenta 23–300 GeV and have pseudorapidity $|\eta| < 0.9$. Isolated direct photons are probes of pQCD via the annihilation ($q\bar{q} \rightarrow \gamma g$) and quark-gluon Compton scattering ($qg \rightarrow \gamma q$) processes, the latter of which is also sensitive to the gluon PDF. The initial state radiation / resummation formalisms are sensitive to the resulting photon p_{\perp} spectrum

Histograms (1):

- p_{\perp} spectrum for leading photon (/REF/D0_2006_S6438750/d01-x01-y01)

7.42 D0_2007_S7075677 [77]

$Z/\gamma^* + X$ cross-section shape, differential in $y(Z)$

Beams: $\bar{p}p$

Energies: (980.0, 980.0) GeV

Experiment: D0 (Tevatron Run 2)

Spires ID: [7075677](#)

Status: VALIDATED

Authors:

- Andy Buckley <andy.buckley@cern.ch>
- Gavin Hesketh <ghesketh@fnal.gov>
- Frank Siegert <frank.siegert@cern.ch>

References:

- Phys.Rev.D76:012003,2007
- arXiv: [hep-ex/0702025](#)

Run details:

- Drell-Yan $p\bar{p} \rightarrow Z/\gamma^* + \text{jets}$ events at $\sqrt{s} = 1960$ GeV. Needs mass cut on lepton pair to avoid photon singularity, looser than $71 < m_{ee} < 111$ GeV

Cross sections as a function of di-electron rapidity $p\bar{p}$ collisions at $\sqrt{s} = 1.96$ TeV, based on an integrated luminosity of 0.4 fb^{-1} .

Histograms (1):

- Inclusive Z boson rapidity ([/REF/D0_2007_S7075677/d01-x01-y01](#))

7.43 D0_2008_S6879055 [78]

Measurement of the ratio $\sigma(Z/\gamma^* + n \text{ jets})/\sigma(Z/\gamma^*)$

Beams: $p\bar{p}$

Energies: (980.0, 980.0) GeV

Experiment: D0 (Tevatron Run 2)

Spires ID: [6879055](#)

Status: VALIDATED

Authors:

- Giulio Lenzi
- Frank Siegert (frank.siegert@cern.ch)

References:

- hep-ex/0608052

Run details:

- $p\bar{p} \rightarrow e^+e^- + \text{jets}$ at 1960 GeV. Needs mass cut on lepton pair to avoid photon singularity, looser than $75 < m_{ee} < 105$ GeV.

Cross sections as a function of p_\perp of the three leading jets and n -jet cross section ratios in $p\bar{p}$ collisions at $\sqrt{s} = 1.96$ TeV, based on an integrated luminosity of 0.4 fb^{-1} .

Histograms (4):

- Inclusive jet multiplicity ([/REF/D0_2008_S6879055/d01-x01-y01](#))
- p_\perp of 1st jet (not detector-corrected!) ([/REF/D0_2008_S6879055/d02-x01-y01](#))
- p_\perp of 2nd jet (not detector-corrected!) ([/REF/D0_2008_S6879055/d03-x01-y01](#))
- p_\perp of 3rd jet (not detector-corrected!) ([/REF/D0_2008_S6879055/d04-x01-y01](#))

7.44 D0_2008_S7554427 [79]

$Z/\gamma^* + X$ cross-section shape, differential in $p_\perp(Z)$

Beams: $\bar{p}p$

Energies: (980.0, 980.0) GeV

Experiment: D0 (Tevatron Run 2)

Spires ID: [7554427](#)

Status: VALIDATED

Authors:

- Andy Buckley <andy.buckley@cern.ch>
- Frank Siegert <frank.siegert@cern.ch>

References:

- arXiv: [0712.0803](#)

Run details:

- * $p\bar{p} \rightarrow e^+e^- + \text{jets}$ at 1960 GeV.
- Needs mass cut on lepton pair to avoid photon singularity, looser than $40 < m_{ee} < 200$ GeV.

Cross sections as a function of p_\perp of the vector boson inclusive and in forward region ($|y| > 2$, $p_\perp < 30$ GeV) in the di-electron channel in $p\bar{p}$ collisions at $\sqrt{s} = 1.96$ TeV, based on an integrated luminosity of 0.98 fb^{-1} .

Histograms (2):

- Z boson pT ([/REF/D0_2008_S7554427/d01-x01-y01](#))
- Z boson pT (forward region only) ([/REF/D0_2008_S7554427/d03-x01-y01](#))

7.45 D0_2008_S7662670 [80]

Measurement of D0 Run II differential jet cross sections

Beams: $p\bar{p}$

Energies: (980.0, 980.0) GeV

Experiment: D0 (Tevatron Run 2)

Spires ID: [7662670](#)

Status: VALIDATED

Authors:

- Andy Buckley <andy.buckley@cern.ch>
- Gavin Hesketh <gavin.hesketh@cern.ch>

References:

- Phys.Rev.Lett.101:062001,2008
- DOI: [10.1103/PhysRevLett.101.062001](https://doi.org/10.1103/PhysRevLett.101.062001)
- arXiv: [0802.2400v3](https://arxiv.org/abs/0802.2400v3)

Run details:

- QCD events at $\sqrt{s} = 1960$ GeV. A p_T^{\min} cut is probably necessary since the lowest jet p_T bin is at 50 GeV

Measurement of the inclusive jet cross section in $p\bar{p}$ collisions at center-of-mass energy $\sqrt{s} = 1.96$ TeV. The data cover jet transverse momenta from 50–600 GeV and jet rapidities in the range -2.4 to 2.4.

Histograms (6):

- Inclusive jet p_T , $0.0 < |y| < 0.4$ ([/REF/D0_2008_S7662670/d01-x01-y01](#))
- Inclusive jet p_T , $0.4 < |y| < 0.8$ ([/REF/D0_2008_S7662670/d02-x01-y01](#))
- Inclusive jet p_T , $0.8 < |y| < 1.2$ ([/REF/D0_2008_S7662670/d03-x01-y01](#))
- Inclusive jet p_T , $1.2 < |y| < 1.6$ ([/REF/D0_2008_S7662670/d04-x01-y01](#))
- Inclusive jet p_T , $1.6 < |y| < 2.0$ ([/REF/D0_2008_S7662670/d05-x01-y01](#))
- Inclusive jet p_T , $2.0 < |y| < 2.4$ ([/REF/D0_2008_S7662670/d06-x01-y01](#))

7.46 D0_2008_S7719523 [81]

Isolated γ + jet cross-sections, differential in $p_{\perp}(\gamma)$ for various y bins

Beams: $\bar{p}p$

Energies: (980.0, 980.0) GeV

Experiment: D0 (Tevatron Run 2)

Spires ID: [7719523](#)

Status: VALIDATED

Authors:

- Andy Buckley <andy.buckley@cern.ch>
- Gavin Hesketh <gavin.hesketh@cern.ch>
- Frank Siegert <frank.siegert@cern.ch>

References:

- Phys.Lett.B666:435-445,2008
- DOI: [10.1016/j.physletb.2008.06.076](https://doi.org/10.1016/j.physletb.2008.06.076)
- arXiv: [0804.1107v2](https://arxiv.org/abs/0804.1107v2)

Run details:

- Produce only gamma + jet (q, \bar{q}, g) hard processes (for Pythia 6, this means MSEL=10 and MSUB indices 14, 29 & 115 enabled). The lowest bin edge is at 30 GeV, so a kinematic p_{\perp} cut is probably required to fill the histograms.

The process $p\bar{p} \rightarrow$ photon + jet + X as studied by the D0 detector at the Fermilab Tevatron collider at center-of-mass energy $\sqrt{s} = 1.96$ TeV. Photons are reconstructed in the central rapidity region $|y_{\gamma}| < 1.0$ with transverse momenta in the range 30–400 GeV, while jets are reconstructed in either the central $|y_{\text{jet}}| < 0.8$ or forward $1.5 < |y_{\text{jet}}| < 2.5$ rapidity intervals with $p_{\perp}^{\text{jet}} > 15$ GeV. The differential cross section $d^3\sigma/dp_{\perp}^{\gamma}dy_{\gamma}dy_{\text{jet}}$ is measured as a function of p_{\perp}^{γ} in four regions, differing by the relative orientations of the photon and the jet. MC predictions have trouble with simultaneously describing the measured normalization and p_{\perp}^{γ} dependence of the cross section in any of the four measured regions.

Histograms (10):

- Leading photon p_{\perp} (central jets, same-sign rapidity) ([/REF/D0_2008_S7719523/d01-x01-y01](#))
- Leading photon p_{\perp} (central jets, opp-sign rapidity) ([/REF/D0_2008_S7719523/d02-x01-y01](#))
- Leading photon p_{\perp} (forward jets, same-sign rapidity) ([/REF/D0_2008_S7719523/d03-x01-y01](#))
- Leading photon p_{\perp} (forward jets, opp-sign rapidity) ([/REF/D0_2008_S7719523/d04-x01-y01](#))
- Differential Cross Section Ratio $\frac{d\sigma(|y^{\text{jet}}|<0.8, y^{\gamma} \cdot y^{\text{jet}} < 0)}{d\sigma(|y^{\text{jet}}|<0.8, y^{\gamma} \cdot y^{\text{jet}} > 0)}$ ([/REF/D0_2008_S7719523/d05-x01-y01](#))

- Differential Cross Section Ratio $\frac{d\sigma(|y^{\text{jet}}|<0.8, y^\gamma \cdot y^{\text{jet}}>0)}{d\sigma(1.5<|y^{\text{jet}}|<2.5, y^\gamma \cdot y^{\text{jet}}>0)}$ ([/REF/D0_2008_S7719523/d06-x01-y01](#))
- Differential Cross Section Ratio $\frac{d\sigma(|y^{\text{jet}}|<0.8, y^\gamma \cdot y^{\text{jet}}>0)}{d\sigma(1.5<|y^{\text{jet}}|<2.5, y^\gamma \cdot y^{\text{jet}}<0)}$ ([/REF/D0_2008_S7719523/d07-x01-y01](#))
- Differential Cross Section Ratio $\frac{d\sigma(1.5<|y^{\text{jet}}|<2.5, y^\gamma \cdot y^{\text{jet}}<0)}{d\sigma(1.5<|y^{\text{jet}}|<2.5, y^\gamma \cdot y^{\text{jet}}>0)}$ ([/REF/D0_2008_S7719523/d08-x01-y01](#))
- Differential Cross Section Ratio $\frac{d\sigma(|y^{\text{jet}}|<0.8, y^\gamma \cdot y^{\text{jet}}<0)}{d\sigma(1.5<|y^{\text{jet}}|<2.5, y^\gamma \cdot y^{\text{jet}}>0)}$ ([/REF/D0_2008_S7719523/d09-x01-y01](#))
- Differential Cross Section Ratio $\frac{d\sigma(|y^{\text{jet}}|<0.8, y^\gamma \cdot y^{\text{jet}}<0)}{d\sigma(1.5<|y^{\text{jet}}|<2.5, y^\gamma \cdot y^{\text{jet}}<0)}$ ([/REF/D0_2008_S7719523/d10-x01-y01](#))

7.47 D0_2008_S7837160 [82]

Measurement of W charge asymmetry from D0 Run II

Beams: $\bar{p}p$

Energies: (980.0, 980.0) GeV

Experiment: D0 (Tevatron Run 2)

Spires ID: [7837160](#)

Status: VALIDATED

Authors:

- Andy Buckley <andy.buckley@cern.ch>
- Gavin Hesketh <gavin.hesketh@cern.ch>

References:

- Phys.Rev.Lett.101:211801,2008
- DOI: [10.1103/PhysRevLett.101.211801](https://doi.org/10.1103/PhysRevLett.101.211801)
- arXiv: [0807.3367v1](https://arxiv.org/abs/0807.3367v1)

Run details:

- * Event type: W production with decay to $e\nu_e$ only
- for Pythia 6: MSEL = 12, MDME(206,1) = 1
- Energy: 1.96 TeV

Measurement of the electron charge asymmetry in $p\bar{p} \rightarrow W + X \rightarrow e\nu_e + X$ events at a center of mass energy of 1.96 TeV. The asymmetry is measured as a function of the electron transverse momentum and pseudorapidity in the interval (-3.2, 3.2). This data is sensitive to proton parton distribution functions due to the valence asymmetry in the incoming quarks which produce the W. Initial state radiation should also affect the p_\perp distribution.

Histograms (3):

- W charge asymmetry for $25 > E_\perp > 35$ GeV ([/REF/D0_2008_S7837160/d01-x01-y01](#))
- W charge asymmetry for $E_\perp > 35$ GeV ([/REF/D0_2008_S7837160/d01-x01-y02](#))
- W charge asymmetry for $E_\perp > 25$ GeV ([/REF/D0_2008_S7837160/d01-x01-y03](#))

7.48 D0_2008_S7863608 [83]

Measurement of differential $Z/\gamma^* + \text{jet} + X$ cross sections

Beams: $\bar{p}p$

Energies: (980.0, 980.0) GeV

Experiment: D0 (Tevatron Run 2)

Spires ID: [7863608](#)

Status: VALIDATED

Authors:

- Andy Buckley <andy.buckley@cern.ch>
- Gavin Hesketh <gavin.hesketh@fnal.gov>
- Frank Siegert <frank.siegert@cern.ch>

References:

- Phys.Lett. B669 (2008) 278-286
- DOI: [10.1016/j.physletb.2008.09.060](https://doi.org/10.1016/j.physletb.2008.09.060)
- arXiv: [0808.1296](https://arxiv.org/abs/0808.1296)

Run details:

- $p\bar{p} \rightarrow \mu^+\mu^- + \text{jets}$ at 1960 GeV. Needs mass cut on lepton pair to avoid photon singularity, looser than $65 < m_{\mu\mu} < 115$ GeV.

Cross sections as a function of p_\perp and rapidity of the boson and p_\perp and rapidity of the leading jet in the di-muon channel in $p\bar{p}$ collisions at $\sqrt{s} = 1.96$ TeV, based on an integrated luminosity of 1.0 fb^{-1} .

Histograms (9):

- Differential cross section in leading jet p_\perp ([/REF/D0_2008_S7863608/d01-x01-y01](#))
- Differential cross section in leading jet p_\perp ([/REF/D0_2008_S7863608/d01-x01-y02](#))
- Differential cross section in leading jet rapidity ([/REF/D0_2008_S7863608/d02-x01-y01](#))
- Differential cross section in leading jet rapidity ([/REF/D0_2008_S7863608/d02-x01-y02](#))
- Differential cross section in Z/γ^* p_\perp ([/REF/D0_2008_S7863608/d03-x01-y01](#))
- Differential cross section in Z/γ^* p_\perp ([/REF/D0_2008_S7863608/d03-x01-y02](#))
- Differential cross section in Z/γ^* rapidity ([/REF/D0_2008_S7863608/d04-x01-y01](#))
- Differential cross section in Z/γ^* rapidity ([/REF/D0_2008_S7863608/d04-x01-y02](#))
- Total $Z + \text{jet}$ cross section ([/REF/D0_2008_S7863608/d05-x01-y01](#))

7.49 D0_2009_S8202443 [84]

$Z/\gamma^* + \text{jet} + X$ cross sections differential in p_\perp (jet 1,2,3)

Beams: $p\bar{p}$

Energies: (980.0, 980.0) GeV

Experiment: D0 (Tevatron Run 2)

Spires ID: [8202443](#)

Status: VALIDATED

Authors:

- Frank Siegert (frank.siegert@cern.ch)

References:

- arXiv: [0903.1748](#)

Run details:

- $p\bar{p} \rightarrow e^+e^- + \text{jets}$ at 1960 GeV. Needs mass cut on lepton pair to avoid photon singularity, looser than $65 < m_{ee} < 115$ GeV.

Cross sections as a function of p_\perp of the three leading jets in $Z/\gamma^*(\rightarrow e^+e^-) + \text{jet} + X$ production in $p\bar{p}$ collisions at $\sqrt{s} = 1.96$ TeV, based on an integrated luminosity of 1.0 fb^{-1} .

Histograms (6):

- pT of 1st jet (constrained electrons) ([/REF/D0_2009_S8202443/d01-x01-y01](#))
- pT of 1st jet ([/REF/D0_2009_S8202443/d02-x01-y01](#))
- pT of 2nd jet (constrained electrons) ([/REF/D0_2009_S8202443/d03-x01-y01](#))
- pT of 2nd jet ([/REF/D0_2009_S8202443/d04-x01-y01](#))
- pT of 3rd jet (constrained electrons) ([/REF/D0_2009_S8202443/d05-x01-y01](#))
- pT of 3rd jet ([/REF/D0_2009_S8202443/d06-x01-y01](#))

7.50 D0_2009_S8320160 [85]

Dijet angular distributions

Beams: $p\bar{p}$

Energies: (980.0, 980.0) GeV

Experiment: D0 (Tevatron Run 2)

Spires ID: 8320160

Status: VALIDATED

Authors:

- Frank Siegert [⟨frank.siegert@cern.ch⟩](mailto:frank.siegert@cern.ch)

References:

- arXiv: [0906.4819](#)

Run details:

- $p\bar{p} \rightarrow$ jets at 1960 GeV

Dijet angular distributions in different bins of dijet mass from 0.25 TeV to above 1.1 TeV in $p\bar{p}$ collisions at $\sqrt{s} = 1.96$ TeV, based on an integrated luminosity of 0.7 fb^{-1} .

Histograms (10):

- Dijet angular distribution in $0.25 < M_{jj}/\text{TeV} < 0.3$ ([/REF/D0_2009_S8320160/d01-x01-y01](#))
- Dijet angular distribution in $0.3 < M_{jj}/\text{TeV} < 0.4$ ([/REF/D0_2009_S8320160/d02-x01-y01](#))
- Dijet angular distribution in $0.4 < M_{jj}/\text{TeV} < 0.5$ ([/REF/D0_2009_S8320160/d03-x01-y01](#))
- Dijet angular distribution in $0.5 < M_{jj}/\text{TeV} < 0.6$ ([/REF/D0_2009_S8320160/d04-x01-y01](#))
- Dijet angular distribution in $0.6 < M_{jj}/\text{TeV} < 0.7$ ([/REF/D0_2009_S8320160/d05-x01-y01](#))
- Dijet angular distribution in $0.7 < M_{jj}/\text{TeV} < 0.8$ ([/REF/D0_2009_S8320160/d06-x01-y01](#))
- Dijet angular distribution in $0.8 < M_{jj}/\text{TeV} < 0.9$ ([/REF/D0_2009_S8320160/d07-x01-y01](#))
- Dijet angular distribution in $0.9 < M_{jj}/\text{TeV} < 1.0$ ([/REF/D0_2009_S8320160/d08-x01-y01](#))
- Dijet angular distribution in $1.0 < M_{jj}/\text{TeV} < 1.1$ ([/REF/D0_2009_S8320160/d09-x01-y01](#))
- Dijet angular distribution in $M_{jj}/\text{TeV} > 1.1$ ([/REF/D0_2009_S8320160/d10-x01-y01](#))

7.51 D0_2009_S8349509 [86]

Z+jets angular distributions

Beams: $\bar{p}p$

Energies: (980.0, 980.0) GeV

Experiment: D0 (Tevatron Run 2)

Spires ID: [8349509](#)

Status: VALIDATED

Authors:

- Frank Siegert (frank.siegert@cern.ch)

References:

- arXiv: [0907.4286](#)

Run details:

- $p\bar{p} \rightarrow \mu^+\mu^- + \text{jets}$ at 1960 GeV. Needs mass cut on lepton pair to avoid photon singularity, looser than $65 < m_{ee} < 115$ GeV.

First measurements at a hadron collider of differential cross sections for $Z(\rightarrow \mu\mu) + \text{jet} + X$ production in $\Delta\phi(Z, j)$, $|\Delta y(Z, j)|$ and $|y_{\text{boost}}(Z, j)|$. Vector boson production in association with jets is an excellent probe of QCD and constitutes the main background to many small cross section processes, such as associated Higgs production. These measurements are crucial tests of the predictions of perturbative QCD and current event generators, which have varied success in describing the data. Using these measurements as inputs in tuning event generators will increase the experimental sensitivity to rare signals.

Histograms (12):

- Azimuthal distribution for $p_\perp^Z > 25$ GeV ([/REF/D0_2009_S8349509/d01-x01-y01](#))
- Azimuthal distribution for $p_\perp^Z > 25$ GeV ([/REF/D0_2009_S8349509/d01-x01-y02](#))
- Azimuthal distribution for $p_\perp^Z > 45$ GeV ([/REF/D0_2009_S8349509/d02-x01-y01](#))
- Azimuthal distribution for $p_\perp^Z > 45$ GeV ([/REF/D0_2009_S8349509/d02-x01-y02](#))
- Rapidity difference for $p_\perp^Z > 25$ GeV ([/REF/D0_2009_S8349509/d03-x01-y01](#))
- Rapidity difference for $p_\perp^Z > 25$ GeV ([/REF/D0_2009_S8349509/d03-x01-y02](#))
- Rapidity difference for $p_\perp^Z > 45$ GeV ([/REF/D0_2009_S8349509/d04-x01-y01](#))
- Rapidity difference for $p_\perp^Z > 45$ GeV ([/REF/D0_2009_S8349509/d04-x01-y02](#))
- Rapidity average for $p_\perp^Z > 25$ GeV ([/REF/D0_2009_S8349509/d05-x01-y01](#))
- Rapidity average for $p_\perp^Z > 25$ GeV ([/REF/D0_2009_S8349509/d05-x01-y02](#))
- Rapidity average for $p_\perp^Z > 45$ GeV ([/REF/D0_2009_S8349509/d06-x01-y01](#))
- Rapidity average for $p_\perp^Z > 45$ GeV ([/REF/D0_2009_S8349509/d06-x01-y02](#))

7.52 D0_2010_S8566488 [87]

Dijet invariant mass

Beams: $\bar{p}p$

Energies: (980.0, 980.0) GeV

Experiment: D0 (Tevatron Run 2)

Spires ID: 8566488

Status: VALIDATED

Authors:

- Frank Siegert <frank.siegert@cern.ch>

References:

- arXiv: [1002.4594](#)

Run details:

- $p\bar{p} \rightarrow$ jets at 1960 GeV. Analysis needs two hard jets above 40 GeV.

The inclusive dijet production double differential cross section as a function of the dijet invariant mass and of the largest absolute rapidity ($|y|_{\max}$) of the two jets with the largest transverse momentum in an event is measured using 0.7 fb^{-1} of data. The measurement is performed in six rapidity regions up to $|y|_{\max} = 2.4$.

Histograms (6):

- Dijet invariant mass for $|y|_{\max} < 0.4$ (/REF/D0_2010_S8566488/d01-x01-y01)
- Dijet invariant mass for $0.4 < |y|_{\max} < 0.8$ (/REF/D0_2010_S8566488/d02-x01-y01)
- Dijet invariant mass for $0.8 < |y|_{\max} < 1.2$ (/REF/D0_2010_S8566488/d03-x01-y01)
- Dijet invariant mass for $1.2 < |y|_{\max} < 1.6$ (/REF/D0_2010_S8566488/d04-x01-y01)
- Dijet invariant mass for $1.6 < |y|_{\max} < 2.0$ (/REF/D0_2010_S8566488/d05-x01-y01)
- Dijet invariant mass for $2.0 < |y|_{\max} < 2.4$ (/REF/D0_2010_S8566488/d06-x01-y01)

7.53 D0_2010_S8570965 [88]

Direct photon pair production

Beams: $\bar{p}p$

Energies: (980.0, 980.0) GeV

Experiment: CDF (Tevatron Run 2)

Spires ID: [8570965](#)

Status: VALIDATED

Authors:

- Frank Siegert <frank.siegert@cern.ch>

References:

- arXiv: [1002.4917](#)

Run details:

- All processes that can produce prompt photon pairs, e.g. $jj \rightarrow jj$, $jj \rightarrow j\gamma$ and $jj \rightarrow \gamma\gamma$. Non-prompt photons from hadron decays like π and η have been corrected for.

Direct photon pair production cross sections are measured using 4.2 fb^{-1} of data. They are binned in diphoton mass, the transverse momentum of the diphoton system, the azimuthal angle between the photons, and the polar scattering angle of the photons. Also available are double differential cross sections considering the last three kinematic variables in three diphoton mass bins. Note, the numbers in version 1 of the arXiv preprint were missing the dM normalisation in the double differential cross sections. This has been reported to and fixed by the authors in v2 and the journal submission. HepData as well as the Rivet analysis have also been updated.

Histograms (13):

- Diphoton mass ([/REF/D0_2010_S8570965/d01-x01-y01](#))
- p_{\perp} of the diphoton system ([/REF/D0_2010_S8570965/d02-x01-y01](#))
- Azimuthal angle between the photons ([/REF/D0_2010_S8570965/d03-x01-y01](#))
- Polar scattering angle of the photons ([/REF/D0_2010_S8570965/d04-x01-y01](#))
- p_{\perp} of the diphoton system ($30 \text{ GeV} < M_{\gamma\gamma} < 50 \text{ GeV}$) ([/REF/D0_2010_S8570965/d05-x01-y01](#))
- Azimuthal angle between the photons ($30 \text{ GeV} < M_{\gamma\gamma} < 50 \text{ GeV}$) ([/REF/D0_2010_S8570965/d06-x01-y01](#))
- Polar scattering angle of the photons ($30 \text{ GeV} < M_{\gamma\gamma} < 50 \text{ GeV}$) ([/REF/D0_2010_S8570965/d07-x01-y01](#))
- p_{\perp} of the diphoton system ($50 \text{ GeV} < M_{\gamma\gamma} < 80 \text{ GeV}$) ([/REF/D0_2010_S8570965/d08-x01-y01](#))

- Azimuthal angle between the photons ($50 \text{ GeV} < M_{\gamma\gamma} < 80 \text{ GeV}$) ([/REF/D0_2010_-s8570965/d09-x01-y01](#))
- Polar scattering angle of the photons ($50 \text{ GeV} < M_{\gamma\gamma} < 80 \text{ GeV}$) ([/REF/D0_2010_-s8570965/d10-x01-y01](#))
- p_{\perp} of the diphoton system ($80 \text{ GeV} < M_{\gamma\gamma} < 350 \text{ GeV}$) ([/REF/D0_2010_s8570965/d11-x01-y01](#))
- Azimuthal angle between the photons ($80 \text{ GeV} < M_{\gamma\gamma} < 350 \text{ GeV}$) ([/REF/D0_2010_-s8570965/d12-x01-y01](#))
- Polar scattering angle of the photons ($80 \text{ GeV} < M_{\gamma\gamma} < 350 \text{ GeV}$) ([/REF/D0_2010_-s8570965/d13-x01-y01](#))

7.54 D0_2010_S8671338 [89]

Measurement of differential Z/γ^* p_\perp

Beams: $p\bar{p}$

Energies: (980.0, 980.0) GeV

Experiment: D0 (Tevatron Run 2)

Spires ID: 8671338

Status: VALIDATED

Authors:

- Flavia Dias <fladias@gmail.com>
- Gavin Hesketh <gavin.hesketh@cern.ch>
- Frank Siegert <frank.siegert@cern.ch>

References:

- arXiv: [1006.0618](#)

Run details:

- $p\bar{p} \rightarrow \mu^+\mu^- + \text{jets}$ at 1960 GeV. Needs mass cut on lepton pair to avoid photon singularity, looser than $65 < m_{\mu\mu} < 115$ GeV. Restrict Z/γ^* mass range to roughly $50 \text{ GeV}/c^2 < m_{\mu\mu} < 120 \text{ GeV}/c^2$ for efficiency. Weighted events and kinematic sampling enhancement can help to fill the p_\perp tail.

Cross section as a function of p_\perp of the Z boson decaying into muons in $p\bar{p}$ collisions at $\sqrt{s} = 1.96$ TeV, based on an integrated luminosity of 0.97 fb^{-1} .

Histograms (2):

- Z boson p_\perp (normalised) ([/REF/D0_2010_S8671338/d01-x01-y01](#))
- Z boson p_\perp (unnormalised) ([/REF/D0_2010_S8671338/d02-x01-y01](#))

7.55 D0_2010_S8821313 [90]

Precise study of Z p_{\perp} using novel technique

Beams: $\bar{p}p$

Energies: (980.0, 980.0) GeV

Experiment: D0 (Tevatron Run 2)

Spires ID: 8821313

Status: VALIDATED

Authors:

- Frank Siegert <frank.siegert@cern.ch>

References:

- arXiv: [1010.0262](#)

Run details:

- Inclusive Z/γ^* production in both electron and muon channels. Cut on invariant lepton mass should be wider than $70 < m_{\ell\ell} < 110$ GeV.

Using 7.3 pb^{-1} the distribution of the variable ϕ^* is measured, which probes the same physical effects as the Z/γ^* boson transverse momentum, but is less susceptible to the effects of experimental resolution and efficiency. Results are presented for both the di-electron and di-muon channel.

Histograms (5):

- Electron channel ($|y_Z| < 1$) ([/REF/D0_2010_S8821313/d01-x01-y01](#))
- Electron channel ($1 < |y_Z| < 2$) ([/REF/D0_2010_S8821313/d01-x01-y02](#))
- Electron channel ($|y_Z| > 2$) ([/REF/D0_2010_S8821313/d01-x01-y03](#))
- Muon channel ($|y_Z| < 1$) ([/REF/D0_2010_S8821313/d02-x01-y01](#))
- Muon channel ($1 < |y_Z| < 2$) ([/REF/D0_2010_S8821313/d02-x01-y02](#))

7.56 D0_2011_I895662 [91]

3-jet invariant mass

Beams: $\bar{p}p$

Energies: (980.0, 980.0) GeV

Experiment: D0 (Tevatron Run 2)

Inspire ID: [895662](#)

Status: VALIDATED

Authors:

- Hendrik Hoeth (hendrik.hoeth@cern.ch)

References:

- arxiv:1104.1986

Run details:

- QCD events, three jets above 40 GeV.

Inclusive three-jet differential cross-section as a function of invariant mass of the three jets with the largest transverse momenta. The measurement is made in three rapidity regions ($|y| < 0.8, 1.6, 2.4$) and with jets above 40, 70, and 100 GeV.

Histograms (5):

- 3-jet mass, $|y| < 0.8, p_{\perp,3} > 40$ GeV ([/REF/D0_2011_I895662/d01-x01-y01](#))
- 3-jet mass, $|y| < 1.6, p_{\perp,3} > 40$ GeV ([/REF/D0_2011_I895662/d02-x01-y01](#))
- 3-jet mass, $|y| < 2.4, p_{\perp,3} > 40$ GeV ([/REF/D0_2011_I895662/d03-x01-y01](#))
- 3-jet mass, $|y| < 2.4, p_{\perp,3} > 70$ GeV ([/REF/D0_2011_I895662/d04-x01-y01](#))
- 3-jet mass, $|y| < 2.4, p_{\perp,3} > 100$ GeV ([/REF/D0_2011_I895662/d05-x01-y01](#))

7.57 E735_1998_S3905616 [92]

Charged particle multiplicity in ppbar collisions at $\sqrt{s} = 1.8$ TeV

Beams: $\bar{p}p$

Energies: (900.0, 900.0) GeV

Experiment: E735 (Tevatron)

Spires ID: [3905616](#)

Status: UNVALIDATED - need trigger etc.

Authors:

- Holger Schulz (holger.schulz@physik.hu-berlin.de)
- Andy Buckley (andy.buckley@cern.ch)

References:

- Phys.Lett.B435:453-457,1998

Run details:

- QCD events, diffractive processes need to be switched on in order to fill the low multiplicity regions. The measurement was done in $|\eta| \lesssim 3.25$ and was extrapolated to full phase space. However, the method of extrapolation remains unclear.

A measurement of the charged multiplicity distribution at $\sqrt{s} = 1.8$ TeV.

Histograms (1):

- Charged multiplicity at $\sqrt{s} = 1800$ GeV ([/REF/E735_1998_S3905616/d01-x01-y01](#))

8. LHC analyses

8.1 ALICE_2010_S8624100 [93]

Charged particle multiplicities at **0.9** and **2.36 TeV** in three different pseudorapidity intervals.

Beams: pp

Energies: (450.0, 450.0), (1180.0, 1180.0) GeV

Experiment: ALICE (LHC)

Spires ID: [8624100](#)

Status: VALIDATED

Authors:

- Holger Schulz (holger.schulz@physik.hu-berlin.de)
- Jan Fiete Grosse-Oetringhaus@cern.ch (Jan.Fiete.Grosse-Oetringhaus@cern.ch)

References:

- Eur.Phys.J.C68:89-108,2010
- arXiv: [1004.3034](#)

Run details:

- QCD and diffractive events at $\sqrt{s} = 0.9$ TeV and $\sqrt{s} = 2.36$ TeV

This is an ALICE analysis where charged particle multiplicities (including the zero bin) have been measured in three different pseudorapidity intervals ($|\eta| < 0.5$; $|\eta| < 1.0$; $|\eta| < 1.3$). Only the INEL distributions have been considered here, i.e. this analysis can only be meaningfully compared to PYTHIA 6 with diffractive processes disabled. The data were taken at 900 and 2360 GeV.

Histograms (6):

- Charged multiplicity, $|\eta| < 0.5$, $\sqrt{s} = 0.9$ TeV (INEL) ([/REF/ALICE_2010_S8624100/d11-x01-y01](#))
- Charged multiplicity, $|\eta| < 1.0$, $\sqrt{s} = 0.9$ TeV (INEL) ([/REF/ALICE_2010_S8624100/d12-x01-y01](#))
- Charged multiplicity, $|\eta| < 1.3$, $\sqrt{s} = 0.9$ TeV (INEL) ([/REF/ALICE_2010_S8624100/d13-x01-y01](#))
- Charged multiplicity, $|\eta| < 0.5$, $\sqrt{s} = 2.36$ TeV (INEL) ([/REF/ALICE_2010_S8624100/d17-x01-y01](#))
- Charged multiplicity, $|\eta| < 1.0$, $\sqrt{s} = 2.36$ TeV (INEL) ([/REF/ALICE_2010_S8624100/d18-x01-y01](#))
- Charged multiplicity, $|\eta| < 1.3$, $\sqrt{s} = 2.36$ TeV (INEL) ([/REF/ALICE_2010_S8624100/d19-x01-y01](#))

8.2 ALICE_2010_S8625980 [94]

Pseudorapidities at three energies, charged multiplicity at 7 TeV.

Beams: pp

Energies: (450.0, 450.0), (1180.0, 1180.0), (3500.0, 3500.0) GeV

Experiment: ALICE (LHC)

Spires ID: [8625980](#)

Status: VALIDATED

Authors:

- Holger Schulz [⟨ holger.schulz@physik.hu-berlin.de ⟩](mailto:holger.schulz@physik.hu-berlin.de)
- Jan Fiete Grosse-Oetringhaus@cern.ch [⟨ Jan.Fiete.Grosse-Oetringhaus@cern.ch ⟩](mailto:Jan.Fiete.Grosse-Oetringhaus@cern.ch)

References:

- Eur.Phys.J. C68 (2010) 345-354
- arXiv: [1004.3514](#)

Run details:

- Diffractive events need to be enabled.

This is an ALICE publication with pseudorapidities for 0.9, 2.36 and 7 TeV and the charged multiplicity at 7 TeV. The analysis requires at least one charged particle in the event. Only the INEL distributions are considered here

Histograms (4):

- Charged Multiplicity $\sqrt(s) = 7$ TeV ([/REF/ALICE_2010_S8625980/d03-x01-y01](#))
- Pseudorapidity $\sqrt(s) = 0.9$ TeV, INEL > 0 ([/REF/ALICE_2010_S8625980/d04-x01-y01](#))
- Pseudorapidity $\sqrt(s) = 2.36$ TeV, INEL > 0 ([/REF/ALICE_2010_S8625980/d05-x01-y01](#))
- Pseudorapidity $\sqrt(s) = 7$ TeV, INEL > 0 ([/REF/ALICE_2010_S8625980/d06-x01-y01](#))

8.3 ALICE_2010_S8706239 [95]

Charged particle $\langle p_{\perp} \rangle$ vs. N_{ch} in pp collisions at 900 GeV

Beams: pp

Energies: (450.0, 450.0) GeV

Experiment: ALICE (LHC)

Spires ID: [8706239](#)

Status: VALIDATED

Authors:

- Holger Schulz (holger.schulz@physik.hu-berlin.de)
- Jan Fiete Grosse-Oetringhaus@cern.ch (Jan.Fiete.Grosse-Oetringhaus@cern.ch)

References:

- Phys.Lett.B693:53-68,2010
- arXiv: [1007.0719](#)

Run details:

- Diffractive events need to be switched on

ALICE measurement of $\langle p_{\perp} \rangle$ vs. N_{ch} and invariant particle yield (as function of p_{\perp}) in proton-proton collisions at $\sqrt{s} = 900$ GeV.

Histograms (3):

- Invariant Yield ([/REF/ALICE_2010_S8706239/d04-x01-y01](#))
- Avg. transv. momentum vs. N_{ch} ($0.15 \leq p_{\perp} \leq 4$ GeV) ([/REF/ALICE_2010_S8706239/d11-x01-y01](#))
- Avg. transv. momentum vs. N_{ch} ($0.5 \leq p_{\perp} \leq 4$ GeV) ([/REF/ALICE_2010_S8706239/d12-x01-y01](#))

8.4 ALICE_2011_S8909580 [96]

Strange particle production in proton-proton collisions at $\sqrt{s} = 0.9$ TeV with ALICE at the LHC.

Beams: pp

Energies: (450.0, 450.0) GeV

Experiment: ALICE (LHC)

Spires ID: [8909580](#)

Status: VALIDATED

Authors:

- Pablo Bueno Gomez <UO189399@uniovi.es>
- Eva Sicking <esicking@cern.ch>

References:

- Eur.Phys.J.C71:1594,2011.

Run details:

- Diffractive events need to be switched on.

Transverse momentum spectra of strange particles (K_S^0 , Λ , ϕ and Ξ) in pp collisions at $\sqrt{s} = 0.9$ TeV with ALICE at the LHC. The ratio of cross-sections as a function of p_\perp for Λ/K_S^0 is also included.

Histograms (6):

- K_s^0 transverse momentum, $|y| < 0.75$, $\sqrt{s} = 0.9$ TeV (INEL) ([/REF/ALICE_2011-S8909580/d01-x01-y01](#))
- Λ transverse momentum, $|y| < 0.75$, $\sqrt{s} = 0.9$ TeV (INEL) ([/REF/ALICE_2011_S8909580/d02-x01-y01](#))
- $\bar{\Lambda}$ transverse momentum, $|y| < 0.75$, $\sqrt{s} = 0.9$ TeV (INEL) ([/REF/ALICE_2011_S8909580/d03-x01-y01](#))
- Ξ transverse momentum, $|y| < 0.8$, $\sqrt{s} = 0.9$ TeV (INEL) ([/REF/ALICE_2011_S8909580/d04-x01-y01](#))
- $\phi(1020)$ transverse momentum, $|y| < 0.6$, $\sqrt{s} = 0.9$ TeV (INEL) ([/REF/ALICE_2011-S8909580/d05-x01-y01](#))
- Λ/K_S^0 ratio, $|y| < 0.75$, $\sqrt{s} = 0.9$ TeV (INEL) ([/REF/ALICE_2011_S8909580/d06-x01-y01](#))

8.5 ALICE_2011_S8945144 [97]

Tranverse momentum spectra of pions, kaons and protons in pp collisions at 0.9 TeV

Beams: pp

Energies: (450.0, 450.0) GeV

Experiment: ALICE (LHC)

Spires ID: [8945144](#)

Status: VALIDATED

Authors:

- Pablo Bueno Gomez UO189399@uniovi.es
- Eva Sicking esicking@cern.ch

References:

- Eur.Phys.J.C71:1655,2011.
- arXiv: [1101.4110](#)

Run details:

- Diffractive events need to be enabled.

Obtaining the transverse momentum spectra of pions, kaons and protons in pp collisions at $\sqrt{s} = 0.9$ TeV with ALICE at the LHC. Mean transverse momentum as a function of the mass of the emitted particle is also included.

Histograms (7):

- π^+ tranverse momentum, $|\eta| < 0.5$, $\sqrt{s} = 0.9$ TeV (INEL) ([/REF/ALICE_2011_S8945144/d01-x01-y01](#))
- π^- tranverse momentum, $|\eta| < 0.5$, $\sqrt{s} = 0.9$ TeV (INEL) ([/REF/ALICE_2011_S8945144/d01-x01-y02](#))
- K^+ tranverse momentum, $|\eta| < 0.5$, $\sqrt{s} = 0.9$ TeV (INEL) ([/REF/ALICE_2011_S8945144/d02-x01-y01](#))
- K^- tranverse momentum, $|\eta| < 0.5$, $\sqrt{s} = 0.9$ TeV (INEL) ([/REF/ALICE_2011_S8945144/d02-x01-y02](#))
- p tranverse momentum, $|\eta| < 0.5$, $\sqrt{s} = 0.9$ TeV (INEL) ([/REF/ALICE_2011_S8945144/d03-x01-y01](#))
- \bar{p} tranverse momentum, $|\eta| < 0.5$, $\sqrt{s} = 0.9$ TeV (INEL) ([/REF/ALICE_2011_S8945144/d03-x01-y02](#))
- Average p_\perp vs mass, $|\eta| < 0.5$, $\sqrt{s} = 0.9$ TeV (INEL) ([/REF/ALICE_2011_S8945144/d04-x01-y01](#))

8.6 ALICE_2012_I1181770 [98]

Measurement of inelastic, single- and double-diffraction cross sections in proton–proton collisions at the LHC with ALICE

Beams: pp

Energies: (450.0, 450.0), (1380.0, 1380.0), (3500.0, 3500.0) GeV

Experiment: ALICE (LHC)

Inspire ID: [1181770](#)

Status: VALIDATED

Authors:

- Martin Poghosyan (Martin.Poghosyan@cern.ch)
- Sercan Sen (Sercan.Sen@cern.ch)
- Burak Bilki (bbilki@gmail.com)
- Andy Buckley (andy.buckley@cern.ch)

References:

- arXiv: [1208.4968](#)

Run details:

- Inelastic events (non-diffractive and inelastic diffractive).

Measurements of cross-sections of inelastic and diffractive processes in proton-proton collisions at $\sqrt{s} = 900, 2760$ and 7000 GeV. The fractions of diffractive processes in inelastic collisions were determined from a study of gaps in charged particle pseudorapidity distributions. Single-diffractive events are selected with $M_X < 200$ GeV/ c^2 and double-diffractive events defined as NSD events with $\Delta\eta > 3$. To measure the inelastic cross-section, beam properties were determined with van der Meer scans using a simulation of diffraction adjusted to data. Note that these are experimental approximations to theoretical concepts – it is not totally clear whether the data point values are model-independent.

Histograms (15):

- Production ratios of SD with $M_X < 200$ GeV/ c^2 to INEL ([/REF/ALICE_2012_I1181770/d01-x01-y01](#))
- Production ratios of SD with $M_X < 200$ GeV/ c^2 to INEL ([/REF/ALICE_2012_I1181770/d01-x01-y02](#))
- Production ratios of SD with $M_X < 200$ GeV/ c^2 to INEL ([/REF/ALICE_2012_I1181770/d01-x01-y03](#))
- Production ratios of DD with $\Delta\eta > 3$ to INEL ([/REF/ALICE_2012_I1181770/d02-x01-y01](#))
- Production ratios of DD with $\Delta\eta > 3$ to INEL ([/REF/ALICE_2012_I1181770/d02-x01-y02](#))
- Production ratios of DD with $\Delta\eta > 3$ to INEL ([/REF/ALICE_2012_I1181770/d02-x01-y03](#))
- Single diffraction cross-section for $M_X < 200$ GeV/ c^2 ([/REF/ALICE_2012_I1181770/d03-x01-y01](#))

- Single diffraction cross-section for $M_X < 200 \text{ GeV}/c^2$ ([/REF/ALICE_2012_I1181770/d03-x01-y02](#))
- Single diffraction cross-section for $M_X < 200 \text{ GeV}/c^2$ ([/REF/ALICE_2012_I1181770/d03-x01-y03](#))
- Double diffraction cross-section for $\Delta\eta > 3$ ([/REF/ALICE_2012_I1181770/d04-x01-y01](#))
- Double diffraction cross-section for $\Delta\eta > 3$ ([/REF/ALICE_2012_I1181770/d04-x01-y02](#))
- Double diffraction cross-section for $\Delta\eta > 3$ ([/REF/ALICE_2012_I1181770/d04-x01-y03](#))
- Inelastic cross-section ([/REF/ALICE_2012_I1181770/d05-x01-y01](#))
- Inelastic cross-section ([/REF/ALICE_2012_I1181770/d05-x01-y02](#))
- Inelastic cross-section ([/REF/ALICE_2012_I1181770/d05-x01-y03](#))

8.7 ATLAS_2010_CONF_2010_049

Cross-section of and fragmentation function in anti-kt track jets

Beams: pp

Energies: (3500.0, 3500.0) GeV

Experiment: ATLAS (LHC 7000GeV)

Spires ID: [None](#)

Status: PRELIMINARY

Authors:

- Hendrik Hoeth (hendrik.hoeth@cern.ch)

References:

- ATLAS-CONF-2010-049

Run details:

- pp QCD interactions at 7000 GeV including diffractive events.

Jets are identified and their properties studied using tracks measured by the ATLAS Inner Detector. Events are selected using a minimum-bias trigger, allowing the emergence of jets at low transverse momentum to be observed and for jets to be studied independently of the calorimeter. Jets are reconstructed using the anti-kt algorithm applied to tracks with two parameter choices, 0.4 and 0.6. An inclusive jet transverse momentum cross section measurement from 4 GeV to 80 GeV is shown, integrated over $|\eta| < 0.57$ and corrected to charged particle-level truth jets. The probability that a particular particle carries a fixed fraction of the jet momentum (fragmentation function) is also measured. All data is corrected to the particle level. ATTENTION - Data read from plots!

Histograms (10):

- Jet x-sec for anti- k_t track jets with $R = 0.6$, $|\eta| < 0.57$, $\sqrt{s} = 7$ TeV ([/REF/ATLAS_2010_CONF_2010_049/d01-x01-y01](#))
- Jet x-sec for anti- k_t track jets with $R = 0.4$, $|\eta| < 0.57$, $\sqrt{s} = 7$ TeV ([/REF/ATLAS_2010_CONF_2010_049/d02-x01-y01](#))
- z in anti- k_t jets, $R = 0.6$, $p_{\perp} \in [4..6]$ GeV, $|\eta| < 0.57$, $\sqrt{s} = 7$ TeV ([/REF/ATLAS_2010_CONF_2010_049/d03-x01-y01](#))
- z in anti- k_t jets, $R = 0.6$, $p_{\perp} \in [6..10]$ GeV, $|\eta| < 0.57$, $\sqrt{s} = 7$ TeV ([/REF/ATLAS_2010_CONF_2010_049/d03-x02-y01](#))
- z in anti- k_t jets, $R = 0.6$, $p_{\perp} \in [10..15]$ GeV, $|\eta| < 0.57$, $\sqrt{s} = 7$ TeV ([/REF/ATLAS_2010_CONF_2010_049/d03-x03-y01](#))
- z in anti- k_t jets, $R = 0.6$, $p_{\perp} \in [15..24]$ GeV, $|\eta| < 0.57$, $\sqrt{s} = 7$ TeV ([/REF/ATLAS_2010_CONF_2010_049/d03-x04-y01](#))

- z in anti- k_t jets, $R = 0.4$, $p_T \in [4..6]$ GeV, $|\eta| < 0.57$, $\sqrt{s} = 7$ TeV ([/REF/ATLAS_2010-CONF_2010_049/d04-x01-y01](#))
- z in anti- k_t jets, $R = 0.4$, $p_T \in [6..10]$ GeV, $|\eta| < 0.57$, $\sqrt{s} = 7$ TeV ([/REF/ATLAS_2010-CONF_2010_049/d04-x02-y01](#))
- z in anti- k_t jets, $R = 0.4$, $p_T \in [10..15]$ GeV, $|\eta| < 0.57$, $\sqrt{s} = 7$ TeV ([/REF/ATLAS_2010_CONF_2010_049/d04-x03-y01](#))
- z in anti- k_t jets, $R = 0.4$, $p_T \in [15..24]$ GeV, $|\eta| < 0.57$, $\sqrt{s} = 7$ TeV ([/REF/ATLAS_2010_CONF_2010_049/d04-x04-y01](#))

8.8 ATLAS_2010_S8591806 [99]

Charged particles at 900 GeV in ATLAS

Beams: pp

Energies: (450.0, 450.0) GeV

Experiment: ATLAS (LHC 900GeV)

Spires ID: [8591806](#)

Status: VALIDATED

Authors:

- Frank Siegert <frank.siegert@cern.ch>

References:

- arXiv: [1003.3124](#)

Run details:

- pp QCD interactions at 900 GeV including diffractive events.

The first measurements with the ATLAS detector at the LHC. Data were collected using a minimum-bias trigger in December 2009 during proton-proton collisions at a centre of mass energy of 900 GeV. The charged- particle density, its dependence on transverse momentum and pseudorapidity, and the relationship between transverse momentum and charged-particle multiplicity are measured for events with at least one charged particle in the kinematic range $|\eta| < 2.5$ and $p_T > 500$ MeV. All data is corrected to the particle level.

Histograms (4):

- Charged particle multiplicity as function of η ([/REF/ATLAS_2010_S8591806/d02-x01-y01](#))
- Charged particle multiplicity as function of p_T ([/REF/ATLAS_2010_S8591806/d03-x01-y01](#))
- Charged particle density ([/REF/ATLAS_2010_S8591806/d04-x01-y01](#))
- Average transverse momentum as function of N_{ch} ([/REF/ATLAS_2010_S8591806/d05-x01-y01](#))

8.9 ATLAS_2010_S8817804 [100]

Inclusive jet cross section and di-jet mass and chi spectra at 7 TeV in ATLAS

Beams: pp

Energies: (3500.0, 3500.0) GeV

Experiment: ATLAS (LHC 7TeV)

Spires ID: [8817804](#)

Status: VALIDATED

Authors:

- James Monk (jmonk@cern.ch)

References:

- arXiv: [1009.5908](#)

Run details:

- pp QCD jet production with a minimum jet p_\perp of 60 GeV (inclusive) or 30 GeV (di-jets) at 7 TeV.

The first jet cross section measurement made with the ATLAS detector at the LHC. Anti-kt jets with $R = 0.4$ and $R = 0.6$ are reconstructed within $|y| < 2.8$ and above 60 GeV for the inclusive jet cross section plots. For the di-jet plots the second jet must have $p_\perp > 30$ GeV. Jet p_\perp and di-jet mass spectra are plotted in bins of rapidity between $|y| = 0.3, 0.8, 1.2, 2.1$, and 2.8 . Di-jet χ spectra are plotted in bins of di-jet mass between 340 GeV, 520 GeV, 800 GeV and 1200 GeV.

Histograms (26):

- Inclusive jet p_T spectrum for $|y| < 0.3$. anti-KT, $R = 0.4$. ([/REF/ATLAS_2010-S8817804/d01-x01-y01](#))
- Inclusive jet p_T spectrum for $0.3 < |y| < 0.8$. anti-KT, $R = 0.4$. ([/REF/ATLAS_2010-S8817804/d02-x01-y01](#))
- Inclusive jet p_T spectrum for $0.8 < |y| < 1.2$. anti-KT, $R = 0.4$. ([/REF/ATLAS_2010-S8817804/d03-x01-y01](#))
- Inclusive jet p_T spectrum for $1.2 < |y| < 2.1$. anti-KT, $R = 0.4$. ([/REF/ATLAS_2010-S8817804/d04-x01-y01](#))
- Inclusive jet p_T spectrum for $2.1 < |y| < 2.8$. anti-KT, $R = 0.4$. ([/REF/ATLAS_2010-S8817804/d05-x01-y01](#))
- Inclusive jet p_T spectrum for $|y| < 0.3$. anti-KT, $R = 0.6$. ([/REF/ATLAS_2010-S8817804/d06-x01-y01](#))
- Inclusive jet p_T spectrum for $0.3 < |y| < 0.8$. anti-KT, $R = 0.6$. ([/REF/ATLAS_2010-S8817804/d07-x01-y01](#))

- Inclusive jet p_T spectrum for $0.8 < |y| < 1.2$. anti-KT, $R = 0.6$. ([/REF/ATLAS_2010-S8817804/d08-x01-y01](#))
- Inclusive jet p_T spectrum for $1.2 < |y| < 2.1$. anti-KT, $R = 0.6$. ([/REF/ATLAS_2010-S8817804/d09-x01-y01](#))
- Inclusive jet p_T spectrum for $2.1 < |y| < 2.8$. anti-KT, $R = 0.6$. ([/REF/ATLAS_2010-S8817804/d10-x01-y01](#))
- Dijet mass spectrum for $|y_{\max}| < 0.3$. anti-KT, $R = 0.4$. ([/REF/ATLAS_2010_S8817804/d11-x01-y01](#))
- Dijet mass spectrum for $0.3 < |y_{\max}| < 0.8$. anti-KT, $R = 0.4$. ([/REF/ATLAS_2010-S8817804/d12-x01-y01](#))
- Dijet mass spectrum for $0.8 < |y_{\max}| < 1.2$. anti-KT, $R = 0.4$. ([/REF/ATLAS_2010-S8817804/d13-x01-y01](#))
- Dijet mass spectrum for $1.2 < |y_{\max}| < 2.1$. anti-KT, $R = 0.4$. ([/REF/ATLAS_2010-S8817804/d14-x01-y01](#))
- Dijet mass spectrum for $2.1 < |y_{\max}| < 2.8$. anti-KT, $R = 0.4$. ([/REF/ATLAS_2010-S8817804/d15-x01-y01](#))
- Dijet mass spectrum for $|y_{\max}| < 0.3$. anti-KT, $R = 0.6$. ([/REF/ATLAS_2010_S8817804/d16-x01-y01](#))
- Dijet mass spectrum for $0.3 < |y_{\max}| < 0.8$. anti-KT, $R = 0.6$. ([/REF/ATLAS_2010-S8817804/d17-x01-y01](#))
- Dijet mass spectrum for $0.8 < |y_{\max}| < 1.2$. anti-KT, $R = 0.6$. ([/REF/ATLAS_2010-S8817804/d18-x01-y01](#))
- Dijet mass spectrum for $1.2 < |y_{\max}| < 2.1$. anti-KT, $R = 0.6$. ([/REF/ATLAS_2010-S8817804/d19-x01-y01](#))
- Dijet mass spectrum for $2.1 < |y_{\max}| < 2.8$. anti-KT, $R = 0.6$. ([/REF/ATLAS_2010-S8817804/d20-x01-y01](#))
- Dijet χ for $340 \text{ GeV} < m_{12} < 520 \text{ GeV}$. anti-KT, $R = 0.4$. ([/REF/ATLAS_2010-S8817804/d21-x01-y01](#))
- Dijet χ for $520 \text{ GeV} < m_{12} < 800 \text{ GeV}$. anti-KT, $R = 0.4$. ([/REF/ATLAS_2010-S8817804/d22-x01-y01](#))
- Dijet χ for $800 \text{ GeV} < m_{12} < 1200 \text{ GeV}$. anti-KT, $R = 0.4$. ([/REF/ATLAS_2010-S8817804/d23-x01-y01](#))
- Dijet χ for $340 \text{ GeV} < m_{12} < 520 \text{ GeV}$. anti-KT, $R = 0.6$. ([/REF/ATLAS_2010-S8817804/d24-x01-y01](#))

- Dijet χ for $520 \text{ GeV} < m_{12} < 800 \text{ GeV}$. anti-KT, $R = 0.6$. ([/REF/ATLAS_2010-s8817804/d25-x01-y01](#))
- Dijet χ for $800 \text{ GeV} < m_{12} < 1200 \text{ GeV}$. anti-KT, $R = 0.6$. ([/REF/ATLAS_2010-s8817804/d26-x01-y01](#))

8.10 ATLAS_2010_S8894728

Track-based underlying event at 900 GeV and 7 TeV in ATLAS

Beams: pp

Energies: (450.0, 450.0), (3500.0, 3500.0) GeV

Experiment: ATLAS (LHC)

Spires ID: [8894728](#)

Status: VALIDATED

Authors:

- Andy Buckley ⟨ andy.buckley@cern.ch ⟩
- Holger Schulz ⟨ holger.schulz@physik.hu-berlin.de ⟩

References:

- arXiv: [1012.0791](#)

Run details:

- pp QCD interactions at 900 GeV and 7 TeV. Diffractive events should be included, but only influence the lowest bins. Multiple kinematic cuts should not be required.

The underlying event measurements with the ATLAS detector at the LHC at the center of mass energies of 900 GeV and 7 TeV. The observables sensitive to the underlying event, i.e the charged particle density and charged p_{\perp} sum, as well as their standard deviations and the average p_{\perp} , are measured as functions of the leading track. A track p_{\perp} cut of 500 MeV is applied for most observables, but the main profile plots are also shown for a lower track cut of 100 MeV, which includes much more of the soft cross-section. The angular distribution of the charged tracks with respect to the leading track is also studied, as are the correlation between mean transverse momentum and charged particle multiplicity, and the ‘plateau’ height as a function of the leading track $|\eta|$.

Histograms (58):

- Transverse N_{chg} density vs. p_{\perp}^{trk1} , $\sqrt{s} = 900$ GeV ([/REF/ATLAS_2010_S8894728/d01-x01-y01](#))
- Toward N_{chg} density vs. p_{\perp}^{trk1} , $\sqrt{s} = 900$ GeV ([/REF/ATLAS_2010_S8894728/d01-x01-y02](#))
- Away N_{chg} density vs. p_{\perp}^{trk1} , $\sqrt{s} = 900$ GeV ([/REF/ATLAS_2010_S8894728/d01-x01-y03](#))
- Transverse N_{chg} density vs. p_{\perp}^{trk1} , $\sqrt{s} = 7$ TeV ([/REF/ATLAS_2010_S8894728/d02-x01-y01](#))
- Toward N_{chg} density vs. p_{\perp}^{trk1} , $\sqrt{s} = 7$ TeV ([/REF/ATLAS_2010_S8894728/d02-x01-y02](#))
- Away N_{chg} density vs. p_{\perp}^{trk1} , $\sqrt{s} = 7$ TeV ([/REF/ATLAS_2010_S8894728/d02-x01-y03](#))
- Transverse $\sum p_{\perp}$ density vs. p_{\perp}^{trk1} , $\sqrt{s} = 900$ GeV ([/REF/ATLAS_2010_S8894728/d03-x01-y01](#))
- Toward $\sum p_{\perp}$ density vs. p_{\perp}^{trk1} , $\sqrt{s} = 900$ GeV ([/REF/ATLAS_2010_S8894728/d03-x01-y02](#))

- Away $\sum p_\perp$ density vs. p_\perp^{trk1} , $\sqrt{s} = 900$ GeV (/REF/ATLAS_2010_S8894728/d03-x01-y03)
- Transverse $\sum p_\perp$ density vs. p_\perp^{trk1} , $\sqrt{s} = 7$ TeV (/REF/ATLAS_2010_S8894728/d04-x01-y01)
- Toward $\sum p_\perp$ density vs. p_\perp^{trk1} , $\sqrt{s} = 7$ TeV (/REF/ATLAS_2010_S8894728/d04-x01-y02)
- Away $\sum p_\perp$ density vs. p_\perp^{trk1} , $\sqrt{s} = 7$ TeV (/REF/ATLAS_2010_S8894728/d04-x01-y03)
- Std. dev. Transverse N_{chg} density vs. p_\perp^{trk1} , $\sqrt{s} = 900$ GeV (/REF/ATLAS_2010_S8894728/d05-x01-y01)
- Std. dev. Transverse N_{chg} density vs. p_\perp^{trk1} , $\sqrt{s} = 7$ TeV (/REF/ATLAS_2010_S8894728/d06-x01-y01)
- Std. dev. Transverse $\sum p_\perp$ density vs. p_\perp^{trk1} , $\sqrt{s} = 900$ GeV (/REF/ATLAS_2010_S8894728/d07-x01-y01)
- Std. dev. Transverse $\sum p_\perp$ density vs. p_\perp^{trk1} , $\sqrt{s} = 7$ TeV (/REF/ATLAS_2010_S8894728/d08-x01-y01)
- Transverse $\langle p_\perp \rangle$ vs. p_\perp^{trk1} , $\sqrt{s} = 900$ GeV (/REF/ATLAS_2010_S8894728/d09-x01-y01)
- Toward $\langle p_\perp \rangle$ vs. p_\perp^{trk1} , $\sqrt{s} = 900$ GeV (/REF/ATLAS_2010_S8894728/d09-x01-y02)
- Away $\langle p_\perp \rangle$ vs. p_\perp^{trk1} , $\sqrt{s} = 900$ GeV (/REF/ATLAS_2010_S8894728/d09-x01-y03)
- Transverse $\langle p_\perp \rangle$ vs. p_\perp^{trk1} , $\sqrt{s} = 7$ TeV (/REF/ATLAS_2010_S8894728/d10-x01-y01)
- Toward $\langle p_\perp \rangle$ vs. p_\perp^{trk1} , $\sqrt{s} = 7$ TeV (/REF/ATLAS_2010_S8894728/d10-x01-y02)
- Away $\langle p_\perp \rangle$ vs. p_\perp^{trk1} , $\sqrt{s} = 7$ TeV (/REF/ATLAS_2010_S8894728/d10-x01-y03)
- Transverse $\langle p_\perp \rangle$ vs. N_{chg} , $\sqrt{s} = 900$ GeV (/REF/ATLAS_2010_S8894728/d11-x01-y01)
- Toward $\langle p_\perp \rangle$ vs. N_{chg} , $\sqrt{s} = 900$ GeV (/REF/ATLAS_2010_S8894728/d11-x01-y02)
- Away $\langle p_\perp \rangle$ vs. N_{chg} , $\sqrt{s} = 900$ GeV (/REF/ATLAS_2010_S8894728/d11-x01-y03)
- Transverse $\langle p_\perp \rangle$ vs. N_{chg} , $\sqrt{s} = 7$ TeV (/REF/ATLAS_2010_S8894728/d12-x01-y01)
- Toward $\langle p_\perp \rangle$ vs. N_{chg} , $\sqrt{s} = 7$ TeV (/REF/ATLAS_2010_S8894728/d12-x01-y02)
- Away $\langle p_\perp \rangle$ vs. N_{chg} , $\sqrt{s} = 7$ TeV (/REF/ATLAS_2010_S8894728/d12-x01-y03)
- N_{chg} density vs. $\Delta\phi$, $p_\perp^{\text{trk1}} > 1.0$ GeV, $\sqrt{s} = 900$ GeV (/REF/ATLAS_2010_S8894728/d13-x01-y01)
- N_{chg} density vs. $\Delta\phi$, $p_\perp^{\text{trk1}} > 1.5$ GeV, $\sqrt{s} = 900$ GeV (/REF/ATLAS_2010_S8894728/d13-x01-y02)
- N_{chg} density vs. $\Delta\phi$, $p_\perp^{\text{trk1}} > 2.0$ GeV, $\sqrt{s} = 900$ GeV (/REF/ATLAS_2010_S8894728/d13-x01-y03)
- N_{chg} density vs. $\Delta\phi$, $p_\perp^{\text{trk1}} > 2.5$ GeV, $\sqrt{s} = 900$ GeV (/REF/ATLAS_2010_S8894728/d13-x01-y04)
- N_{chg} density vs. $\Delta\phi$, $p_\perp^{\text{trk1}} > 1.0$ GeV, $\sqrt{s} = 7$ TeV (/REF/ATLAS_2010_S8894728/d14-x01-y01)

- N_{chg} density vs. $\Delta\phi$, $p_{\perp}^{\text{trk1}} > 2.0 \text{ GeV}$, $\sqrt{s} = 7 \text{ TeV}$ (/REF/ATLAS_2010_S8894728/d14-x01-y02)
- N_{chg} density vs. $\Delta\phi$, $p_{\perp}^{\text{trk1}} > 3.0 \text{ GeV}$, $\sqrt{s} = 7 \text{ TeV}$ (/REF/ATLAS_2010_S8894728/d14-x01-y03)
- N_{chg} density vs. $\Delta\phi$, $p_{\perp}^{\text{trk1}} > 5.0 \text{ GeV}$, $\sqrt{s} = 7 \text{ TeV}$ (/REF/ATLAS_2010_S8894728/d14-x01-y04)
- p_{\perp} density vs. $\Delta\phi$, $p_{\perp}^{\text{trk1}} > 1.0 \text{ GeV}$, $\sqrt{s} = 900 \text{ GeV}$ (/REF/ATLAS_2010_S8894728/d15-x01-y01)
- p_{\perp} density vs. $\Delta\phi$, $p_{\perp}^{\text{trk1}} > 1.5 \text{ GeV}$, $\sqrt{s} = 900 \text{ GeV}$ (/REF/ATLAS_2010_S8894728/d15-x01-y02)
- p_{\perp} density vs. $\Delta\phi$, $p_{\perp}^{\text{trk1}} > 2.0 \text{ GeV}$, $\sqrt{s} = 900 \text{ GeV}$ (/REF/ATLAS_2010_S8894728/d15-x01-y03)
- p_{\perp} density vs. $\Delta\phi$, $p_{\perp}^{\text{trk1}} > 2.5 \text{ GeV}$, $\sqrt{s} = 900 \text{ GeV}$ (/REF/ATLAS_2010_S8894728/d15-x01-y04)
- p_{\perp} density vs. $\Delta\phi$, $p_{\perp}^{\text{trk1}} > 1.0 \text{ GeV}$, $\sqrt{s} = 7 \text{ TeV}$ (/REF/ATLAS_2010_S8894728/d16-x01-y01)
- p_{\perp} density vs. $\Delta\phi$, $p_{\perp}^{\text{trk1}} > 2.0 \text{ GeV}$, $\sqrt{s} = 7 \text{ TeV}$ (/REF/ATLAS_2010_S8894728/d16-x01-y02)
- p_{\perp} density vs. $\Delta\phi$, $p_{\perp}^{\text{trk1}} > 3.0 \text{ GeV}$, $\sqrt{s} = 7 \text{ TeV}$ (/REF/ATLAS_2010_S8894728/d16-x01-y03)
- p_{\perp} density vs. $\Delta\phi$, $p_{\perp}^{\text{trk1}} > 5.0 \text{ GeV}$, $\sqrt{s} = 7 \text{ TeV}$ (/REF/ATLAS_2010_S8894728/d16-x01-y04)
- Transverse N_{chg} density vs. p_{\perp}^{trk1} , $\sqrt{s} = 900 \text{ GeV}$, $p_{\perp} > 100 \text{ MeV}$ (/REF/ATLAS_2010_S8894728/d17-x01-y01)
- Toward N_{chg} density vs. p_{\perp}^{trk1} , $\sqrt{s} = 900 \text{ GeV}$, $p_{\perp} > 100 \text{ MeV}$ (/REF/ATLAS_2010_S8894728/d17-x01-y02)
- Away N_{chg} density vs. p_{\perp}^{trk1} , $\sqrt{s} = 900 \text{ GeV}$, $p_{\perp} > 100 \text{ MeV}$ (/REF/ATLAS_2010_S8894728/d17-x01-y03)
- Transverse N_{chg} density vs. p_{\perp}^{trk1} , $\sqrt{s} = 7 \text{ TeV}$, $p_{\perp} > 100 \text{ MeV}$ (/REF/ATLAS_2010_S8894728/d18-x01-y01)
- Toward N_{chg} density vs. p_{\perp}^{trk1} , $\sqrt{s} = 7 \text{ TeV}$, $p_{\perp} > 100 \text{ MeV}$ (/REF/ATLAS_2010_S8894728/d18-x01-y02)
- Away N_{chg} density vs. p_{\perp}^{trk1} , $\sqrt{s} = 7 \text{ TeV}$, $p_{\perp} > 100 \text{ MeV}$ (/REF/ATLAS_2010_S8894728/d18-x01-y03)
- Transverse $\sum p_{\perp}$ density vs. p_{\perp}^{trk1} , $\sqrt{s} = 900 \text{ GeV}$, $p_{\perp} > 100 \text{ MeV}$ (/REF/ATLAS_2010_S8894728/d19-x01-y01)
- Toward $\sum p_{\perp}$ density vs. p_{\perp}^{trk1} , $\sqrt{s} = 900 \text{ GeV}$, $p_{\perp} > 100 \text{ MeV}$ (/REF/ATLAS_2010_S8894728/d19-x01-y02)
- Away $\sum p_{\perp}$ density vs. p_{\perp}^{trk1} , $\sqrt{s} = 900 \text{ GeV}$, $p_{\perp} > 100 \text{ MeV}$ (/REF/ATLAS_2010_S8894728/d19-x01-y03)
- Transverse $\sum p_{\perp}$ density vs. p_{\perp}^{trk1} , $\sqrt{s} = 7 \text{ TeV}$, $p_{\perp} > 100 \text{ MeV}$ (/REF/ATLAS_2010_S8894728/d20-x01-y01)

- Toward $\sum p_\perp$ density vs. p_\perp^{trk1} , $\sqrt{s} = 7 \text{ TeV}$, $p_\perp > 100 \text{ MeV}$ (/REF/ATLAS_2010_-s8894728/d20-x01-y02)
- Away $\sum p_\perp$ density vs. p_\perp^{trk1} , $\sqrt{s} = 7 \text{ TeV}$, $p_\perp > 100 \text{ MeV}$ (/REF/ATLAS_2010_-s8894728/d20-x01-y03)
- Transverse N_{chg} density vs. $|\eta^{\text{trk1}}|$, $\sqrt{s} = 7 \text{ TeV}$, $p_\perp > 100 \text{ MeV}$ (/REF/ATLAS_2010_-s8894728/d21-x01-y01)
- Transverse $\sum p_\perp$ density vs. $|\eta^{\text{trk1}}|$, $\sqrt{s} = 7 \text{ TeV}$, $p_\perp > 100 \text{ MeV}$ (/REF/ATLAS_2010_-s8894728/d22-x01-y01)

8.11 ATLAS_2010_S8914702 [101]

Inclusive isolated prompt photon analysis

Beams: pp

Energies: (3500.0, 3500.0) GeV

Experiment: ATLAS (LHC 7TeV)

Spires ID: [8914702](#)

Status: VALIDATED

Authors:

- Mike Hance ⟨ michael.hance@cern.ch ⟩

References:

- arXiv: [1012.4389](#)

Run details:

- Inclusive photon+X events (primary gamma+jet events) at $\sqrt{s} = 7$ TeV.

A measurement of the cross section for inclusive isolated photon production at $\sqrt{s} = 7$ TeV. The measurement covers three ranges in $|\eta|$: [0.00,0.60), [0.60,1.37), and [1.52,1.81), for $E_T^\gamma > 15$ GeV. The measurement uses 880 nb⁻¹ of integrated luminosity collected with the ATLAS detector.

Histograms (3):

- Transverse energy of isolated prompt photon, $|\eta| < 0.60$ ([/REF/ATLAS_2010_S8914702/d01-x01-y01](#))
- Transverse energy of isolated prompt photon, $0.60 \leq |\eta| < 1.37$ ([/REF/ATLAS_2010_S8914702/d01-x01-y02](#))
- Transverse energy of isolated prompt photon, $1.52 \leq |\eta| < 1.81$ ([/REF/ATLAS_2010_S8914702/d01-x01-y03](#))

8.12 ATLAS_2010_S8918562

Track-based minimum bias at 900 GeV and 2.36 and 7 TeV in ATLAS

Beams: pp

Energies: (450.0, 450.0), (1180.0, 1180.0), (3500.0, 3500.0) GeV

Experiment: ATLAS (LHC)

Spires ID: [8918562](#)

Status: VALIDATED

Authors:

- Thomas Burgess <thomas.burgess@cern.ch>
- Andy Buckley <andy.buckley@cern.ch>

References:

- arXiv: [1012.5104](#)

Run details:

- pp QCD interactions at 0.9, 2.36, and 7 TeV. Diffractive events should be included. Multiple kinematic cuts should not be required.

Measurements from proton-proton collisions at centre-of-mass energies of $\sqrt{s} = 0.9$, 2.36, and 7 TeV recorded with the ATLAS detector at the LHC. Events were collected using a single-arm minimum-bias trigger. The charged-particle multiplicity, its dependence on transverse momentum and pseudorapidity and the relationship between the mean transverse momentum and charged-particle multiplicity are measured. Measurements in different regions of phase-space are shown, providing diffraction-reduced measurements as well as more inclusive ones. The observed distributions are corrected to well-defined phase-space regions, using model-independent corrections.

Histograms (39):

- Charged particle η at 900 GeV, track $p_{\perp} > 500$ MeV, for $N_{\text{ch}} \geq 1$ ([/REF/ATLAS_2010-S8918562/d01-x01-y01](#))
- Charged particle η at 2360 GeV, track $p_{\perp} > 500$ MeV, for $N_{\text{ch}} \geq 1$ ([/REF/ATLAS_2010-S8918562/d02-x01-y01](#))
- Charged particle η at 7 TeV, track $p_{\perp} > 500$ MeV, for $N_{\text{ch}} \geq 1$ ([/REF/ATLAS_2010-S8918562/d03-x01-y01](#))
- Charged particle η at 900 GeV, track $p_{\perp} > 100$ MeV, for $N_{\text{ch}} \geq 2$ ([/REF/ATLAS_2010-S8918562/d04-x01-y01](#))
- Charged particle η at 7 TeV, track $p_{\perp} > 100$ MeV, for $N_{\text{ch}} \geq 2$ ([/REF/ATLAS_2010-S8918562/d05-x01-y01](#))

- Charged particle η at 900 GeV, track $p_{\perp} > 500$ MeV, for $N_{\text{ch}} \geq 6$ (/REF/ATLAS_2010_-
S8918562/d06-x01-y01)
- Charged particle η at 7 TeV, track $p_{\perp} > 500$ MeV, for $N_{\text{ch}} \geq 6$ (/REF/ATLAS_2010_-
S8918562/d07-x01-y01)
- Charged particle p_{\perp} at 900 GeV, track $p_{\perp} > 500$ MeV, for $N_{\text{ch}} \geq 1$ (/REF/ATLAS_2010_-
S8918562/d08-x01-y01)
- Charged particle p_{\perp} at 2360 GeV, track $p_{\perp} > 500$ MeV, for $N_{\text{ch}} \geq 1$ (/REF/ATLAS_2010_-
S8918562/d09-x01-y01)
- Charged particle p_{\perp} at 7 TeV, track $p_{\perp} > 500$ MeV, for $N_{\text{ch}} \geq 1$ (/REF/ATLAS_2010_-
S8918562/d10-x01-y01)
- Charged particle p_{\perp} at 900 GeV, track $p_{\perp} > 100$ MeV, for $N_{\text{ch}} \geq 2$ (/REF/ATLAS_2010_-
S8918562/d11-x01-y01)
- Charged particle p_{\perp} at 7 TeV, track $p_{\perp} > 100$ MeV, for $N_{\text{ch}} \geq 2$ (/REF/ATLAS_2010_-
S8918562/d12-x01-y01)
- Charged particle p_{\perp} at 900 GeV, track $p_{\perp} > 500$ MeV, for $N_{\text{ch}} \geq 6$ (/REF/ATLAS_2010_-
S8918562/d13-x01-y01)
- Charged particle p_{\perp} at 7 TeV, track $p_{\perp} > 500$ MeV, for $N_{\text{ch}} \geq 6$ (/REF/ATLAS_2010_-
S8918562/d14-x01-y01)
- Charged multiplicity ≥ 1 at 900 GeV, track $p_{\perp} > 500$ MeV (/REF/ATLAS_2010_S8918562/d15-x01-y01)
- Charged multiplicity ≥ 1 at 2360 GeV, track $p_{\perp} > 500$ MeV (/REF/ATLAS_2010_-
S8918562/d16-x01-y01)
- Charged multiplicity ≥ 1 at 7 TeV, track $p_{\perp} > 500$ MeV (/REF/ATLAS_2010_S8918562/d17-x01-y01)
- Charged multiplicity ≥ 2 at 900 GeV, track $p_{\perp} > 100$ MeV (/REF/ATLAS_2010_S8918562/d18-x01-y01)
- Charged multiplicity ≥ 2 at 7 TeV, track $p_{\perp} > 100$ MeV (/REF/ATLAS_2010_S8918562/d19-x01-y01)
- Charged multiplicity ≥ 6 at 900 GeV, track $p_{\perp} > 500$ MeV (/REF/ATLAS_2010_S8918562/d20-x01-y01)
- Charged multiplicity ≥ 6 at 7 TeV, track $p_{\perp} > 500$ MeV (/REF/ATLAS_2010_S8918562/d21-x01-y01)
- Charged $\langle p_{\perp} \rangle$ vs. N_{ch} at 900 GeV, track $p_{\perp} > 500$ MeV, for $N_{\text{ch}} \geq 1$ (/REF/ATLAS_-
2010_S8918562/d22-x01-y01)
- Charged $\langle p_{\perp} \rangle$ vs. N_{ch} at 7 TeV, track $p_{\perp} > 500$ MeV, for $N_{\text{ch}} \geq 1$ (/REF/ATLAS_2010_-
S8918562/d23-x01-y01)
- Charged $\langle p_{\perp} \rangle$ vs. N_{ch} at 900 GeV, track $p_{\perp} > 100$ MeV, for $N_{\text{ch}} \geq 2$ (/REF/ATLAS_-
2010_S8918562/d24-x01-y01)

- Charged $\langle p_{\perp} \rangle$ vs. N_{ch} at 7 TeV, track $p_{\perp} > 100 \text{ MeV}$, for $N_{\text{ch}} \geq 2$ (/REF/ATLAS_2010_-
S8918562/d25-x01-y01)
- Charged particle η at 900 GeV, track $p_{\perp} > 100 \text{ MeV}$, for $N_{\text{ch}} \geq 20$ (/REF/ATLAS_2010_-
S8918562/d26-x01-y01)
- Charged particle η at 7 TeV, track $p_{\perp} > 100 \text{ MeV}$, for $N_{\text{ch}} \geq 20$ (/REF/ATLAS_2010_-
S8918562/d27-x01-y01)
- Charged particle η at 900 GeV, track $p_{\perp} > 2500 \text{ MeV}$, for $N_{\text{ch}} \geq 1$ (/REF/ATLAS_2010_-
S8918562/d28-x01-y01)
- Charged particle η at 7 TeV, track $p_{\perp} > 2500 \text{ MeV}$, for $N_{\text{ch}} \geq 1$ (/REF/ATLAS_2010_-
S8918562/d29-x01-y01)
- Charged particle p_{\perp} at 900 GeV, track $p_{\perp} > 100 \text{ MeV}$, for $N_{\text{ch}} \geq 20$ (/REF/ATLAS_2010_-
S8918562/d30-x01-y01)
- Charged particle p_{\perp} at 7 TeV, track $p_{\perp} > 100 \text{ MeV}$, for $N_{\text{ch}} \geq 20$ (/REF/ATLAS_2010_-
S8918562/d31-x01-y01)
- Charged particle p_{\perp} at 900 GeV, track $p_{\perp} > 2500 \text{ MeV}$, for $N_{\text{ch}} \geq 1$ (/REF/ATLAS_2010_-
S8918562/d32-x01-y01)
- Charged particle p_{\perp} at 7 TeV, track $p_{\perp} > 2500 \text{ MeV}$, for $N_{\text{ch}} \geq 1$ (/REF/ATLAS_2010_-
S8918562/d33-x01-y01)
- Charged multiplicity ≥ 20 at 900 GeV, track $p_{\perp} > 100 \text{ MeV}$ (/REF/ATLAS_2010_-
S8918562/d34-x01-y01)
- Charged multiplicity ≥ 20 at 7 TeV, track $p_{\perp} > 100 \text{ MeV}$ (/REF/ATLAS_2010_S8918562/d35-x01-y01)
- Charged multiplicity ≥ 1 at 900 GeV, track $p_{\perp} > 2500 \text{ MeV}$ (/REF/ATLAS_2010_-
S8918562/d36-x01-y01)
- Charged multiplicity ≥ 1 at 7 TeV, track $p_{\perp} > 2500 \text{ MeV}$ (/REF/ATLAS_2010_S8918562/d37-x01-y01)
- Charged $\langle p_{\perp} \rangle$ vs. N_{ch} at 900 GeV, track $p_{\perp} > 2500 \text{ MeV}$, for $N_{\text{ch}} \geq 1$ (/REF/ATLAS_-
2010_S8918562/d38-x01-y01)
- Charged $\langle p_{\perp} \rangle$ vs. N_{ch} at 7 TeV, track $p_{\perp} > 2500 \text{ MeV}$, for $N_{\text{ch}} \geq 1$ (/REF/ATLAS_2010_-
S8918562/d39-x01-y01)

8.13 ATLAS_2010_S8919674 [102]

$W + \text{jets}$ jet multiplicities and p_{\perp}

Beams: pp

Energies: (3500.0, 3500.0) GeV

Experiment: ATLAS (LHC)

Spires ID: 8919674

Status: VALIDATED

Authors:

- Frank Siegert <frank.siegert@cern.ch>

References:

- arXiv: [1012.5382](#)

Run details:

- $W+jets$ events ideally with matrix element corrections to describe the higher jet multiplicities correctly. Both channels, electron and muon, are part of this analysis and should be run simultaneously.

Cross sections, in both the electron and muon decay modes of the W boson, are presented as a function of jet multiplicity and of the transverse momentum of the leading and next-to-leading jets in the event. Measurements are also presented of the ratio of cross sections for inclusive jet multiplicities. The results, based on an integrated luminosity of 1.3 pb⁻¹, have been corrected for all known detector effects and are quoted in a limited and well-defined range of jet and lepton kinematics.

Histograms (6):

- Inclusive jet multiplicity (electron channel) ([/REF/ATLAS_2010_S8919674/d01-x01-y01](#))
- Inclusive jet multiplicity (muon channel) ([/REF/ATLAS_2010_S8919674/d02-x01-y01](#))
- p_{\perp} of 1st jet (electron channel) ([/REF/ATLAS_2010_S8919674/d05-x01-y01](#))
- p_{\perp} of 1st jet (muon channel) ([/REF/ATLAS_2010_S8919674/d06-x01-y01](#))
- p_{\perp} of 2nd jet (electron channel) ([/REF/ATLAS_2010_S8919674/d07-x01-y01](#))
- p_{\perp} of 2nd jet (muon channel) ([/REF/ATLAS_2010_S8919674/d08-x01-y01](#))

8.14 ATLAS_2011_CONF_2011_090

Single lepton search for supersymmetry

Beams: pp

Energies: (3500.0, 3500.0) GeV

Experiment: ATLAS (LHC)

Spires ID: [~](#)

Status: VALIDATED

Authors:

- Angela Chen (aqchen@fas.harvard.edu)

References:

- ATLAS-CONF-2011-090

Run details:

- BSM signal events at 7000 GeV.

Single lepton search for supersymmetric particles by ATLAS at 7 TeV. Event counts in electron and muon signal regions are implemented as one-bin histograms. Histograms for missing transverse energy and effective mass are implemented for the two signal regions.

8.15 ATLAS_2011_CONF_2011_098

B-jets search for supersymmetry with 0-leptons

Beams: pp

Energies: (3500.0, 3500.0) GeV

Experiment: ATLAS (LHC)

Spires ID: [~](#)

Status: UNVALIDATED

Authors:

- Angela Chen (aqchen@fas.harvard.edu)

References:

- arXiv: [nnnn.nnnn](#)

Run details:

- BSM signal events at 7000 GeV.

Search for supersymmetric particles by ATLAS at 7 TeV in events with b-jets, large missing energy, and no leptons. Event counts in four signal regions (1 b-jet, $m_{eff} > 500$ GeV; 1 b-jet, $m_{eff} > 700$ GeV; 2 b-jets, $m_{eff} > 500$ GeV; 2 b-jets, $m_{eff} > 700$ GeV) are implemented as one-bin histograms. Histograms for missing transverse energy, effective mass, and p_\perp of the leading jet are implemented for the 1 b-tag and 2 b-tag signal regions.

8.16 ATLAS_2011_I894867 [103]

Measurement of the inelastic proton-proton cross-section at $\sqrt{s} = 7$ TeV.

Beams: $p p$

Energies: (3500.0, 3500.0) GeV

Experiment: ATLAS (LHC)

Inspire ID: [894867](#)

Status: VALIDATED

Authors:

- Anton Karneyeu ⟨Anton.Karneyeu@cern.ch⟩
- Sercan Sen ⟨Sercan.Sen@cern.ch⟩

References:

- arXiv: [1104.0326](#)

Run details:

- Inelastic events (non-diffractive and inelastic diffractive).

Inelastic cross-section is measured for $\xi > 5 \times 10^{-6}$, where $\xi = M_X^2/s$ is calculated from the invariant mass, M_X , of hadrons selected using the largest rapidity gap in the event.

Histograms (1):

- σ_{inel} for $\xi > 5 \cdot 10^{-6}$ at $\sqrt{s} = 7$ TeV ([/REF/ATLAS_2011_I894867/d01-x01-y01](#))

8.17 ATLAS_2011_I919017 [104]

Measurement of ATLAS track jet properties at 7 TeV

Beams: pp

Energies: (3500.0, 3500.0) GeV

Experiment: ATLAS (LHC)

Inspire ID: [919017](#)

Status: VALIDATED

Authors:

- Seth Zenz (seth.zenz@cern.ch)
- Andy Buckley (andy.buckley@cern.ch)

References:

- Phys.Rev.D 84 (2011) 054001
- DOI: [10.1103/PhysRevD.84.054001](https://doi.org/10.1103/PhysRevD.84.054001)
- arXiv: [1107.3311](https://arxiv.org/abs/1107.3311)
- ATLAS-STDM-2010-14
- CERN-PH-EP-2011-110

Run details:

- Min bias QCD at 7 TeV.

ATLAS measurement of track jet p_{\perp} , multiplicity per jet, longitudinal fragmentation, transverse momentum, radius w.r.t jet axis distributions, with jets constructed from charged tracks with $p_{\perp} > 300$ MeV, using the anti- k_T jet algorithm with $R = 0.4, 0.6$.

Histograms (208):

- Charged jet cross section vs. p_{\perp} (anti- k_t , $R = 0.4$, y 0.0-0.5) ([/REF/ATLAS_2011-I919017/d01-x01-y01](#))
- Charged jet cross section vs. p_{\perp} (anti- k_t , $R = 0.4$, y 0.5-1.0) ([/REF/ATLAS_2011-I919017/d01-x01-y02](#))
- Charged jet cross section vs. p_{\perp} (anti- k_t , $R = 0.4$, y 1.0-1.5) ([/REF/ATLAS_2011-I919017/d01-x01-y03](#))
- Charged jet cross section vs. p_{\perp} (anti- k_t , $R = 0.4$, y 1.5-1.9) ([/REF/ATLAS_2011-I919017/d01-x01-y04](#))
- Charged jet multiplicity (anti- k_t , $R = 0.4$, y 0.0-1.9, p_{\perp} 4.0-6.0) ([/REF/ATLAS_2011-I919017/d01-x02-y01](#))

- Charged jet multiplicity (anti- k_t , R = 0.4, y 0.0-1.9, p_\perp 6.0-10.0) (/REF/ATLAS_2011-I919017/d01-x02-y02)
- Charged jet multiplicity (anti- k_t , R = 0.4, y 0.0-1.9, p_\perp 10.0-15.0) (/REF/ATLAS_2011-I919017/d01-x02-y03)
- Charged jet multiplicity (anti- k_t , R = 0.4, y 0.0-1.9, p_\perp 15.0-24.0) (/REF/ATLAS_2011-I919017/d01-x02-y04)
- Charged jet multiplicity (anti- k_t , R = 0.4, y 0.0-1.9, p_\perp 24.0-40.0) (/REF/ATLAS_2011-I919017/d01-x02-y05)
- Charged jet multiplicity (anti- k_t , R = 0.4, y 0.0-0.5, p_\perp 4.0-6.0) (/REF/ATLAS_2011-I919017/d01-x02-y06)
- Charged jet multiplicity (anti- k_t , R = 0.4, y 0.0-0.5, p_\perp 6.0-10.0) (/REF/ATLAS_2011-I919017/d01-x02-y07)
- Charged jet multiplicity (anti- k_t , R = 0.4, y 0.0-0.5, p_\perp 10.0-15.0) (/REF/ATLAS_2011-I919017/d01-x02-y08)
- Charged jet multiplicity (anti- k_t , R = 0.4, y 0.0-0.5, p_\perp 15.0-24.0) (/REF/ATLAS_2011-I919017/d01-x02-y09)
- Charged jet multiplicity (anti- k_t , R = 0.4, y 0.0-0.5, p_\perp 24.0-40.0) (/REF/ATLAS_2011-I919017/d01-x02-y10)
- Charged jet multiplicity (anti- k_t , R = 0.4, y 0.5-1.0, p_\perp 4.0-6.0) (/REF/ATLAS_2011-I919017/d01-x02-y11)
- Charged jet multiplicity (anti- k_t , R = 0.4, y 0.5-1.0, p_\perp 6.0-10.0) (/REF/ATLAS_2011-I919017/d01-x02-y12)
- Charged jet multiplicity (anti- k_t , R = 0.4, y 0.5-1.0, p_\perp 10.0-15.0) (/REF/ATLAS_2011-I919017/d01-x02-y13)
- Charged jet multiplicity (anti- k_t , R = 0.4, y 0.5-1.0, p_\perp 15.0-24.0) (/REF/ATLAS_2011-I919017/d01-x02-y14)
- Charged jet multiplicity (anti- k_t , R = 0.4, y 0.5-1.0, p_\perp 24.0-40.0) (/REF/ATLAS_2011-I919017/d01-x02-y15)
- Charged jet multiplicity (anti- k_t , R = 0.4, y 1.0-1.5, p_\perp 4.0-6.0) (/REF/ATLAS_2011-I919017/d01-x02-y16)
- Charged jet multiplicity (anti- k_t , R = 0.4, y 1.0-1.5, p_\perp 6.0-10.0) (/REF/ATLAS_2011-I919017/d01-x02-y17)
- Charged jet multiplicity (anti- k_t , R = 0.4, y 1.0-1.5, p_\perp 10.0-15.0) (/REF/ATLAS_2011-I919017/d01-x02-y18)

- Charged jet multiplicity (anti- k_t , R = 0.4, y 1.0-1.5, p_\perp 15.0-24.0) (/REF/ATLAS_2011_I919017/d01-x02-y19)
- Charged jet multiplicity (anti- k_t , R = 0.4, y 1.0-1.5, p_\perp 24.0-40.0) (/REF/ATLAS_2011_I919017/d01-x02-y20)
- Charged jet multiplicity (anti- k_t , R = 0.4, y 1.5-1.9, p_\perp 4.0-6.0) (/REF/ATLAS_2011_I919017/d01-x02-y21)
- Charged jet multiplicity (anti- k_t , R = 0.4, y 1.5-1.9, p_\perp 6.0-10.0) (/REF/ATLAS_2011_I919017/d01-x02-y22)
- Charged jet multiplicity (anti- k_t , R = 0.4, y 1.5-1.9, p_\perp 10.0-15.0) (/REF/ATLAS_2011_I919017/d01-x02-y23)
- Charged jet multiplicity (anti- k_t , R = 0.4, y 1.5-1.9, p_\perp 15.0-24.0) (/REF/ATLAS_2011_I919017/d01-x02-y24)
- Charged jet multiplicity (anti- k_t , R = 0.4, y 1.5-1.9, p_\perp 24.0-40.0) (/REF/ATLAS_2011_I919017/d01-x02-y25)
- Charged jet z (anti- k_t , R = 0.4, y 0.0-1.9, p_\perp 4.0-6.0) (/REF/ATLAS_2011_I919017/d01-x03-y01)
- Charged jet z (anti- k_t , R = 0.4, y 0.0-1.9, p_\perp 6.0-10.0) (/REF/ATLAS_2011_I919017/d01-x03-y02)
- Charged jet z (anti- k_t , R = 0.4, y 0.0-1.9, p_\perp 10.0-15.0) (/REF/ATLAS_2011_I919017/d01-x03-y03)
- Charged jet z (anti- k_t , R = 0.4, y 0.0-1.9, p_\perp 15.0-24.0) (/REF/ATLAS_2011_I919017/d01-x03-y04)
- Charged jet z (anti- k_t , R = 0.4, y 0.0-1.9, p_\perp 24.0-40.0) (/REF/ATLAS_2011_I919017/d01-x03-y05)
- Charged jet z (anti- k_t , R = 0.4, y 0.0-0.5, p_\perp 4.0-6.0) (/REF/ATLAS_2011_I919017/d01-x03-y06)
- Charged jet z (anti- k_t , R = 0.4, y 0.0-0.5, p_\perp 6.0-10.0) (/REF/ATLAS_2011_I919017/d01-x03-y07)
- Charged jet z (anti- k_t , R = 0.4, y 0.0-0.5, p_\perp 10.0-15.0) (/REF/ATLAS_2011_I919017/d01-x03-y08)
- Charged jet z (anti- k_t , R = 0.4, y 0.0-0.5, p_\perp 15.0-24.0) (/REF/ATLAS_2011_I919017/d01-x03-y09)
- Charged jet z (anti- k_t , R = 0.4, y 0.0-0.5, p_\perp 24.0-40.0) (/REF/ATLAS_2011_I919017/d01-x03-y10)
- Charged jet z (anti- k_t , R = 0.4, y 0.5-1.0, p_\perp 4.0-6.0) (/REF/ATLAS_2011_I919017/d01-x03-y11)
- Charged jet z (anti- k_t , R = 0.4, y 0.5-1.0, p_\perp 6.0-10.0) (/REF/ATLAS_2011_I919017/d01-x03-y12)
- Charged jet z (anti- k_t , R = 0.4, y 0.5-1.0, p_\perp 10.0-15.0) (/REF/ATLAS_2011_I919017/d01-x03-y13)
- Charged jet z (anti- k_t , R = 0.4, y 0.5-1.0, p_\perp 15.0-24.0) (/REF/ATLAS_2011_I919017/d01-x03-y14)
- Charged jet z (anti- k_t , R = 0.4, y 0.5-1.0, p_\perp 24.0-40.0) (/REF/ATLAS_2011_I919017/d01-x03-y15)
- Charged jet z (anti- k_t , R = 0.4, y 1.0-1.5, p_\perp 4.0-6.0) (/REF/ATLAS_2011_I919017/d01-x03-y16)

- Charged jet z (anti- k_t , $R = 0.4$, $y \in [1.0-1.5]$, $p_{\perp} \in [6.0-10.0]$) ([/REF/ATLAS_2011_I919017/d01-x03-y17](#))
- Charged jet z (anti- k_t , $R = 0.4$, $y \in [1.0-1.5]$, $p_{\perp} \in [10.0-15.0]$) ([/REF/ATLAS_2011_I919017/d01-x03-y18](#))
- Charged jet z (anti- k_t , $R = 0.4$, $y \in [1.0-1.5]$, $p_{\perp} \in [15.0-24.0]$) ([/REF/ATLAS_2011_I919017/d01-x03-y19](#))
- Charged jet z (anti- k_t , $R = 0.4$, $y \in [1.0-1.5]$, $p_{\perp} \in [24.0-40.0]$) ([/REF/ATLAS_2011_I919017/d01-x03-y20](#))
- Charged jet z (anti- k_t , $R = 0.4$, $y \in [1.5-1.9]$, $p_{\perp} \in [4.0-6.0]$) ([/REF/ATLAS_2011_I919017/d01-x03-y21](#))
- Charged jet z (anti- k_t , $R = 0.4$, $y \in [1.5-1.9]$, $p_{\perp} \in [6.0-10.0]$) ([/REF/ATLAS_2011_I919017/d01-x03-y22](#))
- Charged jet z (anti- k_t , $R = 0.4$, $y \in [1.5-1.9]$, $p_{\perp} \in [10.0-15.0]$) ([/REF/ATLAS_2011_I919017/d01-x03-y23](#))
- Charged jet z (anti- k_t , $R = 0.4$, $y \in [1.5-1.9]$, $p_{\perp} \in [15.0-24.0]$) ([/REF/ATLAS_2011_I919017/d01-x03-y24](#))
- Charged jet z (anti- k_t , $R = 0.4$, $y \in [1.5-1.9]$, $p_{\perp} \in [24.0-40.0]$) ([/REF/ATLAS_2011_I919017/d01-x03-y25](#))
- Charged jet p_{\perp}^{rel} (anti- k_t , $R = 0.4$, $y \in [0.0-1.9]$, $p_{\perp} \in [4.0-6.0]$) ([/REF/ATLAS_2011_I919017/d01-x04-y01](#))
- Charged jet p_{\perp}^{rel} (anti- k_t , $R = 0.4$, $y \in [0.0-1.9]$, $p_{\perp} \in [6.0-10.0]$) ([/REF/ATLAS_2011_I919017/d01-x04-y02](#))
- Charged jet p_{\perp}^{rel} (anti- k_t , $R = 0.4$, $y \in [0.0-1.9]$, $p_{\perp} \in [10.0-15.0]$) ([/REF/ATLAS_2011_I919017/d01-x04-y03](#))
- Charged jet p_{\perp}^{rel} (anti- k_t , $R = 0.4$, $y \in [0.0-1.9]$, $p_{\perp} \in [15.0-24.0]$) ([/REF/ATLAS_2011_I919017/d01-x04-y04](#))
- Charged jet p_{\perp}^{rel} (anti- k_t , $R = 0.4$, $y \in [0.0-1.9]$, $p_{\perp} \in [24.0-40.0]$) ([/REF/ATLAS_2011_I919017/d01-x04-y05](#))
- Charged jet p_{\perp}^{rel} (anti- k_t , $R = 0.4$, $y \in [0.0-0.5]$, $p_{\perp} \in [4.0-6.0]$) ([/REF/ATLAS_2011_I919017/d01-x04-y06](#))
- Charged jet p_{\perp}^{rel} (anti- k_t , $R = 0.4$, $y \in [0.0-0.5]$, $p_{\perp} \in [6.0-10.0]$) ([/REF/ATLAS_2011_I919017/d01-x04-y07](#))
- Charged jet p_{\perp}^{rel} (anti- k_t , $R = 0.4$, $y \in [0.0-0.5]$, $p_{\perp} \in [10.0-15.0]$) ([/REF/ATLAS_2011_I919017/d01-x04-y08](#))
- Charged jet p_{\perp}^{rel} (anti- k_t , $R = 0.4$, $y \in [0.0-0.5]$, $p_{\perp} \in [15.0-24.0]$) ([/REF/ATLAS_2011_I919017/d01-x04-y09](#))
- Charged jet p_{\perp}^{rel} (anti- k_t , $R = 0.4$, $y \in [0.0-0.5]$, $p_{\perp} \in [24.0-40.0]$) ([/REF/ATLAS_2011_I919017/d01-x04-y10](#))
- Charged jet p_{\perp}^{rel} (anti- k_t , $R = 0.4$, $y \in [0.5-1.0]$, $p_{\perp} \in [4.0-6.0]$) ([/REF/ATLAS_2011_I919017/d01-x04-y11](#))
- Charged jet p_{\perp}^{rel} (anti- k_t , $R = 0.4$, $y \in [0.5-1.0]$, $p_{\perp} \in [6.0-10.0]$) ([/REF/ATLAS_2011_I919017/d01-x04-y12](#))
- Charged jet p_{\perp}^{rel} (anti- k_t , $R = 0.4$, $y \in [0.5-1.0]$, $p_{\perp} \in [10.0-15.0]$) ([/REF/ATLAS_2011_I919017/d01-x04-y13](#))
- Charged jet p_{\perp}^{rel} (anti- k_t , $R = 0.4$, $y \in [0.5-1.0]$, $p_{\perp} \in [15.0-24.0]$) ([/REF/ATLAS_2011_I919017/d01-x04-y14](#))
- Charged jet p_{\perp}^{rel} (anti- k_t , $R = 0.4$, $y \in [0.5-1.0]$, $p_{\perp} \in [24.0-40.0]$) ([/REF/ATLAS_2011_I919017/d01-x04-y15](#))
- Charged jet p_{\perp}^{rel} (anti- k_t , $R = 0.4$, $y \in [1.0-1.5]$, $p_{\perp} \in [4.0-6.0]$) ([/REF/ATLAS_2011_I919017/d01-x04-y16](#))
- Charged jet p_{\perp}^{rel} (anti- k_t , $R = 0.4$, $y \in [1.0-1.5]$, $p_{\perp} \in [6.0-10.0]$) ([/REF/ATLAS_2011_I919017/d01-x04-y17](#))
- Charged jet p_{\perp}^{rel} (anti- k_t , $R = 0.4$, $y \in [1.0-1.5]$, $p_{\perp} \in [10.0-15.0]$) ([/REF/ATLAS_2011_I919017/d01-x04-y18](#))

- Charged jet p_{\perp}^{rel} (anti- k_t , R = 0.4, y 1.0-1.5, p_{\perp} 15.0-24.0) (/REF/ATLAS_2011_I919017/d01-x04-y19)
- Charged jet p_{\perp}^{rel} (anti- k_t , R = 0.4, y 1.0-1.5, p_{\perp} 24.0-40.0) (/REF/ATLAS_2011_I919017/d01-x04-y20)
- Charged jet p_{\perp}^{rel} (anti- k_t , R = 0.4, y 1.5-1.9, p_{\perp} 4.0-6.0) (/REF/ATLAS_2011_I919017/d01-x04-y21)
- Charged jet p_{\perp}^{rel} (anti- k_t , R = 0.4, y 1.5-1.9, p_{\perp} 6.0-10.0) (/REF/ATLAS_2011_I919017/d01-x04-y22)
- Charged jet p_{\perp}^{rel} (anti- k_t , R = 0.4, y 1.5-1.9, p_{\perp} 10.0-15.0) (/REF/ATLAS_2011_I919017/d01-x04-y23)
- Charged jet p_{\perp}^{rel} (anti- k_t , R = 0.4, y 1.5-1.9, p_{\perp} 15.0-24.0) (/REF/ATLAS_2011_I919017/d01-x04-y24)
- Charged jet p_{\perp}^{rel} (anti- k_t , R = 0.4, y 1.5-1.9, p_{\perp} 24.0-40.0) (/REF/ATLAS_2011_I919017/d01-x04-y25)
- Charged jet $\rho_{\text{ch}}(r)$ (anti- k_t , R = 0.4, y 0.0-1.9, p_{\perp} 4.0-6.0) (/REF/ATLAS_2011_I919017/d01-x05-y01)
- Charged jet $\rho_{\text{ch}}(r)$ (anti- k_t , R = 0.4, y 0.0-1.9, p_{\perp} 6.0-10.0) (/REF/ATLAS_2011_I919017/d01-x05-y02)
- Charged jet $\rho_{\text{ch}}(r)$ (anti- k_t , R = 0.4, y 0.0-1.9, p_{\perp} 10.0-15.0) (/REF/ATLAS_2011_I919017/d01-x05-y03)
- Charged jet $\rho_{\text{ch}}(r)$ (anti- k_t , R = 0.4, y 0.0-1.9, p_{\perp} 15.0-24.0) (/REF/ATLAS_2011_I919017/d01-x05-y04)
- Charged jet $\rho_{\text{ch}}(r)$ (anti- k_t , R = 0.4, y 0.0-1.9, p_{\perp} 24.0-40.0) (/REF/ATLAS_2011_I919017/d01-x05-y05)
- Charged jet $\rho_{\text{ch}}(r)$ (anti- k_t , R = 0.4, y 0.0-0.5, p_{\perp} 4.0-6.0) (/REF/ATLAS_2011_I919017/d01-x05-y06)
- Charged jet $\rho_{\text{ch}}(r)$ (anti- k_t , R = 0.4, y 0.0-0.5, p_{\perp} 6.0-10.0) (/REF/ATLAS_2011_I919017/d01-x05-y07)
- Charged jet $\rho_{\text{ch}}(r)$ (anti- k_t , R = 0.4, y 0.0-0.5, p_{\perp} 10.0-15.0) (/REF/ATLAS_2011_I919017/d01-x05-y08)
- Charged jet $\rho_{\text{ch}}(r)$ (anti- k_t , R = 0.4, y 0.0-0.5, p_{\perp} 15.0-24.0) (/REF/ATLAS_2011_I919017/d01-x05-y09)
- Charged jet $\rho_{\text{ch}}(r)$ (anti- k_t , R = 0.4, y 0.0-0.5, p_{\perp} 24.0-40.0) (/REF/ATLAS_2011_I919017/d01-x05-y10)
- Charged jet $\rho_{\text{ch}}(r)$ (anti- k_t , R = 0.4, y 0.5-1.0, p_{\perp} 4.0-6.0) (/REF/ATLAS_2011_I919017/d01-x05-y11)
- Charged jet $\rho_{\text{ch}}(r)$ (anti- k_t , R = 0.4, y 0.5-1.0, p_{\perp} 6.0-10.0) (/REF/ATLAS_2011_I919017/d01-x05-y12)
- Charged jet $\rho_{\text{ch}}(r)$ (anti- k_t , R = 0.4, y 0.5-1.0, p_{\perp} 10.0-15.0) (/REF/ATLAS_2011_I919017/d01-x05-y13)
- Charged jet $\rho_{\text{ch}}(r)$ (anti- k_t , R = 0.4, y 0.5-1.0, p_{\perp} 15.0-24.0) (/REF/ATLAS_2011_I919017/d01-x05-y14)
- Charged jet $\rho_{\text{ch}}(r)$ (anti- k_t , R = 0.4, y 0.5-1.0, p_{\perp} 24.0-40.0) (/REF/ATLAS_2011_I919017/d01-x05-y15)

- Charged jet $\rho_{\text{ch}}(r)$ (anti- k_t , $R = 0.4$, $y \in 1.0\text{-}1.5$, $p_\perp \in 4.0\text{-}6.0$) ([/REF/ATLAS_2011_I919017/d01-x05-y16](#))
- Charged jet $\rho_{\text{ch}}(r)$ (anti- k_t , $R = 0.4$, $y \in 1.0\text{-}1.5$, $p_\perp \in 6.0\text{-}10.0$) ([/REF/ATLAS_2011_I919017/d01-x05-y17](#))
- Charged jet $\rho_{\text{ch}}(r)$ (anti- k_t , $R = 0.4$, $y \in 1.0\text{-}1.5$, $p_\perp \in 10.0\text{-}15.0$) ([/REF/ATLAS_2011_I919017/d01-x05-y18](#))
- Charged jet $\rho_{\text{ch}}(r)$ (anti- k_t , $R = 0.4$, $y \in 1.0\text{-}1.5$, $p_\perp \in 15.0\text{-}24.0$) ([/REF/ATLAS_2011_I919017/d01-x05-y19](#))
- Charged jet $\rho_{\text{ch}}(r)$ (anti- k_t , $R = 0.4$, $y \in 1.0\text{-}1.5$, $p_\perp \in 24.0\text{-}40.0$) ([/REF/ATLAS_2011_I919017/d01-x05-y20](#))
- Charged jet $\rho_{\text{ch}}(r)$ (anti- k_t , $R = 0.4$, $y \in 1.5\text{-}1.9$, $p_\perp \in 4.0\text{-}6.0$) ([/REF/ATLAS_2011_I919017/d01-x05-y21](#))
- Charged jet $\rho_{\text{ch}}(r)$ (anti- k_t , $R = 0.4$, $y \in 1.5\text{-}1.9$, $p_\perp \in 6.0\text{-}10.0$) ([/REF/ATLAS_2011_I919017/d01-x05-y22](#))
- Charged jet $\rho_{\text{ch}}(r)$ (anti- k_t , $R = 0.4$, $y \in 1.5\text{-}1.9$, $p_\perp \in 10.0\text{-}15.0$) ([/REF/ATLAS_2011_I919017/d01-x05-y23](#))
- Charged jet $\rho_{\text{ch}}(r)$ (anti- k_t , $R = 0.4$, $y \in 1.5\text{-}1.9$, $p_\perp \in 15.0\text{-}24.0$) ([/REF/ATLAS_2011_I919017/d01-x05-y24](#))
- Charged jet $\rho_{\text{ch}}(r)$ (anti- k_t , $R = 0.4$, $y \in 1.5\text{-}1.9$, $p_\perp \in 24.0\text{-}40.0$) ([/REF/ATLAS_2011_I919017/d01-x05-y25](#))
- Charged jet cross section vs. p_\perp (anti- k_t , $R = 0.6$, $y \in 0.0\text{-}0.5$) ([/REF/ATLAS_2011_I919017/d02-x01-y01](#))
- Charged jet cross section vs. p_\perp (anti- k_t , $R = 0.6$, $y \in 0.5\text{-}1.0$) ([/REF/ATLAS_2011_I919017/d02-x01-y02](#))
- Charged jet cross section vs. p_\perp (anti- k_t , $R = 0.6$, $y \in 1.0\text{-}1.5$) ([/REF/ATLAS_2011_I919017/d02-x01-y03](#))
- Charged jet cross section vs. p_\perp (anti- k_t , $R = 0.6$, $y \in 1.5\text{-}1.9$) ([/REF/ATLAS_2011_I919017/d02-x01-y04](#))
- Charged jet multiplicity (anti- k_t , $R = 0.6$, $y \in 0.0\text{-}1.9$, $p_\perp \in 4.0\text{-}6.0$) ([/REF/ATLAS_2011_I919017/d02-x02-y01](#))
- Charged jet multiplicity (anti- k_t , $R = 0.6$, $y \in 0.0\text{-}1.9$, $p_\perp \in 6.0\text{-}10.0$) ([/REF/ATLAS_2011_I919017/d02-x02-y02](#))
- Charged jet multiplicity (anti- k_t , $R = 0.6$, $y \in 0.0\text{-}1.9$, $p_\perp \in 10.0\text{-}15.0$) ([/REF/ATLAS_2011_I919017/d02-x02-y03](#))
- Charged jet multiplicity (anti- k_t , $R = 0.6$, $y \in 0.0\text{-}1.9$, $p_\perp \in 15.0\text{-}24.0$) ([/REF/ATLAS_2011_I919017/d02-x02-y04](#))

- Charged jet multiplicity (anti- k_t , R = 0.6, y 0.0-1.9, p_\perp 24.0-40.0) (/REF/ATLAS_2011-I919017/d02-x02-y05)
- Charged jet multiplicity (anti- k_t , R = 0.6, y 0.0-0.5, p_\perp 4.0-6.0) (/REF/ATLAS_2011-I919017/d02-x02-y06)
- Charged jet multiplicity (anti- k_t , R = 0.6, y 0.0-0.5, p_\perp 6.0-10.0) (/REF/ATLAS_2011-I919017/d02-x02-y07)
- Charged jet multiplicity (anti- k_t , R = 0.6, y 0.0-0.5, p_\perp 10.0-15.0) (/REF/ATLAS_2011-I919017/d02-x02-y08)
- Charged jet multiplicity (anti- k_t , R = 0.6, y 0.0-0.5, p_\perp 15.0-24.0) (/REF/ATLAS_2011-I919017/d02-x02-y09)
- Charged jet multiplicity (anti- k_t , R = 0.6, y 0.0-0.5, p_\perp 24.0-40.0) (/REF/ATLAS_2011-I919017/d02-x02-y10)
- Charged jet multiplicity (anti- k_t , R = 0.6, y 0.5-1.0, p_\perp 4.0-6.0) (/REF/ATLAS_2011-I919017/d02-x02-y11)
- Charged jet multiplicity (anti- k_t , R = 0.6, y 0.5-1.0, p_\perp 6.0-10.0) (/REF/ATLAS_2011-I919017/d02-x02-y12)
- Charged jet multiplicity (anti- k_t , R = 0.6, y 0.5-1.0, p_\perp 10.0-15.0) (/REF/ATLAS_2011-I919017/d02-x02-y13)
- Charged jet multiplicity (anti- k_t , R = 0.6, y 0.5-1.0, p_\perp 15.0-24.0) (/REF/ATLAS_2011-I919017/d02-x02-y14)
- Charged jet multiplicity (anti- k_t , R = 0.6, y 0.5-1.0, p_\perp 24.0-40.0) (/REF/ATLAS_2011-I919017/d02-x02-y15)
- Charged jet multiplicity (anti- k_t , R = 0.6, y 1.0-1.5, p_\perp 4.0-6.0) (/REF/ATLAS_2011-I919017/d02-x02-y16)
- Charged jet multiplicity (anti- k_t , R = 0.6, y 1.0-1.5, p_\perp 6.0-10.0) (/REF/ATLAS_2011-I919017/d02-x02-y17)
- Charged jet multiplicity (anti- k_t , R = 0.6, y 1.0-1.5, p_\perp 10.0-15.0) (/REF/ATLAS_2011-I919017/d02-x02-y18)
- Charged jet multiplicity (anti- k_t , R = 0.6, y 1.0-1.5, p_\perp 15.0-24.0) (/REF/ATLAS_2011-I919017/d02-x02-y19)
- Charged jet multiplicity (anti- k_t , R = 0.6, y 1.0-1.5, p_\perp 24.0-40.0) (/REF/ATLAS_2011-I919017/d02-x02-y20)
- Charged jet multiplicity (anti- k_t , R = 0.6, y 1.5-1.9, p_\perp 4.0-6.0) (/REF/ATLAS_2011-I919017/d02-x02-y21)

- Charged jet multiplicity (anti- k_t , R = 0.6, y 1.5-1.9, p_\perp 6.0-10.0) ([/REF/ATLAS_2011_I919017/d02-x02-y22](#))
- Charged jet multiplicity (anti- k_t , R = 0.6, y 1.5-1.9, p_\perp 10.0-15.0) ([/REF/ATLAS_2011_I919017/d02-x02-y23](#))
- Charged jet multiplicity (anti- k_t , R = 0.6, y 1.5-1.9, p_\perp 15.0-24.0) ([/REF/ATLAS_2011_I919017/d02-x02-y24](#))
- Charged jet multiplicity (anti- k_t , R = 0.6, y 1.5-1.9, p_\perp 24.0-40.0) ([/REF/ATLAS_2011_I919017/d02-x02-y25](#))
- Charged jet z (anti- k_t , R = 0.6, y 0.0-1.9, p_\perp 4.0-6.0) ([/REF/ATLAS_2011_I919017/d02-x03-y01](#))
- Charged jet z (anti- k_t , R = 0.6, y 0.0-1.9, p_\perp 6.0-10.0) ([/REF/ATLAS_2011_I919017/d02-x03-y02](#))
- Charged jet z (anti- k_t , R = 0.6, y 0.0-1.9, p_\perp 10.0-15.0) ([/REF/ATLAS_2011_I919017/d02-x03-y03](#))
- Charged jet z (anti- k_t , R = 0.6, y 0.0-1.9, p_\perp 15.0-24.0) ([/REF/ATLAS_2011_I919017/d02-x03-y04](#))
- Charged jet z (anti- k_t , R = 0.6, y 0.0-1.9, p_\perp 24.0-40.0) ([/REF/ATLAS_2011_I919017/d02-x03-y05](#))
- Charged jet z (anti- k_t , R = 0.6, y 0.0-0.5, p_\perp 4.0-6.0) ([/REF/ATLAS_2011_I919017/d02-x03-y06](#))
- Charged jet z (anti- k_t , R = 0.6, y 0.0-0.5, p_\perp 6.0-10.0) ([/REF/ATLAS_2011_I919017/d02-x03-y07](#))
- Charged jet z (anti- k_t , R = 0.6, y 0.0-0.5, p_\perp 10.0-15.0) ([/REF/ATLAS_2011_I919017/d02-x03-y08](#))
- Charged jet z (anti- k_t , R = 0.6, y 0.0-0.5, p_\perp 15.0-24.0) ([/REF/ATLAS_2011_I919017/d02-x03-y09](#))
- Charged jet z (anti- k_t , R = 0.6, y 0.0-0.5, p_\perp 24.0-40.0) ([/REF/ATLAS_2011_I919017/d02-x03-y10](#))
- Charged jet z (anti- k_t , R = 0.6, y 0.5-1.0, p_\perp 4.0-6.0) ([/REF/ATLAS_2011_I919017/d02-x03-y11](#))
- Charged jet z (anti- k_t , R = 0.6, y 0.5-1.0, p_\perp 6.0-10.0) ([/REF/ATLAS_2011_I919017/d02-x03-y12](#))
- Charged jet z (anti- k_t , R = 0.6, y 0.5-1.0, p_\perp 10.0-15.0) ([/REF/ATLAS_2011_I919017/d02-x03-y13](#))
- Charged jet z (anti- k_t , R = 0.6, y 0.5-1.0, p_\perp 15.0-24.0) ([/REF/ATLAS_2011_I919017/d02-x03-y14](#))
- Charged jet z (anti- k_t , R = 0.6, y 0.5-1.0, p_\perp 24.0-40.0) ([/REF/ATLAS_2011_I919017/d02-x03-y15](#))
- Charged jet z (anti- k_t , R = 0.6, y 1.0-1.5, p_\perp 4.0-6.0) ([/REF/ATLAS_2011_I919017/d02-x03-y16](#))
- Charged jet z (anti- k_t , R = 0.6, y 1.0-1.5, p_\perp 6.0-10.0) ([/REF/ATLAS_2011_I919017/d02-x03-y17](#))
- Charged jet z (anti- k_t , R = 0.6, y 1.0-1.5, p_\perp 10.0-15.0) ([/REF/ATLAS_2011_I919017/d02-x03-y18](#))
- Charged jet z (anti- k_t , R = 0.6, y 1.0-1.5, p_\perp 15.0-24.0) ([/REF/ATLAS_2011_I919017/d02-x03-y19](#))
- Charged jet z (anti- k_t , R = 0.6, y 1.0-1.5, p_\perp 24.0-40.0) ([/REF/ATLAS_2011_I919017/d02-x03-y20](#))
- Charged jet z (anti- k_t , R = 0.6, y 1.5-1.9, p_\perp 4.0-6.0) ([/REF/ATLAS_2011_I919017/d02-x03-y21](#))

- Charged jet p_{\perp}^{rel} (anti- k_t , $R = 0.6$, y 1.5-1.9, p_{\perp} 15.0-24.0) ([/REF/ATLAS_2011_I919017/d02-x04-y24](#))
- Charged jet p_{\perp}^{rel} (anti- k_t , $R = 0.6$, y 1.5-1.9, p_{\perp} 24.0-40.0) ([/REF/ATLAS_2011_I919017/d02-x04-y25](#))
- Charged jet $\rho_{\text{ch}}(r)$ (anti- k_t , $R = 0.6$, y 0.0-1.9, p_{\perp} 4.0-6.0) ([/REF/ATLAS_2011_I919017/d02-x05-y01](#))
- Charged jet $\rho_{\text{ch}}(r)$ (anti- k_t , $R = 0.6$, y 0.0-1.9, p_{\perp} 6.0-10.0) ([/REF/ATLAS_2011_I919017/d02-x05-y02](#))
- Charged jet $\rho_{\text{ch}}(r)$ (anti- k_t , $R = 0.6$, y 0.0-1.9, p_{\perp} 10.0-15.0) ([/REF/ATLAS_2011_I919017/d02-x05-y03](#))
- Charged jet $\rho_{\text{ch}}(r)$ (anti- k_t , $R = 0.6$, y 0.0-1.9, p_{\perp} 15.0-24.0) ([/REF/ATLAS_2011_I919017/d02-x05-y04](#))
- Charged jet $\rho_{\text{ch}}(r)$ (anti- k_t , $R = 0.6$, y 0.0-1.9, p_{\perp} 24.0-40.0) ([/REF/ATLAS_2011_I919017/d02-x05-y05](#))
- Charged jet $\rho_{\text{ch}}(r)$ (anti- k_t , $R = 0.6$, y 0.0-0.5, p_{\perp} 4.0-6.0) ([/REF/ATLAS_2011_I919017/d02-x05-y06](#))
- Charged jet $\rho_{\text{ch}}(r)$ (anti- k_t , $R = 0.6$, y 0.0-0.5, p_{\perp} 6.0-10.0) ([/REF/ATLAS_2011_I919017/d02-x05-y07](#))
- Charged jet $\rho_{\text{ch}}(r)$ (anti- k_t , $R = 0.6$, y 0.0-0.5, p_{\perp} 10.0-15.0) ([/REF/ATLAS_2011_I919017/d02-x05-y08](#))
- Charged jet $\rho_{\text{ch}}(r)$ (anti- k_t , $R = 0.6$, y 0.0-0.5, p_{\perp} 15.0-24.0) ([/REF/ATLAS_2011_I919017/d02-x05-y09](#))
- Charged jet $\rho_{\text{ch}}(r)$ (anti- k_t , $R = 0.6$, y 0.0-0.5, p_{\perp} 24.0-40.0) ([/REF/ATLAS_2011_I919017/d02-x05-y10](#))
- Charged jet $\rho_{\text{ch}}(r)$ (anti- k_t , $R = 0.6$, y 0.5-1.0, p_{\perp} 4.0-6.0) ([/REF/ATLAS_2011_I919017/d02-x05-y11](#))
- Charged jet $\rho_{\text{ch}}(r)$ (anti- k_t , $R = 0.6$, y 0.5-1.0, p_{\perp} 6.0-10.0) ([/REF/ATLAS_2011_I919017/d02-x05-y12](#))
- Charged jet $\rho_{\text{ch}}(r)$ (anti- k_t , $R = 0.6$, y 0.5-1.0, p_{\perp} 10.0-15.0) ([/REF/ATLAS_2011_I919017/d02-x05-y13](#))
- Charged jet $\rho_{\text{ch}}(r)$ (anti- k_t , $R = 0.6$, y 0.5-1.0, p_{\perp} 15.0-24.0) ([/REF/ATLAS_2011_I919017/d02-x05-y14](#))
- Charged jet $\rho_{\text{ch}}(r)$ (anti- k_t , $R = 0.6$, y 0.5-1.0, p_{\perp} 24.0-40.0) ([/REF/ATLAS_2011_I919017/d02-x05-y15](#))
- Charged jet $\rho_{\text{ch}}(r)$ (anti- k_t , $R = 0.6$, y 1.0-1.5, p_{\perp} 4.0-6.0) ([/REF/ATLAS_2011_I919017/d02-x05-y16](#))
- Charged jet $\rho_{\text{ch}}(r)$ (anti- k_t , $R = 0.6$, y 1.0-1.5, p_{\perp} 6.0-10.0) ([/REF/ATLAS_2011_I919017/d02-x05-y17](#))
- Charged jet $\rho_{\text{ch}}(r)$ (anti- k_t , $R = 0.6$, y 1.0-1.5, p_{\perp} 10.0-15.0) ([/REF/ATLAS_2011_I919017/d02-x05-y18](#))

- Charged jet $\rho_{\text{ch}}(r)$ (anti- k_t , R = 0.6, y 1.0-1.5, p_\perp 15.0-24.0) ([/REF/ATLAS_2011_I919017/d02-x05-y19](#))
- Charged jet $\rho_{\text{ch}}(r)$ (anti- k_t , R = 0.6, y 1.0-1.5, p_\perp 24.0-40.0) ([/REF/ATLAS_2011_I919017/d02-x05-y20](#))
- Charged jet $\rho_{\text{ch}}(r)$ (anti- k_t , R = 0.6, y 1.5-1.9, p_\perp 4.0-6.0) ([/REF/ATLAS_2011_I919017/d02-x05-y21](#))
- Charged jet $\rho_{\text{ch}}(r)$ (anti- k_t , R = 0.6, y 1.5-1.9, p_\perp 6.0-10.0) ([/REF/ATLAS_2011_I919017/d02-x05-y22](#))
- Charged jet $\rho_{\text{ch}}(r)$ (anti- k_t , R = 0.6, y 1.5-1.9, p_\perp 10.0-15.0) ([/REF/ATLAS_2011_I919017/d02-x05-y23](#))
- Charged jet $\rho_{\text{ch}}(r)$ (anti- k_t , R = 0.6, y 1.5-1.9, p_\perp 15.0-24.0) ([/REF/ATLAS_2011_I919017/d02-x05-y24](#))
- Charged jet $\rho_{\text{ch}}(r)$ (anti- k_t , R = 0.6, y 1.5-1.9, p_\perp 24.0-40.0) ([/REF/ATLAS_2011_I919017/d02-x05-y25](#))

8.18 ATLAS_2011_I925932 [105]

Measurement of the $W p_\perp$ with electrons and muons at 7 TeV

Beams: pp

Energies: (3500.0, 3500.0) GeV

Experiment: ATLAS (LHC)

Inspire ID: [925932](#)

Status: VALIDATED

Authors:

- Elena Yatsenko ⟨elena.yatsenko@desy.de⟩
- Judith Katzy ⟨jkatzy@mail.cern.ch⟩

References:

- arXiv: [1108.6308v1](#)

Run details:

- Run with W decays to $e \nu_e$ and/or $\mu \nu_\mu$.

The $W p_\perp$ at $\sqrt{s} = 7$ TeV is measured using $W \rightarrow e \nu_e$ and $W \rightarrow \mu \nu_\mu$ decay channels. The dressed leptons kinematics calculated from the sum of the post-FSR lepton momentum and the momenta of all photons radiated in a cone around the lepton, while the bare uses the lepton kinematics after all QED radiation.

Histograms (4):

- $W \rightarrow e \nu_e p_\perp$ with "dressed" kinematics ([/REF/ATLAS_2011_I925932/d01-x01-y01](#))
- $W \rightarrow e \nu_e p_\perp$ with "bare" kinematics ([/REF/ATLAS_2011_I925932/d01-x01-y02](#))
- $W \rightarrow \mu \nu_\mu p_\perp$ with "dressed" kinematics ([/REF/ATLAS_2011_I925932/d02-x01-y01](#))
- $W \rightarrow \mu \nu_\mu p_\perp$ with "bare" kinematics ([/REF/ATLAS_2011_I925932/d02-x01-y02](#))

8.19 ATLAS_2011_I926145 [106]

Measurement of electron and muon differential cross-section from heavy-flavour decays

Beams: pp

Energies: (3500.0, 3500.0) GeV

Experiment: ATLAS (LHC)

Inspire ID: [9185208](#)

Status: VALIDATED

Authors:

- Paul Bell (paul.bell@cern.ch)
- Holger Schulz (holger.schulz@physik.hu-berlin.de)

References:

- CERN-PH-EP-2011-108
- arXiv: [1109.0525](#)

Run details:

- pp to electron + X or muon + X at 7 TeV, heavy-flavour (bb and cc) production with $B/D \rightarrow e/\mu$

Measurement of inclusive electron and muon cross sections for $7 < p_\perp < 26$ GeV in $|\eta| < 2.0$, excluding $1.37 < |\eta| < 1.52$, and muon cross section for $4 < p_\perp < 100$ GeV in $|\eta| < 2.50$. The $W/Z/\gamma^*$ component must be subtracted to leave the heavy flavour contribution.

Histograms (3):

- Electron diff. cross-section $|\eta| < 2.0$ excl. $1.37 < |\eta| < 1.52$ ([/REF/ATLAS_2011_I926145/d01-x01-y01](#))
- Muon diff. cross-section $|\eta| < 2.0$ excl. $1.37 < |\eta| < 1.52$ ([/REF/ATLAS_2011_I926145/d02-x01-y01](#))
- Muon differential cross-section $|\eta| < 2.5$ ([/REF/ATLAS_2011_I926145/d03-x01-y01](#))

8.20 ATLAS_2011_I930220 [107]

Inclusive and dijet cross-sections of b -jets in pp collisions at $\sqrt{s} = 7$ TeV with ATLAS

Beams: pp

Energies: (3500.0, 3500.0) GeV

Experiment: ATLAS (LHC)

Inspire ID: [930220](#)

Status: VALIDATED

Authors:

- Stephen Paul Bieniek (stephen.paul.bieniek@cern.ch)

References:

- Eur.Phys.J. C71 (2011) 1846
- arXiv: [1109.6833](#)

Run details:

- QCD events at 7 TeV

The inclusive and dijet production cross-sections have been measured for jets containing b -hadrons (b -jets) in proton–proton collisions at a centre-of-mass energy of $\sqrt{s} = 7$ TeV, using the ATLAS detector at the LHC. The measurements use data corresponding to an integrated luminosity of 34 pb^{-1} . The b -jets are identified using either a lifetime-based method, where secondary decay vertices of b -hadrons in jets are reconstructed using information from the tracking detectors, or a muon-based method where the presence of a muon is used to identify semileptonic decays of b -hadrons inside jets. The inclusive b -jet cross-section is measured as a function of transverse momentum in the range $20 < p_T < 400$ GeV and rapidity in the range $|y| < 2.1$. The $b\bar{b}$ -dijet cross-section is measured as a function of the dijet invariant mass in the range $110 < m_{\text{jj}} < 760$ GeV, the azimuthal angle difference between the two jets and the angular variable χ in two dijet mass regions. The results are compared with next-to-leading-order QCD predictions. Good agreement is observed between the measured cross-sections and the predictions obtained using POWHEG+Pythia6. MC@NLO+Herwig shows good agreement with the measured $b\bar{b}$ -dijet cross-section. However, it does not reproduce the measured inclusive cross-section well, particularly for central b -jets with large transverse momenta.

Histograms (10):

- Lifetime tagged b -jet p_T for $|y| < 0.3$, anti- k_T , $R = 0.4$ ([/REF/ATLAS_2011_I930220/d01-x01-y01](#))
- Lifetime tagged b -jet p_T for $0.3 < |y| < 0.8$, anti- k_T , $R = 0.4$ ([/REF/ATLAS_2011_I930220/d02-x01-y01](#))
- Lifetime tagged b -jet p_T for $0.8 < |y| < 1.2$, anti- k_T , $R = 0.4$ ([/REF/ATLAS_2011_I930220/d03-x01-y01](#))

- Lifetime tagged b -jet p_T for $1.2 < |y| < 2.1$, anti- k_T , $R = 0.4$ ([/REF/ATLAS_2011_I930220/d04-x01-y01](#))
- Lifetime tagged b -jet p_T for $|y| < 2.1$, anti- k_T , $R = 0.4$. ([/REF/ATLAS_2011_I930220/d05-x01-y01](#))
- Muon tagged b -jet p_T for $|y| < 2.1$, anti- k_T , $R = 0.4$ ([/REF/ATLAS_2011_I930220/d06-x01-y01](#))
- Dijet mass spectrum for $|y| < 2.1$, anti- k_T , $R = 0.4$ ([/REF/ATLAS_2011_I930220/d07-x01-y01](#))
- Dijet $\Delta\phi$ for $m_{jj} > 110$ GeV, anti- k_T , $R = 0.4$ ([/REF/ATLAS_2011_I930220/d08-x01-y01](#))
- Dijet χ for $110 < m_{jj} < 370$ GeV, anti- k_T , $R = 0.4$ ([/REF/ATLAS_2011_I930220/d09-x01-y01](#))
- Dijet χ for $370 < m_{jj} < 850$ GeV, anti- k_T , $R = 0.4$ ([/REF/ATLAS_2011_I930220/d10-x01-y01](#))

8.21 ATLAS_2011_I944826 [108]

K_S^0 and Λ production at 0.9 and 7 TeV with ATLAS

Beams: pp

Energies: (450.0, 450.0), (3500.0, 3500.0) GeV

Experiment: ATLAS (LHC)

Inspire ID: [944826](#)

Status: VALIDATED

Authors:

- Holger Schulz (holger.schulz@physik.hu-berlin.de)

References:

- arXiv: [1111.1297v2](#)
- Phys.Rev. D85 (2012) 012001

Run details:

- QCD events, 900 GeV and 7 TeV. Λ and K_S must be able to decay. Allow only charged decay modes to improve efficiency.

The production of K_S and Λ hadrons is studied in inelastic pp collisions at $\sqrt{s} = 0.9$ and 7 TeV collected with the ATLAS detector at the LHC using a minimum-bias trigger. The observed distributions of transverse momentum, rapidity, and multiplicity are corrected to hadron level in a model-independent way within well defined phase-space regions. The distribution of the production ratio of $\bar{\Lambda}$ to Λ baryons is also measured. The results are compared with various Monte Carlo simulation models. Although most of these models agree with data to within 15 percent in the K_S distributions, substantial disagreements with data are found in the Λ distributions of transverse momentum.

Histograms (16):

- K_S^0 transverse momentum, $\sqrt{s} = 7000$ GeV ([/REF/ATLAS_2011_I944826/d01-x01-y01](#))
- K_S^0 rapidity, $\sqrt{s} = 7000$ GeV ([/REF/ATLAS_2011_I944826/d02-x01-y01](#))
- K_S^0 multiplicity, $\sqrt{s} = 7000$ GeV ([/REF/ATLAS_2011_I944826/d03-x01-y01](#))
- K_S^0 transverse momentum, $\sqrt{s} = 900$ GeV ([/REF/ATLAS_2011_I944826/d04-x01-y01](#))
- K_S^0 rapidity, $\sqrt{s} = 900$ GeV ([/REF/ATLAS_2011_I944826/d05-x01-y01](#))
- K_S^0 multiplicity, $\sqrt{s} = 900$ GeV ([/REF/ATLAS_2011_I944826/d06-x01-y01](#))
- Λ transverse momentum, $\sqrt{s} = 7000$ GeV ([/REF/ATLAS_2011_I944826/d07-x01-y01](#))
- Λ rapidity, $\sqrt{s} = 7000$ GeV ([/REF/ATLAS_2011_I944826/d08-x01-y01](#))
- Λ multiplicity, $\sqrt{s} = 7000$ GeV ([/REF/ATLAS_2011_I944826/d09-x01-y01](#))

- Λ transverse momentum, $\sqrt{s} = 900$ GeV ([/REF/ATLAS_2011_I944826/d10-x01-y01](#))
- Λ rapidity, $\sqrt{s} = 900$ GeV ([/REF/ATLAS_2011_I944826/d11-x01-y01](#))
- Λ multiplicity, $\sqrt{s} = 900$ GeV ([/REF/ATLAS_2011_I944826/d12-x01-y01](#))
- Production ratio of $\bar{\Lambda}$ and Λ vs. $|y|$, $\sqrt{s} = 7000$ GeV ([/REF/ATLAS_2011_I944826/d13-x01-y01](#))
- Production ratio of $\bar{\Lambda}$ and Λ vs. p_{\perp} , $\sqrt{s} = 7000$ GeV ([/REF/ATLAS_2011_I944826/d14-x01-y01](#))
- Production ratio of $\bar{\Lambda}$ and Λ vs. $|y|$, $\sqrt{s} = 900$ GeV ([/REF/ATLAS_2011_I944826/d15-x01-y01](#))
- Production ratio of $\bar{\Lambda}$ and Λ vs. p_{\perp} , $\sqrt{s} = 900$ GeV ([/REF/ATLAS_2011_I944826/d16-x01-y01](#))

8.22 ATLAS_2011_I945498 [109]

Z+jets in pp at 7 TeV

Beams: pp

Energies: (3500.0, 3500.0) GeV

Experiment: ATLAS (LHC)

Inspire ID: 945498

Status: VALIDATED

Authors:

- Evelin Meoni (evelin.meoni@cern.ch)
- Holger Schulz
- Roman Lysak (roman.lysak@cern.ch)

References:

- arXiv: [1111.2690v1](#)
- CERN-PH-EP-2011-162

Run details:

- Z+jets, electronic and/or muonic Z-decays. Jets with transverse momentum $p_T > 30$ GeV and jet rapidity $|y| < 4.4$.

Production of jets in association with a Z/γ^* boson in proton–proton collisions at $\sqrt{s} = 7$ TeV with the ATLAS detector. The analysis includes the full 2010 data set, collected with a low rate of multiple proton–proton collisions in the accelerator, corresponding to an integrated luminosity of 36 pb^{-1} . Inclusive jet cross sections in Z/γ^* events, with Z/γ^* decaying into electron or muon pairs, are measured for jets with transverse momentum $p_T > 30$ GeV and jet rapidity $|y| < 4.4$.

Histograms (36):

- $\sigma(\geq N_{\text{jet}}), Z \rightarrow e^+e^-, p_\perp(\text{jet}) > 30 \text{ GeV}, |y_{\text{jet}}| < 4.4$ ([/REF/ATLAS_2011_I945498/d01-x01-y01](#))
- $\sigma(\geq N_{\text{jet}}), Z \rightarrow \mu^+\mu^-, p_\perp(\text{jet}) > 30 \text{ GeV}, |y_{\text{jet}}| < 4.4$ ([/REF/ATLAS_2011_I945498/d01-x01-y02](#))
- $\sigma(\geq N_{\text{jet}}), Z \rightarrow \ell^+\ell^-, p_\perp(\text{jet}) > 30 \text{ GeV}, |y_{\text{jet}}| < 4.4$ ([/REF/ATLAS_2011_I945498/d01-x01-y03](#))
- $\sigma(N_{\text{jet}})/\sigma(N_{\text{jet}} - 1), Z \rightarrow e^+e^-, p_\perp(\text{jet}) > 30 \text{ GeV}, |y_{\text{jet}}| < 4.4$ ([/REF/ATLAS_2011_I945498/d02-x01-y01](#))
- $\sigma(N_{\text{jet}})/\sigma(N_{\text{jet}} - 1), Z \rightarrow \mu^+\mu^-, p_\perp(\text{jet}) > 30 \text{ GeV}, |y_{\text{jet}}| < 4.4$ ([/REF/ATLAS_2011_I945498/d02-x01-y02](#))
- $\sigma(N_{\text{jet}})/\sigma(N_{\text{jet}} - 1), Z \rightarrow \ell^+\ell^-, p_\perp(\text{jet}) > 30 \text{ GeV}, |y_{\text{jet}}| < 4.4$ ([/REF/ATLAS_2011_I945498/d02-x01-y03](#))

- $Z \rightarrow e^+e^-$, $p_\perp(\text{jet}) > 30 \text{ GeV}$, $|y_{\text{jet}}| < 4.4$ (/REF/ATLAS_2011_I945498/d12-x01-y01)
- $Z \rightarrow \mu^+\mu^-$, $p_\perp(\text{jet}) > 30 \text{ GeV}$, $|y_{\text{jet}}| < 4.4$ (/REF/ATLAS_2011_I945498/d12-x01-y02)
- $Z \rightarrow \ell^+\ell^-$, $p_\perp(\text{jet}) > 30 \text{ GeV}$, $|y_{\text{jet}}| < 4.4$ (/REF/ATLAS_2011_I945498/d12-x01-y03)

8.23 ATLAS_2011_I954993 [110]

WZ fiducial cross-section at 7 TeV in ATLAS

Beams: pp

Energies: (3500.0, 3500.0) GeV

Experiment: ATLAS (LHC 7TeV)

Inspire ID: [954993](#)

Status: VALIDATED

Authors:

- Lynn Marx (Lynn.Marx@hep.manchester.ac.uk)
- Roman Lysak (lysak@fzu.cz)

References:

- Phys.Lett. B709 (2012) 341-357
- arXiv: [1111.5570](#)

Run details:

- pp WZ events at 7 TeV with direct e, mu W/Z boson decays (no taus from W/Z)

This is a measurement of WZ production in 1.02 fb^{-1} of pp collision data at $\sqrt{s} = 7 \text{ TeV}$ collected by the ATLAS experiment in 2011. Doubly leptonic decay events are selected with electrons, muons and missing transverse momentum in the final state. The measurement of the combined fiducial cross section for the WZ bosons decaying directly into electrons and muons is performed.

Histograms (1):

- Total fiducial cross-section $WZ \rightarrow \ell\nu\ell\ell$ ([/REF/ATLAS_2011_I954993/d01-x01-y01](#))

8.24 ATLAS_2011_S8924791

Jet shapes at 7 TeV in ATLAS

Beams: pp

Energies: (3500.0, 3500.0) GeV

Experiment: ATLAS (LHC)

Spires ID: [8924791](#)

Status: VALIDATED

Authors:

- Andy Buckley ⟨andy.buckley@cern.ch⟩
- Francesc Vives ⟨fvives@ifae.es⟩
- Judith Katzy ⟨judith.katzy@cern.ch⟩

References:

- arXiv: [1101.0070](#)

Run details:

- pp QCD interactions at 7 TeV GeV, corresponding to JX samples. Matching plots to kinematic p_\perp cut samples, or merging from slices or p_\perp -enhanced sampling is advised.

Measurement of jet shapes in inclusive jet production in pp collisions at 7 TeV based on 3 pb^{-1} of data. Jets are reconstructed in $|\eta| < 5$ using the anti- k_\perp algorithm with $30 < p_\perp < 600 \text{ GeV}$ and $|y| < 2.8$.

Histograms (118):

- Jet shape ρ for $p_\perp \in 30\text{--}40 \text{ GeV}$, $y \in 0.0\text{--}0.3$ ([/REF/ATLAS_2011_S8924791/d01-x01-y01](#))
- Jet shape Ψ for $p_\perp \in 30\text{--}40 \text{ GeV}$, $y \in 0.0\text{--}0.3$ ([/REF/ATLAS_2011_S8924791/d01-x01-y02](#))
- Jet shape ρ for $p_\perp \in 30\text{--}40 \text{ GeV}$, $y \in 0.3\text{--}0.8$ ([/REF/ATLAS_2011_S8924791/d01-x02-y01](#))
- Jet shape Ψ for $p_\perp \in 30\text{--}40 \text{ GeV}$, $y \in 0.3\text{--}0.8$ ([/REF/ATLAS_2011_S8924791/d01-x02-y02](#))
- Jet shape ρ for $p_\perp \in 30\text{--}40 \text{ GeV}$, $y \in 0.8\text{--}1.2$ ([/REF/ATLAS_2011_S8924791/d01-x03-y01](#))
- Jet shape Ψ for $p_\perp \in 30\text{--}40 \text{ GeV}$, $y \in 0.8\text{--}1.2$ ([/REF/ATLAS_2011_S8924791/d01-x03-y02](#))
- Jet shape ρ for $p_\perp \in 30\text{--}40 \text{ GeV}$, $y \in 1.2\text{--}2.1$ ([/REF/ATLAS_2011_S8924791/d01-x04-y01](#))
- Jet shape Ψ for $p_\perp \in 30\text{--}40 \text{ GeV}$, $y \in 1.2\text{--}2.1$ ([/REF/ATLAS_2011_S8924791/d01-x04-y02](#))
- Jet shape ρ for $p_\perp \in 30\text{--}40 \text{ GeV}$, $y \in 2.1\text{--}2.8$ ([/REF/ATLAS_2011_S8924791/d01-x05-y01](#))
- Jet shape Ψ for $p_\perp \in 30\text{--}40 \text{ GeV}$, $y \in 2.1\text{--}2.8$ ([/REF/ATLAS_2011_S8924791/d01-x05-y02](#))
- Jet shape ρ for $p_\perp \in 30\text{--}40 \text{ GeV}$, $y \in 0.0\text{--}2.8$ ([/REF/ATLAS_2011_S8924791/d01-x06-y01](#))

8.25 ATLAS_2011_S8971293 [111]

Dijet azimuthal decorrelations

Beams: pp

Energies: (3500.0, 3500.0) GeV

Experiment: ATLAS (LHC)

Spires ID: [8971293](#)

Status: VALIDATED

Authors:

- Frank Siegert [⟨frank.siegert@cern.ch⟩](mailto:frank.siegert@cern.ch)

References:

- arXiv: [1102.2696](#)

Run details:

- pp QCD interactions at 7000 GeV. The distributions are binned in leading p_{\perp} starting at 110 GeV with the last bin starting at 800 GeV.

Dijet azimuthal decorrelation measured by ATLAS at 7 TeV. Jets are anti- k_t with $R = 0.6$, $p_{\perp} > 100$ GeV, $|\eta| < 0.8$. The analysis is binned in leading jet p_{\perp} bins. All data is fully corrected for detector effects.

Histograms (9):

- Dijet azimuthal decorrelations for $110 < p_{\perp}^{\max}/\text{GeV} < 160$ ([/REF/ATLAS_2011_S8971293/d01-x01-y01](#))
- Dijet azimuthal decorrelations for $160 < p_{\perp}^{\max}/\text{GeV} < 210$ ([/REF/ATLAS_2011_S8971293/d01-x01-y02](#))
- Dijet azimuthal decorrelations for $210 < p_{\perp}^{\max}/\text{GeV} < 260$ ([/REF/ATLAS_2011_S8971293/d01-x01-y03](#))
- Dijet azimuthal decorrelations for $260 < p_{\perp}^{\max}/\text{GeV} < 310$ ([/REF/ATLAS_2011_S8971293/d01-x01-y04](#))
- Dijet azimuthal decorrelations for $310 < p_{\perp}^{\max}/\text{GeV} < 400$ ([/REF/ATLAS_2011_S8971293/d01-x01-y05](#))
- Dijet azimuthal decorrelations for $400 < p_{\perp}^{\max}/\text{GeV} < 500$ ([/REF/ATLAS_2011_S8971293/d01-x01-y06](#))
- Dijet azimuthal decorrelations for $500 < p_{\perp}^{\max}/\text{GeV} < 600$ ([/REF/ATLAS_2011_S8971293/d01-x01-y07](#))
- Dijet azimuthal decorrelations for $600 < p_{\perp}^{\max}/\text{GeV} < 800$ ([/REF/ATLAS_2011_S8971293/d01-x01-y08](#))
- Dijet azimuthal decorrelations for $p_{\perp}^{\max}/\text{GeV} > 800$ ([/REF/ATLAS_2011_S8971293/d01-x01-y09](#))

8.26 ATLAS_2011_S8983313 [112]

0-lepton squark and gluino search

Beams: pp

Energies: (3500.0, 3500.0) GeV

Experiment: ATLAS (LHC)

Spires ID: [8983313](#)

Status: VALIDATED

Authors:

- David Grellscheid [⟨david.grellscheid@durham.ac.uk⟩](mailto:david.grellscheid@durham.ac.uk)

References:

- arXiv: [1102.5290](#)

Run details:

- BSM signal events at 7000 GeV.

0-lepton search for squarks and gluinos by ATLAS at 7 TeV with an integrated luminosity of 35 pb^{-1} . Event counts in four signal regions A-D are implemented as one-bin histograms.

8.27 ATLAS_2011_S8994773

Calo-based underlying event at 900 GeV and 7 TeV in ATLAS

Beams: pp

Energies: (450.0, 450.0), (3500.0, 3500.0) GeV

Experiment: ATLAS (LHC)

Spires ID: [8994773](#)

Status: VALIDATED

Authors:

- Jinlong Zhang ⟨jinlong@mail.cern.ch⟩
- Andy Buckley ⟨andy.buckley@cern.ch⟩

References:

- arXiv: [1103.1816](#)

Run details:

- pp QCD interactions at 900 GeV and 7 TeV. Diffractive events should be included, but only influence the lowest bins. Multiple kinematic cuts should not be required.

Underlying event measurements with the ATLAS detector at the LHC at center-of-mass energies of 900 GeV and 7 TeV, using calorimeter clusters rather than charged tracks.

Histograms (10):

- Transverse N density vs. p_{\perp}^{clus1} , $\sqrt{s} = 900$ GeV ([/REF/ATLAS_2011_S8994773/d01-x01-y01](#))
- Transverse N density vs. p_{\perp}^{clus1} , $\sqrt{s} = 7$ TeV ([/REF/ATLAS_2011_S8994773/d02-x01-y01](#))
- Transverse $\sum p_{\perp}$ density vs. p_{\perp}^{clus1} , $\sqrt{s} = 900$ GeV ([/REF/ATLAS_2011_S8994773/d03-x01-y01](#))
- Transverse $\sum p_{\perp}$ density vs. p_{\perp}^{clus1} , $\sqrt{s} = 7$ TeV ([/REF/ATLAS_2011_S8994773/d04-x01-y01](#))
- N density vs. $\Delta\phi$, $p_{\perp}^{\text{clus1}} > 1.0$ GeV, $\sqrt{s} = 900$ GeV ([/REF/ATLAS_2011_S8994773/d13-x01-y01](#))
- N density vs. $\Delta\phi$, $p_{\perp}^{\text{clus1}} > 2.0$ GeV, $\sqrt{s} = 900$ GeV ([/REF/ATLAS_2011_S8994773/d13-x01-y02](#))
- N density vs. $\Delta\phi$, $p_{\perp}^{\text{clus1}} > 3.0$ GeV, $\sqrt{s} = 900$ GeV ([/REF/ATLAS_2011_S8994773/d13-x01-y03](#))
- N density vs. $\Delta\phi$, $p_{\perp}^{\text{clus1}} > 1.0$ GeV, $\sqrt{s} = 7$ TeV ([/REF/ATLAS_2011_S8994773/d14-x01-y01](#))
- N density vs. $\Delta\phi$, $p_{\perp}^{\text{clus1}} > 2.0$ GeV, $\sqrt{s} = 7$ TeV ([/REF/ATLAS_2011_S8994773/d14-x01-y02](#))
- N density vs. $\Delta\phi$, $p_{\perp}^{\text{clus1}} > 3.0$ GeV, $\sqrt{s} = 7$ TeV ([/REF/ATLAS_2011_S8994773/d14-x01-y03](#))

8.28 ATLAS_2011_S9002537

Muon charge asymmetry in W events at 7 TeV in ATLAS

Beams: pp

Energies: (3500.0, 3500.0) GeV

Experiment: ATLAS (LHC)

Spires ID: [9002537](#)

Status: VALIDATED

Authors:

- Frank Krauss <frank.krauss@durham.ac.uk>
- Hendrik Hoeth <hendrik.hoeth@cern.ch>

References:

- arXiv: [1103.2929](#)

Run details:

- $W \rightarrow \mu\nu$ events at 7 TeV

Measurement of the muon charge asymmetry from W bosons produced in proton-proton collisions at a centre-of-mass energy of 7 TeV with ATLAS. The asymmetry is measured in the $W \rightarrow \mu$ decay mode as a function of the muon pseudorapidity using a data sample corresponding to a total integrated luminosity of 31 pb^{-1} .

Histograms (1):

- Muon charge asymmetry in W decays ([/REF/ATLAS_2011_S9002537/d01-x01-y01](#))

8.29 ATLAS_2011_S9019561 [113]

Two lepton supersymmetry search

Beams: pp

Energies: (3500.0, 3500.0) GeV

Experiment: ATLAS (LHC)

Spires ID: 9019561

Status: VALIDATED

Authors:

- Angela Chen (aqchen@fas.harvard.edu)

References:

- arXiv: [1103.6214](#)

Run details:

- BSM signal events at 7000 GeV.

2-lepton search for supersymmetric particles by ATLAS at 7 TeV. Event counts in signal regions (3 same sign and 3 opposite sign) are implemented as one bin histograms. Histograms for missing transverse energy are implemented.

8.30 ATLAS_2011_S9035664 [114]

Measurement of J/Psi production

Beams: pp

Energies: (3500.0, 3500.0) GeV

Experiment: ATLAS (LHC)

Spires ID: 9035664

Status: VALIDATED

Authors:

•

References:

•

- arXiv: [1104.3038](#)

Run details:

- pp to hadrons including both prompt J/Psi production and the production in B decays

The inclusive J/ψ production cross-section and fraction of J/ψ mesons produced in B-hadron decays are measured in proton-proton collisions at $\sqrt{s} = 7$ TeV with the ATLAS detector at the LHC, as a function of the transverse momentum and rapidity of the J/ψ , using 2.3pb^{-1} of integrated luminosity. The cross section is measured from a minimum p_T of 1 GeV to a maximum of 70 GeV and for rapidities within $|y| < 2.4$ giving the widest reach of any measurement of J/ψ production to date.

8.31 ATLAS_2011_S9041966

1-lepton and 2-lepton search for first or second generation leptoquarks

Beams: pp

Energies: (3500.0, 3500.0) GeV

Experiment: ATLAS (LHC)

Spires ID: [9041966](#)

Status: UNVALIDATED

Authors:

- Angela Chen (aqchen@fas.harvard.edu)

References:

- arXiv: [1104.4481](#)

Run details:

- BSM signal events at 7000 GeV.

Single and dilepton search for first and second generation scalar leptoquarks by ATLAS at 7 TeV. Event counts in four signal regions (single lepton and dilepton for first and second generation) are implemented as one-bin histograms. Histograms for event transverse energy are implemented for dilepton signal regions and histograms for leptoquark mass are implemented for single lepton signal regions. Histograms for observables in six control regions are implemented.

8.32 ATLAS_2011_S9108483 [115]

Long-lived heavy charged particle search

Beams: pp

Energies: (3500.0, 3500.0) GeV

Experiment: ATLAS (LHC)

Spires ID: 9108483

Status: UNVALIDATED

Authors:

- Peter Richardson (Peter.Richardson@durham.ac.uk)

References:

- arXiv: 1106.4495

Run details:

- BSM signal events at 7000 GeV.

ATLAS search for long-lived heavy charged particles for four different mass cuts. Currently only the slepton search is implemented.

8.33 ATLAS_2011_S9120807

Inclusive isolated diphoton analysis

Beams: pp

Energies: (3500.0, 3500.0) GeV

Experiment: ATLAS (LHC 7TeV)

Spires ID: [9120807](#)

Status: VALIDATED

Authors:

- Giovanni Marchiori (giovanni.marchiori@cern.ch)

References:

- arXiv: [1107.0581](#)

Run details:

- Inclusive diphoton + X events at $\sqrt{s} = 7$ TeV.

A measurement of the cross section for inclusive isolated photon production at $\sqrt{s} = 7$ TeV. The measurement is done in bins of $M_{\gamma\gamma}$, $p_{T\gamma\gamma}$, and $\Delta\phi_{\gamma\gamma}$, for isolated photons with $|\eta| < 2.37$ and $E_T^\gamma > 16$ GeV. The measurement uses 37 pb^{-1} of integrated luminosity collected with the ATLAS detector.

Histograms (3):

- Invariant mass of the diphoton system ([/REF/ATLAS_2011_S9120807/d01-x01-y01](#))
- Transverse momentum of the diphoton system ([/REF/ATLAS_2011_S9120807/d02-x01-y01](#))
- Azimuthal separation of the photons ([/REF/ATLAS_2011_S9120807/d03-x01-y01](#))

8.34 ATLAS_2011_S9126244

Measurement of dijet production with a veto on additional central jet activity

Beams: $p p$

Energies: (3500.0, 3500.0) GeV

Experiment: ATLAS (LHC)

Spires ID: [9126244](#)

Status: VALIDATED

Authors:

- Graham Jones (grahamj@cern.ch)

References:

- arXiv: [1107.1641](#)

Run details:

- Require QCD interactions at 7TeV. A substantial number of events are required to populate the large rapidity separation region.

A measurement of the jet activity in rapidity intervals bounded by a dijet system. The fraction of events passing a veto requirement are shown as a function of both the rapidity interval size and the average transverse momentum of the dijet system. The average number of jets above the veto threshold are also shown as a function of the same variables. There are two possible selection criteria applied to data. Either the two highest transverse momentum jets or the jets most forward and backward in rapidity are taken to define the dijet system, where the veto threshold is 20 GeV. Additionally for the latter selection an alternative veto transverse momentum threshold which is equal to the average transverse momentum is applied. Jet selections are based on the anti- k_t algorithm with $R = 0.6$, $p_{\perp} > 20$ GeV and $|y_{\text{jet}}| < 4.4$.

Histograms (72):

- Gap fraction vs $\overline{P_T}$ for $1.0 < |\Delta y| < 2.0$, Leading Jet ([/REF/ATLAS_2011_S9126244/d01-x01-y01](#))
- Gap fraction vs $\overline{P_T}$ for $1.0 < |\Delta y| < 2.0$, Fwd/Bwd ([/REF/ATLAS_2011_S9126244/d01-x01-y02](#))
- Gap fraction vs $\overline{P_T}$ for $2.0 < |\Delta y| < 3.0$, Leading Jet ([/REF/ATLAS_2011_S9126244/d02-x01-y01](#))
- Gap fraction vs $\overline{P_T}$ for $2.0 < |\Delta y| < 3.0$, Fwd/Bwd ([/REF/ATLAS_2011_S9126244/d02-x01-y02](#))
- Gap fraction vs $\overline{P_T}$ for $3.0 < |\Delta y| < 4.0$, Leading Jet ([/REF/ATLAS_2011_S9126244/d03-x01-y01](#))
- Gap fraction vs $\overline{P_T}$ for $3.0 < |\Delta y| < 4.0$, Fwd/Bwd ([/REF/ATLAS_2011_S9126244/d03-x01-y02](#))
- Gap fraction vs $\overline{P_T}$ for $4.0 < |\Delta y| < 5.0$, Leading Jet ([/REF/ATLAS_2011_S9126244/d04-x01-y01](#))
- Gap fraction vs $\overline{P_T}$ for $4.0 < |\Delta y| < 5.0$, Fwd/Bwd ([/REF/ATLAS_2011_S9126244/d04-x01-y02](#))

- Gap fraction vs $\overline{P_T}$ for $5.0 < |\Delta y| < 6.0$, Leading Jet (/REF/ATLAS_2011_S9126244/d05-x01-y01)
- Gap fraction vs $\overline{P_T}$ for $5.0 < |\Delta y| < 6.0$, Fwd/Bwd (/REF/ATLAS_2011_S9126244/d05-x01-y02)
- Gap fraction vs $|\Delta y|$ for $70 < \overline{P_T} < 90$, Leading Jet (/REF/ATLAS_2011_S9126244/d06-x01-y01)
- Gap fraction vs $|\Delta y|$ for $70 < \overline{P_T} < 90$, Fwd/Bwd (/REF/ATLAS_2011_S9126244/d06-x01-y02)
- Gap fraction vs $|\Delta y|$ for $90 < \overline{P_T} < 120$, Leading Jet (/REF/ATLAS_2011_S9126244/d07-x01-y01)
- Gap fraction vs $|\Delta y|$ for $90 < \overline{P_T} < 120$, Fwd/Bwd (/REF/ATLAS_2011_S9126244/d07-x01-y02)
- Gap fraction vs $|\Delta y|$ for $120 < \overline{P_T} < 150$, Leading Jet (/REF/ATLAS_2011_S9126244/d08-x01-y01)
- Gap fraction vs $|\Delta y|$ for $120 < \overline{P_T} < 150$, Fwd/Bwd (/REF/ATLAS_2011_S9126244/d08-x01-y02)
- Gap fraction vs $|\Delta y|$ for $150 < \overline{P_T} < 180$, Leading Jet (/REF/ATLAS_2011_S9126244/d09-x01-y01)
- Gap fraction vs $|\Delta y|$ for $150 < \overline{P_T} < 180$, Fwd/Bwd (/REF/ATLAS_2011_S9126244/d09-x01-y02)
- Gap fraction vs $|\Delta y|$ for $180 < \overline{P_T} < 210$, Leading Jet (/REF/ATLAS_2011_S9126244/d10-x01-y01)
- Gap fraction vs $|\Delta y|$ for $180 < \overline{P_T} < 210$, Fwd/Bwd (/REF/ATLAS_2011_S9126244/d10-x01-y02)
- Gap fraction vs $|\Delta y|$ for $210 < \overline{P_T} < 240$, Leading Jet (/REF/ATLAS_2011_S9126244/d11-x01-y01)
- Gap fraction vs $|\Delta y|$ for $210 < \overline{P_T} < 240$, Fwd/Bwd (/REF/ATLAS_2011_S9126244/d11-x01-y02)
- Gap fraction vs $|\Delta y|$ for $240 < \overline{P_T} < 270$, Leading Jet (/REF/ATLAS_2011_S9126244/d12-x01-y01)
- Gap fraction vs $|\Delta y|$ for $240 < \overline{P_T} < 270$, Fwd/Bwd (/REF/ATLAS_2011_S9126244/d12-x01-y02)
- Gap fraction vs Q_0 for $70 < \overline{P_T} < 90$ $2 < |\Delta y| < 3$, Leading Jet (/REF/ATLAS_2011_S9126244/d13-x01-y01)
- Gap fraction vs Q_0 for $70 < \overline{P_T} < 90$ $2 < |\Delta y| < 3$, Fwd/Bwd (/REF/ATLAS_2011_S9126244/d13-x01-y02)
- Gap fraction vs Q_0 for $70 < \overline{P_T} < 90$ $4 < |\Delta y| < 5$, Leading Jet (/REF/ATLAS_2011_S9126244/d14-x01-y01)
- Gap fraction vs Q_0 for $70 < \overline{P_T} < 90$ $4 < |\Delta y| < 5$, Fwd/Bwd (/REF/ATLAS_2011_S9126244/d14-x01-y02)
- Gap fraction vs Q_0 for $120 < \overline{P_T} < 150$ $2 < |\Delta y| < 3$, Leading Jet (/REF/ATLAS_2011_S9126244/d15-x01-y01)
- Gap fraction vs Q_0 for $120 < \overline{P_T} < 150$ $2 < |\Delta y| < 3$, Fwd/Bwd (/REF/ATLAS_2011_S9126244/d15-x01-y02)
- Gap fraction vs Q_0 for $120 < \overline{P_T} < 150$ $4 < |\Delta y| < 5$, Leading Jet (/REF/ATLAS_2011_S9126244/d16-x01-y01)

- Gap fraction vs Q_0 for $120 < \overline{P_T} < 150$ $4 < |\Delta y| < 5$, Fwd/Bwd ([/REF/ATLAS_2011-S9126244/d16-x01-y02](#))
- Gap fraction vs Q_0 for $210 < \overline{P_T} < 240$ $2 < |\Delta y| < 3$, Leading Jet ([/REF/ATLAS_2011-S9126244/d17-x01-y01](#))
- Gap fraction vs Q_0 for $210 < \overline{P_T} < 240$ $2 < |\Delta y| < 3$, Fwd/Bwd ([/REF/ATLAS_2011-S9126244/d17-x01-y02](#))
- Gap fraction vs Q_0 for $210 < \overline{P_T} < 240$ $4 < |\Delta y| < 5$, Leading Jet ([/REF/ATLAS_2011-S9126244/d18-x01-y01](#))
- Gap fraction vs Q_0 for $210 < \overline{P_T} < 240$ $4 < |\Delta y| < 5$, Fwd/Bwd ([/REF/ATLAS_2011-S9126244/d18-x01-y02](#))
- Gap fraction vs $|\Delta y|$ for $70 < \overline{P_T} < 90$, Fwd/Bwd $Q_0 = \overline{P_T}$ ([/REF/ATLAS_2011-S9126244/d19-x01-y01](#))
- Gap fraction vs $|\Delta y|$ for $90 < \overline{P_T} < 120$, Fwd/Bwd $Q_0 = \overline{P_T}$ ([/REF/ATLAS_2011-S9126244/d20-x01-y01](#))
- Gap fraction vs $|\Delta y|$ for $120 < \overline{P_T} < 150$, Fwd/Bwd $Q_0 = \overline{P_T}$ ([/REF/ATLAS_2011-S9126244/d21-x01-y01](#))
- Gap fraction vs $|\Delta y|$ for $150 < \overline{P_T} < 180$, Fwd/Bwd $Q_0 = \overline{P_T}$ ([/REF/ATLAS_2011-S9126244/d22-x01-y01](#))
- Gap fraction vs $|\Delta y|$ for $180 < \overline{P_T} < 210$, Fwd/Bwd $Q_0 = \overline{P_T}$ ([/REF/ATLAS_2011-S9126244/d23-x01-y01](#))
- Gap fraction vs $|\Delta y|$ for $210 < \overline{P_T} < 240$, Fwd/Bwd $Q_0 = \overline{P_T}$ ([/REF/ATLAS_2011-S9126244/d24-x01-y01](#))
- Gap fraction vs $|\Delta y|$ for $240 < \overline{P_T} < 270$, Fwd/Bwd $Q_0 = \overline{P_T}$ ([/REF/ATLAS_2011-S9126244/d25-x01-y01](#))
- $\overline{N_{jet}}$ vs $\overline{P_T}$ for $1 < |\Delta y| < 2$, Leading Jet ([/REF/ATLAS_2011_S9126244/d26-x01-y01](#))
- $\overline{N_{jet}}$ vs $\overline{P_T}$ for $1 < |\Delta y| < 2$, Fwd/Bwd ([/REF/ATLAS_2011_S9126244/d26-x01-y02](#))
- $\overline{N_{jet}}$ vs $\overline{P_T}$ for $2 < |\Delta y| < 3$, Leading Jet ([/REF/ATLAS_2011_S9126244/d27-x01-y01](#))
- $\overline{N_{jet}}$ vs $\overline{P_T}$ for $2 < |\Delta y| < 3$, Fwd/Bwd ([/REF/ATLAS_2011_S9126244/d27-x01-y02](#))
- $\overline{N_{jet}}$ vs $\overline{P_T}$ for $3 < |\Delta y| < 4$, Leading Jet ([/REF/ATLAS_2011_S9126244/d28-x01-y01](#))
- $\overline{N_{jet}}$ vs $\overline{P_T}$ for $3 < |\Delta y| < 4$, Fwd/Bwd ([/REF/ATLAS_2011_S9126244/d28-x01-y02](#))
- $\overline{N_{jet}}$ vs $\overline{P_T}$ for $4 < |\Delta y| < 5$, Leading Jet ([/REF/ATLAS_2011_S9126244/d29-x01-y01](#))
- $\overline{N_{jet}}$ vs $\overline{P_T}$ for $4 < |\Delta y| < 5$, Fwd/Bwd ([/REF/ATLAS_2011_S9126244/d29-x01-y02](#))

- $\overline{N_{jet}}$ vs $|\Delta y|$ for $70 < \overline{P_T} < 90$, Fwd/Bwd $Q_0 = \overline{P_T}$ (/REF/ATLAS_2011_S9126244/d30-x01-y01)
- $\overline{N_{jet}}$ vs $|\Delta y|$ for $90 < \overline{P_T} < 120$, Fwd/Bwd $Q_0 = \overline{P_T}$ (/REF/ATLAS_2011_S9126244/d31-x01-y01)
- $\overline{N_{jet}}$ vs $|\Delta y|$ for $120 < \overline{P_T} < 150$, Fwd/Bwd $Q_0 = \overline{P_T}$ (/REF/ATLAS_2011_S9126244/d32-x01-y01)
- $\overline{N_{jet}}$ vs $|\Delta y|$ for $150 < \overline{P_T} < 180$, Fwd/Bwd $Q_0 = \overline{P_T}$ (/REF/ATLAS_2011_S9126244/d33-x01-y01)
- $\overline{N_{jet}}$ vs $|\Delta y|$ for $180 < \overline{P_T} < 210$, Fwd/Bwd $Q_0 = \overline{P_T}$ (/REF/ATLAS_2011_S9126244/d34-x01-y01)
- $\overline{N_{jet}}$ vs $|\Delta y|$ for $210 < \overline{P_T} < 240$, Fwd/Bwd $Q_0 = \overline{P_T}$ (/REF/ATLAS_2011_S9126244/d35-x01-y01)
- $\overline{N_{jet}}$ vs $|\Delta y|$ for $240 < \overline{P_T} < 270$, Fwd/Bwd $Q_0 = \overline{P_T}$ (/REF/ATLAS_2011_S9126244/d36-x01-y01)
- $\overline{N_{jet}}$ vs $|\Delta y|$ for $70 < \overline{P_T} < 90$, Leading Jet (/REF/ATLAS_2011_S9126244/d37-x01-y01)
- $\overline{N_{jet}}$ vs $|\Delta y|$ for $70 < \overline{P_T} < 90$, Fwd/Bwd (/REF/ATLAS_2011_S9126244/d37-x01-y02)
- $\overline{N_{jet}}$ vs $|\Delta y|$ for $90 < \overline{P_T} < 120$, Leading Jet (/REF/ATLAS_2011_S9126244/d38-x01-y01)
- $\overline{N_{jet}}$ vs $|\Delta y|$ for $90 < \overline{P_T} < 120$, Fwd/Bwd (/REF/ATLAS_2011_S9126244/d38-x01-y02)
- $\overline{N_{jet}}$ vs $|\Delta y|$ for $120 < \overline{P_T} < 150$, Leading Jet (/REF/ATLAS_2011_S9126244/d39-x01-y01)
- $\overline{N_{jet}}$ vs $|\Delta y|$ for $120 < \overline{P_T} < 150$, Fwd/Bwd (/REF/ATLAS_2011_S9126244/d39-x01-y02)
- $\overline{N_{jet}}$ vs $|\Delta y|$ for $150 < \overline{P_T} < 180$, Leading Jet (/REF/ATLAS_2011_S9126244/d40-x01-y01)
- $\overline{N_{jet}}$ vs $|\Delta y|$ for $150 < \overline{P_T} < 180$, Fwd/Bwd (/REF/ATLAS_2011_S9126244/d40-x01-y02)
- $\overline{N_{jet}}$ vs $|\Delta y|$ for $180 < \overline{P_T} < 210$, Leading Jet (/REF/ATLAS_2011_S9126244/d41-x01-y01)
- $\overline{N_{jet}}$ vs $|\Delta y|$ for $180 < \overline{P_T} < 210$, Fwd/Bwd (/REF/ATLAS_2011_S9126244/d41-x01-y02)
- $\overline{N_{jet}}$ vs $|\Delta y|$ for $210 < \overline{P_T} < 240$, Leading Jet (/REF/ATLAS_2011_S9126244/d42-x01-y01)
- $\overline{N_{jet}}$ vs $|\Delta y|$ for $210 < \overline{P_T} < 240$, Fwd/Bwd (/REF/ATLAS_2011_S9126244/d42-x01-y02)
- $\overline{N_{jet}}$ vs $|\Delta y|$ for $240 < \overline{P_T} < 270$, Leading Jet (/REF/ATLAS_2011_S9126244/d43-x01-y01)
- $\overline{N_{jet}}$ vs $|\Delta y|$ for $240 < \overline{P_T} < 270$, Fwd/Bwd (/REF/ATLAS_2011_S9126244/d43-x01-y02)

8.35 ATLAS_2011_S9128077 [116]

Measurement of multi-jet cross sections

Beams: pp

Energies: (3500.0, 3500.0) GeV

Experiment: ATLAS (LHC)

Spires ID: [9128077](#)

Status: VALIDATED

Authors:

- Frank Siegert <frank.siegert@cern.ch>

References:

- arXiv: [1107.2092](#)

Run details:

- Pure QCD, inclusive enough for jet p_{\perp} down to 60 GeV.

Inclusive multi-jet production is studied using an integrated luminosity of 2.4 pb-1. Results on multi-jet cross sections are presented differential in p_{\perp} of the four leading jets, HT. Additionally three-to-two jet fractions are presented differential in different observables. Jets are anti-kt with $R = 0.4$ and $R = 0.6$, $p_{\perp} > 80(60)$ GeV and $|\eta| < 2.8$.

Histograms (17):

- Inclusive jet multiplicity ($R = 0.4$) ([/REF/ATLAS_2011_S9128077/d01-x01-y01](#))
- Inclusive jet multiplicity ratio $N/N-1$ ($R = 0.4$) ([/REF/ATLAS_2011_S9128077/d02-x01-y01](#))
- Transverse momentum of the leading jet ($R = 0.4$) ([/REF/ATLAS_2011_S9128077/d03-x01-y01](#))
- Transverse momentum of the 2nd leading jet ($R = 0.4$) ([/REF/ATLAS_2011_S9128077/d04-x01-y01](#))
- Transverse momentum of the 3rd leading jet ($R = 0.4$) ([/REF/ATLAS_2011_S9128077/d05-x01-y01](#))
- Transverse momentum of the 4th leading jet ($R = 0.4$) ([/REF/ATLAS_2011_S9128077/d06-x01-y01](#))
- H_T for events with $N_{\text{jet}} \geq 2$ ($R = 0.4$) ([/REF/ATLAS_2011_S9128077/d07-x01-y01](#))
- H_T for events with $N_{\text{jet}} \geq 3$ ($R = 0.4$) ([/REF/ATLAS_2011_S9128077/d08-x01-y01](#))
- H_T for events with $N_{\text{jet}} \geq 4$ ($R = 0.4$) ([/REF/ATLAS_2011_S9128077/d09-x01-y01](#))
- 3-to-2 jet ratio for $p_{\perp}^{\text{jets}} > 60$ GeV ($R = 0.6$) ([/REF/ATLAS_2011_S9128077/d10-x01-y01](#))
- 3-to-2 jet ratio for $p_{\perp}^{\text{jets}} > 80$ GeV ($R = 0.6$) ([/REF/ATLAS_2011_S9128077/d11-x01-y01](#))
- 3-to-2 jet ratio for $p_{\perp}^{\text{jets}} > 110$ GeV ($R = 0.6$) ([/REF/ATLAS_2011_S9128077/d12-x01-y01](#))
- 3-to-2 jet ratio for $p_{\perp}^{\text{jets}} > 60$ GeV ($R = 0.4$) ([/REF/ATLAS_2011_S9128077/d13-x01-y01](#))

- 3-to-2 jet ratio for $p_{\perp}^{\text{jets}} > 80 \text{ GeV}$ ($R = 0.4$) ([/REF/ATLAS_2011_S9128077/d14-x01-y01](#))
- 3-to-2 jet ratio for $p_{\perp}^{\text{jets}} > 110 \text{ GeV}$ ($R = 0.4$) ([/REF/ATLAS_2011_S9128077/d15-x01-y01](#))
- 3-to-2 jet ratio for $p_{\perp}^{\text{jets}} > 60 \text{ GeV}$ ($R = 0.6$) ([/REF/ATLAS_2011_S9128077/d16-x01-y01](#))
- 3-to-2 jet ratio for $p_{\perp}^{\text{jets}} > 60 \text{ GeV}$ ($R = 0.4$) ([/REF/ATLAS_2011_S9128077/d17-x01-y01](#))

8.36 ATLAS_2011_S9131140 [117]

Measurement of the Z p_{\perp} with electrons and muons at 7 TeV

Beams: pp

Energies: (3500.0, 3500.0) GeV

Experiment: ATLAS (LHC)

Spires ID: [9131140](#)

Status: VALIDATED

Authors:

- Elena Yatsenko <elena.yatsenko@desy.de>
- Judith Katzy <jkatzy@mail.cern.ch>

References:

- arXiv: [1107.2381](#)

Run details:

- Run with inclusive Z events, with Z/γ^* decays to electrons and/or muons.

The Z p_{\perp} at $\sqrt{s} = 7$ TeV is measured using electron and muon Z decay channels. The dressed leptons definition uses photons clustered in a cone around the charged leptons, while the bare lepton definition uses the post-FSR charged leptons only in the Z reconstruction. The data used in the bare leptons calculation are based on a forward application of a PHOTOS-based energy loss correction and are hence not quite model-independent.

Histograms (4):

- Z p_{\perp} reconstructed from dressed electrons ([/REF/ATLAS_2011_S9131140/d01-x01-y02](#))
- Z p_{\perp} reconstructed from bare electrons ([/REF/ATLAS_2011_S9131140/d01-x01-y03](#))
- Z p_{\perp} reconstructed from dressed muons ([/REF/ATLAS_2011_S9131140/d02-x01-y02](#))
- Z p_{\perp} reconstructed from bare muons ([/REF/ATLAS_2011_S9131140/d02-x01-y03](#))

8.37 ATLAS_2011_S9212183 [118]

0-lepton squark and gluino search

Beams: pp

Energies: (3500.0, 3500.0) GeV

Experiment: ATLAS (LHC)

Spires ID: 9212183

Status: VALIDATED

Authors:

- Chris Wymant ⟨c.m.wymant@durham.ac.uk⟩
- David Grellscheid ⟨david.grellscheid@durham.ac.uk⟩

References:

- arXiv: [1109.6572](#)

Run details:

- BSM signal events at 7000 GeV.

0-lepton search for squarks and gluinos by ATLAS at 7 TeV with an integrated luminosity of 1.04 fb^{-1} . Event counts in five signal regions are implemented as one-bin histograms.

Histograms (4):

- Effective Mass in the 2 jet Signal Region ([/REF/ATLAS_2011_S9212183/d01-x01-y01](#))
- Effective Mass in the 3 jet Signal Region ([/REF/ATLAS_2011_S9212183/d02-x01-y01](#))
- Effective Mass in the 4 jet Signal Region ([/REF/ATLAS_2011_S9212183/d03-x01-y01](#))
- Effective Mass in the high mass Signal Region ([/REF/ATLAS_2011_S9212183/d04-x01-y01](#))

8.38 ATLAS_2011_S9212353 [119]

Single lepton search for supersymmetry

Beams: pp

Energies: (3500.0, 3500.0) GeV

Experiment: ATLAS (LHC)

Spires ID: 9212353

Status: UNVALIDATED

No authors listed

References:

- Phys. Rev.D85:012006,2012
- arXiv: [1109.6606](#)

Run details:

- BSM signal events at 7000 GeV.

Single lepton search for supersymmetric particles by ATLAS at 7 TeV. Event counts in electron and muon signal regions are implemented as one-bin histograms. Histograms for missing transverse energy and effective mass are implemented for the two signal regions.

8.39 ATLAS_2011_S9225137 [120]

High jet multiplicity squark and gluino search

Beams: pp

Energies: (3500.0, 3500.0) GeV

Experiment: ATLAS (LHC)

Spires ID: [9225137](#)

Status: VALIDATED

Authors:

- Peter Richardson <peter.richardson@durham.ac.uk>

References:

- arXiv: [1110.2299](#)

Run details:

- BSM signal events at 7000 GeV.

Search for SUSY using events with 6 or more jets in association with missing transverse momentum produced in proton-proton collisions at a centre-of-mass energy of 7 TeV. The data sample has a total integrated luminosity of 1.34 fb^{-1} . Distributions in the W and top control regions are not produced, while in addition to the plots from the paper the count of events in the different signal regions is included.

Histograms (36):

- Observed $E_T/\sqrt{H_T}$ for 6 jets with $p_\perp > 55 \text{ GeV}$ ([/REF/ATLAS_2011_S9225137/d01-x01-y01](#))
- Background $E_T/\sqrt{H_T}$ for 6 jets with $p_\perp > 55 \text{ GeV}$ ([/REF/ATLAS_2011_S9225137/d01-x01-y02](#))
- Signal $E_T/\sqrt{H_T}$ for 6 jets with $p_\perp > 55 \text{ GeV}$ ([/REF/ATLAS_2011_S9225137/d01-x01-y03](#))
- Observed $E_T/\sqrt{H_T}$ for 5 jets with $p_\perp > 80 \text{ GeV}$ ([/REF/ATLAS_2011_S9225137/d02-x01-y01](#))
- Background $E_T/\sqrt{H_T}$ for 5 jets with $p_\perp > 80 \text{ GeV}$ ([/REF/ATLAS_2011_S9225137/d02-x01-y02](#))
- Signal $E_T/\sqrt{H_T}$ for 5 jets with $p_\perp > 80 \text{ GeV}$ ([/REF/ATLAS_2011_S9225137/d02-x01-y03](#))
- Observed number of jets with $p_\perp > 55 \text{ GeV}$ for $1.5 < E_T/\sqrt{H_T} < 2 \text{ GeV}^{\frac{1}{2}}$ ([/REF/ATLAS_2011_S9225137/d03-x01-y01](#))
- Background number of jets with $p_\perp > 55 \text{ GeV}$ for $1.5 < E_T/\sqrt{H_T} < 2 \text{ GeV}^{\frac{1}{2}}$ ([/REF/ATLAS_2011_S9225137/d03-x01-y02](#))
- Signal number of jets with $p_\perp > 55 \text{ GeV}$ for $1.5 < E_T/\sqrt{H_T} < 2 \text{ GeV}^{\frac{1}{2}}$ ([/REF/ATLAS_2011_S9225137/d03-x01-y03](#))
- Observed number of jets with $p_\perp > 55 \text{ GeV}$ for $2 < E_T/\sqrt{H_T} < 3 \text{ GeV}^{\frac{1}{2}}$ ([/REF/ATLAS_2011_S9225137/d04-x01-y01](#))

- Background number of jets with $p_{\perp} > 55 \text{ GeV}$ for $2 < E_{\text{T}}/\sqrt{H_{\text{T}}} < 3 \text{ GeV}^{\frac{1}{2}}$ ([/REF/ATLAS_2011_S9225137/d04-x01-y02](#))
- Signal number of jets with $p_{\perp} > 55 \text{ GeV}$ for $2 < E_{\text{T}}/\sqrt{H_{\text{T}}} < 3 \text{ GeV}^{\frac{1}{2}}$ ([/REF/ATLAS_2011_S9225137/d04-x01-y03](#))
- Observed number of jets with $p_{\perp} > 80 \text{ GeV}$ for $1.5 < E_{\text{T}}/\sqrt{H_{\text{T}}} < 2 \text{ GeV}^{\frac{1}{2}}$ ([/REF/ATLAS_2011_S9225137/d05-x01-y01](#))
- Background number of jets with $p_{\perp} > 80 \text{ GeV}$ for $1.5 < E_{\text{T}}/\sqrt{H_{\text{T}}} < 2 \text{ GeV}^{\frac{1}{2}}$ ([/REF/ATLAS_2011_S9225137/d05-x01-y02](#))
- Signal number of jets with $p_{\perp} > 80 \text{ GeV}$ for $1.5 < E_{\text{T}}/\sqrt{H_{\text{T}}} < 2 \text{ GeV}^{\frac{1}{2}}$ ([/REF/ATLAS_2011_S9225137/d05-x01-y03](#))
- Observed number of jets with $p_{\perp} > 80 \text{ GeV}$ for $2 < E_{\text{T}}/\sqrt{H_{\text{T}}} < 3 \text{ GeV}^{\frac{1}{2}}$ ([/REF/ATLAS_2011_S9225137/d06-x01-y01](#))
- Background number of jets with $p_{\perp} > 80 \text{ GeV}$ for $2 < E_{\text{T}}/\sqrt{H_{\text{T}}} < 3 \text{ GeV}^{\frac{1}{2}}$ ([/REF/ATLAS_2011_S9225137/d06-x01-y02](#))
- Signal number of jets with $p_{\perp} > 80 \text{ GeV}$ for $2 < E_{\text{T}}/\sqrt{H_{\text{T}}} < 3 \text{ GeV}^{\frac{1}{2}}$ ([/REF/ATLAS_2011_S9225137/d06-x01-y03](#))
- Observed $E_{\text{T}}/\sqrt{H_{\text{T}}}$ for 7 jets with $p_{\perp} > 55 \text{ GeV}$ ([/REF/ATLAS_2011_S9225137/d13-x01-y01](#))
- Background $E_{\text{T}}/\sqrt{H_{\text{T}}}$ for 7 jets with $p_{\perp} > 55 \text{ GeV}$ ([/REF/ATLAS_2011_S9225137/d13-x01-y02](#))
- Signal $E_{\text{T}}/\sqrt{H_{\text{T}}}$ for 7 jets with $p_{\perp} > 55 \text{ GeV}$ ([/REF/ATLAS_2011_S9225137/d13-x01-y03](#))
- Observed $E_{\text{T}}/\sqrt{H_{\text{T}}}$ for 6 jets with $p_{\perp} > 80 \text{ GeV}$ ([/REF/ATLAS_2011_S9225137/d14-x01-y01](#))
- Background $E_{\text{T}}/\sqrt{H_{\text{T}}}$ for 6 jets with $p_{\perp} > 80 \text{ GeV}$ ([/REF/ATLAS_2011_S9225137/d14-x01-y02](#))
- Signal $E_{\text{T}}/\sqrt{H_{\text{T}}}$ for 6 jets with $p_{\perp} > 80 \text{ GeV}$ ([/REF/ATLAS_2011_S9225137/d14-x01-y03](#))
- Observed $E_{\text{T}}/\sqrt{H_{\text{T}}}$ for 8 jets with $p_{\perp} > 55 \text{ GeV}$ ([/REF/ATLAS_2011_S9225137/d15-x01-y01](#))
- Background $E_{\text{T}}/\sqrt{H_{\text{T}}}$ for 8 jets with $p_{\perp} > 55 \text{ GeV}$ ([/REF/ATLAS_2011_S9225137/d15-x01-y02](#))
- Signal $E_{\text{T}}/\sqrt{H_{\text{T}}}$ for 8 jets with $p_{\perp} > 55 \text{ GeV}$ ([/REF/ATLAS_2011_S9225137/d15-x01-y03](#))
- Observed $E_{\text{T}}/\sqrt{H_{\text{T}}}$ for 7 jets with $p_{\perp} > 80 \text{ GeV}$ ([/REF/ATLAS_2011_S9225137/d16-x01-y01](#))
- Background $E_{\text{T}}/\sqrt{H_{\text{T}}}$ for 7 jets with $p_{\perp} > 80 \text{ GeV}$ ([/REF/ATLAS_2011_S9225137/d16-x01-y02](#))
- Signal $E_{\text{T}}/\sqrt{H_{\text{T}}}$ for 7 jets with $p_{\perp} > 80 \text{ GeV}$ ([/REF/ATLAS_2011_S9225137/d16-x01-y03](#))
- Observed number of jets with $p_{\perp} > 55 \text{ GeV}$ for $3 < E_{\text{T}}/\sqrt{H_{\text{T}}} \text{ GeV}^{\frac{1}{2}}$ ([/REF/ATLAS_2011_S9225137/d17-x01-y01](#))

- Background number of jets with $p_T > 55 \text{ GeV}$ for $3 < E_T/\sqrt{H_T} \text{ GeV}^{\frac{1}{2}}$ ([/REF/ATLAS_2011_S9225137/d17-x01-y02](#))
- Signal number of jets with $p_T > 55 \text{ GeV}$ for $3 < E_T/\sqrt{H_T} \text{ GeV}^{\frac{1}{2}}$ ([/REF/ATLAS_2011_S9225137/d17-x01-y03](#))
- Observed number of jets with $p_T > 80 \text{ GeV}$ for $3 < E_T/\sqrt{H_T} \text{ GeV}^{\frac{1}{2}}$ ([/REF/ATLAS_2011_S9225137/d18-x01-y01](#))
- Background number of jets with $p_T > 80 \text{ GeV}$ for $3 < E_T/\sqrt{H_T} \text{ GeV}^{\frac{1}{2}}$ ([/REF/ATLAS_2011_S9225137/d18-x01-y02](#))
- Signal number of jets with $p_T > 80 \text{ GeV}$ for $3 < E_T/\sqrt{H_T} \text{ GeV}^{\frac{1}{2}}$ ([/REF/ATLAS_2011_S9225137/d18-x01-y03](#))

8.40 ATLAS_2012_CONF_2012_001

4 or more lepton plus missing transverse energy SUSY search

Beams: pp

Energies: (3500.0, 3500.0) GeV

Experiment: ATLAS (LHC)

Status: PRELIMINARY

Authors:

- Peter Richardson (peter.richardson@durham.ac.uk)

References:

- ATLAS-CONF-2012-001
- ATLAS-CONF-2012-035

Run details:

- BSM signal events at 7000 GeV.

Search for SUSY using events with 4 or more leptons in association with missing transverse energy in proton-proton collisions at a centre-of-mass energy of 7 TeV. The data sample has a total integrated luminosity of 2.06 fb^{-1} . There is no reference data and in addition to the control plots from the paper the number of events in the two signal regions, correctly normalized to an integrated luminosity 2.06 fb^{-1} , are calculated.

Histograms (8):

- $E_T^e(p_T^\mu)$ for the leading lepton ([/REF/ATLAS_2012_CONF_2012_001/d01-x01-y01](#))
- $E_T^e(p_T^\mu)$ for the 2nd leading lepton ([/REF/ATLAS_2012_CONF_2012_001/d02-x01-y01](#))
- $E_T^e(p_T^\mu)$ for the 3rd leading lepton ([/REF/ATLAS_2012_CONF_2012_001/d03-x01-y01](#))
- $E_T^e(p_T^\mu)$ for the 4th leading lepton ([/REF/ATLAS_2012_CONF_2012_001/d04-x01-y01](#))
- Number of Jets ([/REF/ATLAS_2012_CONF_2012_001/d05-x01-y01](#))
- Missing Transverse Energy ([/REF/ATLAS_2012_CONF_2012_001/d06-x01-y01](#))
- Mass of SFOF lepton pair closest to the Z^0 mass ([/REF/ATLAS_2012_CONF_2012_001/d07-x01-y01](#))
- Effective Mass ([/REF/ATLAS_2012_CONF_2012_001/d08-x01-y01](#))

8.41 ATLAS_2012_CONF_2012_103

High jet multiplicity squark and gluino search

Beams: pp

Energies: (4000.0, 4000.0) GeV

Experiment: ATLAS (LHC)

Status: UNVALIDATED

Authors:

- Peter Richardson <peter.richardson@durham.ac.uk>

References:

- ATLAS-CONF-2012-103
- arXiv: [1206.1760](#)

Run details:

- BSM signal events at 8000 GeV.

Search for SUSY using events with 6 or more jets in association with missing transverse momentum produced in proton-proton collisions at a centre-of-mass energy of 8 TeV. The data sample has a total integrated luminosity of 5.8 fb^{-1} . Distributions in the W and top control regions are not produced, while in addition to the plots from the paper the count of events in the different signal regions is included. The analysis is identical to the previous 7 TeV paper.

8.42 ATLAS_2012_CONF_2012_104

Search for supersymmetry at 8 TeV in final states with jets, missing transverse momentum and one lepton with the ATLAS detector.

Beams: pp

Energies: (4000.0, 4000.0) GeV

Experiment: ATLAS (LHC)

Status: UNVALIDATED

Authors:

- Peter Richardson (Peter.Richardson@durham.ac.uk)

References:

- ATLAS-CONF-2012-104

Run details:

- BSM signal events at 8000 GeV.

One lepton search for supersymmetric particles by ATLAS at 8 TeV with 5.8 fb^{-1} integrated luminosity. Event counts in the signal regions are implemented as one-bin histograms. Histograms for effective mass are implemented for the two signal hard lepton signal regions and the ratio of missing transverse energy to effective mass for the soft lepton region.

8.43 ATLAS_2012_CONF_2012_105

Search for supersymmetry with 2 same-sign leptons, jets and missing transverse energy

Beams: pp

Energies: (4000.0, 4000.0) GeV

Experiment: ATLAS (LHC)

Status: UNVALIDATED

Authors:

- Peter Richardson (Peter.Richardson@durham.ac.uk)

References:

- ATLAS-CONF-2012-105

Run details:

- BSM signal events at 8000 GeV.

Results of the search for the production of supersymmetric particles decaying into final states with missing transverse momentum and two isolated same-sign leptons, electrons or muons. The analysis uses a data sample collected during the first half of 2012 that corresponds to a total integrated luminosity of 5.8 fb^{-1} of $\sqrt{s} = 8 \text{ TeV}$ proton-proton collisions recorded with the ATLAS detector at the Large Hadron Collider. Opposite-sign and same-sign dilepton events are studied separately.

8.44 ATLAS_2012_CONF_2012_109

0-lepton squark and gluino search

Beams: pp

Energies: (4000.0, 4000.0) GeV

Experiment: ATLAS (LHC)

Inspire ID: [1125961](#)

Status: UNVALIDATED

Authors:

- Peter Richardson ⟨ Peter.Richardson@durham.ac.uk ⟩
- David Grellscheid ⟨ david.grellscheid@durham.ac.uk ⟩
- Chris Wymant ⟨ c.m.wymant@durham.ac.uk ⟩

References:

- arXiv: [1208.0949](#)
- ATLAS-CONF-2012-109

Run details:

- BSM signal events at 8000 GeV.

0-lepton search for squarks and gluinos by ATLAS at 8 TeV. Event counts in five signal regions are implemented as one-bin histograms.

8.45 ATLAS_2012_CONF_2012_153

4 or more lepton plus missing transverse energy SUSY search

Beams: pp

Energies: (4000.0, 4000.0) GeV

Experiment: ATLAS (LHC)

Status: PRELIMINARY

Authors:

- Peter Richardson (peter.richardson@durham.ac.uk)

References:

- ATLAS-CONF-2012-153

Run details:

- BSM signal events at 8000 GeV.

Search for SUSY using events with 4 or more leptons in association with missing transverse energy in proton-proton collisions at a centre-of-mass energy of 8 TeV. The data sample has a total integrated luminosity of 13.0 fb^{-1} . There is no reference data and in addition to the control plots from the paper the number of events in the two signal regions, correctly normalized to an integrated luminosity 13.0 fb^{-1} , are calculated.

8.46 ATLAS_2012_I1082009 [121]

$D^{*\pm}$ production in jets

Beams: pp

Energies: (3500.0, 3500.0) GeV

Experiment: ATLAS (LHC)

Inspire ID: [1082009](#)

Status: UNVALIDATED

Authors:

- Peter Richardson (Peter.Richardson@durham.ac.uk)

References:

- arXiv: [1112.4432](#)

Run details:

- All flavours of quark and gluon jet production at 7 TeV

Measurement of $D^{*\pm}$ meson production in jets from proton-proton collisions at a centre-of-mass energy of $\sqrt{s} = 7$ TeV at the LHC. The measurement is based on a data sample recorded with the ATLAS detector with an integrated luminosity of 0.30 pb^{-1} for jets with transverse momentum between 25 and 70 GeV in the pseudorapidity range $|\eta| < 2.5$.

Histograms (6):

- $R(p_\perp, z)$ for $25 < p_\perp < 30$ GeV ([/REF/ATLAS_2012_I1082009/d08-x01-y01](#))
- $R(p_\perp, z)$ for $30 < p_\perp < 40$ GeV ([/REF/ATLAS_2012_I1082009/d09-x01-y01](#))
- $R(p_\perp, z)$ for $40 < p_\perp < 50$ GeV ([/REF/ATLAS_2012_I1082009/d10-x01-y01](#))
- $R(p_\perp, z)$ for $50 < p_\perp < 60$ GeV ([/REF/ATLAS_2012_I1082009/d11-x01-y01](#))
- $R(p_\perp, z)$ for $60 < p_\perp < 70$ GeV ([/REF/ATLAS_2012_I1082009/d12-x01-y01](#))
- $R(p_\perp, z)$ for $25 < p_\perp < 70$ GeV ([/REF/ATLAS_2012_I1082009/d13-x01-y01](#))

8.47 ATLAS_2012_I1082936 [122]

Inclusive jet and dijet cross sections at 7 TeV

Beams: pp

Energies: (3500.0, 3500.0) GeV

Experiment: ATLAS (LHC)

Inspire ID: [1082936](#)

Status: VALIDATED

Authors:

- Holger Schulz hschulz@physik.hu-berlin.de

References:

- arXiv: [1112.6297v2](#)
- CERN-PH-EP-2011-192

Run details:

- QCD jet production with a minimum leading jet p_\perp of 30 GeV and minimum second jet p_\perp of 20 GeV at 7 TeV.

Inclusive jet and dijet cross sections have been measured in proton-proton collisions at a centre-of-mass energy of 7 TeV using the ATLAS detector at the Large Hadron Collider. The cross sections were measured using jets clustered with the anti- k_T algorithm with parameters $R=0.4$ and $R=0.6$. These measurements are based on the 2010 data sample, consisting of a total integrated luminosity of 37 inverse picobarns. Inclusive jet double-differential cross sections are presented as a function of jet transverse momentum, in bins of jet rapidity. Dijet double-differential cross sections are studied as a function of the dijet invariant mass, in bins of half the rapidity separation of the two leading jets. The measurements are performed in the jet rapidity range $|y| < 4.4$, covering jet transverse momenta from 20 GeV to 1.5 TeV and dijet invariant masses from 70 GeV to 5 TeV. This is the successor analysis of ATLAS_2010_S8817804

Histograms (32):

- Incl. jet double-diff. x-section, anti- k_t 0.4 ($|y| < 0.3$) ([/REF/ATLAS_2012_I1082936/d01-x01-y01](#))
- Incl. jet double-diff. x-section, anti- k_t 0.4 ($0.3 \leq |y| < 0.8$) ([/REF/ATLAS_2012_I1082936/d01-x01-y02](#))
- Incl. jet double-diff. x-section, anti- k_t 0.4 ($0.8 \leq |y| < 1.2$) ([/REF/ATLAS_2012_I1082936/d01-x01-y03](#))
- Incl. jet double-diff. x-section, anti- k_t 0.4 ($1.2 \leq |y| < 2.1$) ([/REF/ATLAS_2012_I1082936/d01-x01-y04](#))

- Incl. jet double-diff. x-section, anti- k_t 0.4 ($2.1 \leq |y| < 2.8$) (/REF/ATLAS_2012_I1082936/d01-x01-y05)
- Incl. jet double-diff. x-section, anti- k_t 0.4 ($2.8 \leq |y| < 3.6$) (/REF/ATLAS_2012_I1082936/d01-x01-y06)
- Incl. jet double-diff. x-section, anti- k_t 0.4 ($3.6 \leq |y| < 4.4$) (/REF/ATLAS_2012_I1082936/d01-x01-y07)
- Incl. jet double-diff. x-section, anti- k_t 0.6 ($|y| < 0.3$) (/REF/ATLAS_2012_I1082936/d02-x01-y01)
- Incl. jet double-diff. x-section, anti- k_t 0.6 ($0.3 \leq |y| < 0.8$) (/REF/ATLAS_2012_I1082936/d02-x01-y02)
- Incl. jet double-diff. x-section, anti- k_t 0.6 ($0.8 \leq |y| < 1.2$) (/REF/ATLAS_2012_I1082936/d02-x01-y03)
- Incl. jet double-diff. x-section, anti- k_t 0.6 ($1.2 \leq |y| < 2.1$) (/REF/ATLAS_2012_I1082936/d02-x01-y04)
- Incl. jet double-diff. x-section, anti- k_t 0.6 ($2.1 \leq |y| < 2.8$) (/REF/ATLAS_2012_I1082936/d02-x01-y05)
- Incl. jet double-diff. x-section, anti- k_t 0.6 ($2.8 \leq |y| < 3.6$) (/REF/ATLAS_2012_I1082936/d02-x01-y06)
- Incl. jet double-diff. x-section, anti- k_t 0.6 ($3.6 \leq |y| < 4.4$) (/REF/ATLAS_2012_I1082936/d02-x01-y07)
- Dijet double-diff. x-section, anti- k_t 0.4 ($y^* < 0.5$) (/REF/ATLAS_2012_I1082936/d03-x01-y01)
- Dijet double-diff. x-section, anti- k_t 0.4 ($0.5 \leq y^* < 1.0$) (/REF/ATLAS_2012_I1082936/d03-x01-y02)
- Dijet double-diff. x-section, anti- k_t 0.4 ($1.0 \leq y^* < 1.5$) (/REF/ATLAS_2012_I1082936/d03-x01-y03)
- Dijet double-diff. x-section, anti- k_t 0.4 ($1.5 \leq y^* < 2.0$) (/REF/ATLAS_2012_I1082936/d03-x01-y04)
- Dijet double-diff. x-section, anti- k_t 0.4 ($2.0 \leq y^* < 2.5$) (/REF/ATLAS_2012_I1082936/d03-x01-y05)
- Dijet double-diff. x-section, anti- k_t 0.4 ($2.5 \leq y^* < 3.0$) (/REF/ATLAS_2012_I1082936/d03-x01-y06)
- Dijet double-diff. x-section, anti- k_t 0.4 ($3.0 \leq y^* < 3.5$) (/REF/ATLAS_2012_I1082936/d03-x01-y07)
- Dijet double-diff. x-section, anti- k_t 0.4 ($3.5 \leq y^* < 4.0$) (/REF/ATLAS_2012_I1082936/d03-x01-y08)
- Dijet double-diff. x-section, anti- k_t 0.4 ($4.0 \leq y^* < 4.4$) (/REF/ATLAS_2012_I1082936/d03-x01-y09)
- Dijet double-diff. x-section, anti- k_t 0.6 ($y^* < 0.5$) (/REF/ATLAS_2012_I1082936/d04-x01-y01)
- Dijet double-diff. x-section, anti- k_t 0.6 ($0.5 \leq y^* < 1.0$) (/REF/ATLAS_2012_I1082936/d04-x01-y02)
- Dijet double-diff. x-section, anti- k_t 0.6 ($1.0 \leq y^* < 1.5$) (/REF/ATLAS_2012_I1082936/d04-x01-y03)

- Dijet double-diff. x-section, anti- k_t 0.6 ($1.5 \leq y^* < 2.0$) (/REF/ATLAS_2012_I1082936/d04-x01-y04)
- Dijet double-diff. x-section, anti- k_t 0.6 ($2.0 \leq y^* < 2.5$) (/REF/ATLAS_2012_I1082936/d04-x01-y05)
- Dijet double-diff. x-section, anti- k_t 0.6 ($2.5 \leq y^* < 3.0$) (/REF/ATLAS_2012_I1082936/d04-x01-y06)
- Dijet double-diff. x-section, anti- k_t 0.6 ($3.0 \leq y^* < 3.5$) (/REF/ATLAS_2012_I1082936/d04-x01-y07)
- Dijet double-diff. x-section, anti- k_t 0.6 ($3.5 \leq y^* < 4.0$) (/REF/ATLAS_2012_I1082936/d04-x01-y08)
- Dijet double-diff. x-section, anti- k_t 0.6 ($4.0 \leq y^* < 4.4$) (/REF/ATLAS_2012_I1082936/d04-x01-y09)

8.48 ATLAS_2012_I1083318 [123]

W+jets production at 7 TeV

Beams: pp

Energies: (3500.0, 3500.0) GeV

Experiment: ATLAS (LHC)

Inspire ID: [1083318](#)

Status: UNVALIDATED

Authors:

- Frank Siegert <frank.siegert@cern.ch>

References:

- arXiv: [1201.1276](#)

Run details:

- W+jet events in either the electron or the muon decay channel (but not both).

Differential cross-sections of properties of the four leading jets in W +jets production, using the full 2010 dataset of 36 pb^{-1} . Observables include jet multiplicities, p_{\perp} , H_T , angular distances, and others. All observables are available using jets with $p_{\perp} > 30$ and $p_{\perp} > 20$ GeV.

Histograms (50):

- Inclusive Jet Multiplicity ([/REF/ATLAS_2012_I1083318/d01-x01-y01](#))
- Inclusive Jet Multiplicity ([/REF/ATLAS_2012_I1083318/d01-x01-y02](#))
- Inclusive Jet Multiplicity Ratio ([/REF/ATLAS_2012_I1083318/d02-x01-y01](#))
- Inclusive Jet Multiplicity Ratio ([/REF/ATLAS_2012_I1083318/d02-x01-y02](#))
- First Jet p_{\perp} ([/REF/ATLAS_2012_I1083318/d03-x01-y01](#))
- First Jet p_{\perp} ([/REF/ATLAS_2012_I1083318/d03-x01-y02](#))
- First Jet p_{\perp} ($W+ \geq 2$ jets) ([/REF/ATLAS_2012_I1083318/d04-x01-y01](#))
- First Jet p_{\perp} ($W+ \geq 2$ jets) ([/REF/ATLAS_2012_I1083318/d04-x01-y02](#))
- First Jet p_{\perp} ($W+ \geq 3$ jets) ([/REF/ATLAS_2012_I1083318/d05-x01-y01](#))
- First Jet p_{\perp} ($W+ \geq 3$ jets) ([/REF/ATLAS_2012_I1083318/d05-x01-y02](#))
- First Jet p_{\perp} ($W+ \geq 4$ jets) ([/REF/ATLAS_2012_I1083318/d06-x01-y01](#))
- First Jet p_{\perp} ($W+ \geq 4$ jets) ([/REF/ATLAS_2012_I1083318/d06-x01-y02](#))
- Second Jet p_{\perp} ([/REF/ATLAS_2012_I1083318/d07-x01-y01](#))

- Second Jet p_{\perp} ([/REF/ATLAS_2012_I1083318/d07-x01-y02](#))
- Second Jet p_{\perp} ($W+ \geq 3$ jets) ([/REF/ATLAS_2012_I1083318/d08-x01-y01](#))
- Second Jet p_{\perp} ($W+ \geq 3$ jets) ([/REF/ATLAS_2012_I1083318/d08-x01-y02](#))
- Second Jet p_{\perp} ($W+ \geq 4$ jets) ([/REF/ATLAS_2012_I1083318/d09-x01-y01](#))
- Second Jet p_{\perp} ($W+ \geq 4$ jets) ([/REF/ATLAS_2012_I1083318/d09-x01-y02](#))
- Third Jet p_{\perp} ([/REF/ATLAS_2012_I1083318/d10-x01-y01](#))
- Third Jet p_{\perp} ([/REF/ATLAS_2012_I1083318/d10-x01-y02](#))
- Third Jet p_{\perp} ($W+ \geq 4$ jets) ([/REF/ATLAS_2012_I1083318/d11-x01-y01](#))
- Third Jet p_{\perp} ($W+ \geq 4$ jets) ([/REF/ATLAS_2012_I1083318/d11-x01-y02](#))
- Fourth Jet p_{\perp} ([/REF/ATLAS_2012_I1083318/d12-x01-y01](#))
- Fourth Jet p_{\perp} ([/REF/ATLAS_2012_I1083318/d12-x01-y02](#))
- H_T ($W+ \geq 1$ jets) ([/REF/ATLAS_2012_I1083318/d13-x01-y01](#))
- H_T ($W+ \geq 1$ jets) ([/REF/ATLAS_2012_I1083318/d13-x01-y02](#))
- H_T ($W+ \geq 2$ jets) ([/REF/ATLAS_2012_I1083318/d14-x01-y01](#))
- H_T ($W+ \geq 2$ jets) ([/REF/ATLAS_2012_I1083318/d14-x01-y02](#))
- H_T ($W+ \geq 3$ jets) ([/REF/ATLAS_2012_I1083318/d15-x01-y01](#))
- H_T ($W+ \geq 3$ jets) ([/REF/ATLAS_2012_I1083318/d15-x01-y02](#))
- H_T ($W+ \geq 4$ jets) ([/REF/ATLAS_2012_I1083318/d16-x01-y01](#))
- H_T ($W+ \geq 4$ jets) ([/REF/ATLAS_2012_I1083318/d16-x01-y02](#))
- Jet Invariant Mass ($W+ \geq 2$ jets) ([/REF/ATLAS_2012_I1083318/d17-x01-y01](#))
- Jet Invariant Mass ($W+ \geq 2$ jets) ([/REF/ATLAS_2012_I1083318/d17-x01-y02](#))
- Jet Invariant Mass ($W+ \geq 3$ jets) ([/REF/ATLAS_2012_I1083318/d18-x01-y01](#))
- Jet Invariant Mass ($W+ \geq 3$ jets) ([/REF/ATLAS_2012_I1083318/d18-x01-y02](#))
- Jet Invariant Mass ($W+ \geq 4$ jets) ([/REF/ATLAS_2012_I1083318/d19-x01-y01](#))
- Jet Invariant Mass ($W+ \geq 4$ jets) ([/REF/ATLAS_2012_I1083318/d19-x01-y02](#))
- First Jet Rapidity ([/REF/ATLAS_2012_I1083318/d20-x01-y01](#))
- First Jet Rapidity ([/REF/ATLAS_2012_I1083318/d20-x01-y02](#))

- Lepton-Jet Rapidity Difference ([/REF/ATLAS_2012_I1083318/d21-x01-y01](#))
- Lepton-Jet Rapidity Difference ([/REF/ATLAS_2012_I1083318/d21-x01-y02](#))
- Lepton-Jet Rapidity Sum ([/REF/ATLAS_2012_I1083318/d22-x01-y01](#))
- Lepton-Jet Rapidity Sum ([/REF/ATLAS_2012_I1083318/d22-x01-y02](#))
- ΔR Distance of Leading Jets ([/REF/ATLAS_2012_I1083318/d23-x01-y01](#))
- ΔR Distance of Leading Jets ([/REF/ATLAS_2012_I1083318/d23-x01-y02](#))
- Rapidity Distance of Leading Jets ([/REF/ATLAS_2012_I1083318/d24-x01-y01](#))
- Rapidity Distance of Leading Jets ([/REF/ATLAS_2012_I1083318/d24-x01-y02](#))
- Azimuthal Distance of Leading Jets ([/REF/ATLAS_2012_I1083318/d25-x01-y01](#))
- Azimuthal Distance of Leading Jets ([/REF/ATLAS_2012_I1083318/d25-x01-y02](#))

8.49 ATLAS_2012_I1084540

Rapidity gap cross sections measured with the ATLAS detector in pp collisions at $\sqrt{s} = 7 \text{ TeV}$.

Beams: pp

Energies: (3500.0, 3500.0) GeV

Experiment: ATLAS (LHC 7TeV)

Inspire ID: [1084540](#)

Status: VALIDATED

Authors:

- Oldrich Kepka ⟨ kepkao@fzu.cz ⟩
- Tim Martin ⟨ tim.martin@cern.ch ⟩
- Paul Newman ⟨ Paul.Newman@cern.ch ⟩
- Pavel Ruzicka ⟨ ruzicka@fzu.cz ⟩

References:

- arXiv: [1201.2808](#)

Run details:

- Minimum bias inelastic pp collision at 7 TeV including diffractive component and overall cross section.

Pseudorapidity gap distributions in proton-proton collisions at $\sqrt{s} = 7 \text{ TeV}$ are studied using a minimum bias data sample with an integrated luminosity of 7.1 inverse microbarns. Cross sections are measured differentially in terms of $\Delta\eta_F$, the larger of the pseudorapidity regions extending to the limits of the ATLAS sensitivity, at $\eta = \pm 4.9$, in which no final state particles are produced above a transverse momentum threshold p_T cut. The measurements span the region $0 < \Delta\eta_F < 8$ for $200 < p_T < 800 \text{ MeV}$. At small $\Delta\eta_F$, the data test the reliability of hadronisation models in describing rapidity and transverse momentum fluctuations in final state particle production. The measurements at larger gap sizes are dominated by contributions from the single diffractive dissociation process ($pp \rightarrow Xp$), enhanced by double dissociation ($pp \rightarrow XY$) where the invariant mass of the lighter of the two dissociation systems satisfies $M_Y \lesssim 7 \text{ GeV}$. The resulting cross section is $d\sigma/d\Delta\eta_F \sim 1 \text{ mb}$ for $\Delta\eta_F \gtrsim 3$. The large rapidity gap data are used to constrain the value of the pomeron intercept appropriate to triple Regge models of soft diffraction. The cross section integrated over all gap sizes is compared with other LHC inelastic cross section measurements.

Histograms (144):

- Rapidity gap size in η starting from $\eta = \pm 4.9$, $p_T > 200 \text{ MeV}$ (/REF/ATLAS_2012_I1084540/d01-x01-y01)

- Rapidity gap size in η starting from $\eta = \pm 4.9$, $p_T > 400$ MeV (/REF/ATLAS_2012-I1084540/d02-x01-y01)
- Rapidity gap size in η starting from $\eta = \pm 4.9$, $p_T > 600$ MeV (/REF/ATLAS_2012-I1084540/d03-x01-y01)
- Rapidity gap size in η starting from $\eta = \pm 4.9$, $p_T > 800$ MeV (/REF/ATLAS_2012-I1084540/d04-x01-y01)
- Rapidity gap size in η starting from $\eta = \pm 4.9$, $p_T > 200$ MeV (/REF/ATLAS_2012-I1084540/d05-x01-y01)
- Rapidity gap size in η starting from $\eta = \pm 4.9$, $p_T > 200$ MeV (/REF/ATLAS_2012-I1084540/d05-x01-y010)
- Rapidity gap size in η starting from $\eta = \pm 4.9$, $p_T > 200$ MeV (/REF/ATLAS_2012-I1084540/d05-x01-y011)
- Rapidity gap size in η starting from $\eta = \pm 4.9$, $p_T > 200$ MeV (/REF/ATLAS_2012-I1084540/d05-x01-y012)
- Rapidity gap size in η starting from $\eta = \pm 4.9$, $p_T > 200$ MeV (/REF/ATLAS_2012-I1084540/d05-x01-y013)
- Rapidity gap size in η starting from $\eta = \pm 4.9$, $p_T > 200$ MeV (/REF/ATLAS_2012-I1084540/d05-x01-y014)
- Rapidity gap size in η starting from $\eta = \pm 4.9$, $p_T > 200$ MeV (/REF/ATLAS_2012-I1084540/d05-x01-y015)
- Rapidity gap size in η starting from $\eta = \pm 4.9$, $p_T > 200$ MeV (/REF/ATLAS_2012-I1084540/d05-x01-y016)
- Rapidity gap size in η starting from $\eta = \pm 4.9$, $p_T > 200$ MeV (/REF/ATLAS_2012-I1084540/d05-x01-y017)
- Rapidity gap size in η starting from $\eta = \pm 4.9$, $p_T > 200$ MeV (/REF/ATLAS_2012-I1084540/d05-x01-y018)
- Rapidity gap size in η starting from $\eta = \pm 4.9$, $p_T > 200$ MeV (/REF/ATLAS_2012-I1084540/d05-x01-y019)
- Rapidity gap size in η starting from $\eta = \pm 4.9$, $p_T > 200$ MeV (/REF/ATLAS_2012-I1084540/d05-x01-y02)
- Rapidity gap size in η starting from $\eta = \pm 4.9$, $p_T > 200$ MeV (/REF/ATLAS_2012-I1084540/d05-x01-y020)
- Rapidity gap size in η starting from $\eta = \pm 4.9$, $p_T > 200$ MeV (/REF/ATLAS_2012-I1084540/d05-x01-y021)

- Rapidity gap size in η starting from $\eta = \pm 4.9$, $p_T > 200$ MeV (/REF/ATLAS_2012-I1084540/d05-x01-y022)
- Rapidity gap size in η starting from $\eta = \pm 4.9$, $p_T > 200$ MeV (/REF/ATLAS_2012-I1084540/d05-x01-y023)
- Rapidity gap size in η starting from $\eta = \pm 4.9$, $p_T > 200$ MeV (/REF/ATLAS_2012-I1084540/d05-x01-y024)
- Rapidity gap size in η starting from $\eta = \pm 4.9$, $p_T > 200$ MeV (/REF/ATLAS_2012-I1084540/d05-x01-y025)
- Rapidity gap size in η starting from $\eta = \pm 4.9$, $p_T > 200$ MeV (/REF/ATLAS_2012-I1084540/d05-x01-y026)
- Rapidity gap size in η starting from $\eta = \pm 4.9$, $p_T > 200$ MeV (/REF/ATLAS_2012-I1084540/d05-x01-y027)
- Rapidity gap size in η starting from $\eta = \pm 4.9$, $p_T > 200$ MeV (/REF/ATLAS_2012-I1084540/d05-x01-y028)
- Rapidity gap size in η starting from $\eta = \pm 4.9$, $p_T > 200$ MeV (/REF/ATLAS_2012-I1084540/d05-x01-y029)
- Rapidity gap size in η starting from $\eta = \pm 4.9$, $p_T > 200$ MeV (/REF/ATLAS_2012-I1084540/d05-x01-y03)
- Rapidity gap size in η starting from $\eta = \pm 4.9$, $p_T > 200$ MeV (/REF/ATLAS_2012-I1084540/d05-x01-y030)
- Rapidity gap size in η starting from $\eta = \pm 4.9$, $p_T > 200$ MeV (/REF/ATLAS_2012-I1084540/d05-x01-y031)
- Rapidity gap size in η starting from $\eta = \pm 4.9$, $p_T > 200$ MeV (/REF/ATLAS_2012-I1084540/d05-x01-y032)
- Rapidity gap size in η starting from $\eta = \pm 4.9$, $p_T > 200$ MeV (/REF/ATLAS_2012-I1084540/d05-x01-y033)
- Rapidity gap size in η starting from $\eta = \pm 4.9$, $p_T > 200$ MeV (/REF/ATLAS_2012-I1084540/d05-x01-y034)
- Rapidity gap size in η starting from $\eta = \pm 4.9$, $p_T > 200$ MeV (/REF/ATLAS_2012-I1084540/d05-x01-y035)
- Rapidity gap size in η starting from $\eta = \pm 4.9$, $p_T > 200$ MeV (/REF/ATLAS_2012-I1084540/d05-x01-y04)
- Rapidity gap size in η starting from $\eta = \pm 4.9$, $p_T > 200$ MeV (/REF/ATLAS_2012-I1084540/d05-x01-y05)

- Rapidity gap size in η starting from $\eta = \pm 4.9$, $p_T > 200$ MeV (/REF/ATLAS_2012-I1084540/d05-x01-y06)
- Rapidity gap size in η starting from $\eta = \pm 4.9$, $p_T > 200$ MeV (/REF/ATLAS_2012-I1084540/d05-x01-y07)
- Rapidity gap size in η starting from $\eta = \pm 4.9$, $p_T > 200$ MeV (/REF/ATLAS_2012-I1084540/d05-x01-y08)
- Rapidity gap size in η starting from $\eta = \pm 4.9$, $p_T > 200$ MeV (/REF/ATLAS_2012-I1084540/d05-x01-y09)
- Rapidity gap size in η starting from $\eta = \pm 4.9$, $p_T > 200$ MeV (/REF/ATLAS_2012-I1084540/d06-x01-y01)
- Rapidity gap size in η starting from $\eta = \pm 4.9$, $p_T > 200$ MeV (/REF/ATLAS_2012-I1084540/d06-x01-y010)
- Rapidity gap size in η starting from $\eta = \pm 4.9$, $p_T > 200$ MeV (/REF/ATLAS_2012-I1084540/d06-x01-y011)
- Rapidity gap size in η starting from $\eta = \pm 4.9$, $p_T > 200$ MeV (/REF/ATLAS_2012-I1084540/d06-x01-y012)
- Rapidity gap size in η starting from $\eta = \pm 4.9$, $p_T > 200$ MeV (/REF/ATLAS_2012-I1084540/d06-x01-y013)
- Rapidity gap size in η starting from $\eta = \pm 4.9$, $p_T > 200$ MeV (/REF/ATLAS_2012-I1084540/d06-x01-y014)
- Rapidity gap size in η starting from $\eta = \pm 4.9$, $p_T > 200$ MeV (/REF/ATLAS_2012-I1084540/d06-x01-y015)
- Rapidity gap size in η starting from $\eta = \pm 4.9$, $p_T > 200$ MeV (/REF/ATLAS_2012-I1084540/d06-x01-y016)
- Rapidity gap size in η starting from $\eta = \pm 4.9$, $p_T > 200$ MeV (/REF/ATLAS_2012-I1084540/d06-x01-y017)
- Rapidity gap size in η starting from $\eta = \pm 4.9$, $p_T > 200$ MeV (/REF/ATLAS_2012-I1084540/d06-x01-y018)
- Rapidity gap size in η starting from $\eta = \pm 4.9$, $p_T > 200$ MeV (/REF/ATLAS_2012-I1084540/d06-x01-y019)
- Rapidity gap size in η starting from $\eta = \pm 4.9$, $p_T > 200$ MeV (/REF/ATLAS_2012-I1084540/d06-x01-y020)

- Rapidity gap size in η starting from $\eta = \pm 4.9$, $p_T > 200$ MeV (/REF/ATLAS_2012-I1084540/d06-x01-y021)
- Rapidity gap size in η starting from $\eta = \pm 4.9$, $p_T > 200$ MeV (/REF/ATLAS_2012-I1084540/d06-x01-y022)
- Rapidity gap size in η starting from $\eta = \pm 4.9$, $p_T > 200$ MeV (/REF/ATLAS_2012-I1084540/d06-x01-y023)
- Rapidity gap size in η starting from $\eta = \pm 4.9$, $p_T > 200$ MeV (/REF/ATLAS_2012-I1084540/d06-x01-y024)
- Rapidity gap size in η starting from $\eta = \pm 4.9$, $p_T > 200$ MeV (/REF/ATLAS_2012-I1084540/d06-x01-y025)
- Rapidity gap size in η starting from $\eta = \pm 4.9$, $p_T > 200$ MeV (/REF/ATLAS_2012-I1084540/d06-x01-y026)
- Rapidity gap size in η starting from $\eta = \pm 4.9$, $p_T > 200$ MeV (/REF/ATLAS_2012-I1084540/d06-x01-y027)
- Rapidity gap size in η starting from $\eta = \pm 4.9$, $p_T > 200$ MeV (/REF/ATLAS_2012-I1084540/d06-x01-y028)
- Rapidity gap size in η starting from $\eta = \pm 4.9$, $p_T > 200$ MeV (/REF/ATLAS_2012-I1084540/d06-x01-y029)
- Rapidity gap size in η starting from $\eta = \pm 4.9$, $p_T > 200$ MeV (/REF/ATLAS_2012-I1084540/d06-x01-y030)
- Rapidity gap size in η starting from $\eta = \pm 4.9$, $p_T > 200$ MeV (/REF/ATLAS_2012-I1084540/d06-x01-y031)
- Rapidity gap size in η starting from $\eta = \pm 4.9$, $p_T > 200$ MeV (/REF/ATLAS_2012-I1084540/d06-x01-y032)
- Rapidity gap size in η starting from $\eta = \pm 4.9$, $p_T > 200$ MeV (/REF/ATLAS_2012-I1084540/d06-x01-y033)
- Rapidity gap size in η starting from $\eta = \pm 4.9$, $p_T > 200$ MeV (/REF/ATLAS_2012-I1084540/d06-x01-y034)
- Rapidity gap size in η starting from $\eta = \pm 4.9$, $p_T > 200$ MeV (/REF/ATLAS_2012-I1084540/d06-x01-y035)
- Rapidity gap size in η starting from $\eta = \pm 4.9$, $p_T > 200$ MeV (/REF/ATLAS_2012-I1084540/d06-x01-y04)

- Rapidity gap size in η starting from $\eta = \pm 4.9$, $p_T > 200$ MeV (/REF/ATLAS_2012-I1084540/d06-x01-y05)
- Rapidity gap size in η starting from $\eta = \pm 4.9$, $p_T > 200$ MeV (/REF/ATLAS_2012-I1084540/d06-x01-y06)
- Rapidity gap size in η starting from $\eta = \pm 4.9$, $p_T > 200$ MeV (/REF/ATLAS_2012-I1084540/d06-x01-y07)
- Rapidity gap size in η starting from $\eta = \pm 4.9$, $p_T > 200$ MeV (/REF/ATLAS_2012-I1084540/d06-x01-y08)
- Rapidity gap size in η starting from $\eta = \pm 4.9$, $p_T > 200$ MeV (/REF/ATLAS_2012-I1084540/d06-x01-y09)
- Rapidity gap size in η starting from $\eta = \pm 4.9$, $p_T > 200$ MeV (/REF/ATLAS_2012-I1084540/d07-x01-y01)
- Rapidity gap size in η starting from $\eta = \pm 4.9$, $p_T > 200$ MeV (/REF/ATLAS_2012-I1084540/d07-x01-y010)
- Rapidity gap size in η starting from $\eta = \pm 4.9$, $p_T > 200$ MeV (/REF/ATLAS_2012-I1084540/d07-x01-y011)
- Rapidity gap size in η starting from $\eta = \pm 4.9$, $p_T > 200$ MeV (/REF/ATLAS_2012-I1084540/d07-x01-y012)
- Rapidity gap size in η starting from $\eta = \pm 4.9$, $p_T > 200$ MeV (/REF/ATLAS_2012-I1084540/d07-x01-y013)
- Rapidity gap size in η starting from $\eta = \pm 4.9$, $p_T > 200$ MeV (/REF/ATLAS_2012-I1084540/d07-x01-y014)
- Rapidity gap size in η starting from $\eta = \pm 4.9$, $p_T > 200$ MeV (/REF/ATLAS_2012-I1084540/d07-x01-y015)
- Rapidity gap size in η starting from $\eta = \pm 4.9$, $p_T > 200$ MeV (/REF/ATLAS_2012-I1084540/d07-x01-y016)
- Rapidity gap size in η starting from $\eta = \pm 4.9$, $p_T > 200$ MeV (/REF/ATLAS_2012-I1084540/d07-x01-y017)
- Rapidity gap size in η starting from $\eta = \pm 4.9$, $p_T > 200$ MeV (/REF/ATLAS_2012-I1084540/d07-x01-y018)
- Rapidity gap size in η starting from $\eta = \pm 4.9$, $p_T > 200$ MeV (/REF/ATLAS_2012-I1084540/d07-x01-y019)
- Rapidity gap size in η starting from $\eta = \pm 4.9$, $p_T > 200$ MeV (/REF/ATLAS_2012-I1084540/d07-x01-y02)

- Rapidity gap size in η starting from $\eta = \pm 4.9$, $p_T > 200$ MeV (/REF/ATLAS_2012-I1084540/d07-x01-y020)
- Rapidity gap size in η starting from $\eta = \pm 4.9$, $p_T > 200$ MeV (/REF/ATLAS_2012-I1084540/d07-x01-y021)
- Rapidity gap size in η starting from $\eta = \pm 4.9$, $p_T > 200$ MeV (/REF/ATLAS_2012-I1084540/d07-x01-y022)
- Rapidity gap size in η starting from $\eta = \pm 4.9$, $p_T > 200$ MeV (/REF/ATLAS_2012-I1084540/d07-x01-y023)
- Rapidity gap size in η starting from $\eta = \pm 4.9$, $p_T > 200$ MeV (/REF/ATLAS_2012-I1084540/d07-x01-y024)
- Rapidity gap size in η starting from $\eta = \pm 4.9$, $p_T > 200$ MeV (/REF/ATLAS_2012-I1084540/d07-x01-y025)
- Rapidity gap size in η starting from $\eta = \pm 4.9$, $p_T > 200$ MeV (/REF/ATLAS_2012-I1084540/d07-x01-y026)
- Rapidity gap size in η starting from $\eta = \pm 4.9$, $p_T > 200$ MeV (/REF/ATLAS_2012-I1084540/d07-x01-y027)
- Rapidity gap size in η starting from $\eta = \pm 4.9$, $p_T > 200$ MeV (/REF/ATLAS_2012-I1084540/d07-x01-y028)
- Rapidity gap size in η starting from $\eta = \pm 4.9$, $p_T > 200$ MeV (/REF/ATLAS_2012-I1084540/d07-x01-y029)
- Rapidity gap size in η starting from $\eta = \pm 4.9$, $p_T > 200$ MeV (/REF/ATLAS_2012-I1084540/d07-x01-y030)
- Rapidity gap size in η starting from $\eta = \pm 4.9$, $p_T > 200$ MeV (/REF/ATLAS_2012-I1084540/d07-x01-y031)
- Rapidity gap size in η starting from $\eta = \pm 4.9$, $p_T > 200$ MeV (/REF/ATLAS_2012-I1084540/d07-x01-y032)
- Rapidity gap size in η starting from $\eta = \pm 4.9$, $p_T > 200$ MeV (/REF/ATLAS_2012-I1084540/d07-x01-y033)
- Rapidity gap size in η starting from $\eta = \pm 4.9$, $p_T > 200$ MeV (/REF/ATLAS_2012-I1084540/d07-x01-y034)
- Rapidity gap size in η starting from $\eta = \pm 4.9$, $p_T > 200$ MeV (/REF/ATLAS_2012-I1084540/d07-x01-y035)

- Rapidity gap size in η starting from $\eta = \pm 4.9$, $p_T > 200$ MeV (/REF/ATLAS_2012-I1084540/d07-x01-y04)
- Rapidity gap size in η starting from $\eta = \pm 4.9$, $p_T > 200$ MeV (/REF/ATLAS_2012-I1084540/d07-x01-y05)
- Rapidity gap size in η starting from $\eta = \pm 4.9$, $p_T > 200$ MeV (/REF/ATLAS_2012-I1084540/d07-x01-y06)
- Rapidity gap size in η starting from $\eta = \pm 4.9$, $p_T > 200$ MeV (/REF/ATLAS_2012-I1084540/d07-x01-y07)
- Rapidity gap size in η starting from $\eta = \pm 4.9$, $p_T > 200$ MeV (/REF/ATLAS_2012-I1084540/d07-x01-y08)
- Rapidity gap size in η starting from $\eta = \pm 4.9$, $p_T > 200$ MeV (/REF/ATLAS_2012-I1084540/d07-x01-y09)
- Rapidity gap size in η starting from $\eta = \pm 4.9$, $p_T > 200$ MeV (/REF/ATLAS_2012-I1084540/d08-x01-y01)
- Rapidity gap size in η starting from $\eta = \pm 4.9$, $p_T > 200$ MeV (/REF/ATLAS_2012-I1084540/d08-x01-y010)
- Rapidity gap size in η starting from $\eta = \pm 4.9$, $p_T > 200$ MeV (/REF/ATLAS_2012-I1084540/d08-x01-y011)
- Rapidity gap size in η starting from $\eta = \pm 4.9$, $p_T > 200$ MeV (/REF/ATLAS_2012-I1084540/d08-x01-y012)
- Rapidity gap size in η starting from $\eta = \pm 4.9$, $p_T > 200$ MeV (/REF/ATLAS_2012-I1084540/d08-x01-y013)
- Rapidity gap size in η starting from $\eta = \pm 4.9$, $p_T > 200$ MeV (/REF/ATLAS_2012-I1084540/d08-x01-y014)
- Rapidity gap size in η starting from $\eta = \pm 4.9$, $p_T > 200$ MeV (/REF/ATLAS_2012-I1084540/d08-x01-y015)
- Rapidity gap size in η starting from $\eta = \pm 4.9$, $p_T > 200$ MeV (/REF/ATLAS_2012-I1084540/d08-x01-y016)
- Rapidity gap size in η starting from $\eta = \pm 4.9$, $p_T > 200$ MeV (/REF/ATLAS_2012-I1084540/d08-x01-y017)
- Rapidity gap size in η starting from $\eta = \pm 4.9$, $p_T > 200$ MeV (/REF/ATLAS_2012-I1084540/d08-x01-y018)
- Rapidity gap size in η starting from $\eta = \pm 4.9$, $p_T > 200$ MeV (/REF/ATLAS_2012-I1084540/d08-x01-y019)

- Rapidity gap size in η starting from $\eta = \pm 4.9$, $p_T > 200$ MeV (/REF/ATLAS_2012-I1084540/d08-x01-y02)
- Rapidity gap size in η starting from $\eta = \pm 4.9$, $p_T > 200$ MeV (/REF/ATLAS_2012-I1084540/d08-x01-y020)
- Rapidity gap size in η starting from $\eta = \pm 4.9$, $p_T > 200$ MeV (/REF/ATLAS_2012-I1084540/d08-x01-y021)
- Rapidity gap size in η starting from $\eta = \pm 4.9$, $p_T > 200$ MeV (/REF/ATLAS_2012-I1084540/d08-x01-y022)
- Rapidity gap size in η starting from $\eta = \pm 4.9$, $p_T > 200$ MeV (/REF/ATLAS_2012-I1084540/d08-x01-y023)
- Rapidity gap size in η starting from $\eta = \pm 4.9$, $p_T > 200$ MeV (/REF/ATLAS_2012-I1084540/d08-x01-y024)
- Rapidity gap size in η starting from $\eta = \pm 4.9$, $p_T > 200$ MeV (/REF/ATLAS_2012-I1084540/d08-x01-y025)
- Rapidity gap size in η starting from $\eta = \pm 4.9$, $p_T > 200$ MeV (/REF/ATLAS_2012-I1084540/d08-x01-y026)
- Rapidity gap size in η starting from $\eta = \pm 4.9$, $p_T > 200$ MeV (/REF/ATLAS_2012-I1084540/d08-x01-y027)
- Rapidity gap size in η starting from $\eta = \pm 4.9$, $p_T > 200$ MeV (/REF/ATLAS_2012-I1084540/d08-x01-y028)
- Rapidity gap size in η starting from $\eta = \pm 4.9$, $p_T > 200$ MeV (/REF/ATLAS_2012-I1084540/d08-x01-y029)
- Rapidity gap size in η starting from $\eta = \pm 4.9$, $p_T > 200$ MeV (/REF/ATLAS_2012-I1084540/d08-x01-y03)
- Rapidity gap size in η starting from $\eta = \pm 4.9$, $p_T > 200$ MeV (/REF/ATLAS_2012-I1084540/d08-x01-y030)
- Rapidity gap size in η starting from $\eta = \pm 4.9$, $p_T > 200$ MeV (/REF/ATLAS_2012-I1084540/d08-x01-y031)
- Rapidity gap size in η starting from $\eta = \pm 4.9$, $p_T > 200$ MeV (/REF/ATLAS_2012-I1084540/d08-x01-y032)
- Rapidity gap size in η starting from $\eta = \pm 4.9$, $p_T > 200$ MeV (/REF/ATLAS_2012-I1084540/d08-x01-y033)
- Rapidity gap size in η starting from $\eta = \pm 4.9$, $p_T > 200$ MeV (/REF/ATLAS_2012-I1084540/d08-x01-y034)

- Rapidity gap size in η starting from $\eta = \pm 4.9$, $p_T > 200$ MeV ([/REF/ATLAS_2012-I1084540/d08-x01-y035](#))
- Rapidity gap size in η starting from $\eta = \pm 4.9$, $p_T > 200$ MeV ([/REF/ATLAS_2012-I1084540/d08-x01-y04](#))
- Rapidity gap size in η starting from $\eta = \pm 4.9$, $p_T > 200$ MeV ([/REF/ATLAS_2012-I1084540/d08-x01-y05](#))
- Rapidity gap size in η starting from $\eta = \pm 4.9$, $p_T > 200$ MeV ([/REF/ATLAS_2012-I1084540/d08-x01-y06](#))
- Rapidity gap size in η starting from $\eta = \pm 4.9$, $p_T > 200$ MeV ([/REF/ATLAS_2012-I1084540/d08-x01-y07](#))
- Rapidity gap size in η starting from $\eta = \pm 4.9$, $p_T > 200$ MeV ([/REF/ATLAS_2012-I1084540/d08-x01-y08](#))
- Rapidity gap size in η starting from $\eta = \pm 4.9$, $p_T > 200$ MeV ([/REF/ATLAS_2012-I1084540/d08-x01-y09](#))

8.50 ATLAS_2012_I1091481 [124]

Azimuthal ordering of charged hadrons

Beams: $p p$

Energies: (450.0, 450.0), (3500.0, 3500.0) GeV

Experiment: ATLAS (LHC)

Inspire ID: [1091481](#)

Status: UNVALIDATED

Authors:

- Sharka Todorova <sarka.todorova@cern.ch>
- Holger Schulz <hschulz@physik.hu-berlin.de>

References:

- CERN-PH-EP-2011-197
- arXiv: [1203.0419](#)

Run details:

- QCD events with diffractives switched on.

Measurement of the ordering of charged hadrons in the azimuthal angle relative to the beam axis at the Large Hadron Collider (LHC). A spectral analysis of correlations between longitudinal and transverse components of the momentum of the charged hadrons is performed. Data were recorded with the ATLAS detector at centre-of-mass energies of $\sqrt{s} = 900$ GeV and $\sqrt{s} = 7$ TeV. The correlations measured in a phase space region dominated by low- p_T particles are not well described by conventional models of hadron production. The measured spectra show features consistent with the fragmentation of a QCD string represented by a helix-like ordered gluon chain.

Histograms (12):

- Power spectrum $p_T > 100\text{MeV}$, $p_T^{\max} < 10\text{GeV}$, $\sqrt{s} = 7\text{TeV}$ ([/REF/ATLAS_2012_I1091481/d01-x01-y01](#))
- Power spectrum $p_T > 100\text{MeV}$, $p_T^{\max} < 1\text{GeV}$, $\sqrt{s} = 7\text{TeV}$ ([/REF/ATLAS_2012_I1091481/d01-x01-y02](#))
- Power spectrum $p_T > 500\text{MeV}$, $p_T^{\max} < 10\text{GeV}$, $\sqrt{s} = 7\text{TeV}$ ([/REF/ATLAS_2012_I1091481/d01-x01-y03](#))
- Power spectrum $p_T > 100\text{MeV}$, $p_T^{\max} < 10\text{GeV}$, $\sqrt{s} = 7\text{TeV}$ ([/REF/ATLAS_2012_I1091481/d01-x02-y01](#))
- Power spectrum $p_T > 100\text{MeV}$, $p_T^{\max} < 1\text{GeV}$, $\sqrt{s} = 7\text{TeV}$ ([/REF/ATLAS_2012_I1091481/d01-x02-y02](#))
- Power spectrum $p_T > 500\text{MeV}$, $p_T^{\max} < 10\text{GeV}$, $\sqrt{s} = 7\text{TeV}$ ([/REF/ATLAS_2012_I1091481/d01-x02-y03](#))

- Power spectrum $p_{\perp} > 100\text{MeV}$, $p_{\perp}^{\max} < 10\text{GeV}$, $\sqrt{s} = 900\text{GeV}$ ([/REF/ATLAS_2012-I1091481/d02-x01-y01](#))
- Power spectrum $p_{\perp} > 100\text{MeV}$, $p_{\perp}^{\max} < 1\text{GeV}$, $\sqrt{s} = 900\text{GeV}$ ([/REF/ATLAS_2012-I1091481/d02-x01-y02](#))
- Power spectrum $p_{\perp} > 500\text{MeV}$, $p_{\perp}^{\max} < 10\text{GeV}$, $\sqrt{s} = 900\text{GeV}$ ([/REF/ATLAS_2012-I1091481/d02-x01-y03](#))
- Power spectrum $p_{\perp} > 100\text{MeV}$, $p_{\perp}^{\max} < 10\text{GeV}$, $\sqrt{s} = 900\text{GeV}$ ([/REF/ATLAS_2012-I1091481/d02-x02-y01](#))
- Power spectrum $p_{\perp} > 100\text{MeV}$, $p_{\perp}^{\max} < 1\text{GeV}$, $\sqrt{s} = 900\text{GeV}$ ([/REF/ATLAS_2012-I1091481/d02-x02-y02](#))
- Power spectrum $p_{\perp} > 500\text{MeV}$, $p_{\perp}^{\max} < 10\text{GeV}$, $\sqrt{s} = 900\text{GeV}$ ([/REF/ATLAS_2012-I1091481/d02-x02-y03](#))

8.51 ATLAS_2012_I1093734 [125]

Forward-backward and ϕ correlations at 900 GeV and 7 TeV

Beams: pp

Energies: (450.0, 450.0), (3500.0, 3500.0) GeV

Experiment: ATLAS (LHC)

Inspire ID: [1093734](#)

Status: VALIDATED

Authors:

- Camille Belanger-Champagne ⟨ camille@physics.mcgill.ca ⟩
- Andy Buckley ⟨ andy.buckley@cern.ch ⟩
- Craig Buttar ⟨ craig.buttar@glasgow.ac.uk ⟩
- Roman Lysak ⟨ lysak@fzu.cz ⟩

References:

- JHEP 1207 (2012) 019
- DOI: [10.1007/JHEP07\(2012\)019](https://doi.org/10.1007/JHEP07(2012)019)
- arXiv: [1203.3100](https://arxiv.org/abs/1203.3100)

Run details:

- QCD events at 7 TeV and 900 GeV. Diffractive events should be included.

Using inelastic proton-proton interactions at $\sqrt{s} = 900$ GeV and 7 TeV, recorded by the ATLAS detector at the LHC, measurements have been made of the correlations between forward and backward charged-particle multiplicities and, for the first time, between forward and backward charged-particle summed transverse momentum. In addition, jet-like structure in the events is studied by means of azimuthal distributions of charged particles relative to the charged particle with highest transverse momentum in a selected kinematic region of the event.

Histograms (27):

- $\sqrt{s} = 900$ GeV, $p_T > 500$ MeV, $|\eta| < 1$ ([/REF/ATLAS_2012_I1093734/d01-x01-y01](#))
- $\sqrt{s} = 7$ TeV, $p_T > 100$ MeV, $|\eta| < 2.5$ ([/REF/ATLAS_2012_I1093734/d01-x02-y01](#))
- $\sqrt{s} = 7$ TeV, $p_T > 500$ MeV, $|\eta| < 1$ ([/REF/ATLAS_2012_I1093734/d02-x01-y01](#))
- $\sqrt{s} = 7$ TeV, $p_T > 200$ MeV, $|\eta| < 2.5$ ([/REF/ATLAS_2012_I1093734/d02-x02-y01](#))
- $\sqrt{s} = 900$ GeV, $p_T > 500$ MeV, $|\eta| < 2$ ([/REF/ATLAS_2012_I1093734/d03-x01-y01](#))
- $\sqrt{s} = 7$ TeV, $p_T > 300$ MeV, $|\eta| < 2.5$ ([/REF/ATLAS_2012_I1093734/d03-x02-y01](#))

- $\sqrt{s} = 7 \text{ TeV}, p_T > 500 \text{ MeV}, |\eta| < 2$ (/REF/ATLAS_2012_I1093734/d04-x01-y01)
- $\sqrt{s} = 7 \text{ TeV}, p_T > 500 \text{ MeV}, |\eta| < 2.5$ (/REF/ATLAS_2012_I1093734/d04-x02-y01)
- $\sqrt{s} = 900 \text{ GeV}, p_T > 500 \text{ MeV}, |\eta| < 2.5$ (/REF/ATLAS_2012_I1093734/d05-x01-y01)
- $\sqrt{s} = 7 \text{ TeV}, p_T > 1000 \text{ MeV}, |\eta| < 2.5$ (/REF/ATLAS_2012_I1093734/d05-x02-y01)
- $\sqrt{s} = 7 \text{ TeV}, p_T > 500 \text{ MeV}, |\eta| < 2.5$ (/REF/ATLAS_2012_I1093734/d06-x01-y01)
- $\sqrt{s} = 7 \text{ TeV}, p_T > 1500 \text{ MeV}, |\eta| < 2.5$ (/REF/ATLAS_2012_I1093734/d06-x02-y01)
- $\sqrt{s} = 900 \text{ GeV}, p_T > 500 \text{ MeV}, |\eta| < 1$ (/REF/ATLAS_2012_I1093734/d07-x01-y01)
- $\sqrt{s} = 7 \text{ TeV}, p_T > 2000 \text{ MeV}, |\eta| < 2.5$ (/REF/ATLAS_2012_I1093734/d07-x02-y01)
- $\sqrt{s} = 7 \text{ TeV}, p_T > 500 \text{ MeV}, |\eta| < 1$ (/REF/ATLAS_2012_I1093734/d08-x01-y01)
- $\sqrt{s} = 7 \text{ TeV}, \eta \text{ interval: } 0.0 - 0.5$ (/REF/ATLAS_2012_I1093734/d08-x02-y01)
- $\sqrt{s} = 900 \text{ GeV}, p_T > 500 \text{ MeV}, |\eta| < 2$ (/REF/ATLAS_2012_I1093734/d09-x01-y01)
- $\sqrt{s} = 7 \text{ TeV}, \eta \text{ interval: } 0.5 - 1.0$ (/REF/ATLAS_2012_I1093734/d09-x02-y01)
- $\sqrt{s} = 7 \text{ TeV}, p_T > 500 \text{ MeV}, |\eta| < 2$ (/REF/ATLAS_2012_I1093734/d10-x01-y01)
- $\sqrt{s} = 7 \text{ TeV}, \eta \text{ interval: } 1.0 - 1.5$ (/REF/ATLAS_2012_I1093734/d10-x02-y01)
- $\sqrt{s} = 900 \text{ GeV}, p_T > 500 \text{ MeV}, |\eta| < 2.5$ (/REF/ATLAS_2012_I1093734/d11-x01-y01)
- $\sqrt{s} = 7 \text{ TeV}, \eta \text{ interval: } 1.5 - 2.0$ (/REF/ATLAS_2012_I1093734/d11-x02-y01)
- $\sqrt{s} = 7 \text{ TeV}, p_T > 500 \text{ MeV}, |\eta| < 2.5$ (/REF/ATLAS_2012_I1093734/d12-x01-y01)
- $\sqrt{s} = 7 \text{ TeV}, \eta \text{ interval: } 2.0 - 2.5$ (/REF/ATLAS_2012_I1093734/d12-x02-y01)
- $\sqrt{s} = 7 \text{ TeV}, p_T > 100 \text{ MeV}, |\eta| < 2.5$ (/REF/ATLAS_2012_I1093734/d13-x02-y01)
- $\sqrt{s} = 900 \text{ GeV}, p_T > 100 \text{ MeV}, |\eta| < 2.5$ (/REF/ATLAS_2012_I1093734/d14-x02-y01)
- $\sqrt{s} = 900 \text{ GeV}, p_T > 100 \text{ MeV}, |\eta| < 2.5$ (/REF/ATLAS_2012_I1093734/d15-x02-y01)

8.52 ATLAS_2012_I1093738 [126]

Isolated prompt photon + jet cross-section

Beams: pp

Energies: (3500.0, 3500.0) GeV

Experiment: ATLAS (LHC)

Inspire ID: [1093738](#)

Status: VALIDATED

Authors:

- Giovanni Marchiori (giovanni.marchiori@cern.ch)

References:

- arXiv: [1203.3161](#)

Run details:

- Inclusive photon+jet+X events at $\sqrt{s} = 7$ TeV.

A measurement of the production cross section for isolated photons in association with jets in pp collisions at $\sqrt{s} = 7$ TeV. Photons with $|\eta| < 1.37$ and $E_T > 25$ GeV and jets with $|y| < 4.4$ and $p_T > 20$ GeV are selected. The differential cross section as a function of the photon transverse energy is measured, for three leading jet rapidity configurations, separately for the cases where the photon and jet rapidities have the same or the opposite sign. The measurement uses 37 pb^{-1} of integrated luminosity collected with the ATLAS detector.

Histograms (6):

- Leading photon E_\perp (central jets, same-sign rapidity) ([/REF/ATLAS_2012_I1093738/d01-x01-y01](#))
- Leading photon E_\perp (forward jets, same-sign rapidity) ([/REF/ATLAS_2012_I1093738/d02-x01-y01](#))
- Leading photon E_\perp (very forward jets, same-sign rapidity) ([/REF/ATLAS_2012_I1093738/d03-x01-y01](#))
- Leading photon E_\perp (central jets, opposite-sign rapidity) ([/REF/ATLAS_2012_I1093738/d04-x01-y01](#))
- Leading photon E_\perp (forward jets, opposite-sign rapidity) ([/REF/ATLAS_2012_I1093738/d05-x01-y01](#))
- Leading photon E_\perp (very forward jets, opposite-sign rapidity) ([/REF/ATLAS_2012_I1093738/d06-x01-y01](#))

8.53 ATLAS_2012_I1094564 [127]

Jet mass and substructure of inclusive jets at 7 TeV

Beams: pp

Energies: (3500.0, 3500.0) GeV

Experiment: ATLAS (LHC 7TeV)

Inspire ID: [1094564](#)

Status: VALIDATED

Authors:

- Karl Nordstrom (1003412n@student.gla.ac.uk)

References:

- JHEP 1205 (2012) 128
- DOI: [10.1007/JHEP05\(2012\)128](https://doi.org/10.1007/JHEP05(2012)128)
- arXiv: [1203.4606](https://arxiv.org/abs/1203.4606)

Run details:

- pp QCD events at 7 TeV

In this analysis, the assumption that the internal substructure of jets generated by QCD radiation is well understood is tested on an inclusive sample of jets recorded with the ATLAS detector in 2010, which corresponds to 35 pb^{-1} of pp collisions delivered by the LHC at $\sqrt{s} = 7 \text{ TeV}$. Jet invariant mass, k_t splitting scales and N -subjettiness variables are presented for anti- k_t $R = 1.0$ jets and Cambridge-Aachen $R = 1.2$ jets. Jet invariant-mass spectra for Cambridge-Aachen $R = 1.2$ jets after a splitting and filtering procedure are also presented.

Histograms (36):

- Cambridge-Aachen jets, R=1.2, $200 \text{ GeV} < p_\perp < 300 \text{ GeV}$ ([/REF/ATLAS_2012_I1094564/d01-x01-y01](#))
- Cambridge-Aachen jets, R=1.2, $300 \text{ GeV} < p_\perp < 400 \text{ GeV}$ ([/REF/ATLAS_2012_I1094564/d02-x01-y01](#))
- Cambridge-Aachen jets, R=1.2, $400 \text{ GeV} < p_\perp < 500 \text{ GeV}$ ([/REF/ATLAS_2012_I1094564/d03-x01-y01](#))
- Cambridge-Aachen jets, R=1.2, $500 \text{ GeV} < p_\perp < 600 \text{ GeV}$ ([/REF/ATLAS_2012_I1094564/d04-x01-y01](#))
- Cambridge-Aachen filtered jets, R=1.2, $200 \text{ GeV} < p_\perp < 300 \text{ GeV}$ ([/REF/ATLAS_2012_I1094564/d05-x01-y01](#))
- Cambridge-Aachen filtered jets, R=1.2, $300 \text{ GeV} < p_\perp < 400 \text{ GeV}$ ([/REF/ATLAS_2012_I1094564/d06-x01-y01](#))
- Cambridge-Aachen filtered jets, R=1.2, $400 \text{ GeV} < p_\perp < 500 \text{ GeV}$ ([/REF/ATLAS_2012_I1094564/d07-x01-y01](#))

- Cambridge-Aachen filtered jets, R=1.2, $500 \text{ GeV} < p_{\perp} < 600 \text{ GeV}$ ([/REF/ATLAS_2012_I1094564/d08-x01-y01](#))
- anti- k_T jets, R=1.0, $200 \text{ GeV} < p_{\perp} < 300 \text{ GeV}$ ([/REF/ATLAS_2012_I1094564/d09-x01-y01](#))
- anti- k_T jets, R=1.0, $300 \text{ GeV} < p_{\perp} < 400 \text{ GeV}$ ([/REF/ATLAS_2012_I1094564/d10-x01-y01](#))
- anti- k_T jets, R=1.0, $400 \text{ GeV} < p_{\perp} < 500 \text{ GeV}$ ([/REF/ATLAS_2012_I1094564/d11-x01-y01](#))
- anti- k_T jets, R=1.0, $500 \text{ GeV} < p_{\perp} < 600 \text{ GeV}$ ([/REF/ATLAS_2012_I1094564/d12-x01-y01](#))
- anti- k_T jets, R=1.0, $200 \text{ GeV} < p_{\perp} < 300 \text{ GeV}$ ([/REF/ATLAS_2012_I1094564/d13-x01-y01](#))
- anti- k_T jets, R=1.0, $300 \text{ GeV} < p_{\perp} < 400 \text{ GeV}$ ([/REF/ATLAS_2012_I1094564/d14-x01-y01](#))
- anti- k_T jets, R=1.0, $400 \text{ GeV} < p_{\perp} < 500 \text{ GeV}$ ([/REF/ATLAS_2012_I1094564/d15-x01-y01](#))
- anti- k_T jets, R=1.0, $500 \text{ GeV} < p_{\perp} < 600 \text{ GeV}$ ([/REF/ATLAS_2012_I1094564/d16-x01-y01](#))
- anti- k_T jets, R=1.0, $200 \text{ GeV} < p_{\perp} < 300 \text{ GeV}$ ([/REF/ATLAS_2012_I1094564/d17-x01-y01](#))
- anti- k_T jets, R=1.0, $300 \text{ GeV} < p_{\perp} < 400 \text{ GeV}$ ([/REF/ATLAS_2012_I1094564/d18-x01-y01](#))
- anti- k_T jets, R=1.0, $400 \text{ GeV} < p_{\perp} < 500 \text{ GeV}$ ([/REF/ATLAS_2012_I1094564/d19-x01-y01](#))
- anti- k_T jets, R=1.0, $500 \text{ GeV} < p_{\perp} < 600 \text{ GeV}$ ([/REF/ATLAS_2012_I1094564/d20-x01-y01](#))
- Cambridge-Aachen jets, R=1.2, $200 \text{ GeV} < p_{\perp} < 300 \text{ GeV}$ ([/REF/ATLAS_2012_I1094564/d21-x01-y01](#))
- Cambridge-Aachen jets, R=1.2, $300 \text{ GeV} < p_{\perp} < 400 \text{ GeV}$ ([/REF/ATLAS_2012_I1094564/d22-x01-y01](#))
- Cambridge-Aachen jets, R=1.2, $400 \text{ GeV} < p_{\perp} < 500 \text{ GeV}$ ([/REF/ATLAS_2012_I1094564/d23-x01-y01](#))
- Cambridge-Aachen jets, R=1.2, $500 \text{ GeV} < p_{\perp} < 600 \text{ GeV}$ ([/REF/ATLAS_2012_I1094564/d24-x01-y01](#))
- Cambridge-Aachen jets, R=1.2, $200 \text{ GeV} < p_{\perp} < 300 \text{ GeV}$ ([/REF/ATLAS_2012_I1094564/d25-x01-y01](#))
- Cambridge-Aachen jets, R=1.2, $300 \text{ GeV} < p_{\perp} < 400 \text{ GeV}$ ([/REF/ATLAS_2012_I1094564/d26-x01-y01](#))
- Cambridge-Aachen jets, R=1.2, $400 \text{ GeV} < p_{\perp} < 500 \text{ GeV}$ ([/REF/ATLAS_2012_I1094564/d27-x01-y01](#))
- Cambridge-Aachen jets, R=1.2, $500 \text{ GeV} < p_{\perp} < 600 \text{ GeV}$ ([/REF/ATLAS_2012_I1094564/d28-x01-y01](#))
- anti k_T jets, R=1.0, $200 \text{ GeV} < p_{\perp} < 300 \text{ GeV}$ ([/REF/ATLAS_2012_I1094564/d29-x01-y01](#))
- anti k_T jets, R=1.0, $300 \text{ GeV} < p_{\perp} < 400 \text{ GeV}$ ([/REF/ATLAS_2012_I1094564/d30-x01-y01](#))
- anti k_T jets, R=1.0, $400 \text{ GeV} < p_{\perp} < 500 \text{ GeV}$ ([/REF/ATLAS_2012_I1094564/d31-x01-y01](#))
- anti k_T jets, R=1.0, $500 \text{ GeV} < p_{\perp} < 600 \text{ GeV}$ ([/REF/ATLAS_2012_I1094564/d32-x01-y01](#))
- anti k_T jets, R=1.0, $200 \text{ GeV} < p_{\perp} < 300 \text{ GeV}$ ([/REF/ATLAS_2012_I1094564/d33-x01-y01](#))

- anti k_T jets, R=1.0, $300 \text{ GeV} < p_{\perp} < 400 \text{ GeV}$ ([/REF/ATLAS_2012_I1094564/d34-x01-y01](#))
- anti k_T jets, R=1.0, $400 \text{ GeV} < p_{\perp} < 500 \text{ GeV}$ ([/REF/ATLAS_2012_I1094564/d35-x01-y01](#))
- anti k_T jets, R=1.0, $500 \text{ GeV} < p_{\perp} < 600 \text{ GeV}$ ([/REF/ATLAS_2012_I1094564/d36-x01-y01](#))

8.54 ATLAS_2012_I1094568 [128]

Measurement of ttbar production with a veto on additional central jet activity

Beams: pp

Energies: (3500.0, 3500.0) GeV

Experiment: ATLAS (LHC)

Inspire ID: [1094568](#)

Status: VALIDATED

Authors:

- Kiran Joshi (kiran.joshi@cern.ch)

References:

- arXiv: [1203.5015](#)
- Eur.Phys.J. C72 (2012) 2043

Run details:

- Require dileptonic ttbar events at 7TeV.

A measurement of the additional jet activity in dileptonic ttbar events. The fraction of events passing a veto requirement are shown as a function the veto scale for four central rapidity intervals. Two veto definitions are used: events are vetoed if they contain an additional jet in the rapidity interval with transverse momentum above a threshold, or alternatively, if the scalar transverse momentum sum of all additional jets in the rapidity interval is above a threshold.

Histograms (8):

- Gap fraction vs. Q_0 for veto region: $|y| < 0.8$ ([/REF/ATLAS_2012_I1094568/d01-x01-y01](#))
- Gap fraction vs. Q_{sum} for veto region: $|y| < 0.8$ ([/REF/ATLAS_2012_I1094568/d01-x02-y01](#))
- Gap fraction vs. Q_0 for veto region: $0.8 < |y| < 1.5$ ([/REF/ATLAS_2012_I1094568/d02-x01-y01](#))
- Gap fraction vs. Q_{sum} for veto region: $0.8 < |y| < 1.5$ ([/REF/ATLAS_2012_I1094568/d02-x02-y01](#))
- Gap fraction vs. Q_0 for veto region: $1.5 < |y| < 2.1$ ([/REF/ATLAS_2012_I1094568/d03-x01-y01](#))
- Gap fraction vs. Q_{sum} for veto region: $1.5 < |y| < 2.1$ ([/REF/ATLAS_2012_I1094568/d03-x02-y01](#))
- Gap fraction vs. Q_0 for veto region: $|y| < 2.1$ ([/REF/ATLAS_2012_I1094568/d04-x01-y01](#))
- Gap fraction vs. Q_{sum} for veto region: $|y| < 2.1$ ([/REF/ATLAS_2012_I1094568/d04-x02-y01](#))

8.55 ATLAS_2012_I1095236 [129]

b-jets search for supersymmetry with 0- and 1-leptons

Beams: pp

Energies: (3500.0, 3500.0) GeV

Experiment: ATLAS (LHC)

Inspire ID: [1095236](#)

Status: UNVALIDATED

Authors:

- Peter Richardson (Peter.Richardson@durham.ac.uk)

References:

- arXiv: [1203.6193](#)

Run details:

- BSM signal events at 7000 GeV.

Search for supersymmetric particles by ATLAS at 7 TeV in events with b-jets, large missing energy, and zero or one leptons. Event counts in six zero lepton and two one lepton signal regions are implemented as one-bin histograms. Histograms for missing transverse energy, and effective mass are also implemented for some signal regions.

8.56 ATLAS_2012_I1112263 [130]

3 lepton plus missing transverse energy SUSY search

Beams: pp

Energies: (3500.0, 3500.0) GeV

Experiment: ATLAS (LHC)

Status: VALIDATED

Authors:

- Peter Richardson <peter.richardson@durham.ac.uk>

References:

- ATLAS-CONF-2012-023
- arXiv: [1204.5638](#)

Run details:

- BSM signal events at 7000 GeV.

Search for SUSY using events with 3 leptons in association with missing transverse energy in proton-proton collisions at a centre-of-mass energy of 7 TeV. The data sample has a total integrated luminosity of 2.06 fb^{-1} . There is no reference data and in addition to the control plots from the paper the number of events in the two signal regions, correctly normalized to an integrated luminosity 2.06 fb^{-1} , are calculated.

8.57 ATLAS_2012_I1117704

High jet multiplicity squark and gluino search

Beams: pp

Energies: (3500.0, 3500.0) GeV

Experiment: ATLAS (LHC)

Status: VALIDATED

Authors:

- Peter Richardson (peter.richardson@durham.ac.uk)

References:

- arXiv: [1206.1760](#)

Run details:

- BSM signal events at 7000 GeV.

Search for SUSY using events with 6 or more jets in association with missing transverse momentum produced in proton-proton collisions at a centre-of-mass energy of 7 TeV. The data sample has a total integrated luminosity of 4.7 fb^{-1} . Distributions in the W and top control regions are not produced, while in addition to the plots from the paper the count of events in the different signal regions is included.

8.58 ATLAS_2012_I1118269 [131]

b-hadron production cross-section using decays to $D^*\mu^-X$ at $\sqrt{s} = 7$ TeV

Beams: pp

Energies: (3500.0, 3500.0) GeV

Experiment: ATLAS (LHC)

Inspire ID: [1118269](#)

Status: VALIDATED

Authors:

- Andy Buckley ⟨ andy.buckley@ed.ac.uk ⟩
- Sercan Sen ⟨ sercan.sen@cern.ch ⟩
- Peter Skands ⟨ Peter.Skands@cern.ch ⟩

References:

- arXiv: [1206.3122](#)

Run details:

- pp to b-hadron + X at 7 TeV, i.e. switch on "HardQCD:gg2bbbar" and "HardQCD:qbar2bbbar" flags in Pythia8.

Measurement of *b*-hadron production cross section using 3.3 pb^{-1} of integrated luminosity, collected during the 2010 LHC run. The *b*-hadrons are selected by partially reconstructing $D^*\mu^-X$ final states using only direct semileptonic decays of *b* to $D^*\mu^-X$. Differential cross sections as functions of p_\perp and $|\eta|$.

Histograms (2):

- *b* hadron p_\perp at $\sqrt{s} = 7$ TeV ([/REF/ATLAS_2012_I1118269/d01-x01-y01](#))
- *b* hadron η at $\sqrt{s} = 7$ TeV ([/REF/ATLAS_2012_I1118269/d02-x01-y01](#))

8.59 ATLAS_2012_I1119557 [132]

Jet shapes and jet masses

Beams: pp

Energies: (3500.0, 3500.0) GeV

Experiment: ATLAS (LHC 7TeV)

Inspire ID: [1119557](#)

Status: VALIDATED

Authors:

- Lily Asquith (lasquith@hep.anl.gov)
- Roman Lysak (lysak@fzu.cz)

References:

- Phys.Rev. D86 (2012) 072006
- DOI: [10.1103/PhysRevD.86.072006](https://doi.org/10.1103/PhysRevD.86.072006)
- arXiv: [1206.5369](https://arxiv.org/abs/1206.5369)

Run details:

- QCD events at 7 TeV, leading- p_T jets with $p_T > 300 \text{ GeV}$.

Measurements are presented of the properties of high transverse momentum jets, produced in proton-proton collisions at a center-of-mass energy of $\sqrt{s} = 7 \text{ TeV}$. Jet mass, width, eccentricity, planar flow and angularity are measured for jets reconstructed using the anti- k_T algorithm with distance parameters $R = 0.6$ and 1.0 , with transverse momentum $p_T > 300 \text{ GeV}$ and pseudorapidity $|\eta| < 2$.

Histograms (6):

- Anti- k_T jets, $R = 0.6$, $p_T > 300 \text{ GeV}$, $|\eta| < 2$ ([/REF/ATLAS_2012_I1119557/d01-x01-y01](#))
- Anti- k_T jets, $R = 1.0$, $p_T > 300 \text{ GeV}$, $|\eta| < 2$ ([/REF/ATLAS_2012_I1119557/d01-x02-y01](#))
- Anti- k_T jets, $R = 0.6$, $p_T > 300 \text{ GeV}$, $|\eta| < 2$ ([/REF/ATLAS_2012_I1119557/d02-x01-y01](#))
- Anti- k_T jets, $R = 1.0$, $p_T > 300 \text{ GeV}$, $|\eta| < 2$ ([/REF/ATLAS_2012_I1119557/d02-x02-y01](#))
- Anti- k_T jets, $R = 1.0$, $p_T > 300 \text{ GeV}$, $|\eta| < 0.7$, $130 < M < 210 \text{ GeV}$ ([/REF/ATLAS_2012_I1119557/d04-x02-y01](#))
- Anti- k_T jets, $R = 0.6$, $p_T > 300 \text{ GeV}$, $|\eta| < 0.7$, $100 < M < 130 \text{ GeV}$ ([/REF/ATLAS_2012_I1119557/d05-x01-y01](#))

8.60 ATLAS_2012_I1124167 [133]

Measurement of charged-particle event shape variables

Beams: pp

Energies: (3500.0, 3500.0) GeV

Experiment: ATLAS (LHC)

Inspire ID: [1124167](#)

Status: VALIDATED

Authors:

- Deepak Kar (deepak.kar@cern.ch)

References:

- arXiv: [1207.6915](#)
- Phys.Rev. D88 (2013) 032004
- [10.1103/PhysRevD.88.032004](https://doi.org/10.1103/PhysRevD.88.032004)

Run details:

- Minimum bias events with at least 6 charged particles at 7 TeV

The measurement of charged-particle event shape variables is presented in inclusive inelastic pp collisions at a center-of-mass energy of 7 TeV using the ATLAS detector at the LHC. The observables studied are the transverse thrust, thrust minor, and transverse sphericity, each defined using the final-state charged particles momentum components perpendicular to the beam direction. Events with at least six charged particles are selected by a minimum-bias trigger. In addition to the differential distributions, the evolution of each event shape variable as a function of the leading charged-particle transverse momentum, charged-particle multiplicity, and summed transverse momentum is presented.

Histograms (33):

- Transverse thrust for $0.5 \text{ GeV} < p_T^{\text{lead}} \leq 2.5 \text{ GeV}$ ([/REF/ATLAS_2012_I1124167/d01-x01-y01](#))
- Transverse thrust for $2.5 \text{ GeV} < p_T^{\text{lead}} \leq 5 \text{ GeV}$ ([/REF/ATLAS_2012_I1124167/d01-x01-y02](#))
- Transverse thrust for $5 \text{ GeV} < p_T^{\text{lead}} \leq 7.5 \text{ GeV}$ ([/REF/ATLAS_2012_I1124167/d01-x01-y03](#))
- Transverse thrust for $7.5 \text{ GeV} < p_T^{\text{lead}} \leq 10 \text{ GeV}$ ([/REF/ATLAS_2012_I1124167/d01-x01-y04](#))
- Transverse thrust for $p_T^{\text{lead}} > 0.5 \text{ GeV}$ ([/REF/ATLAS_2012_I1124167/d02-x01-y01](#))
- Transverse thrust for $p_T^{\text{lead}} > 2.5 \text{ GeV}$ ([/REF/ATLAS_2012_I1124167/d02-x01-y02](#))
- Transverse thrust for $p_T^{\text{lead}} > 5 \text{ GeV}$ ([/REF/ATLAS_2012_I1124167/d02-x01-y03](#))
- Transverse thrust for $p_T^{\text{lead}} > 7.5 \text{ GeV}$ ([/REF/ATLAS_2012_I1124167/d02-x01-y04](#))

- Transverse thrust for $p_T^{\text{lead}} > 10 \text{ GeV}$ (/REF/ATLAS_2012_I1124167/d02-x01-y05)
- Transverse thrust minor for $0.5 \text{ GeV} < p_T^{\text{lead}} \leq 2.5 \text{ GeV}$ (/REF/ATLAS_2012_I1124167/d03-x01-y01)
- Transverse thrust minor for $2.5 \text{ GeV} < p_T^{\text{lead}} \leq 5 \text{ GeV}$ (/REF/ATLAS_2012_I1124167/d03-x01-y02)
- Transverse thrust minor for $5 \text{ GeV} < p_T^{\text{lead}} \leq 7.5 \text{ GeV}$ (/REF/ATLAS_2012_I1124167/d03-x01-y03)
- Transverse thrust minor for $7.5 \text{ GeV} < p_T^{\text{lead}} \leq 10 \text{ GeV}$ (/REF/ATLAS_2012_I1124167/d03-x01-y04)
- Transverse thrust minor for $p_T^{\text{lead}} > 0.5 \text{ GeV}$ (/REF/ATLAS_2012_I1124167/d04-x01-y01)
- Transverse thrust minor for $p_T^{\text{lead}} > 2.5 \text{ GeV}$ (/REF/ATLAS_2012_I1124167/d04-x01-y02)
- Transverse thrust minor for $p_T^{\text{lead}} > 5 \text{ GeV}$ (/REF/ATLAS_2012_I1124167/d04-x01-y03)
- Transverse thrust minor for $p_T^{\text{lead}} > 7.5 \text{ GeV}$ (/REF/ATLAS_2012_I1124167/d04-x01-y04)
- Transverse thrust minor for $p_T^{\text{lead}} > 10 \text{ GeV}$ (/REF/ATLAS_2012_I1124167/d04-x01-y05)
- Transverse sphericity for $0.5 \text{ GeV} < p_T^{\text{lead}} \leq 2.5 \text{ GeV}$ (/REF/ATLAS_2012_I1124167/d05-x01-y01)
- Transverse sphericity for $2.5 \text{ GeV} < p_T^{\text{lead}} \leq 5 \text{ GeV}$ (/REF/ATLAS_2012_I1124167/d05-x01-y02)
- Transverse sphericity for $5 \text{ GeV} < p_T^{\text{lead}} \leq 7.5 \text{ GeV}$ (/REF/ATLAS_2012_I1124167/d05-x01-y03)
- Transverse sphericity for $7.5 \text{ GeV} < p_T^{\text{lead}} \leq 10 \text{ GeV}$ (/REF/ATLAS_2012_I1124167/d05-x01-y04)
- Transverse sphericity for $p_T^{\text{lead}} > 0.5 \text{ GeV}$ (/REF/ATLAS_2012_I1124167/d06-x01-y01)
- Transverse sphericity for $p_T^{\text{lead}} > 2.5 \text{ GeV}$ (/REF/ATLAS_2012_I1124167/d06-x01-y02)
- Transverse sphericity for $p_T^{\text{lead}} > 5 \text{ GeV}$ (/REF/ATLAS_2012_I1124167/d06-x01-y03)
- Transverse sphericity for $p_T^{\text{lead}} > 7.5 \text{ GeV}$ (/REF/ATLAS_2012_I1124167/d06-x01-y04)
- Transverse sphericity for $p_T^{\text{lead}} > 10 \text{ GeV}$ (/REF/ATLAS_2012_I1124167/d06-x01-y05)
- Average transverse thrust vs. multiplicity (/REF/ATLAS_2012_I1124167/d07-x01-y01)
- Average transverse thrust minor vs. multiplicity (/REF/ATLAS_2012_I1124167/d07-x01-y02)
- Average transverse sphericity vs. multiplicity (/REF/ATLAS_2012_I1124167/d07-x01-y03)
- Average transverse thrust vs. transverse $\sum p_T$ (/REF/ATLAS_2012_I1124167/d08-x01-y01)
- Average transverse thrust minor vs. transverse $\sum p_T$ (/REF/ATLAS_2012_I1124167/d08-x01-y02)
- Average transverse sphericity vs. transverse $\sum p_T$ (/REF/ATLAS_2012_I1124167/d08-x01-y03)

8.61 ATLAS_2012_I1125575 [134]

Studies of the underlying event at 7 TeV with track-jets

Beams: pp

Energies: (3500.0, 3500.0) GeV

Experiment: ATLAS (LHC)

Inspire ID: [1125575](#)

Status: VALIDATED

Authors:

- Kiran Joshi (kiran.joshi@cern.ch)

References:

- arXiv: [1208.0563](#)

Run details:

- Minimum bias events at 7 TeV.

Distributions sensitive to the underlying event are studied in events containing one or more charged particles. Jets are reconstructed using the anti- k_t algorithm with radius parameter R varying between 0.2 and 1.0. Distributions of the charged-particle multiplicity, the scalar sum of the transverse momentum of charged particles, and the average charged-particle p_\perp are measured as functions of p_\perp^{jet} in regions transverse to and opposite the leading jet for $4\text{GeV} < p_\perp^{\text{jet}} < 100\text{GeV}$. In addition, the R -dependence of the mean values of these observables is studied.

Histograms (330):

- Mean N_{ch} vs. leading jet p_\perp , $R = 0.2$, Away region ([/REF/ATLAS_2012_I1125575/d01-x01-y01](#))
- Mean N_{ch} vs. leading jet p_\perp , $R = 0.2$, Transverse region ([/REF/ATLAS_2012_I1125575/d01-x01-y02](#))
- Mean N_{ch} vs. leading jet p_\perp , $R = 0.4$, Away region ([/REF/ATLAS_2012_I1125575/d01-x02-y01](#))
- Mean N_{ch} vs. leading jet p_\perp , $R = 0.4$, Transverse region ([/REF/ATLAS_2012_I1125575/d01-x02-y02](#))
- Mean N_{ch} vs. leading jet p_\perp , $R = 0.6$, Away region ([/REF/ATLAS_2012_I1125575/d01-x03-y01](#))
- Mean N_{ch} vs. leading jet p_\perp , $R = 0.6$, Transverse region ([/REF/ATLAS_2012_I1125575/d01-x03-y02](#))
- Mean N_{ch} vs. leading jet p_\perp , $R = 0.8$, Away region ([/REF/ATLAS_2012_I1125575/d01-x04-y01](#))
- Mean N_{ch} vs. leading jet p_\perp , $R = 0.8$, Transverse region ([/REF/ATLAS_2012_I1125575/d01-x04-y02](#))
- Mean N_{ch} vs. leading jet p_\perp , $R = 1.0$, Away region ([/REF/ATLAS_2012_I1125575/d01-x05-y01](#))
- Mean N_{ch} vs. leading jet p_\perp , $R = 1.0$, Transverse region ([/REF/ATLAS_2012_I1125575/d01-x05-y02](#))
- Mean p_\perp vs. leading jet p_\perp , $R = 0.2$, Away region ([/REF/ATLAS_2012_I1125575/d02-x01-y01](#))

- Mean p_\perp vs. leading jet p_\perp , $R = 0.2$, Transverse region (/REF/ATLAS_2012_I1125575/d02-x01-y02)
- Mean p_\perp vs. leading jet p_\perp , $R = 0.4$, Away region (/REF/ATLAS_2012_I1125575/d02-x02-y01)
- Mean p_\perp vs. leading jet p_\perp , $R = 0.4$, Transverse region (/REF/ATLAS_2012_I1125575/d02-x02-y02)
- Mean p_\perp vs. leading jet p_\perp , $R = 0.6$, Away region (/REF/ATLAS_2012_I1125575/d02-x03-y01)
- Mean p_\perp vs. leading jet p_\perp , $R = 0.6$, Transverse region (/REF/ATLAS_2012_I1125575/d02-x03-y02)
- Mean p_\perp vs. leading jet p_\perp , $R = 0.8$, Away region (/REF/ATLAS_2012_I1125575/d02-x04-y01)
- Mean p_\perp vs. leading jet p_\perp , $R = 0.8$, Transverse region (/REF/ATLAS_2012_I1125575/d02-x04-y02)
- Mean p_\perp vs. leading jet p_\perp , $R = 1.0$, Away region (/REF/ATLAS_2012_I1125575/d02-x05-y01)
- Mean p_\perp vs. leading jet p_\perp , $R = 1.0$, Transverse region (/REF/ATLAS_2012_I1125575/d02-x05-y02)
- Mean $\sum p_\perp$ vs. leading jet p_\perp , $R = 0.2$, Away region (/REF/ATLAS_2012_I1125575/d03-x01-y01)
- Mean $\sum p_\perp$ vs. leading jet p_\perp , $R = 0.2$, Transverse region (/REF/ATLAS_2012_I1125575/d03-x01-y02)
- Mean $\sum p_\perp$ vs. leading jet p_\perp , $R = 0.4$, Away region (/REF/ATLAS_2012_I1125575/d03-x02-y01)
- Mean $\sum p_\perp$ vs. leading jet p_\perp , $R = 0.4$, Transverse region (/REF/ATLAS_2012_I1125575/d03-x02-y02)
- Mean $\sum p_\perp$ vs. leading jet p_\perp , $R = 0.6$, Away region (/REF/ATLAS_2012_I1125575/d03-x03-y01)
- Mean $\sum p_\perp$ vs. leading jet p_\perp , $R = 0.6$, Transverse region (/REF/ATLAS_2012_I1125575/d03-x03-y02)
- Mean $\sum p_\perp$ vs. leading jet p_\perp , $R = 0.8$, Away region (/REF/ATLAS_2012_I1125575/d03-x04-y01)
- Mean $\sum p_\perp$ vs. leading jet p_\perp , $R = 0.8$, Transverse region (/REF/ATLAS_2012_I1125575/d03-x04-y02)
- Mean $\sum p_\perp$ vs. leading jet p_\perp , $R = 1.0$, Away region (/REF/ATLAS_2012_I1125575/d03-x05-y01)
- Mean $\sum p_\perp$ vs. leading jet p_\perp , $R = 1.0$, Transverse region (/REF/ATLAS_2012_I1125575/d03-x05-y02)
- N_{ch} for $4 \leq p_\perp^{\text{jet}} < 5$ GeV, $R = 0.2$, Away region (/REF/ATLAS_2012_I1125575/d04-x01-y01)
- N_{ch} for $4 \leq p_\perp^{\text{jet}} < 5$ GeV, $R = 0.2$, Transverse region (/REF/ATLAS_2012_I1125575/d04-x01-y02)
- N_{ch} for $5 \leq p_\perp^{\text{jet}} < 6$ GeV, $R = 0.2$, Away region (/REF/ATLAS_2012_I1125575/d04-x01-y03)
- N_{ch} for $5 \leq p_\perp^{\text{jet}} < 6$ GeV, $R = 0.2$, Transverse region (/REF/ATLAS_2012_I1125575/d04-x01-y04)
- N_{ch} for $6 \leq p_\perp^{\text{jet}} < 8$ GeV, $R = 0.2$, Away region (/REF/ATLAS_2012_I1125575/d04-x01-y05)
- N_{ch} for $6 \leq p_\perp^{\text{jet}} < 8$ GeV, $R = 0.2$, Transverse region (/REF/ATLAS_2012_I1125575/d04-x01-y06)
- N_{ch} for $8 \leq p_\perp^{\text{jet}} < 11$ GeV, $R = 0.2$, Away region (/REF/ATLAS_2012_I1125575/d04-x01-y07)
- N_{ch} for $8 \leq p_\perp^{\text{jet}} < 11$ GeV, $R = 0.2$, Transverse region (/REF/ATLAS_2012_I1125575/d04-x01-y08)

- N_{ch} for $11 \leq p_{\perp}^{\text{jet}} < 14$ GeV, $R = 0.2$, Away region ([/REF/ATLAS_2012_I1125575/d04-x01-y09](#))
- N_{ch} for $11 \leq p_{\perp}^{\text{jet}} < 14$ GeV, $R = 0.2$, Transverse region ([/REF/ATLAS_2012_I1125575/d04-x01-y10](#))
- N_{ch} for $14 \leq p_{\perp}^{\text{jet}} < 19$ GeV, $R = 0.2$, Away region ([/REF/ATLAS_2012_I1125575/d04-x01-y11](#))
- N_{ch} for $14 \leq p_{\perp}^{\text{jet}} < 19$ GeV, $R = 0.2$, Transverse region ([/REF/ATLAS_2012_I1125575/d04-x01-y12](#))
- N_{ch} for $19 \leq p_{\perp}^{\text{jet}} < 24$ GeV, $R = 0.2$, Away region ([/REF/ATLAS_2012_I1125575/d04-x01-y13](#))
- N_{ch} for $19 \leq p_{\perp}^{\text{jet}} < 24$ GeV, $R = 0.2$, Transverse region ([/REF/ATLAS_2012_I1125575/d04-x01-y14](#))
- N_{ch} for $24 \leq p_{\perp}^{\text{jet}} < 31$ GeV, $R = 0.2$, Away region ([/REF/ATLAS_2012_I1125575/d04-x01-y15](#))
- N_{ch} for $24 \leq p_{\perp}^{\text{jet}} < 31$ GeV, $R = 0.2$, Transverse region ([/REF/ATLAS_2012_I1125575/d04-x01-y16](#))
- N_{ch} for $31 \leq p_{\perp}^{\text{jet}} < 50$ GeV, $R = 0.2$, Away region ([/REF/ATLAS_2012_I1125575/d04-x01-y17](#))
- N_{ch} for $31 \leq p_{\perp}^{\text{jet}} < 50$ GeV, $R = 0.2$, Transverse region ([/REF/ATLAS_2012_I1125575/d04-x01-y18](#))
- N_{ch} for $50 \leq p_{\perp}^{\text{jet}} < 100$ GeV, $R = 0.2$, Away region ([/REF/ATLAS_2012_I1125575/d04-x01-y19](#))
- N_{ch} for $50 \leq p_{\perp}^{\text{jet}} < 100$ GeV, $R = 0.2$, Transverse region ([/REF/ATLAS_2012_I1125575/d04-x01-y20](#))
- N_{ch} for $4 \leq p_{\perp}^{\text{jet}} < 5$ GeV, $R = 0.4$, Away region ([/REF/ATLAS_2012_I1125575/d04-x02-y01](#))
- N_{ch} for $4 \leq p_{\perp}^{\text{jet}} < 5$ GeV, $R = 0.4$, Transverse region ([/REF/ATLAS_2012_I1125575/d04-x02-y02](#))
- N_{ch} for $5 \leq p_{\perp}^{\text{jet}} < 6$ GeV, $R = 0.4$, Away region ([/REF/ATLAS_2012_I1125575/d04-x02-y03](#))
- N_{ch} for $5 \leq p_{\perp}^{\text{jet}} < 6$ GeV, $R = 0.4$, Transverse region ([/REF/ATLAS_2012_I1125575/d04-x02-y04](#))
- N_{ch} for $6 \leq p_{\perp}^{\text{jet}} < 8$ GeV, $R = 0.4$, Away region ([/REF/ATLAS_2012_I1125575/d04-x02-y05](#))
- N_{ch} for $6 \leq p_{\perp}^{\text{jet}} < 8$ GeV, $R = 0.4$, Transverse region ([/REF/ATLAS_2012_I1125575/d04-x02-y06](#))
- N_{ch} for $8 \leq p_{\perp}^{\text{jet}} < 11$ GeV, $R = 0.4$, Away region ([/REF/ATLAS_2012_I1125575/d04-x02-y07](#))
- N_{ch} for $8 \leq p_{\perp}^{\text{jet}} < 11$ GeV, $R = 0.4$, Transverse region ([/REF/ATLAS_2012_I1125575/d04-x02-y08](#))
- N_{ch} for $11 \leq p_{\perp}^{\text{jet}} < 14$ GeV, $R = 0.4$, Away region ([/REF/ATLAS_2012_I1125575/d04-x02-y09](#))
- N_{ch} for $11 \leq p_{\perp}^{\text{jet}} < 14$ GeV, $R = 0.4$, Transverse region ([/REF/ATLAS_2012_I1125575/d04-x02-y10](#))
- N_{ch} for $14 \leq p_{\perp}^{\text{jet}} < 19$ GeV, $R = 0.4$, Away region ([/REF/ATLAS_2012_I1125575/d04-x02-y11](#))
- N_{ch} for $14 \leq p_{\perp}^{\text{jet}} < 19$ GeV, $R = 0.4$, Transverse region ([/REF/ATLAS_2012_I1125575/d04-x02-y12](#))
- N_{ch} for $19 \leq p_{\perp}^{\text{jet}} < 24$ GeV, $R = 0.4$, Away region ([/REF/ATLAS_2012_I1125575/d04-x02-y13](#))
- N_{ch} for $19 \leq p_{\perp}^{\text{jet}} < 24$ GeV, $R = 0.4$, Transverse region ([/REF/ATLAS_2012_I1125575/d04-x02-y14](#))
- N_{ch} for $24 \leq p_{\perp}^{\text{jet}} < 31$ GeV, $R = 0.4$, Away region ([/REF/ATLAS_2012_I1125575/d04-x02-y15](#))

- N_{ch} for $24 \leq p_{\perp}^{\text{jet}} < 31$ GeV, $R = 0.4$, Transverse region ([/REF/ATLAS_2012_I1125575/d04-x02-y16](#))
- N_{ch} for $31 \leq p_{\perp}^{\text{jet}} < 50$ GeV, $R = 0.4$, Away region ([/REF/ATLAS_2012_I1125575/d04-x02-y17](#))
- N_{ch} for $31 \leq p_{\perp}^{\text{jet}} < 50$ GeV, $R = 0.4$, Transverse region ([/REF/ATLAS_2012_I1125575/d04-x02-y18](#))
- N_{ch} for $50 \leq p_{\perp}^{\text{jet}} < 100$ GeV, $R = 0.4$, Away region ([/REF/ATLAS_2012_I1125575/d04-x02-y19](#))
- N_{ch} for $50 \leq p_{\perp}^{\text{jet}} < 100$ GeV, $R = 0.4$, Transverse region ([/REF/ATLAS_2012_I1125575/d04-x02-y20](#))
- N_{ch} for $4 \leq p_{\perp}^{\text{jet}} < 5$ GeV, $R = 0.6$, Away region ([/REF/ATLAS_2012_I1125575/d04-x03-y01](#))
- N_{ch} for $4 \leq p_{\perp}^{\text{jet}} < 5$ GeV, $R = 0.6$, Transverse region ([/REF/ATLAS_2012_I1125575/d04-x03-y02](#))
- N_{ch} for $5 \leq p_{\perp}^{\text{jet}} < 6$ GeV, $R = 0.6$, Away region ([/REF/ATLAS_2012_I1125575/d04-x03-y03](#))
- N_{ch} for $5 \leq p_{\perp}^{\text{jet}} < 6$ GeV, $R = 0.6$, Transverse region ([/REF/ATLAS_2012_I1125575/d04-x03-y04](#))
- N_{ch} for $6 \leq p_{\perp}^{\text{jet}} < 8$ GeV, $R = 0.6$, Away region ([/REF/ATLAS_2012_I1125575/d04-x03-y05](#))
- N_{ch} for $6 \leq p_{\perp}^{\text{jet}} < 8$ GeV, $R = 0.6$, Transverse region ([/REF/ATLAS_2012_I1125575/d04-x03-y06](#))
- N_{ch} for $8 \leq p_{\perp}^{\text{jet}} < 11$ GeV, $R = 0.6$, Away region ([/REF/ATLAS_2012_I1125575/d04-x03-y07](#))
- N_{ch} for $8 \leq p_{\perp}^{\text{jet}} < 11$ GeV, $R = 0.6$, Transverse region ([/REF/ATLAS_2012_I1125575/d04-x03-y08](#))
- N_{ch} for $11 \leq p_{\perp}^{\text{jet}} < 14$ GeV, $R = 0.6$, Away region ([/REF/ATLAS_2012_I1125575/d04-x03-y09](#))
- N_{ch} for $11 \leq p_{\perp}^{\text{jet}} < 14$ GeV, $R = 0.6$, Transverse region ([/REF/ATLAS_2012_I1125575/d04-x03-y10](#))
- N_{ch} for $14 \leq p_{\perp}^{\text{jet}} < 19$ GeV, $R = 0.6$, Away region ([/REF/ATLAS_2012_I1125575/d04-x03-y11](#))
- N_{ch} for $14 \leq p_{\perp}^{\text{jet}} < 19$ GeV, $R = 0.6$, Transverse region ([/REF/ATLAS_2012_I1125575/d04-x03-y12](#))
- N_{ch} for $19 \leq p_{\perp}^{\text{jet}} < 24$ GeV, $R = 0.6$, Away region ([/REF/ATLAS_2012_I1125575/d04-x03-y13](#))
- N_{ch} for $19 \leq p_{\perp}^{\text{jet}} < 24$ GeV, $R = 0.6$, Transverse region ([/REF/ATLAS_2012_I1125575/d04-x03-y14](#))
- N_{ch} for $24 \leq p_{\perp}^{\text{jet}} < 31$ GeV, $R = 0.6$, Away region ([/REF/ATLAS_2012_I1125575/d04-x03-y15](#))
- N_{ch} for $24 \leq p_{\perp}^{\text{jet}} < 31$ GeV, $R = 0.6$, Transverse region ([/REF/ATLAS_2012_I1125575/d04-x03-y16](#))
- N_{ch} for $31 \leq p_{\perp}^{\text{jet}} < 50$ GeV, $R = 0.6$, Away region ([/REF/ATLAS_2012_I1125575/d04-x03-y17](#))
- N_{ch} for $31 \leq p_{\perp}^{\text{jet}} < 50$ GeV, $R = 0.6$, Transverse region ([/REF/ATLAS_2012_I1125575/d04-x03-y18](#))
- N_{ch} for $50 \leq p_{\perp}^{\text{jet}} < 100$ GeV, $R = 0.6$, Away region ([/REF/ATLAS_2012_I1125575/d04-x03-y19](#))
- N_{ch} for $50 \leq p_{\perp}^{\text{jet}} < 100$ GeV, $R = 0.6$, Transverse region ([/REF/ATLAS_2012_I1125575/d04-x03-y20](#))
- N_{ch} for $4 \leq p_{\perp}^{\text{jet}} < 5$ GeV, $R = 0.8$, Away region ([/REF/ATLAS_2012_I1125575/d04-x04-y01](#))
- N_{ch} for $4 \leq p_{\perp}^{\text{jet}} < 5$ GeV, $R = 0.8$, Transverse region ([/REF/ATLAS_2012_I1125575/d04-x04-y02](#))

- N_{ch} for $5 \leq p_{\perp}^{\text{jet}} < 6$ GeV, $R = 0.8$, Away region ([/REF/ATLAS_2012_I1125575/d04-x04-y03](#))
- N_{ch} for $5 \leq p_{\perp}^{\text{jet}} < 6$ GeV, $R = 0.8$, Transverse region ([/REF/ATLAS_2012_I1125575/d04-x04-y04](#))
- N_{ch} for $6 \leq p_{\perp}^{\text{jet}} < 8$ GeV, $R = 0.8$, Away region ([/REF/ATLAS_2012_I1125575/d04-x04-y05](#))
- N_{ch} for $6 \leq p_{\perp}^{\text{jet}} < 8$ GeV, $R = 0.8$, Transverse region ([/REF/ATLAS_2012_I1125575/d04-x04-y06](#))
- N_{ch} for $8 \leq p_{\perp}^{\text{jet}} < 11$ GeV, $R = 0.8$, Away region ([/REF/ATLAS_2012_I1125575/d04-x04-y07](#))
- N_{ch} for $8 \leq p_{\perp}^{\text{jet}} < 11$ GeV, $R = 0.8$, Transverse region ([/REF/ATLAS_2012_I1125575/d04-x04-y08](#))
- N_{ch} for $11 \leq p_{\perp}^{\text{jet}} < 14$ GeV, $R = 0.8$, Away region ([/REF/ATLAS_2012_I1125575/d04-x04-y09](#))
- N_{ch} for $11 \leq p_{\perp}^{\text{jet}} < 14$ GeV, $R = 0.8$, Transverse region ([/REF/ATLAS_2012_I1125575/d04-x04-y10](#))
- N_{ch} for $14 \leq p_{\perp}^{\text{jet}} < 19$ GeV, $R = 0.8$, Away region ([/REF/ATLAS_2012_I1125575/d04-x04-y11](#))
- N_{ch} for $14 \leq p_{\perp}^{\text{jet}} < 19$ GeV, $R = 0.8$, Transverse region ([/REF/ATLAS_2012_I1125575/d04-x04-y12](#))
- N_{ch} for $19 \leq p_{\perp}^{\text{jet}} < 24$ GeV, $R = 0.8$, Away region ([/REF/ATLAS_2012_I1125575/d04-x04-y13](#))
- N_{ch} for $19 \leq p_{\perp}^{\text{jet}} < 24$ GeV, $R = 0.8$, Transverse region ([/REF/ATLAS_2012_I1125575/d04-x04-y14](#))
- N_{ch} for $24 \leq p_{\perp}^{\text{jet}} < 31$ GeV, $R = 0.8$, Away region ([/REF/ATLAS_2012_I1125575/d04-x04-y15](#))
- N_{ch} for $24 \leq p_{\perp}^{\text{jet}} < 31$ GeV, $R = 0.8$, Transverse region ([/REF/ATLAS_2012_I1125575/d04-x04-y16](#))
- N_{ch} for $31 \leq p_{\perp}^{\text{jet}} < 50$ GeV, $R = 0.8$, Away region ([/REF/ATLAS_2012_I1125575/d04-x04-y17](#))
- N_{ch} for $31 \leq p_{\perp}^{\text{jet}} < 50$ GeV, $R = 0.8$, Transverse region ([/REF/ATLAS_2012_I1125575/d04-x04-y18](#))
- N_{ch} for $50 \leq p_{\perp}^{\text{jet}} < 100$ GeV, $R = 0.8$, Away region ([/REF/ATLAS_2012_I1125575/d04-x04-y19](#))
- N_{ch} for $50 \leq p_{\perp}^{\text{jet}} < 100$ GeV, $R = 0.8$, Transverse region ([/REF/ATLAS_2012_I1125575/d04-x04-y20](#))
- N_{ch} for $4 \leq p_{\perp}^{\text{jet}} < 5$ GeV, $R = 1.0$, Away region ([/REF/ATLAS_2012_I1125575/d04-x05-y01](#))
- N_{ch} for $4 \leq p_{\perp}^{\text{jet}} < 5$ GeV, $R = 1.0$, Transverse region ([/REF/ATLAS_2012_I1125575/d04-x05-y02](#))
- N_{ch} for $5 \leq p_{\perp}^{\text{jet}} < 6$ GeV, $R = 1.0$, Away region ([/REF/ATLAS_2012_I1125575/d04-x05-y03](#))
- N_{ch} for $5 \leq p_{\perp}^{\text{jet}} < 6$ GeV, $R = 1.0$, Transverse region ([/REF/ATLAS_2012_I1125575/d04-x05-y04](#))
- N_{ch} for $6 \leq p_{\perp}^{\text{jet}} < 8$ GeV, $R = 1.0$, Away region ([/REF/ATLAS_2012_I1125575/d04-x05-y05](#))
- N_{ch} for $6 \leq p_{\perp}^{\text{jet}} < 8$ GeV, $R = 1.0$, Transverse region ([/REF/ATLAS_2012_I1125575/d04-x05-y06](#))
- N_{ch} for $8 \leq p_{\perp}^{\text{jet}} < 11$ GeV, $R = 1.0$, Away region ([/REF/ATLAS_2012_I1125575/d04-x05-y07](#))
- N_{ch} for $8 \leq p_{\perp}^{\text{jet}} < 11$ GeV, $R = 1.0$, Transverse region ([/REF/ATLAS_2012_I1125575/d04-x05-y08](#))
- N_{ch} for $11 \leq p_{\perp}^{\text{jet}} < 14$ GeV, $R = 1.0$, Away region ([/REF/ATLAS_2012_I1125575/d04-x05-y09](#))

- N_{ch} for $11 \leq p_{\perp}^{\text{jet}} < 14$ GeV, $R = 1.0$, Transverse region ([/REF/ATLAS_2012_I1125575/d04-x05-y10](#))
- N_{ch} for $14 \leq p_{\perp}^{\text{jet}} < 19$ GeV, $R = 1.0$, Away region ([/REF/ATLAS_2012_I1125575/d04-x05-y11](#))
- N_{ch} for $14 \leq p_{\perp}^{\text{jet}} < 19$ GeV, $R = 1.0$, Transverse region ([/REF/ATLAS_2012_I1125575/d04-x05-y12](#))
- N_{ch} for $19 \leq p_{\perp}^{\text{jet}} < 24$ GeV, $R = 1.0$, Away region ([/REF/ATLAS_2012_I1125575/d04-x05-y13](#))
- N_{ch} for $19 \leq p_{\perp}^{\text{jet}} < 24$ GeV, $R = 1.0$, Transverse region ([/REF/ATLAS_2012_I1125575/d04-x05-y14](#))
- N_{ch} for $24 \leq p_{\perp}^{\text{jet}} < 31$ GeV, $R = 1.0$, Away region ([/REF/ATLAS_2012_I1125575/d04-x05-y15](#))
- N_{ch} for $24 \leq p_{\perp}^{\text{jet}} < 31$ GeV, $R = 1.0$, Transverse region ([/REF/ATLAS_2012_I1125575/d04-x05-y16](#))
- N_{ch} for $31 \leq p_{\perp}^{\text{jet}} < 50$ GeV, $R = 1.0$, Away region ([/REF/ATLAS_2012_I1125575/d04-x05-y17](#))
- N_{ch} for $31 \leq p_{\perp}^{\text{jet}} < 50$ GeV, $R = 1.0$, Transverse region ([/REF/ATLAS_2012_I1125575/d04-x05-y18](#))
- N_{ch} for $50 \leq p_{\perp}^{\text{jet}} < 100$ GeV, $R = 1.0$, Away region ([/REF/ATLAS_2012_I1125575/d04-x05-y19](#))
- N_{ch} for $50 \leq p_{\perp}^{\text{jet}} < 100$ GeV, $R = 1.0$, Transverse region ([/REF/ATLAS_2012_I1125575/d04-x05-y20](#))
- p_{\perp} for $4 \leq p_{\perp}^{\text{jet}} < 5$ GeV, $R = 0.2$, Away region ([/REF/ATLAS_2012_I1125575/d05-x01-y01](#))
- p_{\perp} for $4 \leq p_{\perp}^{\text{jet}} < 5$ GeV, $R = 0.2$, Transverse region ([/REF/ATLAS_2012_I1125575/d05-x01-y02](#))
- p_{\perp} for $5 \leq p_{\perp}^{\text{jet}} < 6$ GeV, $R = 0.2$, Away region ([/REF/ATLAS_2012_I1125575/d05-x01-y03](#))
- p_{\perp} for $5 \leq p_{\perp}^{\text{jet}} < 6$ GeV, $R = 0.2$, Transverse region ([/REF/ATLAS_2012_I1125575/d05-x01-y04](#))
- p_{\perp} for $6 \leq p_{\perp}^{\text{jet}} < 8$ GeV, $R = 0.2$, Away region ([/REF/ATLAS_2012_I1125575/d05-x01-y05](#))
- p_{\perp} for $6 \leq p_{\perp}^{\text{jet}} < 8$ GeV, $R = 0.2$, Transverse region ([/REF/ATLAS_2012_I1125575/d05-x01-y06](#))
- p_{\perp} for $8 \leq p_{\perp}^{\text{jet}} < 11$ GeV, $R = 0.2$, Away region ([/REF/ATLAS_2012_I1125575/d05-x01-y07](#))
- p_{\perp} for $8 \leq p_{\perp}^{\text{jet}} < 11$ GeV, $R = 0.2$, Transverse region ([/REF/ATLAS_2012_I1125575/d05-x01-y08](#))
- p_{\perp} for $11 \leq p_{\perp}^{\text{jet}} < 14$ GeV, $R = 0.2$, Away region ([/REF/ATLAS_2012_I1125575/d05-x01-y09](#))
- p_{\perp} for $11 \leq p_{\perp}^{\text{jet}} < 14$ GeV, $R = 0.2$, Transverse region ([/REF/ATLAS_2012_I1125575/d05-x01-y10](#))
- p_{\perp} for $14 \leq p_{\perp}^{\text{jet}} < 19$ GeV, $R = 0.2$, Away region ([/REF/ATLAS_2012_I1125575/d05-x01-y11](#))
- p_{\perp} for $14 \leq p_{\perp}^{\text{jet}} < 19$ GeV, $R = 0.2$, Transverse region ([/REF/ATLAS_2012_I1125575/d05-x01-y12](#))
- p_{\perp} for $19 \leq p_{\perp}^{\text{jet}} < 24$ GeV, $R = 0.2$, Away region ([/REF/ATLAS_2012_I1125575/d05-x01-y13](#))
- p_{\perp} for $19 \leq p_{\perp}^{\text{jet}} < 24$ GeV, $R = 0.2$, Transverse region ([/REF/ATLAS_2012_I1125575/d05-x01-y14](#))
- p_{\perp} for $24 \leq p_{\perp}^{\text{jet}} < 31$ GeV, $R = 0.2$, Away region ([/REF/ATLAS_2012_I1125575/d05-x01-y15](#))
- p_{\perp} for $24 \leq p_{\perp}^{\text{jet}} < 31$ GeV, $R = 0.2$, Transverse region ([/REF/ATLAS_2012_I1125575/d05-x01-y16](#))

- p_{\perp} for $31 \leq p_{\perp}^{\text{jet}} < 50$ GeV, $R = 0.2$, Away region ([/REF/ATLAS_2012_I1125575/d05-x01-y17](#))
- p_{\perp} for $31 \leq p_{\perp}^{\text{jet}} < 50$ GeV, $R = 0.2$, Transverse region ([/REF/ATLAS_2012_I1125575/d05-x01-y18](#))
- p_{\perp} for $50 \leq p_{\perp}^{\text{jet}} < 100$ GeV, $R = 0.2$, Away region ([/REF/ATLAS_2012_I1125575/d05-x01-y19](#))
- p_{\perp} for $50 \leq p_{\perp}^{\text{jet}} < 100$ GeV, $R = 0.2$, Transverse region ([/REF/ATLAS_2012_I1125575/d05-x01-y20](#))
- p_{\perp} for $4 \leq p_{\perp}^{\text{jet}} < 5$ GeV, $R = 0.4$, Away region ([/REF/ATLAS_2012_I1125575/d05-x02-y01](#))
- p_{\perp} for $4 \leq p_{\perp}^{\text{jet}} < 5$ GeV, $R = 0.4$, Transverse region ([/REF/ATLAS_2012_I1125575/d05-x02-y02](#))
- p_{\perp} for $5 \leq p_{\perp}^{\text{jet}} < 6$ GeV, $R = 0.4$, Away region ([/REF/ATLAS_2012_I1125575/d05-x02-y03](#))
- p_{\perp} for $5 \leq p_{\perp}^{\text{jet}} < 6$ GeV, $R = 0.4$, Transverse region ([/REF/ATLAS_2012_I1125575/d05-x02-y04](#))
- p_{\perp} for $6 \leq p_{\perp}^{\text{jet}} < 8$ GeV, $R = 0.4$, Away region ([/REF/ATLAS_2012_I1125575/d05-x02-y05](#))
- p_{\perp} for $6 \leq p_{\perp}^{\text{jet}} < 8$ GeV, $R = 0.4$, Transverse region ([/REF/ATLAS_2012_I1125575/d05-x02-y06](#))
- p_{\perp} for $8 \leq p_{\perp}^{\text{jet}} < 11$ GeV, $R = 0.4$, Away region ([/REF/ATLAS_2012_I1125575/d05-x02-y07](#))
- p_{\perp} for $8 \leq p_{\perp}^{\text{jet}} < 11$ GeV, $R = 0.4$, Transverse region ([/REF/ATLAS_2012_I1125575/d05-x02-y08](#))
- p_{\perp} for $11 \leq p_{\perp}^{\text{jet}} < 14$ GeV, $R = 0.4$, Away region ([/REF/ATLAS_2012_I1125575/d05-x02-y09](#))
- p_{\perp} for $11 \leq p_{\perp}^{\text{jet}} < 14$ GeV, $R = 0.4$, Transverse region ([/REF/ATLAS_2012_I1125575/d05-x02-y10](#))
- p_{\perp} for $14 \leq p_{\perp}^{\text{jet}} < 19$ GeV, $R = 0.4$, Away region ([/REF/ATLAS_2012_I1125575/d05-x02-y11](#))
- p_{\perp} for $14 \leq p_{\perp}^{\text{jet}} < 19$ GeV, $R = 0.4$, Transverse region ([/REF/ATLAS_2012_I1125575/d05-x02-y12](#))
- p_{\perp} for $19 \leq p_{\perp}^{\text{jet}} < 24$ GeV, $R = 0.4$, Away region ([/REF/ATLAS_2012_I1125575/d05-x02-y13](#))
- p_{\perp} for $19 \leq p_{\perp}^{\text{jet}} < 24$ GeV, $R = 0.4$, Transverse region ([/REF/ATLAS_2012_I1125575/d05-x02-y14](#))
- p_{\perp} for $24 \leq p_{\perp}^{\text{jet}} < 31$ GeV, $R = 0.4$, Away region ([/REF/ATLAS_2012_I1125575/d05-x02-y15](#))
- p_{\perp} for $24 \leq p_{\perp}^{\text{jet}} < 31$ GeV, $R = 0.4$, Transverse region ([/REF/ATLAS_2012_I1125575/d05-x02-y16](#))
- p_{\perp} for $31 \leq p_{\perp}^{\text{jet}} < 50$ GeV, $R = 0.4$, Away region ([/REF/ATLAS_2012_I1125575/d05-x02-y17](#))
- p_{\perp} for $31 \leq p_{\perp}^{\text{jet}} < 50$ GeV, $R = 0.4$, Transverse region ([/REF/ATLAS_2012_I1125575/d05-x02-y18](#))
- p_{\perp} for $50 \leq p_{\perp}^{\text{jet}} < 100$ GeV, $R = 0.4$, Away region ([/REF/ATLAS_2012_I1125575/d05-x02-y19](#))
- p_{\perp} for $50 \leq p_{\perp}^{\text{jet}} < 100$ GeV, $R = 0.4$, Transverse region ([/REF/ATLAS_2012_I1125575/d05-x02-y20](#))
- p_{\perp} for $4 \leq p_{\perp}^{\text{jet}} < 5$ GeV, $R = 0.6$, Away region ([/REF/ATLAS_2012_I1125575/d05-x03-y01](#))
- p_{\perp} for $4 \leq p_{\perp}^{\text{jet}} < 5$ GeV, $R = 0.6$, Transverse region ([/REF/ATLAS_2012_I1125575/d05-x03-y02](#))
- p_{\perp} for $5 \leq p_{\perp}^{\text{jet}} < 6$ GeV, $R = 0.6$, Away region ([/REF/ATLAS_2012_I1125575/d05-x03-y03](#))

- p_{\perp} for $5 \leq p_{\perp}^{\text{jet}} < 6$ GeV, $R = 0.6$, Transverse region ([/REF/ATLAS_2012_I1125575/d05-x03-y04](#))
- p_{\perp} for $6 \leq p_{\perp}^{\text{jet}} < 8$ GeV, $R = 0.6$, Away region ([/REF/ATLAS_2012_I1125575/d05-x03-y05](#))
- p_{\perp} for $6 \leq p_{\perp}^{\text{jet}} < 8$ GeV, $R = 0.6$, Transverse region ([/REF/ATLAS_2012_I1125575/d05-x03-y06](#))
- p_{\perp} for $8 \leq p_{\perp}^{\text{jet}} < 11$ GeV, $R = 0.6$, Away region ([/REF/ATLAS_2012_I1125575/d05-x03-y07](#))
- p_{\perp} for $8 \leq p_{\perp}^{\text{jet}} < 11$ GeV, $R = 0.6$, Transverse region ([/REF/ATLAS_2012_I1125575/d05-x03-y08](#))
- p_{\perp} for $11 \leq p_{\perp}^{\text{jet}} < 14$ GeV, $R = 0.6$, Away region ([/REF/ATLAS_2012_I1125575/d05-x03-y09](#))
- p_{\perp} for $11 \leq p_{\perp}^{\text{jet}} < 14$ GeV, $R = 0.6$, Transverse region ([/REF/ATLAS_2012_I1125575/d05-x03-y10](#))
- p_{\perp} for $14 \leq p_{\perp}^{\text{jet}} < 19$ GeV, $R = 0.6$, Away region ([/REF/ATLAS_2012_I1125575/d05-x03-y11](#))
- p_{\perp} for $14 \leq p_{\perp}^{\text{jet}} < 19$ GeV, $R = 0.6$, Transverse region ([/REF/ATLAS_2012_I1125575/d05-x03-y12](#))
- p_{\perp} for $19 \leq p_{\perp}^{\text{jet}} < 24$ GeV, $R = 0.6$, Away region ([/REF/ATLAS_2012_I1125575/d05-x03-y13](#))
- p_{\perp} for $19 \leq p_{\perp}^{\text{jet}} < 24$ GeV, $R = 0.6$, Transverse region ([/REF/ATLAS_2012_I1125575/d05-x03-y14](#))
- p_{\perp} for $24 \leq p_{\perp}^{\text{jet}} < 31$ GeV, $R = 0.6$, Away region ([/REF/ATLAS_2012_I1125575/d05-x03-y15](#))
- p_{\perp} for $24 \leq p_{\perp}^{\text{jet}} < 31$ GeV, $R = 0.6$, Transverse region ([/REF/ATLAS_2012_I1125575/d05-x03-y16](#))
- p_{\perp} for $31 \leq p_{\perp}^{\text{jet}} < 50$ GeV, $R = 0.6$, Away region ([/REF/ATLAS_2012_I1125575/d05-x03-y17](#))
- p_{\perp} for $31 \leq p_{\perp}^{\text{jet}} < 50$ GeV, $R = 0.6$, Transverse region ([/REF/ATLAS_2012_I1125575/d05-x03-y18](#))
- p_{\perp} for $50 \leq p_{\perp}^{\text{jet}} < 100$ GeV, $R = 0.6$, Away region ([/REF/ATLAS_2012_I1125575/d05-x03-y19](#))
- p_{\perp} for $50 \leq p_{\perp}^{\text{jet}} < 100$ GeV, $R = 0.6$, Transverse region ([/REF/ATLAS_2012_I1125575/d05-x03-y20](#))
- p_{\perp} for $4 \leq p_{\perp}^{\text{jet}} < 5$ GeV, $R = 0.8$, Away region ([/REF/ATLAS_2012_I1125575/d05-x04-y01](#))
- p_{\perp} for $4 \leq p_{\perp}^{\text{jet}} < 5$ GeV, $R = 0.8$, Transverse region ([/REF/ATLAS_2012_I1125575/d05-x04-y02](#))
- p_{\perp} for $5 \leq p_{\perp}^{\text{jet}} < 6$ GeV, $R = 0.8$, Away region ([/REF/ATLAS_2012_I1125575/d05-x04-y03](#))
- p_{\perp} for $5 \leq p_{\perp}^{\text{jet}} < 6$ GeV, $R = 0.8$, Transverse region ([/REF/ATLAS_2012_I1125575/d05-x04-y04](#))
- p_{\perp} for $6 \leq p_{\perp}^{\text{jet}} < 8$ GeV, $R = 0.8$, Away region ([/REF/ATLAS_2012_I1125575/d05-x04-y05](#))
- p_{\perp} for $6 \leq p_{\perp}^{\text{jet}} < 8$ GeV, $R = 0.8$, Transverse region ([/REF/ATLAS_2012_I1125575/d05-x04-y06](#))
- p_{\perp} for $8 \leq p_{\perp}^{\text{jet}} < 11$ GeV, $R = 0.8$, Away region ([/REF/ATLAS_2012_I1125575/d05-x04-y07](#))
- p_{\perp} for $8 \leq p_{\perp}^{\text{jet}} < 11$ GeV, $R = 0.8$, Transverse region ([/REF/ATLAS_2012_I1125575/d05-x04-y08](#))
- p_{\perp} for $11 \leq p_{\perp}^{\text{jet}} < 14$ GeV, $R = 0.8$, Away region ([/REF/ATLAS_2012_I1125575/d05-x04-y09](#))
- p_{\perp} for $11 \leq p_{\perp}^{\text{jet}} < 14$ GeV, $R = 0.8$, Transverse region ([/REF/ATLAS_2012_I1125575/d05-x04-y10](#))

- p_{\perp} for $14 \leq p_{\perp}^{\text{jet}} < 19$ GeV, $R = 0.8$, Away region ([/REF/ATLAS_2012_I1125575/d05-x04-y11](#))
- p_{\perp} for $14 \leq p_{\perp}^{\text{jet}} < 19$ GeV, $R = 0.8$, Transverse region ([/REF/ATLAS_2012_I1125575/d05-x04-y12](#))
- p_{\perp} for $19 \leq p_{\perp}^{\text{jet}} < 24$ GeV, $R = 0.8$, Away region ([/REF/ATLAS_2012_I1125575/d05-x04-y13](#))
- p_{\perp} for $19 \leq p_{\perp}^{\text{jet}} < 24$ GeV, $R = 0.8$, Transverse region ([/REF/ATLAS_2012_I1125575/d05-x04-y14](#))
- p_{\perp} for $24 \leq p_{\perp}^{\text{jet}} < 31$ GeV, $R = 0.8$, Away region ([/REF/ATLAS_2012_I1125575/d05-x04-y15](#))
- p_{\perp} for $24 \leq p_{\perp}^{\text{jet}} < 31$ GeV, $R = 0.8$, Transverse region ([/REF/ATLAS_2012_I1125575/d05-x04-y16](#))
- p_{\perp} for $31 \leq p_{\perp}^{\text{jet}} < 50$ GeV, $R = 0.8$, Away region ([/REF/ATLAS_2012_I1125575/d05-x04-y17](#))
- p_{\perp} for $31 \leq p_{\perp}^{\text{jet}} < 50$ GeV, $R = 0.8$, Transverse region ([/REF/ATLAS_2012_I1125575/d05-x04-y18](#))
- p_{\perp} for $50 \leq p_{\perp}^{\text{jet}} < 100$ GeV, $R = 0.8$, Away region ([/REF/ATLAS_2012_I1125575/d05-x04-y19](#))
- p_{\perp} for $50 \leq p_{\perp}^{\text{jet}} < 100$ GeV, $R = 0.8$, Transverse region ([/REF/ATLAS_2012_I1125575/d05-x04-y20](#))
- p_{\perp} for $4 \leq p_{\perp}^{\text{jet}} < 5$ GeV, $R = 1.0$, Away region ([/REF/ATLAS_2012_I1125575/d05-x05-y01](#))
- p_{\perp} for $4 \leq p_{\perp}^{\text{jet}} < 5$ GeV, $R = 1.0$, Transverse region ([/REF/ATLAS_2012_I1125575/d05-x05-y02](#))
- p_{\perp} for $5 \leq p_{\perp}^{\text{jet}} < 6$ GeV, $R = 1.0$, Away region ([/REF/ATLAS_2012_I1125575/d05-x05-y03](#))
- p_{\perp} for $5 \leq p_{\perp}^{\text{jet}} < 6$ GeV, $R = 1.0$, Transverse region ([/REF/ATLAS_2012_I1125575/d05-x05-y04](#))
- p_{\perp} for $6 \leq p_{\perp}^{\text{jet}} < 8$ GeV, $R = 1.0$, Away region ([/REF/ATLAS_2012_I1125575/d05-x05-y05](#))
- p_{\perp} for $6 \leq p_{\perp}^{\text{jet}} < 8$ GeV, $R = 1.0$, Transverse region ([/REF/ATLAS_2012_I1125575/d05-x05-y06](#))
- p_{\perp} for $8 \leq p_{\perp}^{\text{jet}} < 11$ GeV, $R = 1.0$, Away region ([/REF/ATLAS_2012_I1125575/d05-x05-y07](#))
- p_{\perp} for $8 \leq p_{\perp}^{\text{jet}} < 11$ GeV, $R = 1.0$, Transverse region ([/REF/ATLAS_2012_I1125575/d05-x05-y08](#))
- p_{\perp} for $11 \leq p_{\perp}^{\text{jet}} < 14$ GeV, $R = 1.0$, Away region ([/REF/ATLAS_2012_I1125575/d05-x05-y09](#))
- p_{\perp} for $11 \leq p_{\perp}^{\text{jet}} < 14$ GeV, $R = 1.0$, Transverse region ([/REF/ATLAS_2012_I1125575/d05-x05-y10](#))
- p_{\perp} for $14 \leq p_{\perp}^{\text{jet}} < 19$ GeV, $R = 1.0$, Away region ([/REF/ATLAS_2012_I1125575/d05-x05-y11](#))
- p_{\perp} for $14 \leq p_{\perp}^{\text{jet}} < 19$ GeV, $R = 1.0$, Transverse region ([/REF/ATLAS_2012_I1125575/d05-x05-y12](#))
- p_{\perp} for $19 \leq p_{\perp}^{\text{jet}} < 24$ GeV, $R = 1.0$, Away region ([/REF/ATLAS_2012_I1125575/d05-x05-y13](#))
- p_{\perp} for $19 \leq p_{\perp}^{\text{jet}} < 24$ GeV, $R = 1.0$, Transverse region ([/REF/ATLAS_2012_I1125575/d05-x05-y14](#))
- p_{\perp} for $24 \leq p_{\perp}^{\text{jet}} < 31$ GeV, $R = 1.0$, Away region ([/REF/ATLAS_2012_I1125575/d05-x05-y15](#))
- p_{\perp} for $24 \leq p_{\perp}^{\text{jet}} < 31$ GeV, $R = 1.0$, Transverse region ([/REF/ATLAS_2012_I1125575/d05-x05-y16](#))
- p_{\perp} for $31 \leq p_{\perp}^{\text{jet}} < 50$ GeV, $R = 1.0$, Away region ([/REF/ATLAS_2012_I1125575/d05-x05-y17](#))

- p_{\perp} for $31 \leq p_{\perp}^{\text{jet}} < 50$ GeV, $R = 1.0$, Transverse region ([/REF/ATLAS_2012_I1125575/d05-x05-y18](#))
- p_{\perp} for $50 \leq p_{\perp}^{\text{jet}} < 100$ GeV, $R = 1.0$, Away region ([/REF/ATLAS_2012_I1125575/d05-x05-y19](#))
- p_{\perp} for $50 \leq p_{\perp}^{\text{jet}} < 100$ GeV, $R = 1.0$, Transverse region ([/REF/ATLAS_2012_I1125575/d05-x05-y20](#))
- $\sum p_{\perp}$ for $4 \leq p_{\perp}^{\text{jet}} < 5$ GeV, $R = 0.2$, Away region ([/REF/ATLAS_2012_I1125575/d06-x01-y01](#))
- $\sum p_{\perp}$ for $4 \leq p_{\perp}^{\text{jet}} < 5$ GeV, $R = 0.2$, Transverse region ([/REF/ATLAS_2012_I1125575/d06-x01-y02](#))
- $\sum p_{\perp}$ for $5 \leq p_{\perp}^{\text{jet}} < 6$ GeV, $R = 0.2$, Away region ([/REF/ATLAS_2012_I1125575/d06-x01-y03](#))
- $\sum p_{\perp}$ for $5 \leq p_{\perp}^{\text{jet}} < 6$ GeV, $R = 0.2$, Transverse region ([/REF/ATLAS_2012_I1125575/d06-x01-y04](#))
- $\sum p_{\perp}$ for $6 \leq p_{\perp}^{\text{jet}} < 8$ GeV, $R = 0.2$, Away region ([/REF/ATLAS_2012_I1125575/d06-x01-y05](#))
- $\sum p_{\perp}$ for $6 \leq p_{\perp}^{\text{jet}} < 8$ GeV, $R = 0.2$, Transverse region ([/REF/ATLAS_2012_I1125575/d06-x01-y06](#))
- $\sum p_{\perp}$ for $8 \leq p_{\perp}^{\text{jet}} < 11$ GeV, $R = 0.2$, Away region ([/REF/ATLAS_2012_I1125575/d06-x01-y07](#))
- $\sum p_{\perp}$ for $8 \leq p_{\perp}^{\text{jet}} < 11$ GeV, $R = 0.2$, Transverse region ([/REF/ATLAS_2012_I1125575/d06-x01-y08](#))
- $\sum p_{\perp}$ for $11 \leq p_{\perp}^{\text{jet}} < 14$ GeV, $R = 0.2$, Away region ([/REF/ATLAS_2012_I1125575/d06-x01-y09](#))
- $\sum p_{\perp}$ for $11 \leq p_{\perp}^{\text{jet}} < 14$ GeV, $R = 0.2$, Transverse region ([/REF/ATLAS_2012_I1125575/d06-x01-y10](#))
- $\sum p_{\perp}$ for $14 \leq p_{\perp}^{\text{jet}} < 19$ GeV, $R = 0.2$, Away region ([/REF/ATLAS_2012_I1125575/d06-x01-y11](#))
- $\sum p_{\perp}$ for $14 \leq p_{\perp}^{\text{jet}} < 19$ GeV, $R = 0.2$, Transverse region ([/REF/ATLAS_2012_I1125575/d06-x01-y12](#))
- $\sum p_{\perp}$ for $19 \leq p_{\perp}^{\text{jet}} < 24$ GeV, $R = 0.2$, Away region ([/REF/ATLAS_2012_I1125575/d06-x01-y13](#))
- $\sum p_{\perp}$ for $19 \leq p_{\perp}^{\text{jet}} < 24$ GeV, $R = 0.2$, Transverse region ([/REF/ATLAS_2012_I1125575/d06-x01-y14](#))
- $\sum p_{\perp}$ for $24 \leq p_{\perp}^{\text{jet}} < 31$ GeV, $R = 0.2$, Away region ([/REF/ATLAS_2012_I1125575/d06-x01-y15](#))
- $\sum p_{\perp}$ for $24 \leq p_{\perp}^{\text{jet}} < 31$ GeV, $R = 0.2$, Transverse region ([/REF/ATLAS_2012_I1125575/d06-x01-y16](#))
- $\sum p_{\perp}$ for $31 \leq p_{\perp}^{\text{jet}} < 50$ GeV, $R = 0.2$, Away region ([/REF/ATLAS_2012_I1125575/d06-x01-y17](#))
- $\sum p_{\perp}$ for $31 \leq p_{\perp}^{\text{jet}} < 50$ GeV, $R = 0.2$, Transverse region ([/REF/ATLAS_2012_I1125575/d06-x01-y18](#))
- $\sum p_{\perp}$ for $50 \leq p_{\perp}^{\text{jet}} < 100$ GeV, $R = 0.2$, Away region ([/REF/ATLAS_2012_I1125575/d06-x01-y19](#))
- $\sum p_{\perp}$ for $50 \leq p_{\perp}^{\text{jet}} < 100$ GeV, $R = 0.2$, Transverse region ([/REF/ATLAS_2012_I1125575/d06-x01-y20](#))
- $\sum p_{\perp}$ for $4 \leq p_{\perp}^{\text{jet}} < 5$ GeV, $R = 0.4$, Away region ([/REF/ATLAS_2012_I1125575/d06-x02-y01](#))
- $\sum p_{\perp}$ for $4 \leq p_{\perp}^{\text{jet}} < 5$ GeV, $R = 0.4$, Transverse region ([/REF/ATLAS_2012_I1125575/d06-x02-y02](#))
- $\sum p_{\perp}$ for $5 \leq p_{\perp}^{\text{jet}} < 6$ GeV, $R = 0.4$, Away region ([/REF/ATLAS_2012_I1125575/d06-x02-y03](#))

- $\sum p_{\perp}$ for $5 \leq p_{\perp}^{\text{jet}} < 6$ GeV, $R = 0.4$, Transverse region ([/REF/ATLAS_2012_I1125575/d06-x02-y04](#))
- $\sum p_{\perp}$ for $6 \leq p_{\perp}^{\text{jet}} < 8$ GeV, $R = 0.4$, Away region ([/REF/ATLAS_2012_I1125575/d06-x02-y05](#))
- $\sum p_{\perp}$ for $6 \leq p_{\perp}^{\text{jet}} < 8$ GeV, $R = 0.4$, Transverse region ([/REF/ATLAS_2012_I1125575/d06-x02-y06](#))
- $\sum p_{\perp}$ for $8 \leq p_{\perp}^{\text{jet}} < 11$ GeV, $R = 0.4$, Away region ([/REF/ATLAS_2012_I1125575/d06-x02-y07](#))
- $\sum p_{\perp}$ for $8 \leq p_{\perp}^{\text{jet}} < 11$ GeV, $R = 0.4$, Transverse region ([/REF/ATLAS_2012_I1125575/d06-x02-y08](#))
- $\sum p_{\perp}$ for $11 \leq p_{\perp}^{\text{jet}} < 14$ GeV, $R = 0.4$, Away region ([/REF/ATLAS_2012_I1125575/d06-x02-y09](#))
- $\sum p_{\perp}$ for $11 \leq p_{\perp}^{\text{jet}} < 14$ GeV, $R = 0.4$, Transverse region ([/REF/ATLAS_2012_I1125575/d06-x02-y10](#))
- $\sum p_{\perp}$ for $14 \leq p_{\perp}^{\text{jet}} < 19$ GeV, $R = 0.4$, Away region ([/REF/ATLAS_2012_I1125575/d06-x02-y11](#))
- $\sum p_{\perp}$ for $14 \leq p_{\perp}^{\text{jet}} < 19$ GeV, $R = 0.4$, Transverse region ([/REF/ATLAS_2012_I1125575/d06-x02-y12](#))
- $\sum p_{\perp}$ for $19 \leq p_{\perp}^{\text{jet}} < 24$ GeV, $R = 0.4$, Away region ([/REF/ATLAS_2012_I1125575/d06-x02-y13](#))
- $\sum p_{\perp}$ for $19 \leq p_{\perp}^{\text{jet}} < 24$ GeV, $R = 0.4$, Transverse region ([/REF/ATLAS_2012_I1125575/d06-x02-y14](#))
- $\sum p_{\perp}$ for $24 \leq p_{\perp}^{\text{jet}} < 31$ GeV, $R = 0.4$, Away region ([/REF/ATLAS_2012_I1125575/d06-x02-y15](#))
- $\sum p_{\perp}$ for $24 \leq p_{\perp}^{\text{jet}} < 31$ GeV, $R = 0.4$, Transverse region ([/REF/ATLAS_2012_I1125575/d06-x02-y16](#))
- $\sum p_{\perp}$ for $31 \leq p_{\perp}^{\text{jet}} < 50$ GeV, $R = 0.4$, Away region ([/REF/ATLAS_2012_I1125575/d06-x02-y17](#))
- $\sum p_{\perp}$ for $31 \leq p_{\perp}^{\text{jet}} < 50$ GeV, $R = 0.4$, Transverse region ([/REF/ATLAS_2012_I1125575/d06-x02-y18](#))
- $\sum p_{\perp}$ for $50 \leq p_{\perp}^{\text{jet}} < 100$ GeV, $R = 0.4$, Away region ([/REF/ATLAS_2012_I1125575/d06-x02-y19](#))
- $\sum p_{\perp}$ for $50 \leq p_{\perp}^{\text{jet}} < 100$ GeV, $R = 0.4$, Transverse region ([/REF/ATLAS_2012_I1125575/d06-x02-y20](#))
- $\sum p_{\perp}$ for $4 \leq p_{\perp}^{\text{jet}} < 5$ GeV, $R = 0.6$, Away region ([/REF/ATLAS_2012_I1125575/d06-x03-y01](#))
- $\sum p_{\perp}$ for $4 \leq p_{\perp}^{\text{jet}} < 5$ GeV, $R = 0.6$, Transverse region ([/REF/ATLAS_2012_I1125575/d06-x03-y02](#))
- $\sum p_{\perp}$ for $5 \leq p_{\perp}^{\text{jet}} < 6$ GeV, $R = 0.6$, Away region ([/REF/ATLAS_2012_I1125575/d06-x03-y03](#))
- $\sum p_{\perp}$ for $5 \leq p_{\perp}^{\text{jet}} < 6$ GeV, $R = 0.6$, Transverse region ([/REF/ATLAS_2012_I1125575/d06-x03-y04](#))
- $\sum p_{\perp}$ for $6 \leq p_{\perp}^{\text{jet}} < 8$ GeV, $R = 0.6$, Away region ([/REF/ATLAS_2012_I1125575/d06-x03-y05](#))
- $\sum p_{\perp}$ for $6 \leq p_{\perp}^{\text{jet}} < 8$ GeV, $R = 0.6$, Transverse region ([/REF/ATLAS_2012_I1125575/d06-x03-y06](#))
- $\sum p_{\perp}$ for $8 \leq p_{\perp}^{\text{jet}} < 11$ GeV, $R = 0.6$, Away region ([/REF/ATLAS_2012_I1125575/d06-x03-y07](#))
- $\sum p_{\perp}$ for $8 \leq p_{\perp}^{\text{jet}} < 11$ GeV, $R = 0.6$, Transverse region ([/REF/ATLAS_2012_I1125575/d06-x03-y08](#))
- $\sum p_{\perp}$ for $11 \leq p_{\perp}^{\text{jet}} < 14$ GeV, $R = 0.6$, Away region ([/REF/ATLAS_2012_I1125575/d06-x03-y09](#))

- $\sum p_{\perp}$ for $11 \leq p_{\perp}^{\text{jet}} < 14$ GeV, $R = 0.6$, Transverse region ([/REF/ATLAS_2012_I1125575/d06-x03-y10](#))
- $\sum p_{\perp}$ for $14 \leq p_{\perp}^{\text{jet}} < 19$ GeV, $R = 0.6$, Away region ([/REF/ATLAS_2012_I1125575/d06-x03-y11](#))
- $\sum p_{\perp}$ for $14 \leq p_{\perp}^{\text{jet}} < 19$ GeV, $R = 0.6$, Transverse region ([/REF/ATLAS_2012_I1125575/d06-x03-y12](#))
- $\sum p_{\perp}$ for $19 \leq p_{\perp}^{\text{jet}} < 24$ GeV, $R = 0.6$, Away region ([/REF/ATLAS_2012_I1125575/d06-x03-y13](#))
- $\sum p_{\perp}$ for $19 \leq p_{\perp}^{\text{jet}} < 24$ GeV, $R = 0.6$, Transverse region ([/REF/ATLAS_2012_I1125575/d06-x03-y14](#))
- $\sum p_{\perp}$ for $24 \leq p_{\perp}^{\text{jet}} < 31$ GeV, $R = 0.6$, Away region ([/REF/ATLAS_2012_I1125575/d06-x03-y15](#))
- $\sum p_{\perp}$ for $24 \leq p_{\perp}^{\text{jet}} < 31$ GeV, $R = 0.6$, Transverse region ([/REF/ATLAS_2012_I1125575/d06-x03-y16](#))
- $\sum p_{\perp}$ for $31 \leq p_{\perp}^{\text{jet}} < 50$ GeV, $R = 0.6$, Away region ([/REF/ATLAS_2012_I1125575/d06-x03-y17](#))
- $\sum p_{\perp}$ for $31 \leq p_{\perp}^{\text{jet}} < 50$ GeV, $R = 0.6$, Transverse region ([/REF/ATLAS_2012_I1125575/d06-x03-y18](#))
- $\sum p_{\perp}$ for $50 \leq p_{\perp}^{\text{jet}} < 100$ GeV, $R = 0.6$, Away region ([/REF/ATLAS_2012_I1125575/d06-x03-y19](#))
- $\sum p_{\perp}$ for $50 \leq p_{\perp}^{\text{jet}} < 100$ GeV, $R = 0.6$, Transverse region ([/REF/ATLAS_2012_I1125575/d06-x03-y20](#))
- $\sum p_{\perp}$ for $4 \leq p_{\perp}^{\text{jet}} < 5$ GeV, $R = 0.8$, Away region ([/REF/ATLAS_2012_I1125575/d06-x04-y01](#))
- $\sum p_{\perp}$ for $4 \leq p_{\perp}^{\text{jet}} < 5$ GeV, $R = 0.8$, Transverse region ([/REF/ATLAS_2012_I1125575/d06-x04-y02](#))
- $\sum p_{\perp}$ for $5 \leq p_{\perp}^{\text{jet}} < 6$ GeV, $R = 0.8$, Away region ([/REF/ATLAS_2012_I1125575/d06-x04-y03](#))
- $\sum p_{\perp}$ for $5 \leq p_{\perp}^{\text{jet}} < 6$ GeV, $R = 0.8$, Transverse region ([/REF/ATLAS_2012_I1125575/d06-x04-y04](#))
- $\sum p_{\perp}$ for $6 \leq p_{\perp}^{\text{jet}} < 8$ GeV, $R = 0.8$, Away region ([/REF/ATLAS_2012_I1125575/d06-x04-y05](#))
- $\sum p_{\perp}$ for $6 \leq p_{\perp}^{\text{jet}} < 8$ GeV, $R = 0.8$, Transverse region ([/REF/ATLAS_2012_I1125575/d06-x04-y06](#))
- $\sum p_{\perp}$ for $8 \leq p_{\perp}^{\text{jet}} < 11$ GeV, $R = 0.8$, Away region ([/REF/ATLAS_2012_I1125575/d06-x04-y07](#))
- $\sum p_{\perp}$ for $8 \leq p_{\perp}^{\text{jet}} < 11$ GeV, $R = 0.8$, Transverse region ([/REF/ATLAS_2012_I1125575/d06-x04-y08](#))
- $\sum p_{\perp}$ for $11 \leq p_{\perp}^{\text{jet}} < 14$ GeV, $R = 0.8$, Away region ([/REF/ATLAS_2012_I1125575/d06-x04-y09](#))
- $\sum p_{\perp}$ for $11 \leq p_{\perp}^{\text{jet}} < 14$ GeV, $R = 0.8$, Transverse region ([/REF/ATLAS_2012_I1125575/d06-x04-y10](#))
- $\sum p_{\perp}$ for $14 \leq p_{\perp}^{\text{jet}} < 19$ GeV, $R = 0.8$, Away region ([/REF/ATLAS_2012_I1125575/d06-x04-y11](#))
- $\sum p_{\perp}$ for $14 \leq p_{\perp}^{\text{jet}} < 19$ GeV, $R = 0.8$, Transverse region ([/REF/ATLAS_2012_I1125575/d06-x04-y12](#))
- $\sum p_{\perp}$ for $19 \leq p_{\perp}^{\text{jet}} < 24$ GeV, $R = 0.8$, Away region ([/REF/ATLAS_2012_I1125575/d06-x04-y13](#))
- $\sum p_{\perp}$ for $19 \leq p_{\perp}^{\text{jet}} < 24$ GeV, $R = 0.8$, Transverse region ([/REF/ATLAS_2012_I1125575/d06-x04-y14](#))
- $\sum p_{\perp}$ for $24 \leq p_{\perp}^{\text{jet}} < 31$ GeV, $R = 0.8$, Away region ([/REF/ATLAS_2012_I1125575/d06-x04-y15](#))

- $\sum p_{\perp}$ for $24 \leq p_{\perp}^{\text{jet}} < 31$ GeV, $R = 0.8$, Transverse region ([/REF/ATLAS_2012_I1125575/d06-x04-y16](#))
- $\sum p_{\perp}$ for $31 \leq p_{\perp}^{\text{jet}} < 50$ GeV, $R = 0.8$, Away region ([/REF/ATLAS_2012_I1125575/d06-x04-y17](#))
- $\sum p_{\perp}$ for $31 \leq p_{\perp}^{\text{jet}} < 50$ GeV, $R = 0.8$, Transverse region ([/REF/ATLAS_2012_I1125575/d06-x04-y18](#))
- $\sum p_{\perp}$ for $50 \leq p_{\perp}^{\text{jet}} < 100$ GeV, $R = 0.8$, Away region ([/REF/ATLAS_2012_I1125575/d06-x04-y19](#))
- $\sum p_{\perp}$ for $50 \leq p_{\perp}^{\text{jet}} < 100$ GeV, $R = 0.8$, Transverse region ([/REF/ATLAS_2012_I1125575/d06-x04-y20](#))
- $\sum p_{\perp}$ for $4 \leq p_{\perp}^{\text{jet}} < 5$ GeV, $R = 1.0$, Away region ([/REF/ATLAS_2012_I1125575/d06-x05-y01](#))
- $\sum p_{\perp}$ for $4 \leq p_{\perp}^{\text{jet}} < 5$ GeV, $R = 1.0$, Transverse region ([/REF/ATLAS_2012_I1125575/d06-x05-y02](#))
- $\sum p_{\perp}$ for $5 \leq p_{\perp}^{\text{jet}} < 6$ GeV, $R = 1.0$, Away region ([/REF/ATLAS_2012_I1125575/d06-x05-y03](#))
- $\sum p_{\perp}$ for $5 \leq p_{\perp}^{\text{jet}} < 6$ GeV, $R = 1.0$, Transverse region ([/REF/ATLAS_2012_I1125575/d06-x05-y04](#))
- $\sum p_{\perp}$ for $6 \leq p_{\perp}^{\text{jet}} < 8$ GeV, $R = 1.0$, Away region ([/REF/ATLAS_2012_I1125575/d06-x05-y05](#))
- $\sum p_{\perp}$ for $6 \leq p_{\perp}^{\text{jet}} < 8$ GeV, $R = 1.0$, Transverse region ([/REF/ATLAS_2012_I1125575/d06-x05-y06](#))
- $\sum p_{\perp}$ for $8 \leq p_{\perp}^{\text{jet}} < 11$ GeV, $R = 1.0$, Away region ([/REF/ATLAS_2012_I1125575/d06-x05-y07](#))
- $\sum p_{\perp}$ for $8 \leq p_{\perp}^{\text{jet}} < 11$ GeV, $R = 1.0$, Transverse region ([/REF/ATLAS_2012_I1125575/d06-x05-y08](#))
- $\sum p_{\perp}$ for $11 \leq p_{\perp}^{\text{jet}} < 14$ GeV, $R = 1.0$, Away region ([/REF/ATLAS_2012_I1125575/d06-x05-y09](#))
- $\sum p_{\perp}$ for $11 \leq p_{\perp}^{\text{jet}} < 14$ GeV, $R = 1.0$, Transverse region ([/REF/ATLAS_2012_I1125575/d06-x05-y10](#))
- $\sum p_{\perp}$ for $14 \leq p_{\perp}^{\text{jet}} < 19$ GeV, $R = 1.0$, Away region ([/REF/ATLAS_2012_I1125575/d06-x05-y11](#))
- $\sum p_{\perp}$ for $14 \leq p_{\perp}^{\text{jet}} < 19$ GeV, $R = 1.0$, Transverse region ([/REF/ATLAS_2012_I1125575/d06-x05-y12](#))
- $\sum p_{\perp}$ for $19 \leq p_{\perp}^{\text{jet}} < 24$ GeV, $R = 1.0$, Away region ([/REF/ATLAS_2012_I1125575/d06-x05-y13](#))
- $\sum p_{\perp}$ for $19 \leq p_{\perp}^{\text{jet}} < 24$ GeV, $R = 1.0$, Transverse region ([/REF/ATLAS_2012_I1125575/d06-x05-y14](#))
- $\sum p_{\perp}$ for $24 \leq p_{\perp}^{\text{jet}} < 31$ GeV, $R = 1.0$, Away region ([/REF/ATLAS_2012_I1125575/d06-x05-y15](#))
- $\sum p_{\perp}$ for $24 \leq p_{\perp}^{\text{jet}} < 31$ GeV, $R = 1.0$, Transverse region ([/REF/ATLAS_2012_I1125575/d06-x05-y16](#))
- $\sum p_{\perp}$ for $31 \leq p_{\perp}^{\text{jet}} < 50$ GeV, $R = 1.0$, Away region ([/REF/ATLAS_2012_I1125575/d06-x05-y17](#))
- $\sum p_{\perp}$ for $31 \leq p_{\perp}^{\text{jet}} < 50$ GeV, $R = 1.0$, Transverse region ([/REF/ATLAS_2012_I1125575/d06-x05-y18](#))
- $\sum p_{\perp}$ for $50 \leq p_{\perp}^{\text{jet}} < 100$ GeV, $R = 1.0$, Away region ([/REF/ATLAS_2012_I1125575/d06-x05-y19](#))
- $\sum p_{\perp}$ for $50 \leq p_{\perp}^{\text{jet}} < 100$ GeV, $R = 1.0$, Transverse region ([/REF/ATLAS_2012_I1125575/d06-x05-y20](#))

8.62 ATLAS_2012_I1125961

0-lepton squark and gluino search

Beams: pp

Energies: (3500.0, 3500.0) GeV

Experiment: ATLAS (LHC)

Inspire ID: [1125961](#)

Status: VALIDATED

Authors:

- Peter Richardson ⟨ Peter.Richardson@durham.ac.uk ⟩
- David Grellscheid ⟨ david.grellscheid@durham.ac.uk ⟩
- Chris Wymant ⟨ c.m.wymant@durham.ac.uk ⟩

References:

- arXiv: [1208.0949](#)

Run details:

- BSM signal events at 7000 GeV.

0-lepton search for squarks and gluinos by ATLAS at 7 TeV. Event counts in five signal regions are implemented as one-bin histograms.

8.63 ATLAS_2012_I1126136

SUSY Top partner search in jets with missing transverse momentum

Beams: pp

Energies: (3500.0, 3500.0) GeV

Experiment: ATLAS (LHC)

Inspire ID: [1126136](#)

Status: UNVALIDATED

Authors:

- Peter Richardson (peter.richardson@durham.ac.uk)

References:

- arXiv: [1208.1447](#)

Run details:

- BSM signal events at 7000 GeV.

Search for direct pair production of supersymmetric top squarks, assuming the stop_1 decays into a top quark and the lightest supersymmetric particle, and that both top quarks decay to purely hadronic final states. This search has an integrated luminosity of 4.7 fb^{-1} at $\sqrt{s} = 8 \text{ TeV}$.

8.64 ATLAS_2012_I1180197

Search for supersymmetry at 7 TeV in final states with jets, missing transverse momentum and isolated leptons with the ATLAS detector.

Beams: pp

Energies: (3500.0, 3500.0) GeV

Experiment: ATLAS (LHC)

Inspire ID: [1180197](#)

Status: UNVALIDATED

Authors:

- Peter Richardson (Peter.Richardson@durham.ac.uk)

References:

- ATLAS-CONF-2012-041
- arXiv: [1208.4688](#)

Run details:

- BSM signal events at 7000 GeV.

One and two lepton search for supersymmetric particles by ATLAS at 7 TeV. Event counts in the signal regions are implemented as one-bin histograms. Histograms for effective mass are implemented for the two signal hard lepton signal regions and the ratio of missing transverse energy to effective mass for the soft lepton region. Only the one lepton plots are currently implemented as taken from a conf note originally.

8.65 ATLAS_2012_I1183818 [135]

Pseudorapidity dependence of the total transverse energy at 7 TeV

Beams: pp

Energies: (3500.0, 3500.0) GeV

Experiment: ATLAS (LHC 7TeV)

Inspire ID: [1183818](#)

Status: VALIDATED

Authors:

- Robindra Prabhu (prabhu@cern.ch)
- Peter Wijeratne (paw@hep.ucl.ac.uk)
- Roman Lysak (lysak@fzu.cz)

References:

- arXiv: [1208.6256](#)

Run details:

- pp QCD interactions at 7 TeV, min bias and di-jet events

The measurement of the sum of the transverse energy of particles as a function of particle pseudorapidity, eta, in proton-proton collisions at a centre-of-mass energy, $\sqrt{s} = 7$ TeV using the ATLAS detector at the Large Hadron Collider. The measurements are performed in the region $|\eta| < 4.8$ for two event classes: those requiring the presence of particles with a low transverse momentum and those requiring particles with a significant transverse momentum (dijet events where both jets have $E_T > 20$ GeV). In the second dataset measurements are made in the region transverse to the hard scatter.

Histograms (14):

- E_\perp density for the minimum bias selection ([/REF/ATLAS_2012_I1183818/d01-x01-y01](#))
- E_\perp density for the dijet selection in the transverse region ([/REF/ATLAS_2012_I1183818/d02-x01-y01](#))
- $\sum E_\perp$ for the minimum bias selection, $0.0 < |\eta| < 0.8$ ([/REF/ATLAS_2012_I1183818/d03-x01-y01](#))
- $\sum E_\perp$ for the minimum bias selection, $0.8 < |\eta| < 1.6$ ([/REF/ATLAS_2012_I1183818/d04-x01-y01](#))
- $\sum E_\perp$ for the minimum bias selection, $1.6 < |\eta| < 2.4$ ([/REF/ATLAS_2012_I1183818/d05-x01-y01](#))
- $\sum E_\perp$ for the minimum bias selection, $2.4 < |\eta| < 3.2$ ([/REF/ATLAS_2012_I1183818/d06-x01-y01](#))
- $\sum E_\perp$ for the minimum bias selection, $3.2 < |\eta| < 4.0$ ([/REF/ATLAS_2012_I1183818/d07-x01-y01](#))
- $\sum E_\perp$ for the minimum bias selection, $4.0 < |\eta| < 4.8$ ([/REF/ATLAS_2012_I1183818/d08-x01-y01](#))
- $\sum E_\perp$ for the dijet selection, $0.0 < |\eta| < 0.8$ ([/REF/ATLAS_2012_I1183818/d09-x01-y01](#))

- $\sum E_{\perp}$ for the dijet selection, $0.8 < |\eta| < 1.6$ ([/REF/ATLAS_2012_I1183818/d10-x01-y01](#))
- $\sum E_{\perp}$ for the dijet selection, $1.6 < |\eta| < 2.4$ ([/REF/ATLAS_2012_I1183818/d11-x01-y01](#))
- $\sum E_{\perp}$ for the dijet selection, $2.4 < |\eta| < 3.2$ ([/REF/ATLAS_2012_I1183818/d12-x01-y01](#))
- $\sum E_{\perp}$ for the dijet selection, $3.2 < |\eta| < 4.0$ ([/REF/ATLAS_2012_I1183818/d13-x01-y01](#))
- $\sum E_{\perp}$ for the dijet selection, $4.0 < |\eta| < 4.8$ ([/REF/ATLAS_2012_I1183818/d14-x01-y01](#))

8.66 ATLAS_2012_I1186556

Search for a heavy top-quark partner in final states with two leptons.

Beams: pp

Energies: (3500.0, 3500.0) GeV

Experiment: ATLAS (LHC)

Inspire ID: [1186556](#)

Status: UNVALIDATED

Authors:

- Peter Richardson (Peter.Richardson@durham.ac.uk)

References:

- arXiv: [1209.4186](#)

Run details:

- BSM signal events at 7000 GeV.

Search for direct pair production of heavy top-quark partners with 4.7 fb^{-1} integrated luminosity at $\sqrt{s} = 7\text{TeV}$ by the ATLAS experiment. Heavy top-quark partners decaying into a top quark and a neutral non-interacting particle are searched for in events with two leptons in the final state.

8.67 ATLAS_2012_I1188891 [136]

Flavour composition of dijet events at 7 TeV

Beams: pp

Energies: (3500.0, 3500.0) GeV

Experiment: ATLAS (LHC 7TeV)

Inspire ID: [1188891](#)

Status: VALIDATED

Authors:

- Cecile Lapoire ⟨clapoire@cern.ch⟩
- Roman Lysak ⟨lysak@fzu.cz⟩

References:

- arXiv: [1210.0441](#)

Run details:

- pp di-jet events at 7 TeV

The measurement of the flavour composition of dijet events produced in pp collisions at $\sqrt{s} = 7$ TeV using the ATLAS detector. Six possible combinations of light, charm and bottom jets are identified in the dijet events, where the jet flavour is defined by the presence of bottom, charm or solely light flavour hadrons in the jet. The fractions of these dijet flavour states as functions of the leading jet transverse momentum in the range 40 GeV to 500 GeV and jet rapidity $|y| < 2.1$ are measured.

8.68 ATLAS_2012_I1190891

4 or more lepton plus missing transverse energy SUSY search

Beams: pp

Energies: (3500.0, 3500.0) GeV

Experiment: ATLAS (LHC)

Inspire ID: [1190891](#)

Status: UNVALIDATED

Authors:

- Peter Richardson (peter.richardson@durham.ac.uk)

References:

- ATLAS-CONF-2012-001
- ATLAS-CONF-2012-035
- arXiv: [1210.4457](#)

Run details:

- BSM signal events at 7000 GeV.

Search for R-parity violating SUSY using events with 4 or more leptons in association with missing transverse energy in proton-proton collisions at a centre-of-mass energy of 7 TeV. The data sample has a total integrated luminosity of 4.7 fb^{-1} .

8.69 ATLAS_2012_I1203852 [137]

Measurement of the $ZZ(*)$ production cross-section in pp collisions at 7 TeV with ATLAS

Beams: pp

Energies: (3500.0, 3500.0) GeV

Experiment: ATLAS (LHC)

Spires ID: [1203852](#)

Status: VALIDATED

Authors:

- Oldrich Kepka <oldrich.kepka@cern.ch>
- Katerina Moudra <katerina.moudra@cern.ch>

References:

- arXiv: [1211.6096](#)

Run details:

- Run with inclusive Z events, with Z decays to 4 leptons or 2 leptons + MET.

Measurement of the fiducial cross section for $ZZ(*)$ production in proton proton collisions at a centre-of mass energy of 7 TeV, is presented, using data corresponding to an integrated luminosity of 4.6/fb collected by the ATLAS experiment at the Large Hadron Collider. The cross-section is measured using processes with two Z bosons decaying to electrons or muons or with one Z boson decaying to electrons or muons and a second Z boson decaying to neutrinos. The fiducial region contains dressed leptons in restricted p_T and η ranges. The selection has specific requirements for both production processes. A measurement of the normalized fiducial cross-section as a function of ZZ invariant mass, leading Z p_T and angle of two leptons coming from the leading Z is also presented for both signal processes.

Histograms (9):

- Total fiducial cross-section $\sigma_{ZZ \rightarrow 4l}$ ([/REF/ATLAS_2012_I1203852/d01-x01-y01](#))
- Total fiducial cross-section $\sigma_{ZZ^* \rightarrow 4l}$ ([/REF/ATLAS_2012_I1203852/d01-x01-y02](#))
- Total fiducial cross-section $\sigma_{ZZ \rightarrow 2l2nu}$ ([/REF/ATLAS_2012_I1203852/d01-x01-y03](#))
- Differential cross-section for $ZZ \rightarrow 4\ell$ vs. p_\perp^Z ([/REF/ATLAS_2012_I1203852/d03-x01-y01](#))
- Differential cross-section for $ZZ \rightarrow \ell\ell\nu\nu$ vs. p_\perp^Z ([/REF/ATLAS_2012_I1203852/d04-x01-y01](#))
- Differential cross-section for $ZZ \rightarrow 4\ell$ vs. $\Delta\phi(\ell^+, \ell^-)$ ([/REF/ATLAS_2012_I1203852/d05-x01-y01](#))
- Differential cross-section for $ZZ \rightarrow \ell\ell\nu\nu$ vs. $\Delta\phi(\ell^+, \ell^-)$ ([/REF/ATLAS_2012_I1203852/d06-x01-y01](#))
- Differential cross-section for $ZZ \rightarrow 4\ell$ vs. M_T^{ZZ} ([/REF/ATLAS_2012_I1203852/d07-x01-y01](#))
- Differential cross-section for $ZZ \rightarrow \ell\ell\nu\nu$ vs. M_T^{ZZ} ([/REF/ATLAS_2012_I1203852/d08-x01-y01](#))

8.70 ATLAS_2012_I1204447 [138]

Inclusive multi-lepton search

Beams: pp

Energies: (3500.0, 3500.0) GeV

Experiment: ATLAS (LHC)

Inspire ID: [1204447](#)

Status: VALIDATED

Authors:

- Joern Mahlstedt <joern.mahlstedt@cern.ch>

References:

- arXiv: [1211.6312](#)
- Phys. Rev. D 87, 052002 (2013)

Run details:

- Any process producing at least 3 leptons (e.g. pair production of doubly-charged Higgs)

A generic search for anomalous production of events with at least three charged leptons is presented. The search uses a pp -collision data sample at a center-of-mass energy of $\sqrt{s} = 7$ TeV corresponding to 4.6/fb of integrated luminosity collected in 2011 by the ATLAS detector at the CERN Large Hadron Collider. Events are required to contain at least two electrons or muons, while the third lepton may either be an additional electron or muon, or a hadronically decaying tau lepton. Events are categorized by the presence or absence of a reconstructed tau-lepton or Z-boson candidate decaying to leptons. No significant excess above backgrounds expected from Standard Model processes is observed. Results are presented as upper limits on event yields from non-Standard-Model processes producing at least three prompt, isolated leptons, given as functions of lower bounds on several kinematic variables. Fiducial efficiencies for model testing are also provided. This Rivet module implements the event selection and the fiducial efficiencies to test various models for their exclusion based on observed/excluded limits.

8.71 ATLAS_2012_I1204784 [139]

Measurement of angular correlations in Drell-Yan lepton pairs to probe Z/γ^* boson transverse momentum

Beams: pp

Energies: (3500.0, 3500.0) GeV

Experiment: ATLAS (LHC)

Inspire ID: [1204784](#)

Status: VALIDATED

Authors:

- Elena Yatsenko <elena.yatsenko.de@gmail.com>
- Kiran Joshi <kiran.joshi@cern.ch>

References:

- arXiv: [1211.6899](#)

Run details:

- Z/γ^* production with decays to electrons and/or muons.

A measurement of angular correlations in Drell-Yan lepton pairs via the phi-star observable is presented. This variable probes the same physics as the Z/γ^* boson transverse momentum with a better experimental resolution. The $Z/\gamma^* \rightarrow ee$ and $Z/\gamma^* \rightarrow \mu\mu$ decays produced in proton-proton collisions at a centre-of-mass energy of $\sqrt{s} = 7$ TeV are used. Normalised differential cross sections as a function of phi-star are measured separately for electron and muon decay channels. The cross section is also measured double differentially as a function of phi-star for three independent bins of the Z boson rapidity.

Histograms (16):

- ϕ_η^* spectrum, $Z \rightarrow ee$ (bare) ([/REF/ATLAS_2012_I1204784/d01-x01-y01](#))
- ϕ_η^* spectrum, $Z \rightarrow \mu\mu$ (bare) ([/REF/ATLAS_2012_I1204784/d01-x01-y02](#))
- ϕ_η^* spectrum, $Z \rightarrow ee$ (dressed) ([/REF/ATLAS_2012_I1204784/d02-x01-y01](#))
- ϕ_η^* spectrum, $Z \rightarrow \mu\mu$ (dressed) ([/REF/ATLAS_2012_I1204784/d02-x01-y02](#))
- ϕ_η^* spectrum, $Z \rightarrow ee$ (bare), $|y_Z| < 0.8$ ([/REF/ATLAS_2012_I1204784/d03-x01-y01](#))
- ϕ_η^* spectrum, $Z \rightarrow ee$ (bare), $0.8 \leq |y_Z| < 1.6$ ([/REF/ATLAS_2012_I1204784/d03-x01-y02](#))
- ϕ_η^* spectrum, $Z \rightarrow ee$ (bare), $|y_Z| \geq 1.6$ ([/REF/ATLAS_2012_I1204784/d03-x01-y03](#))
- ϕ_η^* spectrum, $Z \rightarrow ee$ (dressed), $|y_Z| < 0.8$ ([/REF/ATLAS_2012_I1204784/d03-x02-y01](#))
- ϕ_η^* spectrum, $Z \rightarrow ee$ (dressed), $0.8 \leq |y_Z| < 1.6$ ([/REF/ATLAS_2012_I1204784/d03-x02-y02](#))

- ϕ_η^* spectrum, Z \rightarrow ee (dressed), $|y_Z| \geq 1.6$ (/REF/ATLAS_2012_I1204784/d03-x02-y03)
- ϕ_η^* spectrum, Z \rightarrow $\mu\mu$ (bare), $|y_Z| < 0.8$ (/REF/ATLAS_2012_I1204784/d04-x01-y01)
- ϕ_η^* spectrum, Z \rightarrow $\mu\mu$ (bare), $0.8 \leq |y_Z| < 1.6$ (/REF/ATLAS_2012_I1204784/d04-x01-y02)
- ϕ_η^* spectrum, Z \rightarrow $\mu\mu$ (bare), $|y_Z| \geq 1.6$ (/REF/ATLAS_2012_I1204784/d04-x01-y03)
- ϕ_η^* spectrum, Z \rightarrow $\mu\mu$ (dressed), $|y_Z| < 0.8$ (/REF/ATLAS_2012_I1204784/d04-x02-y01)
- ϕ_η^* spectrum, Z \rightarrow $\mu\mu$ (dressed), $0.8 \leq |y_Z| < 1.6$ (/REF/ATLAS_2012_I1204784/d04-x02-y02)
- ϕ_η^* spectrum, Z \rightarrow $\mu\mu$ (dressed), $|y_Z| \geq 1.6$ (/REF/ATLAS_2012_I1204784/d04-x02-y03)

8.72 ATLAS_2012_I943401 [140]

Search for supersymmetry with 2 leptons and missing transverse energy

Beams: pp

Energies: (3500.0, 3500.0) GeV

Experiment: ATLAS (LHC)

Inspire ID: [943401](#)

Status: VALIDATED

Authors:

- Peter Richardson (Peter.Richardson@durham.ac.uk)

References:

- arXiv: [1110.6189](#)

Run details:

- BSM signal events at 7000 GeV.

Results of three searches for the production of supersymmetric particles decaying into final states with missing transverse momentum and exactly two isolated leptons, electrons or muons. The analysis uses a data sample collected during the first half of 2011 that corresponds to a total integrated luminosity of 1 fb^{-1} of $\sqrt{s} = 7 \text{ TeV}$ proton-proton collisions recorded with the ATLAS detector at the Large Hadron Collider. Opposite-sign and same-sign dilepton events are studied separately. Additionally, in opposite-sign events, a search is made for an excess of same-flavour over different-flavour lepton pairs.

Histograms (34):

- $m_{\ell\ell}$ for same-sign events (data) ([/REF/ATLAS_2012_I943401/d01-x01-y01](#))
- $m_{\ell\ell}$ for same-sign events (back) ([/REF/ATLAS_2012_I943401/d01-x01-y02](#))
- Missing Transverse Energy for same-sign events (data) ([/REF/ATLAS_2012_I943401/d02-x01-y01](#))
- Missing Transverse Energy for same-sign events (back) ([/REF/ATLAS_2012_I943401/d02-x01-y02](#))
- $m_{\ell\ell}$ for same-sign events with 2 jets (data) ([/REF/ATLAS_2012_I943401/d03-x01-y01](#))
- $m_{\ell\ell}$ for same-sign events with 2 jets (back) ([/REF/ATLAS_2012_I943401/d03-x01-y02](#))
- Number of Jets for same-sign events (data) ([/REF/ATLAS_2012_I943401/d05-x01-y01](#))
- Number of Jets for same-sign events (back) ([/REF/ATLAS_2012_I943401/d05-x01-y02](#))
- p_T of the leading jet for same-sign events (data) ([/REF/ATLAS_2012_I943401/d06-x01-y01](#))
- p_T of the leading jet for same-sign events (back) ([/REF/ATLAS_2012_I943401/d06-x01-y02](#))
- p_T of the second jet for same-sign events (data) ([/REF/ATLAS_2012_I943401/d07-x01-y01](#))

- p_T of the second jet for same-sign events (back) (/REF/ATLAS_2012_I943401/d07-x01-y02)
- p_T of the leading lepton for same-sign events (data) (/REF/ATLAS_2012_I943401/d08-x01-y01)
- p_T of the leading lepton for same-sign events (back) (/REF/ATLAS_2012_I943401/d08-x01-y02)
- p_T of the second lepton for same-sign events (data) (/REF/ATLAS_2012_I943401/d09-x01-y01)
- p_T of the second lepton for same-sign events (back) (/REF/ATLAS_2012_I943401/d09-x01-y02)
- $m_{\ell\ell}$ for opposite-sign events (data) (/REF/ATLAS_2012_I943401/d10-x01-y01)
- $m_{\ell\ell}$ for opposite-sign events (back) (/REF/ATLAS_2012_I943401/d10-x01-y02)
- Missing Transverse Energy for opposite-sign events (data) (/REF/ATLAS_2012_I943401/d11-x01-y01)
- Missing Transverse Energy for opposite-sign events (back) (/REF/ATLAS_2012_I943401/d11-x01-y02)
- Missing Transverse Energy for opposite-sign events with 3 jets (data) (/REF/ATLAS_-2012_I943401/d12-x01-y01)
- Missing Transverse Energy for opposite-sign events with 3 jets (back) (/REF/ATLAS_-2012_I943401/d12-x01-y02)
- Missing Transverse Energy for opposite-sign events with 4 jets (data) (/REF/ATLAS_-2012_I943401/d13-x01-y01)
- Missing Transverse Energy for opposite-sign events with 4 jets (back) (/REF/ATLAS_-2012_I943401/d13-x01-y02)
- Number of Jets for opposite-sign events (data) (/REF/ATLAS_2012_I943401/d14-x01-y01)
- Number of Jets for opposite-sign events (back) (/REF/ATLAS_2012_I943401/d14-x01-y02)
- p_T of the leading jet for opposite-sign events (data) (/REF/ATLAS_2012_I943401/d15-x01-y01)
- p_T of the leading jet for opposite-sign events (back) (/REF/ATLAS_2012_I943401/d15-x01-y02)
- p_T of the second jet for opposite-sign events (data) (/REF/ATLAS_2012_I943401/d16-x01-y01)
- p_T of the second jet for opposite-sign events (back) (/REF/ATLAS_2012_I943401/d16-x01-y02)
- p_T of the leading lepton for opposite-sign events (data) (/REF/ATLAS_2012_I943401/d17-x01-y01)
- p_T of the leading lepton for opposite-sign events (back) (/REF/ATLAS_2012_I943401/d17-x01-y02)
- p_T of the second lepton for opposite-sign events (data) (/REF/ATLAS_2012_I943401/d18-x01-y01)
- p_T of the second lepton for opposite-sign events (back) (/REF/ATLAS_2012_I943401/d18-x01-y02)

8.73 ATLAS_2012_I946427 [141]

Search for supersymmetry with diphotons and mising Transverse Momentum
Beams: pp

Energies: (3500.0, 3500.0) GeV

Experiment: ATLAS (LHC)

Inspire ID: [946427](#)

Status: UNVALIDATED

Authors:

- Peter Richardson (Peter.Richardson@durham.ac.uk)

References:

- arXiv: [1111.4116](#)
- Phys. Lett. B710 (2012) 519-537

Run details:

- BSM signal events at 7000 GeV.

Search for diphoton events with large missing transverse momentum with integrated luminosity 1.07fb^{-1} at $\sqrt{s} = 7$. No excess of events was observed.

8.74 ATLAS_2013_I1190187 [?]

Measurement of the W^+W^- production cross-section at 7 TeV

Beams: pp

Energies: (3500.0, 3500.0) GeV

Experiment: ATLAS (LHC)

Spires ID: [1190187](#)

Status: VALIDATED

Authors:

- Oldrich Kepka <oldrich.kepka@cern.ch>
- Katerina Moudra <katerina.moudra@cern.ch>

References:

- arXiv: [1210.2979](#)

Run details:

- Run with inclusive W^+W^- events, with W decays to electron + MET, muon + MET, or tau + MET.

Measurement of the fiducial cross section for W^+W^- production in proton proton collisions at a centre-of mass energy of 7 TeV, is presented, using data corresponding to an integrated luminosity of 4.6/fb collected by the ATLAS experiment at the Large Hadron Collider. The cross section is measured in the leptonic decay channels, using electron+MET and muon+MET W decays. $W \rightarrow \tau$ processes with the tau decaying into electron + MET or muon + MET are also included in the measurement. The fiducial region contains dressed leptons in restricted p_T and η ranges. The selection has specific requirements for each production channel. A measurement of the normalized fiducial cross section as a function of the leading lepton transverse momentum is also presented.

Histograms (3):

- Total fiducial cross-section $WW \rightarrow e\nu e\nu$ ([/REF/ATLAS_2013_I1190187/d01-x01-y01](#))
- Total fiducial cross-section $WW \rightarrow \mu\nu \mu\nu$ ([/REF/ATLAS_2013_I1190187/d01-x01-y02](#))
- Total fiducial cross-section $WW \rightarrow e\nu \mu\nu$ ([/REF/ATLAS_2013_I1190187/d01-x01-y03](#))

8.75 ATLAS_2013_I1217867 [142]

kT splitting scales in $W \rightarrow l\nu$ events

Beams: pp

Energies: (3500.0, 3500.0) GeV

Experiment: ATLAS (LHC)

Inspire ID: [1217867](#)

Status: VALIDATED

Authors:

- Frank Siegert (frank.siegert@cern.ch)

References:

- arXiv: [1302.1415](#)

Run details:

- $W + \text{jet}$ events in the electron and/or the muon decay channel.

Cluster splitting scales are measured in events containing W bosons decaying to electrons or muons. The measurement comprises the four hardest splitting scales in a kT cluster sequence of the hadronic activity accompanying the W boson, and ratios of these splitting scales.

Histograms (14):

- k_{\perp} scale of $0 \rightarrow 1$ clustering ($W \rightarrow e\nu$) ([/REF/ATLAS_2013_I1217867/d01-x01-y01](#))
- k_{\perp} scale of $0 \rightarrow 1$ clustering ($W \rightarrow \mu\nu$) ([/REF/ATLAS_2013_I1217867/d01-x01-y02](#))
- k_{\perp} scale of $1 \rightarrow 2$ clustering ($W \rightarrow e\nu$) ([/REF/ATLAS_2013_I1217867/d02-x01-y01](#))
- k_{\perp} scale of $1 \rightarrow 2$ clustering ($W \rightarrow \mu\nu$) ([/REF/ATLAS_2013_I1217867/d02-x01-y02](#))
- k_{\perp} scale of $2 \rightarrow 3$ clustering ($W \rightarrow e\nu$) ([/REF/ATLAS_2013_I1217867/d03-x01-y01](#))
- k_{\perp} scale of $2 \rightarrow 3$ clustering ($W \rightarrow \mu\nu$) ([/REF/ATLAS_2013_I1217867/d03-x01-y02](#))
- k_{\perp} scale of $3 \rightarrow 4$ clustering ($W \rightarrow e\nu$) ([/REF/ATLAS_2013_I1217867/d04-x01-y01](#))
- k_{\perp} scale of $3 \rightarrow 4$ clustering ($W \rightarrow \mu\nu$) ([/REF/ATLAS_2013_I1217867/d04-x01-y02](#))
- Ratio of subsequent clustering scales ($W \rightarrow e\nu$) ([/REF/ATLAS_2013_I1217867/d05-x01-y01](#))
- Ratio of subsequent clustering scales ($W \rightarrow \mu\nu$) ([/REF/ATLAS_2013_I1217867/d05-x01-y02](#))
- Ratio of subsequent clustering scales ($W \rightarrow e\nu$) ([/REF/ATLAS_2013_I1217867/d06-x01-y01](#))
- Ratio of subsequent clustering scales ($W \rightarrow \mu\nu$) ([/REF/ATLAS_2013_I1217867/d06-x01-y02](#))
- Ratio of subsequent clustering scales ($W \rightarrow e\nu$) ([/REF/ATLAS_2013_I1217867/d07-x01-y01](#))
- Ratio of subsequent clustering scales ($W \rightarrow \mu\nu$) ([/REF/ATLAS_2013_I1217867/d07-x01-y02](#))

8.76 ATLAS_2013_I1230812 [143]

$Z + \text{jets}$ in pp at 7 TeV

Beams: pp

Energies: (3500.0, 3500.0) GeV

Experiment: ATLAS (LHC)

Inspire ID: [1230812](#)

Status: VALIDATED

Authors:

- Katharina Bierwagen (katharina.bierwagen@cern.ch)
- Frank Siegert (frank.siegert@cern.ch)

References:

- arXiv: [1304.7098](#)
- J. High Energy Phys. 07 (2013) 032

Run details:

- $Z + \text{jets}$, electronic Z -decays (data are a weighted combination of electron/muon).

Measurements of the production of jets of particles in association with a Z boson in pp collisions at $\sqrt{s} = 7$ TeV are presented, using data corresponding to an integrated luminosity of 4.6/fb collected by the ATLAS experiment at the Large Hadron Collider. Inclusive and differential jet cross sections in Z events, with Z decaying into electron or muon pairs, are measured for jets with transverse momentum $p_T > 30$ GeV and rapidity $|y| < 4.4$. This Rivet module implements the event selection for the weighted combination of both decay channels and uses the data from that combination (as in the paper plots). But for simplification of its usage it only requires events with the electronic final state (muonic final state will be ignored). This allows to use it with either pure electronic samples, or mixed electron/muon events. If you want to use it with a pure muon sample, please refer to ATLAS_2013_I1230812_MU.

Histograms (28):

- Inclusive jet multiplicity ([/REF/ATLAS_2013_I1230812/d01-x01-y01](#))
- Inclusive jet multiplicity ratio ([/REF/ATLAS_2013_I1230812/d02-x01-y01](#))
- Exclusive jet multiplicity ([/REF/ATLAS_2013_I1230812/d03-x01-y01](#))
- Exclusive jet multiplicity ratio ([/REF/ATLAS_2013_I1230812/d04-x01-y01](#))
- Exclusive jet multiplicity ($p_{\perp}^{\text{jet1}} > 150$ GeV) ([/REF/ATLAS_2013_I1230812/d05-x01-y01](#))
- Exclusive jet multiplicity ratio ($p_{\perp}^{\text{jet1}} > 150$ GeV) ([/REF/ATLAS_2013_I1230812/d06-x01-y01](#))

- Exclusive jet multiplicity (VBF selection) ([/REF/ATLAS_2013_I1230812/d07-x01-y01](#))
- Exclusive jet multiplicity ratio (VBF selection) ([/REF/ATLAS_2013_I1230812/d08-x01-y01](#))
- Transverse momentum of 1st jet ([/REF/ATLAS_2013_I1230812/d09-x01-y01](#))
- Transverse momentum of 2nd jet ([/REF/ATLAS_2013_I1230812/d10-x01-y01](#))
- Transverse momentum of 3rd jet ([/REF/ATLAS_2013_I1230812/d11-x01-y01](#))
- Transverse momentum of 4th jet ([/REF/ATLAS_2013_I1230812/d12-x01-y01](#))
- Transverse jet momentum in $Z + 1\text{jet}$ events ([/REF/ATLAS_2013_I1230812/d13-x01-y01](#))
- Ratio of jet transverse momenta ([/REF/ATLAS_2013_I1230812/d14-x01-y01](#))
- Transverse momentum of Z -boson ([/REF/ATLAS_2013_I1230812/d15-x01-y01](#))
- Transverse momentum of Z -boson ($Z+1\text{jet}$ events) ([/REF/ATLAS_2013_I1230812/d16-x01-y01](#))
- Rapidity of 1st jet ([/REF/ATLAS_2013_I1230812/d17-x01-y01](#))
- Rapidity of 2nd jet ([/REF/ATLAS_2013_I1230812/d18-x01-y01](#))
- Rapidity of 3rd jet ([/REF/ATLAS_2013_I1230812/d19-x01-y01](#))
- Rapidity of 4th jet ([/REF/ATLAS_2013_I1230812/d20-x01-y01](#))
- Rapidity distance of leading jets ([/REF/ATLAS_2013_I1230812/d21-x01-y01](#))
- Invariant mass of leading jets ([/REF/ATLAS_2013_I1230812/d22-x01-y01](#))
- Azimuthal distance of leading jets ([/REF/ATLAS_2013_I1230812/d23-x01-y01](#))
- ΔR distance of leading jets ([/REF/ATLAS_2013_I1230812/d24-x01-y01](#))
- Transverse momentum of 3rd jet (VBF selection) ([/REF/ATLAS_2013_I1230812/d25-x01-y01](#))
- Rapidity of 3rd jet (VBF selection) ([/REF/ATLAS_2013_I1230812/d26-x01-y01](#))
- Scalar p_{\perp} sum of leptons and jets ([/REF/ATLAS_2013_I1230812/d27-x01-y01](#))
- Scalar p_{\perp} sum of jets ([/REF/ATLAS_2013_I1230812/d28-x01-y01](#))

8.77 ATLAS_2013_I1230812_EL [143]

Z+ jets in pp at 7 TeV (electron channel)

Beams: pp

Energies: (3500.0, 3500.0) GeV

Experiment: ATLAS (LHC)

Inspire ID: [1230812](#)

Status: VALIDATED

Authors:

- Katharina Bierwagen ⟨katharina.bierwagen@cern.ch⟩
- Frank Siegert ⟨frank.siegert@cern.ch⟩

References:

- arXiv: [1304.7098](#)
- J. High Energy Phys. 07 (2013) 032

Run details:

- Z+jets, electronic Z-decays

Measurements of the production of jets of particles in association with a Z boson in pp collisions at $\sqrt{s} = 7$ TeV are presented, using data corresponding to an integrated luminosity of 4.6/fb collected by the ATLAS experiment at the Large Hadron Collider. Inclusive and differential jet cross sections in Z events, with Z decaying into electron or muon pairs, are measured for jets with transverse momentum $p_T > 30$ GeV and rapidity $|y| < 4.4$. This Rivet module implements the event selection for Z decaying into electrons and uses the data measured explicitly in this channel (not the combined results shown in the paper plots). If you want to use muonic events, please refer to ATLAS_2013_I1230812_MU.

Histograms (28):

- Inclusive jet multiplicity ([/REF/ATLAS_2013_I1230812_EL/d01-x01-y02](#))
- Inclusive jet multiplicity ratio ([/REF/ATLAS_2013_I1230812_EL/d02-x01-y02](#))
- Exclusive jet multiplicity ([/REF/ATLAS_2013_I1230812_EL/d03-x01-y02](#))
- Exclusive jet multiplicity ratio ([/REF/ATLAS_2013_I1230812_EL/d04-x01-y02](#))
- Exclusive jet multiplicity ($p_{\perp}^{\text{jet1}} > 150$ GeV) ([/REF/ATLAS_2013_I1230812_EL/d05-x01-y02](#))
- Exclusive jet multiplicity ratio ($p_{\perp}^{\text{jet1}} > 150$ GeV) ([/REF/ATLAS_2013_I1230812_EL/d06-x01-y02](#))
- Exclusive jet multiplicity (VBF selection) ([/REF/ATLAS_2013_I1230812_EL/d07-x01-y02](#))
- Exclusive jet multiplicity ratio (VBF selection) ([/REF/ATLAS_2013_I1230812_EL/d08-x01-y02](#))

- Transverse momentum of 1st jet (`/REF/ATLAS_2013_I1230812_EL/d09-x01-y02`)
- Transverse momentum of 2nd jet (`/REF/ATLAS_2013_I1230812_EL/d10-x01-y02`)
- Transverse momentum of 3rd jet (`/REF/ATLAS_2013_I1230812_EL/d11-x01-y02`)
- Transverse momentum of 4th jet (`/REF/ATLAS_2013_I1230812_EL/d12-x01-y02`)
- Transverse jet momentum in $Z + 1\text{jet}$ events (`/REF/ATLAS_2013_I1230812_EL/d13-x01-y02`)
- Ratio of jet transverse momenta (`/REF/ATLAS_2013_I1230812_EL/d14-x01-y02`)
- Transverse momentum of Z -boson (`/REF/ATLAS_2013_I1230812_EL/d15-x01-y02`)
- Transverse momentum of Z -boson ($Z+1\text{jet}$ events) (`/REF/ATLAS_2013_I1230812_EL/d16-x01-y02`)
- Rapidity of 1st jet (`/REF/ATLAS_2013_I1230812_EL/d17-x01-y02`)
- Rapidity of 2nd jet (`/REF/ATLAS_2013_I1230812_EL/d18-x01-y02`)
- Rapidity of 3rd jet (`/REF/ATLAS_2013_I1230812_EL/d19-x01-y02`)
- Rapidity of 4th jet (`/REF/ATLAS_2013_I1230812_EL/d20-x01-y02`)
- Rapidity distance of leading jets (`/REF/ATLAS_2013_I1230812_EL/d21-x01-y02`)
- Invariant mass of leading jets (`/REF/ATLAS_2013_I1230812_EL/d22-x01-y02`)
- Azimuthal distance of leading jets (`/REF/ATLAS_2013_I1230812_EL/d23-x01-y02`)
- ΔR distance of leading jets (`/REF/ATLAS_2013_I1230812_EL/d24-x01-y02`)
- Transverse momentum of 3rd jet (VBF selection) (`/REF/ATLAS_2013_I1230812_EL/d25-x01-y02`)
- Rapidity of 3rd jet (VBF selection) (`/REF/ATLAS_2013_I1230812_EL/d26-x01-y02`)
- Scalar p_{\perp} sum of leptons and jets (`/REF/ATLAS_2013_I1230812_EL/d27-x01-y02`)
- Scalar p_{\perp} sum of jets (`/REF/ATLAS_2013_I1230812_EL/d28-x01-y02`)

8.78 ATLAS_2013_I1230812_MU [143]

Z+ jets in pp at 7 TeV (muon channel)

Beams: pp

Energies: (3500.0, 3500.0) GeV

Experiment: ATLAS (LHC)

Inspire ID: [1230812](#)

Status: VALIDATED

Authors:

- Katharina Bierwagen ⟨katharina.bierwagen@cern.ch⟩
- Frank Siegert ⟨frank.siegert@cern.ch⟩

References:

- arXiv: [1304.7098](#)
- J. High Energy Phys. 07 (2013) 032

Run details:

- Z+jets, muonic Z-decays

Measurements of the production of jets of particles in association with a Z boson in pp collisions at $\sqrt{s} = 7$ TeV are presented, using data corresponding to an integrated luminosity of 4.6/fb collected by the ATLAS experiment at the Large Hadron Collider. Inclusive and differential jet cross sections in Z events, with Z decaying into electron or muon pairs, are measured for jets with transverse momentum $p_T > 30$ GeV and rapidity $|y| < 4.4$. This Rivet module implements the event selection for Z decaying into muons and uses the data measured explicitly in this channel (not the combined results shown in the paper plots). If you want to use electronic events, please refer to ATLAS_2013_I1230812_EL.

Histograms (28):

- Inclusive jet multiplicity ([/REF/ATLAS_2013_I1230812_MU/d01-x01-y03](#))
- Inclusive jet multiplicity ratio ([/REF/ATLAS_2013_I1230812_MU/d02-x01-y03](#))
- Exclusive jet multiplicity ([/REF/ATLAS_2013_I1230812_MU/d03-x01-y03](#))
- Exclusive jet multiplicity ratio ([/REF/ATLAS_2013_I1230812_MU/d04-x01-y03](#))
- Exclusive jet multiplicity ($p_{\perp}^{\text{jet1}} > 150$ GeV) ([/REF/ATLAS_2013_I1230812_MU/d05-x01-y03](#))
- Exclusive jet multiplicity ratio ($p_{\perp}^{\text{jet1}} > 150$ GeV) ([/REF/ATLAS_2013_I1230812_MU/d06-x01-y03](#))
- Exclusive jet multiplicity (VBF selection) ([/REF/ATLAS_2013_I1230812_MU/d07-x01-y03](#))
- Exclusive jet multiplicity ratio (VBF selection) ([/REF/ATLAS_2013_I1230812_MU/d08-x01-y03](#))

- Transverse momentum of 1st jet (`/REF/ATLAS_2013_I1230812_MU/d09-x01-y03`)
- Transverse momentum of 2nd jet (`/REF/ATLAS_2013_I1230812_MU/d10-x01-y03`)
- Transverse momentum of 3rd jet (`/REF/ATLAS_2013_I1230812_MU/d11-x01-y03`)
- Transverse momentum of 4th jet (`/REF/ATLAS_2013_I1230812_MU/d12-x01-y03`)
- Transverse jet momentum in $Z + 1\text{jet}$ events (`/REF/ATLAS_2013_I1230812_MU/d13-x01-y03`)
- Ratio of jet transverse momenta (`/REF/ATLAS_2013_I1230812_MU/d14-x01-y03`)
- Transverse momentum of Z -boson (`/REF/ATLAS_2013_I1230812_MU/d15-x01-y03`)
- Transverse momentum of Z -boson ($Z+1\text{jet}$ events) (`/REF/ATLAS_2013_I1230812_MU/d16-x01-y03`)
- Rapidity of 1st jet (`/REF/ATLAS_2013_I1230812_MU/d17-x01-y03`)
- Rapidity of 2nd jet (`/REF/ATLAS_2013_I1230812_MU/d18-x01-y03`)
- Rapidity of 3rd jet (`/REF/ATLAS_2013_I1230812_MU/d19-x01-y03`)
- Rapidity of 4th jet (`/REF/ATLAS_2013_I1230812_MU/d20-x01-y03`)
- Rapidity distance of leading jets (`/REF/ATLAS_2013_I1230812_MU/d21-x01-y03`)
- Invariant mass of leading jets (`/REF/ATLAS_2013_I1230812_MU/d22-x01-y03`)
- Azimuthal distance of leading jets (`/REF/ATLAS_2013_I1230812_MU/d23-x01-y03`)
- ΔR distance of leading jets (`/REF/ATLAS_2013_I1230812_MU/d24-x01-y03`)
- Transverse momentum of 3rd jet (VBF selection) (`/REF/ATLAS_2013_I1230812_MU/d25-x01-y03`)
- Rapidity of 3rd jet (VBF selection) (`/REF/ATLAS_2013_I1230812_MU/d26-x01-y03`)
- Scalar p_{\perp} sum of leptons and jets (`/REF/ATLAS_2013_I1230812_MU/d27-x01-y03`)
- Scalar p_{\perp} sum of jets (`/REF/ATLAS_2013_I1230812_MU/d28-x01-y03`)

8.79 ATLAS_2013_I1243871 [144]

Measurement of jet shapes in top quark pair events at $\sqrt{s} = 7$ TeV with ATLAS

Beams: pp

Energies: (3500.0, 3500.0) GeV

Experiment: ATLAS (LHC)

Spires ID: [1243871](#)

Status: VALIDATED

Authors:

- Javier Llorente <javier.llorente.merino@cern.ch>

References:

- arXiv: [1307.5749](#)

Run details:

- Top quark pair production in pp collisions at $\sqrt{s} = 7$ TeV

Measurement of jet shapes in top pair events in the ATLAS 7 TeV run. b-jets are shown to have a wider energy density distribution than light-quark induced jets.

8.80 CMS_2010_S8547297 [145]

Charged particle transverse momentum and pseudorapidity spectra from proton-proton collisions at 900 and 2360 GeV.

Beams: pp

Energies: (450.0, 450.0), (1180.0, 1180.0) GeV

Experiment: CMS (LHC)

Spires ID: [8547297](#)

Status: VALIDATED

Authors:

- A. Knutsson

References:

- JHEP 02 (2010) 041
- DOI: [10.1007/JHEP02\(2010\)041](https://doi.org/10.1007/JHEP02(2010)041)
- arXiv: [1002.0621](https://arxiv.org/abs/1002.0621)

Run details:

- Non-single-diffractive (NSD) events only. Should include double-diffractive (DD) events and non-diffractive (ND) events but NOT single-diffractive (SD) events. Examples, in Pythia6 the SD processes to be turned off are 92 and 93, and in Pythia8 the SD processes are 103 and 104 (also called SoftQCD:singleDiffractive).

Charged particle spectra are measured in proton-proton collisions at center-of-mass energies 900 and 2360 GeV. The spectra are normalized to all non-single-diffractive (NSD) events using corrections for trigger and selection efficiency, acceptance, and branching ratios. There are transverse-momentum (p_\perp) spectra from 0.1 to 2 GeV in bins of pseudorapidity (η) and p_\perp spectra from 0.1 to 4 GeV for $|\eta| < 2.4$. The η spectra come from the average of three methods and cover $|\eta| < 2.5$ and are corrected to include all p_\perp . The data were corrected according to the SD/DD/ND content of the CMS trigger, as predicted by PYTHIA6. The uncertainties connected with correct or incorrect modelling of diffraction were included in the systematic errors.

Histograms (28):

- Charged hadron p_\perp for $|\eta| = 0.1$ at $\sqrt{s} = 0.9$ TeV ([/REF/CMS_2010_S8547297/d01-x01-y01](#))
- Charged hadron p_\perp for $|\eta| = 0.3$ at $\sqrt{s} = 0.9$ TeV ([/REF/CMS_2010_S8547297/d01-x01-y02](#))
- Charged hadron p_\perp for $|\eta| = 0.5$ at $\sqrt{s} = 0.9$ TeV ([/REF/CMS_2010_S8547297/d01-x01-y03](#))
- Charged hadron p_\perp for $|\eta| = 0.7$ at $\sqrt{s} = 0.9$ TeV ([/REF/CMS_2010_S8547297/d01-x01-y04](#))
- Charged hadron p_\perp for $|\eta| = 0.9$ at $\sqrt{s} = 0.9$ TeV ([/REF/CMS_2010_S8547297/d02-x01-y01](#))

- Charged hadron p_\perp for $|\eta| = 1.1$ at $\sqrt{s} = 0.9$ TeV ([/REF/CMS_2010_S8547297/d02-x01-y02](#))
- Charged hadron p_\perp for $|\eta| = 1.3$ at $\sqrt{s} = 0.9$ TeV ([/REF/CMS_2010_S8547297/d02-x01-y03](#))
- Charged hadron p_\perp for $|\eta| = 1.5$ at $\sqrt{s} = 0.9$ TeV ([/REF/CMS_2010_S8547297/d02-x01-y04](#))
- Charged hadron p_\perp for $|\eta| = 1.7$ at $\sqrt{s} = 0.9$ TeV ([/REF/CMS_2010_S8547297/d03-x01-y01](#))
- Charged hadron p_\perp for $|\eta| = 1.9$ at $\sqrt{s} = 0.9$ TeV ([/REF/CMS_2010_S8547297/d03-x01-y02](#))
- Charged hadron p_\perp for $|\eta| = 2.1$ at $\sqrt{s} = 0.9$ TeV ([/REF/CMS_2010_S8547297/d03-x01-y03](#))
- Charged hadron p_\perp for $|\eta| = 2.3$ at $\sqrt{s} = 0.9$ TeV ([/REF/CMS_2010_S8547297/d03-x01-y04](#))
- Charged hadron p_\perp for $|\eta| = 0.1$ at $\sqrt{s} = 2.36$ TeV ([/REF/CMS_2010_S8547297/d04-x01-y01](#))
- Charged hadron p_\perp for $|\eta| = 0.3$ at $\sqrt{s} = 2.36$ TeV ([/REF/CMS_2010_S8547297/d04-x01-y02](#))
- Charged hadron p_\perp for $|\eta| = 0.5$ at $\sqrt{s} = 2.36$ TeV ([/REF/CMS_2010_S8547297/d04-x01-y03](#))
- Charged hadron p_\perp for $|\eta| = 0.7$ at $\sqrt{s} = 2.36$ TeV ([/REF/CMS_2010_S8547297/d04-x01-y04](#))
- Charged hadron p_\perp for $|\eta| = 0.9$ at $\sqrt{s} = 2.36$ TeV ([/REF/CMS_2010_S8547297/d05-x01-y01](#))
- Charged hadron p_\perp for $|\eta| = 1.1$ at $\sqrt{s} = 2.36$ TeV ([/REF/CMS_2010_S8547297/d05-x01-y02](#))
- Charged hadron p_\perp for $|\eta| = 1.3$ at $\sqrt{s} = 2.36$ TeV ([/REF/CMS_2010_S8547297/d05-x01-y03](#))
- Charged hadron p_\perp for $|\eta| = 1.5$ at $\sqrt{s} = 2.36$ TeV ([/REF/CMS_2010_S8547297/d05-x01-y04](#))
- Charged hadron p_\perp for $|\eta| = 1.7$ at $\sqrt{s} = 2.36$ TeV ([/REF/CMS_2010_S8547297/d06-x01-y01](#))
- Charged hadron p_\perp for $|\eta| = 1.9$ at $\sqrt{s} = 2.36$ TeV ([/REF/CMS_2010_S8547297/d06-x01-y02](#))
- Charged hadron p_\perp for $|\eta| = 2.1$ at $\sqrt{s} = 2.36$ TeV ([/REF/CMS_2010_S8547297/d06-x01-y03](#))
- Charged hadron p_\perp for $|\eta| = 2.3$ at $\sqrt{s} = 2.36$ TeV ([/REF/CMS_2010_S8547297/d06-x01-y04](#))
- Charged hadron p_\perp for $|\eta| < 2.4$ at $\sqrt{s} = 0.9$ TeV ([/REF/CMS_2010_S8547297/d07-x01-y01](#))
- Charged hadron p_\perp for $|\eta| < 2.4$ at $\sqrt{s} = 2.36$ TeV ([/REF/CMS_2010_S8547297/d07-x01-y02](#))
- Charged hadron η integrated over p_\perp at $\sqrt{s} = 0.9$ TeV ([/REF/CMS_2010_S8547297/d08-x01-y01](#))
- Charged hadron η integrated over p_\perp at $\sqrt{s} = 2.36$ TeV ([/REF/CMS_2010_S8547297/d08-x01-y02](#))

8.81 CMS_2010_S8656010 [146]

Charged particle transverse momentum and pseudorapidity spectra from proton-proton collisions at 7000 GeV.

Beams: $p p$

Energies: (3500.0, 3500.0) GeV

Experiment: CMS (LHC)

Spires ID: [8656010](#)

Status: VALIDATED

Authors:

- A. Knutsson

References:

- Phys.Rev.Lett.105:022002,2010
- DOI: [10.1103/PhysRevLett.105.022002](https://doi.org/10.1103/PhysRevLett.105.022002)
- arXiv: [1005.3299](https://arxiv.org/abs/1005.3299)

Run details:

- Non-single-diffractive (NSD) events only. Should include double-diffractive (DD) events and non-diffractive (ND) events but NOT single-diffractive (SD) events. For example, in Pythia6 the SD processes to be turned off are 92 and 93, and in Pythia8 the SD processes are 103 and 104 (also called SoftQCD:singleDiffractive).

Charged particle spectra are measured in proton-proton collisions at center-of-mass energies 7000 GeV. The spectra are normalized to all non-single-diffractive (NSD) events using corrections for trigger and selection efficiency, acceptance, and branching ratios. There are transverse-momentum (p_{\perp}) spectra from 0.1 to 2 GeV in bins of pseudorapidity (η) and the p_{\perp} spectrum from 0.1 to 6 GeV for $|\eta| < 2.4$. The η spectra come from the average of three methods and cover $|\eta| < 2.5$ and are corrected to include all p_{\perp} . The data were corrected according to the SD/DD/ND content of the CMS trigger, as predicted by PYTHIA6. The uncertainties connected with correct or incorrect modelling of diffraction were included in the systematic errors.

Histograms (14):

- Charged hadron p_{\perp} for $|\eta| = 0.1$ at $\sqrt{s} = 7$ TeV ([/REF/CMS_2010_S8656010/d01-x01-y01](#))
- Charged hadron p_{\perp} for $|\eta| = 0.3$ at $\sqrt{s} = 7$ TeV ([/REF/CMS_2010_S8656010/d01-x01-y02](#))
- Charged hadron p_{\perp} for $|\eta| = 0.5$ at $\sqrt{s} = 7$ TeV ([/REF/CMS_2010_S8656010/d01-x01-y03](#))
- Charged hadron p_{\perp} for $|\eta| = 0.7$ at $\sqrt{s} = 7$ TeV ([/REF/CMS_2010_S8656010/d01-x01-y04](#))
- Charged hadron p_{\perp} for $|\eta| = 0.9$ at $\sqrt{s} = 7$ TeV ([/REF/CMS_2010_S8656010/d02-x01-y01](#))

- Charged hadron p_{\perp} for $|\eta| = 1.1$ at $\sqrt{s} = 7 \text{ TeV}$ ([/REF/CMS_2010_S8656010/d02-x01-y02](#))
- Charged hadron p_{\perp} for $|\eta| = 1.3$ at $\sqrt{s} = 7 \text{ TeV}$ ([/REF/CMS_2010_S8656010/d02-x01-y03](#))
- Charged hadron p_{\perp} for $|\eta| = 1.5$ at $\sqrt{s} = 7 \text{ TeV}$ ([/REF/CMS_2010_S8656010/d02-x01-y04](#))
- Charged hadron p_{\perp} for $|\eta| = 1.7$ at $\sqrt{s} = 7 \text{ TeV}$ ([/REF/CMS_2010_S8656010/d03-x01-y01](#))
- Charged hadron p_{\perp} for $|\eta| = 1.9$ at $\sqrt{s} = 7 \text{ TeV}$ ([/REF/CMS_2010_S8656010/d03-x01-y02](#))
- Charged hadron p_{\perp} for $|\eta| = 2.1$ at $\sqrt{s} = 7 \text{ TeV}$ ([/REF/CMS_2010_S8656010/d03-x01-y03](#))
- Charged hadron p_{\perp} for $|\eta| = 2.3$ at $\sqrt{s} = 7 \text{ TeV}$ ([/REF/CMS_2010_S8656010/d03-x01-y04](#))
- Charged hadron p_{\perp} for $|\eta| < 2.4$ at $\sqrt{s} = 7 \text{ TeV}$ ([/REF/CMS_2010_S8656010/d04-x01-y01](#))
- Charged hadron η integrated over p_{\perp} at $\sqrt{s} = 7 \text{ TeV}$ ([/REF/CMS_2010_S8656010/d05-x01-y01](#))

8.82 CMS_2011_I954992 [147]

Exclusive photon-photon production of muon pairs in proton-proton collisions at $\sqrt{s} = 7$ TeV

Beams: pp

Energies: (3500.0, 3500.0) GeV

Experiment: CMS (LHC)

Inspire ID: [954992](#)

Status: VALIDATED

Authors:

- David d'Enterria (dde@cern.ch)
- Jonathan Hollar (jjhollar@mail.cern.ch)
- Sercan Sen (Sercan.Sen@cern.ch)

References:

- arXiv: [1111.5536](#)

Run details:

- gamma gamma TO mu+ mu- process.

A measurement of the exclusive two-photon production of muon pairs in proton-proton collisions at a centre-of-mass energy 7 TeV with the final state $\mu^+\mu^-p$, is reported using data corresponding to an integrated luminosity of 40 pb^{-1} collected in 2010. The measured cross section is obtained with a fit to the dimuon p_T distribution for muon pairs with invariant mass greater than 11.5 GeV with each muon $p_T > 4$ GeV and $|\eta| < 2.1$.

Histograms (1):

- Exclusive $\gamma\gamma$ production of muon pairs ([/REF/CMS_2011_I954992/d01-x01-y01](#))

8.83 CMS_2011_S8884919 [148]

Measurement of the NSD charged particle multiplicity at $\sqrt{s} = 0.9$, **2.36**, and **7 TeV** with the CMS detector.

Beams: $p p$

Energies: (450.0, 450.0), (1180.0, 1180.0), (3500.0, 3500.0) GeV

Experiment: CMS (LHC)

Spires ID: [8884919](#)

Status: VALIDATED

Authors:

- Romain Rougny <romain.rougny@cern.ch>

References:

- J. High Energy Phys. 01 (2011) 079
- DOI: [10.1007/JHEP01\(2011\)079](https://doi.org/10.1007/JHEP01(2011)079)
- arXiv: [1011.5531](https://arxiv.org/abs/1011.5531)

Run details:

- Non-single-diffractive (NSD) events only. Should include double-diffractive (DD) events and non-diffractive (ND) events but NOT single-diffractive (SD) events. For example, in Pythia6 the SD processes to be turned off are 92 and 93 and in Pythia8 the SD processes are 103 and 104 (also called SoftQCD:singleDiffractive).

Measurements of primary charged hadron multiplicity distributions are presented for non-single-diffractive events in proton-proton collisions at centre-of-mass energies of $\sqrt{s} = 0.9$, 2.36, and 7 TeV, in five pseudorapidity ranges from $|\eta| < 0.5$ to $|\eta| < 2.4$. The data were collected with the minimum-bias trigger of the CMS experiment during the LHC commissioning runs in 2009 and the 7 TeV run in 2010. The average transverse momentum as a function of the multiplicity is also presented. The measurement of higher-order moments of the multiplicity distribution confirms the violation of Koba-Nielsen-Olesen scaling that has been observed at lower energies.

Histograms (21):

- Charged hadron multiplicity, $|\eta| < 0.5$, $\sqrt{s} = 0.9$ TeV ([/REF/CMS_2011_S8884919/d02-x01-y01](#))
- Charged hadron multiplicity, $|\eta| < 1.0$, $\sqrt{s} = 0.9$ TeV ([/REF/CMS_2011_S8884919/d03-x01-y01](#))
- Charged hadron multiplicity, $|\eta| < 1.5$, $\sqrt{s} = 0.9$ TeV ([/REF/CMS_2011_S8884919/d04-x01-y01](#))
- Charged hadron multiplicity, $|\eta| < 2.0$, $\sqrt{s} = 0.9$ TeV ([/REF/CMS_2011_S8884919/d05-x01-y01](#))
- Charged hadron multiplicity, $|\eta| < 2.4$, $\sqrt{s} = 0.9$ TeV ([/REF/CMS_2011_S8884919/d06-x01-y01](#))
- Charged hadron multiplicity, $|\eta| < 0.5$, $\sqrt{s} = 2.36$ TeV ([/REF/CMS_2011_S8884919/d07-x01-y01](#))

- Charged hadron multiplicity, $|\eta| < 1.0$, $\sqrt{s} = 2.36 \text{ TeV}$ ([/REF/CMS_2011_S8884919/d08-x01-y01](#))
- Charged hadron multiplicity, $|\eta| < 1.5$, $\sqrt{s} = 2.36 \text{ TeV}$ ([/REF/CMS_2011_S8884919/d09-x01-y01](#))
- Charged hadron multiplicity, $|\eta| < 2.0$, $\sqrt{s} = 2.36 \text{ TeV}$ ([/REF/CMS_2011_S8884919/d10-x01-y01](#))
- Charged hadron multiplicity, $|\eta| < 2.4$, $\sqrt{s} = 2.36 \text{ TeV}$ ([/REF/CMS_2011_S8884919/d11-x01-y01](#))
- Charged hadron multiplicity, $|\eta| < 0.5$, $\sqrt{s} = 7 \text{ TeV}$ ([/REF/CMS_2011_S8884919/d12-x01-y01](#))
- Charged hadron multiplicity, $|\eta| < 1.0$, $\sqrt{s} = 7 \text{ TeV}$ ([/REF/CMS_2011_S8884919/d13-x01-y01](#))
- Charged hadron multiplicity, $|\eta| < 1.5$, $\sqrt{s} = 7 \text{ TeV}$ ([/REF/CMS_2011_S8884919/d14-x01-y01](#))
- Charged hadron multiplicity, $|\eta| < 2.0$, $\sqrt{s} = 7 \text{ TeV}$ ([/REF/CMS_2011_S8884919/d15-x01-y01](#))
- Charged hadron multiplicity, $|\eta| < 2.4$, $\sqrt{s} = 7 \text{ TeV}$ ([/REF/CMS_2011_S8884919/d16-x01-y01](#))
- Charged hadron multiplicity, $p_{\perp} > 500 \text{ GeV}$, $|\eta| < 2.4$, $\sqrt{s} = 0.9 \text{ TeV}$ ([/REF/CMS_2011_S8884919/d20-x01-y01](#))
- Charged hadron multiplicity, $p_{\perp} > 500 \text{ GeV}$, $|\eta| < 2.4$, $\sqrt{s} = 2.36 \text{ TeV}$ ([/REF/CMS_2011_S8884919/d21-x01-y01](#))
- Charged hadron multiplicity, $p_{\perp} > 500 \text{ GeV}$, $|\eta| < 2.4$, $\sqrt{s} = 7 \text{ TeV}$ ([/REF/CMS_2011_S8884919/d22-x01-y01](#))
- Mean p_{\perp} vs charged hadron multiplicity, $|\eta| < 2.4$, $\sqrt{s} = 0.9 \text{ TeV}$ ([/REF/CMS_2011_S8884919/d23-x01-y01](#))
- Mean p_{\perp} vs charged hadron multiplicity, $|\eta| < 2.4$, $\sqrt{s} = 2.36 \text{ TeV}$ ([/REF/CMS_2011_S8884919/d24-x01-y01](#))
- Mean p_{\perp} vs charged hadron multiplicity, $|\eta| < 2.4$, $\sqrt{s} = 7 \text{ TeV}$ ([/REF/CMS_2011_S8884919/d25-x01-y01](#))

8.84 CMS_2011_S8941262 [149]

Production cross-sections of muons from b hadron decays in pp collisions

Beams: pp

Energies: (3500.0, 3500.0) GeV

Experiment: CMS (LHC)

Spires ID: [8941262](#)

Status: VALIDATED

Authors:

- Wolfram Erdmann (wolfram.erdmann@psi.ch)

References:

- JHEP 1103,090
- DOI: [10.1007/JHEP03\(2011\)090](https://doi.org/10.1007/JHEP03(2011)090)
- arXiv: [hep-ex/1101.3512](https://arxiv.org/abs/hep-ex/1101.3512)

Run details:

- Inclusive QCD at 7 TeV, with no p_{\perp} cuts.

A measurement of the b -hadron production cross-section in proton-proton collisions at $\sqrt{s} = 7$ TeV. The dataset, corresponding to 85 inverse nanobarns, was recorded with the CMS experiment at the LHC using a low-threshold single-muon trigger. Events are selected by the presence of a muon with transverse momentum greater than 6 GeV with respect to the beam direction and pseudorapidity less than 2.1. The transverse momentum of the muon with respect to the closest jet discriminates events containing b hadrons from background. The inclusive b -hadron production cross section is presented as a function of muon transverse momentum and pseudorapidity.

Histograms (3):

- Inclusive b -hadron production with muons, $p_{\perp}^{\mu} > 6$ GeV, $|\eta^{\mu}| < 2.1$ ([/REF/CMS_2011_S8941262/d01-x01-y01](#))
- Inclusive b -hadron production with muons, $|\eta^{\mu}| < 2.1$ ([/REF/CMS_2011_S8941262/d02-x01-y01](#))
- Inclusive b -hadron production with muons, $p_{\perp}^{\mu} > 6$ GeV ([/REF/CMS_2011_S8941262/d03-x01-y01](#))

8.85 CMS_2011_S8950903 [150]

Dijet azimuthal decorrelations in pp collisions at $\sqrt{s} = 7$ TeV

Beams: pp

Energies: (3500.0, 3500.0) GeV

Experiment: CMS (LHC)

Spires ID: [8950903](#)

Status: VALIDATED

Authors:

- Tomo Umer (tomo.umer@cern.ch)

References:

- Phys. Rev. Lett. 106 (2011) 122003
- arXiv: [1101.5029](#)

Run details:

- Inclusive QCD at $\sqrt{s} = 7$ TeV, p_{\perp} (or equivalent) greater than 20 GeV
Measurements of dijet azimuthal decorrelations in pp collisions at $\sqrt{s} = 7$ TeV using the CMS detector at the CERN LHC are presented. The analysis is based on an inclusive dijet event sample corresponding to an integrated luminosity of 2.9/pb. Jets are anti- k_t with $R = 0.5$, $p_{\perp} > 80(30)$ GeV and $|\eta| < 1.1$.

Histograms (5):

- Di-jet azimuthal decorrelation, $80 < p_T^{\text{leading}} < 110$ GeV ([/REF/CMS_2011_S8950903/d01-x01-y01](#))
- Di-jet azimuthal decorrelation, $110 < p_T^{\text{leading}} < 140$ GeV ([/REF/CMS_2011_S8950903/d02-x01-y01](#))
- Di-jet azimuthal decorrelation, $140 < p_T^{\text{leading}} < 200$ GeV ([/REF/CMS_2011_S8950903/d03-x01-y01](#))
- Di-jet azimuthal decorrelation, $200 < p_T^{\text{leading}} < 300$ GeV ([/REF/CMS_2011_S8950903/d04-x01-y01](#))
- Di-jet azimuthal decorrelation, $p_T^{\text{leading}} > 300$ GeV ([/REF/CMS_2011_S8950903/d05-x01-y01](#))

8.86 CMS_2011_S8957746 [151]

Event shapes

Beams: pp

Energies: (3500.0, 3500.0) GeV

Experiment: CMS (LHC)

Spires ID: 8957746

Status: VALIDATED

Authors:

- Hendrik Hoeth (hendrik.hoeth@cern.ch)

References:

- Phys.Lett.B699:48-67,2011
- arXiv: [1102.0068](#)

Run details:

- pp QCD interactions at 7000 GeV. Particles with $c^*\tau_{\ell} < 10\text{mm}$ are stable.

Central transverse Thrust and Minor have been measured in proton-proton collisions at $\sqrt{s} = 7\text{ TeV}$, with a data sample collected with the CMS detector at the LHC. The sample corresponds to an integrated luminosity of 3.2 inverse picobarns. Input for the variables are anti- k_t jets with $R = 0.5$.

Histograms (6):

- Central Transv. Thrust, $90\text{ GeV} < p_{\perp}^{\text{jet } 1} < 125\text{ GeV}$, $\sqrt{s} = 7\text{ TeV}$ ([/REF/CMS_2011-S8957746/d01-x01-y01](#))
- Central Transv. Minor, $90\text{ GeV} < p_{\perp}^{\text{jet } 1} < 125\text{ GeV}$, $\sqrt{s} = 7\text{ TeV}$ ([/REF/CMS_2011-S8957746/d02-x01-y01](#))
- Central Transv. Thrust, $125\text{ GeV} < p_{\perp}^{\text{jet } 1} < 200\text{ GeV}$, $\sqrt{s} = 7\text{ TeV}$ ([/REF/CMS_2011-S8957746/d03-x01-y01](#))
- Central Transv. Minor, $125\text{ GeV} < p_{\perp}^{\text{jet } 1} < 200\text{ GeV}$, $\sqrt{s} = 7\text{ TeV}$ ([/REF/CMS_2011-S8957746/d04-x01-y01](#))
- Central Transv. Thrust, $p_{\perp}^{\text{jet } 1} > 200\text{ GeV}$, $\sqrt{s} = 7\text{ TeV}$ ([/REF/CMS_2011_S8957746/d05-x01-y01](#))
- Central Transv. Minor, $p_{\perp}^{\text{jet } 1} > 200\text{ GeV}$, $\sqrt{s} = 7\text{ TeV}$ ([/REF/CMS_2011_S8957746/d06-x01-y01](#))

8.87 CMS_2011_S8968497 [152]

Measurement of dijet angular distributions and search for quark compositeness in pp collisions at $\sqrt{s} = 7$ TeV

Beams: pp

Energies: (3500.0, 3500.0) GeV

Experiment: CMS (LHC)

Spires ID: [8968497](#)

Status: VALIDATED

Authors:

- A. Hinzmann

References:

- Phys.Rev.Lett.106:201804,2011
- DOI: [10.1103/PhysRevLett.106.201804](https://doi.org/10.1103/PhysRevLett.106.201804)
- arXiv: [hep-ex/1102.2020](https://arxiv.org/abs/hep-ex/1102.2020)

No run details listed

Measurement of dijet angular distributions in proton-proton collisions at a center-of-mass energy of 7 TeV. The data sample, collected with single jet triggers, has a total integrated luminosity of 36 pb^{-1} , with jets being reconstructed using the anti- k_t clustering algorithm with $R = 0.5$. The data are presented for the variable χ defined as $\chi = \exp(|y_1 - y_2|)$ where y_1 and y_2 are the rapidities of the two leading (highest p_\perp) jets.'

Histograms (9):

- χ_{dijet} for $M_{jj} > 2.2 \text{ TeV}$, $|y_1 + y_2|/2 < 1.11$, $\sqrt{s} = 7 \text{ TeV}$ ([/REF/CMS_2011_S8968497/d01-x01-y01](#))
- χ_{dijet} for $1.8 \text{ TeV} < M_{jj} < 2.2 \text{ TeV}$, $|y_1 + y_2|/2 < 1.11$, $\sqrt{s} = 7 \text{ TeV}$ ([/REF/CMS_2011_S8968497/d02-x01-y01](#))
- χ_{dijet} for $1.4 \text{ TeV} < M_{jj} < 1.8 \text{ TeV}$, $|y_1 + y_2|/2 < 1.11$, $\sqrt{s} = 7 \text{ TeV}$ ([/REF/CMS_2011_S8968497/d03-x01-y01](#))
- χ_{dijet} for $1.1 \text{ TeV} < M_{jj} < 1.4 \text{ TeV}$, $|y_1 + y_2|/2 < 1.11$, $\sqrt{s} = 7 \text{ TeV}$ ([/REF/CMS_2011_S8968497/d04-x01-y01](#))
- χ_{dijet} for $0.85 \text{ TeV} < M_{jj} < 1.1 \text{ TeV}$, $|y_1 + y_2|/2 < 1.11$, $\sqrt{s} = 7 \text{ TeV}$ ([/REF/CMS_2011_S8968497/d05-x01-y01](#))
- χ_{dijet} for $0.65 \text{ TeV} < M_{jj} < 0.85 \text{ TeV}$, $|y_1 + y_2|/2 < 1.11$, $\sqrt{s} = 7 \text{ TeV}$ ([/REF/CMS_2011_S8968497/d06-x01-y01](#))
- χ_{dijet} for $0.5 \text{ TeV} < M_{jj} < 0.65 \text{ TeV}$, $|y_1 + y_2|/2 < 1.11$, $\sqrt{s} = 7 \text{ TeV}$ ([/REF/CMS_2011_S8968497/d07-x01-y01](#))

- χ_{dijet} for $0.35 \text{ TeV} < M_{jj} < 0.5 \text{ TeV}$, $|y_1 + y_2|/2 < 1.11$, $\sqrt{s} = 7 \text{ TeV}$ ([/REF/CMS_2011-S8968497/d08-x01-y01](#))
- χ_{dijet} for $0.25 \text{ TeV} < M_{jj} < 0.35 \text{ TeV}$, $|y_1 + y_2|/2 < 1.11$, $\sqrt{s} = 7 \text{ TeV}$ ([/REF/CMS_2011-S8968497/d09-x01-y01](#))

8.88 CMS_2011_S8973270 [153]

B/\bar{B} angular correlations based on secondary vertex reconstruction in pp collisions

Beams: pp

Energies: (3500.0, 3500.0) GeV

Experiment: CMS (LHC)

Spires ID: [8973270](#)

Status: VALIDATED

Authors:

- Lukas Wehrli ⟨ wehrli@cern.ch ⟩

References:

- JHEP 1103 136
- DOI: [10.1007/JHEP03\(2011\)136](https://doi.org/10.1007/JHEP03(2011)136)
- arXiv: [hep-ex/1102.3194](https://arxiv.org/abs/hep-ex/1102.3194)

Run details:

- Inclusive QCD at 7 TeV. A \hat{p}_\perp cut (or similar) is recommended since a leading jet $p_\perp > 56$ GeV is required.

The differential $B\bar{B}$ cross-section is measured as a function of the opening angle ΔR and $\Delta\phi$ using data collected with the CMS detector during 2010 and corresponding to an integrated luminosity of 3.1 pb^{-1} . The measurement is performed for three different event energy scales, characterized by the transverse momentum of the leading jet in the event (above 56 GeV, above 84 GeV and above 120 GeV). Simulated events are normalised in the region $\Delta R > 2.4$ and $\Delta\phi > 3/4\pi$ respectively.

Histograms (6):

- $B\bar{B}$ production cross-section (leading jet $p_\perp > 56$ GeV) ([/REF/CMS_2011_S8973270/d01-x01-y01](#))
- $B\bar{B}$ production cross-section (leading jet $p_\perp > 84$ GeV) ([/REF/CMS_2011_S8973270/d02-x01-y01](#))
- $B\bar{B}$ production cross-section (leading jet $p_\perp > 120$ GeV) ([/REF/CMS_2011_S8973270/d03-x01-y01](#))
- $B\bar{B}$ production cross-section (leading jet $p_\perp > 56$ GeV) ([/REF/CMS_2011_S8973270/d04-x01-y01](#))
- $B\bar{B}$ production cross-section (leading jet $p_\perp > 84$ GeV) ([/REF/CMS_2011_S8973270/d05-x01-y01](#))
- $B\bar{B}$ production cross-section (leading jet $p_\perp > 120$ GeV) ([/REF/CMS_2011_S8973270/d06-x01-y01](#))

8.89 CMS_2011_S8978280 [154]

K_s , Λ , and Cascade– transverse momentum and rapidity spectra at 900 and 7000 GeV.

Beams: pp

Energies: (450.0, 450.0), (3500.0, 3500.0) GeV

Experiment: CMS (LHC)

Spires ID: [8978280](#)

Status: VALIDATED

Authors:

- Kevin Stenson (kevin.stenson@colorado.edu)

References:

- JHEP 05 (2011) 064
- DOI: [10.1007/JHEP05\(2011\)064](https://doi.org/10.1007/JHEP05(2011)064)
- arXiv: [1102.4282](https://arxiv.org/abs/1102.4282)

Run details:

- Non-single-diffractive (NSD) events only. Should include double-diffractive (DD) events and non-diffractive (ND) events but NOT single-diffractive (SD) events. For example, in Pythia6 the SD processes to be turned off are 92 and 93, and in Pythia8 the SD processes are 103 and 104 (also called SoftQCD:singleDiffractive).

The spectra of K_S , Λ , and Cascade– particles were measured versus transverse-momentum (p_\perp) and rapidity (y) in proton-proton collisions at center-of-mass energies 900 and 7000 GeV. The production is normalized to all non-single-diffractive (NSD) events using corrections for trigger and selection efficiency, acceptance, and branching ratios. The results cover a rapidity range of $|y| < 2$ and a p_\perp range from 0 to 10 GeV (K_S and Λ) and 0 to 6 GeV (Cascade–). Antiparticles are included in all measurements so only the sums of Λ and $\bar{\Lambda}$, and Cascade– and anti-Cascade– are given. The rapidity distributions are shown versus $|y|$ but normalized to a unit of y . Ratios of Λ/K_S and Cascade–/ Λ production versus p_\perp and $|y|$ are also given, with somewhat smaller systematic uncertainties than obtained from taking the ratio of the individual distributions.¹ The data were corrected according to the SD/DD/ND content of the CMS trigger, as predicted by PYTHIA6. The uncertainties connected with correct or uncorrect modelling of diffraction were included in the systematic errors.

Histograms (20):

- K_S^0 rapidity distribution at $\sqrt{s} = 0.9$ TeV ([/REF/CMS_2011_S8978280/d01-x01-y01](#))
- K_S^0 rapidity distribution at $\sqrt{s} = 7$ TeV ([/REF/CMS_2011_S8978280/d01-x01-y02](#))
- K_S^0 transverse momentum distribution at $\sqrt{s} = 0.9$ TeV ([/REF/CMS_2011_S8978280/d02-x01-y01](#))

- K_S^0 transverse momentum distribution at $\sqrt{s} = 7$ TeV ([/REF/CMS_2011_S8978280/d02-x01-y02](#))
- Λ rapidity distribution at $\sqrt{s} = 0.9$ TeV ([/REF/CMS_2011_S8978280/d03-x01-y01](#))
- Λ rapidity distribution at $\sqrt{s} = 7$ TeV ([/REF/CMS_2011_S8978280/d03-x01-y02](#))
- Λ transverse momentum distribution at $\sqrt{s} = 0.9$ TeV ([/REF/CMS_2011_S8978280/d04-x01-y01](#))
- Λ transverse momentum distribution at $\sqrt{s} = 7$ TeV ([/REF/CMS_2011_S8978280/d04-x01-y02](#))
- Ξ^- rapidity distribution at $\sqrt{s} = 0.9$ TeV ([/REF/CMS_2011_S8978280/d05-x01-y01](#))
- Ξ^- rapidity distribution at $\sqrt{s} = 7$ TeV ([/REF/CMS_2011_S8978280/d05-x01-y02](#))
- Ξ^- transverse momentum distribution at $\sqrt{s} = 0.9$ TeV ([/REF/CMS_2011_S8978280/d06-x01-y01](#))
- Ξ^- transverse momentum distribution at $\sqrt{s} = 7$ TeV ([/REF/CMS_2011_S8978280/d06-x01-y02](#))
- Λ/K_S^0 versus transverse momentum at $\sqrt{s} = 0.9$ TeV ([/REF/CMS_2011_S8978280/d07-x01-y01](#))
- Λ/K_S^0 versus transverse momentum at $\sqrt{s} = 7$ TeV ([/REF/CMS_2011_S8978280/d07-x01-y02](#))
- Ξ^-/Λ versus transverse momentum at $\sqrt{s} = 0.9$ TeV ([/REF/CMS_2011_S8978280/d08-x01-y01](#))
- Ξ^-/Λ versus transverse momentum at $\sqrt{s} = 7$ TeV ([/REF/CMS_2011_S8978280/d08-x01-y02](#))
- Λ/K_S^0 versus rapidity at $\sqrt{s} = 0.9$ TeV ([/REF/CMS_2011_S8978280/d09-x01-y01](#))
- Λ/K_S^0 versus rapidity at $\sqrt{s} = 7$ TeV ([/REF/CMS_2011_S8978280/d09-x01-y02](#))
- Ξ^-/Λ versus rapidity at $\sqrt{s} = 0.9$ TeV ([/REF/CMS_2011_S8978280/d10-x01-y01](#))
- Ξ^-/Λ versus rapidity at $\sqrt{s} = 7$ TeV ([/REF/CMS_2011_S8978280/d10-x01-y02](#))

8.90 CMS_2011_S9086218 [155]

Measurement of the inclusive jet cross-section in pp collisions at $\sqrt{s} = 7$ TeV

Beams: pp

Energies: (3500.0, 3500.0) GeV

Experiment: CMS (LHC)

Spires ID: 9086218

Status: VALIDATED

Authors:

- Rasmus Sloth Hansen rsh07@phys.au.dk

References:

- <http://cdsweb.cern.ch/record/1355680>

Run details:

- Inclusive QCD at 7TeV comEnergy, ptHat (or equivalent) greater than 10 GeV

The inclusive jet cross section is measured in pp collisions with a center-of-mass energy of 7 TeV at the LHC using the CMS experiment. The data sample corresponds to an integrated luminosity of 34 inverse picobarns. The measurement is made for jet transverse momenta in the range 18-1100 GeV and for absolute values of rapidity less than 3. Jets are anti-kt with $R = 0.5$, $p_{\perp} > 18$ GeV and $|y| < 3.0$.

Histograms (6):

- Inclusive jets, $0.0 < |y| < 0.5$ ([/REF/CMS_2011_S9086218/d01-x01-y01](#))
- Inclusive jets, $0.5 < |y| < 1.0$ ([/REF/CMS_2011_S9086218/d02-x01-y01](#))
- Inclusive jets, $1.0 < |y| < 1.5$ ([/REF/CMS_2011_S9086218/d03-x01-y01](#))
- Inclusive jets, $1.5 < |y| < 2.0$ ([/REF/CMS_2011_S9086218/d04-x01-y01](#))
- Inclusive jets, $2.0 < |y| < 2.5$ ([/REF/CMS_2011_S9086218/d05-x01-y01](#))
- Inclusive jets, $2.5 < |y| < 3.0$ ([/REF/CMS_2011_S9086218/d06-x01-y01](#))

8.91 CMS_2011_S9088458 [156]

Measurement of ratio of the 3-jet over 2-jet cross section in pp collisions at $\sqrt{s} = 7$ TeV

Beams: pp

Energies: (3500.0, 3500.0) GeV

Experiment: CMS (LHC)

Spires ID: [9088458](#)

Status: VALIDATED

Authors:

- Tomo Umer (tomo.umer@cern.ch)

References:

- Phys. Lett. B 702 (2011) 336

Run details:

- Inclusive QCD at 7 TeV. p_T^γ (or equivalent) greater than 30 GeV

A measurement of the ratio of the inclusive 3-jet to 2-jet cross sections as a function of the total jet transverse momentum, H_T , in the range $0.2 < H_T < 2.5$ TeV is presented. The data have been collected at a proton–proton centre-of-mass energy of 7 TeV with the CMS detector at the LHC, and correspond to an integrated luminosity of 36/pb. Jets are anti- k_t with $R = 0.5$, $p_T > 50$ GeV and $|\eta| < 2.5$.

Histograms (1):

- 3 jets over 2 jets ratio ([/REF/CMS_2011_S9088458/d01-x01-y01](#))

8.92 CMS_2011_S9120041 [157]

Traditional leading jet UE measurement at $\sqrt{s} = 0.9$ and 7 TeV

Beams: pp

Energies: (450.0, 450.0), (3500.0, 3500.0) GeV

Experiment: CMS (LHC)

Spires ID: 9120041

Status: VALIDATED

Authors:

- Mohammed Zakaria (mzakaria@ufl.edu)

References:

- J. High Energy Phys 09 (2011) 109

Run details:

- Requires inclusive inelastic events (non-diffractive and inelastic diffractive). The profile plots require large statistics.

A measurement of the underlying activity in scattering processes with a hard scale in the several-GeV region is performed in proton-proton collisions at Energies of 0.9 and 7 TeV, using data collected by the CMS experiment at the LHC. The production of charged particles with pseudorapidity $-|\eta| < 2$ and transverse momentum $p_T > 0.5$ GeV/ c is studied in the azimuthal region transverse to that of the leading set of charged particles forming a track-jet. Various comparisons are made between the two different energies and also between two sets of cuts on p_T for leading track jet p_T -leading > 3 GeV and p_T -leading > 20 GeV. The activity is studied using 5 types of plots. Two profile plots for the multiplicity of charged particles and the scalar sum of p_T , and three distributions for the two previous quantities as well as p_T for all the particles in the transverse region.

Histograms (13):

- Transverse N_{ch} density vs. $p_T^{\text{jet } 1}$, $\sqrt{s} = 7000$ GeV ([/REF/CMS_2011_S9120041/d01-x01-y01](#))
- Transverse $\sum p_T$ density vs. $p_T^{\text{jet } 1}$, $\sqrt{s} = 7000$ GeV ([/REF/CMS_2011_S9120041/d02-x01-y01](#))
- Transverse N_{ch} density vs. $p_T^{\text{jet } 1}$, $\sqrt{s} = 900$ GeV ([/REF/CMS_2011_S9120041/d03-x01-y01](#))
- Transverse $\sum p_T$ density vs. $p_T^{\text{jet } 1}$, $\sqrt{s} = 900$ GeV ([/REF/CMS_2011_S9120041/d04-x01-y01](#))
- Transverse charged multiplicity, $p_T^{\text{jet } 1} > 3$ GeV, $\sqrt{s} = 7000$ GeV ([/REF/CMS_2011_S9120041/d05-x01-y01](#))
- Transverse $\sum p_T$, $p_T^{\text{jet } 1} > 3$ GeV, $\sqrt{s} = 7000$ GeV ([/REF/CMS_2011_S9120041/d06-x01-y01](#))
- Transverse p_T , $p_T^{\text{jet } 1} > 3$ GeV, $\sqrt{s} = 7000$ GeV ([/REF/CMS_2011_S9120041/d07-x01-y01](#))

- Transverse charged multiplicity, $p_{\perp}^{\text{jet } 1} > 20 \text{ GeV}, \sqrt{s} = 7000 \text{ GeV}$ ([/REF/CMS_2011_S9120041/d08-x01-y01](#))
- Transverse $\sum p_{\perp}, p_{\perp}^{\text{jet } 1} > 20 \text{ GeV}, \sqrt{s} = 7000 \text{ GeV}$ ([/REF/CMS_2011_S9120041/d09-x01-y01](#))
- Transverse $p_{\perp}, p_{\perp}^{\text{jet } 1} > 20 \text{ GeV}, \sqrt{s} = 7000 \text{ GeV}$ ([/REF/CMS_2011_S9120041/d10-x01-y01](#))
- Transverse charged multiplicity, $p_{\perp}^{\text{jet } 1} > 3 \text{ GeV}, \sqrt{s} = 900 \text{ GeV}$ ([/REF/CMS_2011_S9120041/d11-x01-y01](#))
- Transverse $\sum p_{\perp}, p_{\perp}^{\text{jet } 1} > 3 \text{ GeV}, \sqrt{s} = 900 \text{ GeV}$ ([/REF/CMS_2011_S9120041/d12-x01-y01](#))
- Transverse $p_{\perp}, p_{\perp}^{\text{jet } 1} > 3 \text{ GeV}, \sqrt{s} = 900 \text{ GeV}$ ([/REF/CMS_2011_S9120041/d13-x01-y01](#))

8.93 CMS_2011_S9215166 [158]

Forward energy flow in MB and dijet events at 0.9 and 7 TeV

Beams: pp

Energies: (450.0, 450.0), (3500.0, 3500.0) GeV

Experiment: CMS (LHC)

Spires ID: [9215166](#)

Status: VALIDATED

Authors:

- S. Dooling <samantha.dooling@cern.ch>
- A. Knutsson <albert.knutsson@cern.ch>

References:

- JHEP 1111 148
- DOI: [10.1007/JHEP11\(2011\)148](https://doi.org/10.1007/JHEP11(2011)148)
- arXiv: [hep-ex/1110.0211](https://arxiv.org/abs/hep-ex/1110.0211)

Run details:

- pp MB and QCD interactions at 0.9 and 7 TeV. No p_{\perp} -cuts.

Forward energy flow measured by CMS at $\sqrt{s} = 0.9$ and 7 TeV in MB and dijet events.

Histograms (4):

- Energy flow in MB events, $\sqrt{s} = 0.9$ TeV ([/REF/CMS_2011_S9215166/d01-x01-y01](#))
- Energy flow in dijet events, $\sqrt{s} = 0.9$ TeV, $p_{\perp}^{\text{jets}} > 8$ GeV ([/REF/CMS_2011_S9215166/d02-x01-y01](#))
- Energy flow in MB events, $\sqrt{s} = 7$ TeV ([/REF/CMS_2011_S9215166/d03-x01-y01](#))
- Energy flow in dijet events, $\sqrt{s} = 7$ TeV, $p_{\perp}^{\text{jets}} > 20$ GeV ([/REF/CMS_2011_S9215166/d04-x01-y01](#))

8.94 CMS_2012_I1087342 [159]

Measurement of forward and forward+central jets at $\sqrt{s} = 7$ TeV

Beams: pp

Energies: (3500.0, 3500.0) GeV

Experiment: CMS (LHC)

Inspire ID: [1087342](#)

Status: VALIDATED

Authors:

- Albert Knutsson <albert.knutsson@cern.ch>
- Rasmus Sloth Hansen <rsh07@phys.au.dk>
- Bo Zhu

References:

- JHEP 1206 (2012) 036
- CMS-FWD-11-002
- CERN-PH-EP-2011-179
- doi [10.1007/JHEP06\(2012\)036](https://doi.org/10.1007/JHEP06(2012)036)
- arXiv: [1202.0704](#)

Run details:

- pp QCD interactions at 7 TeV.

Inclusive forward jets and forward+central jets measured by CMS at $\sqrt{s} = 7$ TeV.

Histograms (3):

- Measurement of forward jets in pp collisions at $\sqrt{s} = 7$ TeV ([/REF/CMS_2012_I1087342/d01-x01-y01](#))
- Measurement of forward+central jets at $\sqrt{s} = 7$ TeV ([/REF/CMS_2012_I1087342/d02-x01-y01](#))
- Measurement of forward+central jets at $\sqrt{s} = 7$ TeV ([/REF/CMS_2012_I1087342/d03-x01-y01](#))

8.95 CMS_2012_I1090423 [160]

Dijet angular distributions in pp collisions at $\sqrt{s} = 7$ TeV

Beams: pp

Energies: (3500.0, 3500.0) GeV

Experiment: CMS (LHC)

Spires ID: [1090423](#)

Status: VALIDATED

Authors:

- A. Hinzmann

References:

- JHEP 05 (2012) 055
- DOI: [10.1007/JHEP05\(2012\)055](https://doi.org/10.1007/JHEP05(2012)055)
- arXiv: [hep-ex/1202.5535](https://arxiv.org/abs/hep-ex/1202.5535)

No run details listed

Measurement of dijet angular distributions in proton-proton collisions at a center-of-mass energy of 7 TeV. The data sample has a total integrated luminosity of 2.2 inverse femtobarns, recorded by the CMS experiment at the LHC. Normalized dijet angular distributions have been measured for dijet invariant masses from 0.4 TeV to above 3 TeV.

Histograms (9):

- χ_{dijet} for $M_{jj} > 3.0$ TeV, $|y_1 + y_2|/2 < 1.11$, $\sqrt{s} = 7$ TeV ([/REF/CMS_2012_I1090423/d01-x01-y01](#))
- χ_{dijet} for $2.4 \text{ TeV} < M_{jj} < 3.0 \text{ TeV}$, $|y_1 + y_2|/2 < 1.11$, $\sqrt{s} = 7$ TeV ([/REF/CMS_2012_I1090423/d02-x01-y01](#))
- χ_{dijet} for $1.9 \text{ TeV} < M_{jj} < 2.4 \text{ TeV}$, $|y_1 + y_2|/2 < 1.11$, $\sqrt{s} = 7$ TeV ([/REF/CMS_2012_I1090423/d03-x01-y01](#))
- χ_{dijet} for $1.5 \text{ TeV} < M_{jj} < 1.9 \text{ TeV}$, $|y_1 + y_2|/2 < 1.11$, $\sqrt{s} = 7$ TeV ([/REF/CMS_2012_I1090423/d04-x01-y01](#))
- χ_{dijet} for $1.2 \text{ TeV} < M_{jj} < 1.5 \text{ TeV}$, $|y_1 + y_2|/2 < 1.11$, $\sqrt{s} = 7$ TeV ([/REF/CMS_2012_I1090423/d05-x01-y01](#))
- χ_{dijet} for $1.0 \text{ TeV} < M_{jj} < 1.2 \text{ TeV}$, $|y_1 + y_2|/2 < 1.11$, $\sqrt{s} = 7$ TeV ([/REF/CMS_2012_I1090423/d06-x01-y01](#))
- χ_{dijet} for $0.8 \text{ TeV} < M_{jj} < 1.0 \text{ TeV}$, $|y_1 + y_2|/2 < 1.11$, $\sqrt{s} = 7$ TeV ([/REF/CMS_2012_I1090423/d07-x01-y01](#))

- χ_{dijet} for $0.6 \text{ TeV} < M_{jj} < 0.8 \text{ TeV}$, $|y_1 + y_2|/2 < 1.11$, $\sqrt{s} = 7 \text{ TeV}$ ([/REF/CMS_2012-I1090423/d08-x01-y01](#))
- χ_{dijet} for $0.4 \text{ TeV} < M_{jj} < 0.6 \text{ TeV}$, $|y_1 + y_2|/2 < 1.11$, $\sqrt{s} = 7 \text{ TeV}$ ([/REF/CMS_2012-I1090423/d09-x01-y01](#))

8.96 CMS_2012_I1102908 [161]

Measurement of inclusive and exclusive dijet production ratio at large rapidity intervals at center-of-mass energy 7 TeV.

Beams: pp

Energies: (3500.0, 3500.0) GeV

Experiment: CMS (LHC)

Inspire ID: [1102908](#)

Status: VALIDATED

Authors:

- Grzegorz Brona
- Vladimir Gavrilov
- Hannes Jung
- Victor Kim
- Victor Murzin
- Vadim Oreshkin
- Grigory Pivovarov
- Ivan Pozdnyakov
- Grigory Safronov

References:

- CMS-FWD-10-014
- CERN-PH-EP-2012-088
- arXiv: [1204.0696](#)
- Submitted to the EPJ C

Run details:

- Inclusive QCD at 7TeV comEnergy, ptHat (or equivalent) greater than 15 GeV

This is a measurement of the ratio of inclusive to exclusive dijet production as a function of the absolute distance in rapidity, Δy , between jets. The ratio of the Mueller-Navelet to exclusive dijet production is also measured. These measurements were performed with the CMS detector in proton-proton collisions at $\sqrt{s} = 7$ TeV for jets with $p_T > 35$ GeV and $|y| < 4.7$ taken from a mixture of two data samples, one of which containing dijets with moderate rapidity separation and the other containing dijets with large rapidity separation, with integrated luminosity of 33/nb and 5/pb respectively. The measured observables are corrected for detector effects.

Histograms (2):

- Inclusive to exclusive dijet production ratio ([/REF/CMS_2012_I1102908/d01-x01-y01](#))
- Mueller-Navelet to exclusive dijet production ratio ([/REF/CMS_2012_I1102908/d02-x01-y01](#))

8.97 CMS_2012_I1107658 [162]

Measurement of the underlying event activity in the Drell-Yan process at a centre-of-mass energy of 7 TeV

Beams: $p p$

Energies: (3500.0, 3500.0) GeV

Experiment: CMS (LHC)

Inspire ID: [1107658](#)

Status: VALIDATED

Authors:

- Sunil Bansal (sunil.bansal@cern.ch)

References:

- CMS-QCD-11-012
- CERN-PH-EP-2012-085
- arXiv: [1204.1411](#)

Run details:

- Drell-Yan events with $Z/\gamma^* \rightarrow \mu\mu$. $m(\mu, \mu) > 20$ GeV

A measurement of the underlying event activity using Drell-Yan events using muonic final state. The production of charged particles with pseudorapidity $|\eta| < 2$ and transverse momentum $p_{\perp} > 0.5$ GeV/c is studied in towards, transverse and away region w.r.t. to the direction of di-muon system. The UE activity is measured in terms of a particle density and an energy density. The particle density is computed as the average number of primary charged particles per unit pseudorapidity and per unit azimuth. The energy density is expressed in terms of the average of the scalar sum of the transverse momenta of primary charged particles per unit pseudorapidity and azimuth. The ratio of the energy and particle density is also reported in 3 regions. UE activity is studied as a function of invariant mass of muon pair ($M_{\mu\mu}$) by limiting the ISR contribution by requiring transverse momentum of muon pair $p_{\perp}(\mu\mu) < 5$ GeV/c. The $p_{\perp}(\mu\mu)$ dependence is studied for the events having $M_{\mu\mu}$ in window of 81–101 GeV/c. The normalized charged particle multiplicity and p_{\perp} spectrum of the charged particles in three regions also been reported for events having $M_{\mu\mu}$ in window of 81–101 GeV/c. Multiplicity and p_{\perp} spectra in the transverse region are also reported, for events having $p_{\perp}(\mu\mu) < 5$ GeV/c.

Histograms (20):

- Toward N_{chg} density vs $p_{\perp}^{\mu\mu}$ ([/REF/CMS_2012_I1107658/d01-x01-y01](#))
- Transverse N_{chg} density vs $p_{\perp}^{\mu\mu}$ ([/REF/CMS_2012_I1107658/d02-x01-y01](#))
- Away N_{chg} density vs $p_{\perp}^{\mu\mu}$ ([/REF/CMS_2012_I1107658/d03-x01-y01](#))

- Toward $\sum p_\perp$ density vs $p_\perp^{\mu\mu}$ (/REF/CMS_2012_I1107658/d04-x01-y01)
- Transverse $\sum p_\perp$ density vs $p_\perp^{\mu\mu}$ (/REF/CMS_2012_I1107658/d05-x01-y01)
- Away $\sum p_\perp$ density vs $p_\perp^{\mu\mu}$ (/REF/CMS_2012_I1107658/d06-x01-y01)
- Toward $\langle p_\perp \rangle$ vs $p_\perp^{\mu\mu}$ (/REF/CMS_2012_I1107658/d07-x01-y01)
- Transverse $\langle p_\perp \rangle$ vs $p_\perp^{\mu\mu}$ (/REF/CMS_2012_I1107658/d08-x01-y01)
- Away $\langle p_\perp \rangle$ vs $p_\perp^{\mu\mu}$ (/REF/CMS_2012_I1107658/d09-x01-y01)
- Towards + transverse N_{chg} density vs $m_{\mu\mu}, p_\perp^{\mu\mu} < 5 \text{ GeV}$ (/REF/CMS_2012_I1107658/d10-x01-y01)
- Towards + transverse $\sum p_\perp$ density vs $m_{\mu\mu}, p_\perp^{\mu\mu} < 5 \text{ GeV}$ (/REF/CMS_2012_I1107658/d11-x01-y01)
- Towards + transverse $\langle p_\perp \rangle$ vs $m_{\mu\mu}, p_\perp^{\mu\mu} < 5 \text{ GeV}$ (/REF/CMS_2012_I1107658/d12-x01-y01)
- Toward N_{chg} (/REF/CMS_2012_I1107658/d13-x01-y01)
- Transverse N_{chg} (/REF/CMS_2012_I1107658/d14-x01-y01)
- Away N_{chg} (/REF/CMS_2012_I1107658/d15-x01-y01)
- Toward p_\perp (/REF/CMS_2012_I1107658/d16-x01-y01)
- Transverse p_\perp (/REF/CMS_2012_I1107658/d17-x01-y01)
- Away p_\perp (/REF/CMS_2012_I1107658/d18-x01-y01)
- Transverse $N_{\text{chg}}, p_\perp(\mu\mu) < 5 \text{ GeV}$ (/REF/CMS_2012_I1107658/d19-x01-y01)
- Transverse $p_\perp, p_\perp(\mu\mu) < 5 \text{ GeV}$ (/REF/CMS_2012_I1107658/d20-x01-y01)

8.98 CMS_2012_I1184941 [163]

Measurement of the differential cross section for inclusive dijet production as a function of ξ in 7 TeV proton-proton collisions.

Beams: pp

Energies: (3500.0, 3500.0) GeV

Experiment: CMS (LHC)

Inspire ID: [1184941](#)

Status: VALIDATED

Authors:

- Sercan Sen (ssen@cern.ch)
- Alexander Proskuryakov (aproskur@mail.cern.ch)

References:

- arXiv: [1209.1805](#)
- Submitted to Phys. Rev. D

Run details:

- High statistics is needed to observe events in the lowest (ξ) bin. Distributions are presented for hard QCD events (i.e. with p_T^\perp greater than 15 GeV) and diffractive-enhanced events.

Measurement of the differential cross section for inclusive dijet production as a function of ξ which approximates the fractional momentum loss of the scattered proton in single-diffraction events. The data used has a total integrated luminosity of 2.7 nb^{-1} collected during 2010 with low instantaneous luminosity. Events are selected with at least two jets in $|\eta| < 4.4$ with $p_T^\perp > 20 \text{ GeV}$ and all final states particles are used for the reconstruction of ξ .

Histograms (1):

- $\sqrt{s} = 7 \text{ TeV}, pp \rightarrow \text{jet}_1\text{jet}_2, |\eta^{j_1,j_2}| < 4.4, p_T^{j_1,j_2} > 20 \text{ GeV}$ (/REF/CMS_2012_I1184941/d01-x01-y01)

8.99 CMS_2012_I1193338 [164]

Measurement of the inelastic proton-proton cross section at $\sqrt{s} = 7$ TeV

Beams: pp

Energies: (3500.0, 3500.0) GeV

Experiment: CMS (LHC)

Inspire ID: [1193338](#)

Status: VALIDATED

Authors:

- Sercan Sen (ssen@cern.ch)

References:

- arXiv: [1210.6718](#)

Run details:

- Inelastic events (non-diffractive and inelastic diffractive).

The inelastic cross-section is measured through two independent methods based on information from (i) forward calorimetry (for pseudorapidity $3 < |\eta| < 5$), in collisions where at least one proton loses more than $\xi > 5 \cdot 10^{-6}$ of its longitudinal momentum, and (ii) the central tracker ($|\eta| < 2.4$), in collisions containing an interaction vertex with more than 1, 2, or 3 tracks with $p_{\perp} > 200$ MeV/ c .

Histograms (1):

- σ_{inel} at $\sqrt{s} = 7$ TeV ([/REF/CMS_2012_I1193338/d01-x01-y01](#))

8.100 CMS_2012_I941555 [165]

Measurement of differential Z/γ^* p_T and y

Beams: pp

Energies: (3500.0, 3500.0) GeV

Experiment: CMS (LHC)

Spires ID: [941555](#)

Status: VALIDATED

Authors:

- Luca Perrozzi (luca.perrozzi@cern.ch)
- Justin Hugon (justin.hugon@cern.ch)

References:

- Phys.Rev. D85 (2012) 032002
- arXiv: [1110.4973](#)
- CMS-EWK-10-010
- CERN-PH-EP-2011-169

Run details:

- $pp \rightarrow \mu^+\mu^- + X$ 7 TeV. Needs mass cut on lepton pair to avoid photon singularity, restrict Z/γ^* mass range to roughly $50 \text{ GeV}/c^2 < m_{\mu\mu} < 130 \text{ GeV}/c^2$ for efficiency. Result is corrected for QED FSR (i.e. leptons are dressed), so turn off in generator.

Cross section as a function of p_T and y of the Z boson decaying into muons in $p p$ collisions at $\sqrt{s} = 7$ TeV. p_T and y cross sections are measured for $60 < m_{\mu\mu} < 120$ GeV. The p_T cross section is measured for lepton $p_T > 20$ GeV and $\eta < 2.1$, while the y cross section is extrapolated to all lepton p_T and η . This measurement was performed using 36 pb^{-1} of data collected during 2010 with the CMS detector at the LHC.

Histograms (9):

- Z boson y with dressed muons ([/REF/CMS_2012_I941555/d01-x01-y01](#))
- Z boson y with dressed electrons ([/REF/CMS_2012_I941555/d01-x01-y02](#))
- Z boson y with dressed leptons ([/REF/CMS_2012_I941555/d01-x01-y03](#))
- Z boson p_T with dressed muons ([/REF/CMS_2012_I941555/d02-x01-y01](#))
- Z boson p_T with dressed electrons ([/REF/CMS_2012_I941555/d02-x01-y02](#))
- Z boson p_T with dressed leptons ([/REF/CMS_2012_I941555/d02-x01-y03](#))
- Z boson p_T with dressed muons ([/REF/CMS_2012_I941555/d03-x01-y01](#))
- Z boson p_T with dressed electrons ([/REF/CMS_2012_I941555/d03-x01-y02](#))
- Z boson p_T with dressed leptons ([/REF/CMS_2012_I941555/d03-x01-y03](#))

8.101 CMS_2012_PAS_QCD_11_010 [166]

Strange particle production in underlying events in proton–proton collisions at $\sqrt{s} = 7$ TeV

Beams: pp

Energies: (3500.0, 3500.0) GeV

Experiment: CMS (LHC)

Inspire ID: [~](#)

Status: PRELIMINARY

Authors:

- Sercan Sen (Sercan.Sen@cern.ch)

References:

- CMS-PAS-QCD-11-010
- <http://cdsweb.cern.ch/record/1463352>

Run details:

- Inelastic events (non-diffractive and inelastic diffractive) at $\sqrt{s} = 7$ TeV.

Measurements of the production of K_S^0 , Λ and $\bar{\Lambda}$ particles in the underlying activity of events with a p_\perp scale ranging from 1 to 50 GeV/ c in pp collisions at $\sqrt{s} = 7$ TeV.

Histograms (4):

- Transverse $\Lambda + \bar{\Lambda}$ particle density at $\sqrt{s} = 7$ TeV, $p_\perp > 1.5$ GeV ([/REF/CMS_2012_PAS_QCD_11_010/d01-x01-y01](#))
- Transverse K_s^0 particle density at $\sqrt{s} = 7$ TeV, $p_\perp > 0.6$ GeV ([/REF/CMS_2012_PAS_QCD_11_010/d02-x01-y01](#))
- Transverse $\sum p_\perp(\Lambda + \bar{\Lambda})$ at $\sqrt{s} = 7$ TeV, $p_\perp > 1.5$ GeV ([/REF/CMS_2012_PAS_QCD_11_010/d03-x01-y01](#))
- Transverse $\sum p_\perp(K_s^0)$ at $\sqrt{s} = 7$ TeV, $p_\perp > 0.6$ GeV ([/REF/CMS_2012_PAS_QCD_11_010/d04-x01-y01](#))

8.102 CMS_2013_I1209721 [167]

Azimuthal correlations and event shapes in $Z + \text{jets}$ in pp collisions at 7 TeV

Beams: pp

Energies: (3500.0, 3500.0) GeV

Experiment: CMS (LHC)

Spires ID: [1209721](#)

Status: VALIDATED

Authors:

- Io Odderskov <io.odderskov@gmail.com>

References:

- <http://cms.cern.ch/iCMS/analysisadmin/cadi?ancode=EWK-11-021>
- <https://cds.cern.ch/record/1503578>
- <http://inspirehep.net/record/1209721>
- arXiv: [1301.1646](#)
- Submitted to Phys. Lett. B

Run details:

- Run MC generators with Z decaying to leptonic modes at 7TeV comEnergy

Measurements are presented of event shapes and azimuthal correlations in the inclusive production of a Z boson in association with jets in proton-proton collisions. The data correspond to an integrated luminosity of 5.0/fb, collected with the CMS detector at the CERN LHC at $\sqrt{s} = 7$ TeV. This to test perturbative QCD predictions and evaluate a substantial background to most physics channels. Studies performed as a function of jet multiplicity for inclusive Z boson production and for Z bosons with transverse-momenta greater than 150 GeV, are compared to predictions from Monte Carlo event generators that include leading-order multiparton matrix-element (with up to four hard partons in the final state) and next-to-leading-order simulations of $Z + 1$ -jet events. The results are corrected for detector effects, and can therefore be used as input to improve models for describing these processes.

Histograms (18):

- CMS, $\Delta\phi(Z, J1)$, $\sqrt{s} = 7$ TeV ([/REF/CMS_2013_I1209721/d01-x01-y01](#))
- CMS, $\Delta\phi(Z, J1)$, ≥ 2 jets, $\sqrt{s} = 7$ TeV ([/REF/CMS_2013_I1209721/d02-x01-y01](#))
- CMS, $\Delta\phi(Z, J3)$, ≥ 3 jets, $\sqrt{s} = 7$ TeV ([/REF/CMS_2013_I1209721/d03-x01-y01](#))
- CMS, $\Delta\phi(Z, J1)$, ≥ 3 jets, $\sqrt{s} = 7$ TeV ([/REF/CMS_2013_I1209721/d04-x01-y01](#))

- CMS, $\Delta\phi(Z, J2)$, ≥ 3 jets, $\sqrt{s} = 7$ TeV ([/REF/CMS_2013_I1209721/d05-x01-y01](#))
- CMS, $\Delta\phi(J1, J2)$, ≥ 3 jets, $\sqrt{s} = 7$ TeV ([/REF/CMS_2013_I1209721/d06-x01-y01](#))
- CMS, $\Delta\phi(J1, J3)$, ≥ 3 jets, $\sqrt{s} = 7$ TeV ([/REF/CMS_2013_I1209721/d07-x01-y01](#))
- CMS, $\Delta\phi(J2, J3)$, ≥ 3 jets, $\sqrt{s} = 7$ TeV ([/REF/CMS_2013_I1209721/d08-x01-y01](#))
- CMS, Thrust, $\sqrt{s} = 7$ TeV ([/REF/CMS_2013_I1209721/d09-x01-y01](#))
- CMS, $\Delta\phi(Z, J1)$, boosted regime, $\sqrt{s} = 7$ TeV ([/REF/CMS_2013_I1209721/d10-x01-y01](#))
- CMS, $\Delta\phi(Z, J1)$, ≥ 2 jets, boosted regime, $\sqrt{s} = 7$ TeV ([/REF/CMS_2013_I1209721/d11-x01-y01](#))
- CMS, $\Delta\phi(Z, J3)$, ≥ 3 jets, boosted regime, $\sqrt{s} = 7$ TeV ([/REF/CMS_2013_I1209721/d12-x01-y01](#))
- CMS, $\Delta\phi(Z, J1)$, ≥ 3 jets, boosted regime, $\sqrt{s} = 7$ TeV ([/REF/CMS_2013_I1209721/d13-x01-y01](#))
- CMS, $\Delta\phi(Z, J2)$, ≥ 3 jets, boosted regime, $\sqrt{s} = 7$ TeV ([/REF/CMS_2013_I1209721/d14-x01-y01](#))
- CMS, $\Delta\phi(J1, J2)$, ≥ 3 jets, boosted regime, $\sqrt{s} = 7$ TeV ([/REF/CMS_2013_I1209721/d15-x01-y01](#))
- CMS, $\Delta\phi(J1J3)$, ≥ 3 jets, boosted regime, $\sqrt{s} = 7$ TeV ([/REF/CMS_2013_I1209721/d16-x01-y01](#))
- CMS, $\Delta\phi(J2, J3)$, ≥ 3 jets, boosted regime, $\sqrt{s} = 7$ TeV ([/REF/CMS_2013_I1209721/d17-x01-y01](#))
- CMS, thrust, boosted regime, $\sqrt{s} = 7$ TeV ([/REF/CMS_2013_I1209721/d18-x01-y01](#))

8.103 CMS_2013_I1218372 [168]

Study of the underlying event at forward rapidity in proton–proton collisions at the LHC

Beams: pp

Energies: (450.0, 450.0), (1380.0, 1380.0), (3500.0, 3500.0) GeV

Experiment: CMS (LHC)

Spires ID: [1218372](#)

Status: VALIDATED

Authors:

- Samantha Dooling (samantha.dooling@desy.de)

References:

- JHEP 1304 (2013) 072
- [10.1007/JHEP04\(2013\)072](https://doi.org/10.1007/JHEP04(2013)072)
- CMS-FWD-11-003
- arXiv: [1302.2394](#)

Run details:

- Inelastic events (non-diffractive and diffractive) at $\sqrt{s} = 0.9, 2.76$ and 7 TeV.

Ratio of the energy deposited in the pseudorapidity range $-6.6 < \eta < -5.2$ for events with a charged particle jet with $|\eta| < 2$ with respect to the energy in inclusive events, as a function of charged particle jet transverse momentum for $\sqrt{s} = 0.9, 2.76$ and 7 TeV.

Histograms (3):

- Ratio of energy deposited in $-6.6 < \eta < -5.2$ for $\sqrt{s} = 0.9$ TeV ([/REF/CMS_2013_I1218372/d01-x01-y01](#))
- Ratio of energy deposited in $-6.6 < \eta < -5.2$ for $\sqrt{s} = 2.76$ TeV ([/REF/CMS_2013_I1218372/d02-x01-y01](#))
- Ratio of energy deposited in $-6.6 < \eta < -5.2$ for $\sqrt{s} = 7$ TeV ([/REF/CMS_2013_I1218372/d03-x01-y01](#))

8.104 CMS_2013_I1224539_DIJET [169]

CMS jet mass measurement in dijet events

Beams: pp

Energies: (3500.0, 3500.0) GeV

Experiment: CMS (LHC)

Inspire ID: [1224539](#)

Status: VALIDATED

Authors:

- salvatore.rappoccio@cern.ch
- ntran@fnal.gov
- kalanand@fnal.gov
- dlopes@mail.cern.ch

References:

- arXiv: [1303.4811](#)

Run details:

- 7 TeV pp collisions. Events are required to have at least 2 jets with $(p_{\perp 1} + p_{\perp 2})/2.0 > 220$ GeV with both jets satisfying $|y| < 2.4$.

Measurements of the mass spectra of the jets in dijet and W/Z +jet events from proton–proton collisions at a centre-of-mass energy of 7 TeV using a data sample of integrated luminosity of 5 fb^{-1} . The jets are reconstructed using the both the anti- k_T algorithm with $R = 0.7$ (AK7) and the Cambridge-Aachen algorithm with $R = 0.8$ (CA8) and $R = 1.2$ (CA12) with several grooming techniques applied (ungroomed, filtered, pruned and trimmed). See the text of the paper for more details. For the dijet events the distributions are presented as a function of the mean mass of the two leading jets in bins of the mean p_{\perp} of the two jets.

Histograms (28):

- Ungroomed AK7 dijets, $(p_T^1 + p_T^2)/2 = 220\text{--}300$ GeV ([/REF/CMS_2013_I1224539_DIJET/d01-x01-y01](#))
- Ungroomed AK7 dijets, $(p_T^1 + p_T^2)/2 = 300\text{--}450$ GeV ([/REF/CMS_2013_I1224539_DIJET/d02-x01-y01](#))
- Ungroomed AK7 dijets, $(p_T^1 + p_T^2)/2 = 450\text{--}500$ GeV ([/REF/CMS_2013_I1224539_DIJET/d03-x01-y01](#))
- Ungroomed AK7 dijets, $(p_T^1 + p_T^2)/2 = 500\text{--}600$ GeV ([/REF/CMS_2013_I1224539_DIJET/d04-x01-y01](#))
- Ungroomed AK7 dijets, $(p_T^1 + p_T^2)/2 = 600\text{--}800$ GeV ([/REF/CMS_2013_I1224539_DIJET/d05-x01-y01](#))
- Ungroomed AK7 dijets, $(p_T^1 + p_T^2)/2 = 800\text{--}1000$ GeV ([/REF/CMS_2013_I1224539_DIJET/d06-x01-y01](#))

- Ungroomed AK7 dijets, $(p_T^1 + p_T^2)/2 = 1000\text{--}1500 \text{ GeV}$ ([/REF/CMS_2013_I1224539_DIJET/d07-x01-y01](#))
- Filtered AK7 dijets, $(p_T^1 + p_T^2)/2 = 220\text{--}300 \text{ GeV}$ ([/REF/CMS_2013_I1224539_DIJET/d08-x01-y01](#))
- Filtered AK7 dijets, $(p_T^1 + p_T^2)/2 = 300\text{--}450 \text{ GeV}$ ([/REF/CMS_2013_I1224539_DIJET/d09-x01-y01](#))
- Filtered AK7 dijets, $(p_T^1 + p_T^2)/2 = 450\text{--}500 \text{ GeV}$ ([/REF/CMS_2013_I1224539_DIJET/d10-x01-y01](#))
- Filtered AK7 dijets, $(p_T^1 + p_T^2)/2 = 500\text{--}600 \text{ GeV}$ ([/REF/CMS_2013_I1224539_DIJET/d11-x01-y01](#))
- Filtered AK7 dijets, $(p_T^1 + p_T^2)/2 = 600\text{--}800 \text{ GeV}$ ([/REF/CMS_2013_I1224539_DIJET/d12-x01-y01](#))
- Filtered AK7 dijets, $(p_T^1 + p_T^2)/2 = 800\text{--}1000 \text{ GeV}$ ([/REF/CMS_2013_I1224539_DIJET/d13-x01-y01](#))
- Filtered AK7 dijets, $(p_T^1 + p_T^2)/2 = 1000\text{--}1500 \text{ GeV}$ ([/REF/CMS_2013_I1224539_DIJET/d14-x01-y01](#))
- Trimmed AK7 dijets, $(p_T^1 + p_T^2)/2 = 220\text{--}300 \text{ GeV}$ ([/REF/CMS_2013_I1224539_DIJET/d15-x01-y01](#))
- Trimmed AK7 dijets, $(p_T^1 + p_T^2)/2 = 300\text{--}450 \text{ GeV}$ ([/REF/CMS_2013_I1224539_DIJET/d16-x01-y01](#))
- Trimmed AK7 dijets, $(p_T^1 + p_T^2)/2 = 450\text{--}500 \text{ GeV}$ ([/REF/CMS_2013_I1224539_DIJET/d17-x01-y01](#))
- Trimmed AK7 dijets, $(p_T^1 + p_T^2)/2 = 500\text{--}600 \text{ GeV}$ ([/REF/CMS_2013_I1224539_DIJET/d18-x01-y01](#))
- Trimmed AK7 dijets, $(p_T^1 + p_T^2)/2 = 600\text{--}800 \text{ GeV}$ ([/REF/CMS_2013_I1224539_DIJET/d19-x01-y01](#))
- Trimmed AK7 dijets, $(p_T^1 + p_T^2)/2 = 800\text{--}1000 \text{ GeV}$ ([/REF/CMS_2013_I1224539_DIJET/d20-x01-y01](#))
- Trimmed AK7 dijets, $(p_T^1 + p_T^2)/2 = 1000\text{--}1500 \text{ GeV}$ ([/REF/CMS_2013_I1224539_DIJET/d21-x01-y01](#))
- Pruned AK7 dijets, $(p_T^1 + p_T^2)/2 = 220\text{--}300 \text{ GeV}$ ([/REF/CMS_2013_I1224539_DIJET/d22-x01-y01](#))
- Pruned AK7 dijets, $(p_T^1 + p_T^2)/2 = 300\text{--}450 \text{ GeV}$ ([/REF/CMS_2013_I1224539_DIJET/d23-x01-y01](#))
- Pruned AK7 dijets, $(p_T^1 + p_T^2)/2 = 450\text{--}500 \text{ GeV}$ ([/REF/CMS_2013_I1224539_DIJET/d24-x01-y01](#))
- Pruned AK7 dijets, $(p_T^1 + p_T^2)/2 = 600\text{--}800 \text{ GeV}$ ([/REF/CMS_2013_I1224539_DIJET/d25-x01-y01](#))
- Pruned AK7 dijets, $(p_T^1 + p_T^2)/2 = 600\text{--}800 \text{ GeV}$ ([/REF/CMS_2013_I1224539_DIJET/d26-x01-y01](#))
- Pruned AK7 dijets, $(p_T^1 + p_T^2)/2 = 800\text{--}1000 \text{ GeV}$ ([/REF/CMS_2013_I1224539_DIJET/d27-x01-y01](#))
- Pruned AK7 dijets, $(p_T^1 + p_T^2)/2 = 1000\text{--}1500 \text{ GeV}$ ([/REF/CMS_2013_I1224539_DIJET/d28-x01-y01](#))

8.105 CMS_2013_I1224539_WJET [169]

CMS jet mass measurement in $W +$ jet events

Beams: pp

Energies: (3500.0, 3500.0) GeV

Experiment: CMS (LHC)

Inspire ID: [1224539](#)

Status: VALIDATED

Authors:

- salvatore.rappoccio@cern.ch
- ntran@fnal.gov
- kalanand@fnal.gov
- dlopes@mail.cern.ch

References:

- arXiv: [1303.4811](#)

Run details:

- 7 TeV pp collisions. Events are required to have a electron channel W with $p_{\perp} > 120$ GeV, and at least 1 jet opposed to the W with $p_{\perp} > 50$ GeV and $|y| < 2.4$.

Measurements of the mass spectra of the jets in dijet and $W/Z+jet$ events from proton–proton collisions at a centre-of-mass energy of 7 TeV using a data sample of integrated luminosity of 5 fb^{-1} . The jets are reconstructed using the both the anti- k_T algorithm with $R = 0.7$ (AK7) and the Cambridge-Aachen algorithm with $R = 0.8$ (CA8) and $R = 1.2$ (CA12) with several grooming techniques applied (ungroomed, filtered, pruned and trimmed). See the text of the paper for more details. For the dijet events the distributions are presented as a function of the mean Mass of the two leading jets in bins of the mean p_{\perp} of the two jets.

Histograms (23):

- Ungroomed AK7 $W+jets$, $p_{T,j} = 125\text{--}150$ GeV ([/REF/CMS_2013_I1224539_WJET/d52-x01-y01](#))
- Ungroomed AK7 $W+jets$, $p_{T,j} = 150\text{--}220$ GeV ([/REF/CMS_2013_I1224539_WJET/d53-x01-y01](#))
- Ungroomed AK7 $W+jets$, $p_{T,j} = 220\text{--}300$ GeV ([/REF/CMS_2013_I1224539_WJET/d54-x01-y01](#))
- Ungroomed AK7 $W+jets$, $p_{T,j} = 300\text{--}450$ GeV ([/REF/CMS_2013_I1224539_WJET/d55-x01-y01](#))
- Filtered AK7 $W+jets$, $p_{T,j} = 125\text{--}150$ GeV ([/REF/CMS_2013_I1224539_WJET/d56-x01-y01](#))
- Filtered AK7 $W+jets$, $p_{T,j} = 150\text{--}220$ GeV ([/REF/CMS_2013_I1224539_WJET/d57-x01-y01](#))
- Filtered AK7 $W+jets$, $p_{T,j} = 220\text{--}300$ GeV ([/REF/CMS_2013_I1224539_WJET/d58-x01-y01](#))

- Filtered AK7 $W+jets$, $p_{T,j} = 300\text{--}450$ GeV ([/REF/CMS_2013_I1224539_WJET/d59-x01-y01](#))
- Trimmed AK7 $W+jets$, $p_{T,j} = 125\text{--}150$ GeV ([/REF/CMS_2013_I1224539_WJET/d60-x01-y01](#))
- Trimmed AK7 $W+jets$, $p_{T,j} = 150\text{--}220$ GeV ([/REF/CMS_2013_I1224539_WJET/d61-x01-y01](#))
- Trimmed AK7 $W+jets$, $p_{T,j} = 220\text{--}300$ GeV ([/REF/CMS_2013_I1224539_WJET/d62-x01-y01](#))
- Trimmed AK7 $W+jets$, $p_{T,j} = 300\text{--}450$ GeV ([/REF/CMS_2013_I1224539_WJET/d63-x01-y01](#))
- Pruned AK7 $W+jets$, $p_{T,j} = 125\text{--}150$ GeV ([/REF/CMS_2013_I1224539_WJET/d64-x01-y01](#))
- Pruned AK7 $W+jets$, $p_{T,j} = 150\text{--}220$ GeV ([/REF/CMS_2013_I1224539_WJET/d65-x01-y01](#))
- Pruned AK7 $W+jets$, $p_{T,j} = 220\text{--}300$ GeV ([/REF/CMS_2013_I1224539_WJET/d66-x01-y01](#))
- Pruned AK7 $W+jets$, $p_{T,j} = 300\text{--}450$ GeV ([/REF/CMS_2013_I1224539_WJET/d67-x01-y01](#))
- Pruned CA8 $W+jets$, $p_{T,j} = 125\text{--}150$ GeV ([/REF/CMS_2013_I1224539_WJET/d68-x01-y01](#))
- Pruned CA8 $W+jets$, $p_{T,j} = 150\text{--}220$ GeV ([/REF/CMS_2013_I1224539_WJET/d69-x01-y01](#))
- Pruned CA8 $W+jets$, $p_{T,j} = 220\text{--}300$ GeV ([/REF/CMS_2013_I1224539_WJET/d70-x01-y01](#))
- Pruned CA8 $W+jets$, $p_{T,j} = 300\text{--}450$ GeV ([/REF/CMS_2013_I1224539_WJET/d71-x01-y01](#))
- Filtered CA12 $W+jets$, $p_{T,j} = 150\text{--}220$ GeV ([/REF/CMS_2013_I1224539_WJET/d72-x01-y01](#))
- Filtered CA12 $W+jets$, $p_{T,j} = 220\text{--}300$ GeV ([/REF/CMS_2013_I1224539_WJET/d73-x01-y01](#))
- Filtered CA12 $W+jets$, $p_{T,j} = 300\text{--}450$ GeV ([/REF/CMS_2013_I1224539_WJET/d74-x01-y01](#))

8.106 CMS_2013_I1224539_ZJET [169]

CMS jet mass measurement in $Z +$ jet events

Beams: pp

Energies: (3500.0, 3500.0) GeV

Experiment: CMS (LHC)

Inspire ID: [1224539](#)

Status: VALIDATED

Authors:

- salvatore.rappoccio@cern.ch
- ntran@fnal.gov
- kalanand@fnal.gov
- dlopes@mail.cern.ch

References:

- arXiv: [1303.4811](#)

Run details:

- 7 TeV pp collisions. Events are required to have a electron channel Z with $p_{\perp} > 120$ GeV, and at least 1 jet opposed to the Z with $p_{\perp} > 50$ GeV and $|y| < 2.4$.

Measurements of the mass spectra of the jets in dijet and $W/Z+jet$ events from proton–proton collisions at a centre-of-mass energy of 7 TeV using a data sample of integrated luminosity of 5 fb^{-1} . The jets are reconstructed using the both the anti- k_T algorithm with $R = 0.7$ (AK7) and the Cambridge-Aachen algorithm with $R = 0.8$ (CA8) and $R = 1.2$ (CA12) with several grooming techniques applied (ungroomed, filtered, pruned and trimmed). See the text of the paper for more details. For the dijet events the distributions are presented as a function of the mean Mass of the two leading jets in bins of the mean p_{\perp} of the two jets.

Histograms (23):

- Ungroomed AK7 $Z+jet$, $p_{T,j} = 125\text{--}150$ GeV ([/REF/CMS_2013_I1224539_ZJET/d29-x01-y01](#))
- Ungroomed AK7 $Z+jet$, $p_{T,j} = 150\text{--}220$ GeV ([/REF/CMS_2013_I1224539_ZJET/d30-x01-y01](#))
- Ungroomed AK7 $Z+jet$, $p_{T,j} = 220\text{--}300$ GeV ([/REF/CMS_2013_I1224539_ZJET/d31-x01-y01](#))
- Ungroomed AK7 $Z+jet$, $p_{T,j} = 300\text{--}450$ GeV ([/REF/CMS_2013_I1224539_ZJET/d32-x01-y01](#))
- Filtered AK7 $Z+jet$, $p_{T,j} = 125\text{--}150$ GeV ([/REF/CMS_2013_I1224539_ZJET/d33-x01-y01](#))
- Filtered AK7 $Z+jet$, $p_{T,j} = 150\text{--}220$ GeV ([/REF/CMS_2013_I1224539_ZJET/d34-x01-y01](#))
- Filtered AK7 $Z+jet$, $p_{T,j} = 220\text{--}300$ GeV ([/REF/CMS_2013_I1224539_ZJET/d35-x01-y01](#))

- Filtered AK7 Z +jets, $p_{T,j} = 300\text{--}450$ GeV ([/REF/CMS_2013_I1224539_ZJET/d36-x01-y01](#))
- Trimmed AK7 Z +jets, $p_{T,j} = 125\text{--}150$ GeV ([/REF/CMS_2013_I1224539_ZJET/d37-x01-y01](#))
- Trimmed AK7 Z +jets, $p_{T,j} = 150\text{--}220$ GeV ([/REF/CMS_2013_I1224539_ZJET/d38-x01-y01](#))
- Trimmed AK7 Z +jets, $p_{T,j} = 220\text{--}300$ GeV ([/REF/CMS_2013_I1224539_ZJET/d39-x01-y01](#))
- Trimmed AK7 Z +jets, $p_{T,j} = 300\text{--}450$ GeV ([/REF/CMS_2013_I1224539_ZJET/d40-x01-y01](#))
- Pruned AK7 Z +jets, $p_{T,j} = 125\text{--}150$ GeV ([/REF/CMS_2013_I1224539_ZJET/d41-x01-y01](#))
- Pruned AK7 Z +jets, $p_{T,j} = 150\text{--}220$ GeV ([/REF/CMS_2013_I1224539_ZJET/d42-x01-y01](#))
- Pruned AK7 Z +jets, $p_{T,j} = 220\text{--}300$ GeV ([/REF/CMS_2013_I1224539_ZJET/d43-x01-y01](#))
- Pruned AK7 Z +jets, $p_{T,j} = 300\text{--}450$ GeV ([/REF/CMS_2013_I1224539_ZJET/d44-x01-y01](#))
- Pruned CA8 Z +jets, $p_{T,j} = 125\text{--}150$ GeV ([/REF/CMS_2013_I1224539_ZJET/d45-x01-y01](#))
- Pruned CA8 Z +jets, $p_{T,j} = 150\text{--}220$ GeV ([/REF/CMS_2013_I1224539_ZJET/d46-x01-y01](#))
- Pruned CA8 Z +jets, $p_{T,j} = 220\text{--}300$ GeV ([/REF/CMS_2013_I1224539_ZJET/d47-x01-y01](#))
- Pruned CA8 Z +jets, $p_{T,j} = 300\text{--}450$ GeV ([/REF/CMS_2013_I1224539_ZJET/d48-x01-y01](#))
- Filtered CA12 Z +jets, $p_{T,j} = 150\text{--}220$ GeV ([/REF/CMS_2013_I1224539_ZJET/d49-x01-y01](#))
- Filtered CA12 Z +jets, $p_{T,j} = 220\text{--}300$ GeV ([/REF/CMS_2013_I1224539_ZJET/d50-x01-y01](#))
- Filtered CA12 Z +jets, $p_{T,j} = 300\text{--}450$ GeV ([/REF/CMS_2013_I1224539_ZJET/d51-x01-y01](#))

8.107 CMS_2013_I1256943 [170]

Cross-section and angular correlations in Z boson with b -hadrons events at $\sqrt{s} = 7$ TeV

Beams: pp

Energies: (3500.0, 3500.0) GeV

Experiment: CMS (LHC)

Inspire ID: [1256943](#)

Status: VALIDATED

Authors:

- Lorenzo Viliani ⟨ lorenzo.viliani@cern.ch ⟩
- Piergiulio Lenzi ⟨ piergiulio.lenzi@cern.ch ⟩

References:

- 10.1007 / JHEP12(2013)039
- arXiv: [1310.1349](#)
- CERN-PH-EP-2013-153
- CMS-EWK-11-015

Run details:

- pp collisions with $\sqrt{s} = 7$ TeV. Selection of events with exactly two b -hadrons and a lepton pair from the Z boson decay. Each lepton has $p_T > 20$ GeV and $|\eta| < 2.4$ and the dilepton invariant mass is $81 < M_{\ell\ell} < 101$ GeV. The b -hadrons have $p_T > 15$ GeV and $|\eta| < 2$. The differential cross sections are measured for $p_T > 0$ and $p_T > 50$ GeV.

A study of proton-proton collisions in which two b -hadrons are produced in association with a Z boson is reported. The collisions were recorded at a centre-of-mass energy of 7 TeV with the CMS detector at the LHC, for an integrated luminosity of 5.2/fb. The b -hadrons are identified by means of displaced secondary vertices, without the use of reconstructed jets, permitting the study of b -hadron pair production at small angular separation. Differential cross sections are presented as a function of the angular separation of the b -hadrons and the Z boson. In addition, inclusive measurements are presented. For both the inclusive and differential studies,different ranges of Z boson momentum are considered.

Histograms (9):

- CMS, $\sqrt{s} = 7$ TeV, 5.2 fb^{-1} , all p_T^Z ([/REF/CMS_2013_I1256943/d01-x01-y01](#))
- CMS, $\sqrt{s} = 7$ TeV, 5.2 fb^{-1} , all p_T^Z ([/REF/CMS_2013_I1256943/d02-x01-y01](#))
- CMS, $\sqrt{s} = 7$ TeV, 5.2 fb^{-1} , all p_T^Z ([/REF/CMS_2013_I1256943/d03-x01-y01](#))

- CMS, $\sqrt{s} = 7$ TeV, 5.2 fb^{-1} , all p_T^Z ([/REF/CMS_2013_I1256943/d04-x01-y01](#))
- CMS, $\sqrt{s} = 7$ TeV, 5.2 fb^{-1} , $p_T^Z > 50$ GeV ([/REF/CMS_2013_I1256943/d05-x01-y01](#))
- CMS, $\sqrt{s} = 7$ TeV, 5.2 fb^{-1} , $p_T^Z > 50$ GeV ([/REF/CMS_2013_I1256943/d06-x01-y01](#))
- CMS, $\sqrt{s} = 7$ TeV, 5.2 fb^{-1} , $p_T^Z > 50$ GeV ([/REF/CMS_2013_I1256943/d07-x01-y01](#))
- CMS, $\sqrt{s} = 7$ TeV, 5.2 fb^{-1} , $p_T^Z > 50$ GeV ([/REF/CMS_2013_I1256943/d08-x01-y01](#))
- CMS, $\sqrt{s} = 7$ TeV, 5.2 fb^{-1} ([/REF/CMS_2013_I1256943/d09-x01-y01](#))

8.108 CMS_2013_I1258128 [171]

Rapidity distributions in exclusive $Z + \text{jet}$ and $\gamma + \text{jet}$ events in pp collisions at $\sqrt{s} = 7 \text{ TeV}$

Beams: pp

Energies: (3500.0, 3500.0) GeV

Experiment: CMS (LHC)

Inspire ID: [I1258128](#)

Status: VALIDATED

Authors:

- Steve Linn <linn@cern.ch>
- Shin-Shan Eiko Yu <syu@cern.ch>
- Anil Sing Pratap <singh.ap79@gmail.com>
- Lovedeep Kaur Saini <lvdeep9@gmail.com>
- Kittikul Kovitanggoon <kovitang.cern@gmail.com>
- Luis Lebolo <luis.lebolo@cern.ch>
- Vanessa Gaultney Werner <vgaul001@fiu.edu>
- Yun-Ju Lu <Yun-Ju.Lu@cern.ch>
- Syue-Wei Li <Syue-Wei.Li@cern.ch>
- Yu-Hsiang Chang <index0192@yahoo.com.tw>
- Sung-Won Lee <Sungwon.Lee@ttu.edu>
- Pete E.C. Markowitz <markowit@fiu.edu>
- Darko Mekterovic <Darko.Mekterovic@cern.ch>
- Jorge Rodriguez <jrodriguez@cern.ch>
- Bhawan Uppal

References:

- arXiv: [1310.3082](#)
- <https://twiki.cern.ch/twiki/bin/view/CMSPublic/PhysicsResultsSMP12004>
- Submitted to Phys. Rev. Lett

Run details:

- Run MC generators with Z decaying to leptonic modes + jets and photon + jets at 7 TeV centre-of-mass energy.

Rapidity distributions are presented for events containing either a Z boson or a photon in association with a single jet in proton-proton collisions produced at the CERN LHC. The data, collected with the CMS detector at $\sqrt{s} = 7$ TeV, correspond to an integrated luminosity of 5.0/fb. The individual rapidity distributions of the boson and the jet are consistent within 5% with expectations from perturbative QCD. However, QCD predictions for the sum and the difference in rapidities of the two final-state objects show significant discrepancies with CMS data. In particular, next-to-leading-order QCD calculations, and two Monte Carlo event generators using different methods to merge matrix-element partons with evolved parton showers, appear inconsistent with the data as well as with each other.

Histograms (8):

- CMS, $|y_Z|$, $\sqrt{s} = 7$ TeV, $L=5 \text{ fb}^{-1}$ ([/REF/CMS_2013_I1258128/d01-x01-y01](#))
- CMS, $|y_{\text{jet}}|$, $\sqrt{s} = 7$ TeV, $L=5 \text{ fb}^{-1}$ ([/REF/CMS_2013_I1258128/d02-x01-y01](#))
- CMS, y_{sum} , $\sqrt{s} = 7$ TeV, $L=5 \text{ fb}^{-1}$ ([/REF/CMS_2013_I1258128/d03-x01-y01](#))
- CMS, y_{dif} , $\sqrt{s} = 7$ TeV, $L=5 \text{ fb}^{-1}$ ([/REF/CMS_2013_I1258128/d04-x01-y01](#))
- CMS, $|y_\gamma|$, $\sqrt{s} = 7$ TeV, $L=4.9 \text{ pb}^{-1}$ ([/REF/CMS_2013_I1258128/d05-x01-y01](#))
- CMS, $|y_{\text{jet}}|$, $\sqrt{s} = 7$ TeV, $L=4.9 \text{ pb}^{-1}$ ([/REF/CMS_2013_I1258128/d06-x01-y01](#))
- CMS, y_{sum} , $\sqrt{s} = 7$ TeV, $L=4.9 \text{ pb}^{-1}$ ([/REF/CMS_2013_I1258128/d07-x01-y01](#))
- CMS, y_{dif} , $\sqrt{s} = 7$ TeV, $L=4.9 \text{ pb}^{-1}$ ([/REF/CMS_2013_I1258128/d08-x01-y01](#))

8.109 CMS_2013_I1261026 [172]

Jet and underlying event properties as a function of particle multiplicity

Beams: $p p$

Energies: (3500.0, 3500.0) GeV

Experiment: CMS (LHC)

Spires ID: [1261026](#)

Status: VALIDATED

Authors:

- Maxim Azarkin (Maksim.Azarkin@cern.ch)

References:

- Eur.Phys.J. C73 (2013) 2674
- arXiv: [1310.4554](#)
- CMS-FSQ-12-022,
- CERN-PH-EP-2013-195

Run details:

- QCD MB

Characteristics of multi-particle production in proton-proton collisions at $\sqrt{s} = 7$ TeV are studied as a function of the charged-particle multiplicity (N_{ch}). The produced particles are separated into two classes: those belonging to jets and those belonging to the underlying event. Charged particles are measured with pseudorapidity $|\eta| < 2.4$ and transverse momentum $p_T > 0.25$ GeV. Jets are reconstructed from charged-particles only and required to have $p_T > 5$ GeV. The distributions of jet p_T , average p_T of charged particles belonging to the underlying event or to jets, jet rates, and jet shapes are presented as functions of N_{ch} .

Histograms (17):

- Mean p_\perp , all charged particles ([/REF/CMS_2013_I1261026/d01-x01-y01](#))
- Mean p_\perp , UE charged particles ([/REF/CMS_2013_I1261026/d02-x01-y01](#))
- Mean p_\perp , in-jet charged particles ([/REF/CMS_2013_I1261026/d03-x01-y01](#))
- Mean p_\perp , leading in-jet charged particle ([/REF/CMS_2013_I1261026/d04-x01-y01](#))
- Mean p_\perp , charged particle jets, $p_T^{ch.jet} > 5$ GeV, $|\eta^{ch.jet}| < 1.9$ ([/REF/CMS_2013_I1261026/d05-x01-y01](#))
- Charged jet rate, $p_T^{ch.jet} > 5$ GeV, $|\eta^{ch.jet}| < 1.9$ ([/REF/CMS_2013_I1261026/d06-x01-y01](#))
- Charged jet rate, $p_T^{ch.jet} > 30$ GeV, $|\eta^{ch.jet}| < 1.9$ ([/REF/CMS_2013_I1261026/d07-x01-y01](#))

- Jet p_T spectrum, $|\eta^{ch.jet}| < 1.9$, $10 < N_{\text{ch}} \leq 30$ ([/REF/CMS_2013_I1261026/d08-x01-y01](#))
- Jet p_T spectrum, $|\eta^{ch.jet}| < 1.9$, $30 < N_{\text{ch}} \leq 50$ ([/REF/CMS_2013_I1261026/d09-x01-y01](#))
- Jet p_T spectrum, $|\eta^{ch.jet}| < 1.9$, $50 < N_{\text{ch}} \leq 80$ ([/REF/CMS_2013_I1261026/d10-x01-y01](#))
- Jet p_T spectrum, $|\eta^{ch.jet}| < 1.9$, $80 < N_{\text{ch}} \leq 110$ ([/REF/CMS_2013_I1261026/d11-x01-y01](#))
- Jet p_T spectrum, $|\eta^{ch.jet}| < 1.9$, $110 < N_{\text{ch}} \leq 140$ ([/REF/CMS_2013_I1261026/d12-x01-y01](#))
- Inrajet ring p_T density, $10 < N_{\text{ch}} \leq 30$ ([/REF/CMS_2013_I1261026/d13-x01-y01](#))
- Inrajet ring p_T density, $30 < N_{\text{ch}} \leq 50$ ([/REF/CMS_2013_I1261026/d14-x01-y01](#))
- Inrajet ring p_T density, $50 < N_{\text{ch}} \leq 80$ ([/REF/CMS_2013_I1261026/d15-x01-y01](#))
- Inrajet ring p_T density, $80 < N_{\text{ch}} \leq 110$ ([/REF/CMS_2013_I1261026/d16-x01-y01](#))
- Inrajet ring p_T density, $110 < N_{\text{ch}} \leq 140$ ([/REF/CMS_2013_I1261026/d17-x01-y01](#))

8.110 CMS_2013_I1265659 [173]

Probing color coherence effects in pp collisions at $\sqrt{s} = 7$ TeV

Beams: pp

Energies: (3500.0, 3500.0) GeV

Experiment: CMS (LHC)

Inspire ID: [1265659](#)

Status: VALIDATED

Authors:

- Maxime Gouzevitch mgouzevi@cern.ch
- Chawon Park parknkim@gmail.com
- Inkyu Park inkyu.park@cern.ch

References:

- CMS-SMP-12-010
- CERN-PH-EP-2013-200
- arXiv: [1311.5815](#)

Run details:

- pp QCD interactions at $\sqrt{s} = 7$ TeV. Data collected by CMS during the year 2010.

A study of color coherence effects in pp collisions at a center-of-mass energy of 7 TeV is presented. The data used in the analysis were collected in 2010 with the CMS detector at the LHC and correspond to an integrated luminosity of 36/pb. Events are selected that contain at least three jets and where the two jets with the largest transverse momentum exhibit a back-to-back topology. The measured angular correlation between the second- and third-leading jet is shown to be sensitive to color coherence effects, and is compared to the predictions of Monte Carlo models with various implementations of color coherence. None of the models describe the data satisfactorily.

Histograms (2):

- CMS, $\sqrt{s} = 7$ TeV, central jet 2–3 correlation, $|\eta_2| < 0.8$ ([/REF/CMS_2013_I1265659/d01-x01-y01](#))
- CMS, $\sqrt{s} = 7$ TeV, jet 2–3 correlation, $0.8 < |\eta_2| < 2.5$ ([/REF/CMS_2013_I1265659/d01-x01-y02](#))

8.111 CMS_2013_I1272853 [174]

Study of observables sensitive to double parton scattering in $W + 2$ jets process in pp collisions at $\sqrt{s} = 7$ TeV

Beams: pp

Energies: (3500.0, 3500.0) GeV

Experiment: CMS (LHC)

Spires ID: [1272853](#)

Status: VALIDATED

Authors:

- Sunil Bansal (sunil.bansal@cern.ch)

References:

- CMS-FSQ-12-028
- CERN-PH-EP-2013-224
- arXiv: [1312.5729](#)
- Submitted to JHEP

Run details:

- Only muonic decay of W boson

Double parton scattering is investigated in proton-proton collisions at $\sqrt{s} = 7$ TeV where the final state includes a W boson, which decays into a muon and a neutrino, and two jets. The data sample corresponds to an integrated luminosity of 5 inverse femtobarns, collected with the CMS detector at the LHC.

Histograms (2):

- CMS, $\sqrt{s} = 7$ TeV, $W + 2$ -jet ([/REF/CMS_2013_I1272853/d01-x01-y01](#))
- CMS, $\sqrt{s} = 7$ TeV, $W + 2$ -jet ([/REF/CMS_2013_I1272853/d02-x01-y01](#))

8.112 CMS_2013_I1273574 [175]

Studies of 4-jet production in proton-proton collisions at $\sqrt{s} = 7$ TeV

Beams: pp

Energies: (3500.0, 3500.0) GeV

Experiment: CMS (LHC)

Spires ID: [1273574](#)

Status: VALIDATED

Authors:

- P. Gunnellini
- A. Buckley

References:

- CMS-FSQ-12-013
- CERN-PH-EP-2013-229
- arXiv: [1312.6440](#)
- Submitted to Phys. Rev. D

Run details:

- Hard QCD events with p_T cut at generator level of 45 GeV

Measurements are presented of exclusive 4-jet production cross sections as a function of the transverse momentum p_T , pseudorapidity η , as well as of correlations in azimuthal angle and p_T balance among the jets. The data sample was collected at a centre-of-mass energy of 7 TeV with the CMS detector at the LHC, corresponding to an integrated luminosity of 36 pb⁻¹. The jets are reconstructed with the anti- k_T jet algorithm in a range of $|\eta| < 4.7$.

Histograms (11):

- CMS, $\sqrt{s} = 7$ TeV, Leading hard jet η in $pp \rightarrow 4j$ in $|\eta| < 4.7$ ([/REF/CMS_2013_I1273574/d01-x01-y01](#))
- CMS, $\sqrt{s} = 7$ TeV, Leading hard jet p_T in $pp \rightarrow 4j$ in $|\eta| < 4.7$ ([/REF/CMS_2013_I1273574/d02-x01-y01](#))
- CMS, $\sqrt{s} = 7$ TeV, Normalized ΔS in $pp \rightarrow 4j$ in $|\eta| < 4.7$ ([/REF/CMS_2013_I1273574/d03-x01-y01](#))
- CMS, $\sqrt{s} = 7$ TeV, Normalized $\Delta\phi^{soft}$ in $pp \rightarrow 4j$ in $|\eta| < 4.7$ ([/REF/CMS_2013_I1273574/d04-x01-y01](#))
- CMS, $\sqrt{s} = 7$ TeV, Normalized $\Delta_{soft}^{rel} p_T$ in $pp \rightarrow 4j$ in $|\eta| < 4.7$ ([/REF/CMS_2013_I1273574/d05-x01-y01](#))

- CMS, $\sqrt{s} = 7$ TeV, Leading soft jet η in $\text{pp} \rightarrow 4\text{j}$ in $|\eta| < 4.7$ ([/REF/CMS_2013-I1273574/d06-x01-y01](#))
- CMS, $\sqrt{s} = 7$ TeV, Leading soft jet p_T in $\text{pp} \rightarrow 4\text{j}$ in $|\eta| < 4.7$ ([/REF/CMS_2013-I1273574/d07-x01-y01](#))
- CMS, $\sqrt{s} = 7$ TeV, Subleading soft jet η in $\text{pp} \rightarrow 4\text{j}$ in $|\eta| < 4.7$ ([/REF/CMS_2013-I1273574/d08-x01-y01](#))
- CMS, $\sqrt{s} = 7$ TeV, Subleading soft jet p_T in $\text{pp} \rightarrow 4\text{j}$ in $|\eta| < 4.7$ ([/REF/CMS_2013-I1273574/d09-x01-y01](#))
- CMS, $\sqrt{s} = 7$ TeV, Subleading hard jet η in $\text{pp} \rightarrow 4\text{j}$ in $|\eta| < 4.7$ ([/REF/CMS_2013-I1273574/d10-x01-y01](#))
- CMS, $\sqrt{s} = 7$ TeV, Subleading hard jet p_T in $\text{pp} \rightarrow 4\text{j}$ in $|\eta| < 4.7$ ([/REF/CMS_2013-I1273574/d11-x01-y01](#))

8.113 CMS_QCD_10_024 [176]

Pseudorapidity distributions of charged particles at $\sqrt{s} = 0.9$ and 7 TeV

Beams: pp

Energies: (450.0, 450.0), (3500.0, 3500.0) GeV

Experiment: CMS (LHC)

Status: VALIDATED

Authors:

- P. Katsas ⟨ panagiotis.katsas@cern.ch ⟩
- A. Knutsson ⟨ albert.knutsson@cern.ch ⟩

References:

- CMS-PAS-QCD-10-024
- <https://cdsweb.cern.ch/record/1341853?ln=en>

Run details:

- pp collisions at 0.9 and 7 TeV. Minimum bias events.

Pseudorapidity distributions of charged particles in pp collisions at $\sqrt{s} = 0.9$ and 7 TeV with at least one central charged particle.

Histograms (8):

- $n_{\text{ch}} \geq 1$, $p_{\perp} > 0.5$ GeV in $|\eta| < 0.8$; $\sqrt{s} = 7$ TeV ([/REF/CMS_QCD_10_024/d01-x01-y01](#))
- $n_{\text{ch}} \geq 1$, $p_{\perp} > 1$ GeV in $|\eta| < 0.8$; $\sqrt{s} = 7$ TeV ([/REF/CMS_QCD_10_024/d02-x01-y01](#))
- $n_{\text{ch}} \geq 1$, $p_{\perp} > 0.5$ GeV in $|\eta| < 2.4$; $\sqrt{s} = 7$ TeV ([/REF/CMS_QCD_10_024/d03-x01-y01](#))
- $n_{\text{ch}} \geq 1$, $p_{\perp} > 1$ GeV in $|\eta| < 2.4$; $\sqrt{s} = 7$ TeV ([/REF/CMS_QCD_10_024/d04-x01-y01](#))
- $n_{\text{ch}} \geq 1$, $p_{\perp} > 0.5$ GeV in $|\eta| < 0.8$; $\sqrt{s} = 0.9$ TeV ([/REF/CMS_QCD_10_024/d05-x01-y01](#))
- $n_{\text{ch}} \geq 1$, $p_{\perp} > 1$ GeV in $|\eta| < 0.8$; $\sqrt{s} = 0.9$ TeV ([/REF/CMS_QCD_10_024/d06-x01-y01](#))
- $n_{\text{ch}} \geq 1$, $p_{\perp} > 0.5$ GeV in $|\eta| < 2.4$; $\sqrt{s} = 0.9$ TeV ([/REF/CMS_QCD_10_024/d07-x01-y01](#))
- $n_{\text{ch}} \geq 1$, $p_{\perp} > 1$ GeV in $|\eta| < 2.4$; $\sqrt{s} = 0.9$ TeV ([/REF/CMS_QCD_10_024/d08-x01-y01](#))

8.114 LHCb_2010_I867355 [177]

Measurement of $\sigma(pp \rightarrow b\bar{b}X)$ at $\sqrt{s} = 7$ TeV in the forward region

Beams: pp

Energies: (3500.0, 3500.0) GeV

Experiment: LHCb (LHC)

Inspire ID: 867355

Status: VALIDATED

Authors:

- Andy Buckley <andy.buckley@ed.ac.uk>
- Sercan Sen <sercan.sen@cern.ch>
- Peter Skands <Peter.Skands@cern.ch>
- Sheldon Stone <stone@physics.syr.edu>

References:

- arXiv: [1009.2731](#)

Run details:

- pp to b -hadron + X at 7 TeV. i.e., switch on "HardQCD:gg2bbbar" and "HardQCD:qqbar2bbbar" flags in Pythia8.

The average cross-section to produce b -flavoured or \bar{b} -flavoured hadrons is measured in different pseudorapidity intervals over the entire range of p_T , assuming the LEP (and Tevatron) fractions for fragmentation into b -flavoured hadrons.

Histograms (4):

- b production cross-section at $\sqrt{s} = 7$ TeV, with LEP fragmentation fractions ([/REF/LHCb_2010_I867355/d01-x01-y01](#))
- b production cross-section at $\sqrt{s} = 7$ TeV, with Tevatron fragmentation fractions ([/REF/LHCb_2010_I867355/d01-x01-y02](#))
- b production cross-section at $\sqrt{s} = 7$ TeV, with LEP fragmentation fractions ([/REF/LHCb_2010_I867355/d02-x01-y01](#))
- b production cross-section at $\sqrt{s} = 7$ TeV, with Tevatron fragmentation fractions ([/REF/LHCb_2010_I867355/d02-x01-y02](#))

8.115 LHCb_2010_S8758301 [178]

LHCb differential cross section measurement of prompt K_S^0 production in three rapidity windows at $\sqrt{s} = 0.9$ TeV

Beams: pp

Energies: (450.0, 450.0) GeV

Experiment: LHCb (LHC 900 GeV)

Spires ID: [8758301](#)

Status: VALIDATED

Authors:

- Holger Schulz (holger.schulz@physik.hu-berlin.de)
- Alex Grecu (Alex.Grecu@cern.ch)

References:

- Phys.Lett.B693:69-80,2010
- arXiv: [1008.3105\[hep-ex\]](#)

Run details:

- QCD events. See paper for MC discussion.

The paper presents the cross-section and double differential cross-section measurement for prompt K_S^0 production in pp collisions at $\sqrt{s} = 0.9$ TeV. The data were taken during the LHCb run in December 2009 and cover a transversal momentum range from 0 to 1.6 GeV/c. The differential production cross-section is calculated for three rapidity windows $2.5 < y < 3.0$, $3.0 < y < 3.5$ and $3.5 < y < 4.0$ as well as the whole rapidity domain $2.5 < y < 4.0$.

Histograms (7):

- Cross-section for prompt K_S^0 production ($2.5 < y < 3.0$) ([/REF/LHCb_2010_S8758301/d01-x01-y01](#))
- Cross-section for prompt K_S^0 production ($3.0 < y < 3.5$) ([/REF/LHCb_2010_S8758301/d01-x01-y02](#))
- Cross-section for prompt K_S^0 production ($3.5 < y < 4.0$) ([/REF/LHCb_2010_S8758301/d01-x01-y03](#))
- Diff. cross-section for prompt K_S^0 production ($2.5 < y < 3.0$) ([/REF/LHCb_2010_S8758301/d02-x01-y01](#))
- Diff. cross-section for prompt K_S^0 production ($3.0 < y < 3.5$) ([/REF/LHCb_2010_S8758301/d02-x01-y02](#))
- Diff. cross-section for prompt K_S^0 production ($3.5 < y < 4.0$) ([/REF/LHCb_2010_S8758301/d02-x01-y03](#))
- Diff. cross-section for prompt K_S^0 production ($2.5 < y < 4.0$) ([/REF/LHCb_2010_S8758301/d03-x01-y01](#))

8.116 LHCb_2011_I917009 [179]

V^0 production ratios in pp collisions at $\sqrt{s} = 0.9$ and 7 TeV at LHCb

Beams: pp

Energies: (450.0, 450.0), (3500.0, 3500.0) GeV

Experiment: LHCb (LHC)

Inspire ID: [917009](#)

Status: VALIDATED

Authors:

- Alex Grecu (Alex.Grecu@cern.ch)

References:

- JHEP08:034,2011
- arXiv: [1107.0882\[hep-ex\]](#)
- DOI: [10.1007/JHEP08\(2011\)034](#)

Run details:

- QCD events. LHCb minimum bias, Perugia 0 and Perugia NOCR tune events used for reproducing published histograms.

This paper presents the production ratios for $\bar{\Lambda}/\Lambda$ and $\bar{\Lambda}/K_s^0$ measured by LHCb detector in 2010 at $\sqrt{s} = 0.9$ TeV and 7 TeV as functions of the transverse momentum p_\perp and the rapidity y in the ranges $0.15 < p_\perp < 2.50$ GeV/ c and $2.0 < y < 4.5$, respectively. The results for the two energies are merged and represented as a function of rapidity loss $\Delta y = y_{\text{beam}} - y$.

Histograms (24):

- $\bar{\Lambda}/\Lambda$ ratio at $\sqrt{s} = 0.9$ TeV ($0.25 < p_\perp < 0.65$ GeV/ c) ([/REF/LHCb_2011_I917009/d01-x01-y01](#))
- $\bar{\Lambda}/\Lambda$ ratio at $\sqrt{s} = 0.9$ TeV ($0.65 < p_\perp < 1.00$ GeV/ c) ([/REF/LHCb_2011_I917009/d01-x01-y02](#))
- $\bar{\Lambda}/\Lambda$ ratio at $\sqrt{s} = 0.9$ TeV ($1.00 < p_\perp < 2.50$ GeV/ c) ([/REF/LHCb_2011_I917009/d01-x01-y03](#))
- $\bar{\Lambda}/K_s^0$ ratio at $\sqrt{s} = 0.9$ TeV ($0.25 < p_\perp < 0.65$ GeV/ c) ([/REF/LHCb_2011_I917009/d02-x01-y01](#))
- $\bar{\Lambda}/K_s^0$ ratio at $\sqrt{s} = 0.9$ TeV ($0.65 < p_\perp < 1.00$ GeV/ c) ([/REF/LHCb_2011_I917009/d02-x01-y02](#))
- $\bar{\Lambda}/K_s^0$ ratio at $\sqrt{s} = 0.9$ TeV ($1.00 < p_\perp < 2.50$ GeV/ c) ([/REF/LHCb_2011_I917009/d02-x01-y03](#))
- $\bar{\Lambda}/\Lambda$ ratio at $\sqrt{s} = 0.9$ TeV ($0.25 < p_\perp < 2.50$ Gev/ c) ([/REF/LHCb_2011_I917009/d03-x01-y01](#))
- $\bar{\Lambda}/K_s^0$ ratio at $\sqrt{s} = 0.9$ TeV ($0.25 < p_\perp < 2.50$ GeV/ c) ([/REF/LHCb_2011_I917009/d04-x01-y01](#))
- $\bar{\Lambda}/\Lambda$ ratio at $\sqrt{s} = 0.9$ TeV ($2.0 < y < 4.0$) ([/REF/LHCb_2011_I917009/d05-x01-y01](#))

- $\bar{\Lambda}/K_s^0$ ratio at $\sqrt{s} = 0.9$ TeV ($2.0 < y < 4.0$) (/REF/LHCb_2011_I917009/d06-x01-y01)
- $\bar{\Lambda}/\Lambda$ ratio at $\sqrt{s} = 0.9$ TeV ($0.25 < p_\perp < 2.50$ GeV/ c) (/REF/LHCb_2011_I917009/d07-x01-y01)
- $\bar{\Lambda}/K_s^0$ ratio at $\sqrt{s} = 0.9$ TeV ($0.25 < p_\perp < 2.50$ GeV/ c) (/REF/LHCb_2011_I917009/d08-x01-y01)
- $\bar{\Lambda}/\Lambda$ ratio at $\sqrt{s} = 7$ TeV ($0.15 < p_\perp < 0.65$ GeV/ c) (/REF/LHCb_2011_I917009/d09-x01-y01)
- $\bar{\Lambda}/\Lambda$ ratio at $\sqrt{s} = 7$ TeV ($0.65 < p_\perp < 1.00$ GeV/ c) (/REF/LHCb_2011_I917009/d09-x01-y02)
- $\bar{\Lambda}/\Lambda$ ratio at $\sqrt{s} = 7$ TeV ($1.00 < p_\perp < 2.50$ GeV/ c) (/REF/LHCb_2011_I917009/d09-x01-y03)
- $\bar{\Lambda}/K_s^0$ ratio at $\sqrt{s} = 7$ TeV ($0.15 < p_\perp < 0.65$ GeV/ c) (/REF/LHCb_2011_I917009/d10-x01-y01)
- $\bar{\Lambda}/K_s^0$ ratio at $\sqrt{s} = 7$ TeV ($0.65 < p_\perp < 1.00$ GeV/ c) (/REF/LHCb_2011_I917009/d10-x01-y02)
- $\bar{\Lambda}/K_s^0$ ratio at $\sqrt{s} = 7$ TeV ($1.00 < p_\perp < 2.50$ GeV/ c) (/REF/LHCb_2011_I917009/d10-x01-y03)
- $\bar{\Lambda}/\Lambda$ ratio at $\sqrt{s} = 7$ TeV ($0.15 < p_\perp < 2.50$ GeV/ c) (/REF/LHCb_2011_I917009/d11-x01-y01)
- $\bar{\Lambda}/K_s^0$ ratio at $\sqrt{s} = 7$ TeV ($0.15 < p_\perp < 2.5$ GeV/ c) (/REF/LHCb_2011_I917009/d12-x01-y01)
- $\bar{\Lambda}/\Lambda$ ratio at $\sqrt{s} = 7$ TeV ($2.0 < y < 4.5$) (/REF/LHCb_2011_I917009/d13-x01-y01)
- $\bar{\Lambda}/K_s^0$ ratio at $\sqrt{s} = 7$ TeV ($2.0 < y < 4.5$) (/REF/LHCb_2011_I917009/d14-x01-y01)
- $\bar{\Lambda}/\Lambda$ ratio at $\sqrt{s} = 7$ TeV ($0.15 < p_\perp < 2.50$ GeV/ c) (/REF/LHCb_2011_I917009/d15-x01-y01)
- $\bar{\Lambda}/K_s^0$ ratio at $\sqrt{s} = 7$ TeV ($0.15 < p_\perp < 2.50$ GeV/ c) (/REF/LHCb_2011_I917009/d16-x01-y01)

8.117 LHCb_2011_I919315 [180]

Inclusive differential Φ production cross-section as a function of p_T and y

Beams: pp

Energies: (3500.0, 3500.0) GeV

Experiment: LHCb (LHC)

Inspire ID: [919315](#)

Status: VALIDATED

Authors:

- Friederike Blatt (friederike.blatt@tu-dortmund.de)
- Michael Kaballo (michael.kaballo@tu-dortmund.de)
- Till Moritz Karbach (moritz.karbach@tu-dortmund.de)

References:

- Phys.Lett.B703:267-273,2011
- arXiv: [1107.3935](#)

Run details:

- pp collisions, QCD-Events, $\sqrt{s} = 7\text{TeV}$

Measurement of the inclusive differential Φ cross-section in pp collisions at $\sqrt{s} = 7\text{TeV}$ in the rapidity range of $2.44 < y < 4.06$ and the p_T range of $0.6 \text{ GeV}/c < p_T < 5.0 \text{ GeV}/c$.

Histograms (11):

- Transverse momentum of Φ -mesons ([/REF/LHCb_2011_I919315/d02-x01-y01](#))
- Transverse momentum of Φ -mesons ([/REF/LHCb_2011_I919315/d02-x01-y02](#))
- Transverse momentum of Φ -mesons ([/REF/LHCb_2011_I919315/d03-x01-y01](#))
- Transverse momentum of Φ -mesons ([/REF/LHCb_2011_I919315/d03-x01-y02](#))
- Transverse momentum of Φ -mesons ([/REF/LHCb_2011_I919315/d04-x01-y01](#))
- Transverse momentum of Φ -mesons ([/REF/LHCb_2011_I919315/d04-x01-y02](#))
- Transverse momentum of Φ -mesons ([/REF/LHCb_2011_I919315/d05-x01-y01](#))
- Transverse momentum of Φ -mesons ([/REF/LHCb_2011_I919315/d05-x01-y02](#))
- Transverse momentum of Φ -mesons ([/REF/LHCb_2011_I919315/d06-x01-y01](#))
- Transverse momentum of Φ -mesons ([/REF/LHCb_2011_I919315/d07-x01-y01](#))
- Rapidity of Φ -mesons ([/REF/LHCb_2011_I919315/d08-x01-y01](#))

8.118 LHCb_2012_I1119400 [181]

Measurement of prompt hadron production ratios in pp collisions at $\sqrt{s} = 0.9$ and 7 TeV

Beams: pp

Energies: (450.0, 450.0), (3500.0, 3500.0) GeV

Experiment: LHCb (LHC)

Inspire ID: [1119400](#)

Status: UNVALIDATED

Authors:

- Andrea Contu ⟨ Andrea.Contu@cern.ch ⟩
- Alex Grecu ⟨ Alex.Grecu@cern.ch ⟩

References:

- arXiv: [1206.5160](#)

Run details:

- Minimum bias events at $\sqrt{s} = 0.9$ and 7 TeV.

Measurement of the production ratios of prompt charged particles (protons, pions and kaons). Promptness is defined as originating from the primary interaction, either directly, or through the subsequent decay of a resonance.

Histograms (36):

- \bar{p}/p ratio at $\sqrt{s} = 0.9$ TeV ($0.0 < p_\perp < 0.8$ GeV/ c) ([/REF/LHCb_2012_I1119400/d01-x01-y01](#))
- \bar{p}/p ratio at $\sqrt{s} = 0.9$ TeV ($0.8 < p_\perp < 1.2$ GeV/ c) ([/REF/LHCb_2012_I1119400/d01-x01-y02](#))
- \bar{p}/p ratio at $\sqrt{s} = 0.9$ TeV ($p_\perp > 1.2$ GeV/ c) ([/REF/LHCb_2012_I1119400/d01-x01-y03](#))
- \bar{p}/p ratio at $\sqrt{s} = 7$ TeV ($0.0 < p_\perp < 0.8$ GeV/ c) ([/REF/LHCb_2012_I1119400/d02-x01-y01](#))
- \bar{p}/p ratio at $\sqrt{s} = 7$ TeV ($0.8 < p_\perp < 1.2$ GeV/ c) ([/REF/LHCb_2012_I1119400/d02-x01-y02](#))
- \bar{p}/p ratio at $\sqrt{s} = 7$ TeV ($p_\perp > 1.2$ GeV/ c) ([/REF/LHCb_2012_I1119400/d02-x01-y03](#))
- K^-/K^+ ratio at $\sqrt{s} = 0.9$ TeV ($0.0 < p_\perp < 0.8$ GeV/ c) ([/REF/LHCb_2012_I1119400/d03-x01-y01](#))
- K^-/K^+ ratio at $\sqrt{s} = 0.9$ TeV ($0.8 < p_\perp < 1.2$ GeV/ c) ([/REF/LHCb_2012_I1119400/d03-x01-y02](#))
- K^-/K^+ ratio at $\sqrt{s} = 0.9$ TeV ($p_\perp > 1.2$ GeV/ c) ([/REF/LHCb_2012_I1119400/d03-x01-y03](#))
- K^-/K^+ ratio at $\sqrt{s} = 7$ TeV ($0.0 < p_\perp < 0.8$ GeV/ c) ([/REF/LHCb_2012_I1119400/d04-x01-y01](#))
- K^-/K^+ ratio at $\sqrt{s} = 7$ TeV ($0.8 < p_\perp < 1.2$ GeV/ c) ([/REF/LHCb_2012_I1119400/d04-x01-y02](#))
- K^-/K^+ ratio at $\sqrt{s} = 7$ TeV ($p_\perp > 1.2$ GeV/ c) ([/REF/LHCb_2012_I1119400/d04-x01-y03](#))

- π^-/π^+ ratio at $\sqrt{s} = 0.9$ TeV ($0.0 < p_\perp < 0.8$ GeV/ c) (/REF/LHCb_2012_I1119400/d05-x01-y01)
- π^-/π^+ ratio at $\sqrt{s} = 0.9$ TeV ($0.8 < p_\perp < 1.2$ GeV/ c) (/REF/LHCb_2012_I1119400/d05-x01-y02)
- π^-/π^+ ratio at $\sqrt{s} = 0.9$ TeV ($p_\perp > 1.2$ GeV/ c) (/REF/LHCb_2012_I1119400/d05-x01-y03)
- π^-/π^+ ratio at $\sqrt{s} = 7$ TeV ($0.0 < p_\perp < 0.8$ GeV/ c) (/REF/LHCb_2012_I1119400/d06-x01-y01)
- π^-/π^+ ratio at $\sqrt{s} = 7$ TeV ($0.8 < p_\perp < 1.2$ GeV/ c) (/REF/LHCb_2012_I1119400/d06-x01-y02)
- π^-/π^+ ratio at $\sqrt{s} = 7$ TeV ($p_\perp > 1.2$ GeV/ c) (/REF/LHCb_2012_I1119400/d06-x01-y03)
- $(p + \bar{p})/(\pi^+ + \pi^-)$ ratio at $\sqrt{s} = 0.9$ TeV ($0.0 < p_\perp < 0.8$ GeV/ c) (/REF/LHCb_2012_I1119400/d07-x01-y01)
- $(p + \bar{p})/(\pi^+ + \pi^-)$ ratio at $\sqrt{s} = 0.9$ TeV ($0.8 < p_\perp < 1.2$ GeV/ c) (/REF/LHCb_2012_I1119400/d07-x01-y02)
- $(p + \bar{p})/(\pi^+ + \pi^-)$ ratio at $\sqrt{s} = 0.9$ TeV ($p_\perp > 1.2$ GeV/ c) (/REF/LHCb_2012_I1119400/d07-x01-y03)
- $(p + \bar{p})/(\pi^+ + \pi^-)$ ratio at $\sqrt{s} = 7$ TeV ($0.0 < p_\perp < 0.8$ GeV/ c) (/REF/LHCb_2012_I1119400/d08-x01-y01)
- $(p + \bar{p})/(\pi^+ + \pi^-)$ ratio at $\sqrt{s} = 7$ TeV ($0.8 < p_\perp < 1.2$ GeV/ c) (/REF/LHCb_2012_I1119400/d08-x01-y02)
- $(p + \bar{p})/(\pi^+ + \pi^-)$ ratio at $\sqrt{s} = 7$ TeV ($p_\perp > 1.2$ GeV/ c) (/REF/LHCb_2012_I1119400/d08-x01-y03)
- $(K^+ + K^-)/(\pi^+ + \pi^-)$ ratio at $\sqrt{s} = 0.9$ TeV ($0.0 < p_\perp < 0.8$ GeV/ c) (/REF/LHCb_2012_I1119400/d09-x01-y01)
- $(K^+ + K^-)/(\pi^+ + \pi^-)$ ratio at $\sqrt{s} = 0.9$ TeV ($0.8 < p_\perp < 1.2$ GeV/ c) (/REF/LHCb_2012_I1119400/d09-x01-y02)
- $(K^+ + K^-)/(\pi^+ + \pi^-)$ ratio at $\sqrt{s} = 0.9$ TeV ($p_\perp > 1.2$ GeV/ c) (/REF/LHCb_2012_I1119400/d09-x01-y03)
- $(K^+ + K^-)/(\pi^+ + \pi^-)$ ratio at $\sqrt{s} = 7$ TeV ($0.0 < p_\perp < 0.8$ GeV/ c) (/REF/LHCb_2012_I1119400/d10-x01-y01)
- $(K^+ + K^-)/(\pi^+ + \pi^-)$ ratio at $\sqrt{s} = 7$ TeV ($0.8 < p_\perp < 1.2$ GeV/ c) (/REF/LHCb_2012_I1119400/d10-x01-y02)
- $(K^+ + K^-)/(\pi^+ + \pi^-)$ ratio at $\sqrt{s} = 7$ TeV ($p_\perp > 1.2$ GeV/ c) (/REF/LHCb_2012_I1119400/d10-x01-y03)
- $(p + \bar{p})/(K^+ + K^-)$ ratio at $\sqrt{s} = 0.9$ TeV ($0.0 < p_\perp < 0.8$ GeV/ c) (/REF/LHCb_2012_I1119400/d11-x01-y01)

- $(p + \bar{p})/(K^+ + K^-)$ ratio at $\sqrt{s} = 0.9$ TeV ($0.8 < p_\perp < 1.2$ GeV/ c) ([/REF/LHCb_2012-I1119400/d11-x01-y02](#))
- $(p + \bar{p})/(K^+ + K^-)$ ratio at $\sqrt{s} = 0.9$ TeV ($p_\perp > 1.2$ GeV/ c) ([/REF/LHCb_2012-I1119400/d11-x01-y03](#))
- $(p + \bar{p})/(K^+ + K^-)$ ratio at $\sqrt{s} = 7$ TeV ($0.0 < p_\perp < 0.8$ GeV/ c) ([/REF/LHCb_2012-I1119400/d12-x01-y01](#))
- $(p + \bar{p})/(K^+ + K^-)$ ratio at $\sqrt{s} = 7$ TeV ($0.8 < p_\perp < 1.2$ GeV/ c) ([/REF/LHCb_2012-I1119400/d12-x01-y02](#))
- $(p + \bar{p})/(K^+ + K^-)$ ratio at $\sqrt{s} = 7$ TeV ($p_\perp > 1.2$ GeV/ c) ([/REF/LHCb_2012-I1119400/d12-x01-y03](#))

8.119 LHCb_2013_I1208105 [182]

LHCb measurement of energy flow from pp collisions at $\sqrt{s} = 7$ TeV

Beams: pp

Energies: (3500.0, 3500.0) GeV

Experiment: LHCb (LHC)

Inspire ID: [1208105](#)

Status: VALIDATED

Authors:

- Alex Grecu ⟨ Alex.Grecu@cern.ch ⟩
- Dmytro Volyanskyy ⟨ Dmytro.Volyanskyy@cern.ch ⟩
- Michael Schmelling ⟨ Michael.Schmelling@mpi-hd.mpg.de ⟩

References:

- arXiv: [1212.4755](#)
- Eur. Phys. J. C 73 (2012) 2421

Run details:

- Minimum bias events from pp collisions at $\sqrt{s} = 7$ TeV.

The energy flow created in pp collisions at 7 TeV within the fiducial pseudorapidity range of the LHCb detector ($1.9 < \eta < 4.9$) is measured for inclusive minimum bias interactions, hard scattering processes and events with enhanced or suppressed diffractive contribution. Plots for these four event classes are shown separately for all and charged only final state particles, respectively. The total energy flow is measured by combining the charged energy flow and a data-constrained MC estimate of the neutral component. For the two highest eta bins the data-constrained measurements of the neutral energy were extrapolated from the more central region as the LHCb electromagnetic calorimeter has no detection coverage in that phase space domain.

Histograms (8):

- Charged EF – inclusive minimum bias events, $\sqrt{s} = 7$ TeV ([/REF/LHCb_2013_I1208105/d01-x01-y01](#))
- Charged EF – hard scattering events ($p_T > 3$ GeV/c), $\sqrt{s} = 7$ TeV ([/REF/LHCb_2013_I1208105/d02-x01-y01](#))
- Charged EF – diffractive enriched events, $\sqrt{s} = 7$ TeV ([/REF/LHCb_2013_I1208105/d03-x01-y01](#))
- Charged EF – non-diffractive enriched events, $\sqrt{s} = 7$ TeV ([/REF/LHCb_2013_I1208105/d04-x01-y01](#))
- Total EF – inclusive minimum bias events, $\sqrt{s} = 7$ TeV ([/REF/LHCb_2013_I1208105/d05-x01-y01](#))
- Total EF – hard scattering events ($p_T > 3$ GeV/c), $\sqrt{s} = 7$ TeV ([/REF/LHCb_2013_I1208105/d06-x01-y01](#))

- Total EF – diffractive enriched events, $\sqrt{s} = 7$ TeV ([/REF/LHCb_2013_I1208105/d07-x01-y01](#))
- Total EF – non-diffractive enriched events, $\sqrt{s} = 7$ TeV ([/REF/LHCb_2013_I1208105/d08-x01-y01](#))

8.120 LHCb_2013_I1218996 [183]

Charm hadron differential cross-sections in p_\perp and rapidity

Beams: pp

Energies: (3500.0, 3500.0) GeV

Experiment: LHCb (LHC 7TeV)

Inspire ID: [1218996](#)

Status: VALIDATED

Authors:

- Patrick Spradlin (patrick.spradlin@cern.ch)

References:

- Nucl.Phys. B871 (2013) 1-20
- DOI: [10.1016/j.nuclphysb.2013.02.010](https://doi.org/10.1016/j.nuclphysb.2013.02.010)
- arXiv: [1302.2864](https://arxiv.org/abs/1302.2864)
- LHCb-PAPER-2012-041, CERN-PH-EP-2013-009

Run details:

- Minimum bias QCD events, proton–proton interactions at $\sqrt{s} = 7$ TeV.

Measurements of differential production cross-sections with respect to transverse momentum, $d\sigma(H_c + \text{c.c.})/dp_T$, for charm hadron species $H_c \in \{D^0, D^+, D^*(2010)^+, D_s^+, \Lambda_c^+\}$ in proton–proton collisions at center-of-mass energy $\sqrt{s} = 7$ TeV. The differential cross-sections are measured in bins of hadron transverse momentum (p_T) and rapidity (y) with respect to the beam axis in the region $0 < p_T < 8$ GeV/ c and $2.0 < y < 4.5$, where p_T and y are measured in the proton–proton CM frame. In this analysis code, it is assumed that the event coordinate system is in the proton–proton CM frame with the z -axis corresponding to the proton–proton collision axis (as usual). Contributions of charm hadrons from the decays of b -hadrons and other particles with comparably large mean lifetimes have been removed in the measurement. In this analysis code, this is implemented by counting only charm hadrons that do not have an ancestor that contains a b quark.

Histograms (21):

- Prompt $\Lambda_c^+ + \text{c.c.}$ $d\sigma/dp_T$ for rapidity interval $2.0 < y < 4.5$ ([/REF/LHCb_2013_I1218996/d01-x01-y01](#))
- Prompt $D^0 + \text{c.c.}$ $d\sigma/dp_T$ for rapidity interval $2.0 < y < 2.5$ ([/REF/LHCb_2013_I1218996/d02-x01-y01](#))
- Prompt $D^0 + \text{c.c.}$ $d\sigma/dp_T$ for rapidity interval $2.5 < y < 3.0$ ([/REF/LHCb_2013_I1218996/d02-x01-y02](#))

- Prompt $D^0 + \text{c.c. } d\sigma/dp_T$ for rapidity interval $3.0 < y < 3.5$ ([/REF/LHCb_2013-I1218996/d02-x01-y03](#))
- Prompt $D^0 + \text{c.c. } d\sigma/dp_T$ for rapidity interval $3.5 < y < 4.0$ ([/REF/LHCb_2013-I1218996/d02-x01-y04](#))
- Prompt $D^0 + \text{c.c. } d\sigma/dp_T$ for rapidity interval $4.0 < y < 4.5$ ([/REF/LHCb_2013-I1218996/d02-x01-y05](#))
- Prompt $D^+ + \text{c.c. } d\sigma/dp_T$ for rapidity interval $2.0 < y < 2.5$ ([/REF/LHCb_2013-I1218996/d03-x01-y01](#))
- Prompt $D^+ + \text{c.c. } d\sigma/dp_T$ for rapidity interval $2.5 < y < 3.0$ ([/REF/LHCb_2013-I1218996/d03-x01-y02](#))
- Prompt $D^+ + \text{c.c. } d\sigma/dp_T$ for rapidity interval $3.0 < y < 3.5$ ([/REF/LHCb_2013-I1218996/d03-x01-y03](#))
- Prompt $D^+ + \text{c.c. } d\sigma/dp_T$ for rapidity interval $3.5 < y < 4.0$ ([/REF/LHCb_2013-I1218996/d03-x01-y04](#))
- Prompt $D^+ + \text{c.c. } d\sigma/dp_T$ for rapidity interval $4.0 < y < 4.5$ ([/REF/LHCb_2013-I1218996/d03-x01-y05](#))
- Prompt $D^*(2010)^+ + \text{c.c. } d\sigma/dp_T$ for rapidity interval $2 < y < 2.5$ ([/REF/LHCb_2013-I1218996/d04-x01-y01](#))
- Prompt $D^*(2010)^+ + \text{c.c. } d\sigma/dp_T$ for rapidity interval $2.5 < y < 3$ ([/REF/LHCb_2013-I1218996/d04-x01-y02](#))
- Prompt $D^*(2010)^+ + \text{c.c. } d\sigma/dp_T$ for rapidity interval $3 < y < 3.5$ ([/REF/LHCb_2013-I1218996/d04-x01-y03](#))
- Prompt $D^*(2010)^+ + \text{c.c. } d\sigma/dp_T$ for rapidity interval $3.5 < y < 4$ ([/REF/LHCb_2013-I1218996/d04-x01-y04](#))
- Prompt $D^*(2010)^+ + \text{c.c. } d\sigma/dp_T$ for rapidity interval $4 < y < 4.5$ ([/REF/LHCb_2013-I1218996/d04-x01-y05](#))
- Prompt $D_s^+ + \text{c.c. } d\sigma/dp_T$ for rapidity interval $2.0 < y < 2.5$ ([/REF/LHCb_2013-I1218996/d05-x01-y01](#))
- Prompt $D_s^+ + \text{c.c. } d\sigma/dp_T$ for rapidity interval $2.5 < y < 3.0$ ([/REF/LHCb_2013-I1218996/d05-x01-y02](#))
- Prompt $D_s^+ + \text{c.c. } d\sigma/dp_T$ for rapidity interval $3.0 < y < 3.5$ ([/REF/LHCb_2013-I1218996/d05-x01-y03](#))
- Prompt $D_s^+ + \text{c.c. } d\sigma/dp_T$ for rapidity interval $3.5 < y < 4.0$ ([/REF/LHCb_2013-I1218996/d05-x01-y04](#))

- Prompt D_s^+ + c.c. $d\sigma/dp_T$ for rapidity interval $4.0 < y < 4.5$ ([/REF/LHCb_2013-I1218996/d05-x01-y05](#))

8.121 LHCf_2012_I1115479 [184]

Measurement of forward neutral pion transverse momentum spectra for $\sqrt{s} = 7$ TeV proton-proton collisions at LHC

Beams: pp

Energies: (3500.0, 3500.0) GeV

Experiment: LHCf (LHC)

Inspire ID: [1115479](#)

Status: VALIDATED

Authors:

- Sercan Sen (ssen@cern.ch)

References:

- Phys.Rev. D86 (2012) 092001
- arXiv: [1205.4578](#)

Run details:

- Inelastic events (ND+SD+DD) at $\sqrt{s} = 7$ TeV.

The inclusive production rate of neutral pions has been measured by LHCf experiment during $\sqrt{s} = 7$ TeV pp collision operation in early 2010. In order to ensure good event reconstruction efficiency, the range of the π^0 rapidity and p_\perp are limited to $8.9 < y < 11.0$ and $p_\perp < 0.6$ GeV, respectively.

Histograms (6):

- π^0 p_\perp spectrum, $8.9 < y < 9.0$ ([/REF/LHCf_2012_I1115479/d01-x01-y01](#))
- π^0 p_\perp spectrum, $9.0 < y < 9.2$ ([/REF/LHCf_2012_I1115479/d02-x01-y01](#))
- π^0 p_\perp spectrum, $9.2 < y < 9.4$ ([/REF/LHCf_2012_I1115479/d03-x01-y01](#))
- π^0 p_\perp spectrum, $9.4 < y < 9.6$ ([/REF/LHCf_2012_I1115479/d04-x01-y01](#))
- π^0 p_\perp spectrum, $9.6 < y < 10.0$ ([/REF/LHCf_2012_I1115479/d05-x01-y01](#))
- π^0 p_\perp spectrum, $10.0 < y < 11.0$ ([/REF/LHCf_2012_I1115479/d06-x01-y01](#))

8.122 TOTEM_2012_002 [185]

Measurement of proton-proton elastic scattering and total cross section at $\sqrt{s} = 7$ TeV.

Beams: pp

Energies: (3500.0, 3500.0) GeV

Experiment: TOTEM (LHC)

Status: VALIDATED

Authors:

- Sercan Sen (Sercan.Sen@cern.ch)
- Peter Skands (Peter.Skands@cern.ch)

References:

- CERN-PH-EP-2012-239
- <http://cds.cern.ch/record/1472948>

Run details:

- Elastic events only.

Measurement of the elastic differential cross-section in proton-proton interactions at a centre-of-mass energy $\sqrt{s} = 7$ TeV at the LHC. The data, which cover the $|t|$ range $0.005 - 0.2$ GeV 2 , were collected using Roman Pot detectors very close to the outgoing beam in October 2011, allowing the precise extrapolation down to the optical point, $t = 0$, and hence the derivation of the elastic as well as the total cross-section via the optical theorem.

Histograms (3):

- Differential elastic cross-section vs. $|t|$ (low t) (/REF/TOTEM_2012_002/d01-x01-y01)
- Differential elastic cross-section vs. $|t|$ (high t) (/REF/TOTEM_2012_002/d02-x01-y01)
- Total elastic cross-section (/REF/TOTEM_2012_002/d03-x01-y01)

8.123 TOTEM_2012_I1115294 [186]

Forward $dN/d\eta$ at 7 TeV

Beams: pp

Energies: (3500.0, 3500.0) GeV

Experiment: TOTEM (LHC)

Status: VALIDATED

Authors:

- Hendrik Hoeth <hendrik.hoeth@cern.ch>

References:

- Europhys.Lett. 98 (2012) 31002
- arXiv: [1205.4105](#)
- CERN-PH-EP-2012-106
- TOTEM 2012-01

Run details:

- pp QCD interactions at 900 GeV and 7 TeV.

The TOTEM experiment has measured the charged particle pseudorapidity density $dN_{ch}/d\eta$ in pp collisions at $\sqrt{s} = 7$ TeV for $5.3 < |\eta| < 6.4$ in events with at least one charged particle with transverse momentum above 40 MeV/c in this pseudorapidity range.

Histograms (1):

- Charged particle $|\eta|$ at 7 TeV, track $p_\perp > 40$ MeV, for $N_{ch} \geq 1$ ([/REF/TOTEM_2012-I1115294/d01-x01-y01](#))

9. SPS analyses

9.1 UA1_1990_S2044935 [187]

UA1 multiplicities, transverse momenta and transverse energy distributions.

Beams: $\bar{p}p$

Energies: (31.5, 31.5), (100.0, 100.0), (250.0, 250.0), (450.0, 450.0) GeV

Experiment: UA1 (SPS)

Spires ID: [2044935](#)

Status: VALIDATED

Authors:

- Andy Buckley ⟨ andy.buckley@cern.ch ⟩
- Christophe Vaillant ⟨ c.l.j.j.vaillant@durham.ac.uk ⟩

References:

- Nucl.Phys.B353:261,1990

Run details:

- QCD min bias events at $\sqrt{s} = 63, 200, 500$ and 900 GeV.

Particle multiplicities, transverse momenta and transverse energy distributions at the UA1 experiment, at energies of 200, 500 and 900 GeV (with one plot at 63 GeV for comparison).

Histograms (18):

- Multiplicity distribution at $\sqrt{s} = 200$ GeV ([/REF/UA1_1990_S2044935/d01-x01-y01](#))
- Multiplicity distribution at $\sqrt{s} = 500$ GeV ([/REF/UA1_1990_S2044935/d01-x01-y02](#))
- Multiplicity distribution at $\sqrt{s} = 900$ GeV ([/REF/UA1_1990_S2044935/d01-x01-y03](#))
- $E d^3\sigma/dp^3$ at $\eta = 0$, $\sqrt{s} = 200$ GeV ([/REF/UA1_1990_S2044935/d02-x01-y01](#))
- $E d^3\sigma/dp^3$ at $\eta = 0$, $\sqrt{s} = 500$ GeV ([/REF/UA1_1990_S2044935/d02-x01-y02](#))
- $E d^3\sigma/dp^3$ at $\eta = 0$, $\sqrt{s} = 900$ GeV ([/REF/UA1_1990_S2044935/d02-x01-y03](#))
- $E d^3\sigma/dp^3$ at $\eta = 0$, $\sqrt{s} = 900$ GeV ($dn_{ch}/d\eta = 0.8 \dots 4$) ([/REF/UA1_1990_S2044935/d03-x01-y01](#))
- $E d^3\sigma/dp^3$ at $\eta = 0$, $\sqrt{s} = 900$ GeV ($dn_{ch}/d\eta = 4 \dots 8$) ([/REF/UA1_1990_S2044935/d04-x01-y01](#))
- $E d^3\sigma/dp^3$ at $\eta = 0$, $\sqrt{s} = 900$ GeV ($dn_{ch}/d\eta > 8$) ([/REF/UA1_1990_S2044935/d05-x01-y01](#))
- $\langle p_\perp \rangle$ vs. n_{ch} at $\sqrt{s} = 200$ GeV ([/REF/UA1_1990_S2044935/d06-x01-y01](#))
- $\langle p_\perp \rangle$ vs. n_{ch} at $\sqrt{s} = 900$ GeV ([/REF/UA1_1990_S2044935/d07-x01-y01](#))
- $\langle p_\perp \rangle$ vs. n_{ch} at $\sqrt{s} = 63$ GeV ([/REF/UA1_1990_S2044935/d08-x01-y01](#))

- Transverse energy cross section at $\sqrt{s} = 200$ GeV and $|\eta| < 6$ ([/REF/UA1_1990_S2044935/d09-x01-y01](#))
- Transverse energy cross section at $\sqrt{s} = 500$ GeV and $|\eta| < 6$ ([/REF/UA1_1990_S2044935/d10-x01-y01](#))
- Transverse energy cross section at $\sqrt{s} = 900$ GeV and $|\eta| < 6$ ([/REF/UA1_1990_S2044935/d11-x01-y01](#))
- $\langle \Sigma E_{\perp} \rangle$ vs. n_{ch} at $\sqrt{s} = 200$ GeV and $|\eta| < 2.5$ ([/REF/UA1_1990_S2044935/d12-x01-y01](#))
- $\langle \Sigma E_{\perp} \rangle$ vs. n_{ch} at $\sqrt{s} = 500$ GeV and $|\eta| < 2.5$ ([/REF/UA1_1990_S2044935/d12-x01-y02](#))
- $\langle \Sigma E_{\perp} \rangle$ vs. n_{ch} at $\sqrt{s} = 900$ GeV and $|\eta| < 2.5$ ([/REF/UA1_1990_S2044935/d12-x01-y03](#))

9.2 UA5_1982_S875503 [188]

UA5 multiplicity and pseudorapidity distributions for pp and $p\bar{p}$.

Beams: $\bar{p}p$, pp

Energies: (26.5, 26.5) GeV

Experiment: UA5 (SPS)

Spires ID: [875503](#)

Status: VALIDATED

Authors:

- Andy Buckley <andy.buckley@cern.ch>
- Christophe Vaillant <c.l.j.j.vaillant@durham.ac.uk>

References:

- Phys.Lett.112B:183,1982

Run details:

- Min bias QCD events at $\sqrt{s} = 53$ GeV. Run with both pp and $p\bar{p}$ beams.

Comparisons of multiplicity and pseudorapidity distributions for pp and $p\bar{p}$ collisions at 53 GeV, based on the UA5 53 GeV runs in 1982. Data confirms the lack of significant difference between the two beams.

Histograms (4):

- Mean charged multiplicity for pp collisions at $\sqrt{s} = 53$ GeV ([/REF/UA5_1982_S875503/d02-x01-y01](#))
- Mean charged multiplicity for $p\bar{p}$ collisions at $\sqrt{s} = 53$ GeV ([/REF/UA5_1982_S875503/d02-x01-y02](#))
- Pseudorapidity for pp collisions at $\sqrt{s} = 53$ GeV ([/REF/UA5_1982_S875503/d03-x01-y01](#))
- Pseudorapidity for $p\bar{p}$ collisions at $\sqrt{s} = 53$ GeV ([/REF/UA5_1982_S875503/d04-x01-y01](#))

9.3 UA5_1986_S1583476 [189]

Pseudorapidity distributions in $p\bar{p}$ (NSD, NSD+SD) events at $\sqrt{s} = 200$ and 900 GeV

Beams: $p\bar{p}$

Energies: (100.0, 100.0), (450.0, 450.0) GeV

Experiment: UA5 (CERN SPS)

Spires ID: [1583476](#)

Status: VALIDATED

Authors:

- Andy Buckley <andy.buckley@cern.ch>
- Holger Schulz <holger.schulz@physik.hu-berlin.de>
- Christophe Vaillant <c.l.j.j.vaillant@durham.ac.uk>

References:

- Eur. Phys. J. C33, 1, 1986

Run details:

- * Single- and double-diffractive, plus non-diffractive inelastic, events.
- $p\bar{p}$ collider, $\sqrt{s} = 200$ or 900 GeV.
- The trigger implementation for NSD events is the same as in, e.g., the UA5_1989 analysis. No further cuts are needed.

This study comprises measurements of pseudorapidity distributions measured with the UA5 detector at 200 and 900 GeV center of momentum energy. There are distributions for non-single diffractive (NSD) events and also for the combination of single- and double-diffractive events. The NSD distributions are further studied for certain ranges of the events charged multiplicity.

Histograms (19):

- Pseudorapidity η , $\sqrt{s} = 200$ GeV, NSD ([/REF/UA5_1986_S1583476/d01-x01-y01](#))
- Pseudorapidity η , $\sqrt{s} = 200$ GeV, NSD+SD ([/REF/UA5_1986_S1583476/d01-x01-y02](#))
- Pseudorapidity η , $\sqrt{s} = 900$ GeV, NSD ([/REF/UA5_1986_S1583476/d01-x01-y03](#))
- Pseudorapidity η , $\sqrt{s} = 900$ GeV, NSD+SD ([/REF/UA5_1986_S1583476/d01-x01-y04](#))
- Pseudorapidity η , $\sqrt{s} = 200$ GeV, NSD, $2 \leq N_{\text{ch}} < 12$ ([/REF/UA5_1986_S1583476/d02-x01-y01](#))
- Pseudorapidity η , $\sqrt{s} = 200$ GeV, NSD, $12 \leq N_{\text{ch}} < 22$ ([/REF/UA5_1986_S1583476/d02-x01-y02](#))
- Pseudorapidity η , $\sqrt{s} = 200$ GeV, NSD, $22 \leq N_{\text{ch}} < 32$ ([/REF/UA5_1986_S1583476/d02-x01-y03](#))

- Pseudorapidity η , $\sqrt{s} = 200$ GeV, NSD, $32 \leq N_{\text{ch}} < 42$ ([/REF/UA5_1986_S1583476/d02-x01-y04](#))
- Pseudorapidity η , $\sqrt{s} = 200$ GeV, NSD, $42 \leq N_{\text{ch}} < 52$ ([/REF/UA5_1986_S1583476/d02-x01-y05](#))
- Pseudorapidity η , $\sqrt{s} = 200$ GeV, NSD, $N_{\text{ch}} \geq 52$ ([/REF/UA5_1986_S1583476/d02-x01-y06](#))
- Pseudorapidity η , $\sqrt{s} = 900$ GeV, NSD, $2 \leq N_{\text{ch}} < 12$ ([/REF/UA5_1986_S1583476/d03-x01-y01](#))
- Pseudorapidity η , $\sqrt{s} = 900$ GeV, NSD, $12 \leq N_{\text{ch}} < 22$ ([/REF/UA5_1986_S1583476/d03-x01-y02](#))
- Pseudorapidity η , $\sqrt{s} = 900$ GeV, NSD, $22 \leq N_{\text{ch}} < 32$ ([/REF/UA5_1986_S1583476/d03-x01-y03](#))
- Pseudorapidity η , $\sqrt{s} = 900$ GeV, NSD, $32 \leq N_{\text{ch}} < 42$ ([/REF/UA5_1986_S1583476/d03-x01-y04](#))
- Pseudorapidity η , $\sqrt{s} = 900$ GeV, NSD, $42 \leq N_{\text{ch}} < 52$ ([/REF/UA5_1986_S1583476/d03-x01-y05](#))
- Pseudorapidity η , $\sqrt{s} = 900$ GeV, NSD, $52 \leq N_{\text{ch}} < 62$ ([/REF/UA5_1986_S1583476/d03-x01-y06](#))
- Pseudorapidity η , $\sqrt{s} = 900$ GeV, NSD, $62 \leq N_{\text{ch}} < 72$ ([/REF/UA5_1986_S1583476/d03-x01-y07](#))
- Pseudorapidity η , $\sqrt{s} = 900$ GeV, NSD, $72 \leq N_{\text{ch}} < 82$ ([/REF/UA5_1986_S1583476/d03-x01-y08](#))
- Pseudorapidity η , $\sqrt{s} = 900$ GeV, NSD, $N_{\text{ch}} \geq 82$ ([/REF/UA5_1986_S1583476/d03-x01-y09](#))

9.4 UA5_1987_S1640666 [190]

UA5 charged multiplicity measurements at 546 GeV

Beams: $\bar{p}p$

Energies: (273.0, 273.0) GeV

Experiment: UA5 (CERN SPS)

Spires ID: [1640666](#)

Status: VALIDATED

Authors:

- Holger Schulz (holger.schulz@physik.hu-berlin.de)

References:

- Phys.Rept.154:247-383,1987

Run details:

- QCD and diffractive events at 546 GeV

Charged particle multiplicity measurement.

Histograms (2):

- Mean charged multiplicity at $\sqrt{s} = 546$ GeV, $|\eta| < 5.0$ ([/REF/UA5_1987_S1640666/d01-x01-y01](#))
- Charged multiplicity at $\sqrt{s} = 546$ GeV, $|\eta| < 5.0$ ([/REF/UA5_1987_S1640666/d03-x01-y01](#))

9.5 UA5_1988_S1867512 [191]

Charged particle correlations in UA5 $p\bar{p}$ NSD events at $\sqrt{s} = 200, 546$ and 900 GeV

Beams: $p\bar{p}$

Energies: (100.0, 100.0), (273.0, 273.0), (450.0, 450.0) GeV

Experiment: UA5 (CERN SPS)

Spires ID: [1867512](#)

Status: VALIDATED

Authors:

- Holger Schulz (holger.schulz@physik.hu-berlin.de)

References:

- Z.Phys.C37:191-213,1988

Run details:

- ppbar events. Non-single diffractive events need to be switched on. The trigger implementation is the same as in UA5_1989_S1926373. Important: Only the correlation strengths with symmetric eta bins should be used for tuning.

Data on two-particle pseudorapidity and multiplicity correlations of charged particles for non single-diffractive $p\bar{p}$ collisions at c.m. energies of 200, 546 and 900 GeV. Pseudorapidity correlations are interpreted in terms of a cluster model, which has been motivated by this and other experiments, require on average about two charged particles per cluster. The decay width of the clusters in pseudorapidity is approximately independent of multiplicity and of c.m. energy. The investigations of correlations in terms of pseudorapidity gaps confirm the picture of cluster production. The strength of forward–backward multiplicity correlations increases linearly with η and depends strongly on position and size of the pseudorapidity gap separating the forward and backward interval. All our correlation studies can be understood in terms of a cluster model in which clusters contain on average about two charged particles, i.e. are of similar magnitude to earlier estimates from the ISR.

Histograms (6):

- Forward-backward correlation b vs. gap size $\sqrt{s} = 200$ GeV ([/REF/UA5_1988_S1867512/d02-x01-y01](#))
- Forward-backward correlation b vs. gap size $\sqrt{s} = 546$ GeV ([/REF/UA5_1988_S1867512/d02-x01-y02](#))
- Forward-backward correlation b vs. gap size $\sqrt{s} = 900$ GeV ([/REF/UA5_1988_S1867512/d02-x01-y03](#))
- Forward-backward correlation b vs. gap center $\sqrt{s} = 200$ GeV ([/REF/UA5_1988_S1867512/d03-x01-y01](#))
- Forward-backward correlation b vs. gap center $\sqrt{s} = 546$ GeV ([/REF/UA5_1988_S1867512/d03-x01-y02](#))
- Forward-backward correlation b vs. gap center $\sqrt{s} = 900$ GeV ([/REF/UA5_1988_S1867512/d03-x01-y03](#))

9.6 UA5_1989_S1926373 [192]

UA5 charged multiplicity measurements

Beams: $\bar{p}p$

Energies: (100.0, 100.0), (450.0, 450.0) GeV

Experiment: UA5 (CERN SPS)

Spires ID: [1926373](#)

Status: VALIDATED

Authors:

- Holger Schulz (holger.schulz@physik.hu-berlin.de)
- Christophe L. J. Vaillant (c.l.j.j.vaillant@durham.ac.uk)
- Andy Buckley (andy.buckley@cern.ch)

References:

- Z. Phys. C - Particles and Fields 43, 357-374 (1989)
- DOI: [10.1007/BF01506531](#)

Run details:

- Minimum bias events at $\sqrt{s} = 200$ and 900 GeV. Enable single and double diffractive events in addition to non-diffractive processes.

Multiplicity distributions of charged particles produced in non-single-diffractive collisions between protons and antiprotons at centre-of-mass energies of 200 and 900 GeV. The data were recorded in the UA5 streamer chambers at the CERN collider, which was operated in a pulsed mode between the two energies. This analysis confirms the violation of KNO scaling in full phase space found by the UA5 group at an energy of 546 GeV, with similar measurements at 200 and 900 GeV.

Histograms (12):

- Charged multiplicity at $\sqrt{s} = 200$ GeV, $|\eta| < 5.0$ ([/REF/UA5_1989_S1926373/d01-x01-y01](#))
- Charged multiplicity at $\sqrt{s} = 900$ GeV, $|\eta| < 5.0$ ([/REF/UA5_1989_S1926373/d02-x01-y01](#))
- Charged multiplicity at $\sqrt{s} = 200$ GeV, $|\eta| < 0.5$ ([/REF/UA5_1989_S1926373/d03-x01-y01](#))
- Charged multiplicity at $\sqrt{s} = 200$ GeV, $|\eta| < 1.5$ ([/REF/UA5_1989_S1926373/d04-x01-y01](#))
- Charged multiplicity at $\sqrt{s} = 200$ GeV, $|\eta| < 3.0$ ([/REF/UA5_1989_S1926373/d05-x01-y01](#))
- Charged multiplicity at $\sqrt{s} = 200$ GeV, $|\eta| < 5.0$ ([/REF/UA5_1989_S1926373/d06-x01-y01](#))
- Charged multiplicity at $\sqrt{s} = 900$ GeV, $|\eta| < 0.5$ ([/REF/UA5_1989_S1926373/d07-x01-y01](#))
- Charged multiplicity at $\sqrt{s} = 900$ GeV, $|\eta| < 1.5$ ([/REF/UA5_1989_S1926373/d08-x01-y01](#))

- Charged multiplicity at $\sqrt{s} = 900$ GeV, $|\eta| < 3.0$ ([/REF/UA5_1989_S1926373/d09-x01-y01](#))
- Charged multiplicity at $\sqrt{s} = 900$ GeV, $|\eta| < 5.0$ ([/REF/UA5_1989_S1926373/d10-x01-y01](#))
- Mean charged multiplicity at $\sqrt{s} = 200$ GeV, $|\eta| < 5.0$ ([/REF/UA5_1989_S1926373/d11-x01-y01](#))
- Mean charged multiplicity at $\sqrt{s} = 900$ GeV, $|\eta| < 5.0$ ([/REF/UA5_1989_S1926373/d11-x01-y02](#))

10. HERA analyses

10.1 H1_1994_S2919893 [193]

H1 energy flow and charged particle spectra in DIS

Beams: $p e^-$, $p e^+$

Energies: (820.0, 26.7) GeV

Experiment: H1 (HERA)

Spires ID: [2919893](#)

Status: VALIDATED

Authors:

- Peter Richardson <peter.richardson@durham.ac.uk>

References:

- Z.Phys.C63:377-390,1994
- DOI: [10.1007/BF01580319](https://doi.org/10.1007/BF01580319)

Run details:

- $e^- p / e^+ p$ deep inelastic scattering, 820 GeV protons colliding with 26.7 GeV electrons

Global properties of the hadronic final state in deep inelastic scattering events at HERA are investigated. The data are corrected for detector effects. Energy flows in both the laboratory frame and the hadronic centre of mass system, and energy-energy correlations in the laboratory frame are presented. Historically, the Ariadne colour dipole model provided the only satisfactory description of this data, hence making it a useful 'target' analysis for MC shower models.

Histograms (9):

- Transverse energy flow as a function of rapidity, $x < 10^{-3}$ ([/REF/H1_1994_S2919893/d01-x01-y01](#))
- Transverse energy flow as a function of rapidity, $x > 10^{-3}$ ([/REF/H1_1994_S2919893/d01-x01-y02](#))
- Transverse energy-energy correlation for $x < 10^{-3}$ ([/REF/H1_1994_S2919893/d02-x01-y01](#))
- Transverse energy-energy correlation for $x > 10^{-3}$ ([/REF/H1_1994_S2919893/d02-x01-y02](#))
- $50 < W < 100$ ([/REF/H1_1994_S2919893/d03-x01-y01](#))
- $100 < W < 150$ ([/REF/H1_1994_S2919893/d03-x01-y02](#))
- $150 < W < 200$ ([/REF/H1_1994_S2919893/d03-x01-y03](#))
- all W ([/REF/H1_1994_S2919893/d03-x01-y04](#))
- $\langle p_\perp^2 \rangle$ as a function of x_L ([/REF/H1_1994_S2919893/d04-x01-y01](#))

10.2 H1_1995_S3167097 [194]

Transverse energy and forward jet production in the low- x regime at H1

Beams: $p e^-$

Energies: (820.0, 26.7) GeV

Experiment: H1 (HERA Run I)

Spires ID: 3167097

Status: UNVALIDATED

Authors:

- Leif Lonnblad <leif.lonnblad@hep.lu.se>

References:

- Phys.Lett.B356:118,1995
- hep-ex/9506012

Run details:

- 820 GeV protons colliding with 26.7 GeV electrons. DIS events with an outgoing electron energy > 12 GeV. $5 \text{ GeV}^2 < Q^2 < 100 \text{ GeV}^2$, $10^{-4} < x < 10^{-2}$.

DIS events at low x may be sensitive to new QCD dynamics such as BFKL or CCFM radiation. In particular, BFKL is expected to produce more radiation at high transverse energy in the rapidity span between the proton remnant and the struck quark jet. Performing a transverse energy sum in bins of x and η may distinguish between DGLAP and BFKL evolution.

10.3 H1_2000_S4129130 [195]

H1 energy flow in DIS

Beams: $p e^+$

Energies: (820.0, 27.5) GeV

Experiment: H1 (HERA)

Spires ID: 4129130

Status: VALIDATED

Authors:

- Peter Richardson ⟨ peter.richardson@durham.ac.uk ⟩

References:

- Eur.Phys.J.C12:595-607,2000
- DOI: [10.1007/s100520000287](https://doi.org/10.1007/s100520000287)
- arXiv: [hep-ex/9907027v1](https://arxiv.org/abs/hep-ex/9907027v1)

Run details:

- $e^+ p$ deep inelastic scattering with p at 820 GeV, e^+ at 27.5 GeV → $\sqrt{s} = 300$ GeV

Measurements of transverse energy flow for neutral current deep- inelastic scattering events produced in positron-proton collisions at HERA. The kinematic range covers squared momentum transfers Q^2 from 3.2 to 2200 GeV 2 ; the Bjorken scaling variable x from 8×10^{-5} to 0.11 and the hadronic mass W from 66 to 233 GeV. The transverse energy flow is measured in the hadronic centre of mass frame and is studied as a function of Q^2 , x , W and pseudorapidity. The behaviour of the mean transverse energy in the central pseudorapidity region and an interval corresponding to the photon fragmentation region are analysed as a function of Q^2 and W . This analysis is useful for exploring the effect of photon PDFs and for tuning models of parton evolution and treatment of fragmentation and the proton remnant in DIS.

Histograms (34):

- Transverse energy flow for $\langle x \rangle = 0.08 \cdot 10^{-3}$, $\langle Q^2 \rangle = 3.2$ GeV 2 ([/REF/H1_2000_S4129130/d01-x01-y01](#))
- Transverse energy flow for $\langle x \rangle = 0.14 \cdot 10^{-3}$, $\langle Q^2 \rangle = 3.8$ GeV 2 ([/REF/H1_2000_S4129130/d02-x01-y01](#))
- Transverse energy flow for $\langle x \rangle = 0.26 \cdot 10^{-3}$, $\langle Q^2 \rangle = 3.9$ GeV 2 ([/REF/H1_2000_S4129130/d03-x01-y01](#))
- Transverse energy flow for $\langle x \rangle = 0.57 \cdot 10^{-3}$, $\langle Q^2 \rangle = 4.2$ GeV 2 ([/REF/H1_2000_S4129130/d04-x01-y01](#))
- Transverse energy flow for $\langle x \rangle = 0.16 \cdot 10^{-3}$, $\langle Q^2 \rangle = 6.3$ GeV 2 ([/REF/H1_2000_S4129130/d05-x01-y01](#))
- Transverse energy flow for $\langle x \rangle = 0.27 \cdot 10^{-3}$, $\langle Q^2 \rangle = 7.0$ GeV 2 ([/REF/H1_2000_S4129130/d06-x01-y01](#))
- Transverse energy flow for $\langle x \rangle = 0.50 \cdot 10^{-3}$, $\langle Q^2 \rangle = 7.0$ GeV 2 ([/REF/H1_2000_S4129130/d07-x01-y01](#))

- Transverse energy flow for $\langle x \rangle = 1.10 \cdot 10^{-3}, \langle Q^2 \rangle = 7.3 \text{ GeV}^2$ (/REF/H1_2000_S4129130/d08-x01-y01)
- Transverse energy flow for $\langle x \rangle = 0.36 \cdot 10^{-3}, \langle Q^2 \rangle = 13.1 \text{ GeV}^2$ (/REF/H1_2000_S4129130/d09-x01-y01)
- Transverse energy flow for $\langle x \rangle = 0.63 \cdot 10^{-3}, \langle Q^2 \rangle = 14.1 \text{ GeV}^2$ (/REF/H1_2000_S4129130/d10-x01-y01)
- Transverse energy flow for $\langle x \rangle = 1.10 \cdot 10^{-3}, \langle Q^2 \rangle = 14.1 \text{ GeV}^2$ (/REF/H1_2000_S4129130/d11-x01-y01)
- Transverse energy flow for $\langle x \rangle = 2.30 \cdot 10^{-3}, \langle Q^2 \rangle = 14.9 \text{ GeV}^2$ (/REF/H1_2000_S4129130/d12-x01-y01)
- Transverse energy flow for $\langle x \rangle = 0.93 \cdot 10^{-3}, \langle Q^2 \rangle = 28.8 \text{ GeV}^2$ (/REF/H1_2000_S4129130/d13-x01-y01)
- Transverse energy flow for $\langle x \rangle = 2.10 \cdot 10^{-3}, \langle Q^2 \rangle = 31.2 \text{ GeV}^2$ (/REF/H1_2000_S4129130/d14-x01-y01)
- Transverse energy flow for $\langle x \rangle = 4.70 \cdot 10^{-3}, \langle Q^2 \rangle = 33.2 \text{ GeV}^2$ (/REF/H1_2000_S4129130/d15-x01-y01)
- Transverse energy flow for $\langle x \rangle = 2.00 \cdot 10^{-3}, \langle Q^2 \rangle = 59.4 \text{ GeV}^2$ (/REF/H1_2000_S4129130/d16-x01-y01)
- Transverse energy flow for $\langle x \rangle = 7.00 \cdot 10^{-3}, \langle Q^2 \rangle = 70.2 \text{ GeV}^2$ (/REF/H1_2000_S4129130/d17-x01-y01)
- Transverse energy flow for $\langle x \rangle = 0.0043, \langle Q^2 \rangle = 175 \text{ GeV}^2$ (/REF/H1_2000_S4129130/d18-x01-y01)
- Transverse energy flow for $\langle x \rangle = 0.01, \langle Q^2 \rangle = 253 \text{ GeV}^2$ (/REF/H1_2000_S4129130/d19-x01-y01)
- Transverse energy flow for $\langle x \rangle = 0.026, \langle Q^2 \rangle = 283 \text{ GeV}^2$ (/REF/H1_2000_S4129130/d20-x01-y01)
- Transverse energy flow for $\langle x \rangle = 0.012, \langle Q^2 \rangle = 511 \text{ GeV}^2$ (/REF/H1_2000_S4129130/d21-x01-y01)
- Transverse energy flow for $\langle x \rangle = 0.026, \langle Q^2 \rangle = 617 \text{ GeV}^2$ (/REF/H1_2000_S4129130/d22-x01-y01)
- Transverse energy flow for $\langle x \rangle = 0.076, \langle Q^2 \rangle = 682 \text{ GeV}^2$ (/REF/H1_2000_S4129130/d23-x01-y01)
- Transverse energy flow for $\langle x \rangle = 0.11, \langle Q^2 \rangle = 2200 \text{ GeV}^2$ (/REF/H1_2000_S4129130/d24-x01-y01)
- Transverse energy flow for $\langle Q^2 \rangle = 2.5 - 5 \text{ GeV}^2$ (/REF/H1_2000_S4129130/d25-x01-y01)
- Transverse energy flow for $\langle Q^2 \rangle = 5 - 10 \text{ GeV}^2$ (/REF/H1_2000_S4129130/d26-x01-y01)
- Transverse energy flow for $\langle Q^2 \rangle = 10 - 20 \text{ GeV}^2$ (/REF/H1_2000_S4129130/d27-x01-y01)
- Transverse energy flow for $\langle Q^2 \rangle = 20 - 50 \text{ GeV}^2$ (/REF/H1_2000_S4129130/d28-x01-y01)
- Transverse energy flow for $\langle Q^2 \rangle = 50 - 100 \text{ GeV}^2$ (/REF/H1_2000_S4129130/d29-x01-y01)
- Transverse energy flow for $\langle Q^2 \rangle = 100 - 220 \text{ GeV}^2$ (/REF/H1_2000_S4129130/d30-x01-y01)
- Transverse energy flow for $\langle Q^2 \rangle = 220 - 400 \text{ GeV}^2$ (/REF/H1_2000_S4129130/d31-x01-y01)
- Transverse energy flow for $\langle Q^2 \rangle \text{ GeV}^2$ (/REF/H1_2000_S4129130/d32-x01-y01)
- Average E_\perp in the central region (/REF/H1_2000_S4129130/d33-x01-y01)
- Average E_\perp in the forward region (/REF/H1_2000_S4129130/d34-x01-y01)

10.4 ZEUS_2001_S4815815 [196]

Dijet photoproduction analysis

Beams: $p e^+$

Energies: (820.0, 27.5) GeV

Experiment: ZEUS (HERA Run I)

Spires ID: 4815815

Status: UNVALIDATED

Authors:

- Jon Butterworth jmb@hep.ucl.ac.uk

References:

- Eur.Phys.J.C23:615,2002
- DESY 01/220
- hep-ex/0112029

Run details:

- 820 GeV protons colliding with 27.5 GeV positrons; Direct and resolved photoproduction of dijets; Leading jet $p_\perp > 14$ GeV, second jet $p_\perp > 11$ GeV; Jet pseudorapidity $-1 < |\eta| < 2.4$

ZEUS photoproduction of jets from proton–positron collisions at beam energies of 820 GeV on 27.5 GeV. Photoproduction can either be direct, in which case the photon interacts directly with the parton, or resolved, in which case the photon acts as a source of quarks and gluons. A photon-proton centre of mass energy of between 134 GeV and 227 GeV is probed, with values of x_P , the fractional momentum of the partons inside the proton, predominantly in the region between 0.01 and 0.1. The fractional momentum of the partons from the photon, $x\gamma$, is in the region 0.1 to 1. Jets are reconstructed in the range $-1 < |\eta| < 2.4$ using the k_\perp algorithm with an R parameter of 1.0. The minimum p_\perp of the leading jet should be greater than 14 GeV, and at least one other jet must have $p_\perp > 11$ GeV.

11. RHIC analyses

11.1 STAR_2006_S6500200 [197]

Identified hadron spectra in pp at 200 GeV

Beams: pp

Energies: (100.0, 100.0) GeV

Experiment: STAR (RHIC pp 200 GeV)

Spires ID: 6500200

Status: VALIDATED

Authors:

- Bedanga Mohanty (bedanga@rcf.bnl.gov)
- Hendrik Hoeth (hendrik.hoeth@cern.ch)

References:

- Phys. Lett. B637, 161
- arXiv: nucl-ex/0601033

Run details:

- pp at 200 GeV

p_\perp distributions of charged pions and (anti)protons in pp collisions at $\sqrt{s} = 200$ GeV, measured by the STAR experiment at RHIC in non-single-diffractive minbias events.

Histograms (8):

- π^+ transverse momentum (/REF/STAR_2006_S6500200/d01-x01-y01)
- π^- transverse momentum (/REF/STAR_2006_S6500200/d01-x02-y01)
- Proton transverse momentum (/REF/STAR_2006_S6500200/d01-x03-y01)
- Anti-proton transverse momentum (/REF/STAR_2006_S6500200/d01-x04-y01)
- Ratio of π^-/π^+ as function of p_\perp (/REF/STAR_2006_S6500200/d02-x01-y01)
- Ratio of \bar{p}/p as function of p_\perp (/REF/STAR_2006_S6500200/d02-x02-y01)
- Ratio of p/π^+ as function of p_\perp (/REF/STAR_2006_S6500200/d02-x03-y01)
- Ratio of \bar{p}/π^- as function of p_\perp (/REF/STAR_2006_S6500200/d02-x04-y01)

11.2 STAR_2006_S6860818 [198]

Strange particle production in pp at 200 GeV

Beams: pp

Energies: (100.0, 100.0) GeV

Experiment: STAR (RHIC pp 200 GeV)

Spires ID: [6860818](#)

Status: VALIDATED

Authors:

- Hendrik Hoeth (hendrik.hoeth@cern.ch)

References:

- Phys. Rev. C75, 064901
- nucl-ex/0607033

Run details:

- pp at 200 GeV

p_{\perp} distributions of identified strange particles in pp collisions at $\sqrt{s} = 200$ GeV, measured by the STAR experiment at RHIC in non-single-diffractive minbias events. WARNING The $\langle p_{\perp} \rangle$ vs. particle mass plot is not validated yet and might be wrong.

Histograms (11):

- K_s^0 transverse momentum ([/REF/STAR_2006_S6860818/d01-x01-y01](#))
- K^- transverse momentum ([/REF/STAR_2006_S6860818/d01-x02-y01](#))
- K^+ transverse momentum ([/REF/STAR_2006_S6860818/d01-x03-y01](#))
- Λ transverse momentum ([/REF/STAR_2006_S6860818/d01-x04-y01](#))
- $\bar{\Lambda}$ transverse momentum ([/REF/STAR_2006_S6860818/d01-x05-y01](#))
- Ξ^- transverse momentum ([/REF/STAR_2006_S6860818/d01-x06-y01](#))
- Ξ^+ transverse momentum ([/REF/STAR_2006_S6860818/d01-x07-y01](#))
- Anti-baryon over baryon ratio vs strangeness ([/REF/STAR_2006_S6860818/d02-x01-y01](#))
- Ratio of $\bar{\Lambda}/\Lambda$ as function of p_{\perp} ([/REF/STAR_2006_S6860818/d02-x02-y01](#))
- Ratio of Ξ^+/Ξ^- as function of p_{\perp} ([/REF/STAR_2006_S6860818/d02-x03-y01](#))
- Mean p_{\perp} vs particle mass ([/REF/STAR_2006_S6860818/d03-x01-y01](#))

11.3 STAR_2006_S6870392 [199]

Inclusive jet cross-section in pp at 200 GeV

Beams: pp

Energies: (100.0, 100.0) GeV

Experiment: STAR (RHIC pp 200 GeV)

Spires ID: [6870392](#)

Status: VALIDATED

Authors:

- Hendrik Hoeth (hendrik.hoeth@cern.ch)

References:

- Phys. Rev. Lett. 97, 252001
- hep-ex/0608030

Run details:

- pp at 200 GeV

Inclusive jet cross section as a function of p_{\perp} in pp collisions at $\sqrt{s} = 200$ GeV, measured by the STAR experiment at RHIC.

Histograms (2):

- Inclusive jet cross-section, minbias trigger ([/REF/STAR_2006_S6870392/d01-x01-y01](#))
- Inclusive jet cross-section, high tower trigger ([/REF/STAR_2006_S6870392/d02-x01-y01](#))

11.4 STAR_2008_S7869363 [200]

Multiplicities and p_{\perp} spectra from STAR for pp at 200 GeV

Beams: pp

Energies: (100.0, 100.0) GeV

Experiment: STAR (RHIC)

Spires ID: [7869363](#)

Status: UNVALIDATED

Authors:

- Holger Schulz (holger.schulz@physik.hu-berlin.de)

References:

- arXiv: [0808.2041](#)
- <http://drupal.star.bnl.gov/STAR/files/starpublications/124/data.html>

Run details:

- QCD (pp) events at 200 GeV

Charged Multiplicity and identified charged particle spectra

Histograms (7):

- Raw charged multiplicity ($|\eta| < 0.5 \quad p_{\perp} > 0.2$ [GeV]) ([/REF/STAR_2008_S7869363/d01-x01-y01](#))
- π^- p_{\perp} spectrum ([/REF/STAR_2008_S7869363/d02-x01-y01](#))
- π^+ p_{\perp} spectrum ([/REF/STAR_2008_S7869363/d02-x01-y02](#))
- K^- p_{\perp} spectrum ([/REF/STAR_2008_S7869363/d02-x01-y03](#))
- K^+ p_{\perp} spectrum ([/REF/STAR_2008_S7869363/d02-x01-y04](#))
- Antiproton p_{\perp} spectrum ([/REF/STAR_2008_S7869363/d02-x01-y05](#))
- Proton p_{\perp} spectrum ([/REF/STAR_2008_S7869363/d02-x01-y06](#))

11.5 STAR_2008_S7993412 [201]

Di-hadron correlations in d-Au at 200 GeV

Beams: pp

Energies: (100.0, 100.0) GeV

Experiment: STAR (RHIC d-Au 200 GeV)

Spires ID: [7993412](#)

Status: UNVALIDATED

Authors:

- Christine Nattrass (christine.nattrass@yale.edu)
- Hendrik Hoeth (hendrik.hoeth@cern.ch)

References:

- arXiv: [0809.5261](#)

Run details:

- d-Au at 200 GeV (use pp Monte Carlo! See description)

Correlation in η and ϕ between the charged hadron with the highest p_{\perp} (“trigger particle”) and the other charged hadrons in the event (“associated particles”). The data was collected in d-Au collisions at 200 GeV. Nevertheless, it is very proton-proton like and can therefore be compared to pp Monte Carlo (not for tuning, but for qualitative studies.)

Histograms (2):

- Jet yield vs p_T^{trigger} ([/REF/STAR_2008_S7993412/d01-x01-y01](#))
- Jet yield vs $p_T^{\text{associated}}$ ([/REF/STAR_2008_S7993412/d02-x01-y01](#))

11.6 STAR_2009_UE_HELEN

UE measurement in pp at 200 GeV

Beams: pp

Energies: (100.0, 100.0) GeV

Experiment: STAR (RHIC pp 200 GeV)

Spires ID: [None](#)

Status: PRELIMINARY

Authors:

- Helen Caines <helen.caines@yale.edu>
- Hendrik Hoeth <hendrik.hoeth@cern.ch>

References:

- arXiv: [0910.5203](#)
- arXiv: [0907.3460](#)
- WARNING! Mark as "STAR preliminary" and contact authors when using it!

Run details:

- pp at 200 GeV

UE analysis similar to Rick Field's leading jet analysis. SIScone with radius/resolution parameter $R=0.7$ is used. Particles with $p_{\perp} > 0.2$ GeV and $|\eta| < 1$ are included in the analysis. All particles are assumed to have zero mass. Only jets with neutral energy < 0.7 are included. For the transMIN and transMAX $\Delta(\phi)$ is between $\pi/3$ and $2\pi/3$, and $\Delta(\eta) < 2.0$. For the jet region the area of the jet is used for the normalization, i.e. the scaling factor is πR^2 and not $d\phi d\eta$ (this is different from what Rick Field does!). The tracking efficiency is ~ 0.8 , but that is an approximation, as below $p_{\perp} \sim 0.6$ GeV it is falling quite steeply.

Histograms (3):

- TransMAX region charged particle density ([/REF/STAR_2009_UE_HELEN/d01-x01-y01](#))
- TransMIN region charged particle density ([/REF/STAR_2009_UE_HELEN/d02-x01-y01](#))
- Away region charged particle density ([/REF/STAR_2009_UE_HELEN/d03-x01-y01](#))

12. Monte Carlo analyses

12.1 MC_DIJET

Analysis of dijet events at the LHC.

Beams: **

Status: UNVALIDATED

No authors listed

No references listed

Run details:

- Generic QCD events at any energy.

Analysis of dijet events for the upcoming runs at the LHC, specifically studying azimuthal angle, transverse momentum distributions (including for leading jet and secondary jet), as well as charged particle multiplicities and transverse momenta.

12.2 MC_DIPHOTON

Monte Carlo validation observables for diphoton production at LHC

Beams: **

Status: VALIDATED

Authors:

- Frank Siegert (frank.siegert@cern.ch)

No references listed

Run details:

- LHC pp → jet+jet, photon+jet, photon+photon, all with EW+QCD shower

Different observables related to the two photons

12.3 MC_GENERIC

Generic MC testing analysis

Beams: **

Status: VALIDATED

Authors:

- Ian Bruce ⟨ibrace@cern.ch⟩
- Andy Buckley ⟨andy.buckley@cern.ch⟩

No references listed

Run details:

- Any!

Generic analysis of typical event distributions such as η , y , p_{\perp} , ϕ ...

12.4 MC_HINC

Monte Carlo validation observables for $h[\tau^+ \tau^-]$ production

Beams: **

Status: VALIDATED

Authors:

- Frank Siegert (frank.siegert@cern.ch)

No references listed

Run details:

- $h[\rightarrow \tau^+ \tau^-]$.

Monte Carlo validation observables for $h[\tau^+ \tau^-]$ production

12.5 MC_HJETS

Monte Carlo validation observables for $h[\tau^+ \tau^-] + \text{jets}$ production

Beams: **

Status: VALIDATED

Authors:

- Frank Siegert (frank.siegert@cern.ch)

No references listed

Run details:

- $h[\rightarrow \tau^+ \tau^-] + \text{jets}.$

The available observables are the Higgs mass, p_{\perp} of jets 1–4, jet multiplicity, $\Delta\eta(h, \text{jet1})$, $\Delta R(\text{jet2}, \text{jet3})$, differential jet rates 0→1, 1→2, 2→3, 3→4, and integrated 0–4 jet rates.

12.6 MC_HKTSPPLITTINGS

Monte Carlo validation observables for $h[\tau^+ \tau^-] + \text{jets}$ production

Beams: **

Status: VALIDATED

Authors:

- Frank Siegert (frank.siegert@cern.ch)

No references listed

Run details:

- $h[\rightarrow \tau^+ \tau^-] + \text{jets}$.

Monte Carlo validation observables for $h[\tau^+ \tau^-] + \text{jets}$ production

12.7 MC_IDENTIFIED

MC testing analysis for identified particle distributions

Beams: **

Status: VALIDATED

Authors:

- Andy Buckley ⟨andy.buckley@cern.ch⟩

No references listed

Run details:

- Any!

Plotting of distributions of PID codes (all/stable/unstable) and ID-specific distributions such as the $|\eta|$ of K , π and Λ mesons.

12.8 MC_JETS

Monte Carlo validation observables for jet production

Beams: **

Status: VALIDATED

Authors:

- Frank Siegert (frank.siegert@cern.ch)

No references listed

Run details:

- Pure QCD jet production events at an arbitrary collider.

Jets with $p_{\perp} > 20$ GeV are constructed with a k_{\perp} jet finder with $D = 0.7$ and projected onto many different observables.

12.9 MC_LEADJETUE

Underlying event in leading jet events, extended to LHC

Beams: **

Status: VALIDATED

Authors:

- Andy Buckley ⟨andy.buckley@cern.ch⟩

No references listed

Run details:

- LHC pp QCD interactions at 0.9, 10 or 14 TeV. Particles with $c\tau > 10$ mm should be set stable. Several p_T^{\min} cutoffs are probably required to fill the profile histograms.

Rick Field's measurement of the underlying event in leading jet events, extended to the LHC. As usual, the leading jet of the defines an azimuthal toward/transverse/away decomposition, in this case the event is accepted within $|\eta| < 2$, as in the CDF 2008 version of the analysis. Since this isn't the Tevatron, I've chosen to use k_T rather than midpoint jets.

12.10 MC_PDFS

Analysis to study PDF sampling in any MC run

Beams: **

Status: VALIDATED

Authors:

- Andy Buckley ⟨andy.buckley@cern.ch⟩

No references listed

Run details:

- Any!

Plotting of PDF sampling info, such as the Q^2 and both x values of the sampling (aggregated and distinguished as max/min, and some correlations with event properties.

12.11 MC_PHOTONINC

Monte Carlo validation observables for single isolated photon production

Beams: **

Status: VALIDATED

Authors:

- Frank Siegert <frank.siegert@cern.ch>

No references listed

Run details:

- Tevatron Run II ppbar → gamma + jets.

Monte Carlo validation observables for single isolated photon production

12.12 MC_PHOTONJETS

Monte Carlo validation observables for photon + jets production

Beams: **

Status: VALIDATED

Authors:

- Frank Siegert <frank.siegert@cern.ch>

No references listed

Run details:

- Tevatron Run II ppbar → gamma + jets.

Different observables related to the photon and extra jets.

12.13 MC_PHOTONJETUE

Study the usual underlying event observables in photon + jet events

Beams: $pp, \bar{p}p$

Status: UNVALIDATED

Authors:

- Andy Buckley ⟨andy.buckley@cern.ch⟩

No references listed

Run details:

- Photon + jet events at any energy. p_{\perp} cutoff at 10 GeV advised.

Modification of the MC leading jets underlying event analysis to study the UE in hard photon+jet events. This may be of interest, because the leading QCD dipole structure is different from that in either dijet or Drell-Yan hard processes. Observables are also extended to include the variation of transverse activity as a function of jet-photon balance, and using the photon rather than the jet to define the event alignment.

12.14 MC_PHOTONKTSPLITTINGS

Monte Carlo validation observables for photon + jets production

Beams: **

Status: VALIDATED

Authors:

- Frank Siegert (frank.siegert@cern.ch)

No references listed

Run details:

- Tevatron Run II ppbar → gamma + jets.

Monte Carlo validation observables for photon + jets production

12.15 MC_PHOTONS

Monte Carlo validation observables for general photons

Beams: **

Status: VALIDATED

Authors:

- Steve Lloyd
- Andy Buckley ⟨andy.buckley@cern.ch⟩

No references listed

Run details:

- Any event type, but there are many observables for photons associated to (semi-)hard leptons.

Observables for testing general unisolated photon properties, especially those associated with charged leptons (e and mu).

12.16 MC_PRINTEVENT

Print out a dump of each event to standard output

Beams: **

Status: VALIDATED

Authors:

- Andy Buckley ⟨andy.buckley@cern.ch⟩

No references listed

Run details:

- Can be used with any event type.

Print out a dump of the event structure to the terminal standard output, in a conveniently human readable form with e.g. particle names in addition to the usual numerical ID codes.

12.17 MC_QCD_PARTONS

Generic parton-level Monte Carlo validation analysis for $\text{jet} + \text{jets}$.

Beams: **

Status: VALIDATED

Authors:

- Frank Siegert (frank.siegert@cern.ch)

No references listed

Run details:

- Any $\text{jet} + \text{jets}$.

Only partons (excluding top quarks) are taken into account to construct a kt cluster sequence. Thus this analysis can be used as a generic validation tool for QCD activity.

12.18 MC_SUSY

Validate generic SUSY events, including various lepton invariant mass

Beams: **

Status: VALIDATED

Authors:

- Andy Buckley ⟨andy.buckley@cern.ch⟩

No references listed

Run details:

- SUSY events at any energy. p_{\perp} cutoff at 10 GeV may be advised.

Analysis of generic SUSY events at the LHC, based on Atlas Herwig++ validation analysis contents. Plotted are η , ϕ and p_{\perp} observables for charged tracks, photons, isolated photons, electrons, muons, and jets, as well as various dilepton mass ‘edge’ plots for different event selection criteria.

12.19 MC_TTBAR

MC analysis for ttbar studies

Beams: **

Status: VALIDATED

Authors:

- Hendrik Hoeth (hendrik.hoeth@cern.ch)
- Andy Buckley (andy.buckley@cern.ch)
- Dave Mallows
- Michal Kawalec

No references listed

Run details:

- * For Pythia6, set MSEL=6 and fix W^+ and W^- decays to semi-leptonic modes via the MDME array.
- For Fortran Herwig/Jimmy select IPROC=1706.

This is a pure Monte Carlo study for semi-leptonic $t\bar{t}$ production.

12.20 MC_VH2BB

MC unboosted VH2bb validation plots

Beams: **

Status: UNVALIDATED

Authors:

- Ben Smart (bsmart@cern.ch)
- Andy Buckley (andy.buckley@cern.ch)

No references listed

Run details:

- VH with $H \rightarrow b\bar{b}$ and the vector boson decaying to electron or muon channels.

Various plots for characterising the process $VH \rightarrow b\bar{b}$

12.21 MC_WINC

Monte Carlo validation observables for inclusive $W[e\nu]$ production

Beams: **

Status: VALIDATED

Authors:

- Frank Siegert (frank.siegert@cern.ch)

No references listed

Run details:

- $e\nu + \text{jets}$ analysis.

Monte Carlo validation observables for inclusive $W[e\nu]$ production

12.22 MC_WJETS

Monte Carlo validation observables for $W[e\nu] + \text{jets}$ production

Beams: **

Status: VALIDATED

Authors:

- Frank Siegert (frank.siegert@cern.ch)

No references listed

Run details:

- $e\nu + \text{jets}$ analysis.

Monte Carlo validation observables for $W[e\nu] + \text{jets}$ production

12.23 MC_WKTSPLITTINGS

Monte Carlo validation observables for k_{\perp} splitting scales in $W[e\nu] + \text{jets}$ events

Beams: **

Status: VALIDATED

Authors:

- Frank Siegert <frank.siegert@cern.ch>

No references listed

Run details:

- $e\nu + \text{jets}$ analysis.

Monte Carlo validation observables for k_{\perp} splitting scales in $W[e\nu] + \text{jets}$ events

12.24 MC_WPOL

Monte Carlo validation observables for W polarisation

Beams: **

Status: VALIDATED

Authors:

- Frank Siegert (frank.siegert@cern.ch)

No references listed

Run details:

- $W \rightarrow e \nu + \text{jets}$.

Observables sensitive to the polarisation of the W boson: A0, ... A7, fR, fL, f0, separately for W^+ and W^- .

12.25 MC_WWINC

Monte Carlo validation observables for $W^+[e^+\nu]W^-[\mu^-\nu]$ production

Beams: **

Status: VALIDATED

Authors:

- Frank Siegert (frank.siegert@cern.ch)

No references listed

Run details:

- WW analysis.

Monte Carlo validation observables for $W^+[e^+\nu]W^-[\mu^-\nu]$ production

12.26 MC_WWJETS

Monte Carlo validation observables for $W^+[e^+\nu]W^-[\mu^-\nu] + \text{jets}$ production

Beams: **

Status: VALIDATED

Authors:

- Frank Siegert (frank.siegert@cern.ch)

No references listed

Run details:

- $WW + \text{jets}$ analysis.

In addition to the typical jet observables this analysis contains observables related to properties of the WW-pair momentum, correlations between the WW, properties of the W bosons, properties of the leptons, correlations between the opposite charge leptons and correlations with jets.

12.27 MC_WWKTSPPLITTINGS

Monte Carlo validation observables for $W^+[e^+\nu]W^-[\mu^-\nu] + \text{jets}$ production

Beams: **

Status: VALIDATED

Authors:

- Frank Siegert (frank.siegert@cern.ch)

No references listed

Run details:

- $WW + \text{jets}$ analysis.

Monte Carlo validation observables for $W^+[e^+\nu]W^-[\mu^-\nu] + \text{jets}$ production

12.28 MC_XS

MC analysis for process total cross section

Beams: **

Status: VALIDATED

Authors:

- Marek Schoenherr (marek.schoenherr@tu-dresden.de)

No references listed

Run details:

- Suitable for any process.

Analysis for bookkeeping of the total cross section, number of generated events and the ratio of events with positive and negative weights.

12.29 MC_ZINC

Monte Carlo validation observables for $Z[e^+ e^-]$ production

Beams: **

Status: VALIDATED

Authors:

- Frank Siegert (frank.siegert@cern.ch)

No references listed

Run details:

- $e^+ e^-$ analysis. Needs mass cut on lepton pair to avoid photon singularity, e.g. a min range of $66 < m_{ee} < 116$ GeV

Monte Carlo validation observables for $Z[e^+ e^-]$ production

12.30 MC_ZJETS

Monte Carlo validation observables for $Z[e^+ e^-] + \text{jets}$ production

Beams: **

Status: VALIDATED

Authors:

- Frank Siegert (frank.siegert@cern.ch)

No references listed

Run details:

- $e^+ e^- + \text{jets}$ analysis. Needs mass cut on lepton pair to avoid photon singularity, e.g. a min range of $66 < m_{ee} < 116$ GeV

Available observables are Z mass, p_\perp of jets 1-4, jet multiplicity, $\Delta\eta(Z, \text{jet1})$, $\Delta R(\text{jet2}, \text{jet3})$, differential jet rates $0 \rightarrow 1, 1 \rightarrow 2, 2 \rightarrow 3, 3 \rightarrow 4$, integrated 0-4 jet rates.

12.31 MC_ZKTSPLITTINGS

Monte Carlo validation observables for $Z[e^+ e^-] + \text{jets}$ production

Beams: **

Status: VALIDATED

Authors:

- Frank Siegert (frank.siegert@cern.ch)

No references listed

Run details:

- $e^+ e^- + \text{jets}$ analysis. Needs mass cut on lepton pair to avoid photon singularity, e.g. a min range of $66 < m_{ee} < 116$ GeV

Monte Carlo validation observables for $Z[e^+ e^-] + \text{jets}$ production

12.32 MC_ZZINC

Monte Carlo validation observables for $Z[e^+ e^-]Z[\mu^+ \mu^-]$ production

Beams: **

Status: VALIDATED

Authors:

- Frank Siegert (frank.siegert@cern.ch)

No references listed

Run details:

- $ZZ + \text{jets}$ analysis. Needs mass cut on lepton pairs to avoid photon singularity, e.g. a min range of $66 < m_{ee} < 116$ GeV

Monte Carlo validation observables for $Z[e^+ e^-]Z[\mu^+ \mu^-]$ production

12.33 MC_ZZJETS

Monte Carlo validation observables for $Z[e^+ e^-]Z[\mu^+ \mu^-] + \text{jets}$ production

Beams: **

Status: VALIDATED

Authors:

- Frank Siegert (frank.siegert@cern.ch)

No references listed

Run details:

- $ZZ + \text{jets}$ analysis. Needs mass cut on lepton pairs to avoid photon singularity, e.g. a min range of $66 < m_{ee} < 116$ GeV

In addition to the typical jet observables this analysis contains observables related to properties of the ZZ-pair momentum, correlations between the ZZ, properties of the Z bosons, properties of the leptons, correlations between the opposite charge leptons and correlations with jets.

12.34 MC_ZZKTSPLITTINGS

Monte Carlo validation observables for $Z[e^+ e^-]Z[\mu^+ \mu^-] + \text{jets}$ production

Beams: **

Status: VALIDATED

Authors:

- Frank Siegert (frank.siegert@cern.ch)

No references listed

Run details:

- $ZZ + \text{jets}$ analysis. Needs mass cut on lepton pairs to avoid photon singularity, e.g. a min range of $66 < m_{ee} < 116$ GeV

Monte Carlo validation observables for $Z[e^+ e^-]Z[\mu^+ \mu^-] + \text{jets}$ production

13. Example analyses

13.1 EXAMPLE

A demo to show aspects of writing a Rivet analysis

Beams: **

Status: EXAMPLE

Authors:

- Andy Buckley (andy.buckley@cern.ch)

No references listed

Run details:

- All event types will be accepted.

This analysis is a demonstration of the Rivet analysis structure and functionality: booking histograms; the initialisation, analysis and finalisation phases; and a simple loop over event particles. It has no physical meaning, but can be used as a simple pedagogical template for writing real analyses.

14. Misc. analyses

14.1 ARGUS_1993_S2653028 [202]

Inclusive production of charged pions, kaons and protons in $\Upsilon(4S)$ decays.

Beams: $e^+ e^-$

Energies: (5.3, 5.3) GeV

Spires ID: [2653028](#)

Status: VALIDATED

Authors:

- Peter Richardson (Peter.Richardson@durham.ac.uk)

References:

- Z.Phys. C58 (1993) 191-198

Run details:

- $e^+ e^-$ analysis on the $\Upsilon(4S)$ resonance.

Measurement of inclusive production of charged pions, kaons and protons from $\Upsilon(4S)$ decays. Kaon spectra are determined in two different ways using particle identification and detecting decays in-flight. Results are background continuum subtracted. This analysis is useful for tuning B meson decay modes.

Histograms (11):

- π^+ momentum, no Λ , K_S^0 ([/REF/ARGUS_1993_S2653028/d01-x01-y01](#))
- π^+ momentum, including Λ , K_S^0 ([/REF/ARGUS_1993_S2653028/d02-x01-y01](#))
- K^+ momentum ([/REF/ARGUS_1993_S2653028/d03-x01-y01](#))
- Proton momentum, no Λ , K_S^0 ([/REF/ARGUS_1993_S2653028/d04-x01-y01](#))
- Proton momentum, including Λ , K_S^0 ([/REF/ARGUS_1993_S2653028/d05-x01-y01](#))
- K^+ momentum from time-of-flight ([/REF/ARGUS_1993_S2653028/d06-x01-y01](#))
- π^+ multiplicity, no Λ , K_S^0 ([/REF/ARGUS_1993_S2653028/d07-x01-y01](#))
- π^+ multiplicity, including Λ , K_S^0 ([/REF/ARGUS_1993_S2653028/d08-x01-y01](#))
- K^+ multiplicity ([/REF/ARGUS_1993_S2653028/d09-x01-y01](#))
- Proton multiplicity, no Λ , K_S^0 ([/REF/ARGUS_1993_S2653028/d10-x01-y01](#))
- Proton multiplicity, including Λ , K_S^0 ([/REF/ARGUS_1993_S2653028/d11-x01-y01](#))

14.2 ARGUS_1993_S2669951 [203]

Production of the $\eta'(958)$ and $f_0(980)$ in e^+e^- annihilation in the Upsilon region.

Beams: e^+e^-

Energies: (4.7, 4.7), (5.0, 5.0), (5.2, 5.2) GeV

Spires ID: [2669951](#)

Status: VALIDATED

Authors:

- Peter Richardson (Peter.Richardson@durham.ac.uk)

References:

- Z.Phys. C58 (1993) 199-206

Run details:

- e^+e^- analysis near the $\Upsilon(4S)$ resonance.

Measurement of the inclusive production of the $\eta'(958)$ and $f_0(980)$ mesons in e^+e^- annihilation in the Upsilon region. Data are taken on the $\Upsilon(1S)$, $\Upsilon(2S)$ and $\Upsilon(4S)$ resonances and in the nearby continuum (9.36 to 10.45 GeV center-of-mass energy)

Histograms (6):

- η' multiplicity, $x_p > 0.35$ ([/REF/ARGUS_1993_S2669951/d01-x01-y01](#))
- η' multiplicity, $x_p > 0.35$ ([/REF/ARGUS_1993_S2669951/d01-x01-y02](#))
- f_0 scaled momentum, continuum ([/REF/ARGUS_1993_S2669951/d02-x01-y01](#))
- f_0 scaled momentum, $\Upsilon(1S)$ ([/REF/ARGUS_1993_S2669951/d03-x01-y01](#))
- f_0 scaled momentum, $\Upsilon(2S)$ ([/REF/ARGUS_1993_S2669951/d04-x01-y01](#))
- f_0 multiplicity ([/REF/ARGUS_1993_S2669951/d05-x01-y01](#))

14.3 ARGUS_1993_S2789213 [204]

Inclusive production of $K^*(892)$, $\rho^0(770)$, and $\omega(783)$ mesons in the upsilon energy region.

Beams: $e^+ e^-$

Energies: (4.7, 4.7), (5.2, 5.2), (5.3, 5.3) GeV

Spires ID: [2789213](#)

Status: VALIDATED

Authors:

- Peter Richardson (Peter.Richardson@durham.ac.uk)

References:

- Z.Phys. C61 (1994) 1-18

Run details:

- $e^+ e^-$ analysis in the 10 GeV CMS energy range

Measurement of the inclusive production of the vector mesons $K^*(892)$, $\rho^0(770)$ and $\omega(783)$ in $e^+ e^-$ annihilation in the Upsilon region by the Argus Collaboration. Useful for tuning simulations of B meson and bottomium decays.

Histograms (26):

- ω multiplicity, continuum ([/REF/ARGUS_1993_S2789213/d01-x01-y01](#))
- ρ^0 multiplicity, continuum ([/REF/ARGUS_1993_S2789213/d01-x01-y02](#))
- K^{*0} multiplicity, continuum ([/REF/ARGUS_1993_S2789213/d01-x01-y03](#))
- K^{*+} multiplicity, continuum ([/REF/ARGUS_1993_S2789213/d01-x01-y04](#))
- ϕ multiplicity, continuum ([/REF/ARGUS_1993_S2789213/d01-x01-y05](#))
- ω multiplicity, $\Upsilon(1S)$ ([/REF/ARGUS_1993_S2789213/d02-x01-y01](#))
- ρ^0 multiplicity, $\Upsilon(1S)$ ([/REF/ARGUS_1993_S2789213/d02-x01-y02](#))
- K^{*0} multiplicity, $\Upsilon(1S)$ ([/REF/ARGUS_1993_S2789213/d02-x01-y03](#))
- K^{*+} multiplicity, $\Upsilon(1S)$ ([/REF/ARGUS_1993_S2789213/d02-x01-y04](#))
- ϕ multiplicity, $\Upsilon(1S)$ ([/REF/ARGUS_1993_S2789213/d02-x01-y05](#))
- ω multiplicity, $\Upsilon(4S)$ ([/REF/ARGUS_1993_S2789213/d03-x01-y01](#))
- ρ^0 multiplicity, $\Upsilon(4S)$ ([/REF/ARGUS_1993_S2789213/d03-x01-y02](#))
- K^{*0} multiplicity, $\Upsilon(4S)$ ([/REF/ARGUS_1993_S2789213/d03-x01-y03](#))

- K^{*+} multiplicity, $\Upsilon(4S)$ (/REF/ARGUS_1993_S2789213/d03-x01-y04)
- ϕ multiplicity, $\Upsilon(4S)$ (/REF/ARGUS_1993_S2789213/d03-x01-y05)
- K^{*+} scaled momentum, continuum (/REF/ARGUS_1993_S2789213/d04-x01-y01)
- K^{*+} scaled momentum, $\Upsilon(1S)$ (/REF/ARGUS_1993_S2789213/d05-x01-y01)
- K^{*+} scaled momentum, $\Upsilon(4S)$ (/REF/ARGUS_1993_S2789213/d06-x01-y01)
- K^{*0} scaled momentum, continuum (/REF/ARGUS_1993_S2789213/d07-x01-y01)
- K^{*0} scaled momentum, $\Upsilon(1S)$ (/REF/ARGUS_1993_S2789213/d08-x01-y01)
- K^{*0} scaled momentum, $\Upsilon(4S)$ (/REF/ARGUS_1993_S2789213/d09-x01-y01)
- ρ^0 scaled momentum, continuum (/REF/ARGUS_1993_S2789213/d10-x01-y01)
- ρ^0 scaled momentum, $\Upsilon(1S)$ (/REF/ARGUS_1993_S2789213/d11-x01-y01)
- ρ^0 scaled momentum, $\Upsilon(4S)$ (/REF/ARGUS_1993_S2789213/d12-x01-y01)
- ω scaled momentum, continuum (/REF/ARGUS_1993_S2789213/d13-x01-y01)
- ω scaled momentum, $\Upsilon(1S)$ (/REF/ARGUS_1993_S2789213/d14-x01-y01)

14.4 ATLAS_2012_I1199269

Inclusive diphoton + X events at $\sqrt{s} = 7$ TeV

Beams: pp

Energies: (3500.0, 3500.0) GeV

Status: VALIDATED

Authors:

- Giovanni Marchiori (giovanni.marchiori@cern.ch)

References:

- arXiv: [1211.1913](#)
- JHEP 1301 (2013) 086

Run details:

- Inclusive diphoton + X events at $\sqrt{s} = 7$ TeV.

The ATLAS experiment at the LHC has measured the production cross section of events with two isolated photons in the final state, in proton-proton collisions at $\sqrt{s} = 7$ TeV. The full data set collected in 2011, corresponding to an integrated luminosity of 4.9 fb^{-1} , is used. The amount of background, from hadronic jets and isolated electrons, is estimated with data-driven techniques and subtracted. The total cross section, for two isolated photons with transverse energies above 25 GeV and 22 GeV respectively, in the acceptance of the electromagnetic calorimeter ($|\eta| < 1.37$ and $1.52 < |\eta| < 2.37$) and with an angular separation $\Delta R > 0.4$, is $44.0^{+3.2}_{-4.2} \text{ pb}$. The differential cross sections as a function of the di-photon invariant mass, transverse momentum, azimuthal separation, and cosine of the polar angle of the largest transverse energy photon in the Collins–Soper di-photon rest frame are also measured. The results are compared to the prediction of leading-order parton-shower and next-to-leading-order and next-to-next-to-leading-order parton-level generators.

Histograms (4):

- Isolated diphoton cross-section vs diphoton invariant mass ([/REF/ATLAS_2012_I1199269/d01-x01-y01](#))
- Isolated diphoton cross-section vs diphoton transverse momentum ([/REF/ATLAS_2012_I1199269/d02-x01-y01](#))
- Isolated diphoton cross-section vs diphoton azimuthal separation ([/REF/ATLAS_2012_I1199269/d03-x01-y01](#))
- cross-section vs cosine of polar angle in Collins-Soper frame ([/REF/ATLAS_2012_I1199269/d04-x01-y01](#))

14.5 BABAR_2003_I593379 [205]

Measurement of inclusive charmonium production

Beams: $e^+ e^-$

Energies: (3.5, 8.0) GeV

Experiment: BaBar (PEP-II)

Inspire ID: [593379](#)

Status: VALIDATED

Authors:

- Peter Richardson (Peter.Richardson@durham.ac.uk)

References:

- Phys.Rev. D67 032002, 2003
- hep-ex/0207097

Run details:

- Production of charmionum at the $\Upsilon(4S)$ resonace.

Measurement of J/ψ , ψ' , χ_{c1} and χ_{c2} production using a data sample corresponding to an integrated luminosity of 20.3 fb^{-1} collected with the BABAR detector at the SLAC PEP-II electron-positron storage ring operating at a centre-of-mass energy near 10.58 GeV.

Histograms (12):

- $\text{Br}(B \rightarrow J/\psi)$ at the $\Upsilon(4S)$ ([/REF/BABAR_2003_I593379/d01-x01-y01](#))
- $\text{Br}(B \rightarrow J/\psi)$ direct at the $\Upsilon(4S)$ ([/REF/BABAR_2003_I593379/d01-x01-y02](#))
- $\text{Br}(B \rightarrow \chi_{c1})$ at the $\Upsilon(4S)$ ([/REF/BABAR_2003_I593379/d01-x01-y03](#))
- $\text{Br}(B \rightarrow \chi_{c1})$ direct at the $\Upsilon(4S)$ ([/REF/BABAR_2003_I593379/d01-x01-y04](#))
- $\text{Br}(B \rightarrow \chi_{c2})$ at the $\Upsilon(4S)$ ([/REF/BABAR_2003_I593379/d01-x01-y05](#))
- $\text{Br}(B \rightarrow \chi_{c2})$ direct at the $\Upsilon(4S)$ ([/REF/BABAR_2003_I593379/d01-x01-y06](#))
- $\text{Br}(B \rightarrow \psi')$ at the $\Upsilon(4S)$ ([/REF/BABAR_2003_I593379/d01-x01-y07](#))
- $\text{Br}(B \rightarrow J/\psi)$ at the $\Upsilon(4S)$ ([/REF/BABAR_2003_I593379/d06-x01-y01](#))
- $\text{Br}(B \rightarrow \chi_{c1})$ at the $\Upsilon(4S)$ ([/REF/BABAR_2003_I593379/d07-x01-y01](#))
- $\text{Br}(B \rightarrow \chi_{c2})$ at the $\Upsilon(4S)$ ([/REF/BABAR_2003_I593379/d07-x01-y02](#))
- $\text{Br}(B \rightarrow \psi')$ at the $\Upsilon(4S)$ ([/REF/BABAR_2003_I593379/d08-x01-y01](#))
- $\text{Br}(B \rightarrow J/\psi)$ (direct) at the $\Upsilon(4S)$ ([/REF/BABAR_2003_I593379/d10-x01-y01](#))

14.6 BABAR_2005_S6181155 [206]

Production and decay of Ξ_c^0 at BABAR.

Beams: $e^+ e^-$

Energies: (3.5, 8.0), (3.5, 7.9) GeV

Experiment: BaBar (PEP-II)

Spires ID: 6895344

Status: VALIDATED

Authors:

- Peter Richardson (Peter.Richardson@durham.ac.uk)

References:

- Phys.Rev.Lett. 95 (2005) 142003
- hep-ex/0504014

Run details:

- e^+e^- analysis on the $\Upsilon(4S)$ resonance, with CoM boosts of 8.0 GeV (e^-) and 3.5 GeV (e^+)

Analysis of Ξ_c^0 production in B decays and from the $c\bar{c}$ continuum, with the Ξ_c^0 decaying into $\Omega^- K^+$ and $\Xi^- \pi^+$ final states measured using 116.1 fb^{-1} of data collected by the BABAR detector. The normalisation of the data has been modified from that presented in the original paper in order to produce a differential cross section rather than the cross section in each bin. In addition to the data presented in the paper plots are also made with unit normalisation which can be more useful for Monte Carlo tuning.

Histograms (7):

- $\sigma(e^+e^- \rightarrow \Xi_c^0 + \bar{\Xi}_c^0 + X)$ with $\Xi_c^0 \rightarrow \Xi^- \pi^+$ at the $\Upsilon(4S)$ ([/REF/BABAR_2005_S6181155/d01-x01-y01](#))
- $\sigma(e^+e^- \rightarrow \Xi_c^0 + \bar{\Xi}_c^0 + X)$ with $\Xi_c^0 \rightarrow \Xi^- \pi^+$ at the $\Upsilon(4S)$ ([/REF/BABAR_2005_S6181155/d02-x01-y01](#))
- $\sigma(e^+e^- \rightarrow \Xi_c^0 + \bar{\Xi}_c^0 + X)$ with $\Xi_c^0 \rightarrow \Xi^- \pi^+$ in the continuum region ([/REF/BABAR_2005_S6181155/d02-x01-y02](#))
- $\sigma(e^+e^- \rightarrow \Xi_c^0 + \bar{\Xi}_c^0 + X)$ with $\Xi_c^0 \rightarrow \Xi^- \pi^+$ ([/REF/BABAR_2005_S6181155/d03-x01-y01](#))
- $\sigma(e^+e^- \rightarrow \Xi_c^0 + \bar{\Xi}_c^0 + X)$ at the $\Upsilon(4S)$ ([/REF/BABAR_2005_S6181155/d04-x01-y01](#))
- $\sigma(e^+e^- \rightarrow \Xi_c^0 + \bar{\Xi}_c^0 + X)$ at the $\Upsilon(4S)$ ([/REF/BABAR_2005_S6181155/d05-x01-y01](#))
- $\sigma(e^+e^- \rightarrow \Xi_c^0 + \bar{\Xi}_c^0 + X)$ in the continuum region ([/REF/BABAR_2005_S6181155/d05-x01-y02](#))

14.7 BABAR_2007_S6895344 [207]

Inclusive Λ_c^+ Production in e^+e^- Annihilation at $\sqrt{s} = 10.54$ GeV and in $\Upsilon(4S)$ Decays.

Beams: e^+e^-

Energies: (3.5, 8.0), (3.5, 7.9) GeV

Experiment: BaBar (PEP-II)

Spires ID: [6895344](#)

Status: VALIDATED

Authors:

- Peter Richardson (Peter.Richardson@durham.ac.uk)

References:

- Phys.Rev. D75 (2007) 012003
- hep-ex/0609004

Run details:

- e^+e^- analysis on the $\Upsilon(4S)$ resonance, with CoM boosts of 8.0 GeV (e^-) and 3.5 GeV (e^+)

Measurements of the total production rates and momentum distributions of the charmed baryon Λ_c^+ in $e^+e^- \rightarrow$ hadrons at a centre-of-mass energy of 10.54 GeV and in $\Upsilon(4S)$ decays.

Histograms (4):

- Λ_c^+ scaled momentum in the continuum region ([/REF/BABAR_2007_S6895344/d01-x01-y01](#))
- Production rate for $\Lambda_c^+ + \bar{\Lambda}_c^-$ in the continuum region ([/REF/BABAR_2007_S6895344/d02-x01-y01](#))
- Λ_c^+ scaled momentum in the resonance region ([/REF/BABAR_2007_S6895344/d03-x01-y01](#))
- Cross Section for $e^+e^- \rightarrow \Lambda_c^+ + \bar{\Lambda}_c^- + X$ in the resonance region ([/REF/BABAR_2007_S6895344/d04-x01-y01](#))

14.8 BABAR_2007_S7266081 [208]

Measurements of Semi-Leptonic Tau Decays into Three Charged Hadrons

Beams: $e^+ e^-$

Energies: (3.5, 8.0) GeV

Experiment: BaBar (PEP-II)

Spires ID: [7266081](#)

Status: VALIDATED

Authors:

- Peter Richardson (Peter.Richardson@durham.ac.uk)

References:

- Phys.Rev.Lett.100:011801,2008
- arXiv: [0707.2981](#)
- SLAC-R-936

Run details:

- Tau production, can be any process but original data was in $e^+ e^-$ at the $\Upsilon(4S)$ resonance, with CoM boosts of 8.0 GeV (e^-) and 3.5 GeV (e^+)

Measurement of tau decays to three charged hadrons using a data sample corresponding to an integrated luminosity of 342 fb^{-1} collected with the BABAR detector at the SLAC PEP-II electron-positron storage ring operating at a center-of-mass energy near 10.58 GeV.

Histograms (14):

- $\pi^- \pi^- \pi^+$ mass in $\tau^- \rightarrow \pi^- \pi^- \pi^+ \nu_\tau$ decays ([/REF/BABAR_2007_S7266081/d01-x01-y01](#))
- $\pi^- \pi^+$ mass in $\tau^- \rightarrow \pi^- \pi^- \pi^+ \nu_\tau$ decays ([/REF/BABAR_2007_S7266081/d02-x01-y01](#))
- $K^- \pi^- \pi^+$ mass in $\tau^- \rightarrow K^- \pi^- \pi^+ \nu_\tau$ decays ([/REF/BABAR_2007_S7266081/d03-x01-y01](#))
- $K^- \pi^+$ mass in $\tau^- \rightarrow K^- \pi^- \pi^+ \nu_\tau$ decays ([/REF/BABAR_2007_S7266081/d04-x01-y01](#))
- $\pi^- \pi^+$ mass in $\tau^- \rightarrow K^- \pi^- \pi^+ \nu_\tau$ decays ([/REF/BABAR_2007_S7266081/d05-x01-y01](#))
- $K^- \pi^- K^+$ mass in $\tau^- \rightarrow K^- \pi^- K^+ \nu_\tau$ decays ([/REF/BABAR_2007_S7266081/d06-x01-y01](#))
- $K^- K^+$ mass in $\tau^- \rightarrow K^- \pi^- K^+ \nu_\tau$ decays ([/REF/BABAR_2007_S7266081/d07-x01-y01](#))
- $\pi^- K^+$ mass in $\tau^- \rightarrow K^- \pi^- K^+ \nu_\tau$ decays ([/REF/BABAR_2007_S7266081/d08-x01-y01](#))
- $K^- K^- K^+$ mass in $\tau^- \rightarrow K^- K^- K^+ \nu_\tau$ decays ([/REF/BABAR_2007_S7266081/d09-x01-y01](#))
- $K^- K^+$ mass in $\tau^- \rightarrow K^- K^- K^+ \nu_\tau$ decays ([/REF/BABAR_2007_S7266081/d10-x01-y01](#))
- Branching ratio for $\tau^- \rightarrow \pi^- \pi^- \pi^+ \nu_\tau$ decays ([/REF/BABAR_2007_S7266081/d11-x01-y01](#))

- Branching ratio for $\tau^- \rightarrow K^-\pi^-\pi^+\nu_\tau$ decays ([/REF/BABAR_2007_S7266081/d12-x01-y01](#))
- Branching ratio for $\tau^- \rightarrow K^-\pi^-K^+\nu_\tau$ decays ([/REF/BABAR_2007_S7266081/d13-x01-y01](#))
- Branching ratio for $\tau^- \rightarrow K^-K^-K^+\nu_\tau$ decays ([/REF/BABAR_2007_S7266081/d14-x01-y01](#))

14.9 BELLE_2001_S4598261 [209]

Measurement of inclusive production of neutral pions from $\Upsilon(4S)$ decays.

Beams: $e^+ e^-$

Energies: (3.5, 8.0) GeV

Experiment: Belle (KEKB)

Spires ID: 4598261

Status: VALIDATED

Authors:

- Peter Richardson (Peter.Richardson@durham.ac.uk)

References:

- Phys.Rev. D64 (2001) 072001
- hep-ex/0103041

Run details:

- e^+e^- analysis on the $\Upsilon(4S)$ resonance, with CoM boosts of 8.0 GeV (e^-) and 3.5 GeV (e^+)

Measurement of the mean multiplicity and the momentum spectrum of neutral pions from the decays of the Upsilon(4S) resonance using the Belle detector operating at the KEKB e^+e^- storage ring. Useful for tuning B meson decay models.

Histograms (2):

- π^0 momentum (/REF/BELLE_2001_S4598261/d01-x01-y01)
- π^0 multiplicity (/REF/BELLE_2001_S4598261/d02-x01-y01)

14.10 BELLE_2006_S6265367 [210]

Charm hadrons from fragmentation and B decays on the $\Upsilon(4S)$

Beams: $e^+ e^-$

Energies: (3.5, 8.0), (3.5, 7.9) GeV

Experiment: Belle (KEKB)

Spires ID: [6265367](#)

Status: VALIDATED

Authors:

- Jan Eike von Seggern (jan.eike.von.seggern@physik.hu-berlin.de)

References:

- Phys.Rev.D73:032002,2006.
- arXiv: [hep-ex/0506068](#)
- DOI: [10.1103/PhysRevD.73.032002](https://doi.org/10.1103/PhysRevD.73.032002)

Run details:

- $e^+ e^-$ analysis on the $\Upsilon(4S)$ resonance, with CoM boosts of 8.0 GeV (e^-) and 3.5 GeV (e^+)

Analysis of charm quark fragmentation at 10.6 GeV, based on a data sample of 103 fb collected by the Belle detector at the KEKB accelerator. Fragmentation into charm is studied for the main charmed hadron ground states, namely D^0 , D^+ , D_s^+ and Λ_c^+ , as well as the excited states D^{*0} and D^{*+} . This analysis can be used to constrain charm fragmentation in Monte Carlo generators. As the original data are not corrected for the branching ratios of the decay modes used to observed the charm hadrons we also include distributions with unit normalisation which are more useful for Monte Carlo tuning.

Histograms (36):

- Cross Section for $e^+ e^- \rightarrow D^0 + \bar{D}^0 + X$ ([/REF/BELLE_2006_S6265367/d01-x01-y01](#))
- Cross Section for $e^+ e^- \rightarrow D^+ + D^- + X$ ([/REF/BELLE_2006_S6265367/d01-x01-y02](#))
- Cross Section for $e^+ e^- \rightarrow D_s^+ + D_s^- + X$ ([/REF/BELLE_2006_S6265367/d01-x01-y03](#))
- Cross Section for $e^+ e^- \rightarrow \Lambda_c^+ + \bar{\Lambda}_c^- + X$ ([/REF/BELLE_2006_S6265367/d01-x01-y04](#))
- Cross Section for $e^+ e^- \rightarrow D^{*0} + \bar{D}^{*0} + X$ ([/REF/BELLE_2006_S6265367/d01-x01-y05](#))
- Cross Section for $e^+ e^- \rightarrow D^{*+} + D^{*-} + X$ ([/REF/BELLE_2006_S6265367/d01-x01-y06](#))
- Cross Section for $e^+ e^- \rightarrow D^{*+} + D^{*-} + X$ ([/REF/BELLE_2006_S6265367/d01-x01-y07](#))
- Cross Section for $e^+ e^- \rightarrow D^{*+} + D^{*-} + X$ ([/REF/BELLE_2006_S6265367/d01-x01-y08](#))

- $D^{*+} \rightarrow D^0\pi^+$ scaled momentum in the continuum region ([/REF/BELLE_2006_S6265367/d02-x01-y01](#))
- $D^{*+} \rightarrow D^0\pi^+$ scaled momentum in the continuum region ([/REF/BELLE_2006_S6265367/d02-x01-y02](#))
- $D^0 \rightarrow K^-\pi^+$ scaled momentum in the continuum region ([/REF/BELLE_2006_S6265367/d03-x01-y01](#))
- $D^0 \rightarrow K^-\pi^+$ scaled momentum in the continuum region ([/REF/BELLE_2006_S6265367/d03-x01-y02](#))
- $D^+ \rightarrow K^-\pi^+\pi^-$ scaled momentum in the continuum region ([/REF/BELLE_2006_S6265367/d04-x01-y01](#))
- $D^+ \rightarrow K^-\pi^+\pi^-$ scaled momentum in the continuum region ([/REF/BELLE_2006_S6265367/d04-x01-y02](#))
- $D_s^+ \rightarrow \phi\pi^+$ scaled momentum in the continuum region ([/REF/BELLE_2006_S6265367/d05-x01-y01](#))
- $D_s^+ \rightarrow \phi\pi^+$ scaled momentum in the continuum region ([/REF/BELLE_2006_S6265367/d05-x01-y02](#))
- $\Lambda_c^+ \rightarrow p^+K^-\pi^+$ scaled momentum in the continuum region ([/REF/BELLE_2006_S6265367/d06-x01-y01](#))
- $\Lambda_c^+ \rightarrow p^+K^-\pi^+$ scaled momentum in the continuum region ([/REF/BELLE_2006_S6265367/d06-x01-y02](#))
- $D^{*+} \rightarrow D^+\pi^0$ scaled momentum in the continuum region ([/REF/BELLE_2006_S6265367/d07-x01-y01](#))
- $D^{*+} \rightarrow D^+\pi^0$ scaled momentum in the continuum region ([/REF/BELLE_2006_S6265367/d07-x01-y02](#))
- $D^{*0} \rightarrow D^0\pi^0$ scaled momentum in the continuum region ([/REF/BELLE_2006_S6265367/d08-x01-y01](#))
- $D^{*0} \rightarrow D^0\pi^0$ scaled momentum in the continuum region ([/REF/BELLE_2006_S6265367/d08-x01-y02](#))
- $D^{*+} \rightarrow D^0\pi^+$ scaled momentum in the resonance region ([/REF/BELLE_2006_S6265367/d09-x01-y01](#))
- $D^{*+} \rightarrow D^0\pi^+$ scaled momentum in the resonance region ([/REF/BELLE_2006_S6265367/d09-x01-y02](#))
- $D^0 \rightarrow K^-\pi^+$ scaled momentum in the resonance region ([/REF/BELLE_2006_S6265367/d10-x01-y01](#))
- $D^0 \rightarrow K^-\pi^+$ scaled momentum in the resonance region ([/REF/BELLE_2006_S6265367/d10-x01-y02](#))
- $D^+ \rightarrow K^-\pi^+\pi^-$ scaled momentum in the resonance region ([/REF/BELLE_2006_S6265367/d11-x01-y01](#))
- $D^+ \rightarrow K^-\pi^+\pi^-$ scaled momentum in the resonance region ([/REF/BELLE_2006_S6265367/d11-x01-y02](#))
- $D_s^+ \rightarrow \phi\pi^+$ scaled momentum in the resonance region ([/REF/BELLE_2006_S6265367/d12-x01-y01](#))
- $D_s^+ \rightarrow \phi\pi^+$ scaled momentum in the resonance region ([/REF/BELLE_2006_S6265367/d12-x01-y02](#))
- $\Lambda_c^+ \rightarrow p^+K^-\pi^+$ scaled momentum in the resonance region ([/REF/BELLE_2006_S6265367/d13-x01-y01](#))
- $\Lambda_c^+ \rightarrow p^+K^-\pi^+$ scaled momentum in the resonance region ([/REF/BELLE_2006_S6265367/d13-x01-y02](#))
- $D^{*+} \rightarrow D^+\pi^0$ scaled momentum in the resonance region ([/REF/BELLE_2006_S6265367/d14-x01-y01](#))
- $D^{*+} \rightarrow D^+\pi^0$ scaled momentum in the resonance region ([/REF/BELLE_2006_S6265367/d14-x01-y02](#))
- $D^{*0} \rightarrow D^0\pi^0$ scaled momentum in the resonance region ([/REF/BELLE_2006_S6265367/d15-x01-y01](#))
- $D^{*0} \rightarrow D^0\pi^0$ scaled momentum in the resonance region ([/REF/BELLE_2006_S6265367/d15-x01-y02](#))

14.11 CLEO_2004_S5809304 [211]

Charm hadrons from fragmentation near the $\Upsilon(4S)$

Beams: $e^+ e^-$

Energies: (5.3, 5.3) GeV

Spires ID: 6265367

Status: VALIDATED

Authors:

- Peter Richardson (Peter.Richardson@durham.ac.uk)

References:

- Phys.Rev.D70:112001,2004.
- arXiv: [hep-ex/0402040](#)

Run details:

- e^+e^- analysis near the $\Upsilon(4S)$ resonance

Analysis of charm quark fragmentation at 10.5 GeV, based on a data sample of 103 fb collected by the CLEO experiment. Fragmentation into charm is studied for the charmed hadron ground states, namely D^0 , D^+ , as well as the excited states D^{*0} and D^{*+} . This analysis can be used to constrain charm fragmentation in Monte Carlo generators.

Histograms (15):

- Cross Section for $e^+e^- \rightarrow D^+ + D^- + X$ ([/REF/CLEO_2004_S5809304/d01-x01-y01](#))
- Cross Section for $e^+e^- \rightarrow D^0 + \bar{D}^0 + X$ using $D^0 \rightarrow K^-\pi^+$ ([/REF/CLEO_2004_S5809304/d01-x01-y02](#))
- Cross Section for $e^+e^- \rightarrow D^0 + \bar{D}^0 + X$ using $D^0 \rightarrow K^-\pi^+\pi^+\pi^-$ ([/REF/CLEO_2004_S5809304/d01-x01-y03](#))
- Cross Section for $e^+e^- \rightarrow D^{*+} + D^{*-} + X$ using $D^0 \rightarrow K^-\pi^+$ ([/REF/CLEO_2004_S5809304/d01-x01-y04](#))
- Cross Section for $e^+e^- \rightarrow D^{*+} + D^{*-} + X$ using $D^0 \rightarrow K^-\pi^+\pi^+\pi^-$ ([/REF/CLEO_2004_S5809304/d01-x01-y05](#))
- Cross Section for $e^+e^- \rightarrow D^{*0} + \bar{D}^{*0} + X$ using $D^0 \rightarrow K^-\pi^+$ ([/REF/CLEO_2004_S5809304/d01-x01-y06](#))
- Cross Section for $e^+e^- \rightarrow D^{*0} + \bar{D}^{*0} + X$ using $D^0 \rightarrow K^-\pi^+\pi^+\pi^-$ ([/REF/CLEO_2004_S5809304/d01-x01-y07](#))
- D^+ scaled momentum using $D^+ \rightarrow K^-\pi^+\pi^-$ ([/REF/CLEO_2004_S5809304/d02-x01-y01](#))
- D^0 scaled momentum using $D^0 \rightarrow K^-\pi^+$ ([/REF/CLEO_2004_S5809304/d03-x01-y01](#))

- D^0 scaled momentum using $D^0 \rightarrow K^-\pi^+\pi^+\pi^-$ ([/REF/CLEO_2004_S5809304/d04-x01-y01](#))
- D^{*+} scaled momentum using $D^0 \rightarrow K^-\pi^+$ ([/REF/CLEO_2004_S5809304/d05-x01-y01](#))
- D^{*+} scaled momentum using $D^0 \rightarrow K^-\pi^+\pi^+\pi^-$ ([/REF/CLEO_2004_S5809304/d06-x01-y01](#))
- D^{*0} scaled momentum using $D^0 \rightarrow K^-\pi^+$ ([/REF/CLEO_2004_S5809304/d07-x01-y01](#))
- D^{*0} scaled momentum using $D^0 \rightarrow K^-\pi^+\pi^+\pi^-$ ([/REF/CLEO_2004_S5809304/d08-x01-y01](#))
- Average D meson scaled momentum distribution ([/REF/CLEO_2004_S5809304/d09-x01-y01](#))

14.12 JADE_1998_S3612880 [212]

Event shapes for 22, 35 and 44 GeV

Beams: $e^- e^+$

Energies: (11.0, 11.0), (17.5, 17.5), (22.0, 22.0) GeV

Experiment: JADE (PETRA)

Spires ID: 3612880

Status: VALIDATED

Authors:

- Holger Schulz (holger.schulz@physik.hu-berlin.de)

References:

- arXiv: [hep-ex/9708034](#)
- Eur.Phys.J.C1:461-478,1998

Run details:

- Z \rightarrow hadronic final states, bbar contributions have been corrected for as well as ISR Thrust, Jet Mass and Broadenings, Y23 for 35 and 44 GeV and only Y23 at 22 GeV.

Histograms (11):

- 1-Thrust, $\sqrt{s} = 44$ GeV ([/REF/JADE_1998_S3612880/d02-x01-y01](#))
- Heavy Jet Mass, $\sqrt{s} = 44$ GeV ([/REF/JADE_1998_S3612880/d03-x01-y01](#))
- Total Jet Broadening, $\sqrt{s} = 44$ GeV ([/REF/JADE_1998_S3612880/d04-x01-y01](#))
- Wide Jet Broadening, $\sqrt{s} = 44$ GeV ([/REF/JADE_1998_S3612880/d05-x01-y01](#))
- 1-Thrust, $\sqrt{s} = 35$ GeV ([/REF/JADE_1998_S3612880/d06-x01-y01](#))
- Heavy Jet Mass, $\sqrt{s} = 35$ GeV ([/REF/JADE_1998_S3612880/d07-x01-y01](#))
- Total Jet Broadening, $\sqrt{s} = 35$ GeV ([/REF/JADE_1998_S3612880/d08-x01-y01](#))
- Wide Jet Broadening, $\sqrt{s} = 35$ GeV ([/REF/JADE_1998_S3612880/d09-x01-y01](#))
- Differential 2-Jet rate (Durham), $\sqrt{s} = 44$ GeV ([/REF/JADE_1998_S3612880/d10-x01-y01](#))
- Differential 2-Jet rate (Durham), $\sqrt{s} = 35$ GeV ([/REF/JADE_1998_S3612880/d11-x01-y01](#))
- Differential 2-Jet rate (Durham), $\sqrt{s} = 22$ GeV ([/REF/JADE_1998_S3612880/d12-x01-y01](#))

14.13 PDG_HADRON_MULTIPLICITIES [213]

Hadron multiplicities in hadronic e^+e^- events

Beams: e^+e^-

Energies: (5.0, 5.0), (17.5, 17.5), (45.6, 45.6), (88.5, 88.5) GeV

Experiment: PDG (Various)

Spires ID: 7857373

Status: VALIDATED

Authors:

- Hendrik Hoeth (hendrik.hoeth@cern.ch)

References:

- Phys. Lett. B, 667, 1 (2008)

Run details:

- Hadronic events in e^+e^- collisions

Hadron multiplicities in hadronic e^+e^- events, taken from Review of Particle Properties 2008, table 40.1, page 355. Average hadron multiplicities per hadronic e^+e^- annihilation event at $\sqrt{s} \approx 10, 29\text{--}35, 91$, and $130\text{--}200$ GeV. The numbers are averages from various experiments. Correlations of the systematic uncertainties were considered for the calculation of the averages.

Histograms (116):

- Mean π^+ multiplicity (/REF/PDG_HADRON_MULTIPLICITIES/d01-x01-y01)
- Mean π^+ multiplicity (/REF/PDG_HADRON_MULTIPLICITIES/d01-x01-y02)
- Mean π^+ multiplicity (/REF/PDG_HADRON_MULTIPLICITIES/d01-x01-y03)
- Mean π^+ multiplicity (/REF/PDG_HADRON_MULTIPLICITIES/d01-x01-y04)
- Mean π^0 multiplicity (/REF/PDG_HADRON_MULTIPLICITIES/d02-x01-y01)
- Mean π^0 multiplicity (/REF/PDG_HADRON_MULTIPLICITIES/d02-x01-y02)
- Mean π^0 multiplicity (/REF/PDG_HADRON_MULTIPLICITIES/d02-x01-y03)
- Mean K^+ multiplicity (/REF/PDG_HADRON_MULTIPLICITIES/d03-x01-y01)
- Mean K^+ multiplicity (/REF/PDG_HADRON_MULTIPLICITIES/d03-x01-y02)
- Mean K^+ multiplicity (/REF/PDG_HADRON_MULTIPLICITIES/d03-x01-y03)
- Mean K^+ multiplicity (/REF/PDG_HADRON_MULTIPLICITIES/d03-x01-y04)
- Mean K^0 multiplicity (/REF/PDG_HADRON_MULTIPLICITIES/d04-x01-y01)

- Mean K^0 multiplicity (/REF/PDG_HADRON_MULTIPLICITIES/d04-x01-y02)
- Mean K^0 multiplicity (/REF/PDG_HADRON_MULTIPLICITIES/d04-x01-y03)
- Mean K^0 multiplicity (/REF/PDG_HADRON_MULTIPLICITIES/d04-x01-y04)
- Mean η multiplicity (/REF/PDG_HADRON_MULTIPLICITIES/d05-x01-y01)
- Mean η multiplicity (/REF/PDG_HADRON_MULTIPLICITIES/d05-x01-y02)
- Mean η multiplicity (/REF/PDG_HADRON_MULTIPLICITIES/d05-x01-y03)
- Mean $\eta'(958)$ multiplicity (/REF/PDG_HADRON_MULTIPLICITIES/d06-x01-y01)
- Mean $\eta'(958)$ multiplicity (/REF/PDG_HADRON_MULTIPLICITIES/d06-x01-y02)
- Mean $\eta'(958)$ multiplicity (/REF/PDG_HADRON_MULTIPLICITIES/d06-x01-y03)
- Mean D^+ multiplicity (/REF/PDG_HADRON_MULTIPLICITIES/d07-x01-y01)
- Mean D^+ multiplicity (/REF/PDG_HADRON_MULTIPLICITIES/d07-x01-y02)
- Mean D^+ multiplicity (/REF/PDG_HADRON_MULTIPLICITIES/d07-x01-y03)
- Mean D^0 multiplicity (/REF/PDG_HADRON_MULTIPLICITIES/d08-x01-y01)
- Mean D^0 multiplicity (/REF/PDG_HADRON_MULTIPLICITIES/d08-x01-y02)
- Mean D^0 multiplicity (/REF/PDG_HADRON_MULTIPLICITIES/d08-x01-y03)
- Mean D_s^+ multiplicity (/REF/PDG_HADRON_MULTIPLICITIES/d09-x01-y01)
- Mean D_s^+ multiplicity (/REF/PDG_HADRON_MULTIPLICITIES/d09-x01-y02)
- Mean $D^+ s$ multiplicity (/REF/PDG_HADRON_MULTIPLICITIES/d09-x01-y03)
- Mean B^+, B_d^0 multiplicity (/REF/PDG_HADRON_MULTIPLICITIES/d10-x01-y01)
- Mean B_u^+ multiplicity (/REF/PDG_HADRON_MULTIPLICITIES/d11-x01-y01)
- Mean B_s^0 multiplicity (/REF/PDG_HADRON_MULTIPLICITIES/d12-x01-y01)
- Mean $f_0(980)$ multiplicity (/REF/PDG_HADRON_MULTIPLICITIES/d13-x01-y01)
- Mean $f_0(980)$ multiplicity (/REF/PDG_HADRON_MULTIPLICITIES/d13-x01-y02)
- Mean $f_0(980)$ multiplicity (/REF/PDG_HADRON_MULTIPLICITIES/d13-x01-y03)
- Mean $a_0^+(980)$ multiplicity (/REF/PDG_HADRON_MULTIPLICITIES/d14-x01-y01)
- Mean $\rho^0(770)$ multiplicity (/REF/PDG_HADRON_MULTIPLICITIES/d15-x01-y01)
- Mean $\rho^0(770)$ multiplicity (/REF/PDG_HADRON_MULTIPLICITIES/d15-x01-y02)

- Mean $\rho^0(770)$ multiplicity (/REF/PDG_HADRON_MULTIPLICITIES/d15-x01-y03)
- Mean $\rho^+(770)$ multiplicity (/REF/PDG_HADRON_MULTIPLICITIES/d16-x01-y01)
- Mean $\omega(782)$ multiplicity (/REF/PDG_HADRON_MULTIPLICITIES/d17-x01-y01)
- Mean $\omega(782)$ multiplicity (/REF/PDG_HADRON_MULTIPLICITIES/d17-x01-y02)
- Mean $K^{*+}(892)$ multiplicity (/REF/PDG_HADRON_MULTIPLICITIES/d18-x01-y01)
- Mean $K^{*+}(892)$ multiplicity (/REF/PDG_HADRON_MULTIPLICITIES/d18-x01-y02)
- Mean $K^{*+}(892)$ multiplicity (/REF/PDG_HADRON_MULTIPLICITIES/d18-x01-y03)
- Mean $K^{*0}(892)$ multiplicity (/REF/PDG_HADRON_MULTIPLICITIES/d19-x01-y01)
- Mean $K^{*0}(892)$ multiplicity (/REF/PDG_HADRON_MULTIPLICITIES/d19-x01-y02)
- Mean $K^{*0}(892)$ multiplicity (/REF/PDG_HADRON_MULTIPLICITIES/d19-x01-y03)
- Mean $\phi(1020)$ multiplicity (/REF/PDG_HADRON_MULTIPLICITIES/d20-x01-y01)
- Mean $\phi(1020)$ multiplicity (/REF/PDG_HADRON_MULTIPLICITIES/d20-x01-y02)
- Mean $\phi(1020)$ multiplicity (/REF/PDG_HADRON_MULTIPLICITIES/d20-x01-y03)
- Mean $D^{*+}(2010)$ multiplicity (/REF/PDG_HADRON_MULTIPLICITIES/d21-x01-y01)
- Mean $D^{*+}(2010)$ multiplicity (/REF/PDG_HADRON_MULTIPLICITIES/d21-x01-y02)
- Mean $D^{*+}(2010)$ multiplicity (/REF/PDG_HADRON_MULTIPLICITIES/d21-x01-y03)
- Mean $D^{*0}(2007)$ multiplicity (/REF/PDG_HADRON_MULTIPLICITIES/d22-x01-y01)
- Mean $D^{*0}(2007)$ multiplicity (/REF/PDG_HADRON_MULTIPLICITIES/d22-x01-y02)
- Mean $D_s^{*+}(2112)$ multiplicity (/REF/PDG_HADRON_MULTIPLICITIES/d23-x01-y01)
- Mean $D_s^{*+}(2112)$ multiplicity (/REF/PDG_HADRON_MULTIPLICITIES/d23-x01-y02)
- Mean B^* multiplicity (/REF/PDG_HADRON_MULTIPLICITIES/d24-x01-y01)
- Mean $J/\psi(1S)$ multiplicity (/REF/PDG_HADRON_MULTIPLICITIES/d25-x01-y01)
- Mean $J/\psi(1S)$ multiplicity (/REF/PDG_HADRON_MULTIPLICITIES/d25-x01-y02)
- Mean $\psi(2S)$ multiplicity (/REF/PDG_HADRON_MULTIPLICITIES/d26-x01-y01)
- Mean $\Upsilon(1S)$ multiplicity (/REF/PDG_HADRON_MULTIPLICITIES/d27-x01-y01)
- Mean $f_1(1285)$ multiplicity (/REF/PDG_HADRON_MULTIPLICITIES/d28-x01-y01)
- Mean $f_1(1420)$ multiplicity (/REF/PDG_HADRON_MULTIPLICITIES/d29-x01-y01)

- Mean $\chi_{c1}(3510)$ multiplicity (/REF/PDG_HADRON_MULTIPLICITIES/d30-x01-y01)
- Mean $f_2(1270)$ multiplicity (/REF/PDG_HADRON_MULTIPLICITIES/d31-x01-y01)
- Mean $f_2(1270)$ multiplicity (/REF/PDG_HADRON_MULTIPLICITIES/d31-x01-y02)
- Mean $f_2(1270)$ multiplicity (/REF/PDG_HADRON_MULTIPLICITIES/d31-x01-y03)
- Mean $f'_2(1525)$ multiplicity (/REF/PDG_HADRON_MULTIPLICITIES/d32-x01-y01)
- Mean $K_2^{*+}(1430)$ multiplicity (/REF/PDG_HADRON_MULTIPLICITIES/d33-x01-y01)
- Mean $K_2^{*0}(1430)$ multiplicity (/REF/PDG_HADRON_MULTIPLICITIES/d34-x01-y01)
- Mean $K_2^{*0}(1430)$ multiplicity (/REF/PDG_HADRON_MULTIPLICITIES/d34-x01-y02)
- Mean B^{*+} multiplicity (/REF/PDG_HADRON_MULTIPLICITIES/d35-x01-y01)
- Mean D_{s1}^+ multiplicity (/REF/PDG_HADRON_MULTIPLICITIES/d36-x01-y01)
- Mean D_{s2}^+ multiplicity (/REF/PDG_HADRON_MULTIPLICITIES/d37-x01-y01)
- Mean p multiplicity (/REF/PDG_HADRON_MULTIPLICITIES/d38-x01-y01)
- Mean p multiplicity (/REF/PDG_HADRON_MULTIPLICITIES/d38-x01-y02)
- Mean p multiplicity (/REF/PDG_HADRON_MULTIPLICITIES/d38-x01-y03)
- Mean p multiplicity (/REF/PDG_HADRON_MULTIPLICITIES/d38-x01-y04)
- Mean Λ multiplicity (/REF/PDG_HADRON_MULTIPLICITIES/d39-x01-y01)
- Mean Λ multiplicity (/REF/PDG_HADRON_MULTIPLICITIES/d39-x01-y02)
- Mean Λ multiplicity (/REF/PDG_HADRON_MULTIPLICITIES/d39-x01-y03)
- Mean Λ multiplicity (/REF/PDG_HADRON_MULTIPLICITIES/d39-x01-y04)
- Mean Σ^0 multiplicity (/REF/PDG_HADRON_MULTIPLICITIES/d40-x01-y01)
- Mean Σ^0 multiplicity (/REF/PDG_HADRON_MULTIPLICITIES/d40-x01-y02)
- Mean Σ^- multiplicity (/REF/PDG_HADRON_MULTIPLICITIES/d41-x01-y01)
- Mean Σ^+ multiplicity (/REF/PDG_HADRON_MULTIPLICITIES/d42-x01-y01)
- Mean Σ^\pm multiplicity (/REF/PDG_HADRON_MULTIPLICITIES/d43-x01-y01)
- Mean Ξ^- multiplicity (/REF/PDG_HADRON_MULTIPLICITIES/d44-x01-y01)
- Mean Ξ^- multiplicity (/REF/PDG_HADRON_MULTIPLICITIES/d44-x01-y02)
- Mean Ξ^- multiplicity (/REF/PDG_HADRON_MULTIPLICITIES/d44-x01-y03)

- Mean $\Delta^{++}(1232)$ multiplicity (/REF/PDG_HADRON_MULTIPLICITIES/d45-x01-y01)
- Mean $\Delta^{++}(1232)$ multiplicity (/REF/PDG_HADRON_MULTIPLICITIES/d45-x01-y02)
- Mean $\Sigma^-(1385)$ multiplicity (/REF/PDG_HADRON_MULTIPLICITIES/d46-x01-y01)
- Mean $\Sigma^-(1385)$ multiplicity (/REF/PDG_HADRON_MULTIPLICITIES/d46-x01-y02)
- Mean $\Sigma^-(1385)$ multiplicity (/REF/PDG_HADRON_MULTIPLICITIES/d46-x01-y03)
- Mean $\Sigma^+(1385)$ multiplicity (/REF/PDG_HADRON_MULTIPLICITIES/d47-x01-y01)
- Mean $\Sigma^+(1385)$ multiplicity (/REF/PDG_HADRON_MULTIPLICITIES/d47-x01-y02)
- Mean $\Sigma^+(1385)$ multiplicity (/REF/PDG_HADRON_MULTIPLICITIES/d47-x01-y03)
- Mean $\Sigma^\pm(1385)$ multiplicity (/REF/PDG_HADRON_MULTIPLICITIES/d48-x01-y01)
- Mean $\Sigma^\pm(1385)$ multiplicity (/REF/PDG_HADRON_MULTIPLICITIES/d48-x01-y02)
- Mean $\Sigma^\pm(1385)$ multiplicity (/REF/PDG_HADRON_MULTIPLICITIES/d48-x01-y03)
- Mean $\Xi^0(1530)$ multiplicity (/REF/PDG_HADRON_MULTIPLICITIES/d49-x01-y01)
- Mean $\Xi^0(1530)$ multiplicity (/REF/PDG_HADRON_MULTIPLICITIES/d49-x01-y02)
- Mean Ω^- multiplicity (/REF/PDG_HADRON_MULTIPLICITIES/d50-x01-y01)
- Mean Ω^- multiplicity (/REF/PDG_HADRON_MULTIPLICITIES/d50-x01-y02)
- Mean Ω^- multiplicity (/REF/PDG_HADRON_MULTIPLICITIES/d50-x01-y03)
- Mean Λ_c^+ multiplicity (/REF/PDG_HADRON_MULTIPLICITIES/d51-x01-y01)
- Mean Λ_c^+ multiplicity (/REF/PDG_HADRON_MULTIPLICITIES/d51-x01-y02)
- Mean Λ_c^+ multiplicity (/REF/PDG_HADRON_MULTIPLICITIES/d51-x01-y03)
- Mean Λ_b^0 multiplicity (/REF/PDG_HADRON_MULTIPLICITIES/d52-x01-y01)
- Mean $\Sigma_c^{++}, \Sigma_c^0$ multiplicity (/REF/PDG_HADRON_MULTIPLICITIES/d53-x01-y01)
- Mean $\Lambda(1520)$ multiplicity (/REF/PDG_HADRON_MULTIPLICITIES/d54-x01-y01)
- Mean $\Lambda(1520)$ multiplicity (/REF/PDG_HADRON_MULTIPLICITIES/d54-x01-y02)

14.14 PDG_HADRON_MULTIPLICITIES RATIOS [213]

Ratios (w.r.t. π^+/π^-) of hadron multiplicities in hadronic e^+e^- events

Beams: e^+e^-

Energies: (5.0, 5.0), (17.5, 17.5), (45.6, 45.6), (88.5, 88.5) GeV

Experiment: PDG (Various)

Spires ID: [7857373](#)

Status: VALIDATED

Authors:

- Holger Schulz (holger.schulz@physik.hu-berlin.de)

References:

- Phys. Lett. B, 667, 1 (2008)

Run details:

- Hadronic events in e^+e^- collisions

Ratios (w.r.t. π^+/π^-) of hadron multiplicities in hadronic e^+e^- events, taken from Review of Particle Properties 2008, table 40.1, page 355. Average hadron multiplicities per hadronic e^+e^- annihilation event at $\sqrt{s} \approx 10, 29\text{--}35, 91$, and $130\text{--}200$ GeV, normalised to the pion multiplicity. The numbers are averages from various experiments. Correlations of the systematic uncertainties were considered for the calculation of the averages.

Histograms (112):

- Ratio (w.r.t. π^\pm) of mean π^0 multiplicity ([/REF/PDG_HADRON_MULTIPLICITIES_RATIOS/d02-x01-y01](#))
- Ratio (w.r.t. π^\pm) of mean π^0 multiplicity ([/REF/PDG_HADRON_MULTIPLICITIES_RATIOS/d02-x01-y02](#))
- Ratio (w.r.t. π^\pm) of mean π^0 multiplicity ([/REF/PDG_HADRON_MULTIPLICITIES_RATIOS/d02-x01-y03](#))
- Ratio (w.r.t. π^\pm) of mean K^+ multiplicity ([/REF/PDG_HADRON_MULTIPLICITIES_RATIOS/d03-x01-y01](#))
- Ratio (w.r.t. π^\pm) of mean K^+ multiplicity ([/REF/PDG_HADRON_MULTIPLICITIES_RATIOS/d03-x01-y02](#))
- Ratio (w.r.t. π^\pm) of mean K^+ multiplicity ([/REF/PDG_HADRON_MULTIPLICITIES_RATIOS/d03-x01-y03](#))
- Ratio (w.r.t. π^\pm) of mean K^+ multiplicity ([/REF/PDG_HADRON_MULTIPLICITIES_RATIOS/d03-x01-y04](#))
- Ratio (w.r.t. π^\pm) of mean K^0 multiplicity ([/REF/PDG_HADRON_MULTIPLICITIES_RATIOS/d04-x01-y01](#))
- Ratio (w.r.t. π^\pm) of mean K^0 multiplicity ([/REF/PDG_HADRON_MULTIPLICITIES_RATIOS/d04-x01-y02](#))
- Ratio (w.r.t. π^\pm) of mean K^0 multiplicity ([/REF/PDG_HADRON_MULTIPLICITIES_RATIOS/d04-x01-y03](#))
- Ratio (w.r.t. π^\pm) of mean K^0 multiplicity ([/REF/PDG_HADRON_MULTIPLICITIES_RATIOS/d04-x01-y04](#))
- Ratio (w.r.t. π^\pm) of mean η multiplicity ([/REF/PDG_HADRON_MULTIPLICITIES_RATIOS/d05-x01-y01](#))

- Ratio (w.r.t. π^\pm) of mean η multiplicity (/REF/PDG_HADRON_MULTIPLICITIES RATIOS/d05-x01-y02)
- Ratio (w.r.t. π^\pm) of mean η multiplicity (/REF/PDG_HADRON_MULTIPLICITIES RATIOS/d05-x01-y03)
- Ratio (w.r.t. π^\pm) of mean $\eta'(958)$ multiplicity (/REF/PDG_HADRON_MULTIPLICITIES RATIOS/d06-x01-y01)
- Ratio (w.r.t. π^\pm) of mean $\eta'(958)$ multiplicity (/REF/PDG_HADRON_MULTIPLICITIES RATIOS/d06-x01-y02)
- Ratio (w.r.t. π^\pm) of mean $\eta'(958)$ multiplicity (/REF/PDG_HADRON_MULTIPLICITIES RATIOS/d06-x01-y03)
- Ratio (w.r.t. π^\pm) of mean D^+ multiplicity (/REF/PDG_HADRON_MULTIPLICITIES RATIOS/d07-x01-y01)
- Ratio (w.r.t. π^\pm) of mean D^+ multiplicity (/REF/PDG_HADRON_MULTIPLICITIES RATIOS/d07-x01-y02)
- Ratio (w.r.t. π^\pm) of mean D^+ multiplicity (/REF/PDG_HADRON_MULTIPLICITIES RATIOS/d07-x01-y03)
- Ratio (w.r.t. π^\pm) of mean D^0 multiplicity (/REF/PDG_HADRON_MULTIPLICITIES RATIOS/d08-x01-y01)
- Ratio (w.r.t. π^\pm) of mean D^0 multiplicity (/REF/PDG_HADRON_MULTIPLICITIES RATIOS/d08-x01-y02)
- Ratio (w.r.t. π^\pm) of mean D^0 multiplicity (/REF/PDG_HADRON_MULTIPLICITIES RATIOS/d08-x01-y03)
- Ratio (w.r.t. π^\pm) of mean D_s^+ multiplicity (/REF/PDG_HADRON_MULTIPLICITIES RATIOS/d09-x01-y01)
- Ratio (w.r.t. π^\pm) of mean D_s^+ multiplicity (/REF/PDG_HADRON_MULTIPLICITIES RATIOS/d09-x01-y02)
- Ratio (w.r.t. π^\pm) of mean D_s^+ multiplicity (/REF/PDG_HADRON_MULTIPLICITIES RATIOS/d09-x01-y03)
- Ratio (w.r.t. π^\pm) of mean B^+, B_d^0 multiplicity (/REF/PDG_HADRON_MULTIPLICITIES RATIOS/d10-x01-y01)
- Ratio (w.r.t. π^\pm) of mean B_u^+ multiplicity (/REF/PDG_HADRON_MULTIPLICITIES RATIOS/d11-x01-y01)
- Ratio (w.r.t. π^\pm) of mean B_s^0 multiplicity (/REF/PDG_HADRON_MULTIPLICITIES RATIOS/d12-x01-y01)
- Ratio (w.r.t. π^\pm) of mean $f_0(980)$ multiplicity (/REF/PDG_HADRON_MULTIPLICITIES RATIOS/d13-x01-y01)
- Ratio (w.r.t. π^\pm) of mean $f_0(980)$ multiplicity (/REF/PDG_HADRON_MULTIPLICITIES RATIOS/d13-x01-y02)
- Ratio (w.r.t. π^\pm) of mean $f_0(980)$ multiplicity (/REF/PDG_HADRON_MULTIPLICITIES RATIOS/d13-x01-y03)
- Ratio (w.r.t. π^\pm) of mean $a_0^+(980)$ multiplicity (/REF/PDG_HADRON_MULTIPLICITIES - RATIOS/d14-x01-y01)
- Ratio (w.r.t. π^\pm) of mean $\rho^0(770)$ multiplicity (/REF/PDG_HADRON_MULTIPLICITIES - RATIOS/d15-x01-y01)
- Ratio (w.r.t. π^\pm) of mean $\rho^0(770)$ multiplicity (/REF/PDG_HADRON_MULTIPLICITIES - RATIOS/d15-x01-y02)
- Ratio (w.r.t. π^\pm) of mean $\rho^0(770)$ multiplicity (/REF/PDG_HADRON_MULTIPLICITIES - RATIOS/d15-x01-y03)

- Ratio (w.r.t. π^\pm) of mean $\rho^+(770)$ multiplicity (/REF/PDG_HADRON_MULTIPLICITIES_- RATIOS/d16-x01-y01)
- Ratio (w.r.t. π^\pm) of mean $\omega(782)$ multiplicity (/REF/PDG_HADRON_MULTIPLICITIES_RATIOS/d17-x01-y01)
- Ratio (w.r.t. π^\pm) of mean $\omega(782)$ multiplicity (/REF/PDG_HADRON_MULTIPLICITIES_RATIOS/d17-x01-y02)
- Ratio (w.r.t. π^\pm) of mean $K^{*+}(892)$ multiplicity (/REF/PDG_HADRON_MULTIPLICITIES_- RATIOS/d18-x01-y01)
- Ratio (w.r.t. π^\pm) of mean $K^{*+}(892)$ multiplicity (/REF/PDG_HADRON_MULTIPLICITIES_- RATIOS/d18-x01-y02)
- Ratio (w.r.t. π^\pm) of mean $K^{*+}(892)$ multiplicity (/REF/PDG_HADRON_MULTIPLICITIES_- RATIOS/d18-x01-y03)
- Ratio (w.r.t. π^\pm) of mean $K^{*0}(892)$ multiplicity (/REF/PDG_HADRON_MULTIPLICITIES_- RATIOS/d19-x01-y01)
- Ratio (w.r.t. π^\pm) of mean $K^{*0}(892)$ multiplicity (/REF/PDG_HADRON_MULTIPLICITIES_- RATIOS/d19-x01-y02)
- Ratio (w.r.t. π^\pm) of mean $K^{*0}(892)$ multiplicity (/REF/PDG_HADRON_MULTIPLICITIES_- RATIOS/d19-x01-y03)
- Ratio (w.r.t. π^\pm) of mean $\phi(1020)$ multiplicity (/REF/PDG_HADRON_MULTIPLICITIES_- RATIOS/d20-x01-y01)
- Ratio (w.r.t. π^\pm) of mean $\phi(1020)$ multiplicity (/REF/PDG_HADRON_MULTIPLICITIES_- RATIOS/d20-x01-y02)
- Ratio (w.r.t. π^\pm) of mean $\phi(1020)$ multiplicity (/REF/PDG_HADRON_MULTIPLICITIES_- RATIOS/d20-x01-y03)
- Ratio (w.r.t. π^\pm) of mean $D^{*+}(2010)$ multiplicity (/REF/PDG_HADRON_MULTIPLICITIES_- RATIOS/d21-x01-y01)
- Ratio (w.r.t. π^\pm) of mean $D^{*+}(2010)$ multiplicity (/REF/PDG_HADRON_MULTIPLICITIES_- RATIOS/d21-x01-y02)
- Ratio (w.r.t. π^\pm) of mean $D^{*+}(2010)$ multiplicity (/REF/PDG_HADRON_MULTIPLICITIES_- RATIOS/d21-x01-y03)
- Ratio (w.r.t. π^\pm) of mean $D^{*0}(2007)$ multiplicity (/REF/PDG_HADRON_MULTIPLICITIES_- RATIOS/d22-x01-y01)
- Ratio (w.r.t. π^\pm) of mean $D^{*0}(2007)$ multiplicity (/REF/PDG_HADRON_MULTIPLICITIES_- RATIOS/d22-x01-y02)

- Ratio (w.r.t. π^\pm) of mean $D_s^{*+}(2112)$ multiplicity ([/REF/PDG_HADRON_MULTIPLICITIES_-_RATIOS/d23-x01-y01](#))
- Ratio (w.r.t. π^\pm) of mean $D_s^{*+}(2112)$ multiplicity ([/REF/PDG_HADRON_MULTIPLICITIES_-_RATIOS/d23-x01-y02](#))
- Ratio (w.r.t. π^\pm) of mean B^* multiplicity ([/REF/PDG_HADRON_MULTIPLICITIES_RATIOS/d24-x01-y01](#))
- Ratio (w.r.t. π^\pm) of mean $J/\psi(1S)$ multiplicity ([/REF/PDG_HADRON_MULTIPLICITIES_-_RATIOS/d25-x01-y01](#))
- Ratio (w.r.t. π^\pm) of mean $J/\psi(1S)$ multiplicity ([/REF/PDG_HADRON_MULTIPLICITIES_-_RATIOS/d25-x01-y02](#))
- Ratio (w.r.t. π^\pm) of mean $\psi(2S)$ multiplicity ([/REF/PDG_HADRON_MULTIPLICITIES_RATIOS/d26-x01-y01](#))
- Ratio (w.r.t. π^\pm) of mean $\Upsilon(1S)$ multiplicity ([/REF/PDG_HADRON_MULTIPLICITIES_RATIOS/d27-x01-y01](#))
- Ratio (w.r.t. π^\pm) of mean $f_1(1285)$ multiplicity ([/REF/PDG_HADRON_MULTIPLICITIES_-_RATIOS/d28-x01-y01](#))
- Ratio (w.r.t. π^\pm) of mean $f_1(1420)$ multiplicity ([/REF/PDG_HADRON_MULTIPLICITIES_-_RATIOS/d29-x01-y01](#))
- Ratio (w.r.t. π^\pm) of mean $\chi_{c1}(3510)$ multiplicity ([/REF/PDG_HADRON_MULTIPLICITIES_-_RATIOS/d30-x01-y01](#))
- Ratio (w.r.t. π^\pm) of mean $f_2(1270)$ multiplicity ([/REF/PDG_HADRON_MULTIPLICITIES_-_RATIOS/d31-x01-y01](#))
- Ratio (w.r.t. π^\pm) of mean $f_2(1270)$ multiplicity ([/REF/PDG_HADRON_MULTIPLICITIES_-_RATIOS/d31-x01-y02](#))
- Ratio (w.r.t. π^\pm) of mean $f_2(1270)$ multiplicity ([/REF/PDG_HADRON_MULTIPLICITIES_-_RATIOS/d31-x01-y03](#))
- Ratio (w.r.t. π^\pm) of mean $f'_2(1525)$ multiplicity ([/REF/PDG_HADRON_MULTIPLICITIES_-_RATIOS/d32-x01-y01](#))
- Ratio (w.r.t. π^\pm) of mean $K_2^{*+}(1430)$ multiplicity ([/REF/PDG_HADRON_MULTIPLICITIES_-_RATIOS/d33-x01-y01](#))
- Ratio (w.r.t. π^\pm) of mean $K_2^{*0}(1430)$ multiplicity ([/REF/PDG_HADRON_MULTIPLICITIES_-_RATIOS/d34-x01-y01](#))
- Ratio (w.r.t. π^\pm) of mean $K_2^{*0}(1430)$ multiplicity ([/REF/PDG_HADRON_MULTIPLICITIES_-_RATIOS/d34-x01-y02](#))
- Ratio (w.r.t. π^\pm) of mean B^{**} multiplicity ([/REF/PDG_HADRON_MULTIPLICITIES_RATIOS/d35-x01-y01](#))

- Ratio (w.r.t. π^\pm) of mean D_{s1}^+ multiplicity (/REF/PDG_HADRON_MULTIPLICITIES RATIOS/d36-x01-y01)
- Ratio (w.r.t. π^\pm) of mean D_{s2}^+ multiplicity (/REF/PDG_HADRON_MULTIPLICITIES RATIOS/d37-x01-y01)
- Ratio (w.r.t. π^\pm) of mean p multiplicity (/REF/PDG_HADRON_MULTIPLICITIES RATIOS/d38-x01-y01)
- Ratio (w.r.t. π^\pm) of mean p multiplicity (/REF/PDG_HADRON_MULTIPLICITIES RATIOS/d38-x01-y02)
- Ratio (w.r.t. π^\pm) of mean p multiplicity (/REF/PDG_HADRON_MULTIPLICITIES RATIOS/d38-x01-y03)
- Ratio (w.r.t. π^\pm) of mean p multiplicity (/REF/PDG_HADRON_MULTIPLICITIES RATIOS/d38-x01-y04)
- Ratio (w.r.t. π^\pm) of mean Λ multiplicity (/REF/PDG_HADRON_MULTIPLICITIES RATIOS/d39-x01-y01)
- Ratio (w.r.t. π^\pm) of mean Λ multiplicity (/REF/PDG_HADRON_MULTIPLICITIES RATIOS/d39-x01-y02)
- Ratio (w.r.t. π^\pm) of mean Λ multiplicity (/REF/PDG_HADRON_MULTIPLICITIES RATIOS/d39-x01-y03)
- Ratio (w.r.t. π^\pm) of mean Λ multiplicity (/REF/PDG_HADRON_MULTIPLICITIES RATIOS/d39-x01-y04)
- Ratio (w.r.t. π^\pm) of mean Σ^0 multiplicity (/REF/PDG_HADRON_MULTIPLICITIES RATIOS/d40-x01-y01)
- Ratio (w.r.t. π^\pm) of mean Σ^0 multiplicity (/REF/PDG_HADRON_MULTIPLICITIES RATIOS/d40-x01-y02)
- Ratio (w.r.t. π^\pm) of mean Σ^- multiplicity (/REF/PDG_HADRON_MULTIPLICITIES RATIOS/d41-x01-y01)
- Ratio (w.r.t. π^\pm) of mean Σ^+ multiplicity (/REF/PDG_HADRON_MULTIPLICITIES RATIOS/d42-x01-y01)
- Ratio (w.r.t. π^\pm) of mean Σ^\pm multiplicity (/REF/PDG_HADRON_MULTIPLICITIES RATIOS/d43-x01-y01)
- Ratio (w.r.t. π^\pm) of mean Ξ^- multiplicity (/REF/PDG_HADRON_MULTIPLICITIES RATIOS/d44-x01-y01)
- Ratio (w.r.t. π^\pm) of mean Ξ^- multiplicity (/REF/PDG_HADRON_MULTIPLICITIES RATIOS/d44-x01-y02)
- Ratio (w.r.t. π^\pm) of mean Ξ^- multiplicity (/REF/PDG_HADRON_MULTIPLICITIES RATIOS/d44-x01-y03)
- Ratio (w.r.t. π^\pm) of mean $\Delta^{++}(1232)$ multiplicity (/REF/PDG_HADRON_MULTIPLICITIES - RATIOS/d45-x01-y01)
- Ratio (w.r.t. π^\pm) of mean $\Delta^{++}(1232)$ multiplicity (/REF/PDG_HADRON_MULTIPLICITIES - RATIOS/d45-x01-y02)
- Ratio (w.r.t. π^\pm) of mean $\Sigma^-(1385)$ multiplicity (/REF/PDG_HADRON_MULTIPLICITIES - RATIOS/d46-x01-y01)
- Ratio (w.r.t. π^\pm) of mean $\Sigma^-(1385)$ multiplicity (/REF/PDG_HADRON_MULTIPLICITIES - RATIOS/d46-x01-y02)
- Ratio (w.r.t. π^\pm) of mean $\Sigma^-(1385)$ multiplicity (/REF/PDG_HADRON_MULTIPLICITIES - RATIOS/d46-x01-y03)
- Ratio (w.r.t. π^\pm) of mean $\Sigma^+(1385)$ multiplicity (/REF/PDG_HADRON_MULTIPLICITIES - RATIOS/d47-x01-y01)

- Ratio (w.r.t. π^\pm) of mean $\Sigma^+(1385)$ multiplicity (`/REF/PDG_HADRON_MULTIPLICITIES_- RATIOS/d47-x01-y02`)
- Ratio (w.r.t. π^\pm) of mean $\Sigma^+(1385)$ multiplicity (`/REF/PDG_HADRON_MULTIPLICITIES_- RATIOS/d47-x01-y03`)
- Ratio (w.r.t. π^\pm) of mean $\Sigma^\pm(1385)$ multiplicity (`/REF/PDG_HADRON_MULTIPLICITIES_- RATIOS/d48-x01-y01`)
- Ratio (w.r.t. π^\pm) of mean $\Sigma^\pm(1385)$ multiplicity (`/REF/PDG_HADRON_MULTIPLICITIES_- RATIOS/d48-x01-y02`)
- Ratio (w.r.t. π^\pm) of mean $\Sigma^\pm(1385)$ multiplicity (`/REF/PDG_HADRON_MULTIPLICITIES_- RATIOS/d48-x01-y03`)
- Ratio (w.r.t. π^\pm) of mean $\Xi^0(1530)$ multiplicity (`/REF/PDG_HADRON_MULTIPLICITIES_- RATIOS/d49-x01-y01`)
- Ratio (w.r.t. π^\pm) of mean $\Xi^0(1530)$ multiplicity (`/REF/PDG_HADRON_MULTIPLICITIES_- RATIOS/d49-x01-y02`)
- Ratio (w.r.t. π^\pm) of mean Ω^- multiplicity (`/REF/PDG_HADRON_MULTIPLICITIES_RATIOS/d50-x01-y01`)
- Ratio (w.r.t. π^\pm) of mean Ω^- multiplicity (`/REF/PDG_HADRON_MULTIPLICITIES_RATIOS/d50-x01-y02`)
- Ratio (w.r.t. π^\pm) of mean Ω^- multiplicity (`/REF/PDG_HADRON_MULTIPLICITIES_RATIOS/d50-x01-y03`)
- Ratio (w.r.t. π^\pm) of mean Λ_c^+ multiplicity (`/REF/PDG_HADRON_MULTIPLICITIES_RATIOS/d51-x01-y01`)
- Ratio (w.r.t. π^\pm) of mean Λ_c^+ multiplicity (`/REF/PDG_HADRON_MULTIPLICITIES_RATIOS/d51-x01-y02`)
- Ratio (w.r.t. π^\pm) of mean Λ_c^+ multiplicity (`/REF/PDG_HADRON_MULTIPLICITIES_RATIOS/d51-x01-y03`)
- Ratio (w.r.t. π^\pm) of mean Λ_b^0 multiplicity (`/REF/PDG_HADRON_MULTIPLICITIES_RATIOS/d52-x01-y01`)
- Ratio (w.r.t. π^\pm) of mean $\Sigma_c^{++}, Sigma_c0$ multiplicity (`/REF/PDG_HADRON_MULTIPLICITIES_- RATIOS/d53-x01-y01`)
- Ratio (w.r.t. π^\pm) of mean $\Lambda(1520)$ multiplicity (`/REF/PDG_HADRON_MULTIPLICITIES_- RATIOS/d54-x01-y01`)
- Ratio (w.r.t. π^\pm) of mean $\Lambda(1520)$ multiplicity (`/REF/PDG_HADRON_MULTIPLICITIES_- RATIOS/d54-x01-y02`)

14.15 SFM_1984_S1178091 [214]

Charged multiplicity distribution in pp interactions at CERN ISR energies

Beams: pp

Energies: (15.2, 15.2), (22.2, 22.2), (26.1, 26.1), (31.1, 31.1) GeV

Experiment: SFM (CERN ISR)

Spires ID: [1178091](#)

Status: UNVALIDATED

Authors:

- Holger Schulz (holger.schulz@physik.hu-berlin.de)
- Andy Buckley (andy.buckley@cern.ch)

References:

- Phys.Rev.D30:528,1984

Run details:

- QCD events, double-diffractive events should be turned on as well.

Charged multiplicities are measured at $\sqrt{s} = 30.4, 44.5, 52.2$ and 62.2 GeV using a minimum-bias trigger. The data is sub-divided into inelastic as well as non-single-diffractive events. However, the implementation of the diffractive events will require some work.

Histograms (8):

- Charged multiplicity at $\sqrt{s} = 30.4$ GeV (inelastic events) ([/REF/SFM_1984_S1178091/d01-x01-y01](#))
- Charged multiplicity at $\sqrt{s} = 44.5$ GeV (inelastic events) ([/REF/SFM_1984_S1178091/d01-x01-y02](#))
- Charged multiplicity at $\sqrt{s} = 52.6$ GeV (inelastic events) ([/REF/SFM_1984_S1178091/d01-x01-y03](#))
- Charged multiplicity at $\sqrt{s} = 62.2$ GeV (inelastic events) ([/REF/SFM_1984_S1178091/d01-x01-y04](#))
- Charged multiplicity at $\sqrt{s} = 30.4$ GeV (NSD events) ([/REF/SFM_1984_S1178091/d02-x01-y01](#))
- Charged multiplicity at $\sqrt{s} = 44.5$ GeV (NSD events) ([/REF/SFM_1984_S1178091/d02-x01-y02](#))
- Charged multiplicity at $\sqrt{s} = 52.6$ GeV (NSD events) ([/REF/SFM_1984_S1178091/d02-x01-y03](#))
- Charged multiplicity at $\sqrt{s} = 62.2$ GeV (NSD events) ([/REF/SFM_1984_S1178091/d02-x01-y04](#))

14.16 TASSO_1990_S2148048 [215]

Event shapes in e^+e^- annihilation at 14–44 GeV

Beams: $e^- e^+$

Energies: (7.0, 7.0), (11.0, 11.0), (17.5, 17.5), (21.9, 21.9) GeV

Experiment: TASSO (PETRA)

Spires ID: [2148048](#)

Status: VALIDATED

Authors:

- Holger Schulz (holger.schulz@physik.hu-berlin.de)

References:

- Z.Phys.C47:187-198,1990
- DESY-90-013

Run details:

- $e^+e^- \rightarrow$ jet jet (+ jets). Kinematic cuts such as CKIN(1) in Pythia need to be set slightly below the CMS energy.

Event shapes Thrust, Sphericity, Aplanarity at four different energies

Histograms (16):

- Scaled momentum distribution ($\sqrt{s} = 14$ GeV) (/REF/TASSO_1990_S2148048/d02-x01-y01)
- Scaled momentum distribution ($\sqrt{s} = 22$ GeV) (/REF/TASSO_1990_S2148048/d02-x01-y02)
- Scaled momentum distribution ($\sqrt{s} = 35$ GeV) (/REF/TASSO_1990_S2148048/d02-x01-y03)
- Scaled momentum distribution ($\sqrt{s} = 44$ GeV) (/REF/TASSO_1990_S2148048/d02-x01-y04)
- Sphericity ($\sqrt{s} = 14$ GeV) (/REF/TASSO_1990_S2148048/d06-x01-y01)
- Sphericity ($\sqrt{s} = 22$ GeV) (/REF/TASSO_1990_S2148048/d06-x01-y02)
- Sphericity ($\sqrt{s} = 35$ GeV) (/REF/TASSO_1990_S2148048/d06-x01-y03)
- Sphericity ($\sqrt{s} = 44$ GeV) (/REF/TASSO_1990_S2148048/d06-x01-y04)
- Aplanarity ($\sqrt{s} = 14$ GeV) (/REF/TASSO_1990_S2148048/d07-x01-y01)
- Aplanarity ($\sqrt{s} = 22$ GeV) (/REF/TASSO_1990_S2148048/d07-x01-y02)
- Aplanarity ($\sqrt{s} = 35$ GeV) (/REF/TASSO_1990_S2148048/d07-x01-y03)
- Aplanarity ($\sqrt{s} = 44$ GeV) (/REF/TASSO_1990_S2148048/d07-x01-y04)
- Thrust ($\sqrt{s} = 14$ GeV) (/REF/TASSO_1990_S2148048/d08-x01-y01)

- Thrust ($\sqrt{s} = 22 \text{ GeV}$) ([/REF/TASSO_1990_S2148048/d08-x01-y02](#))
- Thrust ($\sqrt{s} = 35 \text{ GeV}$) ([/REF/TASSO_1990_S2148048/d08-x01-y03](#))
- Thrust ($\sqrt{s} = 44 \text{ GeV}$) ([/REF/TASSO_1990_S2148048/d08-x01-y04](#))

Part III

How Rivet works

Hopefully by now you’ve run Rivet a few times and got the hang of the command line interface and viewing the resulting analysis data files. Maybe you’ve got some ideas of analyses that you would like to see in Rivet’s library. If so, then you’ll need to know a little about Rivet’s internal workings before you can start coding: with any luck by the end of this section that won’t seem particularly intimidating.

The core objects in Rivet are “projections” and “analyses”. Hopefully “analyses” isn’t a surprise — that’s just the collection of routines that will make histograms to compare with reference data, and the only things that might differ there from experiences with HZTool[216] are the new histogramming system and the fact that we’ve used some object orientation concepts to make life a bit easier. The meaning of “projections”, as applied to event analysis, will probably be less obvious. We’ll discuss them soon, but first a semi-philosophical aside on the “right way” to do physics analyses on and involving simulated data.

15. The science and art of physically valid MC analysis

The world of MC event generators is a wonderfully convenient one for experimentalists: we are provided with fully exclusive events whose most complex correlations can be explored and used to optimise analysis algorithms and some kinds of detector correction effects. It is absolutely true that the majority of data analyses and detector designs in modern collider physics would be very different without MC simulation.

But it is very important to remember that it is just simulation: event generators encode much of known physics and phenomenologically explore the non-perturbative areas of QCD, but only unadulterated experiment can really tell us about how the world behaves. The richness and convenience of MC simulation can be seductive, and it is important that experimental use of MC strives to understand and minimise systematic biases which may result from use of simulated data, and to not “unfold” imperfect models when measuring the real world. The canonical example of the latter effect is the unfolding of hadronisation (a deeply non-perturbative and imperfectly-understood process) at the Tevatron (Run I), based on MC models. Publishing “measured quarks” is not physics — much of the data thus published has proven of little use to either theory or experiment in the following years. In the future we must be alert to such temptation and avoid such gaffes — and much more subtle ones.

These concerns on how MC can be abused in treating measured data also apply to MC validation studies. A key observable in QCD tunings is the p_\perp of the Z boson, which has no phase space at exactly $p_\perp = 0$ but a very sharp peak at $\mathcal{O}(1\text{-}2 \text{ GeV})$. The exact location of this peak is mostly sensitive to the width parameter of a nucleon “intrinsic p_\perp ” in MC generators, plus some soft initial state radiation and QED bremsstrahlung. Unfortunately, all the published Tevatron measurements of this observable have either “unfolded” the QED

effects to the “Z p_\perp ” as attached to the object in the HepMC/HEPEVT event record with a PDG ID code of 23, or have used MC data to fill regions of phase space where the detector could not measure. Accordingly, it is very hard to make an accurate and portable MC analysis to fit this data, without similarly delving into the event record in search of “the boson”. While common practice, this approach intrinsically limits the precision of measured data to the calculational order of the generator — often not analytically well-defined. We can do better.

Away from this philosophical propaganda (which nevertheless we hope strikes some chords in influential places...), there are also excellent pragmatic reasons for MC analyses to avoid treating the MC “truth” record as genuine truth. The key argument is portability: there is no MC generator which is the ideal choice for all scenarios, and an essential tool for understanding sub-leading variability in theoretical approaches to various areas of physics is to use several generators with similar leading accuracies but different sub-leading formalisms. While the HEPEVT record as written by HERWIG and PYTHIA has become familiar to many, there are many ambiguities in how it is filled, from the allowed graph structures to the particle content. Notably, the Sherpa event generator explicitly elides Feynman diagram propagators from the event record, perhaps driven by a desire to protect us from our baser analytical instincts. The Herwig++ event generator takes the almost antipodal approach of expressing different contributing Feynman diagram topologies in different ways (*not* physically meaningful!) and seamlessly integrating shower emissions with the hard process particles. The general trend in MC simulation is to blur the practically-induced line between the sampled matrix element and the Markovian parton cascade, challenging many established assumptions about “how MC works”. In short, if you want to “find” the Z to see what its p_\perp or η spectrum looks like, many new generators may break your honed PYTHIA code... or silently give systematically wrong results. The unfortunate truth is that most of the event record is intended for generator debugging rather than physics interpretation.

Fortunately, the situation is not altogether negative: in practice it is usually as easy to write a highly functional MC analysis using only final state particles and their physically meaningful on-shell decay parents. These are, since the release of HepMC 2.5, standardised to have status codes of 1 and 2 respectively. Z-finding is then a matter of choosing decay lepton candidates, windowing their invariant mass around the known Z mass, and choosing the best Z candidate: effectively a simplified version of an experimental analysis of the same quantity. This is a generally good heuristic for a safe MC analysis! Note that since it’s known that you will be running the analysis on signal events, and there are no detector effects to deal with, almost all the details that make a real analysis hard can be ignored. The one detail that is worth including is summing momentum from photons around the charged leptons, before mass-windowing: this physically corresponds to the indistinguishability of collinear energy deposits in trackers and calorimeters and would be the ideal published experimental measurement of Drell-Yan p_\perp for MC tuning. Note that similar analyses for W bosons have the luxury over a true experiment of being able to exactly identify the decay neutrino rather than having to mess around with missing energy. Similarly, detailed unstable hadron (or tau) reconstruction is unnecessary, due to the presence of these particles in the event record with status code 2. In short, writing an effective analysis which is

automatically portable between generators is no harder than trying to decipher the variable structures and multiple particle copies of the debugging-level event objects. And of course Rivet provides lots of tools to do almost all the standard fiddly bits for you, so there's no excuse!

Good luck, and be careful!

16. Projections

The name “projection” is meant to evoke thoughts of projection operators, low-dimensional slices/views of high-dimensional spaces, and other things that might appeal to physicists who view the world through quantum-tinted lenses. A more mundane, but equally applicable, name would be “observable calculators”, but since that's a long name, the things they return aren't *necessarily* observable, and they all inherit from the `Projection` base class, we'll stick to that name. It doesn't take long to get used to using the name as a synonym for “calculator”, without being intimidated by ideas that they might be some sort of high-powered deep magic. 90% of them is simple and self-explanatory, as a peek under the bonnet of e.g. the all-important `FinalState` projection will reveal.

Projections can be relatively simple things like event shapes (i.e. scalar, vector or tensor quantities), or arbitrarily complex things like lossy or selective views of the event final state. Most users will see them attached to analyses by declarations in each analysis' initialisation, but they can also be recursively “nested” inside other projections² (provided there are no infinite loops in the nesting chain.) Calling a complex projection in an analysis may actually transparently execute many projections on each event.

You can find a list of all existing projections and their inheritance structure in Fig. 1. An up-to-date version of this listing can always be found in the code documentation at <http://rivet.hepforge.org>.

16.1 Projection caching

Aside from semantic issues of how the class design assigns the process of analysing events, projections are important computationally because they live in a framework which automatically stores (“caches”) their results between events. This is a crucial feature for the long-term scalability of Rivet, as the previous experience with HZTool was that HERA validation code ran very slowly due to repeated calculation of the same k_{\perp} clustering algorithm (at that time notorious for scaling as the 3rd power of the number of particles.)

A concrete example may help in understanding how this works. Let's say we have two analyses which have the same run conditions, i.e. incoming beam types, beam energies, etc. Each also uses the thrust event shape measure to define a set of basis vectors for their analysis. For each event that gets passed to Rivet, whichever analysis gets called first will immediately (although maybe indirectly) call a `FinalState` projection to get a list of stable,

²Provided there are no dependency loops in the projection chains! Strictly, only acyclic graphs of projection dependencies are valid, but there is currently no code in Rivet that will attempt to verify this restriction.

physical particles (filtering out the intermediate and book-keeping entries in the HepMC event record). That FS projection is then “attached” to the event. Next, the first analysis will call a **Thrust** projection which internally uses the same final state projection to define the momentum vectors used in calculating the thrust. Once finished, the thrust projection will also be attached to the event.

So far, projections have offered no benefits. However, when the second analysis runs it will similarly try to apply its final state and thrust projections to the event. Rather than repeat the calculations, Rivet’s infrastructure will detect that an equivalent calculation has already been run and will just return references to the already-run projections. Since projections can also contain and use other projections, this model allows some substantial computational savings, without the analysis author even needing to be particularly aware of what is going on.

Observant readers may have noticed a problem with all this projection caching cleverness: what if the final states aren’t defined the same way? One might provide charged final state particles only, or the acceptances (defined in pseudorapidity range and a IR p_{\perp} cutoff) might differ. Rivet handles this by making each projection provide a comparison operator which is used to decide whether the cached version is acceptable or if the calculation must be re-run with different settings. Because projections can be nested, applying a top-level projection to an event can spark off a cascade of comparisons, calculations and cache accesses, making use of existing results wherever possible.

16.2 Using projection caching

So far this is all theory — how does one actually use projections in Rivet? First, you should understand that projections, while semantically stored within each other, are actually all registered with a central **ProjectionHandler** object.³ The reason for this central registration is to ensure that all projections’ lifespans are managed in a consistent way, and to protect projection and analysis authors from some technical subtleties in how C++ polymorphism works.

Inside the constructor of a **Projection** or the **init** method of an **Analysis** class, you must call the **addProjection** function. This takes two arguments, the projection to be registered (by **const** reference), and a name. The name is local to the parent object, so you need not worry about name clashes between objects. A very important point is that the passed **Projection** is not the one that is actually centrally registered — that distinction belongs to a newly created heap object which is created within the **addProjection** method by means of the overloaded **Projection::clone()** method. Hence it is completely safe — and recommended — to use only local (stack) objects in **Projection** and **Analysis** constructors.

³As of version 1.1 onwards — previously, they were stored as class members inside other **Projection**s and **Analysis** classes.



At this point, if you have rightly bought into C++ ideas like super-strong type-safety, this proliferation of dynamic casting may worry you: the compiler can't possibly check if a projection of the requested name has been registered, nor whether the downcast to the requested concrete type is legal. These are very legitimate concerns! In truth, we'd like to have this level of extra safety: who wouldn't? But in the past, when projections were held as members of `ProjectionApplier` classes rather than in the central `ProjectionHandler` repository, the benefits of the strong typing were outweighed by more serious and subtle bugs relating to projection lifetime and object “slicing”. At least when the current approach goes wrong it will throw an unmissable runtime error — until it's fixed, of course! — rather than silently do the wrong thing.

Our problems here are a microcosm of the perpetual language battle between strict and dynamic typing, runtime versus compile time errors. In practice, this manifests itself as a trade-off between the benefits of static type safety and the inconvenience of the type-system gymnastics that it engenders. We take some comfort from the number of very good programs have been and are still written in dynamically typed, interpreted languages like Python, where virtually all error checking (barring first-scan parsing errors) must be done at runtime. By pushing some checking to the domain of runtime errors, Rivet's code is (we believe) in practice safer, and certainly more clear and elegant. However, we believe that with runtime checking should come a culture of unit testing, which is not yet in place in Rivet.

As a final thought, one reason for Rivet's internal complexity is that C++ is just not a very good language for this sort of thing: we are operating on the boundary between event generator codes, number crunching routines (including third party libraries like FastJet) and user routines. The former set unavoidably require native interfaces and benefit from static typing; the latter benefit from interface flexibility, fast prototyping and syntactic clarity. Maybe a future version of Rivet will break through the technical barriers to a hybrid approach and allow users to run compiled projections from interpreted analysis code. For now, however, we hope that our brand of “slightly less safe C++” will be a pleasant compromise.

17. Analyses

17.1 Writing a new analysis

This section provides a recipe that can be followed to write a new analysis using the Rivet projections.

Every analysis must inherit from `Rivet::Analysis` and, in addition to the constructor, must implement a minimum of three methods. Those methods are `init()`, `analyze(const Rivet::Event&)` and `finalize()`, which are called once at the beginning of the analysis, once per event and once at the end of the analysis respectively.

The new analysis should include the header for the base analysis class plus whichever Rivet projections are to be used, and should work under the `Rivet` namespace. Since

analyses are hardly ever intended to be inherited from, they are usually implemented within a single .cc file with no corresponding header. The skeleton of a new analysis named `UserAnalysis` that uses the `FinalState` projection might therefore start off looking like this, in a file named `UserAnalysis.cc`:

```
#include "Rivet/Analysis.hh"

namespace Rivet {

    class UserAnalysis : public Analysis {
public:
    UserAnalysis() : Analysis("USERANA") { }
    void init() { ... }
    void analyze(const Event& event) { ... }
    void finalize() { ... }
};

}
```

The constructor body is usually left empty, as all event loop setup is done in the `init()` method: the one *required* constructor feature is to make a call to its base `Analysis` constructor, passing a string by which the analysis will *register* itself with the Rivet framework. This name is the one exposed to a command-line or API user of this analysis: usually it is the same as the class name, which for official analyses is always in upper case.



Early versions of Rivet required the user to declare allowed beam types, energies, whether a cross-section is required, etc. in the analysis constructor via methods like `setBeams(...)` and `setNeedsCrossSection(...)`. This information is now *much* preferred to be taken from the `.info` file for the analysis, and *must* be done this way in analyses submitted for inclusion in future Rivet releases.

The `init()` method for the `UserAnalysis` class should add to the analysis all of the projections that will be used. Projections can be added to an analysis with a call to `addProjection(Projection, std::string)`, which takes as argument the projection to be added and a name by which that projection can later be referenced. For this example the `FinalState` projection is to be referenced by the string "FS" to provide access to all of the final state particles inside a detector pseudorapidity coverage of ± 5.0 . The syntax to create and add that projection is as follows:

```
init() {
    const FinalState fs(-5.0, 5.0);
    addProjection(fs, "FS");
}
```

A second task of the `init()` method is the booking of all histograms which are later to be filled in the analysis code. Information about the histogramming system can be found in Section 17.3.

17.2 Utility classes

Rivet provides quite a few object types for physics purposes, such as three- and four-vectors, matrices and Lorentz boosts, and convenience proxy objects for e.g. particles and jets. We now briefly summarise the most important features of some of these objects; more complete interface descriptions can be found in the generated Doxygen web pages on the Rivet web site, or simply by browsing the relevant header files.

17.2.1 FourMomentum

The `FourMomentum` class is the main physics vector that you will encounter when writing Rivet analyses. Its functionality and interface are similar to the CLHEP `HepLorentzVector` with which many users will be familiar, but without some of the historical baggage.

Vector components The `FourMomentum E()`, `px()`, `py()`, `pz()` & `mass()` methods are (unsurprisingly) accessors for the vector's energy, momentum components and mass. The `vector3()` method returns a spatial `Vector3` object, i.e. the 3 spatial components of the 4-vector.

Useful properties The `pT()` and `Et()` methods are used to calculate the transverse momentum and transverse energy. Angular variables are accessed via the `eta()`, `phi()` and `theta()` for the pseudorapidity, azimuthal angle and polar angle respectively. More explicitly named versions of these also exist, named `pseudorapidity()`, `azimuthalAngle()` and `polarAngle()`. Finally, the true rapidity is accessed via the `rapidity()` method. Many of these functions are also available as external functions, as are algebraic functions such as `cross(vec3a, vec3b)`, which is perhaps more palatable than `vec3a.cross(vec3b)`.

Distances The η - ϕ distance between any two four-vectors (and/or three-vectors) can be computed using a range of overloaded external functions of the type `deltaR(vec1, vec2)`. Angles between such vectors can be calculated via the similar `angle(vec1, vec2)` functions.

17.2.2 Particle

This class is a wrapper around the HepMC `GenParticle` class. `Particle` objects are usually obtained as a vector from the `particles()` method of a `FinalState` projection. Rather than having to directly use the HepMC objects, and e.g. translate HepMC four-vectors into the Rivet equivalent, several key properties are accessed directly via the `Particle` interface (and more may be added). The main methods of interest are `momentum()`, which returns a `FourMomentum`, and `pdgId()`, which returns the PDG particle ID code. The PDG code can be used to access particle properties by using functions such as `PID::isHadron()`, `PID::threeCharge()`, etc. (these are defined in `Rivet/Tools/ParticleIDMethods.hh`.)

17.2.3 Jet

Jets are obtained from one of the jet accessor methods of a projection that implements the `JetAlg` interface, e.g. `FastJets::jetsByPt()` (this returns the jets sorted by p_\perp , such that the first element in the vector is the hardest jet — usually what you want.) The most useful methods are `particles()`, `momenta()`, `momentum()` (a representative `FourMomentum`), and some checks on the jet contents such as `containsParticleId(pid)`, `containsCharm()` and `containsBottom()`.

17.2.4 Mathematical utilities

The `Rivet/Math/MathUtils.hh` header defines a variety of mathematical utility functions. These include testing functions such as `isZero(a)`, `fuzzyEquals(a, b)` and `inRange(a, low, high)`, whose purpose is hopefully self-evident, and angular range-mapping functions such as `mapAngle0To2Pi(a)`, `mapAngleMPiToPi(a)`, etc.

17.3 Histogramming

Rivet's histogramming uses the AIDA interfaces, composed of abstract classes `IHistogram1D`, `IProfile1D`, `IDataPointSet` etc. which are built by a factories system. Since it's our feeling that much of the factory infrastructure constitutes an abstraction overload, we provide histogram booking functions as part of the `Analysis` class, so that in the `init` method of your analysis you should book histograms with function calls like:

```
void init() {
    _h_one = bookHistogram1D(2,1,1);
    _h_two = bookProfile1D(3,1,2);
    _h_three = bookHistogram1D("d00-x00-y00", 50, 0.0, 1.0);
}
```

Here the first two bookings have a rather cryptic 3-integer sequence as the first arguments. This is the recommended scheme, as it makes use of the exported data files from HepData, in which 1D histograms are constructed from a combination of x and y axes in a dataset d , corresponding to names of the form $d\langle d \rangle - x\langle x \rangle - y\langle y \rangle$. This auto-booking of histograms saves you from having to copy out reams of bin edges and values into your code, and makes sure that any data fixes in HepData are easily propagated to Rivet. The reference data files which are used for these booking methods are distributed and installed with Rivet, you can find them in the `<installdir>/share/Rivet` directory of your installation. The third booking is for a histogram for which there is no such HepData entry: it uses the usual scheme of specifying the name, number of bins and the min/max x -axis limits manually.

Filling the histograms is done in the `MyAnalysis::analyse()` function. Remember to specify the event weight as you fill:

```
void analyse(const Event& e) {
    [projections, cuts, etc.]
    ...
    _h_one->fill(pT, event.weight());
```

```

    _h_two->fill(pT, Nch, event.weight());
    _h_three->fill(fabs(eta), event.weight());
}

```

Finally, histogram normalisations, scalings, divisions etc. are done in the `MyAnalysis::finalize()` method. For normalisations and scalings you will find appropriate convenience methods `Analysis::normalize(histo, norm)` and `Analysis::scale(histo, scaleFactor)`. Many analyses need to be scaled to the generator cross-section, with the number of event weights to pass cuts being included in the normalisation factor: for this you will have to track the passed-cuts weight sum yourself via a member variable, but the analysis class provides `Analysis::crossSection()` and `Analysis::sumOfWeights()` methods to access the pre-cuts cross-section and weight sum respectively.

17.4 Analysis metadata

To keep the analysis source code uncluttered, and to allow for iteration of data plot presentation without re-compilation and/or re-running, Rivet prefers that analysis metadata is provided via separate files rather than hard-coded into the analysis library. There are two such files: an *analysis info* file, with the suffix `.info`, and a *plot styling* file, with the suffix `.plot`.

17.4.1 Analysis info files

The analysis info files are in YAML format: a simple data format intended to be cleaner and more human-readable/writeable than XML. As well as the analysis name (which must coincide with the filename and the name provided to the `Analysis` constructor, this file stores details of the collider, experiment, date of the analysis, Rivet/data analysis authors and contact email addresses, one-line and more complete descriptions of the analysis, advice on how to run it, suggested generator-level cuts, and BibTeX keys and entries for this user manual. It is also where the validation status of the analysis is declared:

See the standard analyses' info files for guidance on how to populate this file. Info files are searched for in the paths known to the `Rivet::getAnalysisInfoPaths()` function, which may be prepended to using the `$RIVET_INFO_PATH` environment variable: the first matching file to be found will be used.

17.4.2 Plot styling files

The `.plot` files are in the header format for the `make-plots` plotting system and are picked up and merged with the plot data by the Rivet `compare-histos` script which produces the `make-plots` input data files. All the analysis' plots should have a `BEGIN PLOT ... END PLOT` section in this file, specifying the title and *x/y*-axis labels (the `Title`, and `XLabel`/`YLabel` directives). In addition, you can use this file to choose whether the *x* and/or *y* axes should be shown with a log scale (`LogX`, `LogY`), to position the legend box to minimise clashes with the data points and MC lines (`LegendXPos`, `LegendYPos`) and any other valid `make-plots` directives including special text labels or forced plot range boundaries. Regular expressions may be used to apply a directive to all analysis names

matching a pattern rather than having to specify the same directive repeatedly for many plots.

See the standard analyses’ plot files and the `make-plots` documentation (e.g. on the Rivet website) for guidance on how to write these files. Plot info files are searched for in the paths known to the `Rivet::getAnalysisPlotPaths()` function, which may be prepended to using the `$RIVET_PLOT_PATH` environment variable. As usual, the first matching file to be found will be used.

17.5 Pluggable analyses

Rivet’s standard analyses are not actually built into the main `libRivet` library: they are loaded dynamically at runtime as an analysis *plugin library*. While you don’t need to worry too much about the technicalities of this, it does mean that you can similarly write analyses of your own, compile them into a similar plugin library and run them from `rivet` without ever having to modify any of the main Rivet sources or build system. This means that you can write and run your own analyses with a system-installed copy of Rivet, and not have to re-patch the main library when a newer version comes out (although chances are you will have to recompile, since the binary interface usually change between releases.)

To get started writing your analysis and understand the plugin system better, you should check out the documentation in the wiki on the Rivet website: <http://rivet.hepforge.org/trac/wiki/>. The standard `rivet-mkanalysis` and `rivet-buildplugin` scripts can respectively be used to make an analysis template with many “boilerplate” details filled in (including bibliographic information from Inspire if available), and to build a plugin library with the appropriate compiler options.

17.5.1 Plugin paths

To load pluggable analyses you will need to set the `$RIVET_ANALYSIS_PATH` environment variable: this is a standard colon-separated UNIX path, specifying directories in which analysis plugin libraries may be found. If it is unspecified, the Rivet loader system will assume that the only entry is the `lib` directory in the Rivet installation area. Specifying the variable adds new paths for searching *before* the standard library area, and they will be searched in the left-to-right order in the path variable.

If analyses with duplicate names are found, a warning message is issued and the first version to have been found will be used. This allows you to override standard analyses with same-named variants of your own, provided they are loaded from different directories.



In Rivet 2.1.0 and later, this `$RIVET_ANALYSIS_PATH` variable (and the others described below) have an special extra syntax feature: if the environment variable ends with a double separator, i.e. `::`, then the default path will not be appended at all. This can be useful if you want to make absolutely certain not to fall back to the default locations, for example to avoid the “duplicate analysis” warnings if you are getting a lot of them.

Several further environment variables are used to load analysis reference data and metadata files:

\$RIVET_REF_PATH: A standard colon-separated path list, whose elements are searched in order for reference histogram files. If the required file is not found in this path, Rivet will fall back to looking in the analysis library paths (for convenience, as it is normal for plugin analysis developers to put analysis library and data files in the same directory and it would be annoying to have to set several variables to make this work), and then the standard Rivet installation data directory.

\$RIVET_INFO_PATH: The path list searched first for analysis `.info` metadata files. The search fallback mechanism works as for **\$RIVET_REF_PATH**.

\$RIVET_PLOT_PATH: The path list searched first for analysis `.plot` presentation style files. The search fallbacks again work as for **\$RIVET_REF_PATH**.

These paths can be accessed from the API using the `Rivet::getAnalysisLibPaths()` etc. functions, and can be searched for files using the Rivet lookup rules via the `Rivet::findAnalysisLibFile(filename)` etc. functions. See the Doxygen documentation for more details. In the lookups using these paths, if the variable ends with a double separator, i.e. `:::`, then the default path will not be appended: this may be useful in some situations. These functions are also available in the Python `rivet` module, with the same behaviours.

18. Using Rivet as a library

You don't have to use Rivet via the provided command-line programmes: for some applications you may want to have more direct control of how Rivet processes events. Here are some possible reasons:

- You need to not waste CPU cycles and I/O resources on rendering HepMC events to a string representation which is immediately read back in. The FIFO idiom (Section 3.1) is not perfect: we use it in circumstances where the convenience and decoupling outweighs the CPU cost.
- You don't want to write out histograms to file, preferring to use them as code objects. Perhaps for applications which want to manipulate histogram data periodically before the end of the run.
- You enjoy tormenting Rivet developers who know their API is far from perfect, by complaining if it changes!
- ... and many more!

The Rivet API (application programming interface) has been designed in the hope of very simple integration into other applications: all you have to do is create a `Rivet::AnalysisHandler` object, tell it which analyses to apply on the events, and then call its `analyse(evt)`

method for each HepMC event – wherever they come from. The API is (we hope) stable, with the exception of the histogramming parts.



The histogramming interfaces in Rivet have long been advertised as marked for replacement, and while progress in that area has lagged far behind our ambitions, it *will* happen with the 2.0.0 release, with unavoidable impact on the related parts of the API. You have been warned!

The API is available for C++ and, in a more restricted form, Python. We will explain the C++ version here; if you wish to operate Rivet (or e.g. use its path-searching capabilities to find Rivet-related files in the standard way) from Python then take a look inside the `rivet` and `rivet-*` Python scripts (e.g. `less ‘which rivet’`) or use the module documentation cf.

```
> python
>>> import rivet
>>> help(rivet)
```

And now the C++ API. The best way to explain is, of course, by example. Here is a simple C++ example based on the `test/testApi.cc` source which we use in development to ensure continuing API functionality:

```
#include "Rivet/AnalysisHandler.hh"
#include "HepMC/GenEvent.h"
#include "HepMC/IO_GenEvent.h"

using namespace std;

int main() {

    // Create analysis handler
    Rivet::AnalysisHandler rivet;

    // Specify the analyses to be used
    rivet.addAnalysis("D0_2008_S7554427");
    vector<string> moreanalyses(1, "D0_2007_S7075677");
    rivet.addAnalyses(moreanalyses);

    // The usual mess of reading from a HepMC file!
    std::istream* file = new std::fstream("testApi.hepmc", std::ios::in);
    HepMC::IO_GenEvent hepmcio(*file);
    HepMC::GenEvent* evt = hepmcio.read_next_event();
    double sum_of_weights = 0.0;
```

```

while (evt) {
    // Analyse the current event
    rivet.analyze(*evt);
    sum_of_weights += evt->weights()[0];

    // Clean up and get next event
    delete evt; evt = 0;
    hepmcio >> evt;
}
delete file; file = 0;

rivet.setCrossSection(1.0);
rivet.setSumOfWeights(sum_of_weights); // not necessary, but allowed
rivet.finalize();
rivet.writeData("out");

return 0;
}

```

Compilation of this, if placed in a file called `myrivet.cc`, into an executable called `myrivet` is simplest and most robust with use of the `rivet-config` script:

```
g++ myrivet.cc -o myrivet `rivet-config --cppflags --ldflags --libs`
```

It should just work!

If you are doing something a bit more advanced, for example using the AGILE package's similar API to generate Fortran generator Pythia events and pass them directly to the Rivet analysis handler, you will need to also add the various compiler and linker flags for the extra libraries, e.g.

```
g++ myrivet.cc -o myrivet \
`rivet-config --cppflags --ldflags --libs` \
`agile-config --cppflags --ldflags --libs`
```

would be needed to compile the following AGILE+Rivet code:

```
#include "AGILE/Loader.hh"
#include "AGILE/Generator.hh"
#include "Rivet/AnalysisHandler.hh"
#include "HepMC/GenEvent.h"
#include "HepMC/IO_GenEvent.h"

using namespace std;

int main() {
```

```

// Have a look what generators are available
AGILE::Loader::initialize();
const vector<string> gens = AGILE::Loader::getAvailableGens();
foreach (const string& gen, gens) {
    cout << gen << endl;
}

// Load libraries for a specific generator and instantiate it
AGILE::Loader::loadGenLibs("Pythia6:425");
AGILE::Generator* generator = AGILE::Loader::createGen();
cout << "Running " << generator->getName()
    << " version " << generator->getVersion() << endl;

// Set generator initial state for LEP
const int particle1 = AGILE::ELECTRON;
const int particle2 = AGILE::POSITRON;
const double sqrts = 91;
generator->setInitialState(particle1, energy1, sqrts/2.0, sqrts/2.0);
generator->setSeed(14283);

// Set some parameters
generator->setParam("MSTP(5)", "320"); //< PYTHIA tune
// ...

// Set up Rivet with a LEP analysis
Rivet::AnalysisHandler rivet;
rivet.addAnalysis("DELPHI_1996_S3430090");

// Run events
const int EVTMAX = 10000;
HepMC::GenEvent evt;
for (int i = 0; i < EVTMAX; ++i) {
    generator->makeEvent(evt);
    rivet.analyze(evt);
}

// Finalize Rivet and generator
rivet.finalize();
rivet.writeData("out.aida");
generator->finalize();

return 0;
}

```

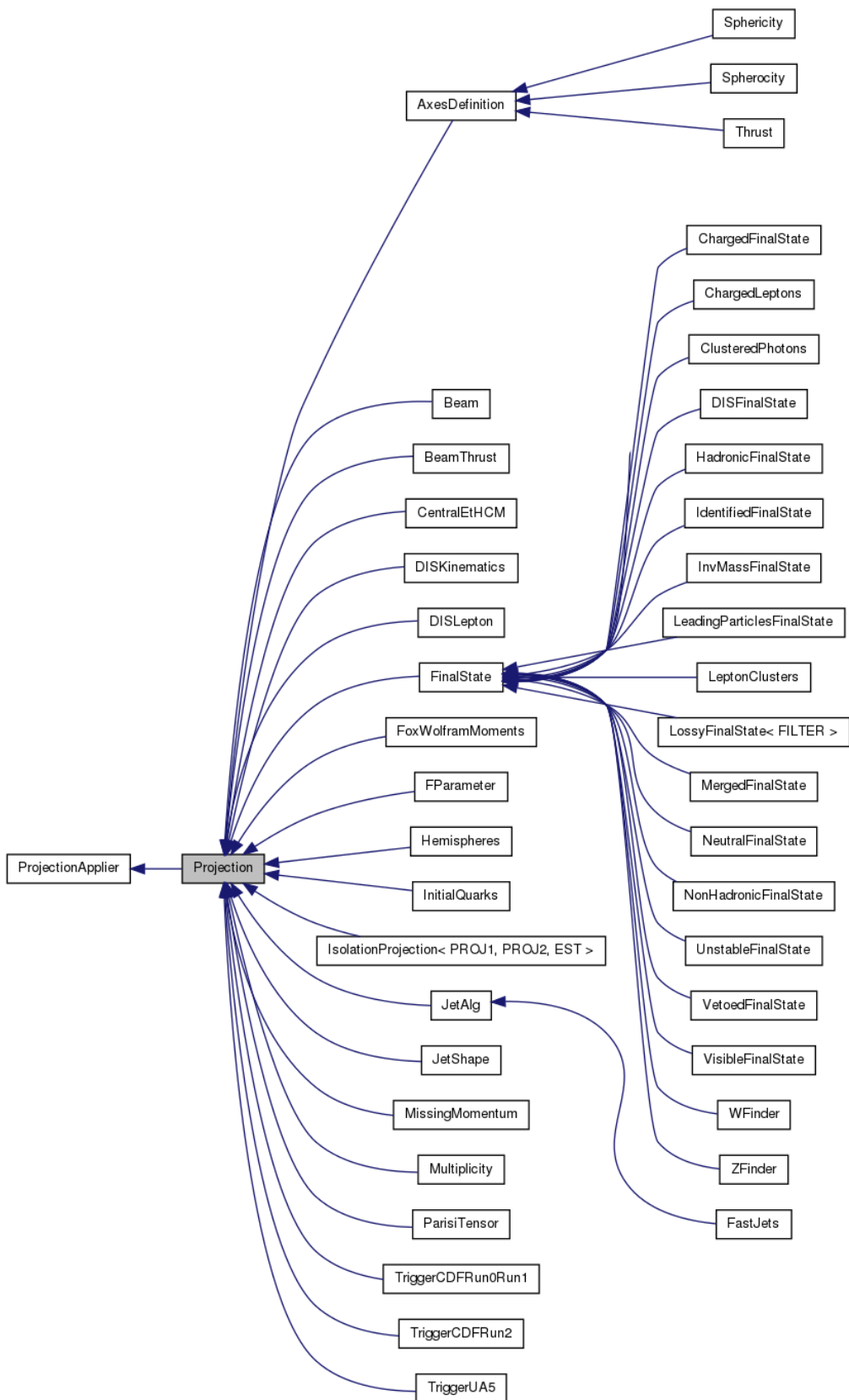


Figure 1: List of available projections and their inheritance structure.

Part IV

Appendices

A. Typical `agile-runmc` commands

- **Simple run:** `agile-runmc Herwig:6510 -P lep1.params --beams=LEP:91.2 \ -n 1000` will use the Fortran Herwig 6.5.10 generator (the `-g` option switch) to generate 1000 events (the `-n` switch) in LEP1 mode, i.e. e^+e^- collisions at $\sqrt{s} = 91.2$ GeV.
- **Parameter changes:** `agile-runmc Pythia6:425 --beams=LEP:91.2 \ -n 1000 -P myrun.params -p "PARJ(82)=5.27"` will generate 1000 events using the Fortran Pythia 6.423 generator, again in LEP1 mode. The `-P` switch is actually the way of specifying a parameters file, with one parameter per line in the format “`<key> <value>`”: in this case, the file `lep1.params` is loaded from the `<installdir>/share/AGILE` directory, if it isn’t first found in the current directory. The `-p` (lower-case) switch is used to change a named generator parameter, here Pythia’s `PARJ(82)`, which sets the parton shower cutoff scale. Being able to change parameters on the command line is useful for scanning parameter ranges from a shell loop, or rapid testing of parameter values without needing to write a parameters file for use with `-P`.
- **Writing out HepMC events:** `agile-runmc Pythia6:425 --beams=LHC:14TeV -n 50 -o out.hepmc -R` will generate 50 LHC events with Pythia. The `-o` switch is being used here to tell `agile-runmc` to write the generated events to the `out.hepmc` file. This file will be a plain text dump of the HepMC event records in the standard HepMC format. Use of filename “`-`” will result in the event stream being written to standard output (i.e. dumping to the terminal).

B. Acknowledgements

Rivet development has been supported by a variety of sources:

- All authors acknowledge support from the EU MCnet research network. MCnet is a Marie Curie Training Network funded under Framework Programme 6 contract MRTN-CT-2006-035606 and Framework Programme 7 contract PITN-GA-2012-315877.
- Andy Buckley has been supported by grants from the UK Science and Technology Facilities Council (Special Project Grant), the Scottish Universities Physics Alliance (Advanced Research Fellowship), the Royal Society (Research Fellowship), the Institute for Particle Physics Phenomenology (Associateship), and a CERN Scientific Associateship.
- Holger Schulz and Frank Siegert acknowledge the support of the German Research Foundation (DFG).

We also wish to thank the CERN MCplots (<http://mcplots.cern.ch>) team, and especially Anton Karneyeu, for doing the pre-release testing since the Rivet 1.5 series and pointing out all the bits that we got wrong: Rivet is a much better system as a result!

Part V

Bibliography

References

- [1] M. Dobbs and J. B. Hansen, Comput. Phys. Commun. **134**, 41 (2001).
- [2] M. R. Whalley, D. Bourilkov, and R. C. Group, (2005), hep-ph/0508110.
- [3] M. Cacciari and G. P. Salam, Phys. Lett. **B641**, 57 (2006), hep-ph/0512210.
- [4] M. Cacciari and G. Salam and G. Soyez, <http://www.fastjet.fr>.
- [5] T. Sjostrand, S. Mrenna, and P. Skands, JHEP **05**, 026 (2006), hep-ph/0603175.
- [6] T. Gleisberg *et al.*, JHEP **0902**, 007 (2009), 0811.4622.
- [7] T. Sjostrand, S. Mrenna, and P. Skands, Comput. Phys. Commun. **178**, 852 (2008), 0710.3820.
- [8] T. Sjostrand, (2008), 0809.0303.
- [9] M. Bahr *et al.*, Eur. Phys. J. **C58**, 639 (2008), 0803.0883.
- [10] DELPHI Collaboration, P. Abreu *et al.*, Z. Phys. **C73**, 11 (1996).
- [11] I. Antcheva *et al.*, Comput. Phys. Commun. **180**, 2499 (2009).
- [12] ALEPH Collaboration, D. Decamp *et al.*, Phys. Lett. **B273**, 181 (1991).
- [13] ALEPH Collaboration, D. Buskulic *et al.*, Z. Phys. **C69**, 365 (1996).
- [14] ALEPH Collaboration, R. Barate *et al.*, Phys. Rept. **294**, 1 (1998).
- [15] ALEPH COLLABORATION Collaboration, R. Barate *et al.*, Eur.Phys.J. **C16**, 597 (2000), hep-ex/9909032.
- [16] ALEPH Collaboration, A. Heister *et al.*, Phys. Lett. **B512**, 30 (2001), hep-ex/0106051.
- [17] ALEPH COLLABORATION Collaboration, A. Heister *et al.*, Phys.Lett. **B528**, 19 (2002), hep-ex/0201012.
- [18] ALEPH Collaboration, A. Heister *et al.*, Eur. Phys. J. **C35**, 457 (2004).
- [19] DELPHI Collaboration, P. Abreu *et al.*, Z. Phys. **C67**, 543 (1995).
- [20] DELPHI Collaboration, P. Abreu *et al.*, Phys. Lett. **B449**, 364 (1999).
- [21] DELPHI Collaboration, P. Abreu *et al.*, Phys. Lett. **B479**, 118 (2000), hep-ex/0103022.
- [22] JADE Collaboration, P. Pfeifenschneider *et al.*, Eur. Phys. J. **C17**, 19 (2000), hep-ex/0001055.
- [23] OPAL Collaboration, P. D. Acton *et al.*, Z. Phys. **C58**, 405 (1993).
- [24] OPAL Collaboration, R. Akers *et al.*, Z. Phys. **C63**, 181 (1994).
- [25] OPAL Collaboration, G. Alexander *et al.*, Phys. Lett. **B358**, 162 (1995).
- [26] OPAL COLLABORATION Collaboration, G. Alexander *et al.*, Z.Phys. **C70**, 197 (1996).
- [27] OPAL Collaboration, G. Alexander *et al.*, Z. Phys. **C73**, 569 (1997).

- [28] OPAL Collaboration, K. Ackerstaff *et al.*, Phys. Lett. **B412**, 210 (1997), hep-ex/9708022.
- [29] OPAL Collaboration, K. Ackerstaff *et al.*, Eur. Phys. J. **C4**, 19 (1998), hep-ex/9802013.
- [30] OPAL Collaboration, K. Ackerstaff *et al.*, Eur. Phys. J. **C5**, 411 (1998), hep-ex/9805011.
- [31] OPAL Collaboration, K. Ackerstaff *et al.*, Eur. Phys. J. **C7**, 369 (1999), hep-ex/9807004.
- [32] OPAL COLLABORATION Collaboration, G. Abbiendi *et al.*, Eur.Phys.J. **C17**, 373 (2000), hep-ex/0007017.
- [33] OPAL Collaboration, G. Abbiendi *et al.*, Eur. Phys. J. **C20**, 601 (2001), hep-ex/0101044.
- [34] OPAL COLLABORATION Collaboration, G. Abbiendi *et al.*, Phys.Lett. **B550**, 33 (2002), hep-ex/0211007, 18 pages, 5 figures Report-no: CERN-EP-2002-0079.
- [35] OPAL Collaboration, G. Abbiendi *et al.*, Eur. Phys. J. **C40**, 287 (2005), hep-ex/0503051.
- [36] SLD Collaboration, K. Abe *et al.*, Phys. Lett. **B386**, 475 (1996), hep-ex/9608008.
- [37] SLD Collaboration, K. Abe *et al.*, Phys. Rev. **D59**, 052001 (1999), hep-ex/9805029.
- [38] SLD Collaboration, K. Abe *et al.*, Phys. Rev. **D65**, 092006 (2002), hep-ex/0202031, [Erratum-ibid.D66:079905,2002].
- [39] SLD Collaboration, K. Abe *et al.*, Phys. Rev. **D69**, 072003 (2004), hep-ex/0310017.
- [40] CDF Collaboration, F. Abe *et al.*, Phys. Rev. Lett. **61**, 1819 (1988).
- [41] CDF Collaboration, F. Abe *et al.*, Phys. Rev. **D41**, 2330 (1990).
- [42] CDF Collaboration, F. Abe *et al.*, Phys. Rev. Lett. **71**, 679 (1993).
- [43] CDF Collaboration, F. Abe *et al.*, Phys. Rev. **D50**, 5562 (1994).
- [44] CDF Collaboration, F. Abe *et al.*, Phys. Rev. Lett. **75**, 608 (1995).
- [45] CDF Collaboration, F. Abe *et al.*, Phys. Rev. **D54**, 4221 (1996), hep-ex/9605004.
- [46] CDF Collaboration, F. Abe *et al.*, Phys. Rev. Lett. **77**, 5336 (1996), hep-ex/9609011.
- [47] CDF Collaboration, F. Abe *et al.*, Phys. Rev. **D56**, 2532 (1997).
- [48] CDF Collaboration, F. Abe *et al.*, Phys. Rev. Lett. **80**, 3461 (1998).
- [49] CDF Collaboration, T. Affolder *et al.*, Phys. Rev. Lett. **84**, 845 (2000), hep-ex/0001021.
- [50] CDF Collaboration, A. A. Affolder *et al.*, Phys. Rev. **D61**, 091101 (2000), hep-ex/9912022.
- [51] CDF Collaboration, A. A. Affolder *et al.*, Phys. Rev. **D64**, 012001 (2001), hep-ex/0012013.
- [52] CDF Collaboration, A. A. Affolder *et al.*, Phys. Rev. **D64**, 032001 (2001), hep-ph/0102074.
- [53] CDF Collaboration, T. Affolder *et al.*, Phys. Rev. **D65**, 092002 (2002).
- [54] CDF Collaboration, D. Acosta *et al.*, Phys. Rev. **D65**, 072005 (2002).
- [55] CDF Collaboration, D. Acosta *et al.*, Phys. Rev. **D70**, 072002 (2004), hep-ex/0404004.
- [56] CDF Collaboration, D. E. Acosta *et al.*, Phys. Rev. Lett. **95**, 022003 (2005), hep-ex/0412050.
- [57] CDF Collaboration, D. E. Acosta *et al.*, Phys. Rev. **D71**, 112002 (2005), hep-ex/0505013.
- [58] CDF Collaboration, A. Abulencia *et al.*, Phys. Rev. **D74**, 071103 (2006), hep-ex/0512020.
- [59] CDF Collaboration, A. Abulencia *et al.*, Phys. Rev. **D74**, 032008 (2006), hep-ex/0605099.

- [60] CDF Collaboration, A. Abulencia *et al.*, Phys. Rev. **D75**, 092006 (2007), hep-ex/0701051.
- [61] CDF Collaboration, T. Aaltonen *et al.*, Phys. Rev. Lett. **100**, 102001 (2008), 0711.3717.
- [62] CDF Collaboration, T. Aaltonen *et al.*, Phys. Rev. **D77**, 011108 (2008), 0711.4044.
- [63] CDF Collaboration, T. Aaltonen *et al.*, Phys. Rev. **D78**, 072005 (2008), 0806.1699.
- [64] CDF Collaboration, T. Aaltonen *et al.*, Phys. Rev. **D78**, 052006 (2008), 0807.2204.
- [65] CDF Collaboration, T. Aaltonen *et al.*, Phys. Rev. **D79**, 112002 (2009), 0812.4036.
- [66] CDF Collaboration, T. Aaltonen *et al.*, Phys. Rev. **D79**, 052008 (2009), 0812.4458.
- [67] CDF Collaboration, T. Aaltonen *et al.*, Phys. Rev. **D79**, 112005 (2009), 0904.1098.
- [68] CDF Collaboration, T. Aaltonen *et al.*, (2009), 0908.3914.
- [69] CDF Collaboration, T. Aaltonen *et al.*, Phys. Rev. **D80**, 111106 (2009), 0910.3623.
- [70] D0 Collaboration, S. Abachi *et al.*, Phys. Rev. **D53**, 6000 (1996), hep-ex/9509005.
- [71] D0 Collaboration, S. Abachi *et al.*, Phys. Rev. Lett. **77**, 595 (1996), hep-ex/9603010.
- [72] D0 COLLABORATION Collaboration, B. Abbott *et al.*, Phys.Lett. **B487**, 264 (2000), hep-ex/9905024.
- [73] D0 Collaboration, B. Abbott *et al.*, Phys. Lett. **B513**, 292 (2001), hep-ex/0010026.
- [74] D0 Collaboration, V. M. Abazov *et al.*, Phys. Lett. **B517**, 299 (2001), hep-ex/0107012.
- [75] D0 Collaboration, V. M. Abazov *et al.*, Phys. Rev. Lett. **94**, 221801 (2005), hep-ex/0409040.
- [76] D0 Collaboration, V. M. Abazov *et al.*, Phys. Lett. **B639**, 151 (2006), hep-ex/0511054.
- [77] D0 Collaboration, V. M. Abazov *et al.*, Phys. Rev. **D76**, 012003 (2007), hep-ex/0702025.
- [78] D0 Collaboration, V. M. Abazov *et al.*, Phys. Lett. **B658**, 112 (2008), hep-ex/0608052.
- [79] D0 Collaboration, V. M. Abazov *et al.*, Phys. Rev. Lett. **100**, 102002 (2008), 0712.0803.
- [80] D0 Collaboration, V. M. Abazov *et al.*, Phys. Rev. Lett. **101**, 062001 (2008), 0802.2400.
- [81] D0 Collaboration, V. M. Abazov *et al.*, Phys. Lett. **B666**, 435 (2008), 0804.1107.
- [82] D0 Collaboration, V. M. Abazov *et al.*, Phys. Rev. Lett. **101**, 211801 (2008), 0807.3367.
- [83] D0 Collaboration, V. M. Abazov *et al.*, Phys. Lett. **B669**, 278 (2008), 0808.1296.
- [84] D0 Collaboration, V. M. Abazov *et al.*, Phys. Lett. **B678**, 45 (2009), 0903.1748.
- [85] D0 Collaboration, V. M. Abazov *et al.*, Phys. Rev. Lett. **103**, 191803 (2009), 0906.4819.
- [86] D0 Collaboration, V. M. Abazov *et al.*, Phys. Lett. **B682**, 370 (2010), 0907.4286.
- [87] D0 Collaboration, V. M. Abazov *et al.*, (2010), 1002.4594.
- [88] D0 Collaboration, V. M. Abazov *et al.*, (2010), 1002.4917.
- [89] D0 Collaboration, V. M. Abazov *et al.*, (2010), 1006.0618.
- [90] D0 Collaboration, V. M. Abazov *et al.*, (2010), 1010.0262.
- [91] D0 COLLABORATION Collaboration, V. M. Abazov *et al.*, Phys.Lett. **B704**, 434 (2011), 1104.1986.

- [92] T. Alexopoulos *et al.*, Phys. Lett. **B435**, 453 (1998).
- [93] ALICE Collaboration, K. Aamodt *et al.*, Eur. Phys. J. **C68**, 89 (2010), 1004.3034.
- [94] ALICE Collaboration, K. Aamodt *et al.*, Eur.Phys.J. **C68**, 345 (2010), 1004.3514.
- [95] ALICE Collaboration, K. Aamodt *et al.*, Phys. Lett. **B693**, 53 (2010), 1007.0719.
- [96] ALICE COLLABORATION Collaboration, K. Aamodt *et al.*, Eur.Phys.J. **C71**, 1594 (2011), 1012.3257.
- [97] ALICE Collaboration, K. Aamodt *et al.*, Eur.Phys.J. **C71**, 1655 (2011), 1101.4110.
- [98] ALICE COLLABORATION Collaboration, B. Abelev *et al.*, Eur. Phys. J. C (2012), 1208.4968.
- [99] ATLAS Collaboration, G. Aad *et al.*, (2010), 1003.3124.
- [100] ATLAS Collaboration, G. Aad *et al.*, (2010), 1009.5908.
- [101] T. A. Collaboration, (2010), 1012.4389.
- [102] T. A. Collaboration, (2010), 1012.5382.
- [103] ATLAS COLLABORATION Collaboration, G. Aad *et al.*, Nature Commun. **2**, 463 (2011), 1104.0326.
- [104] ATLAS Collaboration, G. Aad *et al.*, (2011), 1107.3311.
- [105] THE ATLAS Collaboration, G. Aad *et al.*, (2011), 1108.6308.
- [106] ATLAS COLLABORATION Collaboration, G. Aad *et al.*, (2011), 1109.0525.
- [107] ATLAS COLLABORATION Collaboration, G. Aad *et al.*, Eur.Phys.J. **C71**, 1846 (2011), 1109.6833.
- [108] ATLAS COLLABORATION Collaboration, G. Aad *et al.*, Phys.Rev. **D85**, 012001 (2012), 1111.1297.
- [109] ATLAS COLLABORATION Collaboration, (2011), 1111.2690.
- [110] ATLAS COLLABORATION Collaboration, G. Aad *et al.*, Phys.Lett. **B709**, 341 (2012), 1111.5570.
- [111] T. A. Collaboration, (2011), 1102.2696.
- [112] ATLAS Collaboration, J. B. G. da Costa *et al.*, (2011), 1102.5290.
- [113] ATLAS Collaboration, G. Aad *et al.*, (2011), 1103.6214.
- [114] ATLAS COLLABORATION Collaboration, G. Aad *et al.*, Nucl.Phys. **B850**, 387 (2011), 1104.3038.
- [115] ATLAS Collaboration, G. Aad *et al.*, Phys. Lett. **B703**, 428 (2011), 1106.4495.
- [116] A. Collaboration, (2011), 1107.2092.
- [117] ATLAS Collaboration, G. Aad *et al.*, (2011), 1107.2381.
- [118] ATLAS Collaboration, G. Aad *et al.*, (2011), 1109.6572.
- [119] ATLAS Collaboration, G. Aad *et al.*, Phys. Rev. **D85**, 012006 (2012), 1109.6606.

- [120] ATLAS COLLABORATION Collaboration, G. Aad *et al.*, JHEP **1111**, 099 (2011), 1110.2299.
- [121] ATLAS COLLABORATION Collaboration, G. Aad *et al.*, Phys.Rev. **D85**, 052005 (2012), 1112.4432, Long author list - awaiting processing.
- [122] ATLAS COLLABORATION Collaboration, G. Aad *et al.*, (2011), 1112.6297.
- [123] ATLAS COLLABORATION Collaboration, G. Aad *et al.*, (2012), 1201.1276.
- [124] ATLAS COLLABORATION Collaboration, G. Aad *et al.*, (2012), 1203.0419.
- [125] ATLAS COLLABORATION Collaboration, G. Aad *et al.*, JHEP **1207**, 019 (2012), 1203.3100.
- [126] ATLAS Collaboration, G. Aad *et al.*, (2012), 1203.3161.
- [127] ATLAS COLLABORATION Collaboration, G. Aad *et al.*, JHEP **1205**, 128 (2012), 1203.4606.
- [128] ATLAS COLLABORATION Collaboration, G. Aad *et al.*, Eur.Phys.J. **C72**, 2043 (2012), 1203.5015.
- [129] ATLAS COLLABORATION Collaboration, G. Aad *et al.*, (2012), 1203.6193, 15 pages plus author list (28 pages total), 11 figures, 8 tables, submitted to Physical Review D.
- [130] ATLAS COLLABORATION Collaboration, G. Aad *et al.*, (2012), 1204.5638, 5 pages plus author list (18 pages total), 2 figures, 1 table, submitted to Physics Review Letters.
- [131] ATLAS COLLABORATION Collaboration, G. Aad *et al.*, Nucl.Phys. **B864**, 341 (2012), 1206.3122.
- [132] ATLAS COLLABORATION Collaboration, G. Aad *et al.*, Phys.Rev. **D86**, 072006 (2012), 1206.5369.
- [133] ATLAS COLLABORATION Collaboration, G. Aad *et al.*, Phys.Rev. **D88**, 032004 (2013), 1207.6915.
- [134] ATLAS COLLABORATION Collaboration, G. Aad *et al.*, Phys.Rev. **D86**, 072004 (2012), 1208.0563.
- [135] ATLAS COLLABORATION Collaboration, G. Aad *et al.*, (2012), 1208.6256.
- [136] ATLAS COLLABORATION Collaboration, G. Aad *et al.*, (2012), 1210.0441.
- [137] ATLAS COLLABORATION Collaboration, G. Aad *et al.*, JHEP **1303**, 128 (2013), 1211.6096.
- [138] ATLAS COLLABORATION Collaboration, G. Aad *et al.*, Phys.Rev. **D87**, 052002 (2013), 1211.6312.
- [139] ATLAS COLLABORATION Collaboration, G. Aad *et al.*, (2012), 1211.6899.
- [140] ATLAS COLLABORATION Collaboration, G. Aad *et al.*, Phys.Lett. **B709**, 137 (2012), 1110.6189.
- [141] ATLAS COLLABORATION Collaboration, G. Aad *et al.*, Phys.Lett. **B710**, 519 (2012), 1111.4116.
- [142] THE ATLAS COLLABORATION Collaboration, G. Aad *et al.*, (2013), 1302.1415.

- [143] ATLAS COLLABORATION Collaboration, G. Aad *et al.*, JHEP **1307**, 032 (2013), 1304.7098.
- [144] ATLAS COLLABORATION Collaboration, G. Aad *et al.*, (2013), 1307.5749.
- [145] CMS Collaboration, V. Khachatryan *et al.*, JHEP **02**, 041 (2010), 1002.0621.
- [146] CMS Collaboration, V. Khachatryan *et al.*, Phys. Rev. Lett. **105**, 022002 (2010), 1005.3299.
- [147] CMS COLLABORATION Collaboration, S. Chatrchyan *et al.*, JHEP **1201**, 052 (2012), 1111.5536.
- [148] CMS Collaboration, V. Khachatryan *et al.*, JHEP **01**, 079 (2011), 1011.5531.
- [149] CMS Collaboration, V. Khachatryan *et al.*, JHEP **03**, 090 (2011), 1101.3512.
- [150] CMS COLLABORATION Collaboration, V. Khachatryan *et al.*, Phys.Rev.Lett. **106**, 122003 (2011), 1101.5029.
- [151] CMS Collaboration, V. Khachatryan *et al.*, Phys. Lett. **B699**, 48 (2011), 1102.0068.
- [152] CMS Collaboration, V. Khachatryan *et al.*, Phys. Rev. Lett. **106**, 201804 (2011), 1102.2020.
- [153] CMS Collaboration, V. Khachatryan *et al.*, JHEP **03**, 136 (2011), 1102.3194.
- [154] CMS Collaboration, V. Khachatryan *et al.*, JHEP **05**, 064 (2011), 1102.4282.
- [155] CMS COLLABORATION Collaboration, S. Chatrchyan *et al.*, Phys. Rev. Lett. **107**, 132001 (2011), 1106.0208, Long author list - awaiting processing.
- [156] CMS COLLABORATION Collaboration, S. Chatrchyan *et al.*, Phys.Lett. **B702**, 336 (2011), 1106.0647.
- [157] CMS COLLABORATION Collaboration, S. Chatrchyan *et al.*, (2011), 1107.0330.
- [158] CMS Collaboration, S. Chatrchyan *et al.*, JHEP **11**, 148 (2011), 1110.0211.
- [159] CMS COLLABORATION Collaboration, S. Chatrchyan *et al.*, JHEP **1206**, 036 (2012), 1202.0704.
- [160] CMS COLLABORATION Collaboration, S. Chatrchyan *et al.*, JHEP **1205**, 055 (2012), 1202.5535.
- [161] CMS COLLABORATION Collaboration, S. Chatrchyan *et al.*, (2012), 1204.0696.
- [162] CMS COLLABORATION Collaboration, S. Chatrchyan *et al.*, (2012), 1204.1411.
- [163] CMS COLLABORATION Collaboration, S. Chatrchyan *et al.*, (2012), 1209.1805.
- [164] CMS COLLABORATION Collaboration, S. Chatrchyan *et al.*, (2012), 1210.6718.
- [165] CMS COLLABORATION Collaboration, S. Chatrchyan *et al.*, Phys.Rev. **D85**, 032002 (2012), 1110.4973.
- [166] (2012).
- [167] CMS COLLABORATION Collaboration, S. Chatrchyan *et al.*, Phys.Lett. **B722**, 238 (2013), 1301.1646.
- [168] CMS COLLABORATION Collaboration, S. Chatrchyan *et al.*, JHEP **1304**, 072 (2013), 1302.2394.
- [169] CMS COLLABORATION Collaboration, S. Chatrchyan *et al.*, (2013), 1303.4811.

- [170] CMS COLLABORATION Collaboration, S. Chatrchyan *et al.*, JHEP **1312**, 039 (2013), 1310.1349.
- [171] CMS COLLABORATION Collaboration, S. Chatrchyan *et al.*, (2013), 1310.3082.
- [172] CMS COLLABORATION Collaboration, S. Chatrchyan *et al.*, Eur.Phys.J. **C73**, 2674 (2013), 1310.4554.
- [173] CMS COLLABORATION Collaboration, S. Chatrchyan *et al.*, (2013), 1311.5815.
- [174] CMS COLLABORATION Collaboration, S. Chatrchyan *et al.*, (2013), 1312.5729.
- [175] CMS COLLABORATION Collaboration, S. Chatrchyan *et al.*, (2013), 1312.6440.
- [176] (2011).
- [177] R. Aaij *et al.*
- [178] LHCb Collaboration, R. Aaij *et al.*, Phys. Lett. **B693**, 69 (2010), 1008.3105.
- [179] LHCb COLLABORATION Collaboration, R. Aaij *et al.*, JHEP **1108**, 034 (2011), 1107.0882.
- [180] LHCb COLLABORATION Collaboration, R. Aaij *et al.*, Phys.Lett. **B703**, 267 (2011), 1107.3935.
- [181] LHCb COLLABORATION Collaboration, R. Aaij *et al.*, Eur.Phys.J. **C72**, 2168 (2012), 1206.5160.
- [182] LHCb COLLABORATION Collaboration, R. Aaij *et al.*, The European Physical Journal C **73**, 2421. 15 p (2013), 1212.4755.
- [183] LHCb COLLABORATION Collaboration, R. Aaij *et al.*, Nucl.Phys. **B871**, 1 (2013), 1302.2864.
- [184] LHCf COLLABORATION Collaboration, O. Adriani *et al.*, Phys.Rev. **D86**, 092001 (2012), 1205.4578.
- [185] TOTEM Collaboration, G. Antchev *et al.*, CERN Report No. CERN-PH-EP-2012-239. TOTEM-2012-002, 2012 (unpublished).
- [186] TOTEM COLLABORATION Collaboration, P. Aspell, Europhys.Lett. **98**, 31002 (2012), 1205.4105.
- [187] UA1 Collaboration, C. Albajar *et al.*, Nucl. Phys. **B335**, 261 (1990).
- [188] UA5 Collaboration, K. Alpgard *et al.*, Phys. Lett. **B112**, 183 (1982).
- [189] UA5 Collaboration, G. J. Alner *et al.*, Z. Phys. **C33**, 1 (1986).
- [190] UA5 Collaboration, G. J. Alner *et al.*, Phys. Rept. **154**, 247 (1987).
- [191] UA5 Collaboration, R. E. Ansorge *et al.*, Z. Phys. **C37**, 191 (1988).
- [192] UA5 Collaboration, R. E. Ansorge *et al.*, Z. Phys. **C43**, 357 (1989).
- [193] H1 Collaboration, I. Abt *et al.*, Z. Phys. **C63**, 377 (1994).
- [194] H1 Collaboration, S. Aid *et al.*, Phys. Lett. **B356**, 118 (1995), hep-ex/9506012.
- [195] H1 Collaboration, C. Adloff *et al.*, Eur. Phys. J. **C12**, 595 (2000), hep-ex/9907027.
- [196] ZEUS Collaboration, S. Chekanov *et al.*, Eur. Phys. J. **C23**, 615 (2002), hep-ex/0112029.
- [197] STAR Collaboration, J. Adams *et al.*, Phys. Lett. **B637**, 161 (2006), nucl-ex/0601033.

- [198] STAR Collaboration, B. I. Abelev *et al.*, Phys. Rev. **C75**, 064901 (2007), nucl-ex/0607033.
- [199] STAR Collaboration, B. I. Abelev *et al.*, Phys. Rev. Lett. **97**, 252001 (2006), hep-ex/0608030.
- [200] STAR Collaboration, B. I. Abelev *et al.*, Phys. Rev. **C79**, 034909 (2009), 0808.2041.
- [201] C. Nattrass, Eur. Phys. J. **C62**, 265 (2009), 0809.5261.
- [202] ARGUS COLLABORATION Collaboration, H. Albrecht *et al.*, Z.Phys. **C58**, 191 (1993).
- [203] ARGUS COLLABORATION Collaboration, H. Albrecht *et al.*, Z.Phys. **C58**, 199 (1993).
- [204] ARGUS COLLABORATION Collaboration, H. Albrecht *et al.*, Z.Phys. **C61**, 1 (1994).
- [205] BABAR COLLABORATION Collaboration, B. Aubert *et al.*, Phys.Rev. **D67**, 032002 (2003), hep-ex/0207097.
- [206] BABAR COLLABORATION Collaboration, B. Aubert *et al.*, Phys.Rev.Lett. **95**, 142003 (2005), hep-ex/0504014.
- [207] BABAR COLLABORATION Collaboration, B. Aubert *et al.*, Phys.Rev. **D75**, 012003 (2007), hep-ex/0609004.
- [208] BABAR Collaboration, B. Aubert *et al.*, Phys. Rev. Lett. **100**, 011801 (2008), 0707.2981.
- [209] BELLE COLLABORATION Collaboration, K. Abe *et al.*, Phys.Rev. **D64**, 072001 (2001), hep-ex/0103041.
- [210] BELLE Collaboration, R. Seuster *et al.*, Phys. Rev. **D73**, 032002 (2006), hep-ex/0506068.
- [211] CLEO Collaboration, M. Artuso *et al.*, Phys. Rev. **D70**, 112001 (2004), hep-ex/0402040.
- [212] JADE Collaboration, P. A. Movilla Fernandez, O. Biebel, S. Bethke, S. Kluth, and P. Pfeifenschneider, Eur. Phys. J. **C1**, 461 (1998), hep-ex/9708034.
- [213] PARTICLE DATA GROUP Collaboration, C. Amsler *et al.*, Phys. Lett. **B667**, 1 (2008).
- [214] AMES-BOLOGNA-CERN-DORTMUND-HEIDELBERG-WARSAW Collaboration, A. Breakstone *et al.*, Phys. Rev. **D30**, 528 (1984).
- [215] TASSO Collaboration, W. Braunschweig *et al.*, Z. Phys. **C47**, 187 (1990).
- [216] J. Bromley *et al.*, (1995), ZEUS and H1 Collaborations.